Mécanismes moléculaires de tolérance des plantes aux xénobiotiques : application à la phytoremédiation des hydrocarbures aromatiques polycycliques (HAPs)

Anne-Sophie Dumas

ANNÉE 2013

THÈSE / UNIVERSITÉ DE RENNES 1

sous le sceau de l'Université Européenne de Bretagne

pour le grade de

DOCTEUR DE L'UNIVERSITÉ DE RENNES 1

Mention : Biologie

Ecole doctorale Vie-Agro-Santé

présentée par

Anne-Sophie DUMAS

Préparée à l'unité mixte de recherche 6553 Ecobio
Ecosystème, Biodiversité, Evolution
CNRS-Université de Rennes 1

Mécanismes moléculaires de tolérance des plantes aux xénobiotiques: Application à la phytoremédiation des Hydrocarbures Aromatiques Polycycliques (HAPs)

Thèse soutenue à Rennes
le 5 décembre 2013

devant le jury composé de :

Jacques BOURGUIGNON
Ingénieur chercheur, CEA Grenoble / *rapporteur*

Bertrand HIREL
Directeur de recherche, INRA-AgroParisTech / *rapporteur*

Malika AINOUCHE
Professeur, Université de Rennes 1 / *examinateur*

Alain BOUCHEREAU
Professeur, Université de Rennes 1 / *examinateur*

Gérard GAILLARD
Executive Vice-President, Axson / *examinateur*

Anis LIMAMI
Professeur, Université d'Angers / *examinateur*

Abdelhak EL AMRANI
Maître de conférence, Université de Rennes 1 / *directeur de thèse*

Richard BERTHOME
Chargé de recherche, INRA Toulouse / *co-directeur de thèse*

Remerciements

Je tiens à remercier en premier lieu la société Axson Coatings et le groupe Axson pour avoir financé le projet ; en particulier Mr Gérard Gaillard, vice-président exécutif, pour avoir lancé le projet, Mr Denys Delcourt pour avoir effectué le suivi de la thèse, Mme Aline Fontaine pour tout l'aspect administratif et enfin Mr Pascal Frichot pour son aide pour son aide sur le terrain.

J'adresse tous mes remerciements à Mr Bourguignon et Mr Hirel pour avoir accepté d'être les rapporteurs de cette thèse ainsi qu'à Mme Ainouche, Mr Bouchereau et Mr Limami pour leur rôle d'examinateur.

Un gros merci à mes encadrants, Richard Berthome et Abdel El Amrani, pour m'avoir accompagnée dans cette aventure qu'est la thèse.

Merci à l'ensemble des gens de l'UMR Ecobio en particulier Delphine Bernard, pour son soutien et sa grande aide dans les expérimentations ; Valérie Gouesbet et Louis Parize pour leur appui technique que ce soit sur le terrain ou au labo ; les stagiaires (Morgan et Jérôme) qui ont fait un gros boulot sur le terrain. Merci à Morgane pour m'avoir aidée à prendre mes repères au sein du labo et puis avoir partagé café, bureau et soutien moral mutuel ! Moez, Rahma, Maria-Dolores et Mounir pour avoir partagé bureaux et labos. Le reste de l'équipe MOB (ancienne ou présente) pour les pauses midi, thé… Julie, Paula, Julien, Mathieu … mais aussi Alexandra et Anne-Antonella et tous les autres ! Merci à Agnès Schermann de m'avoir recueillie pour la fin de ma rédaction avant que je ne sois « sans bureau fixe ». Un grand merci à l'ensemble de l'équipe MOB puis à toutes les autres personnes d'Ecobio que j'ai pu côtoyer à un moment ou à un autre durant ma thèse.

Je tiens aussi à remercier l'ensemble des personnes travaillant à l'URGV pour leur accueil, leur aide et leurs parties de volley qui ont rendu mes quelques semaines dans leur labo très agréables.

Un gros merci à Emile Jardé et Laurent Jeanneau pour leur aide précieuse pour les analyses de HAPs.

Un coucou à toi Aurore pour avoir affirmé que « 2013, année de la thèse », c'est vrai mais après 10 ans tu sais beaucoup de chose !!

Enfin un gros merci à ma famille, mes parents et ma petite sœur (qui n'est plus si petite) pour leur soutient durant cette période de ma vie. Reste à voir ce qui va venir pour la suite…

« La souris est un animal qui, tué en quantité suffisante et dans des conditions contrôlées, produit une thèse de doctorat. »

Woody Allen

Sommaire

Chapitre 1 :
Introduction générale

Partie 1: **Gestion des sols pollués**

1. Introduction

Aujourd'hui, le développement durable est l'une de nos préoccupations majeures. Ce concept a été défini pour la première fois en 1987 comme « un développement qui répond aux besoins du présent sans compromettre la capacité des générations futures à répondre aux leurs » (Giddings et al., 2002). Le développement durable combine à la fois le développement économique avec l'équité sociale et la préservation de l'environnement. Le développement de l'agriculture moderne et l'industrialisation ont permis d'améliorer le niveau de vie de la population mais ont aussi engendré de nombreux problèmes environnementaux. Les marées noires, les rejets industriels, l'utilisation incontrôlée des pesticides et des fertilisants, la gestion des déchets domestiques et industriels qui ont eu lieu par le passé posent actuellement de nombreux problèmes.

2. Des régulations pour contrôler les pollutions

Afin de contrôler ces pollutions, des mesures ont dû être prises par les autorités dans un cadre de protection de l'environnement. En effet, dés 1989, les Etats-Unis mettent en place le premier texte à visée environnementale pour la protection de l'eau : « the Refuse Act for water protection » (Cowdrey, 1975). Le parlement européen a promulgué sa première loi environnementale en 1958, dans le premier traité de la Communauté Economique Européenne (CEE) (Jans and Vedder, 2008).

Pour gérer au mieux les sols pollués, des niveaux-seuils de régulation (RGV=regulatory guidance value) ont été mis en place par la plupart des nations. Ces valeurs sont des recommandations qui permettent aux autorités locales de mettre en place des règlementations pour la gestion des sites contaminés (Jennings, 2012).

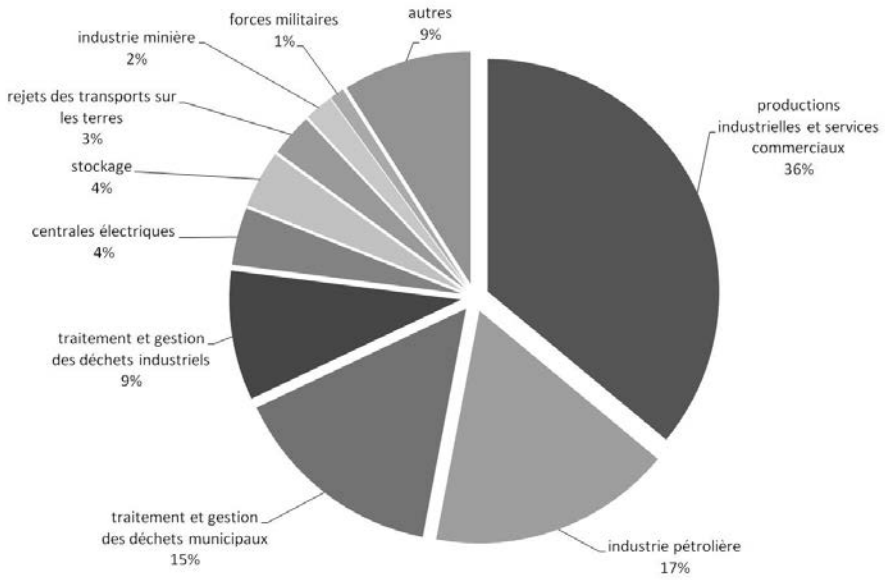

<u>Figure 1</u> : Ensemble des activités responsables de la pollution des sols en Europe (EEA, 2011a)

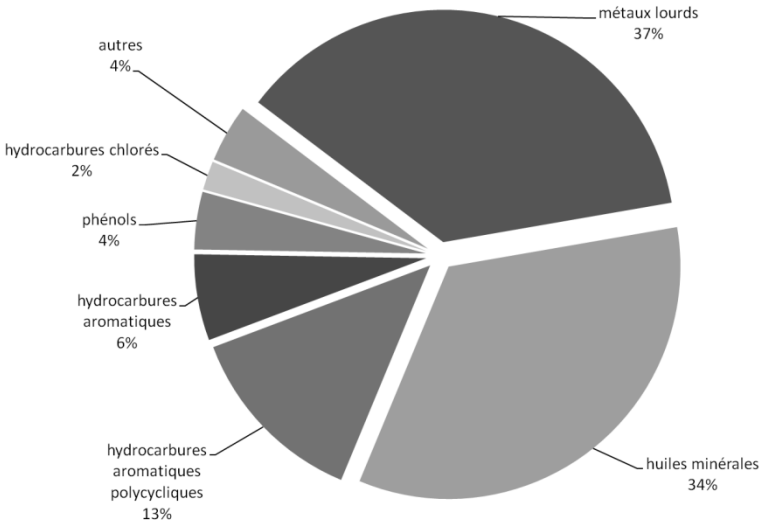

<u>Figure 2</u>

: Ensemble des polluants affectant les sols et les eaux souterraines en Europe (EEA, 2011b)

La régulation de la gestion de l'environnement a conduit à la création d'agences gouvernementales telles que l'Agence Américaine pour l'Environnement (USEPA) en 1970 et de l'Agence Européenne pour l'Environnement (EEA) en 1990. Leur rôle est de guider, d'informer, de prévenir et d'interagir avec les institutions gouvernementales et scientifiques ainsi qu'avec le monde industriel et agricole mais aussi avec l'ensemble de la population.

L'EEA regroupe 32 pays : les 27 Etats-membres de l'Union Européenne (UE) ainsi que l'Islande, le Liechtenstein, la Norvège, le Suisse et la Turquie. L'ensemble des données disponibles sur les pollutions des sols et des eaux souterraines, de ces pays, ont été collectées et publiées par l'EEA. En Europe, la production industrielle et les services commerciaux ainsi que l'industrie pétrolière et le traitement des déchets industriels et municipaux sont à l'origine de plus de ¾ des pollutions de sol (Fig. 1). Ces données soulignent l'impact négatif des activités humaines sur l'environnement.

De plus, les métaux lourds, les huiles minérales et les hydrocarbures aromatiques polycycliques (HAPs) représentent la majorité (84%) des polluants retrouvés dans les sols et eaux souterraines en Europe (Fig. 2). Le pétrole est la source de l'essentiel des pollutions de par la production d'huile minérale, d'HAPs et d'hydrocarbures aromatiques.

Actuellement, l'évaluation des sites pollués (nombre, types de pollution, état des lieux) est réalisée uniquement à un niveau national mais aucune base de données n'a été crée afin d'évaluer à l'échelle mondiale l'ampleur des sols pollués (nombre, localisation, répartition, mesures prises par les autorités…) et ce même si les Nations Unies ont développé un programme environnemental en 1972.

Lors de la conférence de Rio de Janeiro sur l'Environnement et le Développement (1992), les Nations Unies ont créé le principe du « pollueur-payeur » obligeant ainsi les responsables de pollutions à payer les frais de dépollution et de traitement du site pollué (UN, 1992). Ce principe a été adopté par le parlement européen en 2004 avec la directive (directive 2004/35/CE) sur la responsabilité environnementale (UE, 2004). Cette directive a été transposée dans la loi française en 2008 (Parlement Français, 2008). L'USEPA a aussi mis en place cette directive (EPA, 1996).

Tableau 1: Liste des 16 HAPs appartenant à la liste des polluants prioritaires de l'USEPA

Nom	Structure	Formule	Solubilité dans l'eau	PM (g/mol)
Acénaphthène	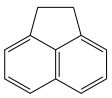	$C_{12}H_{10}$	3,92mg/L	154.21
Acénaphtylène	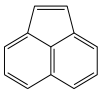	$C_{12}H_8$	3,927mg/L	152.20
Anthracène	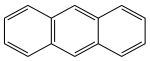	$C_{14}H_{10}$	1,3mg/L	178.23
Benzo[a]anthracène	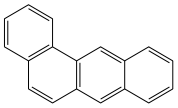	$C_{18}H_{12}$	1,3mg/L	228.29
Benzo[a]pyrène	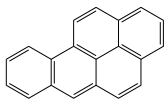	$C_{20}H_{12}$	1,8mg/L	252.31
Benzo[b]fluoranthène	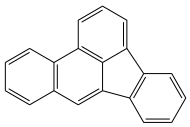	$C_{20}H_{12}$	0,0061mg/L	252.31
Benzo[g,h,i]Perylène	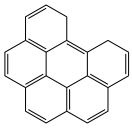	$C_{21}H_{16}$	0,00026mg/L	268.35
Benzo[k]fluoranthène	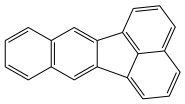	$C_{20}H_{12}$	0,00076mg/L	252.31
Chrysène	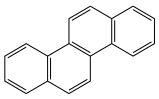	$C_{18}H_{12}$	3,9mg/L	228.29
Dibenzo[a,h]anthracène	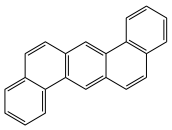	$C_{22}H_{14}$	0,0006mg/L	278.35
Fluoranthène	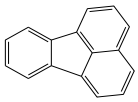	$C_{16}H_{10}$	0,062mg/L	202.26
Fluorène	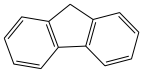	$C_{13}H_{10}$	1,8mg/L	166.22
Indéno[1,2,3cd]pyrène	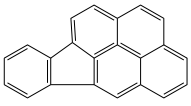	$C_{22}H_{12}$	0,062mg/L	276.33
Naphtalène	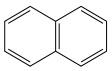	C_8H_{10}	32mg/L	128.19
Phénanthrène	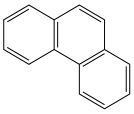	$C_{14}H_{10}$	1,2mg/L	178.23
Pyrène	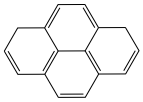	$C_{16}H_{10}$	0,135mg/L	202.26

L'agence américaine pour l'enregistrement des substances toxiques et des maladies qui leur sont associées (ASTDR, USA) établit, tous les deux ans, la liste des polluants nécessitant une action prioritaire de dépollution. Cette liste se base sur des critères tels que la fréquence, la toxicité et l'exposition potentielle de l'homme. De plus, l'USEPA a classé 16 HAPs sur sa liste des polluants nécessitant une action prioritaire (Tableau 1) (Wilson and Jones, 1993). Cette liste a été reprise comme référence par de nombreux autres pays.

3. Les hydrocarbures aromatiques polycycliques (HAPs)

Les HAPs constituent une vaste classe de composés organiques. Ces molécules peuvent être formées naturellement par les volcans ou les feux de forêts mais elles sont surtout produites par les activités industrielles et humaines.

3.1. Caractéristiques physico-chimiques des HAPs

Les HAPs sont constitués uniquement d'atomes de carbone et d'hydrogène assemblés en au moins deux cycles accolés.

Ils sont classés en deux catégories : les alternants qui ne contiennent que des cycles benzéniques (composés chacun de 6 atomes de carbone) et les non-alternants qui sont formés de cycles benzéniques mais aussi de cycles avec un nombre impair d'atomes de carbone.

Si les cycles sont assemblés de façon linéaire, alors le HAP est un acène comme, par exemple, l'anthracène (Tableau 1).

Les HAPs sont souvent classés en fonction de leur poids moléculaire : les HAPs avec deux ou trois cycles sont les HAPs à faible poids moléculaire (LMW HAPs= low molecular weight HAPs) alors que les HAPs avec quatre cycles ou plus sont les HAPs à fort poids moléculaire (HMW HAPs= high molecular weight HAPs) (Mrozik et al., 2003). Leur poids moléculaire influe

fortement sur leurs caractéristiques physico-chimiques comme leur solubilité dans l'eau. Les HMW HAPs, plus gros, sont beaucoup moins solubles dans l'eau que les LMW HAPs (Tableau 1).

De nombreux HAPs contiennent une région appelée « bay-region » et une région appelée « k-region » (Fig. 3) qui sont fortement réactives aussi bien chimiquement que biologiquement. Par exemple, les époxydes formés au niveau de la « k-region » sont bien plus carcinogènes que les HAPs à partir desquels ils ont été formés (Samanta et al., 2002; Mrozik et al., 2003).

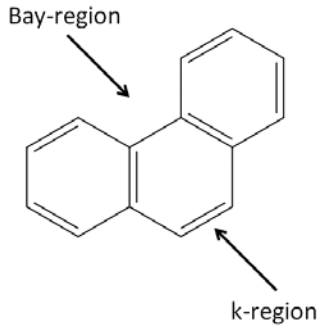

<u>Figure 3</u>: Représentation des régions "bay-region" et "k-region" sur la molécule du phénanthrène

Les propriétés physico-chimiques des HAPs dépendent de la structure de la molécule. Les HAPs sont fortement hydrophobes et possèdent un spectre d'absorption qui dépend du milieu dans lequel la molécule est étudiée.

Habituellement les HAPs fluorescent après avoir été exposés aux UV. Chaque HAP a son spectre d'émission spécifique qui dépend donc de la structure de la molécule. Presque tous les HAPs sont phosphorescents mais cette phosphorescence ne peut pas être détectée à température ambiante dans un milieu fluide (Dabestani and Ivanov, 1999).

3.2. Effets toxiques d'une exposition aux HAPs

Les HAPs sont des polluants organiques persistants (POP) qui sont présents dans l'atmosphère sous forme gazeuse ou particulaire mais aussi dans les sols, les sédiments et les boues. La carcinogénicité de cette famille de molécule a été évaluée et diffère en fonction du type de HAPs.

L'homme est exposé aux HAPs de différentes manières telles que l'inhalation, l'ingestion et le contact par la peau. De plus, il a été montré par Bjoerseth (1983) que la présence d'HAPs dans l'alimentation peut être due aussi bien à une contamination de la chaîne alimentaire qu'aux procédés de fumage et de cuisson des aliments. D'autre part, une étude américaine a révélé que 70% des HAPs reçus par une personne non-fumeuse provient de son alimentation en particulier des céréales, des huiles et matières grasses mais aussi des fruits, des légumes et des sucres. La viande, le poisson, le lait et les boissons ne sont à l'origine que d'un faible apport (Ramesh et al., 2004).

De nombreuses études ont montré que l'exposition de l'homme aux HAPs en milieu industriel et l'occurrence de cancers sont liés. La durée d'exposition (nombre d'années de travail dans ce milieu), le type de molécule, la dose reçue sont autant de paramètres qui sont pris en considération par les autorités pour les études sur l'impact des HAPs sur la santé (Boffetta et al., 1997).

L'effet allergène des HAPs a aussi été démontré. En effet, les émissions routières d'HAPs accentuent directement l'irritation allergique (Schober et al., 2007).

Ramesh et al. (2004) ont montré que les HAPs sont responsables de problèmes neurologiques, reproductifs et développementaux. L'exposition d'une femme enceinte aux HAPs a de nombreux effets sur son bébé. En effet, l'enfant sera plus prédisposé à développer des symptômes respiratoires et de l'asthme à l'âge de 12-24 mois (Miller et al., 2004; Jedrychowski et al., 2005). Les HAPs ont aussi un rôle important dans les premières semaines de grossesse. Une exposition à de fortes doses de HAPs augmente le risque de retard de croissance pour l'enfant (Dejmek et al., 2000). Certaines études ont établi un lien entre une exposition aux HAPs prénatale et un développement cérébral altéré. Des enfants exposés *in-*

utero aux HAPs présentent un retard dans leur développement cérébral à l'âge de trois ans et un QI plus bas que la moyenne à l'âge de cinq ans (Perera et al., 2009).

Les HAPs augmentent le risque de développer certains cancers comme celui du poumon (Smith et al., 2000; Armstrong et al., 2004), du sein (Rundle et al., 2000), de l'œsophage (Kamangar et al., 2005), du pancréas (Ojajärvi et al., 2000), de l'estomac (Ward et al., 1997), du colon (Sivaraman et al., 1994), de la vessie (Bonassi et al., 1989; Clavel et al., 1994), de la peau (Bizub et al., 1986), de la prostate (Rybicki et al., 2006) et du col de l'utérus (Mancini et al., 1999).

4. Les techniques de décontamination des sols pollués par les HAPs

Il existe deux types de traitement des sols : les techniques *in-situ* (Fig. 4A) qui traitent directement le sol pollué et les techniques *ex-situ* (Fig. 4B) qui nécessitent une excavation du sol avant son traitement. Le traitement *ex-situ* peut être fait dans une unité de traitement installée directement sur le site ou dans un centre spécialisé. En France, en 2008, 24% des terres étaient traitées *in-situ*, 21% *ex-situ* directement sur le site et 55% *ex-situ* dans un centre de traitement (ADEME, 2011).

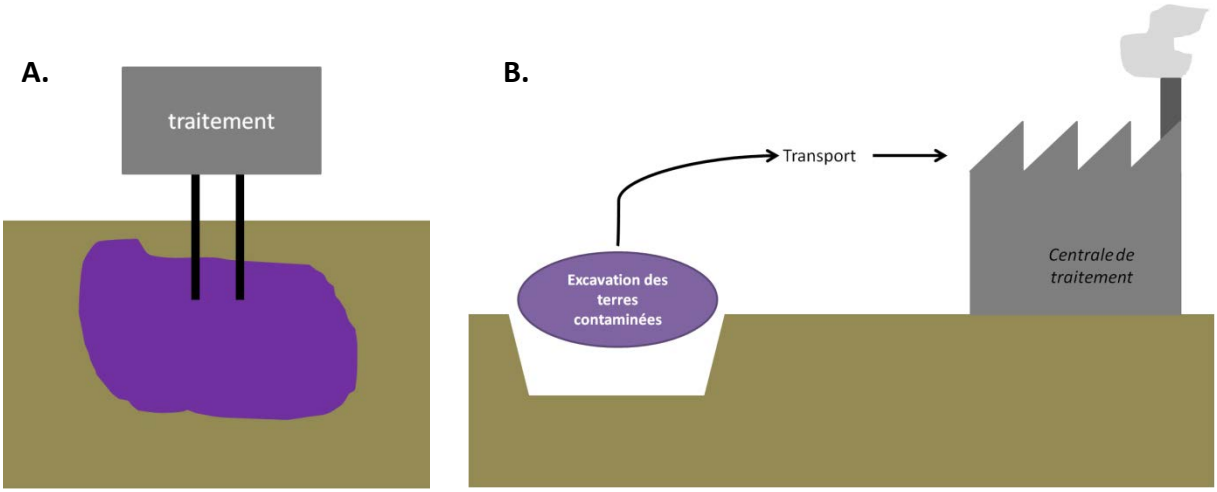

Figure 4: Principes des traitements *in-situ* (A) et *ex-situ* (B).
Dans les techniques *in-situ,* le sol pollué (en violet) est traité directement alors que les techniques *ex-situ* demandent une excavation des terres contaminées qui sont dépolluées dans une centrale de traitement.

4.1. Les techniques de traitement *in-situ*

4.1.1. Par voie biologique

Le bioventing consiste en un apport d'oxygène dans le sol afin de stimuler la dégradation naturelle des HAPs par les microorganismes. C'est l'une des techniques parmi les moins coûteuses (entre 5 et 35€/t traitée) et qui est bien perçue par l'opinion générale. Cette technique reste tout de même lente tout en utilisant des processus naturels (ADEME, 2011).

Il est aussi possible d'améliorer la biodégradation naturelle des HAPs en stimulant l'activité des microorganismes naturellement présents dans le sol par la circulation de solutions nutritives dans le sol contaminé. Cette technique a un des coûts de mise en place parmi les plus faibles (entre 20€ et 75€/t traitée) (FRTR, 2002).

La phytoremédiation est une technique biologique de traitement des sols qui utilise les plantes, leur microflore associée ainsi que les techniques agronomiques pour diminuer la pollution environnementale. On peut distinguer (Pilon-Smits, 2005) :

- La rhizofiltration : les racines filtrent les eaux polluées (Fig. 5A). Les parties aériennes des plantes (les feuilles, en particulier) peuvent aussi servir de filtre de l'air (Fig. 5B).
- La phytoextraction/phytoaccumulation : la plante agit comme une « pompe » et extrait puis stocke directement les polluants du sol sans les modifier ni les conjuguer (Fig. 5C).
- La phytodégradation : la plante seule est capable d'absorber puis de dégrader totalement ou en partie le polluant (Fig. 5C).
- La phytovolatilisation : la plante est capable de libérer le polluant absorbé dans le sol ou un dérivé dans l'atmosphère (Fig. 5C).
- La phytostabilisation : la plante permet de piéger le polluant au niveau de ses racines et d'en diminuer la mobilité, ce qui empêche donc la propagation du polluant notamment dans les eaux souterraines (Fig. 5C).
- La phytostimulation/rhizodégradation : les plantes libèrent des exsudats ou des enzymes qui stimulent l'activité des microorganismes du sol et donc la transformation biochimique du polluant (Fig. 5C).

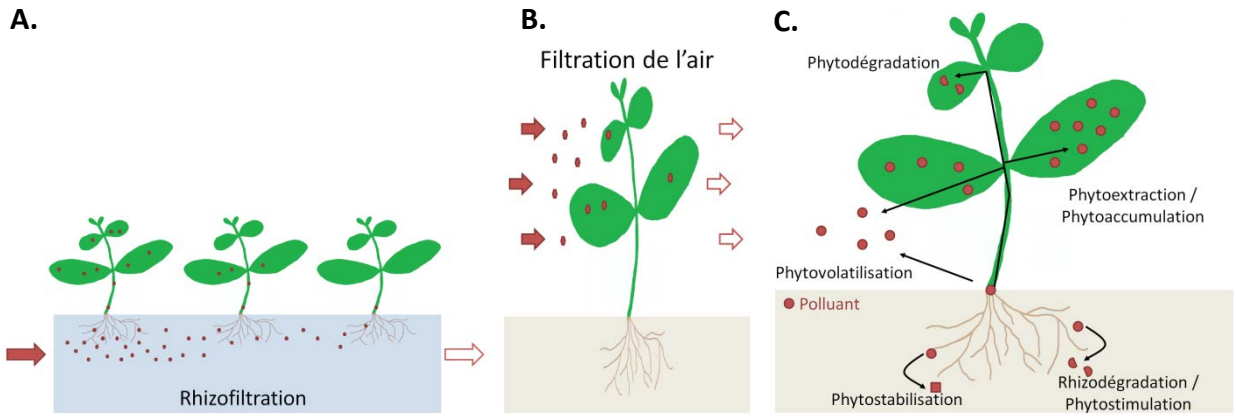

<u>Figure 5</u>: Les technologies de phytoremediation pour la décontamination du sol, de l'eau et de l'air (d'après Pilon-Smits, 2005).

Alors que la phytovolatilisation et la rhizofiltration sont des procédés permettant d'éliminer aussi bien des polluants organiques qu'inorganiques, la phytostabilisation et la phytoaccumulation sont des techniques plutôt adaptées pour les polluants inorganiques tels que les métaux lourds, grâce à l'utilisation de plantes hyperaccumulatrices (Marmiroli et al., 2006). La phytodégradation et la rhizodégradation sont des stratégies parfaitement adaptées aux polluants organiques tels que les HAPs (Ghosh and Singh, 2005).

La popularité de la phytoremédiation est liée à son bon rapport coût/efficacité (en moyenne 30€/m² traité) et à sa bonne perception par la population, car elle est considérée comme une « technologie verte ». Même si la phytoremédiation présente de nombreux avantages, cette technique de dépollution a tout de même quelques limites qui doivent être prises en compte. En effet, c'est un procédé plutôt lent qui dépend des propriétés du sol et des conditions climatiques ; il est plus approprié pour des pollutions peu profondes car son efficacité est limitée par la longueur des racines.

4.1.2. Par des procédés physico-chimiques

Le confinement est une technique permettant de séparer physiquement le sol pollué du reste de l'environnement. Cette technique n'est pas permanente car elle ne permet pas d'éliminer le polluant du sol contaminé. Cette stratégie permet d'éviter la propagation de la pollution (Henner et al., 1997). Cette technique a un faible coût de revient compris entre 35€ et 60€ par tonne traitée (ADEME, 2011).

L'oxydation chimique consiste en l'injection d'un oxydant sous forme liquide ou de gaz dans le sol, de façon à ce qu'il soit en contact direct avec le polluant. Le polluant va être ainsi transformé sous une forme moins toxique ou plus facilement biodégradable. Cette méthode peut aussi s'utiliser *ex-situ* et son coût est compris entre 40€ et 90€ par mètre cube de sol traité (FRTR, 2002).

Le lavage des terres sur site consiste en une extraction des polluants en lavant les terres polluées avec de l'eau ou des solvants. Cette technique peut aussi être utilisée sur des sols excavés. Le coût de cette technique a été évalué entre 15€ et 60€ par tonne de terre traitée (FRTR, 2002; ADEME, 2011).

Il est aussi possible d'extraire les polluants du sol par évaporation. Une pompe à vide est utilisée afin de créer un gradient de pression/concentration qui induit la volatilisation en phase gazeuse du polluant qui est enlevé du sol grâce à des puits d'extraction. Cette technique est une des plus coûteuses : son coût de mise en place est estimé entre 300€/t et 1100€/t (FRTR, 2002).

La stabilisation physico-chimique *in-situ* consiste en une réaction chimique ou physique qui diminue la mobilité du polluant. Cette technique, comme le confinement, ne permet pas d'éliminer le polluant du sol et présente un coût relativement élevé d'environ 80€ par tonne qui peut monter jusqu'à 100€/t (ADEME, 2011).

4.1.3. Par des traitements thermiques

Les techniques thermiques permettent l'élimination des polluants en chauffant le sol pollué afin d'améliorer la désorption du polluant puis de le volatiliser ou l'extraire. Les vapeurs sont récupérées et traitées. Pour traiter une tonne de terre avec cette technique, il faut compter environ 80€.

4.2. Les traitements *ex-situ*

Les techniques *ex-situ* requièrent une excavation préalable des terres polluées, ce qui ajoute des frais de mise en place supplémentaires.

4.2.1. Par des procédés biologiques

Dans les biopiles, les terres polluées sont mélangées avec des amendements puis stockées dans des zones de traitement imperméables. Cette technique utilise les microorganismes afin de dégrader le polluant. C'est une technique à faible coût (environ 50€/t), facile à mettre en œuvre mais qui, comme pour l'ensemble des techniques de dégradation par voie biologique, est relativement lente (ADEME, 2011).

Le compostage consiste à mélanger le sol contaminé avec des amendements organiques et des agents de charge. Il est important avec cette technique d'avoir une bonne gestion des paramètres physico-chimiques du compost afin d'améliorer la dégradation du polluant. Le coût de revient de cette technique est estimé entre 500€ et 600€ par mètre cube traité (FRTR, 2002).

Le landfarming utilise les pratiques agronomiques afin de stimuler la dégradation du polluant. Les terres contaminées sont excavées et puis étalées en couches qui sont régulièrement labourées et enrichies afin d'optimiser au maximum la biodégradation du

polluant (Al-Awadhi et al., 1996; Atagana, 2004; Maila and Cloete, 2004). Le coût total de cette technique n'a pas été évalué mais on estime qu'il faut moins de 75€ par mètre cube de terre afin de mettre en place cette méthode de dépollution.

Il est aussi possible de traiter des terres polluées dans des bioréacteurs. Afin de traiter un mètre cube de terre avec cette technique, il faut compter entre 100 et 150€.

4.2.2. Par des procédés physico-chimiques

L'extraction chimique consiste en un extracteur dans lequel les terres polluées sont mélangées avec un solvant afin de solubiliser le polluant. La solution solvant/polluant ainsi obtenue est placée dans un séparateur qui permet de séparer le solvant et le polluant. Ensuite, le polluant est traité et le solvant peut être réutilisé. L'utilisation d'huiles végétales comme solvant pour extraire les HAPs a été étudiée car ces huiles sont des solvants d'extraction non-toxiques, économiquement rentables et biodégradables (Gan et al., 2009).

L'oxydoréduction chimique est la conversion, par ajout d'un agent oxydant, d'un polluant en une forme moins hasardeuse ou moins dangereuse. Cette technique peut être aussi mise en place *in-situ* (cf. oxydation chimique). Le coût de cette technique est très variable et est compris entre 150€ et 500€ par mètre cube de terre traité (FRTR, 2002).

Les techniques de séparation permettent de concentrer les terres polluées par des procédés chimiques ou physiques tels que la gravité, le magnétisme ou le tamisage afin d'éliminer le polluant du sol.

Le lavage des terres est une technique consistant à extraire les polluants des terres en les lavant avec de l'eau ou des solvants. Cette méthode de traitement est aussi exploitée *in-situ*. L'efficacité de cette technique dépend de du type de solvant utilisé et du ratio terre/solvant appliqué. Un mélange avec 75% de cyclohexane et 25% d'éthanol s'est avéré être

le plus adapté pour éliminer les HAPs à cause de son efficacité et de sa sûreté (Gan et al., 2009). Cette technique coûte entre 50€ et 150€ par mètre cube de terre traité (FRTR, 2002).

Les procédés de stabilisation physico-chimiques utilisés *ex-situ* sont les mêmes que ceux mis en place *in-situ* mais dans ce cas-là ils sont appliqués sur sol excavé. Le coût de cette technique est d'environ 70€ par tonne de terre traitée (ADEME, 2011).

4.2.3. Par des méthodes thermiques

L'incinération est l'utilisation de hautes températures comprises entre 870°C et 1200°C afin de brûler en présence d'oxygène les déchets dangereux tels que les terres polluées. C'est l'une des techniques les plus chères à mettre en place avec un coût situé autour de 330€ par tonne de terre traitée. L'impact écologique de ce type de traitement est important mais cette technique reste malgré tout une des plus efficaces notamment en termes de durée de traitement (ADEME, 2011).

La pyrolyse est une décomposition chimique induite dans les matériaux organiques par la chaleur en absence d'oxygène. Cette technique, un peu moins coûteuse que l'incinération, a un coût estimé à environ 250€ par tonne traitée (ADEME, 2011).

La désorption thermique consiste en la volatilisation de l'eau et du polluant organique qui sont ensuite transportés dans un système de traitement des gaz. Cette technique est la méthode de traitement thermique *ex-situ* la moins chère avec un coût allant de 35€ à 190€ par mètre cube traité (FRTR, 2002).

5. Conclusion

Avec l'augmentation du nombre de sites pollués dans le monde, les autorités ont dû prendre des mesures afin de prévenir les risques de pollution et pour traiter les sites pollués, ce qui a conduit à la création du principe du « pollueur-payeur ». Ce principe est appliqué par l'ensemble des pays membres de l'Organisation de Coopération et de Développement Economique (OCDE) et de l'Union Européenne. Avec ces nouvelles règles, il s'est avéré nécessaire de développer des techniques de traitement.

Parmi les xénobiotiques les plus répandus, les HAPs représentent un intérêt majeur en raison de leur dangerosité pour la santé humaine. De nombreuses méthodes ont été développées afin de décontaminer les environnements pollués par ces molécules. Ces techniques ont toutes leurs avantages et leurs inconvénients. Leur utilisation dépend de nombreux facteurs économiques et techniques. Même si les méthodes *ex-situ* sont actuellement les plus utilisées, les technologies *in-situ* représentent un atout considérable et apportent de nouvelles solutions souvent plus économiques afin de dépolluer l'environnement.

Partie 2: **Mécanismes moléculaires et physiologiques de la biotransformation des Hydrocarbures Aromatiques Polycycliques (HAPs) par les microorganismes et les plantes**

Préambule

L'ingénierie écologique a permis l'émergence de nouvelles technologies telles que la bioremédiation et la phytoremédiation pour nettoyer les pollutions de l'environnement.

Cette introduction sous forme d'article de synthèse résume les dernières connaissances acquises sur les mécanismes moléculaires et physiologiques impliqués dans la biotransformation des hydrocarbures aromatiques polycycliques (HAPs) par les microorganismes du sol et les plantes.

Alors que la plupart des articles de synthèse portent soit sur les microorganismes, soit sur les plantes seules, cet article de synthèse aborde les interactions microbiennes notamment au niveau de la rhizosphère. En effet, les racines des plantes libèrent une grande variété de molécules contrôlant ainsi les populations fongiques et bactériennes, qui jouent un rôle central dans la dégradation des HAPs et d'autres molécules complexes.

L'émergence des approches globales, telles que la métagénomique, la transcriptomique, la métabolomique et la protéomique, sera discutée en mettant l'accent sur comment les approches « -omiques » ont permis de comprendre les mécanismes de bioremédiation afin d'améliorer les stratégies écologiques pour dépolluer les environnements contaminés par les HAPs.

Title: Molecular and physiological mechanisms of the biotransformation of PAHs by plants and microorganisms: contribution of “omics” approaches

Authors: Anne-Sophie Dumas[1], Richard Berthomé[2], Lukas Y. Wick[3] and Abdelhak El Amrani[1]

[1]Université de Rennes 1, CNRS/UMR 6553, Ecosystèmes-Biodiversité-Evolution, 35042 Rennes cedex, France.

[2]Laboratoire des Interactions Plantes Micro-organismes (LIPM), UMR INRA 441/CNRS 2594, CS 52627, 31326 CASTANET TOLOSAN CEDEX, France.

[3]Helmholtz Centre for Environmental Research – UFZ, Department of Environmental Microbiology, Permoserstraße 15, D-04318 Leipzig, Germany.

Corresponding author: Abdelhak El Amrani (abdelhak.elamrani@univ-rennes1.fr)

Abstract

The understanding of genetic and metabolic plasticity of leaving organisms to degrade and accumulate pollutants, allowed the emergence of new technologies such as bioremediation and phytoremediation to clean up environmental pollution. This review summarizes recent knowledge of molecular and physiological mechanisms involved in Polycyclic Aromatic Hydrocarbons (PAHs) biotransformation by micro-organisms and plants. Whereas most of available reviews have focused on PAHs degradation by either plants or micro-organisms separately, this review intends to address the interactions of plants and microbial consortia, present in the rhizosphere. Indeed, plant roots release exudates containing manifold signaling molecules controlling bacterial and fungal populations. These complex populations play a pivotal role in the degradation of high-molecular weight PAHs and other complex molecules. Emerging integrative approaches, such as metagenomic, transcriptomic, metabolomic and proteomic studies, are discussed, emphasizing on how 'omics' approaches bring new insights to decipher molecular mechanisms of PAHs degradation. This knowledge will help to set up integrative bioremediation strategies taking into account the rhizosphere population community and plants.

Key-words: PAHs metabolization, pollution, molecular mechanisms, 'omics'-approaches, bioremediation, phytoremediation.

1. Introduction

Polycyclic aromatic hydrocarbons (PAHs) constitute a large class of persistent and toxic organic compounds; they are generated from different anthropogenic and industrial processes and accidents such as crude oil spills. Their molecular structure contains two or more assembled aromatic rings. Thereby, they are classified into low-molecular weight PAHs (LMW; two to three rings) and high-molecular weight PAHs (HMW; more than three rings) (Mrozik et al., 2003).

In 2011, the Agency for Toxic Substances and Disease Registry (ATSDR, USA) ranked PAHs number 9 on the "CERCLA priority list of hazardous substances" with respect of their frequency, toxicity, human exposure and need of decontamination. Sixteen of the most prevalent PAHs thereby have been classified on the Priority Pollutant List of the USEPA (Wilson and Jones, 1993).

In order to overcome environmental concerns due to PAHs pollution in natural ecosystems, several implementations have been developed for soil treatment: (1) soil can directly be treated *in-situ* or (2) removed before being treated in a treatment center (*ex-situ* treatment), requiring excavation and transport. Traditionally, physico-chemical (solvent extraction, supercritical fluid extraction), chemical (chemical oxidation, photocatalytic degradation, electrokinetic remediation) and thermal (incineration, thermal desorption, thermally enhanced soil vapor extraction) techniques are used to remove PAHs from a contaminated soil (Gan et al., 2009). These techniques are efficient but expensive and impact the environment. Recently, ecological engineering approaches emerged as an alternative to these technologies (Mitsch, 2012). They use the ability of the environment to auto-restore itself with the natural action of living organisms. Indeed, it is common to define bioremediation and phytoremediation as the use of micro-organisms and plants, respectively, to clean up polluted environment. Accordingly, it is of high interest to understand the mechanisms involved in PAHs degradation by these organisms.

In this review, we summarize molecular mechanisms involved in PAHs metabolization by soil micro-organisms and plants and discuss their role in order to improve phyto- and bioremediation approaches of PAHs contaminated environments.

Table 1: Different set-ups used in bioremediation

	Name	description	references
in-situ	Bioventing	This method consist in bringing oxygen into the soil to enhance natural degradation of the contaminant by micro-organism	Lee & Swindoll, 1993; Masten & Davies, 1997; Frutos et al., 2010
	Enhanced Bioremediation	The activity of naturally occurring microbes is stimulated by circulating water-based solutions through contaminated soils contaminants	Liebeg & Cutright, 1999
	Landfarming	This technique uses agronomical techniques to stimulate the degradation of the contaminant (mixing, aeration, moisture and nutrients additions)	Al-Awadhi et al., 1996; Atagana, 2004; Hansen et al., 2004
ex-situ	Bioreactors	This technique uses naturally occurring micro-organisms (i.e. native micro-organisms population of the soil) or inoculated strains with specific metabolic capacities towards the PAH found in the soil to be treated. The bioreactor are designed in order to provide the best medium (nutrients, pH, temperature, oxygenation) for the microbial activity	Pinelli et al. 1997; Janikowski et al. 2002; Mohan et al. 2006
	Composting	It consists in mixing the contaminated soil which was excavated with bulking agents and organic amendments. A good management of the physical and chemical parameters of the compost is essential for the success of this technology	ANTIZAR-LADISLAO, LOPEZ-REAL, and BECK 2004

2. Microbial PAHs degradation

Aerobic microbial PAHs degradation has been intensively studied and showed to require molecular oxygen to initiate the enzymatic attack (Cerniglia, 1992). Contrary, in anaerobic condition nitrate and sulfate are used as terminal electron acceptors, and has been observed only in enriched cultures (Al-Turky, 2009). In addition, little is known on the processes involved (Haritash and Kaushik, 2009). Hence, in this review, we will focus our analyses mainly on aerobic degradation.

This natural process has been used to remove man-made PAHs contamination from the environment. Indeed, technologies listed in table 1 are mostly used to enhance microbial activities. It has been shown that bacteria, fungi and algae share a common pathway for PAHs catabolism. The first step involves the action of a mono or a dioxygenase which introduces atoms of oxygen in the ring forming cis-dihydrodiols. This step implies that PAHs are taken up by the cells. Then, the oxidation of the cis-dihydrodiols forms aromatic dihydroxy compounds that are channeled through the ortho- or the meta cleavage pathway (Johnsen et al., 2005; Haritash and Kaushik, 2009).

2.1. Molecular and biochemical pathways of bacterial PAHs degradation

Till now, most studied bacteria strains degrading PAHs have been isolated from contaminated soil (Haritash and Kaushik, 2009). They belong mainly to a limited number of taxonomic groups such as *Sphingomonas*, *Burkholderia*, *Pseudomonas* and *Mycobacterium* (Johnsen et al., 2005). Indeed, several strains degrading LMW PAHs such as phenanthrene, and HMW such as benzo[a]pyrene, pyrene, acenaphthene, fluorene, anthracene and fluoranthene have been well described (Smith, 1990; Samanta et al., 2002). According to these works, efficient PAHs-degrading strains are likely to be oligotrophic, and are able to highly express genes involved in PAHs catabolism (Johnsen et al., 2005). Overall, it has been shown that enzymes involved in PAHs degradation are often coded by genes located in plasmid DNA. Interestingly several genes were found to be a part or flanked by transposon or transposon like-

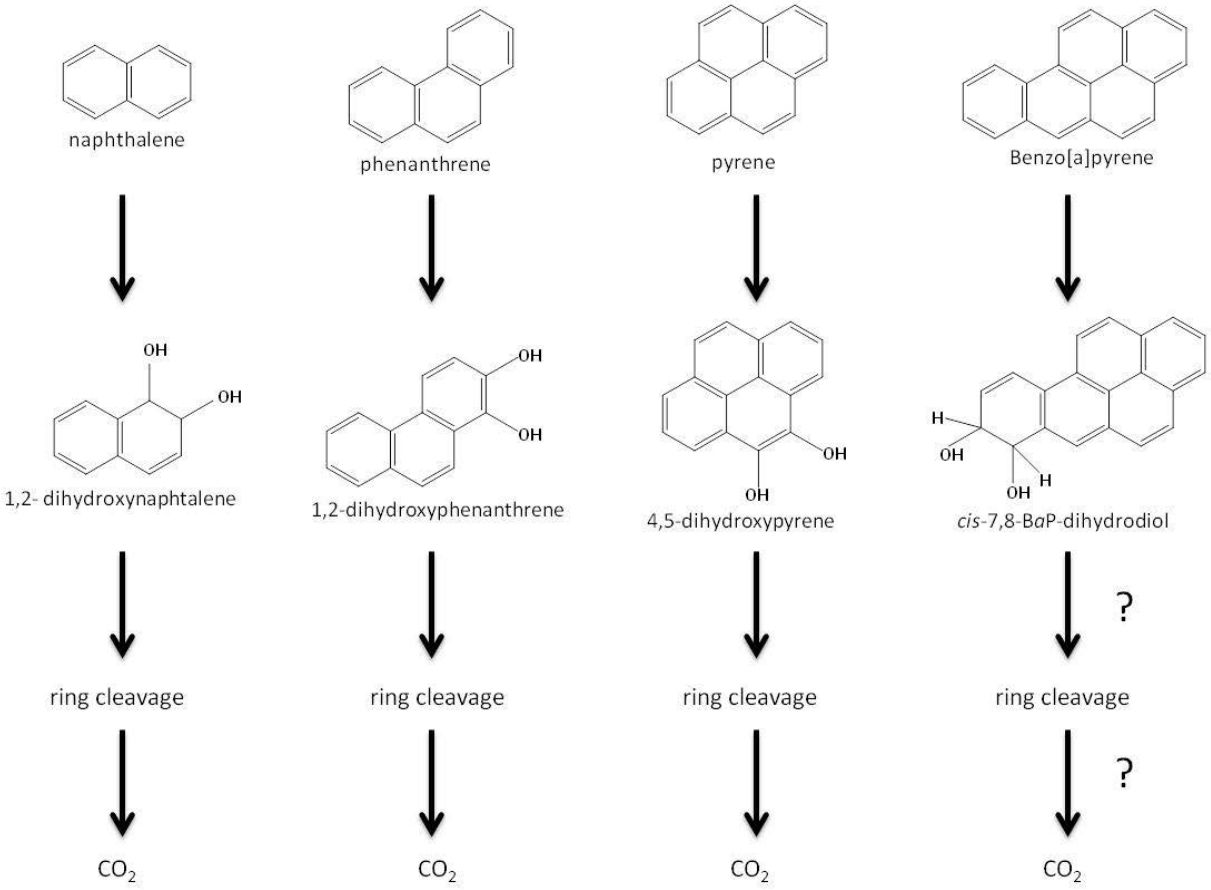

<u>Figure 1</u>: Degradation pathways of different PAH by bacteria

sequences, which suggested that plasmid encoded genes may have high spread activity among different bacterial population. Following are summarized some examples of PAHs degradation pathways identified in bacteria.

- Degradation of naphthalene: Naphthalene degradation is well known because it is the simplest and most soluble PAH. Most of the bacteria degrading naphthalene are from *Pseudomonas* genus. The degradation pathway by *Pseudomonas* was firstly described by Davies and Evans (1964) and is presented in figure 1. The first step is the oxidation of naphthalene by the introduction of both oxygen atoms into the aromatic cycle to form *cis*-1,2-dixydroxy-1,2-dihydronaphthalene by the dioxygenases. The dihydrodiol is then converted to 1,2-dihydroxynaphtalene by the naphthalene(+)-*cis*-dihydrodiol dehydrogenase and then goes under ring cleavage.

- Degradation of phenanthrene: Phenanthrene degradation pathways were described for *Pseudomonas*, *Mycobacterium*, *Arthrobacter*, *Aeromonas*, *Acidovorax*, *Sphingomonas, Staphylococcus* and *Nocardia* genera (Mrozik et al., 2003). *Staphylococcus* sp. Strain PN/Y can use phenanthrene as a sole source of energy. The complete pathway of phenanthrene degradation has been identified for this bacterium (Mallick et al., 2007). This pathway will be described here as an example of phenanthrene degradation by bacteria (Fig. 1). PN/Y initiates the degradation of phenanthrene by a dioxygenation at the C-1 and C-2 position leading to the formation of *cis*-1,2-dihydroxyphenanthrene which goes under a dehydrogenation to form the corresponding diol. Several reactions lead to the formation of catechol which after a ring cleavage goes into the TCA cycle.
  According to the different genus of bacteria, the degradation pathway can vary. The main differences are in the first step during the dioxygenation which can be on the C-1/-2 and on the C-3/-4 positions.

- Degradation of pyrene: Pyrene is a HMW PAHs which has been used as a model compound for HMW PAHs. Bacteria degrading this molecule are mainly members of the *Mycobacterium* and *Rhodococcus* genera. *Mycobacterium vanbaalenii* was reported as the first mineralizing pyrene strain. Kim et al. (2007) described a complete and integrated pyrene degradation using a combination of metabolite identification and genomic and proteomic analyses. Proteomic data and the genome sequence led to the identification of potential enzymes involved in the pyrene mineralization pathway shown in figure 1.

- Degradation of benzo[a]pyrene: Benzo[a]pyrene (BaP) is a HMW-PAHs which degradation has been observed for the genus *Mycobacterium*, *Pseudomonas* and *Bacillus* (Schneider et al., 1996; Kanaly and Harayama, 2000; Mrozik et al., 2003; Lily et al., 2009). Even little is known about bacterial HMW-PAHs degradation, the pathway of BaP degradation by Mycobacterium sp. Strain RJGII-135 is partially described (Fig. 1). BaP degradation starts by the dioxygenation of the molecule at the C-4/5 or C-7/8 or C-9/10 positions leading to the formation of the corresponding dihydrodiol. Then the dihydrodiol goes under ring cleavage. The complete mineralization pathway remains unknown.

Conventionally, PAHs degradation pathways have been elucidated using straightforward "step-by-step" techniques that include analytical chemistry, biochemical characterization for experimental identification of metabolic intermediates and key enzymes. Even if these approaches allowed deciphering several metabolic processes and mechanisms involved in PAHs degradation, most of the metabolic involved steps remains poorly understood.

Interestingly, high-throughput "-omics" approaches clearly revitalized the study of the PAHs catabolism and allowed to bring a global view of the process for PAHs polluted sites. Although, recent reviews listed proteomic approaches that have been used to study bacterial degradation of PAHs (Kim et al., 2007; Loh and Cao, 2008; Kim et al., 2009b), few reports described the real bacterial catabolic diversity of the environment and the *in-situ* functional characterization of catalytic activities.

In parallel, the use of stable isotope probing (SIP) could help to identify bacteria degrading PAHs and the proteins involved in such metabolic pathways. SIP is a method that consists in introducing ^{13}C-labeled substrate, in our case PAHs, into cellular biomarkers such as proteins or DNA and in identifying populations that have integrated the labeled elements. Recently, DNA-based SIP has been already used to identify bacteria degrading phenanthrene, pyrene and naphthalene (Singleton et al., 2005; Singleton et al., 2007; Jones et al., 2011).

In other hand, focused screening using DNA library generated from metagenomic approaches and specific enzymatic activities, such as oxygenases, and their ability to produce yellow or blue coloration depending on the subtract used when expressed in *Escherichia coli* have been also carried out to better understand PAHs catabolism (Vilchez-Vargas et al., 2010). As an exemple, Brennerova et al. (2009) identified several dioxygenase activities in the community of a contaminated site. Interestingly, their results strongly suggested that the effective degradation of a mixture of aromatic compounds could be achieved through a complementary and a community balanced catalytic power against diverse derivatives.

2.2. Biochemical pathways of fungal PAHs degradation: an underestimated system?

Several fungi are known to degrade naphthalene, pyrene, phenanthrene, benzo[a]pyrene, fluoranthene, chrysene. In other hand, mycelial fungi such as *Aspergillus*, *Cladosporium*, *Cunninghamella*, *Penicillium*, *Phanerochaete*, *Pleurotus*, *Syncephalastrum* and yeasts like *Candida*, *Rhodotorula*, *Saccharomyces*, *Torulopsis* are PAHs-degrading fungi found in soil (Zhanf et al., 2006).

In contrast to bacteria, most fungi do not use PAHs as sole source of carbon, but they are significantly involved in PAHs degradation through the production of metabolites with higher water solubility which could enhance microbial activity in the soil (Cerniglia, 1997).

White-rot fungi are able to degrade a wide range of PAHs because of the lignin-degrading system encoded by their genome. *Pleurotus ostrateatus* is a good example of white-rot fungus for which metabolism of phenanthrene degradation is well described (Bezalel et al., 1996b).

However, fungal degradation of PAHs remains poorly understood even if several fungi have been identified as PAHs degraders.

We summarized below known metabolic pathways of fungus PAHs degradation.

- Degradation of phenanthrene*:* Among fungus*, Pleurotus oestreatus* has been described to be able to completely mineralize phenanthrene (Bezalel et al., 1996a; Bezalel et al., 1996b) (Fig. 2). The first step in phenanthrene mineralization is the 0_2 incorporation by the cytochrome P450 monooxygenases (Bezalel et al., 1997). The phenanthrene 9,10-oxide formed is transformed by epoxide hydrolases leading to the synthesis of phenanthrene trans-9,10-dihydrodiol. The involvement of the lignolitic system in the ring cleavage system remains unclear even if experiments with [^{14}C]phenanthrene show its mineralization by the formation of $^{14}CO_2$.

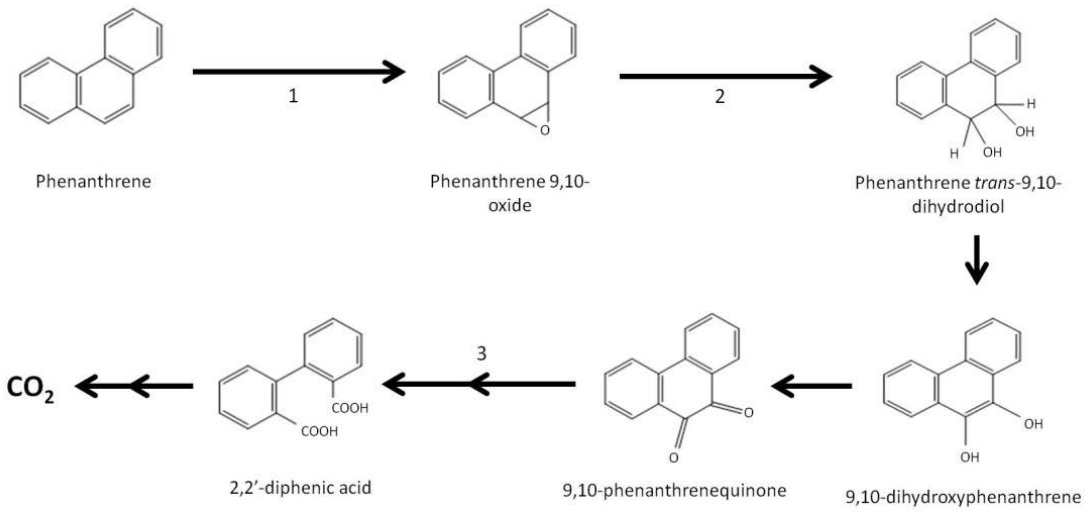

Figure 2: Proposed pathway for phenanthrene degradation by *P. ostrateus*

1, Cytochrome P450; 2, Epoxyde hydrolase; 3, Ring cleavage enzymes. (adapted from Bezalel et al., 1996a; Bezalel et al., 1996b; Bezalel et al., 1997)

- Degradation of other PAHs: The white rot fungi *Bjerkandera* sp. strain BOS55 has been identified to mineralize benzo[a]pyrene but this mineralization is not really efficient and is, most of the time, not complete (Kotterman et al., 1998).

6 cytochromes P450 monooxygenases of the white rot basidiomycetes *Phanerochaete chrysosporium* have been characterized. These enzymes are able to oxidize pyrene, benzo[a]pyrene and phenanthrene which is the first step in PAHs mineralization by micro-organisms (Syed et al., 2010).

Indigenous fungi from a former gasworks site belonging to the *Penicillium* genus are able to use pyrene as the sole carbon source (Saraswathy and Hallberg, 2002).

But, in most described cases degradation of some PAHs is incomplete and could stop after the oxidative step leading to form dead-end products that can sometimes be metabolized by bacteria or have a negative effect on the microbial population of the soil (Andersson and Henrysson, 1996; Andersson et al., 2003).

2.3. Metabolic pathway of algae PAHs degradation

Algal biodegradation of PAHs is useful and has been developed for remediation of aquatic environment. Indeed, prokaryotic and eukaryotic algae, green algae and diatoms are known to metabolize naphthalene (Cerniglia et al., 1980).

Benzo[a]pyrene can be metabolized by marine algae (Warshawsky et al., 1995) within 5 to 6 days and by the freshwater green alga *Selenastrum capricornutum, Scenesdemus acutus* and *Ankistrodesmus reinhardtii* through a dioxygenase pathway to dihydrodiols (Fig. 3) (see Warshawsky et al. 1995). Fluoranthene and pyrene (individually or in mixture) have been reported to be metabolized by *Chlorella vulgaris*, *Scenedesmus platydiscus*, *Scenedesmus quadricauda* and *Scenedesmus capricornutum* (Lei et al., 2007).

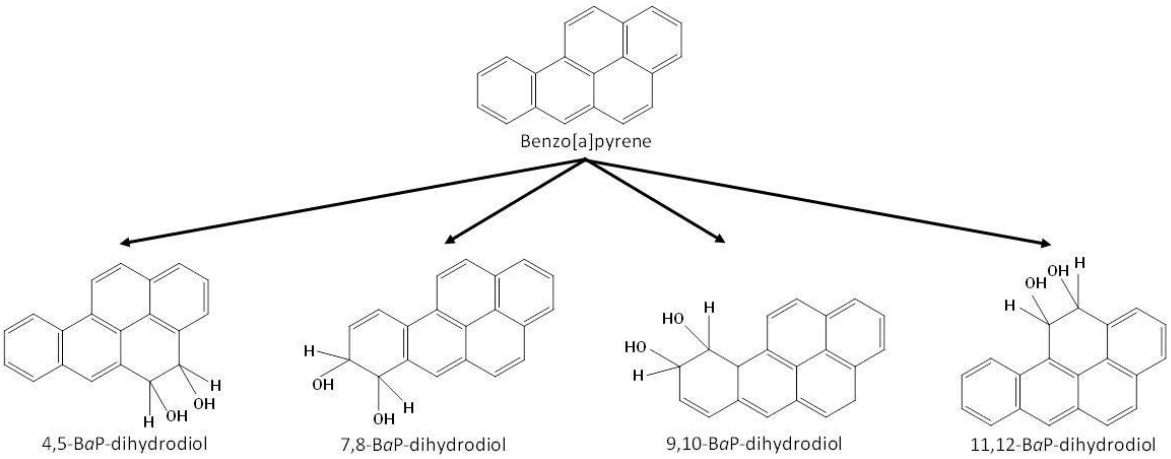

<u>Figure 3</u>: Proposed dioxygenase pathway for benzo[a]pyrene (B*a*P) degradation by freshwater green algae.

The dioxygenation of the benzo[a]pyrene is performed by a dioxygenase enzyme system leading to the formation of dihydrodiol.

Numerous studies showed that algae are suitable for PAHs bioremediation and acts co-metabolically with bacteria (Haritash and Kaushik, 2009). An *in-vitro* study with contaminated soil was carried out using algae *Filamentus chlorophyte* for PAHs removal. The soil with algae was flooded and showed a reduction of more than 90 % of the level of PAHs (Edema et al., 2011). These results showed the potential of algae mediated remediation especially in flooded conditions. Degradation pathways have been partially characterized at least for *Ankistrodesmus reinhardtii,* and several studies showed that the first step was identical to bacteria and fungi leading to the formation of diols (Cerniglia et al., 1980; Narro et al., 1992; Warshawsky et al., 1995).

2.4. PAHs involved meta-cleavage pathways in soil micro-organisms communities: incidence of consortium

Most of the available data explaining molecular and biochemical mechanisms involved in PAHs degradation has been obtained by laboratory studies using isolated pollutant-degrading micro-organisms or model strains. However, it is still misunderstood how such complex molecules are degraded by soil microbial communities.

In-situ technologies have used indigenous mixture of micro-organisms containing several strains of bacteria, fungi and algae which could act as a consortium. The interaction between the members of a consortium seems to be determinant for the PAHs degradation.

Indeed, Juhasz et al. (2000) used a mixture of five bacteria strains in their bioremediation techniques. Boonchan et al. (2000) showed that a fungal–bacterial consortium can degrade benzo[a]pyrene whereas the fungus or the bacteria cannot degrade it alone. These results suggest that there is a mutually dependent relationship between the fungus and the bacteria during the benzo[a]pyrene degradation as it has been as well proposed for bacterial consortium by Brennerova et al. (2009). Furthermore, Trzesicka-Mlynarz and Ward (1995) previously found that a consortium of four fluoranthene-degrading bacteria was more efficient than any individual isolate. It has been suggested that the pre-oxydation of the benzo[a]pyrene performed by the fungus might increase the bioavailability to the bacterial community. Unlike bacteria development, mycelia spread ubiquitously in the soil, penetrate air-water interfaces and cross over air-filled pores between the bacteria and contaminants. In air-filled soil, enhanced homogenization of bacteria and contaminants can be achieved by bridging physical air gaps with fungal hyphae thus enabling substrate-directed mobilization of bacteria along chemical gradients.

Recent studies demonstrated that mycelial dispersal networks influence both the microbial transport and the translocation of polycyclic aromatic hydrocarbons (Furuno et al., 2010; Kohlmeier et al., 2005). They showed that mycelial networks (i) act as effective dispersal networks for both undirected and chemotactic mobilization of contaminant degrading bacteria (termed by authors as ‘fungal highways’), (ii) increase the mobility of a wide range of PAHs due to their translocation in their cytoplasmic streaming (‘fungal pipelines’) with transport rates of

about 0.02 to 1.1 pmol ≙ 4 to 200 pg) per hypha per hour over a distance of 1 cm (figure 4) (Furuno et al., 2012), and thus improve the accessibility of bacteria to soil contaminants and, concomitantly, their biodegradation (Schamfuß et al., 2013a). Given their ubiquity and length of up to 1000 m.g-1 dry soil mycelial networks, fungus appear to play a significant role for the ecology of PAHs biodegradation in contaminated ecosystems (Harms et al., 2011).

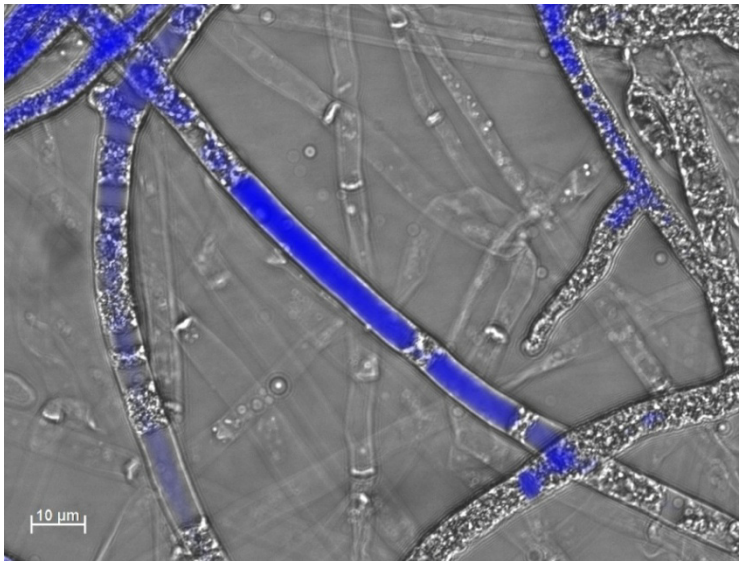

Figure 4: Overlay of a transmission light and fluorescence micrograph (DAPI filter setting) depicting vesicle-bound FLU within hyphae of *P. ultimum* growing over MMA

(Magnification 630x, bar 10 micro m). Micrograph by: S. Schamfuß and L.Y. Wick, UFZ.

Such data highlight the importance of the complementarities, both at the ecological and metabolic level, of the micro-organisms consortium, each component of the mixture being able to catalyze and use different PAHs derivatives.

Sequencing the 16S rDNA and analyzing the PCR-DGGE profiles, HuiJie et al. (2011) demonstrate that the degradation efficiency of a PAHs mixture depends on bacterial strains constituting the consortium and on the type of PAHs found in the contaminated soil. But it remains difficult to identify which species is doing what in a polluted environmental condition. However, such study might be of high interest and could contribute to bring solutions allowing the restoration of bacterial communities often perturbed in polluted soil.

Recently, Guazzaroni et al. (2013) used a metagenomic and a proteomic approaches to identify the strains compositions of communities, their capacity to metabolize PAHs and relative protein abundance, in a soil chronically contaminated by PAHs with or without biostimulation. Results indicate that biostimulation clearly improve soil PAHs decontamination but also strongly modify bacterial communities. Interestingly, metagenomic analyses of highly contaminated aromatic hydrocarbons site, revealed strong enrichment of genes encoding extradiol dioxygnenase, and high diversity and abundance of meta-cleavage pathways, suggesting that micro-organisms communities evolved and acquired selective advantage towards aromatic hydrocarbons degradation (Brennerova et al., 2009).

3. PAHs metabolization by plants

3.1. Molecular mechanisms Involved in plants PAHs detoxification

Description of PAHs absorption by plant organs has been addressed only for one PAH model: the phenanthrene. Alkio et al. (2005) showed that *Arabidopsis thaliana* was able to absorb and internalize phenanthrene. Thereby, its quantification using a GC-MS and the fluorescence characteristics of phenanthrene provides evidence that it was accumulates in plants tissues. Additional data based on fluorescence microscopy observations indicated that phenanthrene accumulates in trichomes of 14 and 21-day-old plants leaves. But it remains unclear if trichomes are an entry point for phenanthrene present in the air or a storage point of the phenanthrene absorbed by the roots and transported to leaves to prevent its toxicity.

Zhan et al. (2010) also studied the absorption of phenanthrene by roots using wheat as plant model. They showed that phenanthrene uptake involved two biological mechanisms: (i) a fast passive diffusion occurring just after the transfer of wheat in the phenanthrene supplemented medium and (ii) a slow active absorption mediated by a transporters that still have to be characterized.

Contrasting with numerous studies describing mechanisms involved in PAHs degradation by bacteria, fungus and algae, little is known about the mechanisms of PAHs metabolization and accumulation in plants.

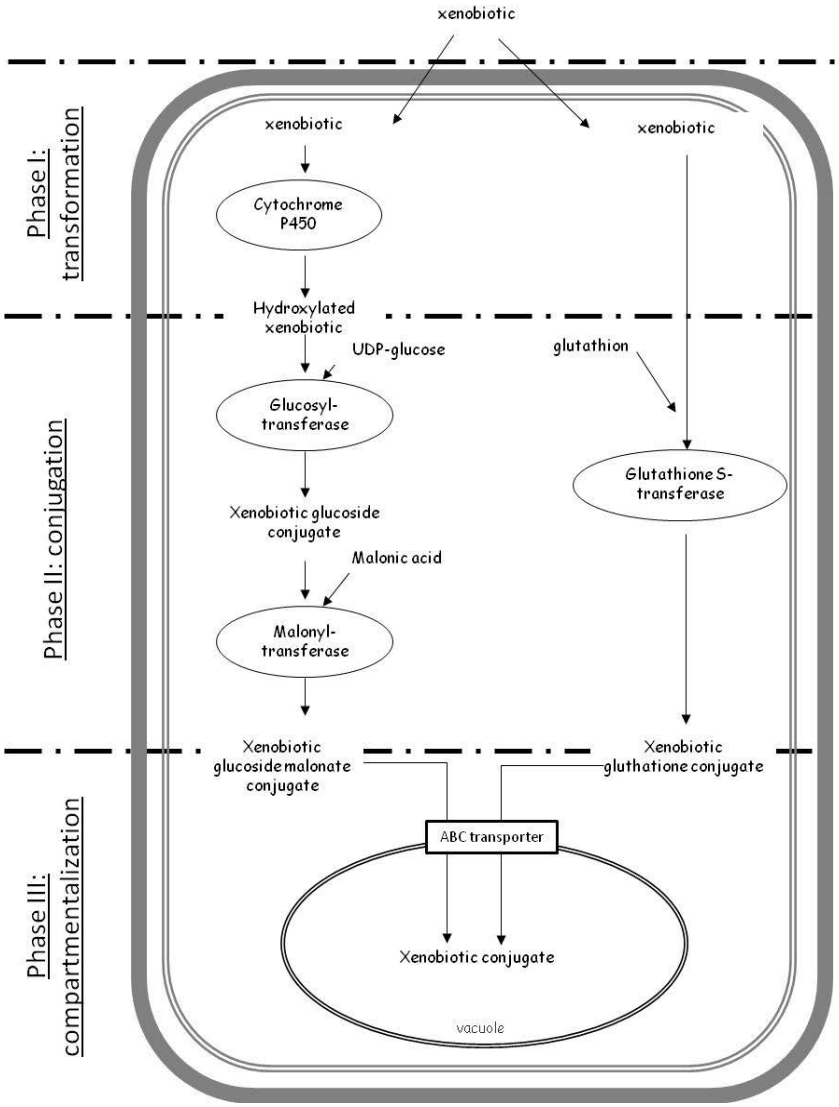

Figure 5: Representation of the plant detoxification system

This model is set in three phases. (i) Transformation: xenobiotics are chemically modified using oxidation, reduction, or hydrolysis, this stage involved cytochrome P450 (CYP). (ii) Conjugation: the xenobiotics are conjugates to endogenous molecules. Glycosyltransferases (UGT) transfer nucleotide-diphosphate-activated sugars like UDP-glucose to low-molecular-weight substrates. The glycosylated xenobiotic is also conjugated with malonic acid by malonyltransferases (MT). The conjugation step can also be performed by the gluthatione-S-transferases (GST) by attaching the tripeptide gluthatione to xenobiotics. (iii) Compartmentalization: The conjugated xenobiotic is transferred to the vacuole or the cell wall by the ATP-binding cassette (ABC) transporters.

However a “green-liver” model (Fig. 5) was proposed for plant organic pollutants detoxification mechanisms by Sandermann Jr (1992). It corresponds to an analogy of the detoxification system described in the mammalian liver. Processes involved in this model have been divided into two steps: (i) detection and signaling, (ii) transport and biotransformation (Sandermann Jr., 1992; Coleman et al., 1997; Edwards et al., 2011). Edwards et al. (2005) also proposed that “the whole expressed genome responsible for the detection, transport and detoxification of xenobiotics in the cell” constitute the xenome. However, even if general models of xenobiotics detoxification by plants are proposed, experimental data demonstrating that they can be applied to plant PAHs detoxification are still missing.

Despite the detection and signaling steps in plant are still unknown, enzymatic activities involved in the green-liver model, and encoded by genes that might belong to the xenome have been proposed. The transformation step which consists in making the xenobiotic more water soluble has been proposed to involve cytochromes P450 (CYPs). Indeed, these enzymes contribute to the phenanthrene degradation in fungi (Bezalel et al., 1996b; Syed et al., 2010). Additionaly, the glycosyltransferases (UGT), the gluthatione-S-transferases (GST) and the malonyltransferases (MT) participate to the conjugation step whereas ATP-binding cassette (ABC) transporters are involved in the compartmentalization step. Except for MT, reported to be encoded by two genes in *Arabidopsis thaliana* (Taguchi et al., 2010), all other components of the green-liver model are encoded by multigenic families. In *A. thaliana*, 244 CYP, 55 GST, 107 UGT and 120 ABC transporters have been respectively annotated (Dixon and Edwards, 2010; Bak et al., 2011; Edwards et al., 2011a)

Among the most promising studies performed to understand molecular mechanisms involved in PAHs remediation, a transcriptomic analysis on 21-days old *Arabidopsis* plants grown *in vitro* on a media supplemented with phenanthrene, showed that phenanthrene treatment induces expression of genes encoding proteins mostly involved in oxidative stress regulation or production (Weisman *et al*. 2010). The authors suggested that following the uptake, the phenanthrene might be oxidized by mono- or di-oxygenases, like the CYP, creating an increase in the reactive oxygen species (ROS) level which is responsible for the oxidative stress. However, it was still unclear if oxidative stress results from the activities linked to the phenanthrene detoxification or if it is an indirect consequence of its own or derivatives phytotoxicity.

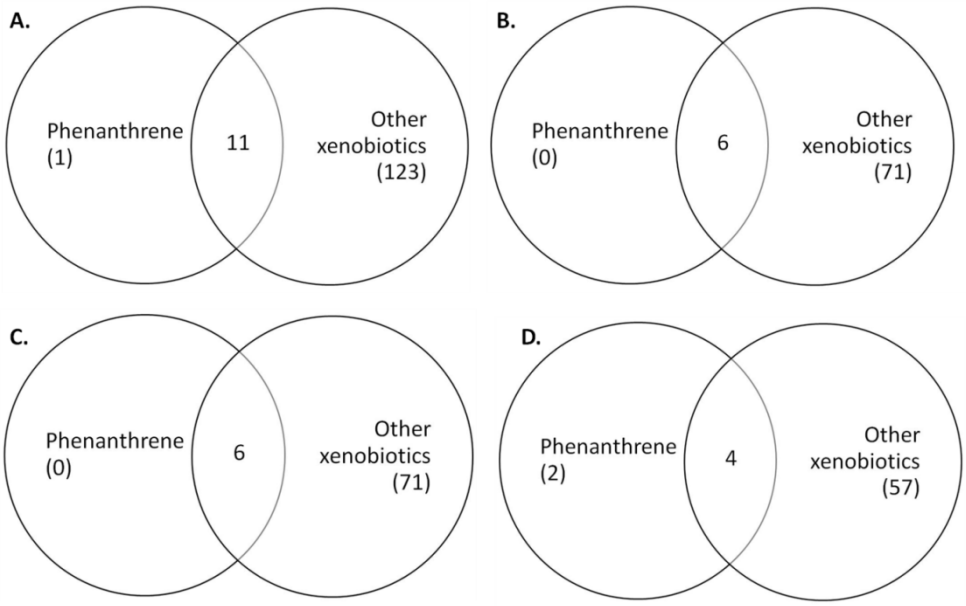

Figure 6: Venn diagram depicting the number of *Arabidopsis* differentially expressed genes compared between data published in Weisman et al. (2010) and the list of potential genes belonging to the xenome extracted from available public data of wide-genome analysis carried out in the presence of xenobiotics experiment. Comparison of cytochromes P450 (A), glutathione-S-transferases (B), glycosyltransferases (C) and ATP-binding cassette transporters (D).

Zhan *et al*. (2010) suggested that several physiological changes might occur very rapidly after phenanthrene exposure. To gain a better understanding of the mechanisms involved in the putative molecular processes involved in PAHs metabolization in plants, it was of high interest to focus on highly regulated genes involved within the few hours after the plant have been transferred to medium supplemented with PAHs. Hence, we performed a genome wide analysis using CATMA array after a short term phenanthrene exposure (data not shown).

Preliminary data indicated that the plant response could be divided in three phases: 1) an early response occurring within the first 30 min in which plant seems to sense phenanthrene rapidly, as genes mainly involved in perception and signalization are differentially expressed within the first 30 minutes, 2) a phase of reaction observed after 2h to 8h of incubation, characterized by regulation of genes involved in detoxification, 3) and a third exhausting phase from 8h where many differentially expressed genes are involved in repression of the secondary metabolism, this later being closely related to those described by Weisman *et al.* (2010).

During this last phase, late plant responsiveness to PAHs was characterized by the induction of numerous genes often regulated in plant response to stresses. In other hand, since no comparative data are available about the specific xenome induced after exposure of PAHs, it is reasonable to speculate that there are common genes shared with other xenobiotic.

Hence, we initiated a preliminary analysis where we collected all information available in public data bases carried out on the xenobiotic. These wide-genome analyses were collected from experiment using aluminum (Goodwin and Sutter, 2009), atrazine (Ramel et al., 2007), BOA (benzoxazolin-2(3H)-one) (Baerson et al., 2005), cadmium (Herbette et al., 2006), PCB (Polychlorinated biphenyl) (Jin et al., 2011), phenol (Xu et al., 2012), selenium (Van Hoewyk et al., 2008) and TNT (trinitrotoluene) (Landa et al., 2010) as xenobiotics. Then we have established a list of all the genes encoding a potential xenome protein (CYP, UGT, MT, GST and ABC transporters) that appeared differentially expressed in at least one transcriptomic analyses after *Arabidopsis* exposure to cited xenobiotics. We have confronted this list to the data obtained by Weisman et al. (2010) and found out that most potential xenome genes involved in phenanthrene detoxification are commonly regulated in other experiments, except for one cytochrome P-450 (AT5G47990) and two ATP-binding cassette transporters (AT1G51500 and AT5G44110) (Fig. 6). These findings suggest that plant xenobiotics detoxification shared

Table 2: List of potential plants for phytoremediation of PAHs

Molecule	Common name	Scientific name	Results obtained	References
anthracene	Poplar	*Populus nigra L. cv. Loenen*	oxidation of anthracene at a higher rate than in an unplanted soil, presence of products of anthracene degradation in the soil	Ballach et al., 2003
benzo[a]pyrene	tall fescue	*Festuca arundinacea*	Residual benzo[a]pyrene lower in soil with plants (44%) than in the absence of plants (53%)	Banks et al., 1999
benzo[b] fluoranthene	arrowhead	*Sagitaria latifolia*	69-83% of benzo[b]fluoranthene removed after 13 months	Euliss et al., 2008
	eastern gamagrass	*Tripsacum dactyloides*	61-68% of benzo[b]fluoranthene removed after 13 months	
	Poplar	*Populus spp.*	33-48% of benzo[b]fluoranthene removed after 13 months	
	sedge	*Carex stricta*	79-86% of benzo[b]fluoranthene removed after 13 months	
	switch grass	*Panicum virgatum*	71-79% of benzo[b]fluoranthène removed after 13 months	
	willow	*Salix exigua*	41-69% of benzo[b]fluoranthène removed after 13 months	
fluoranthene	arrowhead	*Sagitaria latifolia*	81-90% of fluoranthene removed after 13 months	Euliss et al., 2008
	eastern gamagrass	*Tripsacum dactyloides*	84-92% of fluoranthene removed after 13 months	
	Poplar	*Populus spp.*	62-81% of fluoranthene removed after 13 months	
	sedge	*Carex stricta*	91-95% of fluoranthene removed after 13 months	
	switch grass	*Panicum virgatum*	92-97% of fluoranthene removed after 13 months	
	willow	*Salix exigua*	62-95% of fluoranthene removed after 13 months	
naphthalene	tall fescue	*Festuca arundinacea*	mineralization of [^{14}C]naphthalene greater than in bulk soil	Siciliano et al., 2003
phenanthrene	pea soybean sunflower wheat	*Pisum sativum* *Glycine max* *Helianthus annuus* *Triticum aestivum*	significant diminution of the phenanthrene in the growth medium	Liste & Alexander, 1999
	white clover	*Trifolium repens*	81.79–91.80% removal of phenanthrene in 60 days	Xu et al., 2006
		Miscanthus giganteus	almost 98% of phenanthrene disappeared	Técher et al., 2012
	corn	*Zea mays*	92.1% of phenanthrene removed from soil in 60 days	Xu et al., 2006
pyrene	arrowhead	*Sagitaria latifolia*	72-91% of pyrene removed after 13 months	Euliss et al., 2008
	eastern gamagrass	*Tripsacum dactyloides*	80-94% of pyrene removed after 13 months	
	Poplar	*Populus spp.*	52-79% of pyrene removed after 13 months	
	sedge	*Carex stricta*	72-91% of pyrene removed after 13 months	
	switch grass	*Panicum virgatum*	71-79% of pyrene removed after 13 months	
	willow	*Salix exigua*	around 70% of pyrene removed after 13 months	
	dill pepper radish	*Anathum graveolens* *Capsicum annuum* *Raphanus sativus*	52-68% of the total pyrene extractable has disappeared after 28 days	Liste & Alexander, 2000
	jack pine red pine	*Pinus banksiana* *Pinus resinosa*	around 60% of the pyrene removed from the soil at 57 days	
	oat	*Avena sativa*	diminution of 62% of pyrene in soil after 56 days	
	rape	*Brassicca napus*	diminution of 78% of pyrene in soil after 56 days	
		Miscanthus giganteus	around 70% of pyrene disappeared	Técher et al., 2012
	corn	*Zea mays*	88.36% of pyrene removed from soil in 60 days	Xu et al., 2006
	rye grass	*Lolium perenne*	degradation rates of pyrene after 60 days: 70.39%-80.72%	
	white clover	*Trifolium repens*	62.33–88.12% of the total pyrene had disappeared in 60 days	
total PAH	alfalfa	*Medicago sativa*	a reduction of 57% in total PAH concentration after 6 months	Pradhan et al., 1998
	eelgrass	*Zostera marina*	decrease of 73% of the total PAH content	Hueseman et al., 2009
	Salt marsh plants	*Spartina alterniflora*	detection of PAH in roots and shoots	Watts et al., 2006
	switch grass	*Panicum virgatum*	a reduction of 57% in total PAH concentration after 6 months	Pradhan et al., 1998
	willow	*Salix viminalis* L. 'Orm'	23% of reduction of total PAH content in 1.5 years	Vervaeke et al., 2003

common molecular futures. Nevertless, PAHs exposure involved specific genes. Indeed, the identification and the functional characterization of these specific genes will bring new insights about specific detoxification pathway of the PAHs.

3.2. Adapted plant species to PAHs contaminated environment

Even if molecular mechanisms associated to the PAHs metabolization by plants are still under study, number of species have been described to grown on PAHs contaminated soil and to reduce their level in their environment. These species could be considered as potentially degrading PAHs molecules and might be useful for phytoremediation.

Screening of plant species involved in PAHs remediation is often realized *in vitro* using soil or growth medium contaminated with single PAH or a mixture of the 16 PAHs that are on the Priority Pollutant List of the USEPA (Table 1) as a total PAHs content. Mostly, studies evaluate the quantity of PAHs removed from the soil by plant compared to unplanted soil or the amount of PAHs absorbed by the plant to identify plants species adapted for phytoremediation. Table 2 listed potential PAHs degrading plants. Nevertheless, it remains difficult to identify the best plant for PAHs phytoremediation because plants do not remove each PAHs molecule at identical rate. Even if in general, LMW-PAHs are preferentially degraded, higher level of HMW-PAHs degradation rates were observed when combining several plant species compared to each plant alone (Xu et al., 2006; Cheema et al., 2010).

4. Strategies to improve PAHs bioremediation technologies

4.1. Plant-microbe cooperation enhance PAHs degradation : Rhizodegradation

Rhizodegradation (Fig. 7) is the convergence between phytoremediation and microbial bioremediation strategies which leads to a more efficient approach of sustainable remediation technology (Cunningham et al., 1995; Salt et al., 1995; Schnoor et al., 1995; Alkorta and Garbisu, 2001).

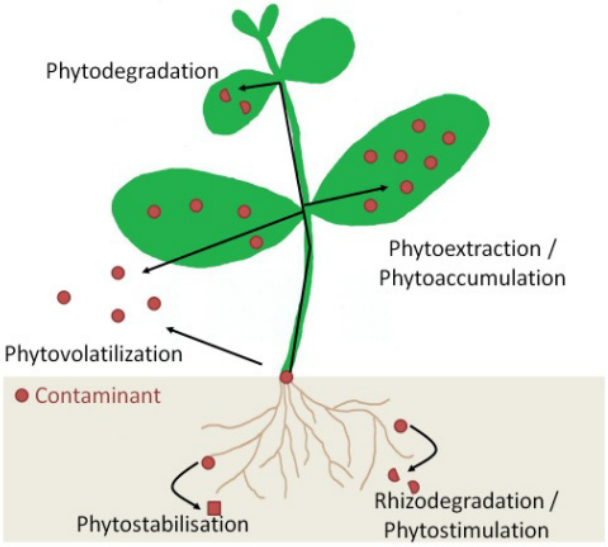

Figure 7: Phytoremediation technologies for decontamination of soil (adapted from Pilon-Smits, 2005).

Field studies mainly showed that rhizodegradation take a predominant place in the process of phytoremediation. Muratova et al. (2003) showed that plants increase the total number of micro-organisms in PAHs-contaminated soil while unplanted soil showed less variety of PAHs degraders. Rhizoremediation occurs naturally because roots release a myriad of compounds, such as flavonoids (Ma et al., 2010) or some fatty acids (Yi and Crowley, 2007), which increase microbial growth and PAHs degradation activity. Indeed, studies have shown that for the initial ring hydroxylation of PAHs, micro-organisms could use roots exudates as a carbon source for the catabolism of HMW-PAHs like benzo[a]pyrene during rhizodegradation (Rentz et al., 2005).

Planted soil with linoleic acid containing plants showed enhanced biodegradation of PAHs compared to unplanted soil. However, its mode of action is still unclear. Liste and Alexander (2000b) found that there is a higher concentration of phenanthrene and pyrene in rhizosphere of some plant species (soybean and rice). It was suggested that plants are responsible for the movement of the PAHs into the root zone, where microbial activity is especially intense. In the *Spartina* rhizosphere, 37 PAHs degrading aerobic bacterial communities were found whereas only 11 were found in unplanted sediment (Launen et al., 2007). Besides chemical compounds released from roots, their growth and death also mechanically enhance PAHs oxidation by allowing soil aeration (Gerhardt et al., 2009).

4.2. Endophytes-assisted phytoremediation: another plant-microbe interaction

The use of bacteria and fungi living within the plant tissues, termed endophytes, present several advantages compared to the free rhizospheric micro-organisms: they are easier to control and they may possibly cause a concentration gradient of the PAHs within the plant tissues, between the organs where the endophytes were localized and the other parts of the plant (Doty, 2008). It may be argued that this strategy may protect meristematic and photosynthetic tissues in order to allow plants to maintain high level of growth, photosynthesis and production of energy, required for protection and cell repair in PAHs induced stress conditions.

Endophytic bacteria showing high tolerance to PAHs and able to use PAHs as sole source of carbon were identified in willow (Doty, 2008). In other hand, some endophytic fungus such *Ceratobasidum stevensii* found in *Bischofia polycarpa* was also able to degrade about 90% of the phenanthrene after 10 days of growth (Dai et al., 2010).

Results obtained by Germaine *et al.* (2009) strongly support that the engineering of PAHs metablizing endophytes, which enhance phytoremediation, constitute a promising strategy. Indeed, they showed that the engineered naphthalene-degrading endophytic strain of *Pseudomonas putida*, an efficient colonizer of plants (pea, annual ryegrass), named VM1441(pNAH7), enhances plant tolerance to naphthalene. Plants containing this endophyte

had a higher naphthalene degradation rate in soil. Indeed, 68% of naphthalene was removed from the soil with inoculated peas compared to unplanted soil, 40% and 37% more when compared to uninoculated plants or to the inoculum alone, respectively.

The use of these new technologies are clearly promising but many efforts have to be done in order to identify and characterize endophytes associated to PAHs degradation, and to better understand the mechanisms involved in these beneficial interactions.

4.3. New tools to improve phyto- and bioremediation

Although micro-organisms play a major role in soil decontamination, PAHs degradation efficiency is limited by (1) the distribution of the cells/communities providing suitable catabolic activity, and (2) the spatio-temporal distribution of catabolically interacting microorganisms. In order to improve soil remediation, it is hence of high interest to understand how microbial populations are distributed in the soil and their role in PAHs degradation activity. Recently, "-omics" approaches emerged as new technologies to address such questions (Desai et al, 2010).

Contrary to classical approaches, metagenomic studies allowed the identification and the monitoring of PAHs degrading microbial populations in the soil. For instance, Layton et al. (2012) were able to monitor the evolution of *Pseudomonas fluorescens* HK44 , its ability to degrade PAHs in the soil following its inoculation, and its impact on the indigenous bacterial population (Layton et al., 2012). Likewise, microbial population dynamic and efficiency of bioremediation processes were monitored also using DNA microarrays (Bae and Park, 2006). Interestingly, pyrosequencing and qPCR assays (Desai et al., 2010) allowed the identification of PAHs degrading bacteria which did not grow on artificial media. In addition, Singleton et al. (2012) successfully monitored bacteria population growing on PAHs contaminated soils, in reactors. They studied the impact of factors such as oxygenation, nutriments, soil depth and duration of treatment, on the bacteria strains development. These promising technologies will bring a global and integrative view about how microbial consortia colonize and adapt to PAHs contaminated ecosystems.

In other hand, recent advances in plant high throughput technologies provide opportunities to decipher mechanisms involved in plant response to PAHs pollution. These global approaches correspond to genome wide association mapping, transcriptomic, metagenomic, proteomic and metabolomic analyses. Indeed, identification of events or actors involved in the perception, absorption, transformation, conjugation and compartmentalization/transport of PAHs should help to create plants enabling a more efficient remediation of pollutants.

Moreover, this knowledge could either allow the improvement of natural occurring methods or the production of transgenic plants harboring an enhanced tolerance to xenobiotics. Several successful incorporation of prokaryotic genes into plants have already been realized especially for decontamination of explosives (Abhilash et al., 2012). Studies using "-omics" approaches designed to investigate the phytoremediation of PAHs still be sparse but will clearly increase in the next future.

Genes degrading PAHs have been identified in bacteria (e.g. Kim et al., 2007; Peng et al., 2008) and fungus (e.g. Syed et al., 2010). They can lead to the creation of transgenic plants to be used for PAHs remediation. As an example, a fungal glutathione-S-transferase gene was introduced into tobacco plants (Dixit et al., 2011). The transgenic plants obtained showed an increased tolerance and higher uptake and metabolization of naphthalene.

Organic pollutants such PAHs are known to be phototoxic and poorly bio-available. Another approach to enhance their phytoremediation would be to use transgenic plants secreting PAHs-degrading enzymes. Even if this strategy is achieved for organic pollutants such as bisphenol A, pentachlorophenol, 2,3-dihydroxybiphenyl and 1-chlorobutane (Doty, 2008), such approaches have not been used for PAHs phytoremediation yet.

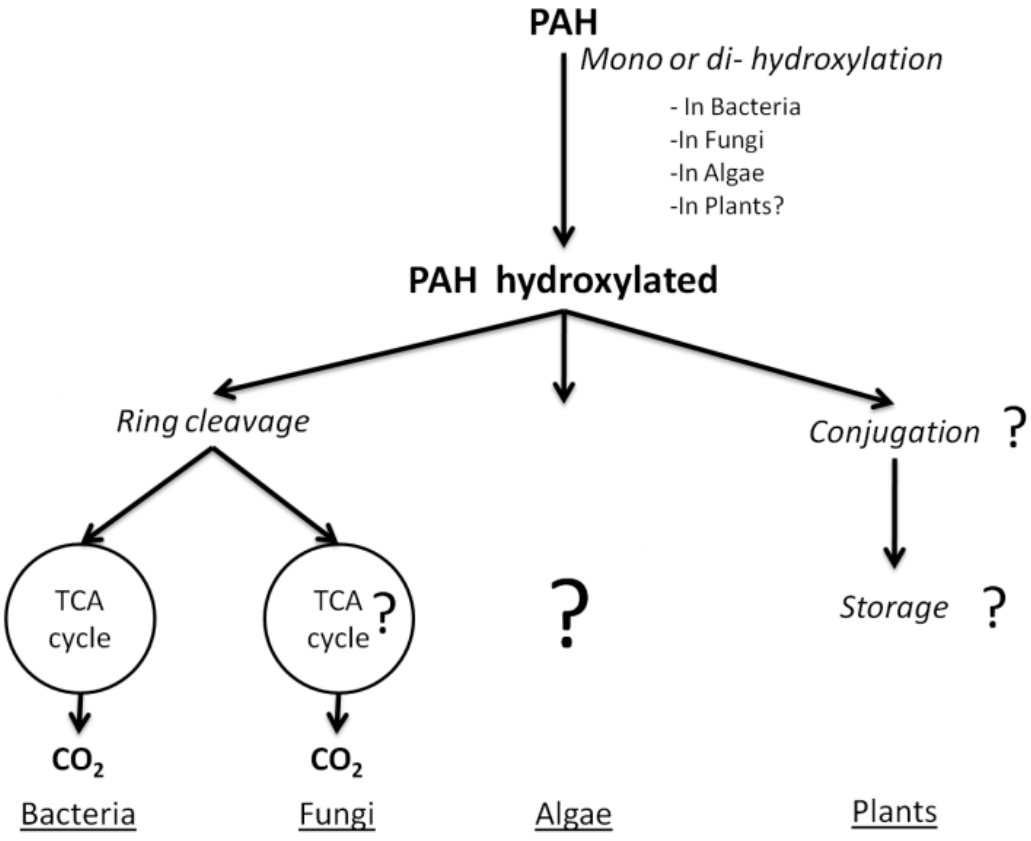

Figure 8: Common and specific PAHs degradation pathways in bacteria, fungi, algae and plants

5. Conclusion

PAHs pollution is a worldwide problem and affects all the components of natural ecosystem. Toxic effects of these molecules conduct most countries to create a regulation of PAHs emissions in the environment. The toxic effects of PAHs and the general concerns highlight the importance of the decontamination of PAHs-contaminated sites.

There is a large variety of decontamination methods ranging from traditional techniques (chemical or thermal) to green technologies. Bioremediation and phytoremediation, classified as green technologies, use the natural capacity of living organisms (plant, fungus, bacteria or algae) to clean up PAHs in the environment. Even if these technologies are slower than thermal treatment, they are easy to set up and demand low capital investment. Moreover, these methods fit in the framework of sustainable development and are widely accepted.

Still far, bacterial remediation is the most developed bioremediation technology and present different strategies that can be set up *in-situ* or *ex-situ*. Indeed, PAHs degradation pathways by bacteria are described and fairly well known. Besides, the PAHs metabolization pathways in fungi and algae are partly described, PAHs degradation in plants was observed but mechanisms involved still have to be identified, even if models of xenobiotic metabolization have been proposed, these processes remain poorly understood.

The emergence of "-omics" tools will help, in the next future, to elucidate the processes of PAHs degradation in plants and also in micro-organisms. Using metabolomic, proteomic and genomic tools, a complete overview of the degradation pathway should be elucidated and could highlight specific events or actors involved in the degradation of PAHs.

Bioremediation technologies are well perceived and promising. Recent metagenomic data show that an efficient PAHs degradation is done mainly by consortium of organisms.

Table 3: List of different combination of remediation technologies

	Molecules	Technologies used	Results	References
combination of biological techniques and agricultural practice	phenanthrene benzo[a] pyrene	soil amendment and bioremediation	Optimization of the carbon source, C/N ratio, soil moisture and aeration conditions are important to enhance PAHs degradation.	Teng et al., 2010
	total PAHs	biosurfactant (ramnolipids), microbial degradation, phytoremediation	Degradation by the combined techniques is 251.83% greater than phytoremediation alone. Better degradation of HMW PAHs.	Zhang et al., 2010
		phytoremediation + landfarming + biodegradation	enhance PAHs removal of 100% more than landfarming, 50% more than bioremediation and 45% more than phytoremediation	Huang et al., 2004
		phytoremediation+ pig manure vermicompost (PMVC)	PMVC increased the shoot and root dry biomasses of S. alfredii by 2.27- and 3.93-fold, PMVC+plants have a higher degradation rate of PAHs than plants or PMVC alone.	Wang et al., 2012
combination of chemical and biological techniques	benzo[a] pyrene	ozonation fallowed by bioremediation	ozonation+bioremediation remove 75-82% of benzo[a]pyrene whereas bioremediation alone remove 35% of the PAHs in 30 days	Russo et al., 2012
	phenanthrene pyrene	solid-liquid 2 phases extraction then bioremediation in a reactor	80% of the original mass of PAHs in the soil has been extracted and after a 14 d period approximately 78%, 62% and 36% of phenanthrene, pyrene, and fluoranthene, respectively, had been desorbed from the polymer and degraded at a laboratory scale.	Rehmann et al., 2008
	total PAHs	solvent pretreatment (acetone or ethanol) then bioremediation	When the soil is pre-treated with solvents, the biodegradation rate of total PAHs is twice the rate without treatment. no difference between the solvents used was observed	Lee et al., 2001
		biodegradation in reactors fallowed by ozonation	shortened the soil remediation from 2-3 months to 1 week	Derudi et al., 2007
		Modified Fenton oxidation and bioremediation as post-treatment	The bioremediation treatment increase up to 10% PAHs degradation compared to the natural attenuation which is usually used after Fenton oxidation. This study shows the compatibility of the 2 treatments.	Venny et al., 2012

To enhance PAHs degradation, it seems important to use different organisms that can act at different stage of the degradation (Fig. 8). Moreover, it is of high interest to understand the mechanisms involved and to improve their efficiency. In order to optimize these techniques, different approaches have been used.

The most promising is the combination of phytoremediation and microbial remediation. The combination of rhizodegradation with chemical (ozonation) or biological (biosurfactant) treatments is also feasible (table 4) and creates the best conditions for soil decontamination. The use of genetically modified plants or micro-organisms for soil decontamination is also a promising alternative in term of increasing decontamination efficiency.

Bibliography

Abhilash, P.C., Powell, J.R., Singh, H.B. and Singh, B.K. (2012) Plant–microbe interactions: novel applications for exploitation in multipurpose remediation technologies. *Trends in Biotechnology*, **30**, 416–420. Available at: [Accessed November 15, 2012].

Al-Awadhi, N., Al-Daher, R., EINawawy, A. and Salba, M.T. (1996) Bioremediation of oil-contaminated soil in Kuwait. I. landfarming to remediate oil-contaminated soil. *Journal of Soil Contamination*, **5**, 243–260. Available at: [Accessed December 3, 2012].

Alkio, M., Tabuchi, T.M., Wang, X. and Colón-Carmona, A. (2005) Stress responses to polycyclic aromatic hydrocarbons in *Arabidopsis* include growth inhibition and hypersensitive response-like symptoms. *Journal of Experimental Botany*, **56**, 2983–2994.

Alkorta, I. and Garbisu, C. (2001) Phytoremediation of organic contaminants in soils. *Bioresource Technology*, **79**, 273–276. Available at: [Accessed July 16, 2012].

Andersson, B.E. and Henrysson, T. (1996) Accumulation and degradation of dead-end metabolites during treatment of soil contaminated with polycyclic aromatic hydrocarbons with five strains of white-rot fungi. *Appl Microbiol Biotechnol*, **46**, 647–652. Available at: [Accessed April 11, 2013].

Andersson, B.E., Lundstedt, S., Tornberg, K., Schnürer, Y., Öberg, L.G. and Mattiasson, B. (2003) Incomplete degradation of polycyclic aromatic hydrocarbons in soil inoculated with wood-rotting fungi and their effect on the indigenous soil bacteria. *Environmental Toxicology and Chemistry*, **22**, 1238–1243. Available at: [Accessed April 11, 2013].

Antizar-Ladislao, B., Lopez-Real, J. and Beck, A. (2004) Bioremediation of Polycyclic Aromatic Hydrocarbon (PAH)-Contaminated Waste Using Composting Approaches. *Critical Reviews in Environmental Science and Technology*, **34**, 249–289. Available at: [Accessed December 3, 2012].

Atagana, H.I. (2004) Bioremediation of creosote-contaminated soil in South Africa by landfarming. *J. Appl. Microbiol.*, **96**, 510–520.

Bae, J.-W. and Park, Y.-H. (2006) Homogeneous versus heterogeneous probes for microbial ecological microarrays. *Trends in Biotechnology*, **24**, 318–323. Available at: [Accessed November 15, 2012].

Baerson, S.R., Sánchez-Moreiras, A., Pedrol-Bonjoch, N., Schulz, M., Kagan, I.A., Agarwal, A.K., Reigosa, M.J. and Duke, S.O. (2005) Detoxification and Transcriptome Response in *Arabidopsis* Seedlings Exposed to the Allelochemical Benzoxazolin-2(3H)-one. *J. Biol. Chem.*, **280**, 21867–21881. Available at: [Accessed September 19, 2012].

Bak, S., Beisson, F., Bishop, G., Hamberger, B., Höfer, R., Paquette, S. and Werck-Reichhart, D. (2011) Cytochromes P450. *The Arabidopsis Book*, e0144. Available at: [Accessed September 19, 2012].

Ballach, H.-J., Kuhn, A. and Wittig, R. (2003) Biodegradation of anthracene in the roots and growth substrate of poplar cuttings. *Environmental Science and Pollution Research*, **10**, 308–316. Available at: [Accessed January 9, 2013].

Banks, M.K., Kulakow, P., Schwab, A.P., Chen, Z. and Rathbone, K. (2003) Degradation of crude oil in the rhizosphere of Sorghum bicolor. *Int J Phytoremediation*, **5**, 225–234.

Banks, M.K., Lee, E. and Schwab, A.P. (1999) Evaluation of Dissipation Mechanisms for Benzo[a]pyrene in the Rhizosphere of Tall Fescue. *Journal of Environmental Quality*, **28**, 294–298. Available at: [Accessed January 9, 2013].

Bezalel, L., Hadar, Y. and Cerniglia, C.E. (1997) Enzymatic Mechanisms Involved in Phenanthrene Degradation by the White Rot Fungus Pleurotus ostreatus. *Appl Environ Microbiol*, **63**, 2495–2501. Available at: [Accessed November 14, 2012].

Bezalel, L., Hadar, Y. and Cerniglia, C.E. (1996) Mineralization of Polycyclic Aromatic Hydrocarbons by the White Rot Fungus Pleurotus ostreatus. *Appl. Environ. Microbiol.*, **62**, 292–295. Available at: [Accessed November 13, 2012].

Bezalel, L., Hadar, Y., Fu, P.P., Freeman, J.P. and Cerniglia, C.E. (1996) Metabolism of phenanthrene by the white rot fungus Pleurotus ostreatus. *Appl Environ Microbiol*, **62**, 2547–2553. Available at: [Accessed October 26, 2012].

Boonchan, S., Britz, M.L. and Stanley, G.A. (2000) Degradation and Mineralization of High-Molecular-Weight Polycyclic Aromatic Hydrocarbons by Defined Fungal-Bacterial Cocultures. *Appl. Environ. Microbiol.*, **66**, 1007–1019. Available at: [Accessed December 3, 2012].

Brennerova, M.V., Josefiova, J., Brenner, V., Pieper, D.H. and Junca, H. (2009) Metagenomics reveals diversity and abundance of meta-cleavage pathways in microbial communities from soil highly contaminated with jet fuel under air-sparging bioremediation. *Environ Microbiol*, **11**, 2216–2227. Available at: [Accessed February 28, 2013].

Cerniglia, C.E. (1992) Biodegradation of polycyclic aromatic hydrocarbons. *Biodegradation*, **3**, 351–368. Available at: [Accessed October 29, 2012].

Cerniglia, C.E. (1997) Fungal metabolism of polycyclic aromatic hydrocarbons: past, present and future applications in bioremediation. *J Ind Microbiol Biotech*, **19**, 324–333. Available at: [Accessed November 13, 2012].

Cerniglia, C.E., Baalen, C.V. and Gibson, D.T. (1980) Metabolism of Naphthalene by the Cyanobacterium Oscillatoria sp., Strain JCM. *J Gen Microbiol*, **116**, 485–494. Available at: [Accessed January 8, 2013].

Cheema, S.A., Imran Khan, M., Shen, C., Tang, X., Farooq, M., Chen, L., Zhang, C. and Chen, Y. (2010) Degradation of phenanthrene and pyrene in spiked soils by single and combined plants cultivation. *Journal of Hazardous Materials*, **177**, 384–389. Available at: [Accessed January 9, 2013].

Coleman, J., Blake-Kalff, M. and Davies, E. (1997) Detoxification of xenobiotics by plants: chemical modification and vacuolar compartmentation. *Trends in Plant Science*, **2**, 144–151. Available at: [Accessed October 16, 2012].

Cunningham, S.D., Berti, W.R. and Huang, J.W. (1995) Phytoremediation of contaminated soils. *Trends in Biotechnology*, **13**, 393–397. Available at: [Accessed November 6, 2012].

Dai, C., Tian, L., Zhao, Y., Chen, Y. and Xie, H. (2010) Degradation of phenanthrene by the endophytic fungus Ceratobasidum stevensii found in Bischofia polycarpa. *Biodegradation*, **21**, 245–255.

Derudi, M., Venturini, G., Lombardi, G., Nano, G. and Rota, R. (2007) Biodegradation combined with ozone for the remediation of contaminated soils. *European Journal of Soil Biology*, **43**, 297–303. Available at: [Accessed January 11, 2013].

Desai, C., Pathak, H. and Madamwar, D. (2010) Advances in molecular and "-omics" technologies to gauge microbial communities and bioremediation at xenobiotic/anthropogen contaminated sites. *Bioresource Technology*, **101**, 1558–1569. Available at: [Accessed November 14, 2012].

Dixit, P., Mukherjee, P.K., Sherkhane, P.D., Kale, S.P. and Eapen, S. (2011) Enhanced tolerance and remediation of anthracene by transgenic tobacco plants expressing a fungal glutathione transferase gene. *Journal of Hazardous Materials*, **192**, 270–276. Available at: [Accessed December 3, 2012].

Dixon, D.P. and Edwards, R. (2010) Glutathione Transferases. *Arabidopsis Book*, **8**. Available at: http://www.ncbi.nlm.nih.gov/pmc/articles/PMC3244946/ [Accessed September 19, 2012].

Doty, S.L. (2008) Enhancing phytoremediation through the use of transgenics and endophytes. *New Phytol.*, **179**, 318–333. Available at: [Accessed June 8, 2012].

Edema, C.U., Idu, T.E. and Edema, M.O. (2011) Remediation of soil contaminated with polycyclic aromatic hydrocarbons from crude oil. *African Journal of Biotechnology*, **10**, 1146–1149. Available at: [Accessed December 3, 2012].

Edwards, R., Brazier-Hicks, M., Dixon, D.P. and Cummins, I. (2005) Chemical Manipulation of Antioxidant Defences in Plants. In J. A. Callow, ed. *Advances in Botanical Research*. Academic Press, pp. 1–32. Available at: http://www.sciencedirect.com/science/article/pii/S0065229605420017 [Accessed October 11, 2012].

Edwards, R., Dixon, D.P., Cummins, I., Brazier-Hicks, M. and Skipsey, M. (2011) New Perspectives on the Metabolism and Detoxification of Synthetic Compounds in Plants. In P. Schröder and C. D. Collins, eds. *Organic Xenobiotics and Plants*. Plant Ecophysiology. Springer Netherlands, pp. 125–148. Available at: http://www.springerlink.com/content/w47665207215u483/abstract/ [Accessed September 14, 2012].

Euliss, K., Ho, C., Schwab, A.P., Rock, S. and Banks, M.K. (2008) Greenhouse and field assessment of phytoremediation for petroleum contaminants in a riparian zone. *Bioresource Technology*, **99**, 1961–1971. Available at: [Accessed January 9, 2013].

Frutos, F.J.G., Escolano, O., García, S., Babín, M. and Fernández, M.D. (2010) Bioventing remediation and ecotoxicity evaluation of phenanthrene-contaminated soil. *Journal of Hazardous Materials*, **183**, 806–813. Available at: [Accessed November 30, 2012].

Furuno, S., Foss, S., Wild, E., Jones, K.C., Semple, K.T., Harms, H. and Wick, L.Y. (2012) Mycelia Promote Active Transport and Spatial Dispersion of Polycyclic Aromatic Hydrocarbons. *Environ. Sci. Technol.*, **46**, 5463–5470. Available at: [Accessed April 11, 2013].

Furuno, S., Päzolt, K., Rabe, C., Neu, T.R., Harms, H. and Wick, L.Y. (2010) Fungal mycelia allow chemotactic dispersal of polycyclic aromatic hydrocarbon-degrading bacteria in water-unsaturated systems. *Environ. Microbiol.*, **12**, 1391–1398.

Gan, S., Lau, E.V. and Ng, H.K. (2009) Remediation of soils contaminated with polycyclic aromatic hydrocarbons (PAHs). *Journal of Hazardous Materials*, **172**, 532–549. Available at: [Accessed September 20, 2012].

Gerhardt, K.E., Huang, X.-D., Glick, B.R. and Greenberg, B.M. (2009) Phytoremediation and rhizoremediation of organic soil contaminants: Potential and challenges. *Plant Science*, **176**, 20–30. Available at: [Accessed November 6, 2012].

Germaine, K.J., Keogh, E., Ryan, D. and Dowling, D.N. (2009) Bacterial endophyte-mediated naphthalene phytoprotection and phytoremediation. *FEMS Microbiology Letters*, **296**, 226–234. Available at: [Accessed December 3, 2012].

Goodwin, S. and Sutter, T. (2009) Microarray analysis of <i>Arabidopsis</i> genome response to aluminum stress. *Biologia Plantarum*, **53**, 85–99. Available at: [Accessed September 19, 2012].

Guazzaroni, M.-E., Herbst, F.-A., Lores, I., *et al.* (2013) Metaproteogenomic insights beyond bacterial response to naphthalene exposure and bio-stimulation. *ISME J*, **7**, 122–136. Available at: [Accessed January 11, 2013].

Hansen, L.D., Nestler, C., Ringelberg, D. and Bajpai, R. (2004) Extended bioremediation of PAH/PCP contaminated soils from the POPILE wood treatment facility. *Chemosphere*, **54**, 1481–1493.

Haritash, A.K. and Kaushik, C.P. (2009) Biodegradation aspects of Polycyclic Aromatic Hydrocarbons (PAHs): A review. *Journal of Hazardous Materials*, **169**, 1–15. Available at: [Accessed August 9, 2012].

Harms, H., Schlosser, D. and Wick, L.Y. (2011) Untapped potential: exploiting fungi in bioremediation of hazardous chemicals. *Nature Reviews Microbiology*, **9**, 177–192. Available at: [Accessed December 3, 2012].

Herbette, S., Taconnat, L., Hugouvieux, V., *et al.* (2006) Genome-wide transcriptome profiling of the early cadmium response of *Arabidopsis* roots and shoots. *Biochimie*, **88**, 1751–1765. Available at: [Accessed September 19, 2012].

Hoewyk, D. Van, Takahashi, H., Inoue, E., Hess, A., Tamaoki, M. and Pilon-Smits, E.A.H. (2008) Transcriptome analyses give insights into selenium-stress responses and selenium tolerance mechanisms in Arabidopsis. *Physiol Plant*, **132**, 236–253. Available at: [Accessed September 19, 2012].

Huang, X.-D., El-Alawi, Y., Penrose, D.M., Glick, B.R. and Greenberg, B.M. (2004) A multi-process phytoremediation system for removal of polycyclic aromatic hydrocarbons from contaminated soils. *Environ. Pollut.*, **130**, 465–476.

Huesemann, M.H., Hausmann, T.S., Fortman, T.J., Thom, R.M. and Cullinan, V. (2009) In situ phytoremediation of PAH- and PCB-contaminated marine sediments with eelgrass (Zostera marina). *Ecological Engineering*, **35**, 1395–1404. Available at: [Accessed January 9, 2013].

HuiJie, L., CaiYun, Y., Yun, T., GuangHui, L. and TianLing, Z. (2011) Using population dynamics analysis by DGGE to design the bacterial consortium isolated from mangrove sediments for biodegradation of PAHs. *International Biodeterioration & Biodegradation*, **65**, 269–275. Available at: [Accessed December 3, 2012].

Janikowski, T., Velicogna, D., Punt, M. and Daugulis, A. (2002) Use of a two-phase partitioning bioreactor for degrading polycyclic aromatic hydrocarbons by a Sphingomonas sp. *Appl Microbiol Biotechnol*, **59**, 368–376. Available at: [Accessed December 3, 2012].

Jin, X.-F., Shuai, J.-J., Peng, R.-H., *et al.* (2011) Identification of candidate genes involved in responses of *Arabidopsis* to polychlorinated biphenyls based on microarray analysis. *Plant Growth Regulation*, **65**, 127–135. Available at: [Accessed September 19, 2012].

Johnsen, A.R., Wick, L.Y. and Harms, H. (2005) Principles of microbial PAH-degradation in soil. *Environmental Pollution*, **133**, 71–84. Available at: [Accessed August 9, 2012].

Jones, M.D., Crandell, D.W., Singleton, D.R. and Aitken, M.D. (2011) Stable-isotope probing of the polycyclic aromatic hydrocarbon-degrading bacterial guild in a contaminated soil. *Environmental Microbiology*, **13**, 2623–2632. Available at: [Accessed April 11, 2013].

Juhasz, A.L., Stanley, G.A. and Britz, M.L. (2000) Degradation of High Molecular Weight PAHs in Contaminated Soil by a Bacterial Consortium: Effects on Microtox and Mutagenicity Bioassays. *Bioremediation Journal*, **4**, 271–283. Available at: [Accessed December 3, 2012].

Kanaly, R.A. and Harayama, S. (2000) Biodegradation of High-Molecular-Weight Polycyclic Aromatic Hydrocarbons by Bacteria. *J. Bacteriol.*, **182**, 2059–2067. Available at: [Accessed August 7, 2012].

Kim, S.-J., Kweon, O. and Cerniglia, C.E. (2009) Proteomic applications to elucidate bacterial aromatic hydrocarbon metabolic pathways. *Current Opinion in Microbiology*, **12**, 301–309. Available at: [Accessed November 16, 2012].

Kim, S.-J., Kweon, O., Jones, R.C., Freeman, J.P., Edmondson, R.D. and Cerniglia, C.E. (2007) Complete and integrated pyrene degradation pathway in Mycobacterium vanbaalenii PYR-1 based on systems biology. *J. Bacteriol.*, **189**, 464–472.

Kohlmeier, S., Smits, T.H.M., Ford, R.M., Keel, C., Harms, H. and Wick, L.Y. (2005) Taking the fungal highway: mobilization of pollutant-degrading bacteria by fungi. *Environ. Sci. Technol.*, **39**, 4640–4646.

Kotterman, M.J.J., Vis, E.H. and Field, J.A. (1998) Successive Mineralization and Detoxification of Benzo[a]pyrene by the White Rot FungusBjerkandera sp. Strain BOS55 and Indigenous Microflora. *Appl. Environ. Microbiol.*, **64**, 2853–2858. Available at: [Accessed November 13, 2012].

Landa, P., Storchova, H., Hodek, J., Vankova, R., Podlipna, R., Marsik, P., Ovesna, J. and Vanek, T. (2010) Transferases and transporters mediate the detoxification and capacity to tolerate trinitrotoluene in Arabidopsis. *Funct. Integr. Genomics*, **10**, 547–559. Available at: [Accessed September 19, 2012].

Launen, L.A., Dutta, J., Turpeinen, R., Eastep, M.E., Dorn, R., Buggs, V.H., Leonard, J.W. and Häggblom, M.M. (2007) Characterization of the indigenous PAH-degrading bacteria of Spartina dominated salt marshes in the New York/New Jersey Harbor. *Biodegradation*, **19**, 347–363. Available at: [Accessed November 9, 2012].

Layton, A., Smart, A.E., Chauhan, A., *et al.* (2012) Ameliorating Risk: Culturable and Metagenomic Monitoring of the 14 Year Decline of a Genetically Engineered Microorganism at a Bioremediation Field Site. *OMICS: Journal of Bioremediation and Biodegradation*, **9**. Available at: http://www.osti.gov/energycitations/product.biblio.jsp?osti_id=1047016 [Accessed January 11, 2013].

Lee, M.D. and Swindoll, C.M. (1993) Bioventing for in situ remediation. *Hydrological Sciences Journal*, **38**, 273–282. Available at: [Accessed November 30, 2012].

Lee, P.-H., Ong, S.K., Golchin, J. and Nelson, G.L. (Sam. (2001) Use of solvents to enhance PAH biodegradation of coal tar-. *Water Research*, **35**, 3941–3949. Available at: [Accessed January 10, 2013].

Lei, A.-P., Hu, Z.-L., Wong, Y.-S. and Tam, N.F.-Y. (2007) Removal of fluoranthene and pyrene by different microalgal species. *Bioresource Technology*, **98**, 273–280. Available at: [Accessed October 26, 2012].

Liebeg, E.W. and Cutright, T.J. (1999) The investigation of enhanced bioremediation through the addition of macro and micro nutrients in a PAH contaminated soil. *International Biodeterioration & Biodegradation*, **44**, 55–64. Available at: [Accessed December 3, 2012].

Lily, M.K., Bahuguna, A., Dangwal, K. and Garg, V. (2009) Degradation of Benzo [a] Pyrene by a novel strain Bacillus subtilis BMT4i (MTCC 9447). *Brazilian Journal of Microbiology*, **40**, 884–892. Available at: [Accessed August 9, 2012].

Liste, H.-H. and Alexander, M. (2000a) Accumulation of phenanthrene and pyrene in rhizosphere soil. *Chemosphere*, **40**, 11–14. Available at: [Accessed November 7, 2012].

Liste, H.-H. and Alexander, M. (2000b) Plant-promoted pyrene degradation in soil. *Chemosphere*, **40**, 7–10. Available at: [Accessed July 3, 2012].

Liste, H.-H. and Alexander, M. (1999) Rapid Screening of Plants Promoting Phenanthrene Degradation. *Journal of Environmental Quality*, **28**, 1376–1377. Available at: [Accessed November 7, 2012].

Loh, K.-C. and Cao, B. (2008) Paradigm in biodegradation using Pseudomonas putida—A review of proteomics studies. *Enzyme and Microbial Technology*, **43**, 1–12. Available at: [Accessed February 28, 2013].

Ma, B., He, Y., Chen, H., Xu, J. and Rengel, Z. (2010) Dissipation of polycyclic aromatic hydrocarbons (PAHs) in the rhizosphere: synthesis through meta-analysis. *Environ. Pollut.*, **158**, 855–861.

Mallick, S., Chatterjee, S. and Dutta, T.K. (2007) A novel degradation pathway in the assimilation of phenanthrene by Staphylococcus sp. strain PN/Y via meta-cleavage of 2-hydroxy-1-naphthoic acid: formation of trans-2,3-dioxo-5-(2'-hydroxyphenyl)-pent-4-enoic acid. *Microbiology (Reading, Engl.)*, **153**, 2104–2115.

Masten, S.J. and Davies, S.H.R. (1997) Efficacy of in-situ for the remediation of PAH contaminated soils. *Journal of Contaminant Hydrology*, **28**, 327–335. Available at:.

Mitsch, W.J. (2012) What is ecological engineering? *Ecological Engineering*, **45**, 5–12. .

Mohan, S.V., Kisa, T., Ohkuma, T., Kanaly, R.A. and Shimizu, Y. (2006) Bioremediation technologies for treatment of PAH-contaminated soil and strategies to enhance process efficiency. *Rev Environ Sci Biotechnol*, **5**, 347–374. Available at: [Accessed December 3, 2012].

Mrozik, A., Piotrowska-Seget, Z. and Łabuzek, S. (2003) Bacterial degradation and bioremediation of polycyclic aromatic hydrocarbons. *Polish Journal of Environmental Studies*, **12**, 15–25.

Muratova, A., Hübner, T., Tischer, S., Turkovskaya, O., Möder, M. and Kuschk, P. (2003) Plant--rhizosphere-microflora association during phytoremediation of PAH-contaminated soil. *Int J Phytoremediation*, **5**, 137–151.

Narro, M.L., Cerniglia, C.E., Baalen, C. Van and Gibson, D.T. (1992) Metabolism of phenanthrene by the marine cyanobacterium Agmenellum quadruplicatum PR-6. *Appl Environ Microbiol*, **58**, 1351–1359. Available at: [Accessed January 8, 2013].

Peng, R.-H., Xiong, A.-S., Xue, Y., Fu, X.-Y., Gao, F., Zhao, W., Tian, Y.-S. and Yao, Q.-H. (2008) Microbial biodegradation of polyaromatic hydrocarbons. *FEMS Microbiology Reviews*, **32**, 927–955. Available at: [Accessed December 3, 2012].

Pinelli, D., Fava, F., Nocentini, M. and Pasquali, G. (1997) Bioremediation of a polycyclic aromatic hydrocarbon-contaminated soil by using different aerobic batch bioreactor systems. *Journal of Soil Contamination*, **6**, 243–256. Available at: [Accessed December 3, 2012].

Pradhan, S.P., Conrad, J.R., Paterek, J.R. and Srivastava, V.J. (1998) Potential of Phytoremediation for Treatment of PAHs in Soil at MGP Sites. *Journal of Soil Contamination*, **7**, 467–480. Available at: [Accessed November 5, 2012].

Ramel, F., Sulmon, C., Cabello-Hurtado, F., Taconnat, L., Martin-Magniette, M.-L., Renou, J.-P., Amrani, A.E., Couée, I. and Gouesbet, G. (2007) Genome-wide interacting effects of sucrose and herbicide-mediated stress in *Arabidopsis thaliana*: novel insights into atrazine toxicity and sucrose-induced tolerance. *BMC Genomics*, **8**, 450. Available at: [Accessed September 19, 2012].

Rehmann, L., Prpich, G.P. and Daugulis, A.J. (2008) Remediation of PAH contaminated soils: Application of a solid–liquid two-phase partitioning bioreactor. *Chemosphere*, **73**, 798–804. Available at: [Accessed December 5, 2012].

Rentz, J.A., Alvarez, P.J.J. and Schnoor, J.L. (2005) Benzo[a]pyrene co-metabolism in the presence of plant root extracts and exudates: Implications for phytoremediation. *Environmental Pollution*, **136**, 477–484. Available at: [Accessed November 5, 2012].

Russo, L., Rizzo, L. and Belgiorno, V. (2012) Ozone oxidation and aerobic biodegradation with spent mushroom compost for detoxification and benzo(a)pyrene removal from contaminated soil. *Chemosphere*, **87**, 595–601. Available at: [Accessed December 5, 2012].

Salt, D.E., Blaylock, M., Kumar, N.P.B.A., Dushenkov, V., Ensley, B.D., Chet, I. and Raskin, I. (1995) Phytoremediation: A Novel Strategy for the Removal of Toxic Metals from the Environment Using Plants. *Nature Biotechnology*, **13**, 468–474. Available at: [Accessed November 6, 2012].

Samanta, S.K., Singh, O.V. and Jain, R.K. (2002) Polycyclic aromatic hydrocarbons: environmental pollution and bioremediation. *Trends in Biotechnology*, **20**, 243–248. Available at: [Accessed August 7, 2012].

Sandermann Jr., H. (1992) Plant metabolism of xenobiotics. *Trends in Biochemical Sciences*, **17**, 82–84. Available at: [Accessed October 4, 2012].

Saraswathy, A. and Hallberg, R. (2002) Degradation of pyrene by indigenous fungi from a former gasworks site. *FEMS Microbiology Letters*, **210**, 227–232. Available at: [Accessed November 20, 2012].

Schamfuß, S., Neu, T.R., Harms, H., Meer, J.R. van der, Tecon, R. and Wick, L.Y. (2013) Mycelial Networks Enhance the Bioavailability of PAH in Water Unsaturated Environments. *Environmental Science & Technology*.

Schneider, J., Grosser, R., Jayasimhulu, K., Xue, W. and Warshawsky, D. (1996) Degradation of pyrene, benz[a]anthracene, and benzo[a]pyrene by Mycobacterium sp. strain RJGII-135, isolated from a former coal gasification site. *Appl. Environ. Microbiol.*, **62**, 13–19. Available at: [Accessed November 13, 2012].

Schnoor, J.L., Licht, L.A., McCutcheon, S.C., Wolfe, N.L. and CARREIRA, L.H. (1995) Phytoremediation of Organic and Nutrient Contaminants. *Environ. Sci. Technol.*, **29**, 318A–323A. Available at: [Accessed November 6, 2012].

Siciliano, S.D., Germida, J.J., Banks, K. and Greer, C.W. (2003) Changes in Microbial Community Composition and Function during a Polyaromatic Hydrocarbon Phytoremediation Field Trial. *Appl. Environ. Microbiol.*, **69**, 483–489. Available at: [Accessed January 9, 2013].

Singleton, D.R., Hunt, M., Powell, S.N., Frontera-Suau, R. and Aitken, M.D. (2007) Stable-isotope probing with multiple growth substrates to determine substrate specificity of uncultivated bacteria. *Journal of Microbiological Methods*, **69**, 180–187. Available at: [Accessed April 11, 2013].

Singleton, D.R., Jones, M.D., Richardson, S.D. and Aitken, M.D. (2012) Pyrosequence analyses of bacterial communities during simulated in situ bioremediation of polycyclic aromatic hydrocarbon-contaminated soil. *Appl. Microbiol. Biotechnol.*

Singleton, D.R., Powell, S.N., Sangaiah, R., Gold, A., Ball, L.M. and Aitken, M.D. (2005) Stable-Isotope Probing of Bacteria Capable of Degrading Salicylate, Naphthalene, or Phenanthrene in a Bioreactor Treating Contaminated Soil. *Appl. Environ. Microbiol.*, **71**, 1202–1209. Available at: [Accessed April 11, 2013].

Smith, M.R. (1990) The biodegradation of aromatic hydrocarbons by bacteria. *Biodegradation*, **1**, 191–206.

Syed, K., Doddapaneni, H., Subramanian, V., Lam, Y.W. and Yadav, J.S. (2010) Genome-to-function characterization of novel fungal P450 monooxygenases oxidizing polycyclic aromatic hydrocarbons (PAHs). *Biochemical and Biophysical Research Communications*, **399**, 492–497. Available at: [Accessed November 20, 2012].

Taguchi, G., Ubukata, T., Nozue, H., Kobayashi, Y., Takahi, M., Yamamoto, H. and Hayashida, N. (2010) Malonylation is a key reaction in the metabolism of xenobiotic phenolic glucosides in *Arabidopsis* and tobacco. *The Plant Journal*, **63**, 1031–1041. Available at: [Accessed February 1, 2013].

Técher, D., Laval-Gilly, P., Henry, S., *et al.* (2011) Contribution of Miscanthus x giganteus root exudates to the biostimulation of PAH degradation: An in vitro study. *Science of The Total Environment*, **409**, 4489–4495. Available at: [Accessed November 8, 2012].

Técher, D., Laval-Gilly, P., Henry, S., Bennasroune, A., Martinez-Chois, C., D'Innocenzo, M. and Falla, J. (2012) Prospects of Miscanthus x giganteus for PAH phytoremediation: A microcosm study. *Industrial Crops and Products*, **36**, 276–281. Available at: [Accessed November 8, 2012].

Teng, Y., Luo, Y., Ping, L., Zou, D., Li, Z. and Christie, P. (2010) Effects of soil amendment with different carbon sources and other factors on the bioremediation of an aged PAH-contaminated soil. *Biodegradation*, **21**, 167–178. Available at: [Accessed December 5, 2012].

Trzesicka-Mlynarz, D. and Ward, O.P. (1995) Degradation of polycyclic aromatic hydrocarbons (PAHs) by a mixed culture and its component pure cultures, obtained from PAH-contaminated soil. *Can. J. Microbiol.*, **41**, 470–476.

Al-Turky, A.I. (2009) Microbial polycyclic aromatic hydrocarbons degradation in soil. *Research Journal of Environmental Toxicology*, **3**, 1–8.

Venny, Gan, S. and Ng, H.K. (2012) Modified Fenton oxidation of polycyclic aromatic hydrocarbon (PAH)-contaminated soils and the potential of bioremediation as post-treatment. *Science of The Total Environment*, **419**, 240–249. Available at: [Accessed December 5, 2012].

Vervaeke, P., Luyssaert, S., Mertens, J., Meers, E., Tack, F.M.. and Lust, N. (2003) Phytoremediation prospects of willow stands on contaminated sediment: a field trial. *Environmental Pollution*, **126**, 275–282. Available at: [Accessed November 8, 2012].

Vilchez-Vargas, R., Junca, H. and Pieper, D.H. (2010) Metabolic networks, microbial ecology and "omics" technologies: towards understanding in situ biodegradation processes. *Environmental Microbiology*, **12**, 3089–3104. Available at: [Accessed November 15, 2012].

Wang, K., Zhang, J., Zhu, Z., Huang, H., Li, T., He, Z., Yang, X. and Alva, A. (2012) Pig manure vermicompost (PMVC) can improve phytoremediation of Cd and PAHs co-contaminated soil by Sedum alfredii. *J Soils Sediments*, **12**, 1089–1099. Available at: [Accessed December 5, 2012].

Warshawsky, D., Cody, T., Radike, M., Reilman, R., Schumann, B., LaDow, K. and Schneider, J. (1995) Biotransformation of benzo[a]pyrene and other polycyclic aromatic hydrocarbons and heterocyclic analogs by several green algae and other algal species under gold and white light. *Chemico-Biological Interactions*, **97**, 131–148. Available at: [Accessed August 13, 2012].

Watts, A.W., Ballestero, T.P. and Gardner, K.H. (2006) Uptake of polycyclic aromatic hydrocarbons (PAHs) in salt marsh plants Spartina alterniflora grown in contaminated sediments. *Chemosphere*, **62**, 1253–1260.

Weisman, D., Alkio, M. and Colón-Carmona, A. (2010) Transcriptional responses to polycyclic aromatic hydrocarbon-induced stress in *Arabidopsis thaliana* reveal the involvement of

hormone and defense signaling pathways. *BMC Plant Biol*, **10**, 59. Available at: [Accessed September 19, 2012].

Wilson, S.C. and Jones, K.C. (1993) Bioremediation of soil contaminated with polynuclear aromatic hydrocarbons (PAHs): A review. *Environmental Pollution*, **81**, 229–249. Available at: [Accessed October 26, 2012].

Xu, J., Su, Z.-H., Chen, C., *et al.* (2012) Stress responses to phenol in *Arabidopsis* and transcriptional changes revealed by microarray analysis. *Planta*, **235**, 399–410. Available at: [Accessed September 21, 2012].

Xu, S.Y., Chen, Y.X., Wu, W.X., Wang, K.X., Lin, Q. and Liang, X.Q. (2006) Enhanced dissipation of phenanthrene and pyrene in spiked soils by combined plants cultivation. *Science of The Total Environment*, **363**, 206–215. Available at: [Accessed November 8, 2012].

Yi, H. and Crowley, D.E. (2007) Biostimulation of PAH Degradation with Plants Containing High Concentrations of Linoleic Acid. *Environ. Sci. Technol.*, **41**, 4382–4388. Available at: [Accessed December 4, 2012].

Zhan, X.-H., Ma, H.-L., Zhou, L.-X., Liang, J.-R., Jiang, T.-H. and Xu, G.-H. (2010) Accumulation of phenanthrene by roots of intact wheat (Triticum acstivnm L.) seedlings: passive or active uptake? *BMC Plant Biology*, **10**, 52. Available at: [Accessed November 5, 2012].

Zhang, J., Yin, R., Lin, X., Liu, W., Chen, R. and Li, X. (2010) Interactive Effect of Biosurfactant and Microorganism to Enhance Phytoremediation for Removal of Aged Polycyclic Aromatic Hydrocarbons from Contaminated Soils. *Journal of Health Science*, **56**, 257–266.

Zhang, X.-X., Cheng, S.-P., Zhu, C.-J. and Sun, S.-L. (2006) Microbial PAH-Degradation in Soil: Degradation Pathways and Contributing Factors. *Pedosphere*, **16**, 555–565. Available at: [Accessed October 26, 2012].

Partie 3: **Les sucres solubles : des molécules-clés impliquées dans la tolérance aux stress abiotiques chez les plantes supérieures**

1. Introduction

En tant qu'organismes cessiles, les plantes sont soumises aux changements de leur environnement et doivent donc mettre en place des processus qui leur permettent de s'adapter à ces modifications. Seules les plantes capables de développer cette capacité à s'adapter ont pu survivre à cette sélection naturelle et se propager. Ces conditions de stress modifient le développement des plantes en affectant plusieurs processus cellulaires tels que le développement, la photosynthèse, le métabolisme des lipides et des sucres, l'expression des gènes, l'équilibre osmotique. Ces perturbations affectent profondément le fonctionnement des plantes entrainant une inhibition de leur croissance.

Une des conséquences les plus communes des stress abiotiques est la production de dérivés actifs de l'oxygène (ROS) dont l'accumulation crée un stress oxydant. Les ROS sont produites continuellement au sein de la plante de par la photosynthèse et la respiration mais leur niveau reste faible grâce à la prise en charge par le système antioxydant. L'augmentation du niveau des ROS due à un stress abiotique est un moyen de signaler à l'ensemble de la plante les modifications dans l'environnement et de provoquer des changements au niveau métabolique. Une accumulation de ces molécules peut causer des dommages cellulaires pouvant aller jusqu'à la mort cellulaire (Foyer and Noctor, 2005).

Les plantes sont des organismes autotrophes et photosynthétiques qui sont capables de produire et de consommer les sucres. Cependant, les sucres ne sont pas seulement des ressources métaboliques et des composés structuraux, ils jouent de nombreux rôles notamment de signalisation et de protection vis-à-vis des stress abiotiques (Rolland et al., 2002; Rosa et al., 2009; Wind et al., 2010).

Le saccharose est un disaccharide représentant la forme majoritaire sous laquelle les sucres sont transportés chez les végétaux supérieurs. Comme la plupart des sucres solubles, il a aussi des caractéristiques autres que métaboliques et induit l'initiation de voies signalétiques qui modifient l'expression des gènes et l'adaptation physiologique de la plante (Wind et al., 2010).

2. Les stress abiotiques modifient la teneur en sucres solubles chez les végétaux

Les plantes doivent s'adapter aux modifications de leur environnement et doivent donc modifier leur métabolisme afin de gérer au mieux ces changements. Ces perturbations, en provoquant une situation de stress abiotique, peuvent entrainer des modifications du métabolisme primaire. Plusieurs études ont notamment montré que, en condition de stress, la concentration en saccharose de la plante est modifiée (Rosa et al., 2009). Ainsi, le stress salin provoque chez le riz une accumulation des sucres solubles, ainsi que d'autres métabolites, afin de rétablir la balance osmotique (Dubey and Singh, 1999). De plus, dans ces conditions, l'activité de la Sucrose Phosphate Synthase (SPS) est augmentée, conduisant à une accumulation de saccharose suite à la dégradation de l'amidon.

Un déficit en eau induit, lui-aussi, une accumulation des sucres solubles chez les plantes. Cette accumulation peut être liée à la diminution de la teneur en eau des cellules végétales (Hsiao, 1973).

Cette accumulation des sucres a été observée chez le coton au niveau des feuilles (Timpa et al., 1986). Alors qu'en condition d'irrigation, les cultivars sensibles et résistants ne présentent pas de différence dans leur teneur en saccharose, la comparant des cultivars sensibles et des cultivars résistants à un déficit en eau, a permi à ces auteurs de montrer que, chez les cotons résistants, la teneur en saccharose est la même en condition de stress ou d'irrigation normale alors que ce n'est pas le cas pour les plantes sensibles. Cette étude a donc montré que le transport du saccharose n'a pu se dérouler normalement chez les cultivars sensibles.

D'autre part, chez des plantes fourragères de zone tropicale, le saccharose peut aussi jouer un rôle dans l'ajustement osmotique en condition de stress hydrique mais cet effet est moindre comparé à d'autres osmolytes (Ford and Wilson, 1981).

Un stress lié à une inondation crée également des modifications dans la teneur en sucre : les sucres s'accumulent dans les parties aériennes alors que les racines présentent un déficit chez l'épicéa et le mélèze (Islam and Macdonald, 2004). Ce résultat montre qu'il y a une interruption du transport des sucres des organes sources (les feuilles) aux organes puits (les racines) probablement due aux conditions d'hypoxie liées à l'inondation.

La présence de métaux lourds (nickel et cadmium) a induit, chez le riz, une accumulation des sucres, notamment du saccharose, au niveau des parties aériennes (Moya et al., 1993). Cette augmentation de la teneur en sucres n'est pas liée à une augmentation de l'activité photosynthétique puisque cette dernière est inhibée par les métaux lourds. Etant donné que la croissance racinaire du riz en présence de cadmium et de nickel est inhibée, il est possible que la répartition entre source et puits soit modifiée avec une accumulation des sucres dans les organes sources, ce qui pourrait souligner une absence de transport ou une inhibition du transport des sucres.

Chez l'épinard, Guy et al. (1992) ont montré qu'une période de froid (3°C) induit l'accumulation de saccharose. Le premier intérêt peut être purement métabolique : le stock de saccharose sert de réserve énergétique facilement utilisable et transportable vers les organes qui en ont besoin. L'accumulation du saccharose est souvent corrélée avec la tolérance au froid car il peut aussi servir de cryoprotecteur, empêchant la formation de glace au sein des cellules. D'autre part, un stress dû à de basses températures induit aussi un stress hydrique impliquant donc l'accumulation d'osmolytes tels que le sucre.

De manière générale, quel que soit le stress, on observe une accumulation de sucres dans les plantes qui peut être due à deux facteurs, pas forcément indépendants : (i) un changement osmotique ou (ii) une rupture du transport des sucres entre les organes puits et les organes sources.

3. Sucres et signalisation

La perception des sucres (« sugar sensing ») résulte de l'interaction entre une molécule de sucre et une protéine-perceptrice couramment appellée « sensor » ce qui permet l'induction de voie de signalisation. En effet, les sucres solubles agiraient comme des phytohormones afin de contrôler l'expression de gènes impliqués dans diverses voies biologiques (Gupta and Kaur, 2005; Gonzali et al., 2006; Rosa et al., 2009). Price et al. (2004) et Thum et al. (2004) ont montré que les sucres modulent une grande variété de gènes impliqués dans les principaux processus cellulaires: le métabolisme des sucres et de l'azote, le métabolisme secondaire, la transduction de signal, le transport des métabolites et la réponse aux stress.

Pour les hexoses, plus particulièrement le glucose, deux systèmes de perception des sucres, coexistant chez les plantes, ont été proposés. Le premier système dit « hexokinase (HXK) dépendant » nécessite la phosphorylation des sucres par l'hexokinase qui joue le rôle de percepteur du signal. Le second système dit « hexokinase indépendant » ne nécessite pas cette étape de phosphorylation. Un récepteur spécifique du glucose, l'hexokinase 1 (HXK 1) a été identifié permettant une meilleure caractérisation du système HXK-dépendant (Ramon et al., 2008).

D'autre part, plusieurs voies de régulation spécifiques au saccharose ont été identifiées.

Le saccharose régule le développement des plantes, notamment au niveau du système racinaire. MacGregor et al. (2008) ont montré que le saccharose modifie l'architecture racinaire en induisant le développement de racines secondaires. La mise en évidence de l'effet signalétique du saccharose sur le développement racinaire a été réalisée grâce à l'application de saccharose sur les parties aériennes. Cette étude a permis de montrer le rôle important des échanges d'informations entre les parties aériennes et les parties racinaires.

Le saccharose réprime la traduction du facteur de transcription bZIP11 entrainant des modifications dans le métabolisme des acides aminés. Le peptide de contrôle du saccharose (SC-peptide), en présence de fortes teneurs en saccharose, inhibe la traduction du facteur de transcription bZIP11 en bloquant le ribosome sur l'ARN messager (ARNm) (Rahmani et al., 2009).

La nitrate reductase 1 (NR1) est connue comme étant activée par la lumière. Cheng et al. (1992) ont montré que le saccharose provoquait une accumulation des ARNm de la NR1, de la même manière que la lumière. Cette action régulatrice du saccharose sur la NR1 permet à la plante de gérer ses réserves en limitant l'action de l'enzyme quand la teneur en sucres est faible. De plus, les auteurs signalent qu'ils ont obtenu le même résultat en substituant le saccharose par le glucose, soulevant l'hypothèse selon laquelle le saccharose n'agirait pas directement mais par l'intermédiaire d'autres métabolites tels que les sucres phosphorylés. D'autre part, ce travail permet de mettre en évidence le lien entre la régulation du métabolisme carboné et celle du métabolisme azoté chez les plantes qui sont, tous deux, dépendant du stade de développement de la plante, du type de cellule et des conditions environnementales (Coruzzi and Zhou, 2001). En condition de stress azoté, on observe, comme dans de nombreux autres stress, une accumulation des sucres (saccharose, glucose et fructose) aussi bien dans les parties aériennes que dans les parties racinaires (Krapp et al., 2011), ce qui met bien en évidence un lien étroit entre carbone et azone chez les plantes.

Karthiketan et al. (2007) ont mis en relation la réponse à un déficit en phosphate et la réponse aux sucres. La présence de saccharose, même à très faible concentration, dans le milieu de culture permet d'augmenter le niveau des transcrits des gènes induits par une privation de phosphate. Par contre, en l'absence de saccharose dans le milieu, ces gènes ne sont pas exprimés. Ces gènes peuvent être aussi régulés par d'autres sucres solubles (glucose, fructose) mais à un niveau réduit.

L'accumulation des anthocyanes a souvent été observée pour des plantes qui ont poussé sur des milieux contenant du saccharose. Solfanelli et al. (2006) ont montré que le saccharose agit comme une molécule-signal sur la voie des anthocyanes : le saccharose induit le facteur de transcription PAP1 qui stimule les gènes de biosynthèse des flavonoïdes. De plus, cette voie de régulation semble être spécifique du saccharose car ni le fructose, ni le glucose n'ont permis d'augmenter le niveau d'ARNm de PAP1.

Plusieurs transporteurs ont été identifiés comme étant spécifiquement régulés par le saccharose. Le saccharose a un effet sur ses propres transporteurs : il régule le niveau d'expression des gènes codant pour SUT2 (Barker et al., 2000) et inhibe l'activité de SUT1 en faisant cesser le transport du saccharose (Wind et al., 2010).

L'action signalétique directe ou indirecte du saccharose se retrouve donc à plusieurs niveaux du fonctionnement de la plante : au niveau du développement de par son influence sur l'architecture racinaire et de la physiologie de par son action sur le métabolisme primaire, sur le métabolisme secondaire et sur les transporteurs.

L'étude des mécanismes moléculaires spécifiques de la signalisation pour une molécule telle que le saccharose est très difficile car ce dernier peut être rapidement hydrolisé en glucose et fructose. A ce stade des connaissances, peu de choses sont connues quant aux mécanismes de perception et de transduction du signal. Chiou et Bush (1998), Barker et al. (2000) et Sivitz (2008) ont suggéré que la fonction « sensor » du saccharose serait assurée par un transporteur de ce dernier. Cependant, aucune donnée expérimentale n'a jusqu'à présent confirmé cette hypothèse.

4. Rôle des sucres dans la phytoremédiation

4.1. Conjugaison avec des sucres solubles pour la modification de la toxicité et l'élimination des polluants organiques

Les polluants organiques sont des molécules chimiques toxiques pour les organismes vivants. Au cours de l'évolution des systèmes de détoxification ont été mis en place selon différentes stratégies adaptatives. En effet, un modèle de détoxification des xénobiotiques chez les plantes a été proposé en s'inspirant du système de détoxification du foie des mammifères (cf. partie 2, Figure 4). Ce modèle, appelé « green-liver », se décompose en 3 étapes : (i) une étape de transformation, (ii) une étape de conjugaison et (iii) une étape de compartimentalisation (Sandermann Jr., 1992; Edwards et al., 2011b).

Dans ce modèle, le glucose sous forme d'UDP-glucose peut servir comme conjugué dans la deuxième étape de détoxification grâce à l'action des glycosyltransferases (UGT) qui conjuguent le groupement glucosyl au xénobiotique organique. Cette étape de glycosylation permet de rendre le xénobiotique moins toxique et plus hydrosoluble ainsi que de le stabiliser (Jones and

Vogt, 2001). Chez *Arabidopsis thaliana*, 107 UGT ont été identifiées (Edwards et al., 2011b). Cette famille multigénique est impliquée dans le métabolisme secondaire mais aussi dans la tolérance aux polluants organiques (Jones and Vogt, 2001).

Après une présélection basée sur des considérations chimiques et structurales, (Meßner et al., 2003) ont identifié la capacité de plusieurs UGT d'Arabidopsis, appartenant aux sous-familles E et L, de conjuguer le 2,4,5-trichlorophénol (TCP) avec de l'UDP-glucose. UGT84B1, UGT72E2 et UGT75D1 ont montré la plus forte affinité vis-à-vis de ce polluant. D'autre part, ces enzymes semblent aussi intervenir dans la voie de synthèse des lignines, ce qui montre un chevauchement entre le métabolisme des plantes et les voies de détoxification (Meßner et al., 2003). Par contre, toutes les UGT des plantes ne présentent pas d'activité face au TCP. En effet, aucune activité de conjugaison n'a pu être détectée pour l'UGT80A2 par exemple.

L'aniline chlorée 3,4-dichloroalanine (DCA) est un xénobiotique issu de la synthèse des pesticides. La conjugaison de ce xénobiotique avec un UDP-glucose a été observée chez *Arabidopsis* (Lao et al., 2003). Une fois conjugué, le xénobiotique est rapidement exporté des racines vers le milieu environnant (Lao et al., 2003). Des études supplémentaires ont permis de caractériser quelle enzyme catalysait cette réaction. Loutre et al. (2003) ont montré que l'UGT72B1 était l'enzyme qui conjugue le DCA et qu'elle présente aussi une activité pour d'autres anilines chlorées et même pour des phénols comme le TCP, ce qui met en évidence le large spectre d'action de cette enzyme. L'UGT72B1 est à la fois une *O*-glucosyltransferase (OGT) et une *N*-glucosyltransferase (NGT), ce qui la rend unique au sein des UGT. Afin de comprendre le fonctionnement de ces deux types d'activité, la structure et la fonction de cette enzyme a été caractérisée et cette UGT présente une activité OGT et NGT vis-à-vis du DCA (Brazier-Hicks et al., 2007).

Les UGT permettent grâce à la conjugaison de limiter les effets toxiques des xénobiotiques. Leur activité est caractérisée pour de nombreux polluants organiques. De plus, leur large spectre de substrat permet de penser que ces enzymes peuvent conjuguer de nombreux autres xénobiotiques organiques tels que les hydrocarbures, par exemple. Selon le modèle du « green-liver » (Sandermann Jr., 1992), le xénobiotique glycosylé est transporté dans la vacuole par les transporteurs à ATP Binding Cassette. Les travaux de Taguchi et al. (2010) sur les composés

phénoliques glycosilés ont permis de mettre en évidence une étape de malonylation du composé phénolique glycosilé précédant l'étape de compartimentalisation du modèle du « green-liver ».

4.2. Les sucres jouent un rôle prédominant dans la tolérance au stress oxydant

Les ROS sont des molécules fortement réactives qui peuvent provoquer la destruction complète des cellules (Mittler et al., 2004). Les organismes ont donc dû mettre en place des systèmes permettant de moduler l'action des ROS. Ces systèmes antioxydants prennent naturellement en charge les ROS produites par la photosynthèse et la respiration. Cependant, en condition de stress abiotique (xénobiotiques, ozone, métaux, salinité), on assiste à une accumulation des ROS car le système antioxydant n'arrive plus à prendre en charge les ROS produites (Keunen et al., 2013).

Les sucres solubles, notamment le fructose, le glucose et le saccharose, ont un double rôle vis-à-vis des ROS : ils entrent dans les voies métaboliques produisant des ROS mais ils ont aussi un effet protecteur face à ces molécules.

Des études ont montré que le saccharose et le glucose (à un niveau moindre) confèrent une meilleure tolérance à l'atrazine, un herbicide qui cause la production d'oxygène triplet (Sulmon et al., 2004; Sulmon et al., 2006). Les études réalisées sur l'effet du saccharose en présence d'atrazine ont permis de montrer que le saccharose semble avoir un effet signalétique sur le système antioxydant. L'apport de saccharose permet d'inhiber la voie métabolique des pentoses phosphates, ce qui limite l'effet des ROS (Couée et al., 2006).

D'autre part, de nombreuses études semblent mettre en évidence l'action des sucres en tant que molécules antioxydantes (Ende and Valluru, 2009; Bolouri-Moghaddam et al., 2010; Ende and Peshev, 2013; Keunen et al., 2013). Des essais biochimiques *in-vitro* ont permis de montrer que le saccharose a un pouvoir antioxydant mais cela n'a pas encore pu être vérifié *in-planta.*

Les sucres jouent un rôle primordial dans la gestion du stress oxydant et des ROS par les plantes, soit directement en tant que molécules antioxydantes ou indirectement en tant que molécule signal. Même si de nombreuses études montrent le rôle protecteur des sucres en conditions de stress oxydant, peu de choses sont actuellement connues sur les mécanismes précis d'action du sucre.

5. Conclusion

Les sucres sont des molécules-clés dans le fonctionnement général des plantes. Ils interviennent à différents niveaux et ne sont pas seulement des métabolites. Leur action en condition de stress abiotique est très large. Ils peuvent agir en tant qu'osmo-protecteur (Ende and Peshev, 2013), protecteurs contre les ROS, dans les voies de signalisation ce qui montre que les sucres ont un rôle clé dans le fonctionnement des plantes.

Les études portant sur l'effet du sucre en conditions de stress ont été réalisées notamment sur des effets climatiques mais peu de choses sont connues quant à l'effet des sucres sur un stress causé par un xénobiotique et rien n'est connu sur les effets du stress liés à des polluants industriels tels que les HAPs. Il paraît intéressant donc de s'intéresser à l'effet des sucres solubles sur les stress causés par les polluants organiques notamment les HAPs qui sont connus comme étant générateur de stress oxydant (Liu et al., 2009). D'autre part, Sulmon et al. (2006) ont montré lors d'un essai en pots que la phytoaccumulation de l'atrazine est améliorée par un apport de saccharose, montrant le potentiel d'un amendement en saccharose pour favoriser la phytoremédiation des polluants organiques d'un sol pollué.

Partie 4 : **Travail de thèse**

Une collaboration a été mise en place entre l'Université de Rennes 1 et l'entreprise Axson-Coatings afin d'évaluer la faisabilité et l'efficacité d'un système de dépollution des HAPs par les plantes d'un site industriel contaminé par les HAPs. C'est dans le cadre d'une convention industrielle de formation par la recherche (CIFRE) que mon projet de thèse a été mis en place.

Le projet porte sur la compréhension des mécanismes de phytoremédiation aussi bien à l'échelle moléculaire qu'*in-situ,* avec une partie réalisée au laboratoire au sein de l'Unité Mixte de Recherche Ecobio (Rennes) et une partie réalisée sur un site pilote qui se situe à Aubevoye (Eure, France).

Des études réalisées au sein de l'UMR Ecobio ont permis de mettre en évidence le rôle protecteur du saccharose dans le processus de tolérance à un herbicide, l'atrazine (Sulmon et al., 2004; Sulmon et al., 2006; Ramel et al., 2007; Ramel et al., 2009). Ces études ont montré le rôle du saccharose dans la réponse à un stress oxydant. D'autre part, le saccharose stimule aussi l'accumulation de l'atrazine dans les plantes (Sulmon et al., 2007a). Ces travaux suggèrent fortement qu'un amendement en saccharose peut améliorer la tolérance des plantes à des polluants organiques, et favoriser sa phytoaccumulation.

L'apport de saccharose apparait donc comme un moyen facile et non dangereux pour l'environnement de stimuler la phytoremédiation d'un polluant organique. A ce stade des recherches, il apparaissait intéressant de voir si le saccharose permet de stimuler la phytoremédiation et de protéger les plantes face à d'autres composés organiques néfastes tels que les HAPs.

Mon travail de thèse s'est articulé autour de trois grandes questions :

(i) La première partie de mon travail a porté sur l'étude des effets des HAPs sur les plantes. Plus particulièrement, ce travail a eu pour objectif d'étudier les mécanismes impliqués dans la réponse des plantes aux HAPs, de déterminer si ces dernières mettent en œuvre des processus de détoxification et d'identifier des acteurs et voies cruciales impliquées dans ce processus pouvant, à moyen terme, faire l'objet de caractérisation fonctionnelle. Cette étude a été réalisée en conditions contrôlées avec la plante modèle *Arabidopsis thaliana* et le phénanthrène, en tant que HAP modèle. L'ensemble des expérimentations a été effectué dans un milieu de culture sans apport de saccharose, contrairement à ce qui est fait précédemment dans d'autres travaux, puisque les résultats obtenus dans notre équipe montrent qu'il a un effet protecteur contre l'atrazine. Les effets du phénanthrène ont été évalués à plusieurs niveaux : d'abord au niveau du développement de la plante sur les parties aériennes et racinaires, ensuite au niveau cellulaire, de son transcriptome, et de son métabolome. Pour les analyses transcriptomiques et métabolomiques, j'ai analysé les effets à court terme (après quelques heures d'incubation) afin d'étudier les premiers évenemments qui sont mis en place et qui sont succeptibles d'apporter des informations précieuses pour comprendre l'induction des différents mécanismes de tolérance. De plus, Zhan et al. (2010) ont montré que le phénanthrène est rapidement absorbé par les plantes. D'autre part les seules données de transcriptome disponibles pour la réponse des plantes au phénanthrène correspondent à des incubations longues, ce qui pourrrait interférer avec des processus de mise en place de senéscence.

(ii) La deuxième partie de mon travail porte sur l'effet protecteur du saccharose en condition de stress induit par le phénanthrène. En effet, les résultats préliminaires obtenus dans le cadre d'un stage de master ont montré que le saccharose permet aux plantes d'*Arabidopsis* de supporter des concentrations de phénanthrène supérieures aux plantes contrôles. Le travail réalisé dans cette partie est parallèle à celui réalisé lors de l'étude des effets du phénanthrène sur les plantes. Dans cette

partie, je me suis intéressée aux effets du saccharose en présence de phénanthrène sur le développement de la plante. Ensuite, une analyse du transcriptome m'a permis de comprendre les effets du sucre en condition de stress et en conditions de culture « standards » mais aussi de voir comment la présence de saccharose modifie l'activité transcriptionnelle de différents groupes de gènes impliqués dans les stresses ou codant pour les gènes impliqués dans le xénome. Mais aussi du métabolome de la plante en présence de phénanthrène. Enfin, j'ai cherché à savoir si un apport de saccharose modifiait l'absorption et la répartition du phénanthrène dans les plantes.

(iii) La dernière partie de mon travail concerne l'utilisation des connaissances obtenues au laboratoire sur un système simple et contrôlé, pour l'amélioration de la phytoremédiation sur un site expérimental. En effet, cette étude *in-situ* porte sur deux grands axes : la comparaison de divers couverts végétaux (arbres, herbacées et aucune végétation plantée) qui permet de chercher quel est l'espèce végétale la plus efficace pour la dépollution des sols et l'étude des effets du saccharose sur la tolérance des plantes aux HAPs dans un écosystème complexe, où coexistent plusieurs communautés microbiennes.

Le manuscrit est organisé de la façon suivante :

- Le chapitre 2 est une présentation de l'ensemble de mes résultats sur l'effet du phénanthrène à court terme sur la plante modèle *Arabidopsis thaliana*.
- Le chapitre 3 décrit l'effet du saccharose en condition de stress lié au phénanthrène.
- Dans le quatrième chapitre, les résultats d'un essai de phytoremédiation sur un site industriel sont présentés.
- Le dernier chapitre est une conclusion générale sur l'ensemble de mon travail.

La partie 2 du chapitre d'introduction a été rédigée en anglais sous forme d'un article de synthèse qui vient d'être soumise au journal Plant Science. Les chapitres 2 et 3 sont rédigés en anglais sous forme d'articles scientifiques dans le but d'une soumission future

Chapitre 2 : **Etude des modifications développementales, transcriptomiques et métabolomiques induites par le stress provoqué par le phénanthrène**

Préambule

Au cours de leur évolution, les organismes sessiles tels que les végétaux supérieurs ont développé des mécanismes moléculaires et physiologiques qui leur permettent de s'adapter aux modifications de leur environnement. En effet, en condition de stress abiotique, les mécanismes de signalisation et le contrôle de l'expression des gènes jouent un rôle majeur pour le maintien du fonctionnement cellulaire.

Les sucres solubles, en particulier le saccharose, ont un impact considérable en condition de stress abiotique et, de par leur action signalétique, modulent fortement la réponse de la plante au stress oxydant (Bolouri-Moghaddam et al., 2010; Keunen et al., 2013). Or, la majorité des études *in-vitro* portant sur les effets d'un stress abiotique, notamment celles sur les effets du phénanthrène (un HAP), sont réalisées sur des milieux supplémentés en saccharose, modifiant ainsi la réponse réelle de la plante au stress. Nous avons donc décidé de travailler en condition d'absence de source carbonée dans le milieu de culture.

D'autre part, Zhan et al. (2010) ont montré que les plantes sont capables d'absorber très rapidement le phénanthrène grâce à un transporteur actif. Ces résultats montrent l'importance des premières heures de contact entre le xénobiotique et les plantes dans la réponse de la plante au xénobiotique.

Dans cet article, nous avons utilisé des approches de transcriptomique et de métabolomique afin de déterminer les premières modifications au niveau du métabolisme et de l'expression des gènes impliquées dans la réponse à un stress induit par le phénanthrène, un produit dangereux issu des activités humaines. Ce travail avait également pour objectif d'identifier des acteurs impliqués dans les étapes précoces de perception et de gestion de ce polluant par la plante. En effet, leur caractérisation fonctionnelle de ces acteurs permettra d'évaluer s'ils pourrontt être utilisés dans des approches biotechnologiques destinées à améliorer le processus de phytorémédiation. Lors de cette étude, les résultats obtenus, nouveaux, montrent que les plantes détectent rapidement la présence du phénanthrène puisque, dés 30 minutes d'incubation, des modifications apparaissent au niveau de la transcription de gènes impliqués principalement dans les voies de signalisation. Les gènes de détoxification et de gestion du stress oxydant, très probalement induits par le phénanthrène, sont régulés plus tardivement jusqu'à 8 heures de

traitement. Enfin, après 8h d'exposition, de très nombreux genes impliqués dans les métabolismes primaires et secondaires sont réprimés alors que ceux intervenant dans les processus de glycolyse, de fermetation et de réponse aux stress sont induits. L'intégration des données de dosage de metabolites montre une forte accumulation d'acides aminés et de sucres solubles, qui sont des indicateurs d'un fonctionnement de la plante en déclin. Le statut énergétique semble être un facteur limitant qui conduit à l'épuisement, lors de la troisième phase de notre modèle.

Running title: Deciphering the early plant response to phenanthrene

Title: New insights into the early *Arabidopsis thaliana* response to phenanthrene exposure

Authors:

Anne-Sophie Dumas[2,*] (anne-sophie.dumas@univ-rennes1.fr)

Evangelos Barbas[1,a,*] (vbarbas@for.auth.gr)

Guillem Rigaill[1] (rigaill@evry.inra.fr)

Delphine Bernard[2,b] (Delphine.Bernard@univ-brest.fr)

Ludivine Taconnat[1] (taconnat@evry.inra.fr)

Abdelhak El Amrani[2,] † (abdelhak.el-amrani@univ-rennes1.fr)

Richard Berthomé[1,c,] †(rberthome@toulouse.inra.fr)

[1]INRA, UMR 1165, Unité de Recherche en Génomique Végétale (URGV), CNRS, ERL 8196, UEVE, 91057, Evry cedex, France.

[2]CNRS, Université de Rennes 1, UMR 6553, Ecosystèmes-Biodiversité-Evolution, 35042 Rennes cedex, France.

Current addresses

a: Laboratory of Forest Genetics and Tree Breeding, AUTH, University Campus, 54124 Thessaloniki, Greece

b : Laboratoire de Génétique Moléculaire et de Génétique Epidémiologique, INSERM U1078, 46, rue Felix Le Dantec, CS 51819, 29218 Brest Cedex 2, France

c : Laboratoire des Interactions Plantes Micro-organismes (LIPM), UMR INRA 441/CNRS 2594, CS 52627, 31326 CASTANET TOLOSAN CEDEX, France

† Corresponding autors:

Richard Berthomé (rberthome@toulouse.inra.fr), tel (33) 5.61.28.55.09

Abstract

Along their evolution, sessile organisms such as higher plants developed molecular and physiological plasticity to cope with environmental cues. Under abiotic stress, signaling mechanisms and control of gene expression play a major role to maintain cellular homeostasis and plant development. In this paper, we used transcriptomic and metabolomic analysis to decipher the early events involved in phenanthrene induced stress, a hazardous polycyclic aromatic hydrocarbon of natural and anthropogenic origins. Our results, are consistent with the earlier studies performed on phenanthrene or others xenobiotics and add a new resolution level by dissecting early plant response during a kinetic ranging from 30m minutes to 24h of treatment. Plant response can be divided in three phases: i) plant sense phenanthrene rapidly, as genes mainly involved in perception and signalization, were differentially expressed within the first 30 minutes, ii) a reaction phase after 2h to 8h of incubation, characterized by regulation of genes involved in detoxification, iii) and a third exhausting phase from 8h where many differentially expressed genes are involved in repression of the secondary metabolism. This study also allowed the identification of new early regulated phenanthrene dependent genes that could be good candidates for further functional characterizations and development of strategies of molecular avoidance for phenanthrene.

Key words: PAH, Arabidopsis, transcriptome, metabolome, xenome, natural xenobiotic

1. Introduction

Polycyclic aromatic hydrocarbons (PAHs) constitute a large class of organic pollutants (POPs) present in the atmosphere in either a gaseous or a particulate form. These chemicals are ultimately deposited within the soil, silt and sediments. The common sources of PAHs in the environment are from both natural (volcanoes eruptions, forest and rangeplant fires) and anthropogenic sources (Haritash and Kaushik, 2009)(1). Human activities generate PAHs through the incomplete combustion processes of organic material such as biomass or of carbon-based fuels as well as from the release of petroleum into the environment (Ravindra et al., 2008; Katsoyiannis et al., 2011; Callén et al., 2012)(2-4). They are highly resistant to biological degradation as their structure contains two or more benzenes rings. There is a concern with these compounds as they are present throughout the environment, and have been shown to have adverse effects on human health since some of them have been described to be carcinogenic, mutagenic or endocrine disrupting compounds (Luch, 2005; Gammon and Santella, 2008; Balabanič et al., 2011)(5-7).

Risks associated to PAHs pollution can be partially overcome by their removal from soil using chemical, physical or thermal treatments. These techniques are efficient but expensive. In addition, they impact the environment and often transfer the pollutant from one compartment to another (Gan et al., 2009)(8). Alternatives emerged with “green technologies” which use of the environment ability to transform the pollutant in a less hazardous compound by the natural action of living organisms (Mitsch, 2012)(9). The development of these green approaches, including bioremediation and phytoremediation tools, brought focus on factors affecting PAHs remediation efficiency. Environmental conditions, plant species used, nature of microbes and plants interactions in the soil, and nature of the pollutant to be degraded have been demonstrated to modulate PAHs remediation (Cheema et al., 2010; Furuno et al., 2010; Furuno et al., 2012; Schamfuß et al., 2013b)(10-13). As for heavy metals or explosives detoxification approaches already in use, improvements in the PAHs bioremediation systems might come from the studies of plant-microbes interactions in the soil and genetic engineering of plants able to stimulate these interactions and/or degrade PAHs (Rylott et al., 2011; Bhargava et al., 2012; Panz and Miksch, 2012; Shim et al., 2013)(14-17). Promising results have been obtained with the engineering a naphthalene-degrading endophytic strain *Pseudomonas putida*

VM1441(pNAH7) that efficiently colonized plants (pea, annual ryegrass) and enhanced plant tolerance to naphthalene (Germaine et al., 2009). Tobacco plants expressing a fungal gluthatione-S-transferase also showed an increased tolerance, higher uptake and transformation of naphthalene (Dixit et al., 2011).

Development of such innovative tools for PAHs phytoremediation remains rare, mainly because cellular and molecular mechanisms involved in plant response to PAHs and their putative uptake and metabolization by the plants are still largely unknown; contrasting with numerous studies performed to elucidate mechanisms involved in PAHs degradation by bacteria, fungus and algae (Cerniglia, 1992; Warshawsky, Cody et al. 1995; Bezalel, Hadar et al. 1997; Kotterman, Vis et al. 1998; Mrozik *et al.*, 2003; Johnsen *et al.*, 2005; Kim *et al.*, 2007; Syed, Doddapaneni et al. 2010). General models for plant xenobiotics detoxification have been based on an analogy of the xenobiotic detoxification system described in the mammalian liver (Sandermann Jr., 1992; Edwards et al., 2005)(18, 19). Edwards et al. (2005) also proposed that "the whole expressed genome responsible for the detection, signalization, transformation, conjugation, compartmentalization and transport of xenobiotics or derivatives in the cell" constitute the xenome.

The phenanthrene, used as PAH model, has been shown to be taken up by both *Arabidopsis* (Alkio et al., 2005)(20) and wheat roots (Zhan et al., 2010)(21) then gone on to be internalized, implying this pollutant or its derivatives being transported in the plants. Moreover, some PAHs were metabolized in cell cultures of different plant species and proposed to be conjugated to soluble sugar or link to glutathione (Sandermann Jr. et al., 1984; Kolb and Harms, 2000)(22, 23). Interestingly, Zhan et al (2010) have shown that the uptake of phenanthrene by roots occurs in a fast passive diffusion just after the transfer of wheat in the phenanthrene supplemented medium and in a slow active absorption probably mediated by a transporter, after 2 hours of incubation. Hence, these observations suggested that the phenanthrene absorption, and its putative transformation, might be quickly regulated by the plant. Physiological, cellular and molecular investigations of plant response to PAHs have been carried out, mostly on long-term expositions to phenanthrene (14-30 days) (Alkio et al., 2005; Liu et al., 2009; Weisman et al., 2010a)(20, 24, 25). After phenanthrene treatments, a concentration dependent reduction of plants size, roots length, chlorophyll content and a delay to set seeds are observed. Phenanthrene induces organelle

structure alteration, up-regulation of antioxidant activities and morphological deformations that could be linked to tissue necrosis (Alkio et al., 2005; Liu et al., 2009)(20, 25). This data sheds light on some features shared between plant responses to phenanthrene, other abiotic stress and pathogen hypersensitive response (HR). More particularly, the production of reactive oxygenes species (ROS) appear to play an important role in stress related phenotypes observed following phenanthrene treatment (Liu et al., 2009)(25). Transcriptional analyses of the plant response to long exposure to phenanthrene support this hypothesis. Weisman et al (2010) proposed that through its putative oxidation by mono- or di-oxygenases, that have to be identified the phenanthrene might trigger an increase in the reactive oxygen species (ROS) level and induce expression of genes encoding proteins mostly involved in oxidative stress regulation or production. However, for phenanthrene it remains unclear if oxidative stress and cell death result from detoxification activities or if it is an indirect consequence of phenanthrene or derivatives phytotoxicity since cell death only appears in location where it accumulates.

ROS are natural byproducts of various metabolic pathways generated in many compartments including organelles, peroxisomes, the endoplasmic reticulum and the plasma membrane. Plant use low levels of ROS as early signaling molecule to restrict pathogen invasion, induce program cell death or regulate stomata closure (Wang and Song, 2008; Zurbriggen et al., 2010)(26, 27). However, the balance between production and scavenging of ROS is disturbed, under various abiotic stress conditions such as UV-radiation, ozone, intense light, drought, decrease or increase in temperature, mechanical stress and xenobiotics stress, leading to irreversible damages that could result in tissue or organ necrosis. To fight against increased levels of ROS, plants use a battery of enzymatic activities and buffering processes (Choudhury et al., 2013)(28). Among them, soluble-sugars originate as true ROS scavengers in plant (Keunen et al., 2013)(29) and also as a tool to improve phytoremediation efficiency through the limitation of ROS production in xenobiotic stress conditions. Exogenous soluble sugars supply, particularly sucrose, has been shown to confer a high level of tolerance to atrazine in *Arabidopsis* (Sulmon et al., 2004; Sulmon et al., 2007a; Sulmon et al., 2007b)(30-32). Interestingly, transcriptome analysis revealed that sensitivity and sucrose-induced tolerance to atrazine were also associated to important modifications of gene expression related to ROS defence mechanisms as for results obtained by Weisman

et al. (2010) in case of long term exposure to phenanthrene (Ramel et al., 2007; Ramel et al., 2009)(33, 34). However, all published data on the plant response to phenanthrene were carried out in medium containing sucrose. As a result the use of these mediums do not allow to discriminate if differential gene expression and process associated to ROS production and scavenging were the result of phenanthrene treatment alone or the consequence of sucrose-induced protection.

In order to characterize mechanisms involved in the phytoremediation process and to decipher molecular determinant of phenanthrene induced injury, a time course genome wide analysis and metabolome profiling were carried out. As sucrose may deeply change genes expression and plant responses, this whole study was performed using sucrose free medium. Results obtained in this study begin to unfold the early events involved in phenanthrene responses. Our results showed that plant response can be divided in three phases: i) Phenanthrene is detected rapidly by plants as genes mainly involved in perception and signalization, were differentially expressed within the first 30 minutes, ii) a reaction phase is observed 2h to 8h after incubation and is characterized by the regulation of genes involved in detoxification, iii) After 8h of exposure to phenanthrene, numerous genes involved photosynthesis, primary and secondary metabolism are repressed, whereas genes mainly involved in glycolysis, fermentation, redox and stress metabolisms are up-regulated. Integration of metabolites titration data indicates a strong accumulation of amino acids and soluble sugars, indicators of functional declines that might lead the exhaustion of the plant. Energy status appears to be the crucial limiting factor that leads the plant to the third phase of our model.

2. Material and methods

2.1. Plant material and growth conditions

Seeds of *Arabidopsis thaliana* ecotype Columbia-0 (Col-0) were used in all the experiments. Seeds were surface sterilized for 10 min with a solution containing 10% (v/v) commercial bleach (BAYROL France SAS, Dardilly, France)) diluted in 95° ethyl alcohol and 0.05% (v/v) Teepol 610 (SERVA Electrophoresis GmbH, Heidelberg, Germany). Seeds were rinsed thoroughly with 95° ethyl alcohol and dried overnight in a sterile hood Seeds were sown on half-strength Murashige and Skoog solid medium (MS/2) containing 0.8% (W/V) agar-agar type E (SIGMA ALDRICH) supplemented with phenanthrene solved in dimethylsulfoxide (DMSO) or DMSO alone used as control. Seeds were germinated in a growth chamber (16-h light/8-h dark cycle 4000 lux, 22°C, 70% hygrometry) after cold treatment for 48 h at 4°C. Phenanthrene stock solution was at 700mM and in each experiment, controls were prepare adding identical volume of DMSO.

2.2. Measurement of seedling growth and development

For root measurement and fresh weight determination, seeds were sown on MS/2 solid medium supplemented with 0, 50, 100, 200 and 400µM of phenanthrene or with DMSO alone as control. Plants were cultivated vertically on square Petri dishes (15x15cm). Primary roots were measured after 10 days of growth using digital photographs acquisitions and Image J v 1.45s software (Abramoff et al., 2004)(73). For each condition, primary root length was measured for 30 independents plants. For rosette fresh weight measurements, plantlets were grown horizontally on circle Petri dishes. Shoots were separated from the roots and weighted after 30 days of growth. Shoots from three plants for two distinct replicates were harvested. Results represent the mean with the standard error (SE). Statistical analyses were carried on using the t-Test in the R software (team RDC, 2013)(74). Levels of chlorophyll were determined using the equations given by Lichtenthaler and Wellburn (1983)(75). Shoots samples previously weighted were ground and incubated for 10 minutes in 80% acetone at room temperature under stirring. Absorbance of these extracts

was measured at three wavelengths (663 nm, 646 nm and 470 nm). Results were given as the mean of the 6 measurements with the standard error (SE). Data were analyzed using the t.Test in the R software (team RDC, 2013)(74).

2.3. Fluorescence microscopy

Analysis were performed at the Imagif plateform, in the Cellular Biology Pole, (CNRS,Gif sur Yvette, France). *Arabidopsis* plantlets used were grown on MS/2 medium for 15 days and then transferred at stage 1.04 (Boyes et al., 2001)(76) on MS/2 medium containing 200µM of phenanthrene or the same volume of DMSO. In order to facilitate the transfer, plants were grown vertically. A sterile and transparent plastic film was applied to the contaminated medium in order to avoid any contact of the vegetative parts of the plantlets with the medium. After 5 days of phenanthrene treatment, leaves and roots from 5 independent plantlets harvested on 3 different petri dishes were observed with a Zeiss LSM510 META microscope under UV-light (excitation 364nm and acquisition with 32 channels between 362nm and 704nm). Data were acquired using Zen2008 software developed by Zeiss (Germany).

2.4. Transcriptome studies

Microarray analysis was carried out at the Research Unit in Plant Genomics in Evry, France, using the CATMA version 5 array containing 31776 gene-specific tags corresponding to 22,089 genes from *Arabidopsis* (Crowe et al., 2003; Hilson et al., 2004)(50, 51). Total RNA extractions from two independent biological replicates were performed using the QIAGEN RNAeasy plant minikit according to the manufacturer's instructions. Each biological replicate was composed of *Arabidopsis* plantlets grown *in-vitro* for 15 days on solid MS/2 medium and transferred at stage 1.04 (Boyes et al., 2001)(76) on liquid MS/2 medium containing 200µM of phenanthrene or the same volume of DMSO. Each biological replicates includes phenanthrene-treated and control plants. Each sample corresponding to 30 plants pooled were harvested after 30 min, 2-, 4-, 8- and 24h of incubation. For all comparisons performed

(Supplemental Figure 1 A), the experiment was done using the dye-switch technique. The labeling of antisense amplified RNA with Cy3-dUTP or Cy5-dUTP (Perkin-Elmer-NEN Life Science Products), the hybridization to the slides, and the scanning were performed as described by Lurin et al. (2004)(77).

2.5. Statistical Analysis of Microarray Data

Experiments were designed in collaboration with the Bioinformatic and Predictive Genomics group at the Research Unit in Plant Genomics in Evry, France. Specific statistics were developed to analyze CATMA hybridizations. For each array, the raw data include the logarithm of median feature pixel intensity (in log base 2) at wavelengths of 635 nm (red) and 532 nm (green). No background was subtracted. The normalization method used was described by Lurin (2004)(77). Differentially expressed genes were determined by performing a paired t-test on the log ratios averaged on the dye switch. A trimmed variance was calculated from spots that did not display extreme variance. The raw P values were adjusted by the Bonferroni method, which controls the family-wise error rate (with a type I error equal to 5%). We also adjusted the raw P values to control a false discovery rate using Benjamini-Yetkutieli at a level of 1%. Nonetheless, in the CATMA analysis pipeline, family-wise error rate proved to be the best solution to balance the estimated number of false positives and false negatives (Ge et al., 2003)(78). As described by Gagnot et al. (2008), when the Bonferroni P value was lower than 0.05, the gene was declared differentially expressed (Gagnot et al., 2008)(79). The complete data set is given as Supplemental Tables 1.

2.6. ANOVA analysis

Normalized intensities for each dye-switch experiment were recovered. A sample is characterized by the time-point of the experiment (0h, 2h, 4h, 8h or 24h), the treatment (none or phenanthrene), the dye used for the experiment (red or green) and the array on which the sample was hybridized (numbered from 1 to 28). For a given gene, we denote Y_{tpda} the expression level of the gene at time-point *t*, with the treatment *p*, using the dye *d* and on

the array *a*. We studied two linear models. The first (see model 1) considers an additive effect of time (α_t) and the treatment (β_p) without interaction. The second model (see model 2) considers an additive effect of time (α_t) and the treatment (β_p) and an interaction between the two (γ_{tp}). In both model we take into account a potential array effect (δ_a). We only analyzed genes for which all 56 data-points were available, in other words genes without missing values.

$Y_{tpda} = \mu + \alpha_t + \beta_p + \delta_a + \varepsilon_{tpda}$ (model 1)

$Y_{tpda} = \mu + \alpha_t + \beta_p + \gamma_{tp} + \delta_a + \varepsilon_{tpda}$ (model 2)

For each gene the parameters of model 1 and 2 were fitted using ordinary least squares. Model 1 has 22 residual degrees of liberty and model 2 only 18. For each gene we used a Fisher test to test the hypothesis H0 that model 1 is true, against the alternative H1 that model 2 is true. We accounted for multiple testing issues using the Benjamini-Hochberg procedure. We considered that genes with an adjusted p-value of less than 5% have an interaction between time and treatment. All these analysis were performed with the R software (team RDC, 2013)(74). Data corresponding to selected genes are presented in Supplemental Table III.

2.7. Biological pathways enrichiment

Lists of genes, with an adjusted p-value of less than 5% have an interaction between time and treatment, were recovered for 30 min, 2-, 4-, 8-, and 24h comparisons. Biological pathways significantly over-represented in lists of differentially expressed genes were identified with the classification superviewer tool of the university of Toronto website (http://bar.utoronto.ca/ntools/cgi-bin/ntools_classification_superviewer.cgi) using MAPMAN classification as a source (Provart T., 2003)(80).

2.8. Clustering

Hierarchical clustering using Pearson correlation as distance calculation were performed. on the Genevestigator Web site (https://www.genevestigator.com/gv/) using

our top list (Table II) and selections of data corresponding to stress, biotic and chemical perturbation.

2.9. cDNA Synthesis and Quantitative Real-Time PCR (qRT-PCR)

The qRT-PCR validation was carried on 11 genes being found to be differentially regulated in phenanthrene treated and control samples described in the microarray section.. Primers were designed using the online software Primers3 (Rozen and Skaletsky, 2000)(81) (http://frodo.wi.mit.edu/, optimal temperature of 60°C, Supplemental Table VI). The primer pairs were first tested on a dilution series of genomic DNA (5, 0.5, 0.05, and 0.005ng) to generate a standard curve and assess their PCR efficiency, which ranged between 90% and 110%. RT was performed on 1µg of total RNA with oligo(dT) primer (18-mer) and the SuperScript II RNase H^- reverse transcriptase according to the manufacturer's instructions (Invitrogen). In every run, at least three replicates PCRs were done for each cDNAs. For each gene investigated using qPCR, a dilution series covering 3 orders of magnitude (1, 1/10 and 1/100) of the cDNA stock solution was prepared. Three replicates of each of the three standards were used in qPCR experiment together with three no-template controls. qPCR was performed in 5 µL, with 0.5 µL of RT reaction (1/100 dilution), 900 nM final concentration of each primer pair, and 2,5µL of MESA GREEN qPCR MasterMix Plus for SYBR® Assay (Eurogentec). Corresponding minus-RT controls were performed with each primer pair. All reactions were performed with the CFX384 Touch™ Real-Time PCR Detection System (Bio-Rad) as follows: 95°C for 5 min; 40x95°C for 10 s and 60°C for 30 s ; and a dissociation step to discriminate primer dimers from the PCR product. Using CFX Manager™ Software version 3.0 provided by the manufacturer, the optimal cycle threshold (Ct) was determined from the dilution series, with the raw expression data derived. Six housekeeping genes were assessed in this experiment, and the two best control genes, consistently expressed, were selected to calculate the average normalization factor: *AT4G13615* and *AT5G21090* for each sample pair. Normalized (Norm) ΔCt for each differentially expressed gene was calculated as following: Norm ΔCt = - (rawΔCt - Norm factor). Microarray data from this article were deposited at Gene Expression Omnibus (http://www.ncbi.nlm.nih.gov/geo/), accession no. GSE48181) and at CATdb

(http://urgv.evry.inra.fr/CATdb/; Project: AU10-04_phytoremediation) according to the "Minimum Information About a Microarray Experiment" standards.

2.10. Targeted analysis of metabolites

Analysis were realized at the CORSAIRE platform (Biogenouest, INRA UMR 1349 IGEPP, Le Rheu, France). *Arabidopsis* plants used for this analysis were grown on MS/2 medium for 15 days and then transferred at stage 1.04 (Boyes et al., 2001)(76) on liquid MS/2 medium containing 200µM of phenanthrene or the same volume of DMSO. After 24 hours of incubation, plants were harvested, frost in liquid nitrogen, lyophilized and ground. A total of 10mg of dry plant material was extracted in 500µL of extraction solvent and 250µL of chloroform. The extraction solvent is composed of 5% of methanol and 95% of beta amino benzoic acid (10mM) – adonitol (20mM) concentrated solution. Samples were shaken 10 min at room temperature then 500µL of ultra pure water were added. All samples were vortexed for 30s and then centrifugated for 5 min at 12000g and 15°C. The entire liquid phase was transferred to a new tube. For amino acids analysis, 50µL of the extract was dried under vacuum and 50µL of water were added. Samples were derivated using the AccQTag method (Waters) and analyzed by Ultra Performance Liquid Chromatography (UPLC, Waters). For the sugars, organic acids, alcohol and ammonium quantification, 50µL of the extract supplemented with 50µL of internal standard were dried under vacuum. 50µL of methoxamine in pyridine (concentration 20mg/mL) were added to the dried samples which were incubated 90min at 30°C. 50µL of MSTFA (N-Methyl-N-(trimethylsilyl)trifluoroacetamide) were added to each sample which are incubated for 30min at 37°C and than analyzed by GC-MS.

3. Results-discussion

3.1. Phenanthrene altered plant development in a dose dependant manner

In order to estimate the phenanthrene concentration to be used in our time course analysis and to evaluate its effect on plant development, we investigate the toxicity level of phenanthrene on Arabidopsis. As sucrose has been described as a true ROS scavenger which might act as a signaling molecule modifying plant responses to abiotic responses, these tests were performed on a sucrose free medium. For this purpose, plants were germinated on MS/2 medium, supplemented with 0-, 50-, 100-, 200- and 400µM of phenanthrene. When phenanthrene treatment does not exceed 24h, no macroscopic alterations were induced. However, compared to the control, plants grown for 10 to 30 days on phenanthrene supplemented medium showed altered phenotypes and differences in shoots fresh weight, primary roots length and leaf chlorophyll content, the later well known to be a good indicator of photosynthetic activity, stress and nutrient state (Alena Torres Netto, 2005)(35) (Figure 1).

Thirty days of phenanthrene exposure clearly inhibits the development of plant shoots even at the lower phenanthrene concentration. Plant development was reduced in a dose-dependent manner. The strongest effect was observed at 200µM and 400µM. Plant growth variation was observed with some plants unable to grow. This variation was ever higher at 400µM. Moreover, whereas small plants remained green at 200µM, all of them were chlorotic at 400µM (Figure 1A). In parallel, the mean shoot fresh weight of all treatments were significantly different from the control and decreased by 31%, 57%, 58% and 83% at 50µM, 100µM, 200µM and 400µM of phenanthrene, respectively (Figure 1B). Chlorophyll content, of 30-day-old plants confirmed the chlorotic macroscopic phenotypes observed as it only significantly decrease at 400µM of phenanthrene when compared to the control (Figure 1C). A significant decrease in primary root length was also observed between the untreated plants and those grown on phenanthrene supplemented medium, excepted at 50µM of phenanthrene. At 100µM, 200µM and 400µM of phenanthrene, the primary roots length was reduced about 13%, 55% and 48% in comparison to the control, respectively (Figure 1D). In high salinity stress conditions, toxic effects of salts within the plant lead to inhibition of many biochemical and physiological processes such as nutrient uptake and

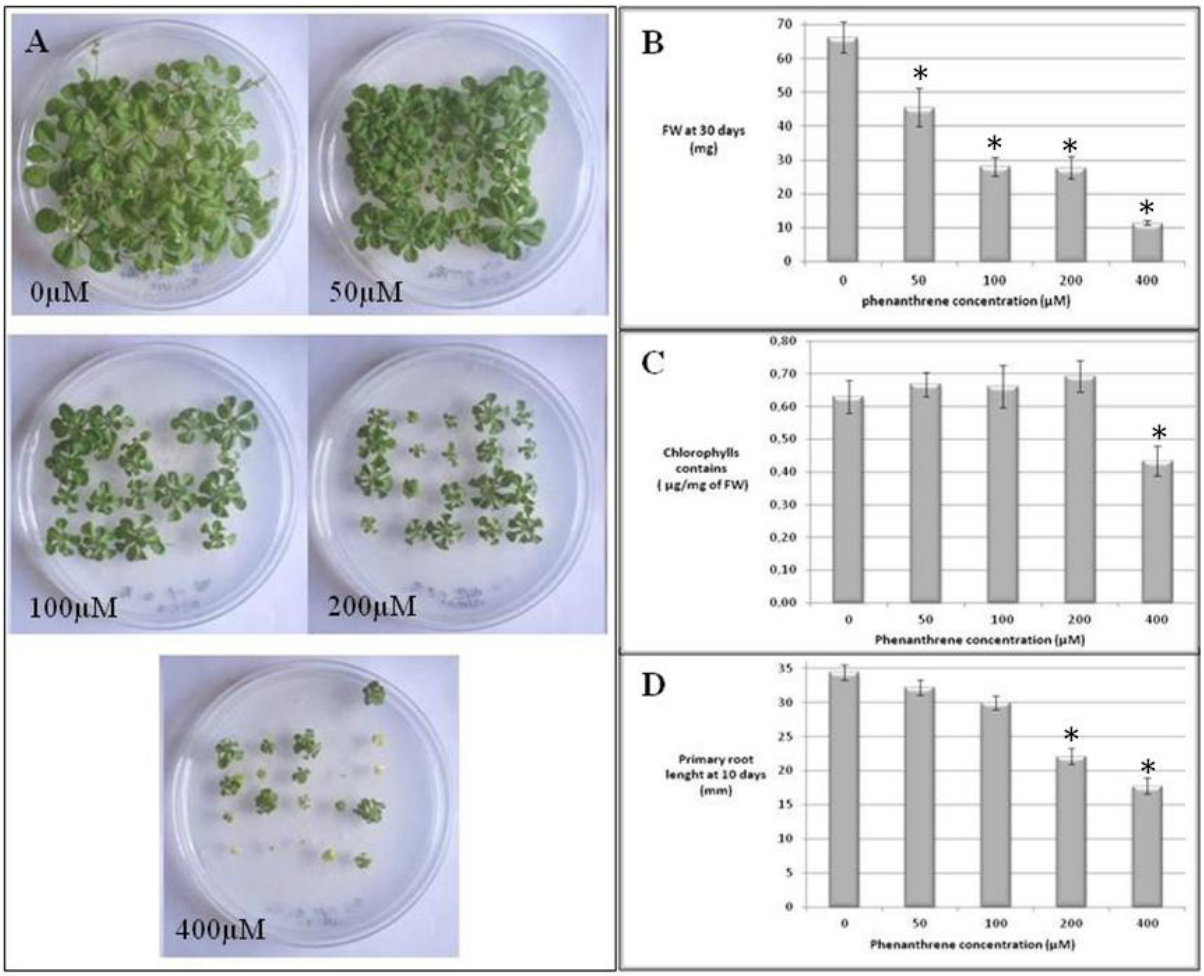

<u>Figure 1</u>: Impact of increasing concentrations of phenanthrene on plant development.

Arabidopsis thaliana plantlets were grown on MS/2 sucrose free medium supplied with 0- (DMSO), 50-, 100-, 200- or 400µM of phenanthrene. 30-days old plantlets were phenotyped (**A**) and harvested to measure their fresh weight (**B**) and chlorophyll contents (**C**). Plantlets were also grown vertically and primary root length measured after 10 days of growth (**D**). The values presents are the means of 30 independents measurements and error bars represent SE. *indicates significant difference between treated and control plants (p-value≤0,05).

assimilation. As a consequence, plant development is altered; shoot growth being more affected as it is more sensitive to salt toxicity than roots growth (Carillo et al., 2011)(36). Phenanthrene uptake and toxicity might induce similar phenomena. Hence, our data showed that shoot growth is more affected than root growth at 50µM. Moreover, the strongest decrease of shoot growth observed at 400µM could be due to the concomitant effects of phenanthrene toxicity and the limited nutrient availability linked to the root growth reduction.

Our results showing a phenanthrene concentration dependent inhibition of roots and shoots development are in accordance with data previously described by Alkio et al. (2005) and Liu et al. (2009) (20, 25). However, several differences were observed in our conditions such as chlorotic phenotypes at 400µM, absence of HR like necrosis on leaves, phenotypic plasticity in the progeny within the same treatment and an absence of saturation of the response between 200- and 400µM of phenanthrene. Rather than differences due to the experimental conditions, we propose that these discrepancies could be linked to the effect of exogenous sucrose supply, with soluble-sugar emerging as true ROS scavengers in plant and limit ROS production in atrazine stress conditions (Sulmon et al., 2006; Sulmon et al., 2007a; Sulmon et al., 2007b)(30-32). A common point with many biotic and abiotic stresses in plant is also the change of bioenergetic status for which plants are mainly dependent on photosynthesis. Abiotic stress such as drought and high salinity toxicity lead to the inhibition of photosynthetic activities. Down regulation of genes involved in photosynthesis also appear to be a common feature of plant response to numerous biotic stresses (Bilgin et al., 2010; Ana Sofia Duque, 2013)(37, 38). In our conditions, at phenanthrene concentrations over 200µM, the lack of sucrose would not enable 30 days old plants to face ROS overproduction associated to phenanthrene metabolism, leading to alteration of photosynthetic activity and ultimately to a decrease of chlorophyll content and the appearance of chlorotic phenotypes. Considering these observations, early incidence of phenanthrene on plant was studied using 200µM phenanthrene concentration.

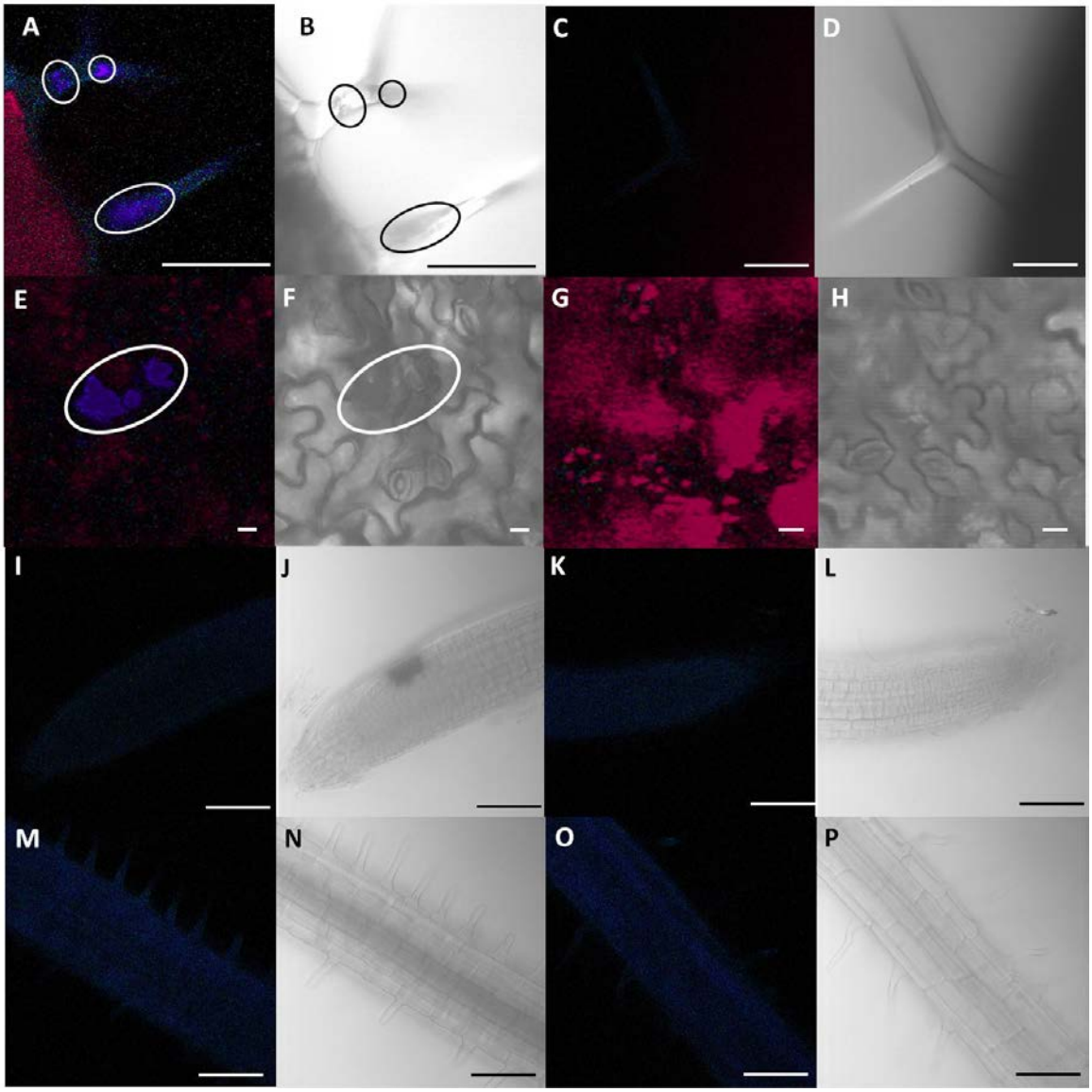

<u>Figure 2</u>: Observations of phenanthrene fluorescence in 20-days-old plantlets.

Plants were grown 15 days on MS/2 sucrose free medium and then transferred for 5 days on a identical medium supplemented with 0.2mM of phenanthrene (A, B, E, F, I, J, M and N) or DMSO as control (C, D, G, H, K, L, O and P). Pictures A to D are an observation of the trichomes, E to H of the underside of the leaves, I to L of the apex of the primary root and M to P of the root hairs of the primary root. 2 consecutives photos (A-B, C-D …) represent the same area. A, C, E, G, I, K, M and O are observations made under UV light and B, D, F, H, J, L, N and P with transmission. Circles show the localization of phenanthrene. All bar scales represent 100µm except for pictures E to H where it represents 10µm.

3.2. Phenanthrene uptake and localization in Arabidopsis

To validate phenanthrene uptake from solid medium in our experimental conditions, gas chromatography and mass spectrometry analysis were performed and confirmed that phenanthrene accumulates only in plants grown on 200µM phenanthrene compared to the control (data not shown).

Using its specific fluorescence spectra under UV light, phenanthrene was also detected *in vivo* in plants tissues. The third leaf and primary root of 15 days old plantlets transferred five days before on solid medium supplemented with 200µM phenanthrene or DMSO were observed (Figure 2).

In control plants, fluorescence was neither detected in leaves nor in roots (Figure 2 C, D, G, H, K, L, O, P). For phenanthrene treated plants, specific fluorescence was only detected in leaves (Figure 2A, B, E, F), not in roots (Figure 2 I, J, M, N). At the adaxial side of leaves, trichomes were the only fluorescent cells detected, signal appearing to be concentrated as bright spots in specific parts of the trichomes (Figure 2 A, B). At the abaxial side of leaves, these spots harbor different shape and seem to be stuck on the epidermis surface (Figure 2 E, F). Our results are consistent with those previously described by Alkio et al. (2005) even if they do not detect the fluorescent signal at the abaxial side of leaves.

In our experiment, we used a transparent sterile plastic film applied to the contaminated medium in order to avoid any contact of the aerial parts of the plants transferred to the medium. This specific device and fluorescent microscopy data strongly suggest that phenanthrene could be absorbed, at least partially from roots, transported and accumulated in specialized cells in leaves. Indeed, Zhan et al (2010) showed, using hydroponic experiments, that the phenanthrene uptake by wheat roots is not only due to a passive diffusion as suggested by Alkio et al. (2005) but also to an active phenanthrene specific symport system. Surprisingly, specific phenanthrene fluorescence was not observed in roots (Figure 2 I, M). An explanation could be that a portion of phenanthrene rapidly moves up to the upper part of the plant. This is in accordance with the adaxial xyleme and the trichome rich adaxial side of *Arabidopsis* leaves (Chitwood et al., 2007). As the majority of organic contaminants absorbed by plants undergoes enzymatic transformation such as reduction, oxidation or hydrolysis that reduce their toxicity and allow their conjugation (Kvesitadze et al., 2009), these processes might also modify their UV absorbance spectra,

making them much more difficult to detect, except in specific locations where they are compartmentalized.

Moreover, even if most of the PAHs are characterized by their low volatility, some studies indicate that phenanthrene is relatively volatile (Sitaras et al., 2004; Schreiber et al., 2008). Thus, in airless conditions such as Petri dishes, we could not exclude that a portion of phenanthrene is volatilized and absorbed by leaves through stomata. Interestingly, in Arabidopsis, most of the stomata are localized at the abaxial side of leaves where bright fluorescent spots were observed (Figure 2 E). In this case, absorption of volatile phenanthrene would also enable its localization in trichome. Obviously, its localization would be expected in most of the stomata, and it is clearly not the case. Alternatively, these fluorescent spot could also correspond to excretion of non-transformed phenanthrene; rather rare process of organic contaminants elimination happening at high concentration of xenobiotic (Kvesitadze et al., 2009). In Arabidopsis, the function of trichome, unicellular and non-glandular, is poorly understood. They are believed to be part of physical defenses but several line of evidence suggests there are involved in detoxification process of heavy metals. In the Zinc hyperaccumulator accession *Arabidopsis hallieri*, trichomes contains by far the largest concentration of Zinc and Cadmiun, metals being localized in specific subcellular compartment at the base of the trichome, as it seems to be the case for phenanthrene or derivatives in our observations (Figure 2 A) (Küpper et al., 2000). In addition, total glutathione content of trichome have been shown to be more than 300-fold higher than in other epidermal cells. Overexpression of metallothioneins in *Arabidopsis* transgenics demonstrates that glutathione are expressed in trichomes, suggesting that trichome functions as a compartment enabeling conjugation and sequestration of heavy metals (Gutiérrez-Alcalá et al., 2000; Guo et al., 2003). Moreover, overexpression of a cystein in Arabidopsis, Atcys-3A, increased level of GSH in leaves in the presence of cadmium and improved its accumulation in trichomes (Domínguez-Solís et al., 2004). In others species such *Nicotiana tabaccum,* trichomes can function as glandular organs and have been demonstrate to participate to heavy metals detoxification through the formation of metal/calcium crystals actively excreted (Choi et al., 2001; Sarret et al., 2006).

The present observations and previous data obtained by Alkio et al (2005) also support that phenanthrene is absorbed and highlighted the role of trichomes in the compartmentalization of native or phenanthrene derivatives and their putative excretion.

3.3. Transcriptome analysis of early plant response to phenanthrene exposure

3.3.1. *Global gene expression studies*

In their natural environment, plants are often subject to external factors, biotic and/or abiotic, causing stress that could strongly affect their development. Additionally plants have also to cope with increasing concentrations of pollutants of both natural and anthropogenic origins, define as natural xenobiotics, among which polycyclic aromatic hydrocarbons constitute a large family. Plants have been shown to be an essential component in the ecological process of phytoremediation leading to the accumulation, the partial or complete degradation and decomposition of pollutants. Hence, the study of plant response to xenobiotics offers the opportunity to engineer efficient ecological detoxification tools. This has been done for phenanthrene at the physiological level as well as, through transcriptome analysis, for only long term treatments (Alkio et al., 2005; Liu et al., 2009; Weisman et al., 2010). Plant response to long term exposure involves metabolic pathways that regulate ROS but also processes linked to plant response to pathogens.

Based on the Sandermann's green liver concept, Edwards et al. (2011) defined the plant xenome as "the biosystem responsible for the detection, transport and detoxification of xenobiotics in the plant cell" (Sandermann Jr., 1992; Skipsey et al., 2011). Analogies with xenobiotics detoxification in mammalian liver suggest that molecular mechanisms in the plant xenome would be involved in two phases: i) early perception and the signaling and ii) the transport and the biotransformation of the xenobiotic. However, even if the model of detoxification of xenobiotic by plants have been proposed, data demonstrating that these processes play a role in PAHs detoxification are still missing.

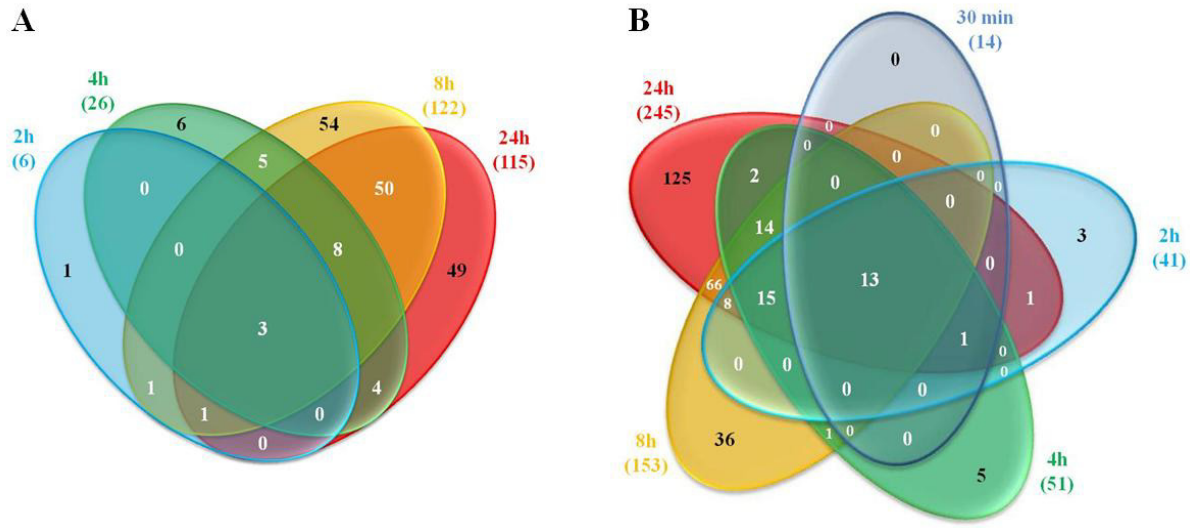

Figure 3: Venn diagram of the total number of differentially expressed genes, selected by ANOVA analysis (p-value < 0.05), showing an interaction between time and treatment.

Lists of compared genes correspond to down-regulated (**A**) and up-regulated genes (**B**) obtained in comparisons between phenanthrene treated samples and control samples at 30 minutes, 2h, 4h, 8h and 24h. Differentially expressed genes used are listed in Supplemental Table III were selected by statistical analysis based on the Bonferroni method using a p-value cut-off of 0.05. Transcriptome data corresponding to hybridizations performed are available in Supplemental Table I.

In order to identify the early molecular events of the plant response to phenanthrene, 15-day-old plantlets grown on solid medium were transferred in liquid media containing either 200µM of phenanthrene or DMSO as control. The transcriptome analysis was performed using CATMA version 5 array containing 31776 gene-specific tags corresponding to 22,089 genes from *Arabidopsis* (Crowe et al., 2003; Hilson et al., 2004). The experimental design was set up to compare 0 minutes to 30 minutes, 30 minutes to 2h, 2h to 4h, 4h to 8h and 8h to 24h of incubation in phenanthrene and DMSO (8h-24h comparison is missing) and to compare phenanthrene treatment to control at each kinetic point (Supplemental Figure 1 A). Two independent biological replicates were performed. Overall, within the comparisons between phenanthrene treated to control samples, 1262 genes were differentially expressed, 58, 130, 174, 650 and 897 genes being differentially expressed at 30 min, 2 h, 4 h, 8 h and 24 h, respectively. Using real time RT-PCR, we confirmed expression changes for 11 genes analysed (Supplemental Figure. 2).

3.3.2. *Plant response to phenanthrene is fast and can be separated in two phases*

An ANOVA analysis was performed on selected differentially expressed genes showing an interaction between time and treatment. Lists of genes corresponding to comparisons between phenanthrene-treated and control samples at 30 minutes, 2h, 4h, 8h and 24h are shown in supplemental Table III and were used for further analysis.

A total of 467 genes were recovered, with 14, 47, 77, 275 and 360 genes differentially expressed after 30 minutes, 2h, 4h, 8h and 24h of phenanthrene treatment, respectively. All the 14 differentially expressed genes at 30 minutes were up-regulated. In general for the other comparisons, up-regulated genes represent the majority of the gene whose expression is modified, (41/47, 51/77, 153/275, 245/360 for 2h, 4h, 8h, 24h comparisons, respectively). If we look at each point of the time course, we can observe an increase in the number of genes differentially expressed between 30 minutes-4h and 8-24h, even stronger trend if we consider the entire gene regulated without ANOVA selection (58, 130, 174, 650 and 897). This result might reflect a sequential response of the plant to phenanthrene. This response

seems to be composed of an early and short phase from 30 minutes to 4h and second phase from 8h to 24h.

Lists of genes whose expression was modified at each time point of the kinetic were compared using Venn diagrams to identify the genes which were specifically induced or repressed after phenanthrene treatment (Figure 3, A-B). Among differentially expressed genes, only five genes encoding a plant thionin, a putative aspartyl protease, the cytochrome P450 protein CYP704B1, the glycosyl hydrolase ATXYN1 and the senescence protein ATWI-12 (*AT1G58370, AT1G66100*, *AT1G69500, AT3G10985, AT5G48430,*) displayed opposing regulation. Strikingly, this regulation occurs between 4h and 24h of treatments for three of them. Few genes are specifically differentially up or down-regulated for 30 minutes, 2h and 4h comparisons (0/3/5 and 0/1/6), contrasting with 8h and 24h comparisons (36/125 and 44/59). Interestingly, 13 out of the 14 genes early up-regulated after 30 minutes are found in common to all comparisons, amount of the corresponding transcript increasing in time. The high number of common gene, differentially up- or down- regulated, between 8h and 24h (66 and 50 respectively) confirm that same pathways are regulated by the plant in response to phenanthrene after 8h and 24h.

Venn diagram analysis performed on differentially expressed genes without ANOVA selection confirms these results (supplementary Figure 1 B, C). Table I shows the 20 mostly differentially expressed genes, when available, for the kinetically different regulated genes.

3.3.3. *Biological processes regulated in response to phenanthrene treatment*

Larcher proposed that physiological response to stress may involved three phases: i) the alarm phase corresponding to early events enabling the perception and the signaling of the stress by the plants; ii) the resistance phase where functional alterations are observed and have to be counteracted to avoid iii) the exhaustion phase (Larcher, 2003).

Even if early events of perception and signaling of xenobiotic are poorly understood, the molecular processes and metabolic pathways involved in their detoxification, which can be assimilated to the resistance phase, have been well described in animal and extrapolated to plants based on the Sandermann's the green liver concept (Sandermann Jr., 1992;

Kvesitadze et al., 2009; Skipsey et al., 2011). The detoxification involves the transformation of the xenobiotics, perfomed by cytochrome P450 (CYP450), peroxidases, phenoloxidases, ascorbatoxidase and catalase. These pollutants undergo oxidation, reduction or hydroxylation to make them more water soluble. Then the conjugation of the xenobiotics to endogenous molecules is realized by transferases such as Glutathione S-transferase (GST), glucuronozyl-O-transferase, malonyl-O-transferase, or glucosyl-O-transferase Glycosyltransferases (UGT). Finally, during the compartmentalization, the conjugated xenobiotic is transferred to the vacuole or the cell wall by ABC transporters.

If we only consider the differentially expressed gene selected using ANOVA analysis and the functional classes in which they are involved in, primary and secondary metabolisms are over-represented. Despite this result, 54 regulatory genes such as transcription factors, receptor kinase and protein phosphatase also showed modified expression during the kinetic in response to phenanthrene treatment. However, in our top lists (Table I), only 11 regulatory genes are listed, 9 up-related and 2 down-regulated. Interestingly, 5 of the most differentially expressed genes are regulated after 30 minutes of treatment whereas all the others, including down-regulated genes, have their expression modified after 8h or 24h. These 5 genes code for three transcriptions factors whose differential expression gradually increase in time, except for *ATMYB4* (*AT4G38620*) showing its highest differential expression at 30 minutes. The two others genes code for a receptor-like kinase protein (RLK) (*AT5G48540*) and the phosphofructokinase 7 (PFK7) (*AT5G56630*) suggesting a fast induction of the glycolysis metabolism after 30 minutes. Such peculiar differential expression pattern for these 5 genes suggests they could be involved in the early phase of sensing and signalization of the phenanthrene by the plant. The RLK would constitute a good candidate of receptor putatively able to bind phenanthrene. This action fits well the model of chemical ligand binding to receptor, described in the case of ABA sensing and suitable for chemical stress such as heavy metal or nutritent depletion stress (Verslues and Zhu, 2005).

Table I: The most differentially expressed genes during the time course in phenantrene treated plants. Of all the differentially expressed genes, a maximum of 20 genes for each different response pattern are listed. AGI identifiers and gene annotation in bold face correspond to genes involved in the "xenome". Expression changes are given as log2. Expression changes in bolt correspond to genes differentially expressed at the significant threshold of Bonferroni p-value<0.05.

AGI ID	Gene annotation	30 min	2h	4h	8h	24h
Rapid up-regulation after 30min of treatment and stay up-regulated throughout the kinetic						
AT1G70800	EHB1__Calcium-dependent lipid-binding (CaLB domain) family protein	**0.64**	**1.23**	**1.91**	**1.97**	**1.19**
AT4G38620	ATMYB4_MYB4__myb domain protein 4	**3.51**	**2.19**	**2.30**	**2.18**	**1.94**
AT2G47950	unknown protein	**1.49**	**2.27**	**2.27**	**2.65**	**1.91**
AT5G48540	receptor-like protein kinase-related family protein	**1.42**	**2.44**	**3.27**	**3.48**	**3.51**
AT5G59820	RHL41_ZAT12__C2H2-type zinc finger family protein	**1.19**	**1.63**	**2.14**	**2.70**	**2.50**
AT2G16900	*Arabidopsis* phospholipase-like protein (PEARLI 4) family	**0.98**	**1.68**	**1.67**	**1.61**	**2.16**
AT1G68620	alpha/beta-Hydrolases superfamily protein	**0.93**	**2.18**	**1.68**	**2.77**	**2.70**
AT5G56630	PFK7__phosphofructokinase 7	**0.91**	**1.59**	**2.41**	**1.54**	**2.53**
AT3G22840	ELIP_ELIP1__Chlorophyll A-B binding family protein	**0.89**	**1.40**	**2.19**	**1.70**	**2.38**
AT1G63840	RING/U-box superfamily protein	**0.83**	**1.80**	**1.64**	**2.10**	**2.16**
AT2G36590	ATPROT3_ProT3__proline transporter 3	**0.79**	**1.42**	**1.93**	**1.80**	**2.24**
AT4G39670	Glycolipid transfer protein (GLTP) family protein	**0.73**	**1.26**	**1.01**	**1.42**	**2.13**
AT4G27657	unknown protein	**0.70**	**1.26**	**1.10**	**1.75**	**0.74**
AT4G15248	B-box type zinc finger family protein	**1.39**	**1.75**	**1.04**	0.35	**1.63**
Genes differentially up-regulated after 2h and stayed high						
AT2G35980	ATNHL10_NHL10_YLS9__Late embryogenesis abundant (LEA) hydroxyproline-rich glycoprotein family	0.56	**1.72**	**1.96**	**1.81**	**2.34**
AT3G22600	Bifunctional inhibitor/lipid-transfer protein/seed storage 2S albumin superfamily protein	0.16	**1.68**	**1.96**	**1.36**	**1.96**
AT4G25640	ATDTX35_DTX35_FFT__detoxifying efflux carrier 35	0.27	**1.66**	**1.40**	**1.98**	**2.11**
AT3G21560	**UGT84A2__UDP-Glycosyltransferase superfamily protein**	0.52	**1.48**	**2.21**	**1.60**	**1.93**
AT1G74010	Calcium-dependent phosphotriesterase superfamily protein	0.46	**1.39**	**1.68**	**1.32**	**2.50**
AT1G75040	PR-5_PR5__pathogenesis-related gene 5	0.21	**1.32**	**1.50**	**1.71**	**1.75**
AT1G30700	FAD-binding Berberine family protein	0.48	**1.26**	**1.06**	**1.56**	**2.28**
AT3G04300	RmlC-like cupins superfamily protein	0.37	**1.25**	**1.73**	**2.08**	**2.25**

AGI ID	Gene annotation	30 min	2h	4h	8h	24h
AT1G18980	RmlC-like cupins superfamily protein	0.20	**1.16**	**1.55**	**1.57**	**1.59**
AT1G76980	unknown protein	0.51	**1.15**	**1.67**	**1.78**	**1.85**
AT5G54500	FQR1__flavodoxin-like quinone reductase 1	0.47	**1.12**	**1.14**	**1.50**	**1.79**
AT1G74450	Protein of unknown function (DUF793)	0.41	**1.09**	**1.16**	**1.06**	**1.10**
AT3G04000	NAD(P)-binding Rossmann-fold superfamily protein	0.06	**0.95**	**1.16**	**1.53**	**1.23**
AT1G27120	Galactosyltransferase family protein	0.00	**0.91**	**2.00**	**2.30**	**2.45**
AT2G17500	Auxin efflux carrier family protein	-0.20	**0.80**	**1.19**	**1.79**	**1.20**
Genes differentially up-regulated from 4 h of treatment						
AT1G78340	**ATGSTU22_GSTU22__glutathione S-transferase TAU 22**	0.04	0.56	**1.62**	**1.75**	**1.69**
AT1G17170	**ATGSTU24_GST_GSTU24__glutathione S-transferase TAU 24**	0.06	0.39	**1.57**	**2.00**	**2.05**
AT3G51660	Tautomerase/MIF superfamily protein	0.10	0.75	**1.47**	**1.80**	**2.27**
AT5G36270	**similar to DHAR2, glutathione dehydrogenase (ascorbate)**	0.00	0.55	**1.38**	**1.56**	**1.74**
AT4G15480	**UGT84A1__UDP-Glycosyltransferase superfamily protein**	0.18	0.47	**1.27**	**1.02**	**1.40**
AT1G78380	**ATGSTU19_GST8_GSTU19__glutathione S-transferase TAU 19**	0.10	0.69	**1.23**	**1.45**	**1.49**
AT2G29500	HSP20-like chaperones superfamily protein	0.16	0.29	**1.15**	**1.11**	**1.53**
AT1G75030	ATLP-3_TLP-3__thaumatin-like protein 3	0.19	0.59	**1.13**	**1.45**	**1.35**
AT1G75270	**DHAR2__dehydroascorbate reductase 2**	0.36	0.78	**1.09**	**1.60**	**1.49**
AT1G64900	**CYP89_CYP89A2__cytochrome P450, family 89, subfamily A, polypeptide 2**	-0.03	0.33	**1.08**	**1.16**	**1.19**
AT3G13520	AGP12_ATAGP12__arabinogalactan protein 12	0.17	0.57	**1.08**	**1.39**	**0.88**
AT2G12190	**Cytochrome P450 superfamily protein**	-0.04	0.43	**1.04**	**0.97**	**0.96**
AT4G13180	NAD(P)-binding Rossmann-fold superfamily protein	0.28	0.29	**1.03**	**1.07**	**1.39**
AT1G05680	**UGT74E2__Uridine diphosphate glycosyltransferase 74E2**	0.14	-0.05	**1.01**	**1.80**	**0.83**
AT2G48140	EDA4__Bifunctional inhibitor/lipid-transfer protein/seed storage 2S albumin superfamily protein	0.02	0.74	**1.20**	**0.73**	0.40
AT3G09270	**ATGSTU8_GSTU8__glutathione S-transferase TAU 8**	-0.12	0.41	**1.15**	0.26	**1.09**
AT1G23490	ARF1_ATARF_ATARF1_ATARFA1A__ADP-ribosylation factor 1	0.48	0.76	**1.04**	0.64	**1.32**
AT1G58370	**ATXYN1_RXF12__glycosyl hydrolase family 10 protein / carbohydrate-binding domain-containing protein**	0.17	0.64	**1.13**	0.08	**-0.86**

AGI ID	Gene annotation	30 min	2h	4h	8h	24h
Genes differentially up-regulated after 8h of treatment						
AT5G22140	FAD/NAD(P)-binding oxidoreductase family protein	0.30	0.02	0.76	**2.15**	**1.97**
AT3G44190	FAD/NAD(P)-binding oxidoreductase family protein	0.03	0.21	0.95	**2.05**	**2.01**
AT2G23110	Late embryogenesis abundant protein, group 6	0.45	0.78	0.51	**1.87**	**2.04**
AT5G64250	Aldolase-type TIM barrel family protein	-0.01	0.35	0.59	**1.62**	**1.55**
AT3G28210	PMZ_SAP12__zinc finger (AN1-like) family protein	0.36	0.52	0.98	**1.60**	**2.09**
AT1G75280	NmrA-like negative transcriptional regulator family protein	0.15	0.62	0.86	**1.56**	**1.37**
AT4G24160	alpha/beta-Hydrolases superfamily protein	-0.01	0.40	0.59	**1.52**	**1.25**
AT3G10500	anac053_NAC053__NAC domain containing protein 53	0.12	0.77	0.66	**1.48**	**1.16**
AT2G01180	ATLPP1_ATPAP1_LPP1_PAP1__phosphatidic acid phosphatase 1	0.20	0.33	0.95	**1.44**	**1.97**
AT5G54206	similar to 12-oxophytodienoate reductase OPR1	0.17	0.15	0.29	**1.41**	**2.04**
AT2G29460	**ATGSTU4_GST22_GSTU4__glutathione S-transferase tau 4**	0.12	0.52	1.00	**1.37**	**0.95**
AT4G34131	**UGT73B3__UDP-glucosyl transferase 73B3**	0.33	0.38	0.89	**1.31**	**1.38**
AT1G05670	Pentatricopeptide repeat (PPR-like) superfamily protein	0.20	0.02	0.71	**1.30**	**0.69**
AT1G77120	ADH_ADH1_ATADH_ATADH1__alcohol dehydrogenase 1	-0.18	0.54	0.25	**1.30**	**1.02**
AT2G21620	RD2__Adenine nucleotide alpha hydrolases-like superfamily protein	-0.01	0.75	0.94	**1.28**	**1.82**
AT1G66580	RPL10C_SAG24__senescence associated gene 24	0.32	0.45	0.63	**1.26**	**1.44**
AT2G36950	Heavy metal transport/detoxification superfamily protein	0.21	0.45	-0.10	**1.26**	**1.01**
AT1G72490	unknown protein	-0.09	0.20	0.02	**1.25**	**1.10**
AT1G67600	Acid phosphatase/vanadium-dependent haloperoxidase-related protein	0.01	0.45	0.50	**1.25**	**1.07**
AT5G27760	Hypoxia-responsive family protein	0.14	0.47	0.83	**1.19**	**1.43**
Genes differentially up-regulated after 24 h of treatment						
AT1G65290	mtACP2__mitochondrial acyl carrier protein 2	0.13	0.06	0.13	0.34	**2.63**
AT4G37990	ATCAD8_CAD-B2_ELI3_ELI3-2__elicitor-activated gene 3-2	0.07	0.30	0.34	0.00	**2.43**
AT5G25260	SPFH/Band 7/PHB domain-containing membrane-associated protein family	-0.10	-0.06	0.30	0.04	**2.07**
AT2G18690	unknown protein	0.11	0.70	0.54	0.66	**1.98**

AGI ID	Gene annotation	30 min	2h	4h	8h	24h
AT4G12490	Bifunctional inhibitor/lipid-transfer protein/seed storage 2S albumin superfamily protein	0.22	0.07	0.66	0.28	**1.90**
AT1G14870	AtPCR2_PCR2__PLANT CADMIUM RESISTANCE 2	-0.03	0.51	0.03	0.48	**1.76**
AT2G23150	ATNRAMP3_NRAMP3__natural resistance-associated macrophage protein 3	-0.17	-0.16	0.01	0.59	**1.69**
AT2G17740	Cysteine/Histidine-rich C1 domain family protein	-0.03	-0.15	0.66	0.20	**1.67**
AT1G66090	Disease resistance protein (TIR-NBS class)	0.36	0.29	0.66	0.55	**1.67**
AT5G06320	NHL3__NDR1/HIN1-like 3	-0.28	0.11	-0.08	0.31	**1.60**
AT2G29350	SAG13__senescence-associated gene 13	-0.17	0.17	0.82	0.59	**1.55**
AT1G13330	AHP2__*Arabidopsis* Hop2 homolog	0.00	-0.09	0.69	0.36	**1.55**
AT5G13320	GDG1_GH3.12_PBS3_WIN3__Auxin-responsive GH3 family protein	-0.10	-0.25	0.11	-0.07	**1.54**
AT5G17380	Thiamine pyrophosphate dependent pyruvate decarboxylase family protein	0.04	0.03	0.35	0.65	**1.48**
AT2G20142	Toll-Interleukin-Resistance (TIR) domain family protein	0.06	0.05	0.21	0.23	**1.47**
AT4G26200	ACS7_ATACS7__1-amino-cyclopropane-1-carboxylate synthase 7	0.22	-0.01	0.18	0.26	**1.44**
AT1G74710	ATICS1_EDS16_ICS1_SID2__ADC synthase superfamily protein	0.05	-0.19	0.14	-0.09	**1.41**
AT4G11890	Protein kinase superfamily protein	0.10	0.19	-0.04	0.56	**1.38**
AT5G25250	SPFH/Band 7/PHB domain-containing membrane-associated protein family	0.07	0.00	0.28	0.40	**1.38**
AT1G26380	FAD-binding Berberine family protein	0.24	0.24	0.34	0.43	**1.38**
	Genes differentially down-regulated from 2 h of treatment and stayed low					
AT1G26810	GALT1__galactosyltransferase1	-0.13	**-1.16**	**-1.71**	**-1.65**	**-1.79**
AT3G19450	ATCAD4_CAD_CAD-C_CAD4__GroES-like zinc-binding alcohol dehydrogenase family protein	0.03	**-0.82**	**-1.22**	**-1.74**	**-1.74**
AT5G48930	HCT__hydroxycinnamoyl-CoA shikimate/quinate hydroxycinnamoyl transferase	-0.20	**-1.17**	**-1.11**	**-1.50**	**-1.18**
	Genes differentially down-regulated from 4 h of treatment and stayed low					
AT1G08630	THA1__threonine aldolase 1	0.06	-0.54	**-1.81**	**-0.92**	**-1.62**
AT1G43160	RAP2.6__related to AP2 6	0.02	-0.57	**-1.57**	**-1.16**	**-0.99**
AT5G49730	ATFRO6_FRO6_FRO6__ferric reduction oxidase 6	-0.05	-0.27	**-1.35**	**-0.79**	**-1.46**
AT5G25460	Protein of unknown function, DUF642	-0.03	-0.55	**-1.30**	**-1.72**	**-1.41**

AGI ID	Gene annotation	30 min	2h	4h	8h	24h
AT4G29905	unknown protein	0.00	0.29	**-1.16**	**-0.76**	**-1.83**
AT1G05240	Peroxidase superfamily protein	0.08	0.19	**-1.07**	**-1.48**	**-0.91**
AT4G23400	PIP1;5_PIP1D__plasma membrane intrinsic protein 1;5	-0.29	-0.16	**-1.06**	**-0.99**	**-1.50**
AT1G69100	Eukaryotic aspartyl protease family protein	0.13	-0.04	**-1.06**	**-1.21**	**-1.03**
AT5G01210	HXXXD-type acyl-transferase family protein	0.05	-0.78	**-1.65**	**-1.37**	-0.38
AT2G45960	ATHH2_PIP1;2_PIP1B_TMP-A__plasma membrane intrinsic protein 1B	-0.17	-0.11	**-1.14**	**-0.77**	-0.37
AT1G65930	cICDH__cytosolic NADP+-dependent isocitrate dehydrogenase	-0.03	-0.29	**-1.13**	**-0.96**	-0.56
AT4G14040	EDA38_SBP2__selenium-binding protein 2	0.21	-0.31	**-1.01**	**-0.70**	-0.60
AT1G64370	unknown protein	-0.15	-0.22	**-1.01**	**-0.77**	-0.16
Genes differentially down-regulated from 8 h of treatment and stayed low						
AT3G03780	ATMS2_MS2__methionine synthase 2	0.15	-0.55	-0.50	**-1.66**	**-2.22**
AT4G22210	LCR85__low-molecular-weight cysteine-rich 85	-0.16	-0.27	-0.69	**-1.56**	**-1.27**
AT4G15390	HXXXD-type acyl-transferase family protein	0.08	-0.44	-0.70	**-1.39**	**-1.54**
AT3G59970	MTHFR1__methylenetetrahydrofolate reductase 1	0.02	-0.54	-0.40	**-1.30**	**-1.06**
AT2G44160	MTHFR2__methylenetetrahydrofolate reductase 2	0.20	-0.28	-0.52	**-1.28**	**-0.95**
AT5G39210	CRR7__chlororespiratory reduction 7	-0.09	0.14	-0.58	**-1.27**	**-0.89**
AT3G19820	CBB1_DIM_DIM1_DWF1_EVE1__cell elongation protein / DWARF1 / DIMINUTO (DIM)	0.07	-0.11	-0.45	**-1.27**	**-1.15**
AT1G29600	Zinc finger C-x8-C-x5-C-x3-H type family protein	-0.10	-0.15	-0.19	**-1.22**	**-1.02**
AT4G12545	Bifunctional inhibitor/lipid-transfer protein/seed storage 2S albumin superfamily protein	-0.03	0.28	-0.70	**-1.20**	**-1.66**
AT1G11860	Glycine cleavage T-protein family	0.00	-0.16	-0.32	**-1.17**	**-1.14**
AT3G60320	Protein of unknown function (DUF630 and DUF632)	0.03	-0.18	-0.72	**-1.10**	**-0.77**
AT5G24760	GroES-like zinc-binding dehydrogenase family protein	-0.04	-0.50	-0.34	**-1.08**	**-1.19**
AT5G17920	ATCIMS_ATMETS_ATMS1__Cobalamin-independent synthase family protein	0.13	-0.26	-0.41	**-1.06**	**-0.99**
AT3G06350	EMB3004_MEE32__dehydroquinate dehydratase, putative / shikimate dehydrogenase, putative	-0.11	-0.25	-0.62	**-1.03**	**-0.85**
AT3G16390	NSP3__nitrile specifier protein 3	0.06	0.20	0.30	**-1.03**	**-1.02**
AT1G29560	Zinc finger C-x8-C-x5-C-x3-H type family protein	0.15	-0.38	-0.45	**-1.00**	**-0.93**
AT5G03300	ADK2__adenosine kinase 2	0.16	-0.30	0.03	**-0.99**	**-0.94**

AGI ID	Gene annotation	30 min	2h	4h	8h	24h
AT1G80830	ATNRAMP1_NRAMP1_PMIT1__natural resistance-associated macrophage protein 1	-0.02	-0.46	-0.93	**-0.99**	**-0.75**
AT4G14890	FdC2__2Fe-2S ferredoxin-like superfamily protein	-0.10	-0.19	-0.48	**-0.97**	**-1.01**
AT5G65010	ASN2__asparagine synthetase 2	-0.03	0.07	-0.15	**-0.97**	**-0.84**
Genes only differentially down-regulated after 24 h of treatment						
AT5G36910	THI2.2__thionin 2.2	-0.16	0.04	-0.38	0.21	**-1.73**
AT2G25510	unknown protein	-0.09	0.23	0.11	-0.40	**-1.52**
AT1G17190	**ATGSTU26_GSTU26__glutathione S-transferase tau 26**	-0.01	-0.19	0.32	-0.31	**-1.41**
AT3G16450	JAL33__Mannose-binding lectin superfamily protein	0.00	0.28	-0.51	-0.67	**-1.30**
AT4G35100	PIP2;7_PIP3_PIP3A_SIMIP__plasma membrane intrinsic protein 3	0.01	0.10	-0.81	-0.67	**-1.26**
AT3G28270	Protein of unknown function (DUF677)	-0.26	0.46	0.25	-0.57	**-1.26**
AT5G51720	2 iron, 2 sulfur cluster binding	-0.06	-0.25	-0.17	-0.38	**-1.24**
AT5G24420	PGL5__6-phosphogluconolactonase 5	0.00	0.05	-0.32	-0.02	**-1.20**
AT4G13870	ATWEX_ATWRNEXO_WEX_WRNEXO__Werner syndrome-like exonuclease	-0.02	0.10	0.61	-0.34	**-1.19**
AT3G02380	ATCOL2_COL2__CONSTANS-like 2	-0.11	-0.60	-0.41	0.04	**-1.15**
AT4G16980	arabinogalactan-protein family	0.07	-0.10	-0.84	-0.54	**-1.14**
AT3G45140	ATLOX2_LOX2__lipoxygenase 2	-0.12	0.51	0.51	-0.24	**-1.11**
AT1G12090	ELP__extensin-like protein	-0.06	-0.04	-0.52	-0.33	**-1.08**
AT1G54000	GLL22__GDSL-like Lipase/Acylhydrolase superfamily protein	0.03	-0.28	-0.77	-0.55	**-1.06**
AT5G58260	NdhN__oxidoreductases, acting on NADH or NADPH, quinone or similar compound as acceptor	0.04	-0.01	-0.14	-0.58	**-1.05**
AT3G16420	JAL30_PBP1__PYK10-binding protein 1	-0.04	0.07	0.01	-0.64	**-1.02**
AT3G16440	ATMLP-300B_MEE36_MLP-300B__myrosinase-binding protein-like protein-300B	-0.24	0.21	-0.37	-0.38	**-0.91**
AT3G15850	ADS3_FAD5_FADB_JB67__fatty acid desaturase 5	-0.21	-0.01	-0.68	-0.06	**-0.91**
AT3G01480	ATCYP38_CYP38__cyclophilin 38	0.07	0.01	-0.76	-0.54	**-0.88**
AT3G11170	AtFAD7_FAD7_FADD__fatty acid desaturase 7	0.03	-0.12	-0.30	-0.63	**-0.87**

To identify differentially expresses genes involved in the xenobiotic detoxification processes, we then recovered AGI identifiers of all CYP450, GST, glycosyl transferase and ABC transporters from the TAIR website (http://www.arabidopsis.org/browse/genefamily/) to constitute a gene list of the putative plant xenome.

Comparing this list to our study reveals that 36 differentially expressed genes belongs to the xenome (Supplemental Table III). These genes have mainly their expression modified from 4h of treatment. Moreover, in our top list (Table I), 16 out 36 are among the highest differentially regulated genes, one being specifically up-regulated after 2h of treatment whereas 11 are differentially up-regulated after 4h. This result suggest that early plant response to phenanthrene follows the Larcher's model (Larcher, 2003). Indeed, after 30 minutes of treatments, the plant seems to sense phenanthrene and induce a cascade of regulation and signalization that leads, in a second phase, to the induction of detoxification processes, mainly between 2h and 4h of treatment.

To identify biological processes which are mostly and significantly regulated by the plant in response to phenanthrene at each time point of our kinetic, lists of genes corresponding to each comparison, were analysed using the classification superviewer tool from the Bio-Array Ressource for Plant Biology (http://www.bar.utoronto.ca/ntools/cgi-bin/ntools_classification_superviewer.cgi) using the MAPMAN classification as source (Figure 4). For up-regulated genes, the number of pathways in which genes are significantly over-represented gradually increase in time, pathways affected from 2h of treatment staying induced at the other kinetic points.

After only 30 minutes of treatment, glycolysis metabolism is induced. At 2h, miscellaneous pathways is induce as for 4h of treatment with the redox metabolism in more. Interestingly, genes corresponding to miscellaneous pathway whose expression is modified in our study encode proteins such as UDP-glycosyltransferase, nitrilase and cytochrome P450, proteins that might be involved in transformation and conjugation of phenanthrene. This analysis seems to confirm that the plant might adapt its response to phenanthrene after 4h of treatment since numerous pathways in which differentially expressed genes are over-represented are induced at 8h and remain regulated at 24h. These pathways include transport, stress, RNA, redox, protein, miscellaneous, hormone, glycolysis and fermentation metabolisms. Compared to up-regulated genes, genes whose steady state expression

decreased were clearly over-represented in different functional classes, mostly involving primary and secondary metabolisms (amino acid , C1, lipid, tetrapyrrole synthesis, metal handling, co-factor and vitamins, TCA, etc). As for up-regulated genes, number of pathways repressed increase in time, pathways affected from 2h of treatment staying repressed at the other kinetic points. Moreover, modification in the plant response after 4h is also illustrated by the increased number of pathways in which differentially repressed genes are significantly over-represented.

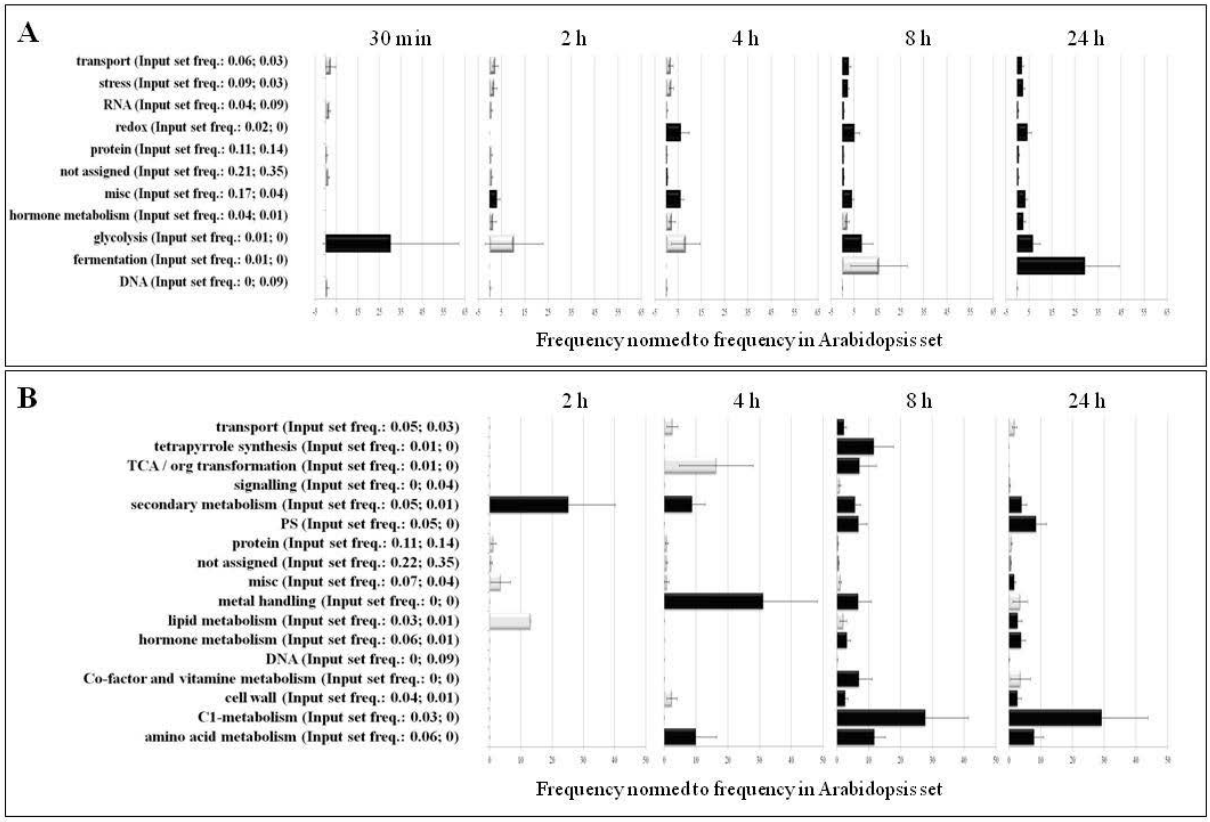

<u>Figure 4</u>: Biological pathways with significant over-representation of up- (A) and down- (B) regulated genes (P-values < 0.05) after 30 min, 2 h, 4 h, 8 h and 24 h of incubation in phenanthrene-treated plants.

Functional enrichment for differentially expressed genes analyzed using the classification superviewer tool from the Bio-Array Resource for Plant Biology (http://www.bar.utoronto.ca/ntools/cgi-bin/ntools_classification_superviewer.cgi) using the MapMan classification as the source. Significant pathways are in bold. PS, Photosynthesis. Misc, miscellaneous.

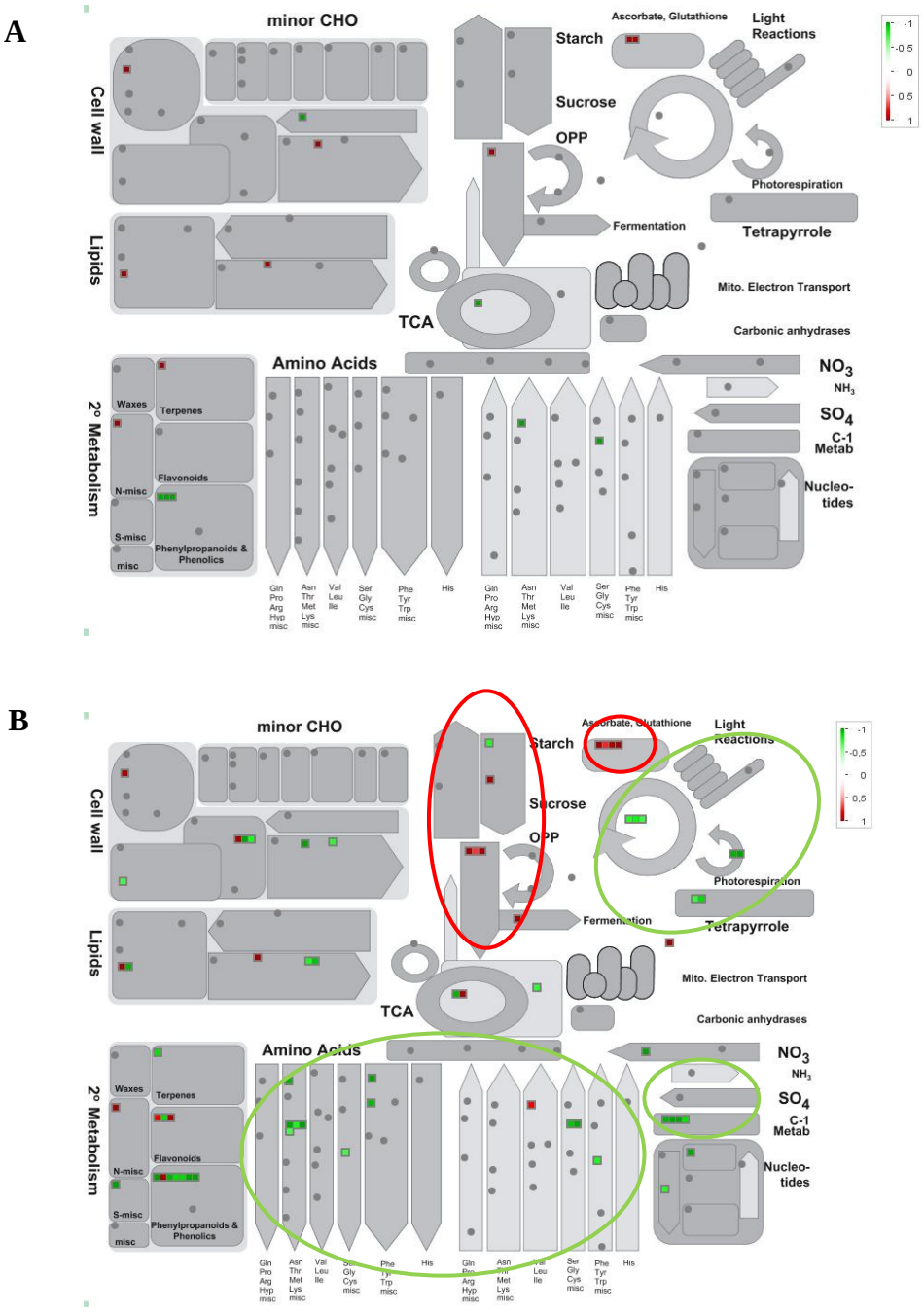

<u>Figure 5</u>: Metabolic gene expression changes at 4 h (A) and 8h (B) of incubation with 0,2mM phenanthrene analyzed by the MapMan tool.

Ratios are given for comparisons phenanthrene-treated to control samples.

3.3.4. *Integration of metabolite data, metabolic changes revealed*

We used the MAPMAN tool to analyse and compare gene expression changes during our time-course. This tool allows the detail visualization and comparison of individual differentially expressed genes onto metabolic pathways.

As an example of recovered information, Figure 5 presents an overview of general metabolism evolutions highlighted for 4h and 8h comparisons. Genes lists corresponding to 4h and 8h comparisons were chosen due to the strong differences in the number of differentially expressed genes that might reflect a modification of plant response to phenanthrene. All the differences at 8h were also confirmed for the 24h kinetic point (Supplemental Figure 3 A).

A first difference was observed for genes involved in light reactions and photorespiration. Whereas no genes are regulated at 4h, some genes involved in the Calvin cycle and photorespirations are repressed at 8h. These changes are in accordance with the known physiological responses to early abiotic stress, well described by Duque et al. (2013). Despite differences in early perception and signalling events between abiotic stress, early stress responses often reduce photosynthetic efficiency, repress transport metabolism or induce accumulation of metabolites and/or uptake-translocation of ions. The stress generated by phenanthrene, proposed by Weisman et al. (2010), originates from its transformation might reduce energy production or increase energy demand to be overcome, as for other abiotic stresses. Consequently, the resulting unbalanced bioenergetic status might affect many other metabolisms.

The glycolysis metabolism produce ATP but also pyruvate for TCA cycle and reductants, such as NADH. Due to the photosynthesis performance reduction, it is not surprising that the number of genes differentially up-regulated involved in glycolysis increase after 8h and 24h.. Some genes involved in ethanolic fermentation are also up-regulated after 24h. These genes encoding alcohol deshydrogenase (ADH) and pyruvate decarboxylase (PDC) have been shown to be hypoxically induced in maize (Ellis et al., 1999). Induction of glycolytic pathway and ethanolic fermentation are part of a strategy developed by the plant to maintain the energy status through the regeneration of NADH in case of oxygen deprivation.

Table 2: Metabolites levels in plants after 24h of phenanthrene treatment. Data are given as the ratio of untreated plants (control). Metabolite contents were determined by GC-MS and HPLC. Data are means of three independent replicates. Citrate, galactinol, galactose, gentibiose, hydroxypiroline, maltose, mannitol, mannose, melibiose, quinate, sorbitol, succinate and trehalose were not detected in both conditions.

Color code (%)

<20	20-49	50-80	81-119	120-200	201-300	>300

Compounds	phenathrene treated plants % of untreated plants
Amino acids	
Alpha-Alanine (Ala)	245%
Arginine (Arg)	132%
Asparagine (Asn)	140%
Aspartate (Asp)	123%
Beta-Alanine	10%
Cystine	150%
GABA	173%
Glutamate (Glu)	125%
Glutamine (Gln)	146%
Glycine (Gly)	140%
Histidine (His)	121%
Isoleucine (Ile)	227%
Leucine (Leu)	233%
Lysine (Lys)	151%
Methionine (Met)	144%
Methylcysteine	55%
Ornithine	111%
Phenylalanine (Phe)	159%
Proline (Pro)	159%
Serine (Ser)	164%
Threonine (Thr)	169%
Tryptophan (Trp)	174%
Tyrosine (Tyr)	127%
Valine (Val)	185%
Alcohols	
Adonitol	132%
Myo-inositol	131%
Organic acids	
Fumarate	0%
Malate	76%
Sugars	
Fructose	115%
Glucose	110%
Sucrose	184%
Inorganic acid	
Ammonium	77%

Moreover, stresses that alter the production of ROS and unbalanced antioxidant networks generate O_2 deprevation. Through its transformation, phenanthrene could strongly affect the plant antioxidant balance and consequently stimulates glycolysis and fermentation metabolisms. However, O_2 deprivation could also results from hypoxic or anoxic conditions. In our study, seedlings were incubated in liquid media before being harvested for transcriptome analysis during which these conditions might have happened. To exclude this possibility, we compared our gene lists to genes differentially regulated by anoxia, hypoxia, and O2 deprivation in the seedlings/shoots of *Arabidopsis* microarray datasets (Pucciariello et al., 2012) and showed that only 3 genes are found in common (Supplemental Table V).

Another difference was observed for genes involved in amino acid synthesis and nucleotide synthesis, only down-regulated at 8h and 24h. Nevertheless, amino acid titration after 24h of phenanthrene treatment suggested the opposite since amino acid accumulates (Table II). This result could be explains by the induction of proteolysis metabolism with increased number of genes whose expression is up-regulated after 8h and 24h of treatment (Supplemental Figure 3 B, Supplemental Figure 4 B). Numerous biochemical studies showed that allosteric enzymes are feedback inhibited by the amino acid they synthesize (Galili, 1995). Accumulation of amino acids in phenanthrene treated plant, due to active proteolysis from 8h to 24h, might reflect a similar situation, feedback inhibition of amino acids synthesis resulting in down-regulation of genes involved in this metabolism. Similar regulations have been described for nucleotides and could explain the repression of genes involved in nucleotide synthesis and C1-metabolism (Zrenner et al., 2006).

Kinetic expression changes of genes classified in the xenome, involved in secondary and the redox metabolisms, shown in Table I and Figure 4, are also supported by visualization of our gene lists onto metabolic pathways (Supplemental Figure 3 and 4). Surprisingly, metabolites titration revealed that sucrose, fructose and glucose accumulate in phenanthrene treated plants at 24h. This result is in accordance with our transcriptome results since numerous known sugar-inducibled genes, such as senescence associated genes (Paul and Pellny, 2003), are differentially up-regulated at 24h. Sugars function as metabolic resources and structural constituents of cells, but also act as signals regulating various processes associated

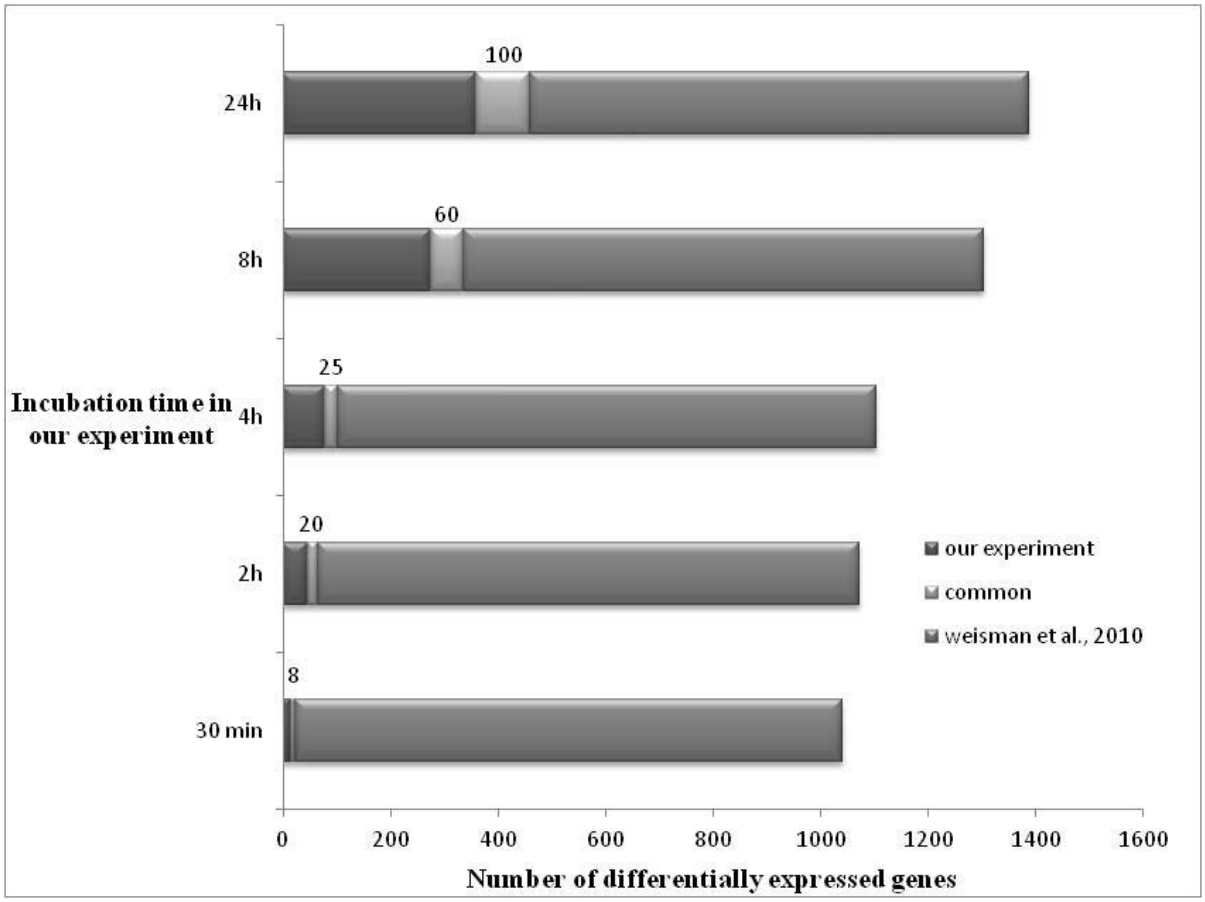

<u>Figure 6</u>: Number of differentially expressed genes found in our experiment, in Weisman et al. (2010) and shared between both experiments.

Numbers above histograms represent the number of differentially expressed genes that are common in both experiments at each kinetic point. 14, 45, 77, 275 and 360 genes found to be differentially expressed in our study after 30 minutes, 2h, 4h, 8h and 24h of treatments with phenanthrene, respectively, were compared to the 1027 differentially expressed genes from the Weisman's (2010) study (24).

with plant growth and development. Accumulation of soluble sugar has also been reported during different biotic and abiotic stress related to oxidative stress (Couée et al., 2006).

3.3.5. *Comparison with public available microarray data*

We first compared the transcriptome data obtained in our study with the only published data on the transcriptome response towards phenanthrene (Supplemental Table V) (Weisman et al., 2010). Weisman et al (2010) performed their transcriptome analysis on 21 days old plants grown on a solid medium supplemented with 250µM of phenanthrene and sucrose. The authors were able to identify PAH-specific response genes involved in xenobiotics detoxification (GST, UGT, CYP450), ROS detoxification mechanisms and also phytohormons metabolism.

In our study approximately 23% (109 out of 467) of the differentially expressed genes were found in common. The majority of these genes have their expression modified after 24h of incubation (100; 27,7%) and are identically differentially regulated at 24h.

Even if some genes belong to important functional classes that characterize the Weisman's transcriptome data (miscellaneous, redox, stress), they are less represented in our study. This is especially the case for genes involved in redox metabolism (ascorbate oxydase, peroxidise, catalase) and pathogen defence response. These discrepancies can be easily explained by differences in the experimental set up used. Indeed, Weisman et al (2010) studied a long term effect of the phenanthrene whereas we studied the 30 minutes-24h plants response.

Hence, results were expected and the fact that most of common genes belongs to our last time point (24h) make sense. However, we cannot exclude that differences could be linked to the scavenger effect of the sucrose, added in the medium in Weisman et al (2010) experiments, or simply to the selectivity of the ANOVA analysis. To test this last hypothesis, we compare the lists of differentially expressed genes obtained before the ANOVA analysis to the Weisman's genes list (data not shown). About 21% of genes (271/1262) were found in common, 24% (215/895) being in common with genes differentially expressed at 24h suggesting that ANOVA analysis do not contribute to differences between studies.

We then compared our differentially expressed genes lists to others transcriptome data sets of analysis performed to study the effect of xenobiotics such as aluminum (60), atrazine (Ramel et al., 2007), BOA (benzoxazolin-2(3H)-one) (Baerson et al., 2005), cadmium (Herbette et al., 2006), PCB (Polychlorinated biphenyl) (Jin et al., 2011), phenol (Xu et al., 2012) selenium (Van Hoewyk et al., 2008) and TNT (trinitrotoluene) (Landa et al., 2010) on higher plants. Differentially expressed genes considered had to be found in common with our genes lists in at least one of all the studies and in one time point in experiments with several time point. Overall, 77,7% (363 out of 467) of differentialy expressed genes were found in common. To summarized, theses comparisons showed that our work is in accordance with the earlier studies performed to decipher the plant response to phenanthrene and to other xenobiotics. Despite differences in gene expression observed between the types of xenobiotics studied, underlying specific molecular responses, this comparison led to the identification of a list of 363 genes, early regulated during phenanthrene exposure, corresponding to a gene network differentially expressed in response to xenobiotic (Supplemental Table V). Among these genes, a consensus group of 36 genes has been classified in the plant ”xenome” and are involved in transformation (CYP450), conjugation (GST, UGT, malonyl transferase) and compartmentalisation (ABC transporters) (Supplemental Table III and V). We thus add a new resolution level by deciphering early response to phenanthrene exposure using a detailed kinetic analysis. In addition, our study adds new phenanthrene regulated genes (Supplemental Tables V) to the present knowledge.

In a second step, we compared the main differentially expressed genes (our study, Table I) with transcriptome data from public genevestigator database to identify either similarities with other transcriptome analysis obtained in response to abiotic, biotic and chemical stimuli (Supplemental Figure 5).

A hierarchical clustering analysis was performed using our top list of differentially regulated genes and all selected data sets. Clustering obtained showed a rather identical pattern of expression of differentially expresses genes from our top list in either abiotic stress conditions (cold, drought, salt and hypoxia stress) or biotic (plant response to pathogenic virus, fungi and bacteria) or chemical stress conditions (Supplemental Figure 5 A, B, C). This result strongly suggest that in response to xenobitotics plant use a common gene

network regulated in response to secondary entities also produced in other biotic or abiotic stress condition as proposed by Ramel et al. (2012) for xenobiotic. In the “biotic selection” (Supplemental Figure 5 B) several experiments showed an opposite regulation pattern. They mainly correspond to comparisons between plants responses to non-pathogenic pathogens such as the mutant bacteria *Pseudomonas syringae pv tomato hrcC*-, deficient in the type III secretion system and unable to infect plant (Deng et al., 1998), and the avirulent mutant bacteria *Pseudomonas syringae pv tomato AvrRpm1,* unable to induce specific resistance associated to the RPS2 plant resistance protein but triggering defence responses after pathogen recognition (Kim et al., 2009). This observation reflect that genes regulated in all these biotic stress may participate in pathogen-associated molecular patterns triggered immunity, mechanism in which photosynthesis seems to play a crucial role (Göhre et al., 2012) as for abiotic stress (Ana Sofia Duque, 2013). Hierarchical clustering with chemical stress experiments enables us to constitute a “chemical selection” inclucing the Weisman’s transciptome data. Even if most of the experiments clustered correspond to plant response to pesticides and herbicides without well described molecular effects on plant, the results obtained confirm that our top list of differentially expressed genes is relevant and representative of plants responses to xenobiotics. These clustering results support that ROS play a major role in the early plant response to phenanthrene since our top list clustered with experiments associated to non enzymatic lipid peroxidation by ROS (phytoprostane A1) (Sattler et al., 2006) or stimulating ROS production (ozone treatment, hydrogen peroxide). Furthermore, similar genes expression pattern observed with a study using fenclorim, known to increase the gluthatione conjugation of the herbicide pretilachlor (Wu et al., 1996) confirm that detoxification process have been activated in our study.

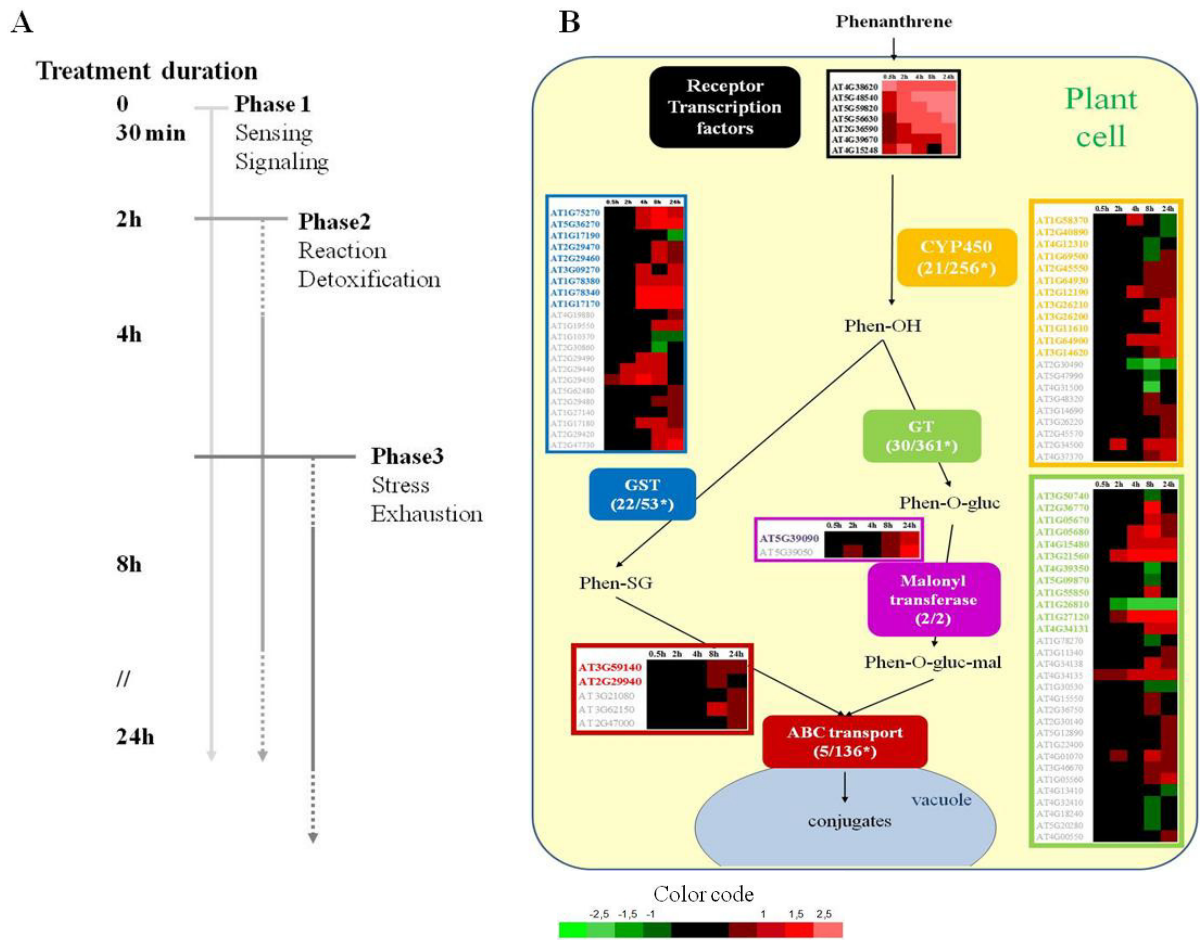

<u>Figure 7</u>: Proposed model of early plant response to phenanthrene exposure.

(**A**) Kinetic representation of the early plant response to phenanthrene. Following the sensing and the signalization of the phenanthrene within the first 30 minutes (phase 1), plant induces from 2h to 24h the expression of genes involved in defence response and detoxification of phenantrene (phase 2). Between 4 and 8h numerous indicators (gene expression and metabolites accumulation) suggest functional declines (phase 3).

(**B**) Representation of genes identified to be involved in the sensing, the signaling and the "xenome" according to the model described by Edwards et al. (2011). Numbers indicate the number of genes belonging to each family, differentially expressed in our study, compared to the total number of genes classified in each family. *: gene members of each family were retrieved from the TAIR website (http://www.arabidopsis.org/browse/genefamily/). Genes in bold face in each family correspond to differentially expressed genes selected after ANOVA analysis.

.

4. Conclusion

This analysis of the early responses of 15 day old *Arabidopsis* plantlets to phenanthrene exposure adds a new resolution level to previous studies on adult plants by dissecting early plant response during a kinetic ranging from 30m minutes to 24h of treatment. Our study is consistent with the earlier studies performed on phenanthrene or others xenobiotics and allowed us to identify a list of 363 genes found in common between our study and at least one of the others works. This study adds new early regulated phenanthrene dependent genes, differently expressed within the first 24h exposure to phenanthrene, Some of them, rapidly expressed after 30min of incubation, are among the most highly differentially expressed genes of the study and correspond to receptor kinase, kinase and transcription factors that could participate to the primary sensing and signalling events preceding detoxification of the phenanthrene. Thus, these genes are good candidates for further functional characterization and development of strategies of molecular avoidance for phenanthrene. A consensus group of 36 genes has been classified in the plant ”xenome” and are putatively involved in transformation (CYP450), conjugation (GST, UGT, malonyl transferase) and compartmentalization (ABC transporters). Eleven of them are also highly up-regulated after 4h of phenanthrene and may be considered in future studies to improve detoxification efficiency.

This study reveals rapid changes in gene expression that might correspond to an adaptive strategy developed by the plant to sense the phenanthrene and activates molecular process devoted to detoxify the pollutant. In a model presented in Figure 7 A, we proposed that the early plant response to phenanthrene could be finally divided in 3 phases. 1) A first phase of sensing and signaling within the first 30 minutes of treatment. Genes encoding receptor, transcription factors and kinase are differentially expressed and continuously regulated during the kinetic (Figure 7 B). 2) A reaction phase with genes involved the putative transformation, conjugation and compartmentalization of phenanthrene have they expression mainly up-regulated from 2 to 8h, some of them being expressed until 24h. Enzymatic activities of proteins encoded by these genes could contribute to increase the level of ROS and thus unbalanced the antioxidant status of cells. Clustering analysis of our top list of differently expressed genes indicates that these genes

are also similarly regulated in numerous transcriptome data sets corresponding to study of plants response to biotic, abiotic or chemical stress. Some of these experiments, using hydrogen peroxide, ozone or molecule that has to be in contact with oxygen singlets to induce similar expression patterns, support this hypothesis. If not counteracted, these free radicals can induce irreversible injuries. Some genes, such as *pfk7*, involved in the glycolysis metabolism, were up-regulated during the first 30 minutes and were continuously over-represented at the other kinetic points suggesting a strong energy and/or reductant demand within the first hours of exposure in order to restore homeostasis. Genes involved in phosynthesis metabolism were also down-regulated after 8h of treatment with phenanthrene. This result suggests that photosynthesis performance declines probably before. However, it remains difficult to known if it is the increase of energy demand or the reduction of energy production, through the repression of the expression genes involved in of the photosynthesis metabolism, that lead to an altered bioenergetics status. However, up-regulation of genes induced in fermentation metabolism at 24h support these decrease biological performances. Thus, energy status appears to be the crucial limiting factor that leads the plant to the third phase of our model. 3) After 8h of exposure to phenanthrene, numerous genes involved in primary and secondary metabolism are repressed, whereas genes mainly involved in glycolysis, fermentation, redox and stress metabolisms are up-regulated. Integration of metabolites titration data indicates a strong accumulation of amino acids and soluble sugars, indicators of functional declines that might lead the exhaustion of the plant.

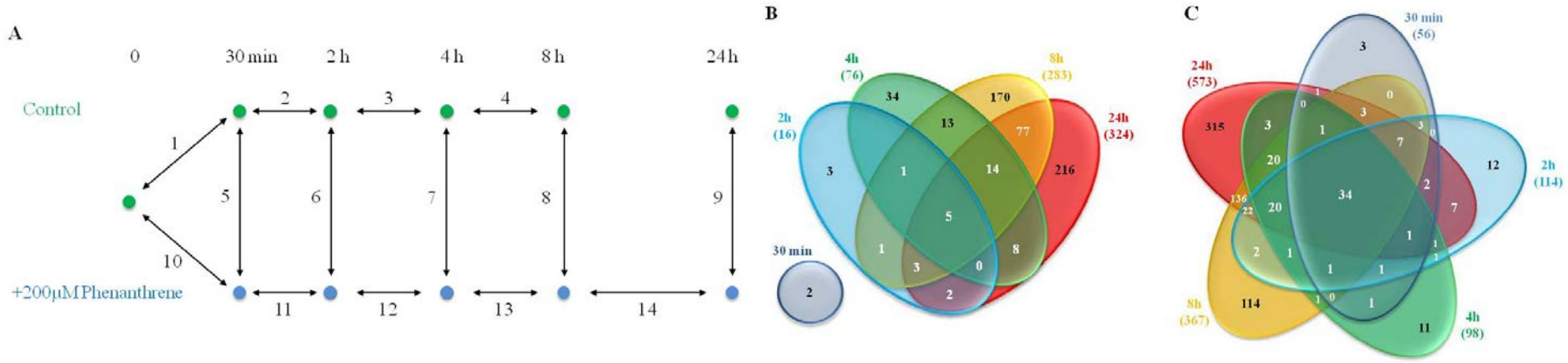

Supplemental Figure 1: (**A**) Schematic representation of the experimental procedure for transcriptome profiling of the *Arabidopsis* response to phenanthrene. Fourteen comparisons (1–14) of control and treated plants with 200µM phenanthrene were performed at five time points (30min, 2 h, 4 h, 8 h and 24 h). Double arrows point to the dye-switch hybridization described in material and method section for the two biological replicates used. In comparisons 1-4, RNAs from control plants from conditions 0, 30 min, 2 h and 4 h were hybridized on the same array with RNAs from control plants in the same condition at 30 min, 2 h, 4 h, 8 h respectively. In comparisons 5-9, RNAs from control plants at 30 min, 2 h, 4 h, 8 h and 24 h were hybridized with RNAs from phenanthrene-treated plants corresponding to the same kinetic point. In comparisons 10-14, RNAs from phenanthrene-treated plants at 0, 30 min, 2 h, 4 h and 8 h were hybridized on the same array with RNAs from treated plants in the 30 min, 2 h, 4 h, 8 h and 24h conditions respectively. (**B**, **C**) Venn diagram showing the total number of differentially expressed genes (p-value < 0.05). Lists of compared genes correspond to down-regulated (B) and up-regulated genes (C) obtained in comparisons between phenanthrene treated samples and control samples at 30 minutes, 2h, 4h, 8h and 24h.

Differentially expressed genes used are listed in Supplemental Table II. Transcriptome data corresponding to hybridizations performed are available in Supplemental Table 1.

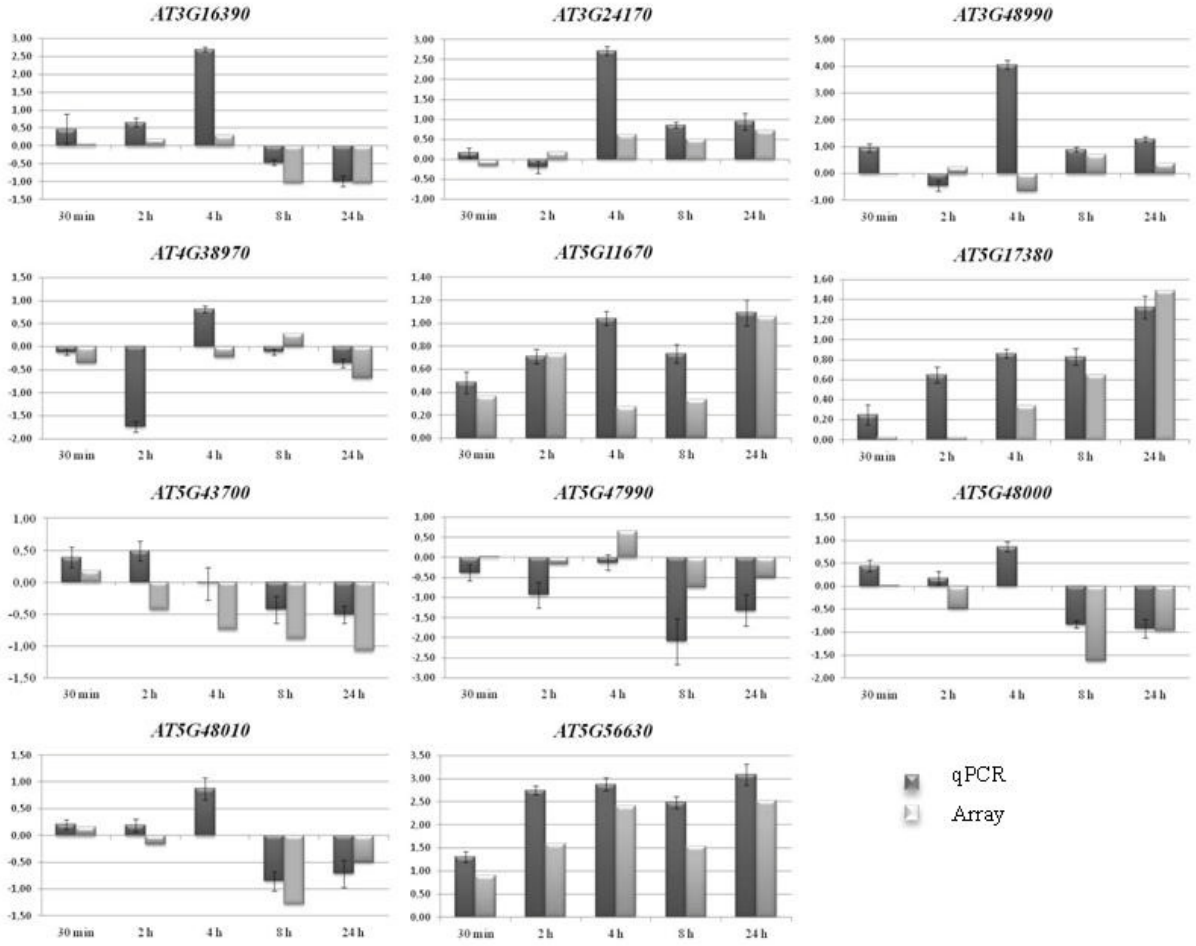

Supplemental Figure 2: QPCR validations of transcriptome data**.** The $\log_2$ ratios from CATMA microarray experiments and subsequent validation by qPCR (ΔC_t) samples for 30 min, 2 h, 4 h, 8 h and 24 h comparisons for 11 selected transcripts. QPCR ΔC_t values are means ±SE of 3 replicates. Normalized ΔCt for each differentially expressed gene were calculated as following: Norm ΔCt =-((C_{t1}-C_{t2})-NF) where the NF corresponds to the average normalization factor calculated on the basis of results obtained for two best control genes chosen to be consistently expressed on CATMA microarray experiments in all samples compared (*AT4G13615* and *AT5G21090*).

A

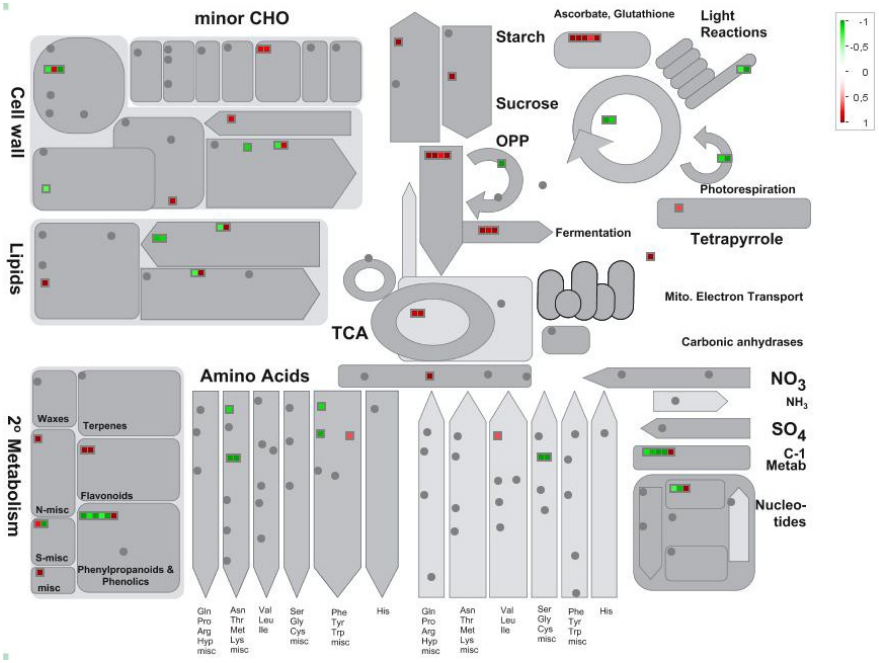

B

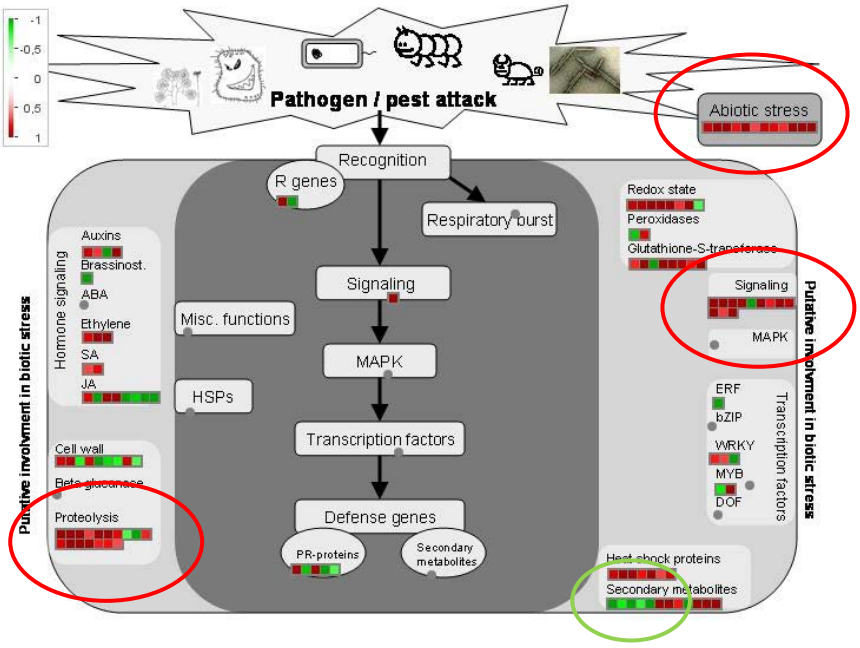

Supplemental Figure 3: Metabolic gene expression changes (**A**), and biotic gene expression overview (**B**), after 24 h of 0,2mM phenanthrene treatment, analyzed by the MapMan tool. Ratios are given for comparisons phenanthrene treated to control samples.

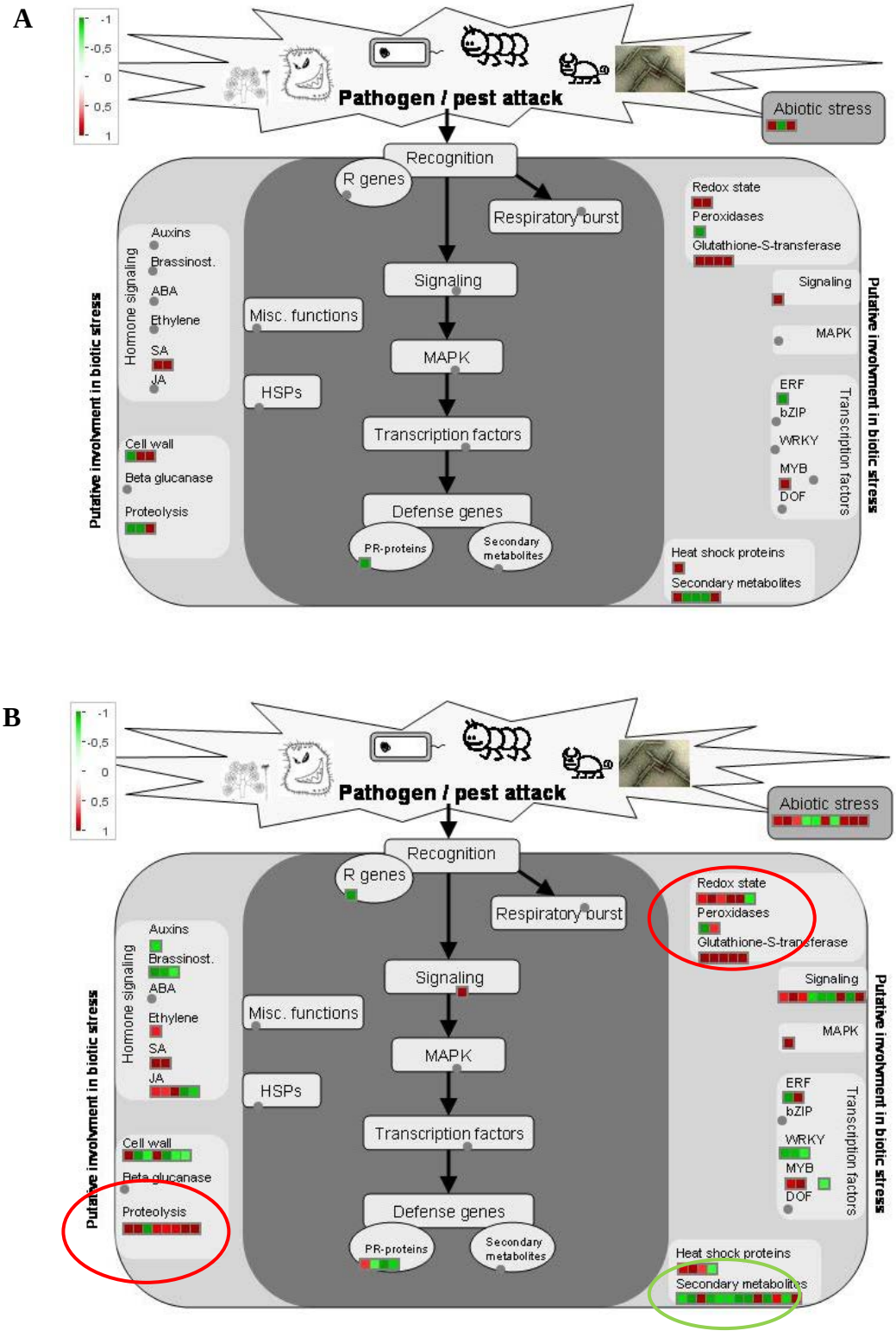

Supplemental Figure 4: Biotic stress genes expression changes after 4h (**A**) and 8h (**B**) of incubation with 0,2mM phenanthrene, analyzed by the MapMan tool. Ratios are given for comparisons phenanthrene treated to control samples.

A: Abiotic selection

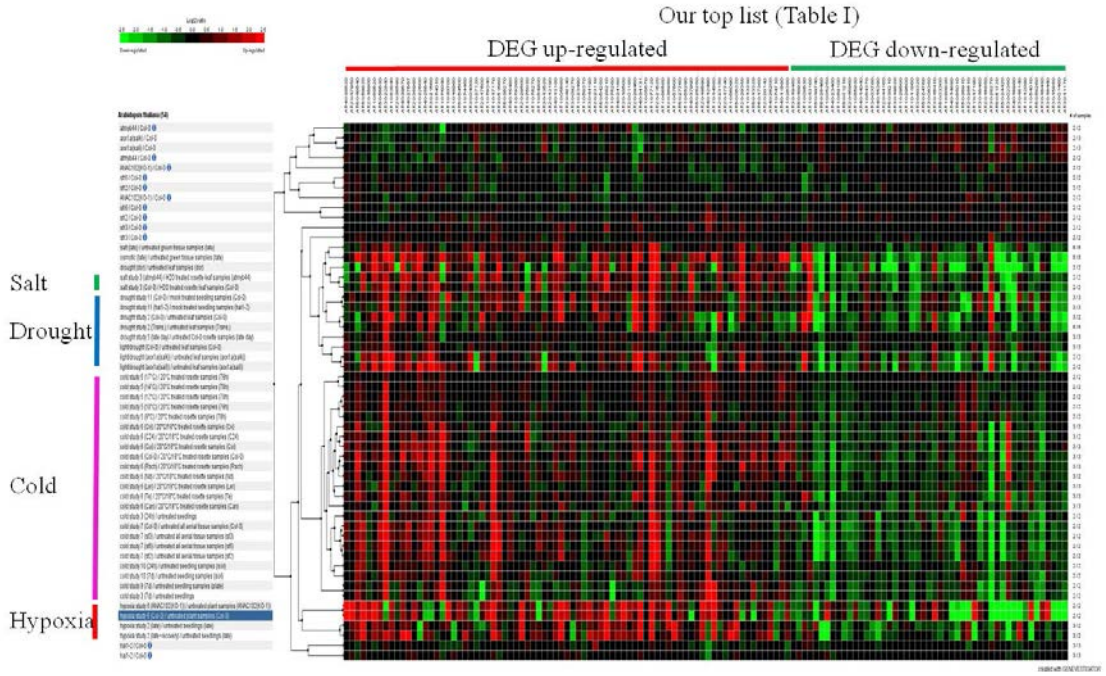

B: biotic selection

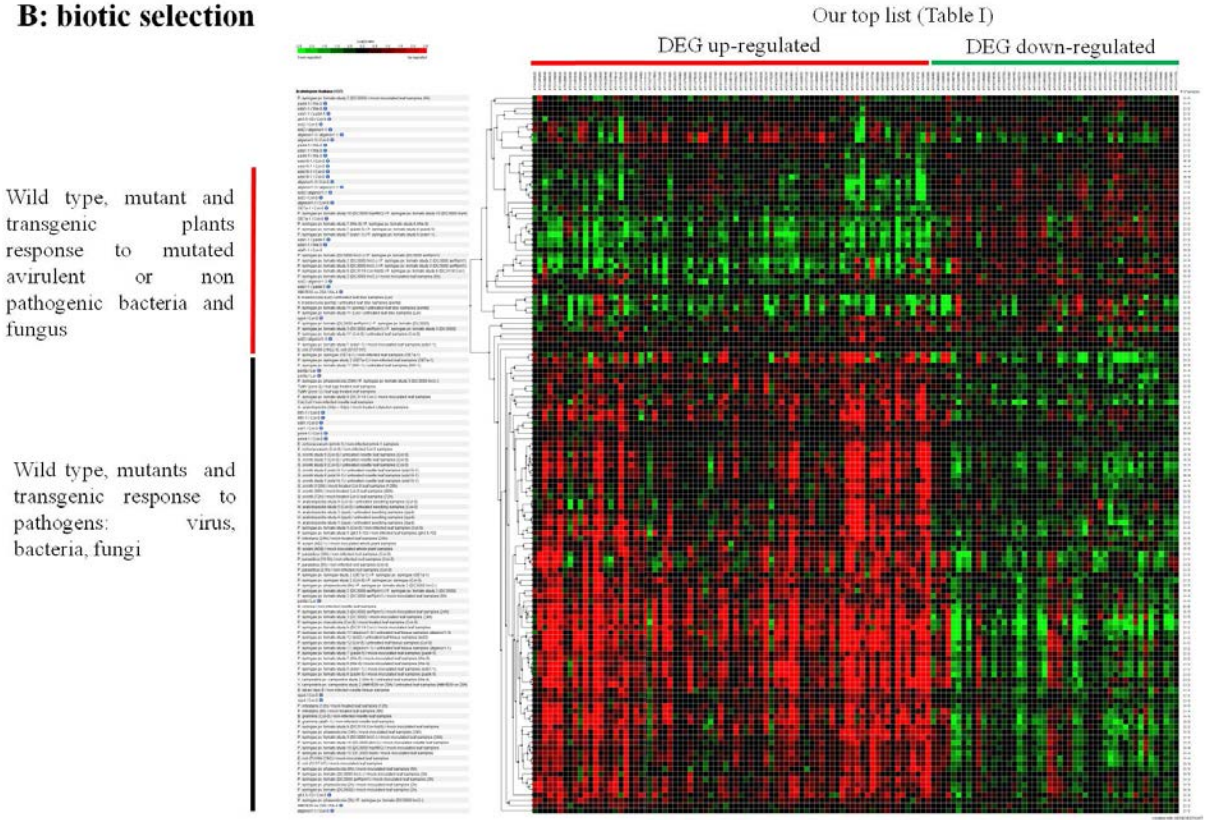

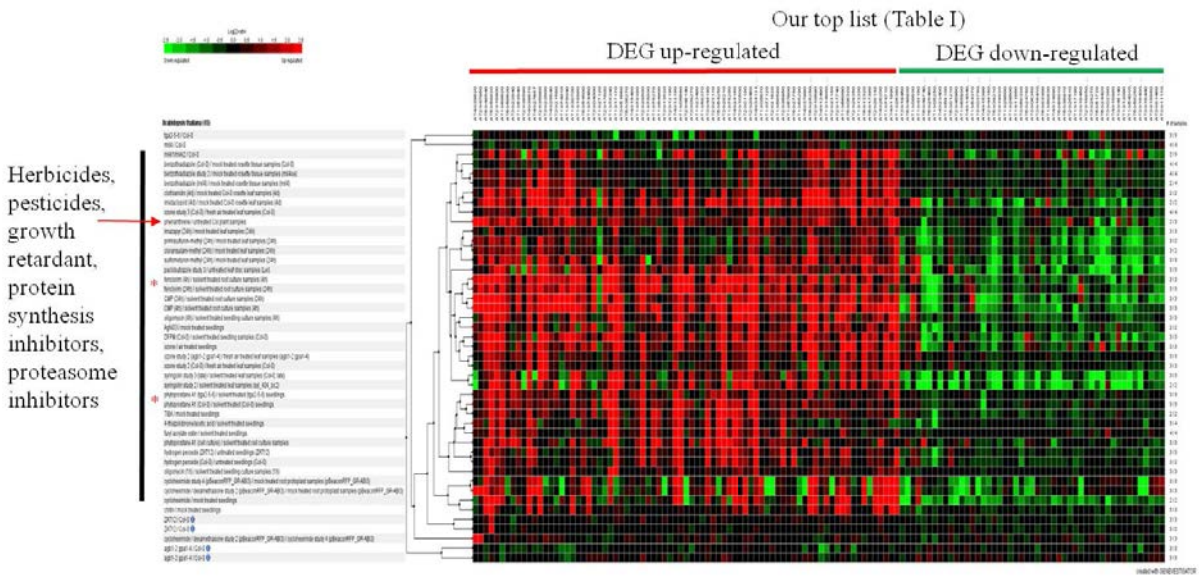

Supplemental Figure 5: Clustering analysis within Genevestigator public data. Clustering analysis was performed using our top list of differentially regulated genes (Table I) using the clustering tool available at www.genenvestigator.com. (**A**) clustering using subset "Abiotic selection", (**B**) clustering using subset "Biotic selection", (**C**) clustering uisng subset "chemical selection". → Weisman et al (2010) study (24).*, Denclorim and phytoprostane A1 examples cited in the article.

Supplemental Table I: Transcriptome data obtained for each comparisons performed. Differentially regulated genes, in bold face, were selected by statistical analysis based on the Bonferroni method using a P value cut-off of 0.05.
(cf. electronic data)

Supplemental Table II: Genes found to be differentially expressed in all the comparisons between phenenthrene-treated and control plants (hybridizations 5-9). Among the 1262 differentially expressed genes corresponding to annotated genes, 58, 130, 174, 650 and 897 genes were expressed at 30 min, 2 h, 4 h, 8 h and 24 h respectively. ns: not significantly differentially expressed. *Arabidopsis* annotation from TAIR, called TAIR10 (most recent versions as of 21 September 2012). Expression changes are given as log2. Expression changes in bolt correspond to genes differentially expressed at the significant threshold of Bonferroni p-value<0.05. ns, not significant.

CATMA identifier	AGI identifier	Gene annotation	30 min	2h	4h	8h	24h
CATMA4A26290_N	AT4G24570	DIC2__dicarboxylate carrier 2	**-0.68**	ns	ns	ns	ns
CATMA1B43120	AT1G52000	Mannose-binding lectin superfamily protein	**-0.65**	ns	ns	ns	ns
CATMA_GFT_02704	AT1G70800	EHB1__Calcium-dependent lipid-binding (CaLB domain) family protein	**0.64**	**1.23**	**1.91**	**1.97**	**1.19**
CATMA4A09435	AT4G09460	AtMYB6_MYB6__myb domain protein 6	**0.64**	**0.91**	ns	**0.75**	ns
CATMA1A16850	AT1G17830	Protein of unknown function (DUF789)	**0.64**	ns	ns	ns	ns
CATMA4C42498	AT4G25810	XTH23_XTR6__xyloglucan endotransglycosylase 6	**0.64**	**0.91**	ns	**0.97**	**1.60**
CATMA1C71994	AT1G65360	AGL23__AGAMOUS-like 23	**0.65**	ns	ns	ns	ns
CATMA1A59790	AT1G70530	CRK3__cysteine-rich RLK (RECEPTOR-like protein kinase) 3	**0.66**	**0.97**	ns	**1.13**	**1.68**
CATMA5A02320	AT5G03210	AtDIP2_DIP2__unknown protein	**0.68**	**1.31**	**1.34**	**0.92**	**1.03**
CATMA1A37730	AT1G44750	ATPUP11_PUP11__purine permease 11	**0.69**	ns	**1.15**	ns	ns
CATMA5A04100	AT5G04930	ALA1__aminophospholipid ATPase 1	**0.69**	**1.07**	**1.11**	**1.18**	**1.39**
CATMA5A12830	AT5G14602	Unknown protein	**0.70**	ns	**1.07**	**0.71**	**0.86**
CATMA4A29300	AT4G27657	unknown protein	**0.70**	**1.26**	**1.10**	**1.75**	**0.74**
CATMA2A35995	AT2G37710	RLK__receptor lectin kinase	**0.70**	**1.23**	**1.85**	**1.45**	**2.34**
CATMA5A22300	AT5G24655	LSU4__response to low sulfur 4	**0.72**	**0.90**	**1.71**	**1.02**	**1.13**
CATMA5A30810	AT5G35580	Protein kinase superfamily protein	**0.72**	ns	ns	**0.98**	**0.92**
CATMA4A41020	AT4G39670	Glycolipid transfer protein (GLTP) family protein	**0.73**	**1.26**	**1.01**	**1.42**	**2.13**
CATMA3A52920	AT3G59900	ARGOS__auxin-regulated gene involved in organ size	**0.73**	ns	ns	ns	**0.83**
CATMA2A27835	AT2G29450	AT103-1A_ATGSTU1_ATGSTU5_GSTU5__glutathione S-transferase tau 5	**0.73**	**1.09**	**1.55**	**1.35**	ns
CATMA1A00730	AT1G01720	ANAC002_ATAF1__NAC (No Apical Meristem) domain transcriptional regulator superfamily protein	**0.73**	ns	ns	**0.80**	**0.86**
CATMA4D01770	AT4G34135	UGT73B2__UDP-glucosyltransferase 73B2	**0.76**	**0.85**	**1.25**	**1.04**	**1.45**
CATMA3A21990	AT3G22060	Receptor-like protein kinase-related family protein	**0.78**	**1.28**	**1.15**	**1.81**	**1.47**
CATMA2A34820	AT2G36590	ATPROT3_ProT3__proline transporter 3	**0.79**	**1.42**	**1.93**	**1.80**	**2.24**
CATMA1A41790	AT1G50740	Transmembrane proteins 14C	**0.80**	**0.99**	ns	**0.75**	**0.96**
CATMA1A08840	AT1G09970	LRR XI-23_RLK7__Leucine-rich receptor-like protein kinase family protein	**0.81**	**0.99**	ns	ns	**1.34**
CATMA1A53060	AT1G63840	RING/U-box superfamily protein	**0.83**	**1.80**	**1.64**	**2.10**	**2.16**
CATMA2A42510	AT2G44080	ARL__ARGOS-like	**0.86**	ns	ns	**0.86**	**1.07**
CATMA3A25100	AT3G25250	AGC2_AGC2-1_AtOXI1_OXI1__AGC (cAMP-dependent, cGMP-dependent and protein kinase C) kinase family protein	**0.87**	**1.03**	**1.33**	**0.83**	**0.84**
CATMA3A22775	AT3G22840	ELIP_ELIP1__Chlorophyll A-B binding family protein	**0.89**	**1.40**	**2.19**	**1.70**	**2.38**
CATMA4A28990	AT4G27410	ANAC072_RD26__NAC (No Apical Meristem) domain transcriptional regulator superfamily protein	**0.89**	**1.26**	ns	**1.27**	ns
CATMA5A52440	AT5G56630	PFK7__phosphofructokinase 7	**0.91**	**1.59**	**2.41**	**1.54**	**2.53**
CATMA1A58000	AT1G68620	alpha/beta-Hydrolases superfamily protein	**0.93**	**2.18**	**1.68**	**2.77**	**2.70**
CATMA1A50830	AT1G61750	Receptor-like protein kinase-related family protein	**0.94**	**1.03**	**1.20**	**0.77**	**1.01**
CATMA1A09000	AT1G10140	Uncharacterised conserved protein UCP031279	**0.98**	**0.89**	ns	**1.02**	**0.79**
CATMA2A15560	AT2G16900	Arabidopsis phospholipase-like protein (PEARLI 4) family	**0.98**	**1.68**	**1.67**	**1.61**	**2.16**
CATMA1A42160	AT1G51090	Heavy metal transport/detoxification superfamily protein	**1.04**	**1.17**	ns	**0.98**	ns
CATMA4C42802	AT4E19530	Unknown protein	**1.06**	**1.16**	**1.64**	**0.79**	**0.91**
CATMA1A59680	AT1G70420	Protein of unknown function (DUF1645)	**1.13**	**1.33**	**1.15**	**1.53**	**1.41**
CATMA5C64297	AT5G18140	Chaperone DnaJ-domain superfamily protein	**1.13**	**1.12**	**1.36**	**1.27**	**1.30**
CATMA1C71184	AT1G13245	DVL4_RTFL17__ROTUNDIFOLIA like 17	**1.14**	**0.87**	ns	**0.98**	**0.69**
CATMA1A22270	AT1G23200	Plant invertase/pectin methylesterase inhibitor superfamily	**1.18**	**2.10**	**2.56**	**2.05**	**2.54**
CATMA5A55595	AT5G59820	RHL41_ZAT12__C2H2-type zinc finger family protein	**1.19**	**1.63**	**2.14**	**2.70**	**2.50**
CATMA1A67660	AT1G78600	BBX22_DBB3_LZF1_STH3__light-regulated zinc finger protein 1	**1.25**	**1.35**	**1.41**	**1.26**	**1.72**
CATMA2A04740	AT2G05940	RIPK__Protein kinase superfamily protein	**1.25**	**1.34**	**1.28**	**1.17**	**1.58**
CATMA3A52950	AT3G59940	Galactose oxidase/kelch repeat superfamily protein	**1.26**	**1.54**	ns	**1.59**	**1.56**
CATMA5A22310	AT5G24660	LSU2__response to low sulfur 2	**1.29**	**1.56**	**2.35**	**1.94**	**2.06**
CATMA1A14680	AT1G15670	Galactose oxidase/kelch repeat superfamily protein	**1.31**	**0.89**	ns	ns	**1.09**
CATMA5A09430	AT5G10695	unknown protein	**1.33**	**1.32**	**1.18**	**1.36**	**1.78**
CATMA1A16150	AT1G17147	VQ motif-containing protein	**1.33**	**1.95**	**1.40**	**1.99**	**1.37**
CATMA1A38140	AT1G47240	ATNRAMP2_NRAMP2__NRAMP metal ion transporter 2	**1.35**	**1.40**	**1.22**	**1.65**	**1.73**
CATMA2A42550	AT2G44140	Peptidase family C54 protein	**1.37**	**3.64**	**2.33**	**3.21**	**3.13**
CATMA4A15850	AT4G15248	B-box type zinc finger family protein	**1.39**	**1.75**	**1.04**	ns	**1.63**
CATMA5A44520	AT5G48540	receptor-like protein kinase-related family protein	**1.42**	**2.44**	**3.27**	**3.48**	**3.51**
CATMA2A46390	AT2G47950	unknown protein	**1.49**	**2.27**	**2.27**	**2.65**	**1.91**
CATMA1A51800	AT1G62690	unknown protein.	**1.52**	**1.81**	**2.07**	**2.12**	**2.83**
CATMA2A15423	AT2G16720	ATMYB7_ATY49_MYB7__myb domain protein 7	**1.62**	**1.25**	ns	**0.75**	**0.88**

CATMA identifier	AGI identifier	Gene annotation	30 min	2h	4h	8h	24h
CATMA3A12420	AT3G13310	Chaperone DnaJ-domain superfamily protein	**1.64**	**1.64**	**1.29**	**1.87**	**1.84**
CATMA4A40092	AT4G38620	ATMYB4_MYB4__myb domain protein 4	**3.51**	**2.19**	**2.30**	**2.18**	**1.94**
CATMA1A19670	AT1E21210	unknown protein	ns	ns	ns	ns	**-0.71**
CATMA1A00310	AT1G01320	Tetratricopeptide repeat (TPR)-like superfamily protein	ns	ns	ns	**-1.14**	ns
CATMA1A00460	AT1G01470	LEA14_LSR3__Late embryogenesis abundant protein	ns	ns	ns	ns	**1.04**
CATMA1C71011	AT1G01790	ATKEA1_KEA1__K+ efflux antiporter 1	ns	ns	ns	**-0.74**	ns
CATMA1A00950	AT1G01960	EDA10__SEC7-like guanine nucleotide exchange family protein	ns	ns	ns	**-0.96**	ns
CATMA1A01610	AT1G02660	alpha/beta-Hydrolases superfamily protein	ns	ns	**-1.18**	ns	ns
CATMA1D02499	AT1G03230	Eukaryotic aspartyl protease family protein	ns	ns	ns	ns	**0.69**
CATMA1C71037	AT1G03700	Uncharacterised protein family (UPF0497)	ns	**0.96**	ns	ns	ns
CATMA1A03115	AT1G04270	RPS15__cytosolic ribosomal protein S15	ns	ns	ns	ns	**-0.67**
CATMA1A03260	AT1G04430	S-adenosyl-L-methionine-dependent methyltransferases superfamily protein	ns	ns	ns	**-0.78**	ns
CATMA1A03520	AT1G04680	Pectin lyase-like superfamily protein	ns	ns	ns	ns	**-0.75**
CATMA1A03570	AT1G04770	Tetratricopeptide repeat (TPR)-like superfamily protein	ns	ns	**1.00**	**0.71**	**0.90**
CATMA1A03970	AT1G05100	MAPKKK18__mitogen-activated protein kinase kinase kinase 18	ns	ns	ns	**0.99**	ns
CATMA_GFT_02501	AT1G05240	Peroxidase superfamily protein	ns	ns	**-1.07**	**-1.48**	**-0.91**
CATMA1C71047	AT1G05340	unknown protein	ns	ns	ns	**0.80**	**1.12**
CATMA1C71051	AT1G05560	UGT1_UGT75B1__UDP-glucosyltransferase 75B1	ns	ns	ns	**0.90**	**1.12**
CATMA1C71052	AT1G05575	unknown protein	ns	ns	ns	**1.21**	ns
CATMA1A04670	AT1G05670	Pentatricopeptide repeat (PPR-like) superfamily protein	ns	ns	ns	**1.30**	**0.69**
CATMA_GFT_00023	AT1G05680	UGT74E2__Uridine diphosphate glycosyltransferase 74E2	ns	ns	**1.01**	**1.80**	**0.83**
CATMA1C71064	AT1G06290	ACX3_ATACX3__acyl-CoA oxidase 3	ns	ns	ns	**0.69**	**0.74**
CATMA1A05580	AT1G06550	ATP-dependent caseinolytic (Clp) protease/crotonase family protein	ns	ns	ns	**-0.77**	ns
CATMA1A05615	AT1G06570	HPD_HPPD_PDS1__phytoene desaturation 1	ns	ns	**-1.23**	ns	ns
CATMA1A06010	AT1G06950	ATTIC110_TIC110__translocon at the inner envelope membrane of chloroplasts 110	ns	ns	ns	**-0.77**	ns
CATMA1A06190	AT1G07135	glycine-rich protein	ns	ns	ns	ns	**0.66**
CATMA1A06330	AT1G07280	Tetratricopeptide repeat (TPR)-like superfamily protein	ns	ns	ns	**-0.92**	ns
CATMA1A06470	AT1G07400	HSP20-like chaperones superfamily protein	ns	ns	**1.24**	**1.18**	**1.23**
CATMA1A06876	AT1G07890	APX1_ATAPX01_ATAPX1_CS1_MEE6__ascorbate peroxidase 1	ns	ns	ns	ns	**0.87**
CATMA1A06950	AT1G07985	Expressed protein	ns	ns	ns	**0.74**	ns
CATMA1C71101	AT1G08360	Ribosomal protein L1p/L10e family	ns	ns	ns	ns	**-0.74**
CATMA1A07491	AT1G08540	ABC1_ATSIG1_ATSIG2_SIG1_SIG2_SIGA_SIGB__RNA polymerase sigma subunit 2	ns	ns	ns	**-0.78**	ns
CATMA1A07550	AT1G08630	THA1__threonine aldolase 1	ns	ns	**-1.81**	**-0.92**	**-1.62**
CATMA1A07793	AT1G08920	ESL1__ERD (early response to dehydration) six-like 1	ns	ns	ns	**0.73**	**0.81**
CATMA1A07895	AT1G09070	(AT)SRC2_SRC2__soybean gene regulated by cold-2	ns	ns	ns	**1.78**	**1.70**
CATMA1A07930	AT1G09130	ATP-dependent caseinolytic (Clp) protease/crotonase family protein	ns	ns	ns	**0.87**	ns
CATMA1C71120	AT1G09340	CRB_CSP41B_HIP1.3__chloroplast RNA binding	ns	ns	ns	ns	**-0.70**
CATMA1C71124	AT1G09400	FMN-linked oxidoreductases superfamily protein	ns	ns	ns	**0.74**	**1.08**
CATMA1C71125	AT1G09500	NAD(P)-binding Rossmann-fold superfamily protein	ns	ns	ns	**0.98**	ns
CATMA1A08395	AT1G09530	PAP3_PIF3_POC1__phytochrome interacting factor 3	ns	ns	ns	**-0.79**	ns
CATMA1A09190	AT1G10340	Ankyrin repeat family protein	ns	ns	ns	ns	**0.93**
CATMA1C71141	AT1G10370	ATGSTU17_ERD9_GST30_GST30B_GSTU17__Glutathione S-transferase family protein	ns	ns	ns	**-0.71**	**-0.78**
CATMA1A09850	AT1G10960	ATFD1_FD1__ferredoxin 1	ns	ns	ns	**-0.70**	ns
CATMA1C71155	AT1G11610	CYP71A18__cytochrome P450, family 71, subfamily A, polypeptide 18	ns	ns	ns	ns	**1.12**
CATMA1A10860	AT1G11850	unknown protein	ns	ns	ns	ns	**-0.72**
CATMA1A10870	AT1G11860	Glycine cleavage T-protein family	ns	ns	ns	**-1.17**	**-1.14**
CATMA1A10930	AT1G11910	APA1_ATAPA1__aspartic proteinase A1	ns	ns	ns	ns	**0.84**
CATMA1A11060	AT1G12010	2-oxoglutarate (2OG) and Fe(II)-dependent oxygenase superfamily protein	ns	ns	ns	**-0.72**	**-0.80**
CATMA1A11135	AT1G12090	ELP__extensin-like protein	ns	ns	ns	ns	**-1.08**
CATMA1A11765	AT1G12780	ATUGE1_UGE1__UDP-D-glucose/UDP-D-galactose 4-epimerase 1	ns	ns	**-1.06**	ns	ns
CATMA1A11780	AT1G12800	Nucleic acid-binding, OB-fold-like protein	ns	ns	ns	**-0.82**	ns
CATMA1A11900	AT1G12900	GAPA-2__glyceraldehyde 3-phosphate dehydrogenase A subunit 2	ns	ns	ns	ns	**-0.89**
CATMA1A12340	AT1G13330	AHP2__Arabidopsis Hop2 homolog	ns	ns	ns	ns	**1.55**
CATMA1A13090	AT1G14120	2-oxoglutarate (2OG) and Fe(II)-dependent oxygenase superfamily protein	ns	ns	**1.08**	ns	ns
CATMA1C71197	AT1G14130	2-oxoglutarate (2OG) and Fe(II)-dependent oxygenase superfamily protein	ns	ns	ns	**1.04**	**0.86**
CATMA1A13300	AT1G14290	SBH2__sphingoid base hydroxylase 2	ns	ns	ns	ns	**-0.82**
CATMA1A13550	AT1G14540	Peroxidase superfamily protein	ns	ns	ns	ns	**0.75**
CATMA1C71209	AT1G14870	AtPCR2_PCR2__PLANT CADMIUM RESISTANCE 2	ns	ns	ns	ns	**1.76**
CATMA1A13910	AT1G14880	AtPCR1_PCR1__PLANT CADMIUM RESISTANCE 1	ns	ns	ns	ns	**0.66**
CATMA1A14290	AT1G15290	Tetratricopeptide repeat (TPR)-like superfamily protein	ns	ns	ns	**-0.97**	ns

CATMA identifier	AGI identifier	Gene annotation	30 min	2h	4h	8h	24h
CATMA1A14450	AT1G15415	The protein encoded by this gene was identified as a part of pollen proteome by mass spec analysis. It has weak homology to LEA (late embryo abundant) proteins.	ns	ns	ns	**0.74**	ns
CATMA1A14525	AT1G15500	Encodes protein phosphatase 2A (PP2A) B'gamma subunit. Targeted to nucleus and cytosol. ATNTT2__TLC ATP/ADP transporter	ns	ns	ns	**-0.69**	ns
CATMA1C71226	AT1G15750	TPL_WSIP1__Transducin family protein / WD-40 repeat family protein	ns	ns	ns	**0.78**	ns
CATMA1A14990	AT1G15930	Ribosomal protein L7Ae/L30e/S12e/Gadd45 family protein	ns	ns	ns	ns	**-0.71**
CATMA1A15040	AT1G16030	Hsp70b__heat shock protein 70B	ns	ns	ns	ns	**0.70**
CATMA1A15340	AT1G16350	Aldolase-type TIM barrel family protein	ns	ns	ns	**-0.74**	ns
CATMA1A15380	AT1G16390	ATOCT3_OCT3__organic cation/carnitine transporter 3	ns	ns	ns	ns	**-0.83**
CATMA1A15690	AT1G16720	HCF173__high chlorophyll fluorescence phenotype 173	ns	ns	**-1.31**	ns	ns
CATMA1C71257	AT1G17170	ATGSTU24_GST_GSTU24__glutathione S-transferase TAU 24	ns	ns	**1.57**	**2.00**	**2.05**
CATMA1C71258	AT1G17180	ATGSTU25_GSTU25__glutathione S-transferase TAU 25	ns	ns	**1.50**	**1.07**	**0.99**
CATMA1A16200	AT1G17190	ATGSTU26_GSTU26__glutathione S-transferase tau 26	ns	ns	ns	ns	**-1.41**
CATMA1A16230	AT1G17220	FUG1__Translation initiation factor 2, small GTP-binding protein	ns	ns	ns	**-0.85**	ns
CATMA1A16880	AT1G17860	Kunitz family trypsin and protease inhibitor protein	ns	ns	ns	**1.10**	**1.06**
CATMA1A16990	AT1G18020	FMN-linked oxidoreductases superfamily protein	ns	ns	ns	**0.92**	ns
CATMA1A17300	AT1G18290	unknown protein	ns	ns	ns	ns	**-0.83**
CATMA1C71277	AT1G18390	Protein kinase superfamily protein	ns	ns	ns	ns	**0.82**
CATMA1A17560	AT1G18510	TET16__tetraspanin 16	ns	ns	ns	**1.26**	ns
CATMA1A17615	AT1G18570	AtMYB51_BW51A_BW51B_HIG1_MYB51__myb domain protein 51	ns	ns	ns	**-0.74**	ns
CATMA1A17740	AT1G18700	DNAJ heat shock N-terminal domain-containing protein	ns	ns	ns	**0.77**	**0.83**
CATMA1A17860	AT1G18810	phytochrome kinase substrate-related	ns	ns	ns	**-1.27**	ns
CATMA1B17945	AT1G18880	NRT1.9__Major facilitator superfamily protein	ns	ns	ns	ns	**0.76**
CATMA1A18010	AT1G18980	RmlC-like cupins superfamily protein	ns	**1.16**	**1.55**	**1.57**	**1.59**
CATMA1A18090	AT1G19050	ARR7__response regulator 7	ns	ns	ns	**-0.72**	ns
CATMA1A18130	AT1G19100	Histidine kinase-, DNA gyrase B-, and HSP90-like ATPase family protein	ns	ns	ns	**-0.69**	ns
CATMA1A18260	AT1G19220	ARF11_ARF19_IAA22__auxin response factor 19	ns	ns	ns	ns	**0.82**
CATMA1A18400	AT1G19380	Protein of unknown function (DUF1195)	ns	ns	ns	ns	**0.87**
CATMA_GFT_02523	AT1G19550	Glutathione S-transferase family protein	ns	ns	ns	**1.05**	**1.20**
CATMA1A18780	AT1G19770	ATPUP14_PUP14__purine permease 14	ns	ns	**-1.01**	ns	ns
CATMA1A19470	AT1G20470	SAUR-like auxin-responsive protein family	ns	ns	ns	**0.71**	ns
CATMA1A19955	AT1G20900	AHL27_ESC_ORE7__Predicted AT-hook DNA-binding family protein	ns	ns	ns	ns	**-1.02**
CATMA1C71316	AT1G21000	PLATZ transcription factor family protein	ns	ns	ns	**0.73**	ns
CATMA1A20325	AT1G21270	WAK2__wall-associated kinase 2	ns	ns	ns	ns	**0.74**
CATMA1A20370	AT1G21320	nucleotide binding;nucleic acid binding	ns	ns	ns	**-0.70**	ns
CATMA1A20530	AT1G21480	Exostosin family protein	ns	ns	ns	**-0.77**	**-1.08**
CATMA1A20650	AT1G21570	unknown protein	ns	ns	ns	**-1.57**	ns
CATMA1A20760	AT1G21670	unknown protein.	ns	**0.97**	ns	**1.20**	**1.79**
CATMA1A20815	AT1G21720	PBC1__proteasome beta subunit C1	ns	ns	ns	**0.74**	ns
CATMA1A20840	AT1G21750	ATPDI5_ATPDIL1-1_PDI5_PDIL1-1__PDI-like 1-1	ns	ns	ns	ns	**0.93**
CATMA1C72301	AT1G22350	unknown protein	ns	ns	ns	ns	**0.76**
CATMA1C71339	AT1G22400	ATUGT85A1_UGT85A1__UDP-Glycosyltransferase superfamily protein	ns	ns	ns	ns	**0.81**
CATMA1C71343	AT1G22500	AtATL15_ATL15__RING/U-box superfamily protein	ns	ns	ns	**0.88**	ns
CATMA1A21725	AT1G22640	ATMYB3_MYB3__myb domain protein 3	ns	ns	ns	ns	**-0.83**
CATMA1A21785_N	AT1G22710	ATSUC2_SUC2_SUT1__sucrose-proton symporter 2	ns	ns	ns	**0.87**	**1.27**
CATMA1C71357	AT1G22840	ATCYTC-A_CYTC-1__CYTOCHROME C-1	ns	ns	ns	ns	**0.70**
CATMA1A21975	AT1G22920	AJH1_CSN5A_JAB1__COP9 signalosome 5A	ns	ns	ns	ns	**-0.87**
CATMA1A22180	AT1G23120	Polyketide cyclase/dehydrase and lipid transport superfamily protein	ns	ns	ns	**-0.76**	ns
CATMA1A22430	AT1G23350	Plant invertase/pectin methylesterase inhibitor superfamily protein	ns	ns	**-1.13**	**-0.69**	ns
CATMA1C71370	AT1G23490	ARF1_ATARF_ATARF1_ATARFA1A__ADP-ribosylation factor 1	ns	ns	**1.04**	ns	**1.32**
CATMA1A22740	AT1G23880	NHL domain-containing protein	ns	ns	ns	ns	**0.78**
CATMA1A22750	AT1G23890	NHL domain-containing protein	ns	ns	ns	**1.26**	ns
CATMA1A22830	AT1G23980	RING/U-box superfamily protein	ns	ns	ns	ns	**0.75**
CATMA1A23910	AT1G25260	Ribosomal protein L10 family protein	ns	ns	ns	ns	**-0.74**
CATMA1C71401	AT1G26380	FAD-binding Berberine family protein	ns	ns	ns	ns	**1.38**
CATMA1A24650	AT1G26410	FAD-binding Berberine family protein	ns	ns	ns	ns	**0.66**
CATMA1A24860	AT1G26630	ATELF5A-2_ELF5A-2_FBR12__Eukaryotic translation initiation factor 5A-1 (eIF-5A 1) protein	ns	ns	ns	ns	**1.36**
CATMA1A24990	AT1G26761	Arabinanase/levansucrase/invertase	ns	ns	**-1.09**	ns	ns
CATMA1A25030	AT1G26810	GALT1__galactosyltransferase1	ns	**-1.16**	**-1.71**	**-1.65**	**-1.79**
CATMA1A25300	AT1G27080	NRT1.6__nitrate transporter 1.6	ns	ns	ns	ns	**0.88**
CATMA1A25350	AT1G27120	Galactosyltransferase family protein	ns	**0.91**	**2.00**	**2.30**	**2.45**
CATMA1A25370	AT1G27140	ATGSTU14_GST13_GSTU14__glutathione S-transferase tau 14	ns	ns	ns	ns	**0.79**
CATMA1A25440	AT1G27190	Leucine-rich repeat protein kinase family protein	ns	ns	ns	**1.96**	ns
CATMA1A26000	AT1G27760	ATSAT32_SAT32__interferon-related developmental regulator family protein / IFRD protein family	ns	ns	ns	**0.69**	**0.76**
CATMA1A27020	AT1G29050	TBL38__TRICHOME BIREFRINGENCE-LIKE 38	ns	ns	ns	**-0.77**	ns

CATMA identifier	AGI identifier	Gene annotation	30 min	2h	4h	8h	24h
CATMA1A27110	AT1G29140	Pollen Ole e 1 allergen and extensin family protein	ns	ns	ns	ns	**0.75**
CATMA1A27180	AT1G29200	O-fucosyltransferase family protein	ns	ns	ns	ns	**-0.85**
CATMA1A27260	AT1G29280	ATWRKY65_WRKY65__WRKY DNA-binding protein 65	ns	ns	ns	**-0.95**	ns
CATMA1C71449	AT1G29310	SecY protein transport family protein	ns	ns	ns	ns	**0.68**
CATMA1A27510	AT1G29560	Zinc finger C-x8-C-x5-C-x3-H type family protein	ns	ns	ns	**-1.00**	**-0.93**
CATMA1A27550	AT1G29600	Zinc finger C-x8-C-x5-C-x3-H type family protein	ns	ns	ns	**-1.22**	**-1.02**
CATMA1A27560	AT1G29630	5'-3' exonuclease family protein	ns	ns	ns	**-0.80**	**-0.72**
CATMA1D00214	AT1G29910	AB180_CAB3_LHCB1.2__chlorophyll A/B binding protein 3	ns	ns	ns	ns	**-1.15**
CATMA1D00215	AT1G29920	AB165_CAB2_LHCB1.1__chlorophyll A/B-binding protein 2	ns	ns	ns	ns	**-0.89**
CATMA1A28300	AT1G30270	ATCIPK23_CIPK23_LKS1_PKS17_SnRK3.23__CBL-interacting protein kinase 23	ns	ns	ns	**0.69**	ns
CATMA1A28370	AT1G30360	ERD4__Early-responsive to dehydration stress protein (ERD4)	ns	ns	**-1.15**	ns	**-0.89**
CATMA1A28550	AT1G30530	UGT78D1__UDP-glucosyl transferase 78D1	ns	ns	ns	**-0.85**	**-0.67**
CATMA1A28670	AT1G30620	HSR8_MUR4_UXE1__NAD(P)-binding Rossmann-fold superfamily protein	ns	ns	ns	ns	**1.01**
CATMA1A28750	AT1G30700	FAD-binding Berberine family protein	ns	**1.26**	**1.06**	**1.56**	**2.28**
CATMA1A29810	AT1G31580	CXC750__ECS1	ns	ns	ns	**-1.12**	ns
CATMA1A30210	AT1G31940	unknown protein	ns	ns	ns	**0.81**	ns
CATMA1A30550	AT1G32200	ACT1_ATS1__phospholipid/glycerol acyltransferase family protein	ns	**-0.84**	ns	ns	**-0.74**
CATMA1A31040	AT1G32700	PLATZ transcription factor family protein	ns	ns	ns	**-0.69**	ns
CATMA1A31170	AT1G32870	ANAC013_ANAC13_NAC13__NAC domain protein 13	ns	ns	ns	ns	**0.70**
CATMA1C71521	AT1G32940	ATSBT3.5_SBT3.5__Subtilase family protein	ns	ns	ns	ns	**1.06**
CATMA1C71522	AT1G32960	ATSBT3.3_SBT3.3__Subtilase family protein	ns	ns	ns	ns	**1.27**
CATMA1A31460	AT1G33110	MATE efflux family protein	ns	ns	ns	**0.85**	ns
CATMA1A31830	AT1G33560	ADR1__Disease resistance protein (CC-NBS-LRR class) family	ns	ns	ns	ns	**0.70**
CATMA1C71536	AT1G33590	Leucine-rich repeat (LRR) family protein	ns	ns	ns	**0.73**	**1.43**
CATMA1A31880	AT1G33610	Leucine-rich repeat (LRR) family protein	ns	ns	ns	**1.70**	**1.78**
CATMA1A32330	AT1G34047	Defensin-like (DEFL) family protein	ns	ns	ns	**0.82**	**0.82**
CATMA1A32770	AT1G34440	unknown protein	ns	ns	ns	ns	**-0.75**
CATMA1A32980	AT1G34630	FUNCTIONS IN: molecular_function unknown; INVOLVED IN: biological_process unknown; LOCATED IN: cellular_component unknown; EXPRESSED IN: 25 plant structures; EXPRESSED DURING: 15 growth stages; BEST Arabidopsis thaliana protein match is: Mitochondrial import inner membrane translocase subunit Tim17/Tim22/Tim23 family protein (TAIR:AT5G51150.1); (source: NCBI BLink).	ns	**1.06**	ns	ns	ns
CATMA1A33100	AT1G34790	TT1_WIP1__C2H2 and C2HC zinc fingers superfamily protein	ns	ns	ns	**-0.73**	ns
CATMA1C71568	AT1G35350	EXS (ERD1/XPR1/SYG1) family protein	ns	ns	ns	ns	**0.95**
CATMA1A33690	AT1G35515	HOS10_MYB8__high response to osmotic stress 10	ns	ns	ns	**-0.73**	ns
CATMA1A34330	AT1G36230	unknown protein	ns	ns	ns	**-0.84**	ns
CATMA_GFT_02596	AT1G36580	BEST Arabidopsis thaliana protein match is: short-chain dehydrogenase-reductase B (TAIR:AT3G12800.1); Has 109 Blast hits to 109 proteins in 14 species: Archae - 0; Bacteria - 0; Metazoa - 0; Fungi - 0; Plants - 107; Viruses - 0; Other Eukaryotes - 2 (source: NCBI BLink).	ns	ns	ns	**0.87**	**0.84**
CATMA1C72346	AT1G36622	unknown protein	ns	ns	ns	ns	**1.12**
CATMA1B35155	AT1G37130	ATNR2_B29_CHL3_NIA2_NIA2-1_NR_NR2__nitrate reductase 2	ns	ns	ns	**1.17**	ns
CATMA1A36330	AT1G42990	ATBZIP60_BZIP60_BZIP60__basic region/leucine zipper motif 60	ns	ns	ns	ns	**1.34**
CATMA1A36590	AT1G43160	RAP2.6__related to AP2 6	ns	ns	**-1.57**	**-1.16**	**-0.99**
CATMA1A36595	AT1G43170	ARP1_emb2207_RP1_RPL3A__ribosomal protein 1	ns	ns	ns	ns	**-0.75**
CATMA1C71613	AT1G44350	ILL6__IAA-leucine resistant (ILR)-like gene 6	ns	ns	ns	**0.79**	ns
CATMA1C71618	AT1G44575	CP22_NPQ4_PSBS__Chlorophyll A-B binding family protein	ns	ns	ns	ns	**-0.75**
CATMA1C71632	AT1G45201	ATTLL1_TLL1__triacylglycerol lipase-like 1	ns	ns	ns	**-0.76**	ns
CATMA1A38770	AT1G47720	OSB1__Primosome PriB/single-strand DNA-binding	ns	ns	ns	**0.71**	**0.82**
CATMA1A38970	AT1G47890	AtRLP7_RLP7__receptor like protein 7	ns	ns	ns	**-0.70**	**-0.92**
CATMA1A39400	AT1G48320	Thioesterase superfamily protein	ns	**-0.80**	ns	**-0.93**	ns
CATMA1A40900	AT1G49820	ATMTK_MTK_MTK1__S-methyl-5-thioribose kinase	ns	ns	ns	ns	**0.88**
CATMA1A41950	AT1G50910	unknown protein	ns	ns	ns	ns	**-0.76**
CATMA1A42700	AT1G51570	Calcium-dependent lipid-binding (CaLB domain) plant phosphoribosyltransferase family protein	ns	ns	ns	ns	**-0.71**
CATMA1A42750	AT1G51620	Protein kinase superfamily protein	ns	ns	ns	ns	**0.71**
CATMA1A42790	AT1G51700	ADOF1_DOF1__DOF zinc finger protein 1	ns	ns	ns	ns	**0.74**
CATMA1A42890	AT1G51800	IOS1__Leucine-rich repeat protein kinase family protein	ns	ns	ns	ns	**0.72**
CATMA1D00376	AT1G51820	Leucine-rich repeat protein kinase family protein	ns	ns	ns	ns	**1.21**
CATMA1A43060	AT1G51940	protein kinase family protein / peptidoglycan-binding LysM domain-containing protein	ns	ns	ns	**-0.87**	**-1.13**
CATMA1A43630	AT1G52580	ATRBL5_RBL5__RHOMBOID-like protein 5	ns	ns	ns	**-1.10**	**-0.66**
CATMA1A43790	AT1G52730	Transducin/WD40 repeat-like superfamily protein	ns	ns	ns	**1.03**	**1.24**
CATMA1A44030	AT1G53010	RING/U-box superfamily protein	ns	ns	ns	ns	**-0.78**
CATMA1A44350	AT1G53320	AtTLP7_TLP7__tubby like protein 7	ns	ns	ns	**1.19**	ns
CATMA1A44596	AT1G53580	ETHE1_GLX2-3_GLY3__glyoxalase II 3	ns	ns	ns	**1.07**	ns
CATMA1C71795	AT1G53625	unknown protein	ns	ns	ns	ns	**0.72**

CATMA identifier	AGI identifier	Gene annotation	30 min	2h	4h	8h	24h
CATMA1A45100	AT1G54000	GLL22__GDSL-like Lipase/Acylhydrolase superfamily protein	ns	ns	ns	ns	**-1.06**
CATMA1A45145	AT1G54040	ESP_ESR_TASTY__epithiospecifier protein	ns	ns	ns	**0.70**	ns
CATMA1A45820	AT1G54740	Protein of unknown function (DUF3049)	ns	ns	**-1.12**	ns	ns
CATMA1A46090	AT1G55050	unknown protein.	ns	ns	**-1.01**	ns	**-0.81**
CATMA1A46140	AT1G55110	AtIDD7_IDD7__indeterminate(ID)-domain 7	ns	ns	ns	**-0.71**	ns
CATMA1A46180	AT1G55152	unknown protein	ns	ns	ns	ns	**-0.71**
CATMA1A46400	AT1G55320	AAE18__acyl-activating enzyme 18	ns	ns	ns	**-0.69**	ns
CATMA1C71832	AT1G55330	AGP21_ATAGP21__arabinogalactan protein 21	ns	ns	ns	**0.75**	ns
CATMA1B46590	AT1G55490	CPN60B_Cpn60beta1_LEN1__chaperonin 60 beta	ns	ns	ns	**-0.79**	ns
CATMA1A46603	AT1G55510	BCDH BETA1__branched-chain alpha-keto acid decarboxylase E1 beta subunit	ns	ns	ns	**0.83**	ns
CATMA_GFT_02657	AT1G55720	ATCAX6_CAX6__cation exchanger 6	ns	ns	ns	ns	**0.80**
CATMA1A47044	AT1G55850	ATCSLE1_CSLE1__cellulose synthase like E1	ns	ns	ns	**1.17**	ns
CATMA1C71857	AT1G56060	unknown protein	ns	ns	ns	ns	**0.97**
CATMA1A47290	AT1G56190	Phosphoglycerate kinase family protein	ns	ns	ns	ns	**-0.69**
CATMA1A47320	AT1G56220	Dormancy/auxin associated family protein	ns	ns	**-1.32**	**-0.70**	ns
CATMA1A47890	AT1G57590	Pectinacetylesterase family protein	ns	ns	ns	**0.73**	ns
CATMA1A48498	AT1G58370	ATXYN1_RXF12__glycosyl hydrolase family 10 protein / carbohydrate-binding domain-containing protein	ns	ns	**1.13**	ns	**-0.86**
CATMA1A48650	AT1G59590	ZCF37	ns	ns	ns	ns	**0.77**
CATMA1A48850	AT1G59800	Cullin family protein	ns	ns	ns	ns	**-0.83**
CATMA1A48920	AT1G59860	HSP20-like chaperones superfamily protein	ns	ns	ns	ns	**0.91**
CATMA1C71892	AT1G60680	NAD(P)-linked oxidoreductase superfamily protein	ns	ns	ns	ns	**0.91**
CATMA1C71893	AT1G60690	NAD(P)-linked oxidoreductase superfamily protein	ns	ns	ns	ns	**1.03**
CATMA1A49705	AT1G60710	ATB2__NAD(P)-linked oxidoreductase superfamily protein	ns	ns	ns	ns	**0.72**
CATMA1A49740	AT1G60750	NAD(P)-linked oxidoreductase superfamily protein	ns	ns	ns	**1.15**	**1.21**
CATMA1C71897	AT1G60950	ATFD2_FED A__2Fe-2S ferredoxin-like superfamily protein	ns	ns	ns	ns	**-0.72**
CATMA1A50390	AT1G61340	F-box family protein	ns	ns	ns	ns	**0.78**
CATMA1A50430	AT1G61380	SD1-29__S-domain-1 29	ns	ns	ns	ns	**0.90**
CATMA1A50605	AT1G61520	LHCA3__photosystem I light harvesting complex gene 3	ns	ns	ns	ns	**-0.75**
CATMA1A50730	AT1G61630	ATENT7_ENT7__equilibrative nucleoside transporter 7	ns	ns	ns	ns	**0.80**
CATMA1A50870	AT1G61790	Oligosaccharyltransferase complex/magnesium transporter family protein	ns	ns	ns	**0.74**	ns
CATMA1A50880	AT1G61800	ATGPT2_GPT2__glucose-6-phosphate/phosphate translocator 2	ns	ns	ns	ns	**0.83**
CATMA1C71919	AT1G61820	BGLU46__beta glucosidase 46	ns	ns	ns	**-0.93**	ns
CATMA1A51440	AT1G62320	ERD (early-responsive to dehydration stress) family protein	ns	**0.98**	ns	**0.94**	**0.85**
CATMA1A51690	AT1G62570	FMO GS-OX4__flavin-monooxygenase glucosinolate S-oxygenase 4	ns	ns	ns	ns	**0.78**
CATMA1A52120	AT1G62960	ACS10__ACC synthase 10	ns	ns	ns	ns	**-0.98**
CATMA1A53050	AT1G63830	PLAC8 family protein	ns	ns	ns	ns	**0.87**
CATMA1A53235	AT1G63980	D111/G-patch domain-containing protein	ns	ns	ns	ns	**-0.69**
CATMA1A53640	AT1G64355	unknown protein	ns	ns	ns	ns	**0.97**
CATMA1A53660	AT1G64370	unknown protein	ns	ns	**-1.01**	**-0.77**	ns
CATMA1A53750	AT1G64450	Glycine-rich protein family	ns	ns	**-1.05**	**-0.84**	ns
CATMA1A54050	AT1G64740	TUA1__alpha-1 tubulin	ns	ns	ns	**-0.83**	ns
CATMA1A54205	AT1G64900	CYP89_CYP89A2__cytochrome P450, family 89, subfamily A, polypeptide 2	ns	ns	**1.08**	**1.16**	**1.19**
CATMA1C71981	AT1G64930	CYP89A7__cytochrome P450, family 87, subfamily A, polypeptide 7	ns	ns	ns	**0.85**	**0.94**
CATMA1A54390	AT1G65110	Ubiquitin carboxyl-terminal hydrolase-related protein	ns	ns	ns	**0.79**	**1.18**
CATMA1A54570	AT1G65280	DNAJ heat shock N-terminal domain-containing protein	ns	ns	ns	**0.89**	**1.56**
CATMA1A54580	AT1G65290	mtACP2__mitochondrial acyl carrier protein 2	ns	ns	ns	ns	**2.63**
CATMA1A54830	AT1G65490	unknown protein	ns	ns	ns	ns	**-0.67**
CATMA1A54970	AT1G65690	Late embryogenesis abundant (LEA) hydroxyproline-rich glycoprotein family	ns	**1.01**	ns	**1.13**	**1.54**
CATMA1C72001	AT1G65845	unknown protein	ns	ns	ns	ns	**0.81**
CATMA1A55220	AT1G65930	cICDH__cytosolic NADP+-dependent isocitrate dehydrogenase	ns	ns	**-1.13**	**-0.96**	ns
CATMA1A55350	AT1G66090	Disease resistance protein (TIR-NBS class)	ns	ns	ns	ns	**1.67**
CATMA1A55360	AT1G66100	Plant thionin	ns	ns	ns	**0.82**	**-1.11**
CATMA1A55410	AT1G66160	ATCMPG1_CMPG1__CYS, MET, PRO, and GLY protein 1	ns	ns	ns	ns	**0.75**
CATMA1A55440	AT1G66180	Eukaryotic aspartyl protease family protein	ns	ns	**-1.07**	ns	**-0.68**
CATMA1A55460	AT1G66200	ATGSR2_GLN1;2_GSR2__glutamine synthase clone F11	ns	ns	ns	**-1.18**	ns
CATMA_GFT_02693	AT1G66570	ATSUC7_SUC7__sucrose-proton symporter 7	ns	ns	ns	**0.73**	ns
CATMA1A55860	AT1G66580	RPL10C_SAG24__senescence associated gene 24	ns	ns	ns	**1.26**	**1.44**
CATMA1A55946	AT1G66670	CLPP3_NCLPP3__CLP protease proteolytic subunit 3	ns	ns	ns	ns	**0.69**
CATMA1A56210	AT1G66920	Protein kinase superfamily protein	ns	ns	ns	ns	**0.77**
CATMA1A56880	AT1G67530	ARM repeat superfamily protein	ns	ns	ns	**0.69**	**1.01**
CATMA1A56950	AT1G67600	Acid phosphatase/vanadium-dependent haloperoxidase-related protein	ns	ns	ns	**1.25**	**1.07**
CATMA1C72047	AT1G67970	AT-HSFA8_HSFA8__heat shock transcription factor A8	ns	ns	ns	ns	**0.71**
CATMA1A57396_N	AT1G67980	CCOAMT__caffeoyl-CoA 3-O-methyltransferase	ns	ns	ns	ns	**1.14**
CATMA1A57406_N	AT1G68010	ATHPR1_HPR__hydroxypyruvate reductase	ns	ns	ns	**-0.82**	**-0.71**
CATMA1A57530	AT1G68160	Protein of unknown function (DUF3755)	ns	ns	ns	**0.70**	ns
CATMA1A57790	AT1G68410	Protein phosphatase 2C family protein	ns	ns	ns	**0.96**	ns

CATMA identifier	AGI identifier	Gene annotation	30 min	2h	4h	8h	24h
CATMA1A57900	AT1G68520	B-box type zinc finger protein with CCT domain	ns	ns	ns	**-0.76**	ns
CATMA1A57940	AT1G68570	Major facilitator superfamily protein	ns	ns	ns	ns	**1.14**
CATMA1A58250	AT1G68850	Peroxidase superfamily protein	ns	**0.86**	**1.01**	ns	ns
CATMA1A58470	AT1G69100	Eukaryotic aspartyl protease family protein	ns	ns	**-1.06**	**-1.21**	**-1.03**
CATMA1A58493	AT1G69170	Squamosa promoter-binding protein-like (SBP domain) transcription factor family protein	ns	ns	ns	ns	**-0.74**
CATMA1A58810	AT1G69500	CYP704B1__cytochrome P450, family 704, subfamily B, polypeptide 1	ns	ns	ns	**-0.71**	**0.71**
CATMA1C72074	AT1G69520	S-adenosyl-L-methionine-dependent methyltransferases superfamily protein	ns	ns	ns	**-0.69**	ns
CATMA1A59020	AT1G69710	Regulator of chromosome condensation (RCC1) family with FYVE zinc finger domain	ns	ns	ns	ns	**-0.76**
CATMA_GFT_02702	AT1G69750	ATCOX19-2_COX19-2__cytochrome c oxidase 19-2	ns	ns	**1.15**	**1.19**	**0.68**
CATMA1A59420	AT1G70140	ATFH8_FH8__formin 8	ns	ns	ns	ns	**0.70**
CATMA1A59450	AT1G70170	MMP__matrix metalloproteinase	ns	**0.85**	ns	**0.79**	**1.05**
CATMA1A59560	AT1G70280	NHL domain-containing protein	ns	ns	ns	**-0.90**	ns
CATMA1A59760	AT1G70490	ARFA1D_ATARFA1D__Ras-related small GTP-binding family protein	ns	ns	ns	ns	**1.04**
CATMA1A59940	AT1G70660	MMZ2_UEV1B__MMS ZWEI homologue 2	ns	ns	ns	ns	**-0.87**
CATMA1A60040	AT1G70770	Protein of unknown function DUF2359, transmembrane	ns	ns	ns	ns	**-0.71**
CATMA1A60070	AT1G70790	Calcium-dependent lipid-binding (CaLB domain) family protein	ns	ns	ns	**0.72**	ns
CATMA1C72092	AT1G70810	Calcium-dependent lipid-binding (CaLB domain) family protein	ns	ns	ns	**0.88**	**1.01**
CATMA1A60130	AT1G70850	MLP34__MLP-like protein 34	ns	ns	ns	ns	**-0.77**
CATMA1A60820	AT1G71500	Rieske (2Fe-2S) domain-containing protein	ns	ns	ns	ns	**-0.76**
CATMA1A60830	AT1G71520	Integrase-type DNA-binding superfamily protein	ns	ns	ns	**1.47**	ns
CATMA1A60840	AT1G71530	Protein kinase superfamily protein	ns	ns	ns	**0.70**	ns
CATMA1A61280	AT1G72060	serine-type endopeptidase inhibitors	ns	ns	ns	ns	**-0.67**
CATMA1A61300	AT1G72090	Methylthiotransferase	ns	ns	ns	**-0.74**	ns
CATMA1A61380	AT1G72150	PATL1__PATELLIN 1	ns	ns	**-1.36**	ns	ns
CATMA1A61710	AT1G72490	unknown protein	ns	ns	ns	**1.25**	**1.10**
CATMA1A61835	AT1G72610	ATGER1_GER1_GLP1__germin-like protein 1	ns	ns	ns	**-0.82**	**-1.15**
CATMA1A61900	AT1G72680	ATCAD1_CAD1__cinnamyl-alcohol dehydrogenase	ns	ns	ns	**0.81**	**1.37**
CATMA1C72125	AT1G72930	TIR__toll/interleukin-1 receptor-like	ns	ns	ns	**-1.33**	ns
CATMA1A62510	AT1G73220	AtOCT1_OCT1__organic cation/carnitine transporter1	ns	ns	ns	ns	**-0.74**
CATMA1A62540	AT1G73260	ATKTI1_KTI1__kunitz trypsin inhibitor 1	ns	ns	**-1.74**	ns	ns
CATMA1A62800	AT1G73490	RNA-binding (RRM/RBD/RNP motifs) family protein	ns	ns	ns	**0.77**	ns
CATMA1A63360	AT1G74010	Calcium-dependent phosphotriesterase superfamily protein	ns	**1.39**	**1.68**	**1.32**	**2.50**
CATMA1A63370	AT1G74020	SS2__strictosidine synthase 2	ns	**1.02**	ns	**1.43**	**1.40**
CATMA1A63440	AT1G74070	Cyclophilin-like peptidyl-prolyl cis-trans isomerase family protein	ns	ns	ns	ns	**-0.74**
CATMA1A63850	AT1G74450	Protein of unknown function (DUF793)	ns	**1.09**	**1.16**	**1.06**	**1.10**
CATMA1A64075	AT1G74710	ATICS1_EDS16_ICS1_SID2__ADC synthase superfamily protein	ns	ns	ns	ns	**1.41**
CATMA1C72158	AT1G75030	ATLP-3_TLP-3__thaumatin-like protein 3	ns	ns	**1.13**	**1.45**	**1.35**
CATMA1A64376	AT1G75040	PR-5_PR5__pathogenesis-related gene 5	ns	**1.32**	**1.50**	**1.71**	**1.75**
CATMA1A64610	AT1G75270	DHAR2__dehydroascorbate reductase 2	ns	ns	**1.09**	**1.60**	**1.49**
CATMA1A64615	AT1G75280	NmrA-like negative transcriptional regulator family protein	ns	ns	ns	**1.56**	**1.37**
CATMA1D02716	AT1G75290	NAD(P)-binding Rossmann-fold superfamily protein	ns	ns	ns	**0.92**	**0.86**
CATMA1C72164	AT1G75490	Integrase-type DNA-binding superfamily protein	ns	ns	ns	ns	**-0.78**
CATMA1A64990	AT1G75690	LQY1__DnaJ/Hsp40 cysteine-rich domain superfamily protein	ns	ns	ns	ns	**-0.97**
CATMA1C72165	AT1G75750	GASA1__GAST1 protein homolog 1	ns	ns	**-1.23**	ns	ns
CATMA1A65090	AT1G75800	Pathogenesis-related thaumatin superfamily protein	ns	ns	ns	ns	**-0.66**
CATMA1A65170	AT1G75900	GDSL-like Lipase/Acylhydrolase superfamily protein	ns	**1.31**	**1.60**	**1.36**	**1.02**
CATMA1A65300	AT1G76070	unknown protein	ns	ns	ns	**0.90**	**0.68**
CATMA1A65370	AT1G76150	ATECH2_ECH2__enoyl-CoA hydratase 2	ns	ns	ns	ns	**0.78**
CATMA1A65380	AT1G76160	sks5__SKU5 similar 5	ns	ns	ns	**-1.08**	ns
CATMA1A65720	AT1G76520	Auxin efflux carrier family protein	ns	ns	ns	**0.87**	**0.66**
CATMA1A65730	AT1G76530	Auxin efflux carrier family protein	ns	ns	ns	**0.90**	**0.88**
CATMA1A65800	AT1G76600	unknown protein	ns	ns	ns	**1.06**	**0.70**
CATMA1C72183	AT1G76680	ATOPR1_OPR1__12-oxophytodienoate reductase 1	ns	ns	ns	**1.22**	**2.04**
CATMA1A66220	AT1G76980	unknown protein	ns	**1.15**	**1.67**	**1.78**	**1.85**
CATMA1A66320	AT1G77120	ADH_ADH1_ATADH_ATADH1__alcohol dehydrogenase 1	ns	ns	ns	**1.30**	**1.02**
CATMA1A66420	AT1G77210	AtSTP14_STP14__sugar transporter 14	ns	ns	ns	**-0.72**	**-0.86**
CATMA1A66550	AT1G77330	2-oxoglutarate (2OG) and Fe(II)-dependent oxygenase superfamily protein	ns	**-0.80**	ns	ns	ns
CATMA1A66600	AT1G77380	AAP3_ATAAP3__amino acid permease 3	ns	ns	ns	**-0.91**	ns
CATMA1C72199	AT1G77510	ATPDI6_ATPDIL1-2_PDI6_PDIL1-2__PDI-like 1-2	ns	ns	ns	ns	**0.96**
CATMA1A66910	AT1G77760	GNR1_NIA1_NR1__nitrate reductase 1	ns	ns	**-1.38**	ns	ns
CATMA1A67090	AT1G77940	Ribosomal protein L7Ae/L30e/S12e/Gadd45 family protein	ns	ns	ns	ns	**-0.73**
CATMA1A67360	AT1G78240	OSU1_QUA2_TSD2__S-adenosyl-L-methionine-dependent methyltransferases superfamily protein	ns	ns	ns	**-0.82**	ns
CATMA1A67380	AT1G78270	AtUGT85A4_UGT85A4__UDP-glucosyl transferase 85A4	ns	ns	ns	**-0.79**	ns
CATMA1C72216	AT1G78340	ATGSTU22_GSTU22__glutathione S-transferase TAU 22	ns	ns	**1.62**	**1.75**	**1.69**
CATMA1A67475	AT1G78380	ATGSTU19_GST8_GSTU19__glutathione S-transferase TAU 19	ns	ns	**1.23**	**1.45**	**1.49**
CATMA1A67640	AT1G78570	ATRHM1_RHM1_ROL1__rhamnose biosynthesis 1	ns	ns	ns	ns	**0.76**
CATMA1A67730	AT1G78660	ATGGH1_GGH1__gamma-glutamyl hydrolase 1	ns	**1.98**	ns	**1.96**	**1.27**
CATMA1A67740	AT1G78670	ATGGH3_GGH3__gamma-glutamyl hydrolase 3	ns	ns	ns	**0.97**	**0.80**

CATMA identifier	AGI identifier	Gene annotation	30 min	2h	4h	8h	24h
CATMA1A67745	AT1G78680	ATGGH2_GGH2__gamma-glutamyl hydrolase 2	ns	**1.24**	ns	**1.53**	**1.00**
CATMA1A68110	AT1G78995	unknown protein	ns	ns	ns	**-0.88**	**-0.73**
CATMA1A68510	AT1G79410	AtOCT5_OCT5__organic cation/carnitine transporter5	ns	ns	ns	**1.49**	**1.35**
CATMA1A69225	AT1G80050	APT2_ATAPT2_PHT1.1__adenine phosphoribosyl transferase 2	ns	ns	ns	ns	**-0.70**
CATMA1A69240	AT1G80070	EMB14_EMB177_EMB33_SUS2__Pre-mRNA-processing-splicing factor	ns	ns	ns	**-0.69**	ns
CATMA1A69430	AT1G80240	Protein of unknown function, DUF642	ns	ns	ns	ns	**0.95**
CATMA1A69530	AT1G80330	ATGA3OX4_GA3OX4__gibberellin 3-oxidase 4	ns	ns	ns	ns	**0.83**
CATMA1A70055	AT1G80830	ATNRAMP1_NRAMP1_PMIT1__natural resistance-associated macrophage protein 1	ns	ns	ns	**-0.99**	**-0.75**
CATMA2A00260	AT2G01180	ATLPP1_ATPAP1_LPP1_PAP1__phosphatidic acid phosphatase 1	ns	ns	ns	**1.44**	**1.97**
CATMA2A00720	AT2G01670	atnudt17_NUDT17__nudix hydrolase homolog 17	ns	ns	ns	ns	**1.19**
CATMA2A00905	AT2G01850	ATXTH27_EXGT-A3_XTH27__endoxyloglucan transferase A3	ns	ns	**-1.26**	ns	ns
CATMA2B00960	AT2G01910	ATMAP65-6_MAP65-6__Microtubule associated protein (MAP65/ASE1) family protein	ns	ns	ns	**-0.71**	ns
CATMA2A01060	AT2G02000	GAD3__glutamate decarboxylase 3	ns	ns	ns	ns	**0.71**
CATMA2A01260	AT2G02180	TOM3__tobamovirus multiplication protein 3	ns	ns	ns	**0.78**	ns
CATMA2A01645	AT2G02760	ATUBC2_UBC2_UBC2__ubiquiting-conjugating enzyme 2	ns	ns	ns	**0.73**	ns
CATMA2A01705	AT2G02800	APK2B_Kin2__protein kinase 2B	ns	ns	ns	**0.71**	**0.71**
CATMA2A01885	AT2G02990	ATRNS1_RNS1__ribonuclease 1	ns	ns	**1.14**	ns	**1.23**
CATMA2A02140	AT2G03240	EXS (ERD1/XPR1/SYG1) family protein	ns	ns	ns	**-0.71**	ns
CATMA2A02770	AT2G03890	ATPI4K GAMMA 7_PI4K GAMMA 7_UBDK GAMMA 7__phosphoinositide 4-kinase gamma 7	ns	ns	ns	**-0.75**	ns
CATMA2A04100	AT2G05220	Ribosomal S17 family protein	ns	ns	ns	ns	**-0.86**
CATMA2A04160	AT2G05310	unknown protein	ns	ns	ns	ns	**-0.69**
CATMA2A04205	AT2G05380	GRP3S__glycine-rich protein 3 short isoform	ns	ns	ns	**1.00**	**1.85**
CATMA2A04295	AT2G05520	ATGRP-3_ATGRP3_GRP-3_GRP3__glycine-rich protein 3	ns	ns	ns	**0.70**	**1.61**
CATMA2C47087	AT2G05530	Glycine-rich protein family	ns	ns	ns	**0.85**	**1.73**
CATMA2A04450	AT2G05710	ACO3__aconitase 3	ns	ns	ns	**0.69**	**0.81**
CATMA2A04625	AT2G05840	PAA2__20S proteasome subunit PAA2	ns	ns	ns	ns	**0.77**
CATMA2A04765	AT2G05990	ENR1_MOD1__NAD(P)-binding Rossmann-fold superfamily protein	ns	ns	ns	ns	**-0.72**
CATMA2A05190	AT2G06520	PSBX__photosystem II subunit X	ns	ns	ns	ns	**-0.67**
CATMA2A05540	AT2G06850	EXGT-A1_EXT_XTH4__xyloglucan endotransglucosylase/hydrolase 4	ns	ns	ns	**-0.84**	ns
CATMA2A05825	AT2G07050	CAS1__cycloartenol synthase 1	ns	ns	ns	**-0.96**	ns
CATMA2A06390	AT2G07671	ATP synthase subunit C family protein	ns	ns	ns	**0.86**	**0.82**
CATMA_GFT_02404	AT2G07699	unknown protein	ns	ns	ns	ns	**0.81**
CATMA2A06650	AT2G07811	unknown protein	ns	ns	ns	**1.01**	ns
CATMA_GFT_00745	AT2G12190	Cytochrome P450 superfamily protein	ns	ns	**1.04**	**0.97**	**0.96**
CATMA2A10730	AT2G12557	unknown protein	ns	ns	ns	**0.81**	ns
CATMA2A13650	AT2G14920	ATST4A_ST4A__sulfotransferase 4A	ns	ns	ns	ns	**-0.73**
CATMA2A13890	AT2G15090	KCS8__3-ketoacyl-CoA synthase 8	ns	ns	ns	ns	**-0.66**
CATMA2C47189	AT2G15220	Plant basic secretory protein (BSP) family protein	ns	ns	ns	ns	**0.85**
CATMA2D02807	AT2G15240	UNC-50 family protein	ns	ns	ns	ns	**1.02**
CATMA2C47194	AT2G15500	RNA-binding protein	ns	ns	ns	**0.76**	**0.90**
CATMA2A14420	AT2G15530	RING/U-box superfamily protein	ns	**0.81**	ns	**1.71**	**2.15**
CATMA2A15240	AT2G16430	ATPAP10_PAP10__purple acid phosphatase 10	ns	ns	ns	ns	**0.96**
CATMA2C47224	AT2G16500	ADC1_ARGDC_ARGDC1_SPE1__arginine decarboxylase 1	ns	ns	ns	**1.85**	**1.23**
CATMA2D02819	AT2G16586	unknown protein	ns	ns	ns	**0.69**	ns
CATMA2A15360	AT2G16640	ATTOC132_TOC132__multimeric translocon complex in the outer envelope membrane 132	ns	ns	ns	**-0.79**	ns
CATMA2A16180	AT2G17500	Auxin efflux carrier family protein	ns	**0.80**	**1.19**	**1.79**	**1.20**
CATMA2A16420	AT2G17740	Cysteine/Histidine-rich C1 domain family protein	ns	ns	ns	ns	**1.67**
CATMA2A16500	AT2G17840	ERD7__Senescence/dehydration-associated protein-related	ns	ns	ns	ns	**0.85**
CATMA2A16860	AT2G18193	P-loop containing nucleoside triphosphate hydrolases superfamily protein	ns	ns	ns	**0.90**	**0.87**
CATMA2A17100	AT2G18450	SDH1-2__succinate dehydrogenase 1-2	ns	ns	ns	ns	**0.78**
CATMA2A17330	AT2G18680	unknown protein	ns	ns	ns	**0.75**	**1.97**
CATMA2A17340_N	AT2G18690	unknown protein	ns	ns	ns	ns	**1.98**
CATMA2A17545	AT2G18960	AHA1_HA1_OST2_PMA__H(+)-ATPase 1	ns	ns	ns	**-0.91**	ns
CATMA2A18290	AT2G19750	Ribosomal protein S30 family protein	ns	ns	ns	ns	**-0.76**
CATMA2C47318	AT2G20050	protein serine/threonine phosphatases;protein kinases;catalytics;cAMP-dependent protein kinase regulators;ATP binding;protein serine/threonine phosphatases	ns	ns	ns	**-0.79**	ns
CATMA_GFT_00812	AT2G20142	Toll-Interleukin-Resistance (TIR) domain family protein	ns	ns	ns	ns	**1.47**
CATMA2A19320	AT2G20760	Clathrin light chain protein	ns	ns	ns	ns	**0.70**
CATMA2A19595	AT2G20960	pEARLI4__Arabidopsis phospholipase-like protein (PEARLI 4) family	ns	ns	ns	**0.75**	ns
CATMA2A19870	AT2G21210	SAUR-like auxin-responsive protein family	ns	ns	ns	ns	**-0.78**
CATMA2A20020	AT2G21330	FBA1__fructose-bisphosphate aldolase 1	ns	ns	ns	ns	**-0.89**
CATMA2A20280	AT2G21620	RD2__Adenine nucleotide alpha hydrolases-like superfamily protein	ns	ns	ns	**1.28**	**1.82**
CATMA2A20680	AT2G22122	unknown protein	ns	ns	ns	**-1.00**	**-0.96**
CATMA2A20690	AT2G22125	CSI1_POM2__binding	ns	ns	ns	**-0.76**	ns

CATMA identifier	AGI identifier	Gene annotation	30 min	2h	4h	8h	24h
CATMA2A21020	AT2G22500	ATPUMP5_DIC1_UCP5__uncoupling protein 5	ns	ns	ns	ns	**0.87**
CATMA2A21470	AT2G22980	SCPL13__serine carboxypeptidase-like 13	ns	ns	ns	ns	**-0.66**
CATMA2A21610	AT2G23110	Late embryogenesis abundant protein, group 6	ns	ns	ns	**1.87**	**2.04**
CATMA2A21620	AT2G23120	Late embryogenesis abundant protein, group 6	ns	ns	ns	ns	**1.23**
CATMA2A21655	AT2G23150	ATNRAMP3_NRAMP3__natural resistance-associated macrophage protein 3	ns	ns	ns	ns	**1.69**
CATMA2C47379	AT2G23170	GH3.3__Auxin-responsive GH3 family protein	ns	ns	ns	ns	**0.73**
CATMA2A22070	AT2G23680	Cold acclimation protein WCOR413 family	ns	ns	ns	**0.88**	**1.12**
CATMA2A22170	AT2G23810	TET8__tetraspanin8	ns	ns	ns	ns	**1.15**
CATMA2A22600	AT2G24270	ALDH11A3__aldehyde dehydrogenase 11A3	ns	ns	ns	ns	**-0.70**
CATMA2A22825	AT2G24500	FZF__Zinc finger protein 622	ns	ns	ns	**1.13**	**0.76**
CATMA2A22930	AT2G24600	Ankyrin repeat family protein	ns	ns	ns	**-0.92**	ns
CATMA2A23310	AT2G25000	ATWRKY60_WRKY60__WRKY DNA-binding protein 60	ns	ns	ns	**-0.93**	ns
CATMA2A23850	AT2G25510	unknown protein	ns	ns	ns	ns	**-1.52**
CATMA2A24710	AT2G26380	Leucine-rich repeat (LRR) family protein	ns	ns	ns	**1.69**	**1.59**
CATMA2A24760	AT2G26440	Plant invertase/pectin methylesterase inhibitor superfamily	ns	ns	ns	**-0.72**	**0.68**
CATMA2A24825	AT2G26500	cytochrome b6f complex subunit (petM), putative	ns	ns	ns	ns	**-0.68**
CATMA2A25790	AT2G27385	Pollen Ole e 1 allergen and extensin family protein	ns	ns	**-1.40**	ns	**-1.00**
CATMA2C47453	AT2G27402	unknown protein	ns	ns	ns	ns	**-1.04**
CATMA2B25830	AT2G27420	Cysteine proteinases superfamily protein	ns	ns	ns	ns	**-1.47**
CATMA2C47455	AT2G27530	PGY1__Ribosomal protein L1p/L10e family	ns	ns	ns	ns	**-0.74**
CATMA2A26000	AT2G27580	A20/AN1-like zinc finger family protein	ns	ns	ns	**0.75**	ns
CATMA2C47460	AT2G27720	60S acidic ribosomal protein family	ns	ns	ns	ns	**-0.66**
CATMA2A27030	AT2G28605	Photosystem II reaction center PsbP family protein	ns	ns	ns	ns	**-0.80**
CATMA2A27320	AT2G28930	APK1B_PK1B__protein kinase 1B	ns	ns	ns	ns	**0.70**
CATMA2B27340	AT2G28950	ATEXP6_ATEXPA6_ATHEXP ALPHA 1.8_EXPA6__expansin A6	ns	ns	ns	ns	**-1.02**
CATMA_GFT_02855	AT2G29310	NAD(P)-binding Rossmann-fold superfamily protein	ns	ns	**-1.07**	**-0.92**	ns
CATMA2A27740	AT2G29340	NAD-dependent epimerase/dehydratase family protein	ns	ns	**-1.17**	ns	ns
CATMA2A27750	AT2G29350	SAG13__senescence-associated gene 13	ns	ns	ns	ns	**1.55**
CATMA2A27810	AT2G29420	ATGSTU7_GST25_GSTU7__glutathione S-transferase tau 7	ns	ns	ns	**1.49**	**1.36**
CATMA2A27830	AT2G29440	ATGSTU6_GST24_GSTU6__glutathione S-transferase tau 6	ns	**1.24**	**1.32**	**1.45**	ns
CATMA2D02856	AT2G29460	ATGSTU4_GST22_GSTU4__glutathione S-transferase tau 4	ns	ns	ns	**1.37**	**0.95**
CATMA2C47487	AT2G29470	ATGSTU3_GST21_GSTU3__glutathione S-transferase tau 3	ns	ns	ns	**1.14**	**0.76**
CATMA2C47488	AT2G29480	ATGSTU2_GST20_GSTU2__glutathione S-transferase tau 2	ns	ns	ns	**0.91**	**0.73**
CATMA2C47489	AT2G29490	ATGSTU1_GST19_GSTU1__glutathione S-transferase TAU 1	ns	ns	**1.34**	**1.00**	ns
CATMA2A27880	AT2G29500	HSP20-like chaperones superfamily protein	ns	ns	**1.15**	**1.11**	**1.53**
CATMA2A28010	AT2G29630	PY_THIC__thiaminC	ns	ns	ns	**-0.71**	ns
CATMA2A28280	AT2G29940	ABCG31_ATPDR3_PDR3__pleiotropic drug resistance 3	ns	ns	ns	**0.96**	ns
CATMA2A28340	AT2G30010	TBL45__TRICHOME BIREFRINGENCE-LIKE 45	ns	ns	ns	ns	**-0.66**
CATMA2A28440	AT2G30140	UDP-Glycosyltransferase superfamily protein	ns	ns	ns	ns	**0.67**
CATMA2A28685	AT2G30390	ATFC-II_FC-II_FC2__ferrochelatase 2	ns	ns	ns	**-0.80**	ns
CATMA2A28715	AT2G30440	Plsp2B_TPP__thylakoid processing peptide	ns	ns	ns	ns	**0.73**
CATMA2A28746	AT2G30490	ATC4H_C4H_CYP73A5_REF3__cinnamate-4-hydroxylase	ns	ns	**-1.19**	**-1.50**	**-1.21**
CATMA2A28860	AT2G30600	BTB/POZ domain-containing protein	ns	ns	**-1.07**	ns	ns
CATMA2C47512	AT2G30670	NAD(P)-binding Rossmann-fold superfamily protein	ns	ns	ns	**-0.73**	ns
CATMA2C47515	AT2G30860	ATGSTF7_ATGSTF9_GLUTTR_GSTF9__glutathione S-transferase PHI 9	ns	ns	ns	**-1.31**	ns
CATMA2A29670	AT2G31430	Plant invertase/pectin methylesterase inhibitor superfamily protein	ns	ns	ns	ns	**0.66**
CATMA2A29880	AT2G31660	EMA1_SAD2_URM9__ARM repeat superfamily protein	ns	ns	ns	ns	**0.68**
CATMA2A30110	AT2G31865	PARG2__poly(ADP-ribose) glycohydrolase 2	ns	ns	ns	ns	**1.17**
CATMA2A30340	AT2G32060	Ribosomal protein L7Ae/L30e/S12e/Gadd45 family protein	ns	ns	ns	ns	**-0.89**
CATMA2C47548	AT2G32190	unknown protein	ns	ns	ns	ns	**1.33**
CATMA2D02863	AT2G32200	unknown protein	ns	ns	ns	ns	**0.93**
CATMA2A30800	AT2G32510	MAPKKK17__mitogen-activated protein kinase kinase kinase 17	ns	**0.94**	ns	ns	ns
CATMA2A30970	AT2G32720	ATCB5-B_B5 #4_CB5-B__cytochrome B5 isoform B	ns	ns	ns	**-1.04**	**-1.08**
CATMA2A31025	AT2G32800	AP4.3A__protein kinase family protein	ns	**0.88**	ns	ns	**1.05**
CATMA2A31295	AT2G33120	ATVAMP722_SAR1_VAMP722__synaptobrevin-related protein 1	ns	ns	ns	ns	**0.81**
CATMA2A31305	AT2G33150	KAT2_PED1_PKT3__peroxisomal 3-ketoacyl-CoA thiolase 3	ns	ns	ns	**0.84**	**0.68**
CATMA2A31540	AT2G33380	AtCLO3_CLO-3_CLO3_RD20__Caleosin-related family protein	ns	ns	ns	ns	**0.77**
CATMA2A31850	AT2G33690	Late embryogenesis abundant protein, group 6	ns	ns	ns	ns	**0.68**
CATMA2A32070	AT2G33850	unknown protein	ns	ns	ns	ns	**-0.66**
CATMA2A32200	AT2G34070	TBL37__TRICHOME BIREFRINGENCE-LIKE 37	ns	ns	ns	**0.99**	ns
CATMA2A32300	AT2G34180	ATWL2_CIPK13_SnRK3.7_WL2__CBL-interacting protein kinase 13	ns	ns	ns	ns	**0.75**
CATMA2A32490	AT2G34355	Major facilitator superfamily protein	ns	ns	ns	**1.07**	ns
CATMA2A32620	AT2G34480	Ribosomal protein L18ae/LX family protein	ns	ns	ns	ns	**-0.75**
CATMA2A32640	AT2G34500	CYP710A1__cytochrome P450, family 710, subfamily A, polypeptide 1	ns	**1.17**	ns	**1.13**	**1.07**
CATMA2A32650	AT2G34510	Protein of unknown function, DUF642	ns	ns	ns	**-0.78**	ns

CATMA identifier	AGI identifier	Gene annotation	30 min	2h	4h	8h	24h
CATMA2A32895	AT2G34770	ATFAH1_FAH1__fatty acid hydroxylase 1	ns	ns	ns	**0.69**	ns
CATMA2C47605	AT2G35620	FEI2__Leucine-rich repeat protein kinase family protein	ns	ns	ns	**-0.73**	ns
CATMA2A33980	AT2G35800	SAMTL__mitochondrial substrate carrier family protein	ns	ns	ns	**-0.74**	ns
CATMA2A34180	AT2G35980	ATNHL10_NHL10_YLS9__Late embryogenesis abundant (LEA) hydroxyproline-rich glycoprotein family	ns	**1.72**	**1.96**	**1.81**	**2.34**
CATMA2A34320	AT2G36120	DOT1__Glycine-rich protein family	ns	ns	ns	ns	**-0.67**
CATMA2A34710	AT2G36460	Aldolase superfamily protein	ns	ns	ns	**0.72**	**1.08**
CATMA2A34850	AT2G36620	RPL24A__ribosomal protein L24	ns	ns	ns	ns	**-0.81**
CATMA2A34860	AT2G36630	Sulfite exporter TauE/SafE family protein	ns	ns	ns	ns	**-0.79**
CATMA2A34910	AT2G36690	2-oxoglutarate (2OG) and Fe(II)-dependent oxygenase superfamily protein	ns	**-1.13**	ns	ns	ns
CATMA2A34980	AT2G36750	UGT73C1__UDP-glucosyl transferase 73C1	ns	ns	ns	**0.99**	ns
CATMA_GFT_02874	AT2G36770	UDP-Glycosyltransferase superfamily protein	ns	ns	ns	**1.65**	ns
CATMA2A35230	AT2G36950	Heavy metal transport/detoxification superfamily protein	ns	ns	ns	**1.26**	**1.01**
CATMA2A35330	AT2G37040	ATPAL1_PAL1__PHE ammonia lyase 1	ns	**-1.09**	ns	**-0.69**	**-1.21**
CATMA2A35400	AT2G37110	PLAC8 family protein	ns	ns	ns	ns	**0.94**
CATMA2A35430	AT2G37130	Peroxidase superfamily protein	ns	ns	**-1.05**	**-1.04**	**-0.67**
CATMA2C47630_N	AT2G37170	PIP2;2_PIP2B__plasma membrane intrinsic protein 2	ns	ns	ns	**-0.98**	ns
CATMA2A35456	AT2G37180	PIP2;3_PIP2C_RD28__Aquaporin-like superfamily protein	ns	ns	ns	**-0.87**	**-0.82**
CATMA2A35500	AT2G37220	RNA-binding (RRM/RBD/RNP motifs) family protein	ns	ns	ns	ns	**-0.85**
CATMA2A35880	AT2G37600	Ribosomal protein L36e family protein	ns	ns	ns	ns	**-0.82**
CATMA2A35920	AT2G37640	ATEXP3_ATEXPA3_ATHEXP ALPHA 1.9_EXP3__Barwin-like endoglucanases superfamily protein	ns	ns	ns	**-0.88**	**-0.71**
CATMA2A36040	AT2G37760	AKR4C8__NAD(P)-linked oxidoreductase superfamily protein	ns	ns	ns	ns	**0.82**
CATMA2A36240	AT2G37940	AtIPCS2_ERH1__Arabidopsis Inositol phosphorylceramide synthase 2	ns	ns	ns	ns	**0.79**
CATMA2A36270	AT2G37970	SOUL-1__SOUL heme-binding family protein	ns	ns	ns	**0.83**	**0.74**
CATMA2A36560	AT2G38250	Homeodomain-like superfamily protein	ns	ns	ns	**0.71**	ns
CATMA2A36760	AT2G38470	ATWRKY33_WRKY33__WRKY DNA-binding protein 33	ns	ns	ns	ns	**0.99**
CATMA2A37026	AT2G38750	ANNAT4__annexin 4	ns	ns	**1.11**	ns	ns
CATMA2A37130	AT2G38870	Serine protease inhibitor, potato inhibitor I-type family protein	ns	ns	ns	ns	**1.18**
CATMA2A37430	AT2G39200	ATMLO12_MLO12__Seven transmembrane MLO family protein	ns	ns	ns	ns	**1.17**
CATMA2A37735	AT2G39460	ATRPL23A_RPL23A_RPL23A1_RPL23AA__ribosomal protein L23AA	ns	ns	ns	ns	**-0.86**
CATMA2A37780	AT2G39510	nodulin MtN21 /EamA-like transporter family protein	ns	**0.84**	ns	ns	ns
CATMA2A37790	AT2G39520	unknown protein	ns	ns	ns	ns	**0.74**
CATMA2A37967	AT2G39730	RCA__rubisco activase	ns	ns	ns	**-0.71**	**-0.88**
CATMA2A38220	AT2G40000	ATHSPRO2_HSPRO2__ortholog of sugar beet HS1 PRO-1 2	ns	ns	**-1.03**	ns	ns
CATMA2A38330	AT2G40095	Alpha/beta hydrolase related protein	ns	ns	ns	**0.84**	ns
CATMA2A38380	AT2G40140	ATSZF2_CZF1_SZF2_ZFAR1__zinc finger (CCCH-type) family protein	ns	ns	ns	ns	**1.06**
CATMA2A38620	AT2G40340	AtERF48_DREB2C__Integrase-type DNA-binding superfamily protein	ns	ns	ns	**1.10**	**0.85**
CATMA2A39220	AT2G40890	CYP98A3__cytochrome P450, family 98, subfamily A, polypeptide 3	ns	ns	ns	ns	**-0.74**
CATMA2A39435	AT2G41090	Calcium-binding EF-hand family protein	ns	ns	ns	**-0.69**	**0.70**
CATMA2C47695	AT2G41100	ATCAL4_TCH3__Calcium-binding EF hand family protein	ns	ns	ns	ns	**1.10**
CATMA2A39530	AT2G41180	SIB2__VQ motif-containing protein	ns	ns	ns	**0.75**	ns
CATMA2A39750	AT2G41380	S-adenosyl-L-methionine-dependent methyltransferases superfamily protein	ns	ns	ns	**0.87**	**1.99**
CATMA2A39780	AT2G41410	Calcium-binding EF-hand family protein	ns	ns	ns	ns	**0.84**
CATMA2A39960	AT2G41560	ACA4__autoinhibited Ca(2+)-ATPase, isoform 4	ns	ns	ns	**-0.95**	ns
CATMA2B40960	AT2G42530	COR15B__cold regulated 15b	ns	ns	ns	**0.88**	ns
CATMA2C47720	AT2G42540	COR15_COR15A__cold-regulated 15a	ns	ns	**1.10**	**0.79**	ns
CATMA2A41170	AT2G42740	RPL16A__ribosomal protein large subunit 16A	ns	ns	ns	ns	**-0.66**
CATMA2A41220	AT2G42790	CSY3__citrate synthase 3	ns	ns	ns	ns	**0.76**
CATMA2C47735	AT2G43290	MSS3__Calcium-binding EF-hand family protein	ns	ns	ns	ns	**0.71**
CATMA2A41775	AT2G43360	BIO2_BIOB__Radical SAM superfamily protein	ns	ns	ns	**-0.95**	ns
CATMA2C47736	AT2G43445	F-box and associated interaction domains-containing protein	ns	ns	ns	**0.73**	ns
CATMA2A41920	AT2G43510	ATTI1_TI1__trypsin inhibitor protein 1	ns	ns	ns	ns	**0.77**
CATMA2C47737	AT2G43535	Scorpion toxin-like knottin superfamily protein	ns	ns	ns	ns	**-0.79**
CATMA2B42010	AT2G43590	Chitinase family protein	ns	ns	ns	ns	**1.09**
CATMA2A42040	AT2G43620	Chitinase family protein	ns	ns	ns	ns	**1.46**
CATMA2A42575	AT2G44160	MTHFR2__methylenetetrahydrofolate reductase 2	ns	ns	ns	**-1.28**	**-0.95**
CATMA2A42660	AT2G44230	Plant protein of unknown function (DUF946)	ns	ns	ns	ns	**-1.03**
CATMA2C47752	AT2G44290	Bifunctional inhibitor/lipid-transfer protein/seed storage 2S albumin superfamily protein	ns	ns	ns	ns	**1.13**
CATMA2A42760	AT2G44350	ATCS_CSY4__Citrate synthase family protein	ns	ns	ns	ns	**0.91**
CATMA2A42780	AT2G44370	Cysteine/Histidine-rich C1 domain family protein	ns	ns	ns	ns	**0.79**
CATMA2A42890	AT2G44460	BGLU28__beta glucosidase 28	ns	ns	ns	**0.74**	**0.70**
CATMA2A43610	AT2G45220	Plant invertase/pectin methylesterase inhibitor superfamily	ns	ns	ns	ns	**0.70**
CATMA2A43760	AT2G45360	Protein of unknown function (DUF1442)	ns	**-0.89**	ns	**-0.93**	**-0.88**
CATMA2A43870	AT2G45470	AGP8_FLA8__FASCICLIN-like arabinogalactan protein 8	ns	ns	ns	ns	**-0.77**

CATMA identifier	AGI identifier	Gene annotation	30 min	2h	4h	8h	24h
CATMA2A43960	AT2G45550	CYP76C4__cytochrome P450, family 76, subfamily C, polypeptide 4	ns	ns	ns	**0.91**	**0.89**
CATMA2A43970	AT2G45570	CYP76C2__cytochrome P450, family 76, subfamily C, polypeptide 2	ns	ns	ns	ns	**0.90**
CATMA2A44365	AT2G45960	ATHH2_PIP1;2_PIP1B_TMP-A__plasma membrane intrinsic protein 1B	ns	ns	**-1.14**	**-0.77**	ns
CATMA2A44610	AT2G46220	Uncharacterized conserved protein (DUF2358)	ns	ns	ns	**0.96**	ns
CATMA2C47791	AT2G46390	SDH8__unknown protein	ns	ns	ns	ns	**0.73**
CATMA2A44770	AT2G46400	ATWRKY46_WRKY46__WRKY DNA-binding protein 46	ns	ns	ns	ns	**0.76**
CATMA2A44780	AT2G46420	Plant protein 1589 of unknown function	ns	ns	ns	**-0.72**	ns
CATMA2A45030	AT2G46600	Calcium-binding EF-hand family protein	ns	ns	ns	ns	**0.90**
CATMA2A45470	AT2G47000	ABCB4_ATPGP4_MDR4_PGP4__ATP binding cassette subfamily B4	ns	ns	ns	ns	**0.72**
CATMA2A45700	AT2G47240	CER8_LACS1__AMP-dependent synthetase and ligase family protein	ns	ns	ns	**-0.93**	ns
CATMA2A45920	AT2G47480	Protein of unknown function (DUF3511)	ns	ns	ns	ns	**0.77**
CATMA2A46140	AT2G47710	Adenine nucleotide alpha hydrolases-like superfamily protein	ns	ns	ns	ns	**0.78**
CATMA2A46160	AT2G47730	ATGSTF5_ATGSTF8_GST6_GSTF8__glutathione S-transferase phi 8	ns	ns	ns	**1.34**	**1.80**
CATMA2A46310	AT2G47890	B-box type zinc finger protein with CCT domain	ns	ns	ns	**0.98**	ns
CATMA2A46380	AT2G47940	DEGP2_EMB3117__DEGP protease 2	ns	ns	ns	**0.73**	ns
CATMA2A46540	AT2G48130	Bifunctional inhibitor/lipid-transfer protein/seed storage 2S albumin superfamily protein	ns	**0.94**	ns	ns	ns
CATMA2A46550	AT2G48140	EDA4__Bifunctional inhibitor/lipid-transfer protein/seed storage 2S albumin superfamily protein	ns	ns	**1.20**	**0.73**	ns
CATMA3A00185	AT3G01190	Peroxidase superfamily protein	ns	**-0.89**	**-1.01**	**-1.66**	**-1.02**
CATMA3A00350	AT3G01370	ATCFM2_CFM2__CRM family member 2	ns	ns	ns	**-0.72**	ns
CATMA3A00390	AT3G01420	ALPHA-DOX1_DIOX1_DOX1_PADOX-1__Peroxidase superfamily protein	ns	ns	ns	ns	**0.77**
CATMA3A00470	AT3G01480	ATCYP38_CYP38__cyclophilin 38	ns	ns	ns	ns	**-0.88**
CATMA3A00490	AT3G01500	ATBCA1_ATSABP3_CA1_SABP3__carbonic anhydrase 1	ns	ns	ns	ns	**-0.68**
CATMA3A00640	AT3G01640	ATGLCAK_GLCAK__glucuronokinase G	ns	ns	ns	**0.75**	ns
CATMA3A00690	AT3G01690	alpha/beta-Hydrolases superfamily protein	ns	ns	ns	ns	**-0.70**
CATMA3C57014	AT3G01930	Major facilitator superfamily protein	ns	ns	**-1.18**	ns	**-0.71**
CATMA3A00955	AT3G01970	ATWRKY45_WRKY45__WRKY DNA-binding protein 45	ns	ns	ns	**0.71**	ns
CATMA3A01030	AT3G02040	AtGDPD1_GDPD1_SRG3__senescence-related gene 3	ns	ns	ns	**0.71**	ns
CATMA3A01070	AT3G02080	Ribosomal protein S19e family protein	ns	ns	ns	ns	**-0.69**
CATMA3A01355	AT3G02380	ATCOL2_COL2__CONSTANS-like 2	ns	ns	ns	ns	**-1.15**
CATMA3A01530_N	AT3G02560	Ribosomal protein S7e family protein	ns	ns	ns	ns	**-0.80**
CATMA3A01800	AT3G02875	ILR1__Peptidase M20/M25/M40 family protein	ns	ns	ns	ns	**0.73**
CATMA3C57042	AT3G03150	unknown protein	ns	ns	**-1.17**	**-0.82**	ns
CATMA3C57935	AT3G03341	unknown protein	ns	ns	**1.15**	ns	ns
CATMA3A02720	AT3G03780	ATMS2_MS2__methionine synthase 2	ns	ns	ns	**-1.66**	**-2.22**
CATMA3A02970	AT3G04000	NAD(P)-binding Rossmann-fold superfamily protein	ns	**0.95**	**1.16**	**1.53**	**1.23**
CATMA3A02980	AT3G04010	O-Glycosyl hydrolases family 17 protein	ns	ns	ns	**0.90**	**0.66**
CATMA3A03070	AT3G04120	GAPC_GAPC-1_GAPC1__glyceraldehyde-3-phosphate dehydrogenase C subunit 1	ns	ns	ns	**1.09**	**1.11**
CATMA3A03260	AT3G04290	ATLTL1_LTL1__Li-tolerant lipase 1	ns	ns	ns	ns	**-0.81**
CATMA3A03265	AT3G04300	RmlC-like cupins superfamily protein	ns	**1.25**	**1.73**	**2.08**	**2.25**
CATMA3A03370	AT3G04400	emb2171__Ribosomal protein L14p/L23e family protein	ns	ns	ns	ns	**-0.67**
CATMA3A03743	AT3G04720	HEL_PR-4_PR4__pathogenesis-related 4	ns	ns	ns	ns	**1.00**
CATMA3A03860	AT3G04840	Ribosomal protein S3Ae	ns	ns	ns	ns	**-0.81**
CATMA3A03955	AT3G04940	ATCYSD1_CYSD1__cysteine synthase D1	ns	ns	ns	**-0.70**	ns
CATMA3A04215	AT3G05200	ATL6__RING/U-box superfamily protein	ns	ns	ns	**0.75**	ns
CATMA3A04930	AT3G05900	neurofilament protein-related	ns	ns	ns	ns	**-1.15**
CATMA3A05430	AT3G06350	EMB3004_MEE32__dehydroquinate dehydratase, putative / shikimate dehydrogenase, putative	ns	ns	ns	**-1.03**	**-0.85**
CATMA3A05500	AT3G06420	ATG8H__Ubiquitin-like superfamily protein	ns	ns	ns	**0.84**	ns
CATMA3A05650	AT3G06510	ATSFR2_SFR2__Glycosyl hydrolase superfamily protein	ns	ns	ns	**-0.76**	ns
CATMA3A05810	AT3G06650	ACLB-1__ATP-citrate lyase B-1	ns	ns	ns	**-0.73**	ns
CATMA3C57105	AT3G06750	hydroxyproline-rich glycoprotein family protein	ns	ns	ns	ns	**-0.68**
CATMA3A05990	AT3G06770	Pectin lyase-like superfamily protein	ns	ns	ns	ns	**-0.68**
CATMA3A06180	AT3G06980	DEA(D/H)-box RNA helicase family protein	ns	ns	ns	**-0.99**	ns
CATMA3A06550	AT3G07310	Protein of unknown function (DUF760)	ns	ns	**-1.12**	ns	ns
CATMA3A07410	AT3G08590	iPGAM2__Phosphoglycerate mutase, 2,3-bisphosphoglycerate-independent	ns	ns	ns	ns	**0.94**
CATMA3A07510	AT3G08690	ATUBC11_UBC11__ubiquitin-conjugating enzyme 11	ns	ns	ns	**0.69**	ns
CATMA3A07540	AT3G08740	elongation factor P (EF-P) family protein	ns	ns	ns	ns	**-0.95**
CATMA3A08125	AT3G09260	BGLU23_LEB_PSR3.1_PYK10__Glycosyl hydrolase superfamily protein	ns	ns	ns	**-0.85**	**-0.81**
CATMA3A08130	AT3G09270	ATGSTU8_GSTU8__glutathione S-transferase TAU 8	ns	ns	**1.15**	ns	**1.09**
CATMA3A08210	AT3G09350	Fes1A	ns	ns	ns	**0.70**	ns
CATMA3A08275	AT3G09390	ATMT-1_ATMT-K_MT2A__metallothionein 2A	ns	ns	ns	ns	**0.81**
CATMA3C57134	AT3G09440	Heat shock protein 70 (Hsp 70) family protein	ns	ns	ns	ns	**1.36**
CATMA3A08690	AT3G09820	ADK1_ATADK1__adenosine kinase 1	ns	ns	ns	**-0.97**	**-0.75**
CATMA3A08820	AT3G09940	ATMDAR3_MDAR2_MDAR3_MDHAR__monodehydroascorbate reductase	ns	ns	ns	ns	**0.98**
CATMA3A09500	AT3G10500	anac053_NAC053__NAC domain containing protein 53	ns	ns	ns	**1.48**	**1.16**
CATMA3A09650	AT3G10610	Ribosomal S17 family protein	ns	ns	ns	ns	**-0.67**

CATMA identifier	AGI identifier	Gene annotation	30 min	2h	4h	8h	24h
CATMA3A10050	AT3G10985	ATWI-12_SAG20_WI12__senescence associated gene 20	ns	ns	**-1.07**	ns	**0.74**
CATMA3A10205	AT3G11170	AtFAD7_FAD7_FADD__fatty acid desaturase 7	ns	ns	ns	ns	**-0.87**
CATMA3A10360	AT3G11340	UGT76B1__UDP-Glycosyltransferase superfamily protein	ns	ns	ns	ns	**0.73**
CATMA3A10470	AT3G11510	Ribosomal protein S11 family protein	ns	ns	ns	ns	**-0.83**
CATMA3A10755	AT3G11820	AT-SYR1_ATSYP121_ATSYR1_PEN1_SYP121_SYR1__syntaxin of plants 121	ns	ns	ns	ns	**0.77**
CATMA3A11535	AT3G12580	ATHSP70_HSP70__heat shock protein 70	ns	ns	ns	**0.77**	**1.42**
CATMA3A11910	AT3G12930	Lojap-related protein	ns	ns	ns	ns	**-0.67**
CATMA3C57188	AT3G13320	atcax2_CAX2__cation exchanger 2	ns	**0.87**	ns	ns	**0.89**
CATMA3A12620	AT3G13470	Cpn60beta2__TCP-1/cpn60 chaperonin family protein	ns	ns	ns	**-0.74**	ns
CATMA3A12660	AT3G13520	AGP12_ATAGP12__arabinogalactan protein 12	ns	ns	**1.08**	**1.39**	**0.88**
CATMA3C57193	AT3G13620	Amino acid permease family protein	ns	ns	ns	ns	**0.81**
CATMA3A13170	AT3G13950	unknown protein	ns	ns	ns	ns	**1.12**
CATMA3A13230	AT3G14000	ATBRXL2_BRX-LIKE2__DZC (Disease resistance/zinc finger/chromosome condensation-like region) domain containing protein	ns	ns	ns	**0.91**	ns
CATMA3A13460	AT3G14200	Chaperone DnaJ-domain superfamily protein	ns	ns	ns	**0.77**	ns
CATMA3A13520	AT3G14240	Subtilase family protein	ns	ns	ns	**-0.83**	ns
CATMA3A13690	AT3G14415	Aldolase-type TIM barrel family protein	ns	ns	ns	**-0.74**	ns
CATMA3A13940	AT3G14620	CYP72A8__cytochrome P450, family 72, subfamily A, polypeptide 8	ns	ns	ns	**0.86**	**1.40**
CATMA3C57211	AT3G14690	CYP72A15__cytochrome P450, family 72, subfamily A, polypeptide 15	ns	ns	ns	**0.70**	**0.66**
CATMA3A14120	AT3G14770	AtSWEET2_SWEET2__Nodulin MtN3 family protein	ns	ns	ns	**1.02**	ns
CATMA3A14930	AT3G15518	unknown protein	ns	ns	ns	ns	**0.83**
CATMA3A14940	AT3G15520	Cyclophilin-like peptidyl-prolyl cis-trans isomerase family protein	ns	ns	ns	ns	**-0.70**
CATMA3A15240	AT3G15850	ADS3_FAD5_FADB_JB67__fatty acid desaturase 5	ns	ns	ns	ns	**-0.91**
CATMA3A15360	AT3G15950	NAI2__DNA topoisomerase-related	ns	ns	ns	**-0.94**	**-1.30**
CATMA3A15500	AT3G16080	Zinc-binding ribosomal protein family protein	ns	ns	ns	ns	**-0.69**
CATMA3A15560	AT3G16150	ASPGB1__N-terminal nucleophile aminohydrolases (Ntn hydrolases) superfamily protein	ns	ns	**-1.48**	ns	ns
CATMA_GFT_02931	AT3G16390	NSP3__nitrile specifier protein 3	ns	ns	ns	**-1.03**	**-1.02**
CATMA3C57236	AT3G16400	ATMLP-470_ATNSP1_NSP1__nitrile specifier protein 1	ns	ns	ns	ns	**-1.11**
CATMA3C57238	AT3G16420	JAL30_PBP1__PYK10-binding protein 1	ns	ns	ns	ns	**-1.02**
CATMA3C57239	AT3G16430	JAL31__jacalin-related lectin 31	ns	ns	ns	ns	**-0.87**
CATMA3A15865	AT3G16440	ATMLP-300B_MEE36_MLP-300B__myrosinase-binding protein-like protein-300B	ns	ns	ns	ns	**-0.91**
CATMA3A15870	AT3G16450	JAL33__Mannose-binding lectin superfamily protein	ns	ns	ns	ns	**-1.30**
CATMA3A15880	AT3G16460	JAL34__Mannose-binding lectin superfamily protein	ns	ns	ns	**-0.89**	**-1.53**
CATMA3C57243	AT3G16690	AtSWEET16_SWEET16__Nodulin MtN3 family protein	ns	ns	ns	ns	**-0.81**
CATMA3A16175	AT3G16770	ATEBP_EBP_ERF72_RAP2.3__ethylene-responsive element binding protein	ns	ns	**-1.16**	**-0.76**	**-0.71**
CATMA3A16580	AT3G17170	RFC3__Translation elongation factor EF1B/ribosomal protein S6 family protein	ns	ns	ns	**-0.72**	**-0.79**
CATMA3A16820	AT3G17390	MAT4_MTO3_SAMS3__S-adenosylmethionine synthetase family protein	ns	ns	ns	**-0.85**	ns
CATMA3A16940	AT3G17510	CIPK1_SnRK3.16__CBL-interacting protein kinase 1	ns	ns	ns	ns	**-0.76**
CATMA3A17290	AT3G17790	ATACP5_ATPAP17_PAP17__purple acid phosphatase 17	ns	ns	ns	ns	**0.86**
CATMA3A17310	AT3G17810	PYD1__pyrimidine 1	ns	ns	ns	ns	**0.72**
CATMA3A17790	AT3G18250	Putative membrane lipoprotein	ns	ns	ns	ns	**0.71**
CATMA3A17960	AT3G18390	EMB1865__CRS1 / YhbY (CRM) domain-containing protein	ns	ns	ns	**-0.83**	**-0.76**
CATMA3A18350	AT3G18740	RLK902__Ribosomal protein L7Ae/L30e/S12e/Gadd45 family protein	ns	ns	ns	ns	**-0.67**
CATMA3A19045	AT3G19450	ATCAD4_CAD_CAD-C_CAD4__GroES-like zinc-binding alcohol dehydrogenase family protein	ns	**-0.82**	**-1.22**	**-1.74**	**-1.74**
CATMA3A19070	AT3G19480	D-3-phosphoglycerate dehydrogenase	ns	ns	ns	ns	**-0.77**
CATMA3A19415	AT3G19820	CBB1_DIM_DIM1_DWF1_EVE1__cell elongation protein / DWARF1 / DIMINUTO (DIM)	ns	ns	ns	**-1.27**	**-1.15**
CATMA3A19545	AT3G19930	ATSTP4_STP4__sugar transporter 4	ns	ns	**-1.18**	ns	ns
CATMA3A20050	AT3G20370	TRAF-like family protein	ns	ns	ns	**-0.94**	**-1.06**
CATMA3A20070	AT3G20390	endoribonuclease L-PSP family protein	ns	ns	ns	ns	**-0.78**
CATMA3A20080	AT3G20395	RING/U-box superfamily protein	ns	ns	ns	ns	**-0.71**
CATMA3A20210	AT3G20500	ATPAP18_PAP18__purple acid phosphatase 18	ns	ns	ns	ns	**0.68**
CATMA3A20220	AT3G20510	Transmembrane proteins 14C	ns	ns	ns	ns	**0.96**
CATMA3A20560	AT3G20820	Leucine-rich repeat (LRR) family protein	ns	ns	ns	ns	**-0.86**
CATMA3A20880	AT3G21055	PSBTN__photosystem II subunit T	ns	ns	ns	**-1.01**	ns
CATMA3A20920	AT3G21080	ABC transporter-related	ns	ns	ns	ns	**0.87**
CATMA3A21390	AT3G21520	AtDMP1_DMP1__DUF679 domain membrane protein 1	ns	**1.10**	ns	**0.92**	**0.97**
CATMA3A21430	AT3G21560	UGT84A2__UDP-Glycosyltransferase superfamily protein	ns	**1.48**	**2.21**	**1.60**	**1.93**
CATMA3A21590	AT3G21720	ICL__isocitrate lyase	ns	ns	ns	**0.72**	ns
CATMA3C57319	AT3G22210	unknown protein	ns	ns	ns	ns	**-0.74**
CATMA3A22365	AT3G22370	AOX1A_ATAOX1A_AtHSR3_HSR3__alternative oxidase 1A	ns	ns	ns	**0.99**	**1.18**
CATMA3A22410	AT3G22420	ATWNK2_WNK2_ZIK3__with no lysine (K) kinase 2	ns	ns	ns	**-0.70**	**-1.04**
CATMA3A22520	AT3G22530	unknown protein	ns	ns	ns	**0.72**	ns
CATMA3C57326	AT3G22600	Bifunctional inhibitor/lipid-transfer protein/seed storage 2S albumin superfamily protein	ns	**1.68**	**1.96**	**1.36**	**1.96**

CATMA identifier	AGI identifier	Gene annotation	30 min	2h	4h	8h	24h
CATMA3A22590	AT3G22620	Bifunctional inhibitor/lipid-transfer protein/seed storage 2S albumin superfamily protein	ns	**1.35**	ns	**0.82**	**1.00**
CATMA3A22910	AT3G22960	PKP-ALPHA_PKP1__Pyruvate kinase family protein	ns	ns	ns	**-0.70**	ns
CATMA3A23300	AT3G23300	S-adenosyl-L-methionine-dependent methyltransferases superfamily protein	ns	ns	ns	**-0.72**	ns
CATMA3A23320	AT3G23390	Zinc-binding ribosomal protein family protein	ns	ns	ns	ns	**-0.77**
CATMA3A23470	AT3G23560	ALF5__MATE efflux family protein	ns	ns	ns	ns	**0.82**
CATMA3A23830	AT3G23880	F-box and associated interaction domains-containing protein	ns	**-0.81**	ns	ns	ns
CATMA3A23850	AT3G23920	BAM1_BMY7_TR-BAMY__beta-amylase 1	ns	ns	ns	ns	**0.77**
CATMA3A23870	AT3G23940	dehydratase family	ns	ns	ns	**-0.87**	ns
CATMA3A24096	AT3G24170	ATGR1_GR1__glutathione-disulfide reductase	ns	ns	ns	ns	**0.73**
CATMA3A24390	AT3G24500	ATMBF1C_MBF1C__multiprotein bridging factor 1C	ns	ns	ns	**0.77**	ns
CATMA3A24400	AT3G24503	ALDH1A_ALDH2C4_REF1__aldehyde dehydrogenase 2C4	ns	ns	ns	ns	**1.13**
CATMA3A24500	AT3G24540	AtPERK3_PERK3__Protein kinase superfamily protein	ns	ns	ns	ns	**0.81**
CATMA3C57381	AT3G25610	ATPase E1-E2 type family protein / haloacid dehalogenase-like hydrolase family protein	ns	ns	ns	**1.02**	**1.78**
CATMA3A25470	AT3G25690	AtCHUP1_CHUP1__Hydroxyproline-rich glycoprotein family protein	ns	ns	**-1.05**	ns	ns
CATMA_GFT_01090	AT3G25830	ATTPS-CIN_TPS-CIN_TPS-CIN__terpene synthase-like sequence-1,8-cineole	ns	ns	**1.19**	ns	ns
CATMA3A25860	AT3G26060	ATPRX Q_PRXQ__Thioredoxin superfamily protein	ns	ns	ns	**-0.79**	**-0.67**
CATMA3A26050	AT3G26200	CYP71B22__cytochrome P450, family 71, subfamily B, polypeptide 22	ns	ns	ns	**1.07**	**1.07**
CATMA3A26060	AT3G26210	CYP71B23__cytochrome P450, family 71, subfamily B, polypeptide 23	ns	ns	ns	ns	**1.01**
CATMA3C57399	AT3G26220	CYP71B3__cytochrome P450, family 71, subfamily B, polypeptide 3	ns	ns	ns	ns	**0.70**
CATMA_GFT_01102	AT3G26450	Polyketide cyclase/dehydrase and lipid transport superfamily protein	ns	ns	**1.04**	ns	ns
CATMA3A26310	AT3G26470	Powdery mildew resistance protein, RPW8 domain	ns	ns	ns	**0.73**	**1.26**
CATMA3A26416	AT3G26650	GAPA_GAPA-1__glyceraldehyde 3-phosphate dehydrogenase A subunit	ns	ns	ns	**-0.77**	**-0.69**
CATMA3A26630	AT3G26890	unknown protein	ns	ns	ns	**-0.70**	ns
CATMA3A27240	AT3G27380	SDH2-1__succinate dehydrogenase 2-1	ns	ns	ns	**0.99**	**0.95**
CATMA3C57427	AT3G27690	LHCB2_LHCB2.3_LHCB2.4__photosystem II light harvesting complex gene 2.3	ns	ns	ns	ns	**-1.00**
CATMA3A27615	AT3G27770	unknown protein	ns	ns	ns	**0.78**	ns
CATMA3A27690	AT3G27880	Protein of unknown function (DUF1645)	ns	**0.94**	ns	**0.71**	ns
CATMA3A27830	AT3G28040	Leucine-rich receptor-like protein kinase family protein	ns	ns	ns	ns	**-0.80**
CATMA3A28035	AT3G28210	PMZ_SAP12__zinc finger (AN1-like) family protein	ns	ns	ns	**1.60**	**2.09**
CATMA3A28050	AT3G28220	TRAF-like family protein	ns	ns	ns	ns	**-0.91**
CATMA3A28100	AT3G28270	Protein of unknown function (DUF677)	ns	ns	ns	ns	**-1.26**
CATMA3A28190	AT3G28340	GATL10_GolS8__galacturonosyltransferase-like 10	ns	ns	ns	**0.92**	**0.67**
CATMA3C57443	AT3G28740	CYP81D11__Cytochrome P450 superfamily protein	ns	ns	ns	**0.88**	**0.92**
CATMA3A28845	AT3G28910	ATMYB30_MYB30__myb domain protein 30	ns	ns	ns	**0.89**	ns
CATMA3A29010	AT3G29000	Calcium-binding EF-hand family protein	ns	ns	ns	ns	**0.69**
CATMA3A29325_N	AT3G29200	ATCM1_CM1__chorismate mutase 1	ns	ns	ns	**-0.95**	**-0.96**
CATMA3A29390	AT3G29250	AtSDR4_SDR4__NAD(P)-binding Rossmann-fold superfamily protein	ns	ns	ns	**-1.26**	ns
CATMA3C57461	AT3G29360	UGD2__UDP-glucose 6-dehydrogenase family protein	ns	ns	ns	ns	**0.87**
CATMA3A31275	AT3G30775	AT-POX_ATPDH_ATPOX_ERD5_PDH1_PRO1_PRODH__ Methylenetetrahydrofolate reductase family protein	ns	ns	**-1.57**	ns	ns
CATMA3A36600	AT3G43720	Bifunctional inhibitor/lipid-transfer protein/seed storage 2S albumin superfamily protein	ns	ns	ns	**-0.71**	**-0.86**
CATMA3A37080	AT3G44190	FAD/NAD(P)-binding oxidoreductase family protein	ns	ns	ns	**2.05**	**2.01**
CATMA3A37360	AT3G44430	unknown protein	ns	ns	ns	**0.76**	ns
CATMA3A37900	AT3G44880	ACD1_LLS1_PAO__Pheophorbide a oxygenase family protein with Rieske [2Fe-2S] domain	ns	ns	ns	ns	**0.68**
CATMA3A38175	AT3G45140	ATLOX2_LOX2__lipoxygenase 2	ns	ns	ns	ns	**-1.11**
CATMA3A38190	AT3G45160	Putative membrane lipoprotein	ns	ns	ns	ns	**-0.68**
CATMA3C57563	AT3G45180	Ubiquitin-like superfamily protein	ns	ns	ns	**0.86**	**0.87**
CATMA3C57579	AT3G45700	Major facilitator superfamily protein	ns	ns	ns	**-0.91**	**-0.93**
CATMA3C57580	AT3G45710	Major facilitator superfamily protein	ns	ns	ns	**-0.73**	ns
CATMA3C57581	AT3G45730	unknown protein	ns	ns	**-1.05**	**-0.71**	**-1.52**
CATMA_GFT_01303	AT3G46070	C2H2-type zinc finger family protein	ns	ns	ns	**0.88**	**1.29**
CATMA_GFT_01304	AT3G46080	C2H2-type zinc finger family protein	ns	**1.03**	ns	**1.39**	**1.72**
CATMA3A39230	AT3G46230	ATHSP17.4_HSP17.4__heat shock protein 17.4	ns	ns	ns	ns	**0.95**
CATMA3A39300	AT3G46280	protein kinase-related	ns	ns	ns	ns	**0.73**
CATMA3A39760	AT3G46670	UGT76E11__UDP-glucosyl transferase 76E11	ns	ns	ns	**0.79**	**0.90**
CATMA3A40150	AT3G47070	Unknown protein	ns	ns	ns	**-0.76**	ns
CATMA3C57618	AT3G47470	CAB4_LHCA4__light-harvesting chlorophyll-protein complex I subunit A4	ns	ns	ns	ns	**-0.71**
CATMA3A40490	AT3G47480	Calcium-binding EF-hand family protein	ns	ns	ns	ns	**0.93**
CATMA3A40980	AT3G47960	Major facilitator superfamily protein	ns	ns	ns	**-1.24**	ns
CATMA3A41100	AT3G48070	RING/U-box superfamily protein	ns	ns	ns	ns	**0.84**
CATMA_GFT_01324	AT3G48320	CYP71A21__cytochrome P450, family 71, subfamily A, polypeptide 21	ns	ns	ns	**0.88**	ns
CATMA3A41720	AT3G48730	GSA2__glutamate-1-semialdehyde 2,1-aminomutase 2	ns	ns	ns	**-0.72**	ns
CATMA3A41875	AT3G48870	ATCLPC_ATHSP93-III_ClpC2_HSP93-III__Clp ATPase	ns	ns	ns	**-0.85**	ns

CATMA identifier	AGI identifier	Gene annotation	30 min	2h	4h	8h	24h
CATMA3A41910	AT3G48930	EMB1080__Nucleic acid-binding, OB-fold-like protein	ns	ns	ns	ns	**-0.68**
CATMA3A41980	AT3G48990	AMP-dependent synthetase and ligase family protein	ns	ns	ns	**0.70**	ns
CATMA3A42560	AT3G49530	ANAC062_NAC062_NTL6__NAC domain containing protein 62	ns	ns	ns	ns	**1.28**
CATMA3C57667	AT3G49570	LSU3__response to low sulfur 3	ns	ns	**1.04**	ns	ns
CATMA3A42710	AT3G49670	BAM2__Leucine-rich receptor-like protein kinase family protein	ns	ns	ns	**-0.93**	**-0.76**
CATMA3A42990	AT3G49940	LBD38__LOB domain-containing protein 38	ns	ns	ns	ns	**-0.69**
CATMA3A43500	AT3G50440	ATMES10_MES10__methyl esterase 10	ns	**0.96**	ns	ns	**1.12**
CATMA3A43600	AT3G50560	NAD(P)-binding Rossmann-fold superfamily protein	ns	**1.05**	ns	ns	ns
CATMA3A43687	AT3G50685	unknown protein	ns	ns	ns	ns	**-0.66**
CATMA3A43750	AT3G50740	UGT72E1__UDP-glucosyl transferase 72E1	ns	ns	ns	**-0.88**	ns
CATMA3C57691	AT3G50770	CML41__calmodulin-like 41	ns	ns	ns	**-0.72**	**1.10**
CATMA3A43920	AT3G50910	unknown protein	ns	ns	ns	**0.86**	**0.66**
CATMA3A43940	AT3G50930	BCS1__cytochrome BC1 synthesis	ns	ns	ns	ns	**0.76**
CATMA3A43980	AT3G50970	LTI30_XERO2__dehydrin family protein	ns	**0.92**	ns	**1.16**	ns
CATMA3A44140	AT3G51130	unknown protein	ns	ns	ns	**0.83**	**0.67**
CATMA3A44230	AT3G51240	F3'H_F3H_TT6__flavanone 3-hydroxylase	ns	ns	**1.09**	ns	ns
CATMA3A44245	AT3G51260	PAD1__20S proteasome alpha subunit PAD1	ns	ns	ns	ns	**0.71**
CATMA3A44640	AT3G51660	Tautomerase/MIF superfamily protein	ns	ns	**1.47**	**1.80**	**2.27**
CATMA3A44650	AT3G51670	SEC14 cytosolic factor family protein / phosphoglyceride transfer family protein	ns	ns	ns	ns	**1.15**
CATMA3A44970	AT3G52060	Core-2/I-branching beta-1,6-N-acetylglucosaminyltransferase family protein	ns	ns	ns	**0.70**	ns
CATMA3A45070	AT3G52150	RNA-binding (RRM/RBD/RNP motifs) family protein	ns	ns	ns	ns	**-0.82**
CATMA3A45345	AT3G52430	ATPAD4_PAD4__alpha/beta-Hydrolases superfamily protein	ns	ns	ns	ns	**0.79**
CATMA3A45773	AT3G52840	BGAL2__beta-galactosidase 2	ns	ns	ns	**-0.78**	ns
CATMA3A45870	AT3G52930	Aldolase superfamily protein	ns	ns	ns	ns	**0.81**
CATMA3A46180_N	AT3G53260	ATPAL2_PAL2__phenylalanine ammonia-lyase 2	ns	**-0.99**	ns	ns	**-0.97**
CATMA3A46410_N	AT3G53460	CP29__chloroplast RNA-binding protein 29	ns	ns	**-1.04**	ns	ns
CATMA3A46760	AT3G53810	Concanavalin A-like lectin protein kinase family protein	ns	ns	ns	ns	**0.94**
CATMA3A46865	AT3G53920	SIG3_SIGC__RNApolymerase sigma-subunit C	ns	ns	ns	**-0.69**	ns
CATMA3A46990	AT3G54040	PAR1 protein	ns	ns	**-1.20**	ns	ns
CATMA3A47000	AT3G54050	HCEF1__high cyclic electron flow 1	ns	ns	ns	ns	**-0.72**
CATMA3A47350	AT3G54420	ATCHITIV_ATEP3_CHIV_EP3__homolog of carrot EP3-3 chitinase	ns	ns	ns	**0.98**	**2.05**
CATMA3A47520	AT3G54580	Proline-rich extensin-like family protein	ns	ns	ns	**-0.91**	**-0.82**
CATMA3C57794	AT3G54590	ATHRGP1_HRGP1__hydroxyproline-rich glycoprotein	ns	ns	ns	**-0.91**	**-0.74**
CATMA3A47540	AT3G54600	Class I glutamine amidotransferase-like superfamily protein	ns	ns	ns	**-0.77**	ns
CATMA3A47730	AT3G54810	BME3_BME3-ZF_GATA8__Plant-specific GATA-type zinc finger transcription factor family protein	ns	ns	ns	ns	**0.76**
CATMA3A47740	AT3G54820	PIP2;5_PIP2D__plasma membrane intrinsic protein 2;5	ns	**0.98**	ns	**0.77**	**1.01**
CATMA3A47840	AT3G54880	unknown protein	ns	ns	ns	ns	**-0.81**
CATMA3A48130	AT3G55120	A11_CFI_TT5__Chalcone-flavanone isomerase family protein	ns	ns	ns	ns	**-0.69**
CATMA3A48330	AT3G55330	PPL1__PsbP-like protein 1	ns	ns	ns	ns	**-0.88**
CATMA3A48400	AT3G55430	O-Glycosyl hydrolases family 17 protein	ns	ns	ns	**0.73**	ns
CATMA3B48595	AT3G55610	P5CS2__delta 1-pyrroline-5-carboxylate synthase 2	ns	ns	ns	ns	**-0.66**
CATMA3A48610	AT3G55630	ATDFD_DFD_FPGS3__DHFS-FPGS homolog D	ns	ns	ns	**-0.86**	**-1.06**
CATMA3A48860	AT3G55880	SUE4__Alpha/beta hydrolase related protein	ns	ns	ns	**0.82**	**0.94**
CATMA3A48940	AT3G55970	ATJRG21_JRG21__jasmonate-regulated gene 21	ns	ns	ns	**1.12**	**1.21**
CATMA3A48950	AT3G55980	ATSZF1_SZF1__salt-inducible zinc finger 1	ns	ns	ns	ns	**0.98**
CATMA3A49200	AT3G56260	unknown protein	ns	ns	ns	ns	**0.88**
CATMA3A49380	AT3G56400	ATWRKY70_WRKY70__WRKY DNA-binding protein 70	ns	ns	ns	ns	**0.70**
CATMA3A49680	AT3G56710	SIB1__sigma factor binding protein 1	ns	ns	ns	**0.75**	ns
CATMA3A49900	AT3G56910	PSRP5__plastid-specific 50S ribosomal protein 5	ns	ns	ns	ns	**-0.75**
CATMA3A50026	AT3G57050	CBL__cystathionine beta-lyase	ns	ns	ns	**-0.77**	ns
CATMA3A50400	AT3G57400	unknown protein	ns	ns	ns	**0.82**	ns
CATMA3A50520	AT3G57520	AtSIP2_RS2_SIP2__seed imbibition 2	ns	ns	ns	ns	**-0.78**
CATMA3A50680	AT3G57670	NTT_WIP2__C2H2-type zinc finger family protein	ns	ns	ns	ns	**0.85**
CATMA3A51750	AT3G58750	CSY2__citrate synthase 2	ns	ns	ns	ns	**0.76**
CATMA3A52190	AT3G59140	ABCC10_ATMRP14_MRP14__multidrug resistance-associated protein 14	ns	ns	ns	**0.76**	**0.67**
CATMA3A52725	AT3G59700	ATHLECRK_HLECRK_LECRK1__lectin-receptor kinase	ns	ns	ns	ns	**0.99**
CATMA3A52975	AT3G59970	MTHFR1__methylenetetrahydrofolate reductase 1	ns	ns	ns	**-1.30**	**-1.06**
CATMA3A53225	AT3G60190	ADL1E_ADL4_ADLP2_DL1E_DRP1E_EDR3__DYNAMIN-like 1E	ns	**0.82**	ns	ns	**1.11**
CATMA3A53335	AT3G60320	Protein of unknown function (DUF630 and DUF632)	ns	ns	ns	**-1.10**	**-0.77**
CATMA3A53430	AT3G60420	Phosphoglycerate mutase family protein	ns	ns	ns	ns	**1.16**
CATMA3A53460	AT3G60450	Phosphoglycerate mutase family protein	ns	ns	ns	ns	**0.95**
CATMA3A54593	AT3G61430	ATPIP1_PIP1_PIP1;1_PIP1A__plasma membrane intrinsic protein 1A	ns	ns	**-1.16**	**-0.94**	ns
CATMA3A54980	AT3G61820	Eukaryotic aspartyl protease family protein	ns	**1.06**	**1.35**	ns	**1.30**
CATMA3A55250	AT3G62110	Pectin lyase-like superfamily protein	ns	ns	ns	**-0.88**	ns
CATMA3A55290	AT3G62150	ABCB21_PGP21__P-glycoprotein 21	ns	ns	ns	**1.00**	**0.71**

CATMA identifier	AGI identifier	Gene annotation	30 min	2h	4h	8h	24h
CATMA3A55410	AT3G62260	Protein phosphatase 2C family protein	ns	ns	ns	ns	**0.81**
CATMA3A55700	AT3G62530	ARM repeat superfamily protein	ns	ns	ns	ns	**-0.81**
CATMA3A55770	AT3G62600	ATERDJ3B_ERDJ3B__DNAJ heat shock family protein	ns	ns	ns	ns	**0.79**
CATMA3A56350	AT3G63160	Unknown protein	ns	ns	ns	**-0.92**	ns
CATMA4C42011	AT4G00550	DGD2__digalactosyl diacylglycerol deficient 2	ns	ns	ns	ns	**0.66**
CATMA4A00800	AT4G00750	S-adenosyl-L-methionine-dependent methyltransferases superfamily protein	ns	ns	ns	**0.95**	ns
CATMA4A01250	AT4G01070	GT72B1_UGT72B1__UDP-Glycosyltransferase superfamily protein	ns	**0.84**	ns	**1.03**	**0.86**
CATMA4A01430	AT4G01250	AtWRKY22_WRKY22__WRKY family transcription factor	ns	ns	ns	ns	**0.77**
CATMA4C42026	AT4G01265	Unknown protein	ns	ns	**-1.34**	ns	ns
CATMA_GFT_01425	AT4G01770	RGXT1__rhamnogalacturonan xylosyltransferase 1	ns	ns	ns	ns	**0.95**
CATMA4C42043	AT4G01800	AGY1_AtcpSecA_SECA1__Albino or Glassy Yellow 1	ns	ns	ns	**-0.81**	ns
CATMA4A02680	AT4G02380	AtLEA5_SAG21__senescence-associated gene 21	ns	ns	ns	ns	**1.17**
CATMA4A03280	AT4G02940	oxidoreductase, 2OG-Fe(II) oxygenase family protein	ns	ns	**1.00**	**1.30**	**0.87**
CATMA4A03586_N	AT4G03280	PETC_PGR1__photosynthetic electron transfer C	ns	ns	ns	ns	**-0.69**
CATMA4C42083	AT4G03320	AtTic20-IV_Tic20-IV__translocon at the inner envelope membrane of chloroplasts 20-IV	ns	ns	ns	**1.00**	**0.82**
CATMA4A03800	AT4G03450	Ankyrin repeat family protein	ns	ns	ns	ns	**0.76**
CATMA4C42092	AT4G03540	Uncharacterised protein family (UPF0497)	ns	ns	**1.09**	ns	ns
CATMA4A05135	AT4G04610	APR_APR1_ATAPR1_PRH19__APS reductase 1	ns	ns	ns	**1.09**	**0.98**
CATMA4C42113	AT4G04745	unknown protein	ns	ns	**1.01**	ns	ns
CATMA4A05940	AT4G05310	Ubiquitin-like superfamily protein	ns	ns	ns	ns	**-0.71**
CATMA4C42144	AT4G06744	Leucine-rich repeat (LRR) family protein	ns	ns	ns	**-0.73**	ns
CATMA4A09810	AT4G09750	NAD(P)-binding Rossmann-fold superfamily protein	ns	ns	ns	ns	**0.71**
CATMA4A10160	AT4G10110	RNA-binding (RRM/RBD/RNP motifs) family protein	ns	ns	ns	ns	**0.95**
CATMA4A10410	AT4G10380	AtNIP5;1_NIP5;1_NLM6_NLM8__NOD26-like intrinsic protein 5;1	ns	ns	ns	ns	**0.85**
CATMA4A10490	AT4G10450	Ribosomal protein L6 family	ns	ns	ns	**-0.71**	ns
CATMA4C42222	AT4G11310	Papain family cysteine protease	ns	ns	ns	**-0.75**	ns
CATMA4A11720	AT4G11570	Haloacid dehalogenase-like hydrolase (HAD) superfamily protein	ns	ns	ns	**0.78**	ns
CATMA4A11745	AT4G11600	ATGPX6_GPX6_LSC803_PHGPX__glutathione peroxidase 6	ns	ns	ns	**1.03**	**1.95**
CATMA4A11780_N	AT4G11650	ATOSM34_OSM34__osmotin 34	ns	**0.93**	ns	ns	**1.31**
CATMA4A12000	AT4G11890	Protein kinase superfamily protein	ns	ns	ns	ns	**1.38**
CATMA_GFT_01594	AT4G12310	CYP706A5__cytochrome P450, family 706, subfamily A, polypeptide 5	ns	ns	ns	**-0.88**	ns
CATMA4A12530	AT4G12420	SKU5__Cupredoxin superfamily protein	ns	ns	ns	**-1.07**	ns
CATMA4C42251	AT4G12480	EARLI1_pEARLI 1__Bifunctional inhibitor/lipid-transfer protein/seed storage 2S albumin superfamily protein	ns	ns	ns	ns	**1.19**
CATMA4C42252	AT4G12490	Bifunctional inhibitor/lipid-transfer protein/seed storage 2S albumin superfamily protein	ns	ns	ns	ns	**1.90**
CATMA4C42253	AT4G12500	Bifunctional inhibitor/lipid-transfer protein/seed storage 2S albumin superfamily protein	ns	ns	ns	ns	**1.32**
CATMA4D03132	AT4G12545	Bifunctional inhibitor/lipid-transfer protein/seed storage 2S albumin superfamily protein	ns	ns	ns	**-1.20**	**-1.66**
CATMA4A12760	AT4G12600	Ribosomal protein L7Ae/L30e/S12e/Gadd45 family protein	ns	ns	ns	ns	**-0.92**
CATMA4A12860	AT4G12720	AtNUDT7_GFG1_NUDT7__MutT/nudix family protein	ns	ns	ns	ns	**1.07**
CATMA4A13280	AT4G13180	NAD(P)-binding Rossmann-fold superfamily protein	ns	ns	**1.03**	**1.07**	**1.39**
CATMA4A13370	AT4G13250	NYC1__NAD(P)-binding Rossmann-fold superfamily protein	ns	ns	ns	ns	**1.08**
CATMA4C42276	AT4G13410	ATCSLA15_CSLA15__Nucleotide-diphospho-sugar transferases superfamily protein	ns	ns	ns	ns	**-0.77**
CATMA4A14010	AT4G13840	HXXXD-type acyl-transferase family protein	ns	ns	ns	ns	**-0.79**
CATMA4A14040	AT4G13870	ATWEX_ATWRNEXO_WEX_WRNEXO__Werner syndrome-like exonuclease	ns	ns	ns	ns	**-1.19**
CATMA4A14135	AT4G13940	ATSAHH1_EMB1395_HOG1_MEE58_SAHH1__S-adenosyl-L-homocysteine hydrolase	ns	ns	ns	**-0.82**	ns
CATMA4A14250	AT4G14040	EDA38_SBP2__selenium-binding protein 2	ns	ns	**-1.01**	**-0.70**	ns
CATMA4A14375	AT4G14130	XTH15_XTR7__xyloglucan endotransglucosylase/hydrolase 15	ns	ns	ns	ns	**-0.67**
CATMA4A14640	AT4G14320	Zinc-binding ribosomal protein family protein	ns	ns	ns	ns	**-0.70**
CATMA4A14700	AT4G14365	XBAT34__XB3 ortholog 4 in Arabidopsis thaliana	ns	ns	ns	ns	**1.36**
CATMA4A15020	AT4G14630	GLP9__germin-like protein 9	ns	ns	ns	ns	**1.09**
CATMA4A15350	AT4G14890	FdC2__2Fe-2S ferredoxin-like superfamily protein	ns	ns	ns	**-0.97**	**-1.01**
CATMA4A15480	AT4G15000	Ribosomal L27e protein family	ns	ns	ns	ns	**-0.70**
CATMA4A15700	AT4G15160	Bifunctional inhibitor/lipid-transfer protein/seed storage 2S albumin superfamily protein	ns	ns	ns	ns	**-0.75**
CATMA4A15970	AT4G15340	04C11_ATPEN1_PEN1__pentacyclic triterpene synthase 1	ns	ns	ns	**-0.80**	ns
CATMA4D03142	AT4G15390	HXXXD-type acyl-transferase family protein	ns	ns	ns	**-1.39**	**-1.54**
CATMA4A16210	AT4G15480	UGT84A1__UDP-Glycosyltransferase superfamily protein	ns	ns	**1.27**	**1.02**	**1.40**
CATMA4A16293	AT4G15550	IAGLU__indole-3-acetate beta-D-glucosyltransferase	ns	ns	ns	**0.91**	ns
CATMA4D03144	AT4G15630	Uncharacterised protein family (UPF0497)	ns	ns	ns	ns	**-0.79**
CATMA4A16545	AT4G15760	MO1__monooxygenase 1	ns	ns	ns	ns	**0.75**
CATMA4C42335	AT4G16146	cAMP-regulated phosphoprotein 19-related protein	ns	ns	ns	**-0.80**	ns
CATMA4A16980	AT4G16190	Papain family cysteine protease	ns	ns	ns	**0.91**	**0.66**
CATMA4A17500	AT4G16563	Eukaryotic aspartyl protease family protein	ns	ns	**-1.06**	**-0.73**	ns
CATMA4A17600	AT4G16660	heat shock protein 70 (Hsp 70) family protein	ns	ns	ns	ns	**0.72**
CATMA4A17800	AT4G16830	Hyaluronan / mRNA binding family	ns	ns	ns	**-0.82**	ns

CATMA identifier	AGI identifier	Gene annotation	30 min	2h	4h	8h	24h
CATMA4C42351	AT4G16860	RPP4__Disease resistance protein (TIR-NBS-LRR class) family	ns	ns	ns	ns	**0.74**
CATMA_GFT_01632	AT4G16920	Disease resistance protein (TIR-NBS-LRR class) family	ns	ns	ns	**0.76**	**0.68**
CATMA4A18000	AT4G16980	arabinogalactan-protein family	ns	ns	ns	ns	**-1.14**
CATMA4A18330	AT4G17280	Auxin-responsive family protein	ns	**0.89**	ns	ns	ns
CATMA4A18370	AT4G17340	DELTA-TIP2_TIP2;2__tonoplast intrinsic protein 2;2	ns	ns	ns	ns	**0.94**
CATMA4A18440	AT4G17390	Ribosomal protein L23/L15e family protein	ns	ns	ns	ns	**-0.70**
CATMA4A18485	AT4G17460	HAT1__Homeobox-leucine zipper protein 4 (HB-4) / HD-ZIP protein	ns	ns	ns	ns	**-0.83**
CATMA4A18580	AT4G17560	Ribosomal protein L19 family protein	ns	ns	ns	ns	**-0.66**
CATMA4A18645	AT4G17615	ATCBL1_CBL1_SCABP5__calcineurin B-like protein 1	ns	ns	ns	**1.10**	**0.73**
CATMA4A18850	AT4G17810	C2H2 and C2HC zinc fingers superfamily protein	ns	ns	ns	**-0.78**	**-1.03**
CATMA4A18870	AT4G17840	unknown protein	ns	ns	ns	**0.99**	ns
CATMA4A19280	AT4G18240	ATSS4_SS4_SSIV__starch synthase 4	ns	ns	ns	**-0.77**	ns
CATMA4A19570	AT4G18480	CH-42_CH42_CHL11_CHLI-1_CHLI1__P-loop containing nucleoside triphosphate hydrolases superfamily protein	ns	ns	ns	**-0.73**	ns
CATMA4A19590	AT4G18510	CLE2__CLAVATA3/ESR-related 2	ns	ns	ns	**-0.92**	ns
CATMA4A20400	AT4G19200	proline-rich family protein	ns	ns	ns	**0.69**	**1.10**
CATMA4C42396	AT4G19420	Pectinacetylesterase family protein	ns	ns	ns	**-0.71**	ns
CATMA4C42406	AT4G19880	Glutathione S-transferase family protein	ns	ns	ns	ns	**0.98**
CATMA4A22340	AT4G20830	FAD-binding Berberine family protein	ns	ns	ns	**0.87**	**1.20**
CATMA4A22370	AT4G20860	FAD-binding Berberine family protein	ns	**0.91**	ns	**1.45**	**1.79**
CATMA4A22690	AT4G21120	AAT1_CAT1__amino acid transporter 1	ns	ns	ns	ns	**0.76**
CATMA4A23540	AT4G21870	HSP20-like chaperones superfamily protein	ns	ns	ns	ns	**-0.88**
CATMA4A23655	AT4G21960	PRXR1__Peroxidase superfamily protein	ns	ns	ns	**-0.76**	ns
CATMA4C42448	AT4G22210	LCR85__low-molecular-weight cysteine-rich 85	ns	ns	ns	**-1.56**	**-1.27**
CATMA4A24100	AT4G22380	Ribosomal protein L7Ae/L30e/S12e/Gadd45 family protein	ns	ns	ns	ns	**-0.69**
CATMA4A24750	AT4G23010	ATUTR2_UTR2__UDP-galactose transporter 2	ns	ns	ns	ns	**0.72**
CATMA4A24800	AT4G23050	PAS domain-containing protein tyrosine kinase family protein	ns	ns	ns	**0.81**	ns
CATMA4A24945	AT4G23190	AT-RLK3_CRK11__cysteine-rich RLK (RECEPTOR-like protein kinase) 11	ns	ns	ns	**0.80**	**1.38**
CATMA4A25210	AT4G23400	PIP1;5_PIP1D__plasma membrane intrinsic protein 1;5	ns	ns	**-1.06**	**-0.99**	**-1.50**
CATMA4A25290	AT4G23470	PLAC8 family protein	ns	ns	ns	ns	**1.14**
CATMA4A25390	AT4G23550	ATWRKY29_WRKY29__WRKY family transcription factor	ns	ns	ns	**-0.76**	**-1.01**
CATMA4C42473	AT4G23680	Polyketide cyclase/dehydrase and lipid transport superfamily protein	ns	ns	ns	ns	**0.76**
CATMA4A25530	AT4G23700	ATCHX17_CHX17__cation/H+ exchanger 17	ns	ns	ns	ns	**0.97**
CATMA4A25590	AT4G23770	unknown protein	ns	ns	ns	ns	**0.75**
CATMA4A25640	AT4G23820	Pectin lyase-like superfamily protein	ns	ns	ns	**-0.74**	**-0.76**
CATMA4A25880	AT4G24160	alpha/beta-Hydrolases superfamily protein	ns	ns	ns	**1.52**	**1.25**
CATMA4A25970	AT4G24230	ACBP3__acyl-CoA-binding domain 3	ns	ns	**-1.22**	ns	ns
CATMA4A26240	AT4G24510	CER2_VC-2_VC2__HXXXD-type acyl-transferase family protein	ns	ns	ns	ns	**-0.76**
CATMA4A26400	AT4G24690	AtNBR1_NBR1__ubiquitin-associated (UBA)/TS-N domain-containing protein / octicosapeptide/Phox/Bemp1 (PB1) domain-containing protein	ns	ns	ns	ns	**0.93**
CATMA4A26430	AT4G24730	Calcineurin-like metallo-phosphoesterase superfamily protein	ns	ns	ns	**0.69**	ns
CATMA4A26465	AT4G24770	ATRBP31_ATRBP33_CP31_RBP31__31-kDa RNA binding protein	ns	ns	ns	ns	**-0.70**
CATMA4A26470	AT4G24780	Pectin lyase-like superfamily protein	ns	ns	ns	**-1.20**	**-1.15**
CATMA4A26620	AT4G24930	thylakoid lumenal 17.9 kDa protein, chloroplast	ns	ns	ns	ns	**-0.78**
CATMA4A26750	AT4G25050	ACP4__acyl carrier protein 4	ns	ns	ns	ns	**-0.84**
CATMA4A26770	AT4G25080	CHLM__magnesium-protoporphyrin IX methyltransferase	ns	ns	**-1.06**	**-0.76**	**-0.68**
CATMA4A26790	AT4G25100	ATFSD1_FSD1__Fe superoxide dismutase 1	ns	ns	ns	ns	**-0.89**
CATMA4A26860	AT4G25170	Uncharacterised conserved protein (UCP012943)	ns	ns	**-1.13**	ns	ns
CATMA4A27330	AT4G25640	ATDTX35_DTX35_FFT__detoxifying efflux carrier 35	ns	**1.66**	**1.40**	**1.98**	**2.11**
CATMA4A27360	AT4G25672	CPuORF12__conserved peptide upstream open reading frame 12	ns	ns	ns	ns	**0.84**
CATMA4A27430	AT4G25740	RNA binding Plectin/S10 domain-containing protein	ns	ns	ns	ns	**-0.86**
CATMA4A27590	AT4G25890	60S acidic ribosomal protein family	ns	ns	ns	ns	**-0.72**
CATMA4A27600	AT4G25900	Galactose mutarotase-like superfamily protein	ns	ns	ns	ns	**0.82**
CATMA4A27720	AT4G26200	ACS7_ATACS7__1-amino-cyclopropane-1-carboxylate synthase 7	ns	ns	ns	ns	**1.44**
CATMA4A28100	AT4G26530	Aldolase superfamily protein	ns	ns	**-1.32**	**-1.03**	**-1.31**
CATMA4A28430	AT4G26850	VTC2__mannose-1-phosphate guanylyltransferase (GDP)s	ns	ns	ns	ns	**0.84**
CATMA4C42516	AT4G27090	Ribosomal protein L14	ns	ns	ns	ns	**-0.71**
CATMA4C42519	AT4G27270	Quinone reductase family protein	ns	**0.98**	**1.20**	**1.69**	**1.56**
CATMA4C42532	AT4G28080	Tetratricopeptide repeat (TPR)-like superfamily protein	ns	ns	ns	**-0.78**	ns
CATMA4A29880	AT4G28240	Wound-responsive family protein	ns	ns	**-1.01**	ns	ns
CATMA4A29890	AT4G28250	ATEXPB3_ATHEXP BETA 1.6_EXPB3__expansin B3	ns	ns	ns	**-0.77**	**-0.87**
CATMA4A30310	AT4G28660	PSB28__photosystem II reaction center PSB28 protein	ns	ns	ns	ns	**-0.71**
CATMA4A30705	AT4G29040	RPT2a__regulatory particle AAA-ATPase 2A	ns	ns	ns	ns	**0.79**
CATMA4A30720	AT4G29060	emb2726__elongation factor Ts family protein	ns	ns	ns	**-1.07**	ns
CATMA4A31300	AT4G29670	ACHT2__atypical CYS HIS rich thioredoxin 2	ns	ns	ns	**0.80**	ns
CATMA4A31560	AT4G29905	unknown protein	ns	ns	**-1.16**	**-0.76**	**-1.83**
CATMA4A31820	AT4G30190	AHA2_HA2_PMA2__H(+)-ATPase 2	ns	ns	ns	**-1.12**	**0.68**

CATMA identifier	AGI identifier	Gene annotation	30 min	2h	4h	8h	24h
CATMA_GFT_01747	AT4G30280	ATXTH18_XTH18__xyloglucan endotransglucosylase/hydrolase 18	ns	ns	ns	ns	**1.86**
CATMA4A32100	AT4G30480	AtTPR1_TPR1__Tetratricopeptide repeat (TPR)-like superfamily protein	ns	ns	ns	**1.01**	**0.87**
CATMA4A32140	AT4G30530	GGP1__Class I glutamine amidotransferase-like superfamily protein	ns	ns	ns	**-0.69**	ns
CATMA4C42566	AT4G30670	Putative membrane lipoprotein	ns	ns	ns	ns	**-0.71**
CATMA4A32330	AT4G30720	PDE327__FAD/NAD(P)-binding oxidoreductase family protein	ns	ns	ns	**-0.74**	ns
CATMA4A33066	AT4G31380	FLP1__FPF1-like protein 1	ns	ns	ns	**0.70**	ns
CATMA4A33145	AT4G31500	ATR4_CYP83B1_RED1_RNT1_SUR2__cytochrome P450, family 83, subfamily B, polypeptide 1	ns	ns	ns	**-1.51**	ns
CATMA4A33440	AT4G31800	ATWRKY18_WRKY18__WRKY DNA-binding protein 18	ns	ns	ns	ns	**0.90**
CATMA4A33510	AT4G31850	PGR3__proton gradient regulation 3	ns	ns	ns	**1.09**	**0.79**
CATMA4C42596	AT4G32410	AtCESA1_CESA1_RSW1__cellulose synthase 1	ns	ns	ns	**-0.75**	ns
CATMA4A34760	AT4G33010	AtGLDP1_GLDP1__glycine decarboxylase P-protein 1	ns	ns	ns	**-0.97**	**-0.83**
CATMA4A34830	AT4G33090	APM1_ATAPM1__aminopeptidase M1	ns	ns	ns	**-0.75**	ns
CATMA4A35030	AT4G33300	ADR1-L1__ADR1-like 1	ns	ns	ns	ns	**0.82**
CATMA4A35140	AT4G33420	Peroxidase superfamily protein	ns	ns	ns	**0.74**	**0.85**
CATMA4A35270	AT4G33540	metallo-beta-lactamase family protein	ns	ns	ns	ns	**0.77**
CATMA_GFT_01764	AT4G33610	glycine-rich protein	ns	**1.24**	**1.49**	**0.69**	**0.80**
CATMA4A35720	AT4G33920	Protein phosphatase 2C family protein	ns	**0.81**	ns	**0.76**	**1.06**
CATMA4A35845	AT4G34050	CCoAOMT1__S-adenosyl-L-methionine-dependent methyltransferases superfamily protein	ns	ns	ns	**-1.80**	**-1.30**
CATMA4A35910	AT4G34120	CBSX2_CDCP1_LEJ1__Cystathionine beta-synthase (CBS) family protein	ns	ns	ns	**0.77**	**0.86**
CATMA4A35920	AT4G34131	UGT73B3__UDP-glucosyl transferase 73B3	ns	ns	ns	**1.31**	**1.38**
CATMA4A35950	AT4G34138	UGT73B1__UDP-glucosyl transferase 73B1	ns	ns	ns	**1.00**	**0.87**
CATMA4A35980	AT4G34150	Calcium-dependent lipid-binding (CaLB domain) family protein	ns	ns	ns	ns	**0.78**
CATMA4A36070	AT4G34250	KCS16__3-ketoacyl-CoA synthase 16	ns	ns	ns	**0.70**	ns
CATMA4A36120	AT4G34290	SWIB/MDM2 domain superfamily protein	ns	ns	ns	ns	**-0.74**
CATMA4A36210	AT4G34380	Transducin/WD40 repeat-like superfamily protein	ns	ns	ns	ns	**0.69**
CATMA4A36220	AT4G34390	XLG2__extra-large GTP-binding protein 2	ns	ns	ns	ns	**0.71**
CATMA4A36460	AT4G34620	SSR16__small subunit ribosomal protein 16	ns	ns	ns	ns	**-0.85**
CATMA4A36493	AT4G34670	Ribosomal protein S3Ae	ns	ns	ns	ns	**-0.76**
CATMA4A36503	AT4G34710	ADC2_ATADC2_SPE2__arginine decarboxylase 2	ns	ns	ns	**0.93**	**1.40**
CATMA4A36600	AT4G34830	MRL1_PDE346__Pentatricopeptide repeat (PPR) superfamily protein	ns	ns	ns	**-0.78**	ns
CATMA4A36827	AT4G35100	PIP2;7_PIP3_PIP3A_SIMIP__plasma membrane intrinsic protein 3	ns	ns	ns	ns	**-1.26**
CATMA4A37120	AT4G35430	unknown protein	ns	ns	ns	**-0.83**	ns
CATMA4A37660	AT4G36010	Pathogenesis-related thaumatin superfamily protein	ns	ns	**1.26**	**1.24**	**0.95**
CATMA4A37700	AT4G36050	endonuclease/exonuclease/phosphatase family protein	ns	ns	ns	**0.77**	ns
CATMA4A38150	AT4G36610	alpha/beta-Hydrolases superfamily protein	ns	**1.43**	ns	ns	ns
CATMA4A38190	AT4G36640	Sec14p-like phosphatidylinositol transfer family protein	ns	ns	ns	ns	**0.75**
CATMA4A38320	AT4G36760	APP1_ATAPP1__aminopeptidase P1	ns	ns	ns	ns	**0.74**
CATMA4A38440	AT4G36850	PQ-loop repeat family protein / transmembrane family protein	ns	ns	**-1.17**	ns	**-0.95**
CATMA4A38575	AT4G36990	AT-HSFB1_ATHSF4_HSF4_HSFB1__heat shock factor 4	ns	**1.32**	ns	**1.81**	**1.72**
CATMA4A38880	AT4G37300	MEE59__maternal effect embryo arrest 59	ns	ns	ns	**-0.94**	ns
CATMA4C42674	AT4G37370	CYP81D8__cytochrome P450, family 81, subfamily D, polypeptide 8	ns	ns	ns	**0.86**	**1.07**
CATMA4A39300	AT4G37800	XTH7__xyloglucan endotransglucosylase/hydrolase 7	ns	ns	ns	**-0.69**	ns
CATMA4A39440	AT4G37925	NDH-M_NdhM__subunit NDH-M of NAD(P)H:plastoquinone dehydrogenase complex	ns	ns	ns	**-0.83**	**-1.07**
CATMA4A39445	AT4G37930	SHM1_SHMT1_STM__serine transhydroxymethyltransferase 1	ns	ns	ns	ns	**-0.81**
CATMA4C42686	AT4G37990	ATCAD8_CAD-B2_ELI3_ELI3-2__elicitor-activated gene 3-2	ns	ns	ns	ns	**2.43**
CATMA4A39600	AT4G38080	hydroxyproline-rich glycoprotein family protein	ns	**0.83**	ns	ns	ns
CATMA4A39680	AT4G38160	pde191__Mitochondrial transcription termination factor family protein	ns	ns	ns	**-0.92**	**-0.79**
CATMA4A40030	AT4G38520	Protein phosphatase 2C family protein	ns	ns	ns	**-0.80**	ns
CATMA4A40036	AT4G38540	FAD/NAD(P)-binding oxidoreductase family protein	ns	ns	ns	ns	**0.81**
CATMA4A40040	AT4G38550	Arabidopsis phospholipase-like protein (PEARLI 4) family	ns	ns	ns	ns	**0.68**
CATMA4A40140	AT4G38690	PLC-like phosphodiesterases superfamily protein	ns	ns	ns	ns	**-0.71**
CATMA4A40230	AT4G38810	Calcium-binding EF-hand family protein	ns	ns	ns	**0.88**	ns
CATMA4C42695	AT4G38840	SAUR-like auxin-responsive protein family	ns	ns	ns	**-0.84**	**-1.31**
CATMA4A40290	AT4G38860	SAUR-like auxin-responsive protein family	ns	ns	ns	ns	**-0.70**
CATMA4A40580	AT4G39090	RD19_RD19A__Papain family cysteine protease	ns	ns	ns	ns	**0.72**
CATMA4C42701	AT4G39330	ATCAD9_CAD9__cinnamyl alcohol dehydrogenase 9	ns	ns	ns	**-0.82**	ns
CATMA4A40743	AT4G39350	ATCESA2_ATH-A_CESA2__cellulose synthase A2	ns	ns	ns	**-1.10**	ns
CATMA4A41030	AT4G39675	unknown protein	ns	ns	**-1.04**	ns	ns
CATMA4A41393	AT4G39980	DHS1__3-deoxy-D-arabino-heptulosonate 7-phosphate synthase 1	ns	**-0.98**	**-1.02**	**-1.76**	**-1.19**
CATMA5A00030	AT5G01015	unknown protein	ns	ns	ns	**-0.78**	**-1.03**
CATMA5A00240	AT5G01210	HXXXD-type acyl-transferase family protein	ns	ns	**-1.65**	**-1.37**	ns
CATMA5A00600	AT5G01540	LECRKA4.1__lectin receptor kinase a4.1	ns	ns	ns	ns	**1.17**
CATMA5A00790	AT5G01740	Nuclear transport factor 2 (NTF2) family protein	ns	ns	ns	**0.72**	ns
CATMA5A00800	AT5G01750	Protein of unknown function (DUF567)	ns	ns	ns	ns	**0.72**

CATMA identifier	AGI identifier	Gene annotation	30 min	2h	4h	8h	24h
CATMA5A00870	AT5G01820	ATCIPK14_ATSR1_CIPK14_PKS24_SnRK3.15_SR1__serine/threonine protein kinase 1	ns	ns	ns	ns	**0.69**
CATMA5A01340	AT5G02260	ATEXP9_ATEXPA9_ATHEXP ALPHA 1.10_EXP9_EXPA9__expansin A9	ns	ns	ns	ns	**-0.93**
CATMA5A01530	AT5G02450	Ribosomal protein L36e family protein	ns	ns	ns	ns	**-0.90**
CATMA5A01570	AT5G02490	AtHsp70-2_Hsp70-2__Heat shock protein 70 (Hsp 70) family protein	ns	ns	ns	ns	**1.16**
CATMA5A01910	AT5G02820	BIN5_RHL2__Spo11/DNA topoisomerase VI, subunit A protein	ns	ns	ns	**-0.73**	ns
CATMA5A02060	AT5G02960	Ribosomal protein S12/S23 family protein	ns	ns	ns	ns	**-0.67**
CATMA5A02260	AT5G03150	JKD__C2H2-like zinc finger protein	ns	ns	ns	ns	**0.82**
CATMA5A02400	AT5G03290	IDH-V__isocitrate dehydrogenase V	ns	ns	ns	ns	**0.71**
CATMA5A02410	AT5G03300	ADK2__adenosine kinase 2	ns	ns	ns	**-0.99**	**-0.94**
CATMA5A02790	AT5G03610	GDSL-like Lipase/Acylhydrolase superfamily protein	ns	ns	ns	ns	**1.15**
CATMA5A02810	AT5G03630	ATMDAR2__Pyridine nucleotide-disulphide oxidoreductase family protein	ns	ns	ns	**0.75**	**1.80**
CATMA5A03320	AT5G04140	FD-GOGAT_GLS1_GLU1_GLUS__glutamate synthase 1	ns	ns	ns	ns	**-0.70**
CATMA5A03420	AT5G04230	ATPAL3_PAL3__phenyl alanine ammonia-lyase 3	ns	ns	ns	**-0.88**	**-0.81**
CATMA5A03450	AT5G04250	Cysteine proteinases superfamily protein	ns	ns	ns	**0.73**	ns
CATMA5A03550	AT5G04340	C2H2_CZF2_ZAT6__zinc finger of Arabidopsis thaliana 6	ns	**0.96**	ns	ns	ns
CATMA5C64056	AT5G04410	anac078_NAC2__NAC domain containing protein 2	ns	ns	ns	ns	**0.75**
CATMA5A03660	AT5G04430	BTR1_BTR1L_BTR1S__binding to TOMV RNA 1L (long form)	ns	ns	ns	ns	**-0.72**
CATMA5A03750	AT5G04530	KCS19__3-ketoacyl-CoA synthase 19	ns	ns	ns	ns	**-0.66**
CATMA5A04460	AT5G05270	Chalcone-flavanone isomerase family protein	ns	ns	ns	ns	**-1.10**
CATMA5A04585	AT5G05410	DREB2_DREB2A__DRE-binding protein 2A	ns	ns	ns	**1.64**	**1.26**
CATMA5A05530	AT5G06320	NHL3__NDR1/HIN1-like 3	ns	ns	ns	ns	**1.60**
CATMA5C64099	AT5G06860	ATPGIP1_PGIP1__polygalacturonase inhibiting protein 1	ns	ns	ns	ns	**0.90**
CATMA5A06270	AT5G07090	Ribosomal protein S4 (RPS4A) family protein	ns	ns	ns	ns	**-0.80**
CATMA5A06560	AT5G07340	Calreticulin family protein	ns	ns	ns	**-0.96**	ns
CATMA5A07120	AT5G07870	HXXXD-type acyl-transferase family protein	ns	ns	ns	**1.20**	ns
CATMA_GFT_01848	AT5G09590	HSC70-5_MTHSC70-2__mitochondrial HSO70 2	ns	ns	ns	**0.71**	**0.96**
CATMA5A08637	AT5G09870	CESA5__cellulose synthase 5	ns	ns	ns	**-0.76**	ns
CATMA5A09290	AT5G10560	Glycosyl hydrolase family protein	ns	ns	ns	**-1.00**	ns
CATMA5A09510	AT5G10770	Eukaryotic aspartyl protease family protein	ns	ns	ns	ns	**0.67**
CATMA5A09830	AT5G11070	unknown protein	ns	ns	ns	**-1.05**	ns
CATMA5A09870	AT5G11110	ATSPS2F_KNS2_SPS1_SPS2F_SPSA2__sucrose phosphate synthase 2F	ns	**1.20**	ns	ns	**0.84**
CATMA5A10190	AT5G11420	Protein of unknown function, DUF642	ns	ns	ns	**-0.79**	**-0.71**
CATMA5A10285	AT5G11520	ASP3_YLS4__aspartate aminotransferase 3	ns	ns	ns	**0.72**	ns
CATMA5A10440	AT5G11670	ATNADP-ME2_NADP-ME2__NADP-malic enzyme 2	ns	ns	ns	ns	**1.06**
CATMA5A11120	AT5G12890	UDP-Glycosyltransferase superfamily protein	ns	ns	ns	ns	**0.67**
CATMA_GFT_03239	AT5G12960	Putative glycosyl hydrolase of unknown function (DUF1680)	ns	**1.12**	ns	ns	ns
CATMA5A11290	AT5G13080	ATWRKY75_WRKY75__WRKY DNA-binding protein 75	ns	ns	ns	**1.14**	ns
CATMA5A11330	AT5G13120	ATCYP20-2_CYP20-2_Pnsl5__cyclophilin 20-2	ns	ns	ns	ns	**-0.67**
CATMA5A11350	AT5G13140	Pollen Ole e 1 allergen and extensin family protein	ns	ns	ns	ns	**-0.78**
CATMA5C64213	AT5G13190	AtGILP_GILP__CONTAINS InterPro DOMAIN/s: LPS-induced tumor necrosis factor alpha factor	ns	**0.80**	ns	**0.69**	**1.22**
CATMA5A11410	AT5G13200	GRAM domain family protein	ns	**0.80**	ns	ns	**0.69**
CATMA5C64215	AT5G13320	GDG1_GH3.12_PBS3_WIN3__Auxin-responsive GH3 family protein	ns	ns	ns	ns	**1.54**
CATMA5A11620	AT5G13420	Aldolase-type TIM barrel family protein	ns	ns	ns	**-0.89**	ns
CATMA5A11720	AT5G13490	AAC2__ADP/ATP carrier 2	ns	ns	ns	**0.69**	**1.00**
CATMA5A11860	AT5G13630	ABAR_CCH_CCH1_CHLH_GUN5__magnesium-chelatase subunit chlH, chloroplast, putative / Mg-protoporphyrin IX chelatase, putative (CHLH)	ns	ns	ns	**-0.79**	ns
CATMA5A11990	AT5G13750	ZIFL1__zinc induced facilitator-like 1	ns	ns	ns	**1.40**	**0.91**
CATMA5A12150	AT5G13930	ATCHS_CHS_TT4__Chalcone and stilbene synthase family protein	ns	ns	ns	ns	**-0.90**
CATMA5A12210	AT5G13980	Glycosyl hydrolase family 38 protein	ns	ns	ns	**-0.88**	ns
CATMA5A12350	AT5G14120	Major facilitator superfamily protein	ns	ns	**-2.20**	ns	**-0.90**
CATMA5A12650	AT5G14410	unknown protein	ns	ns	ns	**-0.98**	**-1.15**
CATMA5A12710	AT5G14470	GHMP kinase family protein	ns	ns	ns	**0.98**	ns
CATMA5A12950	AT5G14730	Unknown protein	ns	ns	ns	**0.77**	ns
CATMA5C64237	AT5G14740	BETA CA2_CA18_CA2__carbonic anhydrase 2	ns	ns	ns	ns	**-0.95**
CATMA5A13000	AT5G14780	FDH__formate dehydrogenase	ns	ns	ns	ns	**1.33**
CATMA5A13200	AT5G14930	SAG101__senescence-associated gene 101	ns	ns	ns	ns	**0.98**
CATMA5A13675	AT5G15410	ATCNGC2_CNGC2_DND1__Cyclic nucleotide-regulated ion channel family protein	ns	ns	ns	**-0.78**	ns
CATMA5A13890	AT5G15640	Mitochondrial substrate carrier family protein	ns	ns	ns	**1.19**	ns
CATMA5C64254	AT5G15970	AtCor6.6_COR6.6_KIN2__stress-responsive protein (KIN2) / stress-induced protein (KIN2) / cold-responsive protein (COR6.6) / cold-regulated protein (COR6.6)	ns	ns	ns	ns	**0.78**
CATMA5A14290	AT5G16010	3-oxo-5-alpha-steroid 4-dehydrogenase family protein	ns	ns	ns	ns	**1.01**
CATMA5A14420	AT5G16130	Ribosomal protein S7e family protein	ns	ns	ns	ns	**-0.97**
CATMA_GFT_01871	AT5G16970	AER_AT-AER__alkenal reductase	ns	ns	ns	**1.15**	**1.28**
CATMA5C64275	AT5G17000	Zinc-binding dehydrogenase family protein	ns	ns	ns	**1.02**	**1.09**
CATMA5A15505	AT5G17230	PSY__PHYTOENE SYNTHASE	ns	ns	ns	**-0.86**	ns
CATMA5A15570	AT5G17300	RVE1__Homeodomain-like superfamily protein	ns	ns	ns	ns	**-0.88**
CATMA5A15640	AT5G17380	Thiamine pyrophosphate dependent pyruvate decarboxylase family protein	ns	ns	ns	ns	**1.48**

CATMA identifier	AGI identifier	Gene annotation	30 min	2h	4h	8h	24h
CATMA5A15960	AT5G17670	alpha/beta-Hydrolases superfamily protein	ns	ns	ns	ns	**-0.66**
CATMA5A16060	AT5G17760	P-loop containing nucleoside triphosphate hydrolases superfamily protein	ns	ns	ns	ns	**0.91**
CATMA5A16140	AT5G17860	CAX7__calcium exchanger 7	ns	ns	ns	ns	**0.66**
CATMA5A16195	AT5G17920	ATCIMS_ATMETS_ATMS1__Cobalamin-independent synthase family protein	ns	ns	ns	**-1.06**	**-0.99**
CATMA5A16780	AT5G18480	PGSIP6__plant glycogenin-like starch initiation protein 6	ns	ns	ns	ns	**1.05**
CATMA5A17020	AT5G18670	BAM9_BMY3__beta-amylase 3	ns	ns	ns	ns	**-1.17**
CATMA5A17550	AT5G19140	AILP1_ATAILP1__Aluminium induced protein with YGL and LRDR motifs	ns	ns	**-1.03**	ns	ns
CATMA5A17870	AT5G19440	NAD(P)-binding Rossmann-fold superfamily protein	ns	ns	ns	ns	**1.28**
CATMA5A17990	AT5G19550	AAT2_ASP2__aspartate aminotransferase 2	ns	ns	ns	ns	**1.26**
CATMA5C64314	AT5G19800	hydroxyproline-rich glycoprotein family protein	ns	ns	ns	ns	**0.67**
CATMA5A18280	AT5G19855	AtRbcX2_RbcX2__Chaperonin-like RbcX protein	ns	ns	ns	**0.73**	ns
CATMA5A18380	AT5G19940	Plastid-lipid associated protein PAP / fibrillin family protein	ns	ns	ns	ns	**-0.74**
CATMA5A18440	AT5G20000	AAA-type ATPase family protein	ns	ns	ns	ns	**0.79**
CATMA5A18670	AT5G20230	ATBCB_BCB_BCB_SAG14__blue-copper-binding protein	ns	ns	ns	ns	**0.72**
CATMA5A18720	AT5G20280	ATSPS1F_SPS1F_SPSA1__sucrose phosphate synthase 1F	ns	ns	ns	**-0.72**	ns
CATMA5C64324	AT5G20400	2-oxoglutarate (2OG) and Fe(II)-dependent oxygenase superfamily protein	ns	ns	ns	ns	**1.03**
CATMA5A19130	AT5G20630	ATGER3_GER3_GLP3_GLP3A_GLP3B__germin 3	ns	ns	ns	**-0.84**	ns
CATMA5C64371	AT5G22140	FAD/NAD(P)-binding oxidoreductase family protein	ns	ns	ns	**2.15**	**1.97**
CATMA5A19778	AT5G22350	ELM1__Protein of unknown function (DUF1022)	ns	ns	ns	ns	**0.73**
CATMA5A19900	AT5G22440	Ribosomal protein L1p/L10e family	ns	ns	ns	ns	**-0.80**
CATMA5A20120	AT5G22640	emb1211__MORN (Membrane Occupation and Recognition Nexus) repeat-containing protein	ns	ns	ns	**-0.90**	ns
CATMA5A20350	AT5G22850	Eukaryotic aspartyl protease family protein	ns	ns	ns	ns	**0.69**
CATMA5A20510	AT5G23020	IMS2_MAM-L_MAM3__2-isopropylmalate synthase 2	ns	ns	ns	**-0.86**	ns
CATMA5A21060	AT5G23540	Mov34/MPN/PAD-1 family protein	ns	ns	ns	ns	**0.68**
CATMA5A21225	AT5G23740	RPS11-BETA__ribosomal protein S11-beta	ns	ns	ns	ns	**-0.87**
CATMA5A21620	AT5G24090	ATCHIA_CHIA__chitinase A	ns	**1.01**	ns	**1.50**	**1.48**
CATMA5A21750	AT5G24200	alpha/beta-Hydrolases superfamily protein	ns	ns	ns	ns	**1.03**
CATMA5A21760	AT5G24210	alpha/beta-Hydrolases superfamily protein	ns	ns	ns	ns	**1.32**
CATMA5A21890	AT5G24314	PDE225_PTAC7__plastid transcriptionally active7	ns	ns	ns	**-0.72**	ns
CATMA5A22030	AT5G24420	PGL5__6-phosphogluconolactonase 5	ns	ns	ns	ns	**-1.20**
CATMA5A22430	AT5G24760	GroES-like zinc-binding dehydrogenase family protein	ns	ns	ns	**-1.08**	**-1.19**
CATMA5A22960	AT5G25250	SPFH/Band 7/PHB domain-containing membrane-associated protein family	ns	ns	ns	ns	**1.38**
CATMA5C64427	AT5G25260	SPFH/Band 7/PHB domain-containing membrane-associated protein family	ns	ns	ns	ns	**2.07**
CATMA5C64436	AT5G25460	Protein of unknown function, DUF642	ns	ns	**-1.30**	**-1.72**	**-1.41**
CATMA5A23590	AT5G25930	Protein kinase family protein with leucine-rich repeat domain	ns	ns	ns	**1.18**	**1.06**
CATMA5A23675	AT5G26030	ATFC-I_FC-I_FC1__ferrochelatase 1	ns	ns	ns	ns	**0.69**
CATMA5C64456	AT5G26260	TRAF-like family protein	ns	ns	ns	**-0.78**	**-0.99**
CATMA_GFT_01923	AT5G26280	TRAF-like family protein	ns	ns	**-1.02**	ns	**-0.86**
CATMA5C64457	AT5G26290	TRAF-like family protein	ns	**-0.87**	ns	**-1.50**	**-1.36**
CATMA5A24060	AT5G26570	ATGWD3_OK1_PWD__catalytics;carbohydrate kinases;phosphoglucan, water dikinases	ns	ns	ns	**-0.75**	ns
CATMA5A24080	AT5G26740	Protein of unknown function (DUF300)	ns	ns	ns	ns	**-0.66**
CATMA5A24850	AT5G27420	ATL31_CNI1__carbon/nitrogen insensitive 1	ns	**0.91**	ns	**1.50**	**1.39**
CATMA5A24910	AT5G27520	AtPNC2_PNC2__peroxisomal adenine nucleotide carrier 2	ns	ns	ns	**0.72**	ns
CATMA5A25170	AT5G27760	Hypoxia-responsive family protein	ns	ns	ns	**1.19**	**1.43**
CATMA5A25280	AT5G27850	Ribosomal protein L18e/L15 superfamily protein	ns	ns	ns	ns	**-0.92**
CATMA5A26920	AT5G28840	GME__GDP-D-mannose 3',5'-epimerase	ns	ns	**-1.01**	ns	ns
CATMA5C64535	AT5G33320	ARAPPT_CUE1_PPT__Glucose-6-phosphate/phosphate translocator-related	ns	ns	ns	**-0.87**	ns
CATMA5C64549	AT5G35480	unknown protein	ns	ns	ns	ns	**-0.68**
CATMA5A30990	AT5G35690	unknown protein	ns	ns	ns	**0.83**	**0.86**
CATMA5A31080	AT5G35735	Auxin-responsive family protein	ns	**1.01**	**1.09**	**1.15**	**1.12**
CATMA5A31830	AT5G36270	Unknown protein	ns	ns	**1.38**	**1.56**	**1.74**
CATMA5A32135	AT5G36910	THI2.2__thionin 2.2	ns	ns	ns	ns	**-1.73**
CATMA5A32230	AT5G36960	unknown protein	ns	ns	ns	ns	**0.68**
CATMA5A32930	AT5G37600	ATGLN1;1_ATGSR1_GLN1;1_GSR 1__glutamine synthase clone R1	ns	ns	ns	ns	**1.29**
CATMA5C64593	AT5G37920	Family of unknown function (DUF577)	ns	ns	ns	**0.80**	**0.79**
CATMA5C64595	AT5G38020	S-adenosyl-L-methionine-dependent methyltransferases superfamily protein	ns	ns	**1.15**	ns	ns
CATMA5A33960	AT5G38410	Ribulose bisphosphate carboxylase (small chain) family protein	ns	ns	ns	ns	**-0.81**
CATMA5C64608	AT5G38430	Ribulose bisphosphate carboxylase (small chain) family protein	ns	ns	ns	**-0.74**	**-0.98**
CATMA5A34050	AT5G38520	alpha/beta-Hydrolases superfamily protein	ns	ns	ns	ns	**-0.69**
CATMA5A34060	AT5G38530	TSBtype2__tryptophan synthase beta type 2	ns	ns	ns	ns	**0.68**
CATMA5A34590	AT5G38980	unknown protein	ns	ns	ns	**-0.96**	**-1.09**
CATMA5A34660	AT5G39050	PMAT1__HXXXD-type acyl-transferase family protein	ns	**0.86**	ns	**0.86**	**1.57**
CATMA5A34710	AT5G39090	HXXXD-type acyl-transferase family protein	ns	ns	ns	**0.82**	**1.05**
CATMA5A34820	AT5G39210	CRR7__chlororespiratory reduction 7	ns	ns	ns	**-1.27**	**-0.89**
CATMA5A35160	AT5G39580	Peroxidase superfamily protein	ns	ns	**-1.78**	ns	**1.01**

CATMA identifier	AGI identifier	Gene annotation	30 min	2h	4h	8h	24h
CATMA5A35200	AT5G39610	ANAC092_ATNAC2_ATNAC6_NAC2_NAC6_ORE1__NAC domain containing protein 6	ns	ns	ns	ns	**0.82**
CATMA5A35240	AT5G39670	Calcium-binding EF-hand family protein	ns	ns	ns	ns	**1.38**
CATMA5A36030	AT5G40370	GRXC2__Glutaredoxin family protein	ns	ns	ns	ns	**0.79**
CATMA5A36458	AT5G40780	LHT1__lysine histidine transporter 1	ns	ns	ns	**-0.85**	**0.93**
CATMA5A36700	AT5G41040	HXXXD-type acyl-transferase family protein	ns	**0.91**	ns	ns	ns
CATMA5A37020	AT5G41390	PLAC8 family protein	ns	ns	ns	ns	**0.79**
CATMA5A37030	AT5G41400	RING/U-box superfamily protein	ns	**0.91**	**1.04**	**0.85**	**0.91**
CATMA5A37770	AT5G42050	DCD (Development and Cell Death) domain protein	ns	ns	ns	ns	**1.41**
CATMA5A37800	AT5G42090	Lung seven transmembrane receptor family protein	ns	ns	ns	ns	**0.69**
CATMA5A37820	AT5G42100	ATBG_PPAP_BG_PPAP__beta-1,3-glucanase_putative	ns	ns	ns	**-0.77**	ns
CATMA5A37830	AT5G42110	unknown protein	ns	ns	ns	ns	**-0.76**
CATMA5C64706	AT5G42300	UBL5__ubiquitin-like protein 5	ns	ns	ns	**0.81**	**1.23**
CATMA5A39130	AT5G43260	chaperone protein dnaJ-related	ns	ns	ns	**0.71**	ns
CATMA5A39290	AT5G43430	ETFBETA__electron transfer flavoprotein beta	ns	ns	ns	**0.86**	ns
CATMA5A39530	AT5G43700	ATAUX2-11_IAA4__AUX/IAA transcriptional regulator family protein	ns	ns	ns	**-0.89**	**-1.08**
CATMA5A40380	AT5G44580	unknown protein	ns	ns	ns	**-0.81**	ns
CATMA5A40400	AT5G44585	unknown protein	ns	ns	**-1.48**	**-0.99**	ns
CATMA5A41300	AT5G45350	proline-rich family protein	ns	ns	ns	ns	**0.84**
CATMA5A41430	AT5G45490	P-loop containing nucleoside triphosphate hydrolases superfamily protein	ns	ns	ns	**-0.89**	**-0.68**
CATMA5A41930	AT5G45930	CHL I2_CHLI-2_CHLI2__magnesium chelatase i2	ns	ns	ns	**-0.88**	ns
CATMA5A42580	AT5G46580	pentatricopeptide (PPR) repeat-containing protein	ns	ns	ns	**-0.93**	ns
CATMA5A42810	AT5G46800	BOU__Mitochondrial substrate carrier family protein	ns	ns	ns	ns	**-0.69**
CATMA5C64809	AT5G47120	ATBI-1_ATBI1_BI-1_BI1__BAX inhibitor 1	ns	ns	ns	ns	**1.21**
CATMA5A43120	AT5G47130	Bax inhibitor-1 family protein	ns	ns	ns	ns	**1.16**
CATMA5A43190	AT5G47200	ATRAB1A_ATRABD2B_RAB1A__RAB GTPase homolog 1A	ns	ns	ns	ns	**0.76**
CATMA5A43205	AT5G47220	ATERF-2_ATERF2_ERF2__ethylene responsive element binding factor 2	ns	ns	ns	ns	**0.80**
CATMA5A43920	AT5G47950	HXXXD-type acyl-transferase family protein	ns	ns	ns	**-0.96**	**-1.11**
CATMA5C64822	AT5G47990	CYP705A5_THAD_THAD1__cytochrome P450, family 705, subfamily A, polypeptide 5	ns	ns	ns	**-0.75**	ns
CATMA5A44340	AT5G48380	BIR1__BAK1-interacting receptor-like kinase 1	ns	ns	ns	ns	**0.74**
CATMA_GFT_02191	AT5G48400	ATGLR1.2_GLR1.2__Glutamate receptor family protein	ns	ns	ns	**0.77**	**1.54**
CATMA5A44410	AT5G48430	Eukaryotic aspartyl protease family protein	ns	ns	**-1.12**	ns	**1.47**
CATMA5A44460	AT5G48485	DIR1__Bifunctional inhibitor/lipid-transfer protein/seed storage 2S albumin superfamily protein	ns	ns	ns	ns	**-0.74**
CATMA5A44530	AT5G48545	HINT3__histidine triad nucleotide-binding 3	ns	ns	ns	ns	**-0.68**
CATMA5A44660	AT5G48657	defense protein-related	ns	ns	ns	ns	**0.80**
CATMA5C64839	AT5G48810	ATB5-B_ATCB5-D_B5 #3_CB5-D__cytochrome B5 isoform D	ns	ns	ns	**-0.71**	ns
CATMA5A44840	AT5G48930	HCT__hydroxycinnamoyl-CoA shikimate/quinate hydroxycinnamoyl transferase	ns	**-1.17**	**-1.11**	**-1.50**	**-1.18**
CATMA5A44970	AT5G49030	OVA2__tRNA synthetase class I (I, L, M and V) family protein	ns	ns	ns	**-0.77**	ns
CATMA5A45465	AT5G49480	ATCP1_CP1__Ca2+-binding protein 1	ns	ns	ns	**0.96**	ns
CATMA5A45500	AT5G49520	ATWRKY48_WRKY48__WRKY DNA-binding protein 48	ns	ns	ns	**0.74**	**1.05**
CATMA5A45660	AT5G49730	ATFRO6_FRO6_FRO6__ferric reduction oxidase 6	ns	ns	**-1.35**	**-0.79**	**-1.46**
CATMA5A45825	AT5G49910	cpHsc70-2_HSC70-7__chloroplast heat shock protein 70-2	ns	ns	ns	**-0.71**	ns
CATMA5A46160	AT5G50200	ATNRT3.1_NRT3.1_WR3__nitrate transmembrane transporters	ns	ns	ns	**0.92**	**1.17**
CATMA5A46170	AT5G50210	OLD5_QS_SUFE3__quinolinate synthase	ns	ns	ns	**0.75**	**1.02**
CATMA5A46355	AT5G50375	CPI1__cyclopropyl isomerase	ns	ns	ns	**-0.76**	ns
CATMA5A46860	AT5G50920	ATHSP93-V_CLPC1_DCA1_HSP93-V__CLPC homologue 1	ns	ns	ns	**-0.86**	ns
CATMA5A46970	AT5G51040	unknown protein	ns	ns	ns	ns	**0.83**
CATMA5A46995	AT5G51070	CLPD_ERD1_SAG15__Clp ATPase	ns	ns	ns	ns	**0.72**
CATMA5A47350	AT5G51440	HSP20-like chaperones superfamily protein	ns	ns	ns	**0.90**	ns
CATMA5A47480	AT5G51550	EXL3__EXORDIUM like 3	ns	ns	ns	**-0.94**	**-0.90**
CATMA5A47660	AT5G51720	2 iron, 2 sulfur cluster binding	ns	ns	ns	ns	**-1.24**
CATMA5A47700	AT5G51770	Protein kinase superfamily protein	ns	ns	ns	ns	**1.00**
CATMA5A47760	AT5G51830	pfkB-like carbohydrate kinase family protein	ns	ns	ns	**1.07**	**1.10**
CATMA5A48130	AT5G52190	Sugar isomerase (SIS) family protein	ns	ns	ns	ns	**-0.73**
CATMA5A48515	AT5G52640	ATHS83_AtHsp90-1_ATHSP90.1_HSP81-1_HSP81.1_HSP83_HSP90.1__heat shock protein 90.1	ns	ns	ns	ns	**1.13**
CATMA5A48640	AT5G52780	Protein of unknown function (DUF3464)	ns	ns	ns	**-0.88**	ns
CATMA5A48670	AT5G52810	NAD(P)-binding Rossmann-fold superfamily protein	ns	ns	ns	ns	**1.00**
CATMA5A49030	AT5G53120	ATSPDS3_SPDS3_SPMS__spermidine synthase 3	ns	ns	ns	ns	**0.88**
CATMA5A49070	AT5G53160	PYL8_RCAR3__regulatory components of ABA receptor 3	ns	ns	ns	ns	**-0.76**
CATMA5A49080	AT5G53170	FTSH11__FTSH protease 11	ns	ns	ns	**-0.69**	ns
CATMA5A49360	AT5G53460	GLT1__NADH-dependent glutamate synthase 1	ns	ns	ns	**-1.16**	ns
CATMA5A49390	AT5G53490	Tetratricopeptide repeat (TPR)-like superfamily protein	ns	ns	ns	ns	**-0.83**
CATMA5A49490	AT5G53590	SAUR-like auxin-responsive protein family	ns	ns	ns	**0.73**	**0.83**
CATMA5A49880	AT5G53970	TAT7__Tyrosine transaminase family protein	ns	ns	ns	**0.84**	ns
CATMA5A50126	AT5G54206	0	ns	ns	ns	**1.41**	**2.04**
CATMA5C64941	AT5G54500	FQR1__flavodoxin-like quinone reductase 1	ns	**1.12**	**1.14**	**1.50**	**1.79**

CATMA identifier	AGI identifier	Gene annotation	30 min	2h	4h	8h	24h
CATMA5C64943	AT5G54640	ATHTA1_HTA1_RAT5__Histone superfamily protein	ns	ns	ns	**0.94**	ns
CATMA5C64946	AT5G54710	Ankyrin repeat family protein	ns	ns	ns	ns	**1.15**
CATMA5A50595	AT5G54770	THI1_THI4_TZ__thiazole biosynthetic enzyme, chloroplast (ARA6) (THI1) (THI4)	ns	ns	ns	**-0.75**	**-0.89**
CATMA5A50760	AT5G54960	PDC2__pyruvate decarboxylase-2	ns	ns	ns	ns	**0.90**
CATMA5A50820	AT5G55050	GDSL-like Lipase/Acylhydrolase superfamily protein	ns	ns	ns	ns	**0.69**
CATMA5A50990	AT5G55230	ATMAP65-1_MAP65-1_MAP65-1__microtubule-associated proteins 65-1	ns	ns	ns	**-1.06**	ns
CATMA5A51370	AT5G55620	unknown protein	ns	ns	ns	ns	**-1.11**
CATMA5C64969	AT5G55750	hydroxyproline-rich glycoprotein family protein	ns	ns	ns	**0.95**	**1.62**
CATMA5A51710	AT5G55930	ATOPT1_OPT1__oligopeptide transporter 1	ns	ns	ns	**-1.07**	ns
CATMA5A51750	AT5G55970	RING/U-box superfamily protein	ns	ns	ns	**0.82**	ns
CATMA5C64978	AT5G56030	AtHsp90.2_ERD8_HSP81-2_HSP81.2_HSP90.2__heat shock protein 81-2	ns	ns	ns	ns	**0.70**
CATMA5A51870	AT5G56100	glycine-rich protein / oleosin	ns	ns	ns	ns	**-0.98**
CATMA5A52490	AT5G56710	Ribosomal protein L31e family protein	ns	ns	ns	ns	**-0.70**
CATMA5A53440	AT5G57710	Double Clp-N motif-containing P-loop nucleoside triphosphate hydrolases superfamily protein	ns	ns	ns	ns	**0.91**
CATMA5C65014	AT5G57887	unknown protein	ns	ns	**-1.02**	ns	ns
CATMA5A54020	AT5G58260	NdhN__oxidoreductases, acting on NADH or NADPH, quinone or similar compound as acceptor	ns	ns	ns	ns	**-1.05**
CATMA5A54045	AT5G58290	RPT3__regulatory particle triple-A ATPase 3	ns	ns	ns	ns	**0.69**
CATMA_GFT_03391	AT5G58570	unknown protein	ns	ns	ns	ns	**0.70**
CATMA5A54650	AT5G58900	Homeodomain-like transcriptional regulator	ns	ns	ns	**-0.72**	ns
CATMA5A54840	AT5G59090	ATSBT4.12_SBT4.12__subtilase 4.12	ns	ns	ns	**-0.73**	ns
CATMA5A55310	AT5G59570	BOA__Homeodomain-like superfamily protein	ns	ns	ns	**1.32**	ns
CATMA5A55565	AT5G59780	ATMYB59_ATMYB59-1_ATMYB59-2_ATMYB59-3_MYB59__myb domain protein 59	ns	ns	ns	ns	**-0.67**
CATMA5A55640	AT5G59870	HTA6__histone H2A 6	ns	ns	ns	ns	**-0.78**
CATMA5A55646	AT5G59890	ADF4_ATADF4__actin depolymerizing factor 4	ns	ns	ns	ns	**0.70**
CATMA5A56030	AT5G60270	Concanavalin A-like lectin protein kinase family protein	ns	ns	ns	ns	**0.80**
CATMA5A56105	AT5G60360	AALP_ALP_SAG2__aleurain-like protease	ns	ns	ns	ns	**0.77**
CATMA5A56140	AT5G60400	unknown protein	ns	ns	ns	**-0.84**	**-0.93**
CATMA5A56360	AT5G60640	ATPDI2_ATPDIL1-4_PDI2_PDIL1-4__PDI-like 1-4	ns	ns	ns	**-0.73**	ns
CATMA5A56650	AT5G61010	ATEXO70E2_EXO70E2__exocyst subunit exo70 family protein E2	ns	ns	ns	ns	**0.70**
CATMA5A57025	AT5G61380	APRR1_AtTOC1_PRR1_TOC1__CCT motif -containing response regulator protein	ns	ns	ns	**-0.71**	ns
CATMA5A57390	AT5G61790	ATCNX1_CNX1__calnexin 1	ns	ns	ns	ns	**0.72**
CATMA5A57420	AT5G61820	unknown protein	ns	ns	ns	**0.96**	**1.25**
CATMA5A57490	AT5G61900	BON_BON1_CPN1__Calcium-dependent phospholipid-binding Copine family protein	ns	ns	ns	ns	**0.68**
CATMA5A57623	AT5G62020	AT-HSFB2A_HSFB2A__heat shock transcription factor B2A	ns	**0.96**	ns	**1.07**	**0.95**
CATMA5C65085	AT5G62480	ATGSTU9_GST14_GST14B_GSTU9__glutathione S-transferase tau 9	ns	ns	ns	ns	**0.70**
CATMA5A58220	AT5G62630	HIPL2__hipl2 protein precursor	ns	ns	ns	ns	**1.21**
CATMA5A58260	AT5G62670	AHA11_HA11__H(+)-ATPase 11	ns	ns	ns	ns	**-0.77**
CATMA5A58310	AT5G62720	Integral membrane HPP family protein	ns	ns	ns	**0.91**	ns
CATMA5A58590	AT5G63030	GRXC1__Thioredoxin superfamily protein	ns	ns	ns	ns	**0.87**
CATMA5A58780	AT5G63180	Pectin lyase-like superfamily protein	ns	ns	ns	ns	**-0.79**
CATMA5A58950	AT5G63420	emb2746__RNA-metabolising metallo-beta-lactamase family protein	ns	ns	ns	**-0.74**	ns
CATMA5A59230	AT5G63680	Pyruvate kinase family protein	ns	ns	ns	ns	**0.79**
CATMA5A59330	AT5G63790	ANAC102_NAC102__NAC domain containing protein 102	ns	ns	ns	ns	**0.90**
CATMA5A59535	AT5G64040	PSAN__photosystem I reaction center subunit PSI-N, chloroplast, putative / PSI-N, putative (PSAN)	ns	ns	ns	ns	**-0.86**
CATMA5A59575_N	AT5G64100	Peroxidase superfamily protein	ns	**-0.84**	**-1.70**	**-0.69**	ns
CATMA5A59660	AT5G64200	At-SC35_ATSC35_SC35__ortholog of human splicing factor SC35	ns	ns	ns	**-0.84**	ns
CATMA5C65119	AT5G64250	Aldolase-type TIM barrel family protein	ns	ns	ns	**1.62**	**1.55**
CATMA5A59763	AT5G64310	AGP1_ATAGP1__arabinogalactan protein 1	ns	ns	ns	**0.72**	ns
CATMA5A60320	AT5G64890	PROPEP2__elicitor peptide 2 precursor	ns	ns	ns	**1.07**	ns
CATMA5A60423	AT5G65010	ASN2__asparagine synthetase 2	ns	ns	ns	**-0.97**	**-0.84**
CATMA_GFT_03400	AT5G66052	unknown protein	ns	ns	ns	**0.75**	ns
CATMA5A61460	AT5G66070	RING/U-box superfamily protein	ns	ns	ns	ns	**0.68**
CATMA5A61750	AT5G66420	unknown protein	ns	**-0.83**	**-1.22**	ns	**0.89**
CATMA5A61900	AT5G66540	Unknown protein	ns	ns	**-1.00**	ns	ns
CATMA5A62120	AT5G66720	Protein phosphatase 2C family protein	ns	ns	ns	ns	**-0.88**
CATMA5A62765	AT5G67300	ATMYB44_ATMYBR1_MYB44_MYBR1__myb domain protein r1	ns	ns	ns	**0.76**	**0.71**
CATMA5A62800	AT5G67350	unknown protein	ns	ns	ns	**0.96**	ns
CATMA5A62810	AT5G67360	ARA12__Subtilase family protein	ns	ns	ns	**-0.85**	ns
CATMA5C65166	AT5G67600	WIH1__unknown protein; LOCATED IN: plasma membrane	ns	ns	ns	**0.96**	ns

Supplemental Table III: Genes found to be differentially expressed in all the comparisons between phenanthrene-treated and control plants (hybridizations 5-9), selected after ANOVA analysis. Among the 467 differentially expressed genes, 14, 47, 77, 275 and 360 genes were expressed at 30 min, 2 h, 4 h, 8 h and 24 h, respectively. *Arabidopsis* annotation from TAIR, called TAIR10 (most recent versions as of 21 September 2012). Expression changes are given as log2. Expression changes in bolt correspond to genes differentially expressed at the significant threshold of Bonferroni p-value<0.05. AGI and gene annotation in bold face correspond to gene involved in the "xenome".

AGI identifier	Gene annotation	30 min	2h	4h	8h	24h
AT4G38620	ATMYB4_MYB4__myb domain protein 4	**3.51**	**2.19**	**2.30**	**2.18**	**1.94**
AT2G47950	unknown protein	**1.49**	**2.27**	**2.27**	**2.65**	**1.91**
AT5G48540	receptor-like protein kinase-related family protein	**1.42**	**2.44**	**3.27**	**3.48**	**3.51**
AT4G15248	B-box type zinc finger family protein	**1.39**	**1.75**	**1.04**	0.35	**1.63**
AT5G59820	RHL41_ZAT12__C2H2-type zinc finger family protein	**1.19**	**1.63**	**2.14**	**2.70**	**2.50**
AT2G16900	*Arabidopsis* phospholipase-like protein (PEARLI 4) family	**0.98**	**1.68**	**1.67**	**1.61**	**2.16**
AT1G68620	alpha/beta-Hydrolases superfamily protein	**0.93**	**2.18**	**1.68**	**2.77**	**2.70**
AT5G56630	PFK7__phosphofructokinase 7	**0.91**	**1.59**	**2.41**	**1.54**	**2.53**
AT3G22840	ELIP_ELIP1__Chlorophyll A-B binding family protein	**0.89**	**1.40**	**2.19**	**1.70**	**2.38**
AT1G63840	RING/U-box superfamily protein	**0.83**	**1.80**	**1.64**	**2.10**	**2.16**
AT2G36590	ATPROT3_ProT3__proline transporter 3	**0.79**	**1.42**	**1.93**	**1.80**	**2.24**
AT4G39670	Glycolipid transfer protein (GLTP) family protein	**0.73**	**1.26**	**1.01**	**1.42**	**2.13**
AT4G27657	unknown protein	**0.70**	**1.26**	**1.10**	**1.75**	**0.74**
AT1G70800	EHB1__Calcium-dependent lipid-binding (CaLB domain) family protein	**0.64**	**1.23**	**1.91**	**1.97**	**1.19**
AT3G21560	**UGT84A2__UDP-Glycosyltransferase superfamily protein**	0.52	**1.48**	**2.21**	**1.60**	**1.93**
AT1G27120	**Galactosyltransferase family protein**	0.00	**0.91**	**2.00**	**2.30**	**2.45**
AT3G22600	Bifunctional inhibitor/lipid-transfer protein/seed storage 2S albumin superfamily protein	0.16	**1.68**	**1.96**	**1.36**	**1.96**
AT2G35980	ATNHL10_NHL10_YLS9__Late embryogenesis abundant (LEA) hydroxyproline-rich glycoprotein family	0.56	**1.72**	**1.96**	**1.81**	**2.34**
AT3G04300	RmlC-like cupins superfamily protein	0.37	**1.25**	**1.73**	**2.08**	**2.25**
AT1G74010	Calcium-dependent phosphotriesterase superfamily protein	0.46	**1.39**	**1.68**	**1.32**	**2.50**
AT1G76980	unknown protein	0.51	**1.15**	**1.67**	**1.78**	**1.85**
AT1G18980	RmlC-like cupins superfamily protein	0.20	**1.16**	**1.55**	**1.57**	**1.59**
AT1G75040	PR-5_PR5__pathogenesis-related gene 5	0.21	**1.32**	**1.50**	**1.71**	**1.75**

AGI identifier	Gene annotation	30 min	2h	4h	8h	24h
AT4G25640	ATDTX35_DTX35_FFT_detoxifying efflux carrier 35	0.27	**1.66**	**1.40**	**1.98**	**2.11**
AT2G17500	Auxin efflux carrier family protein	-0.20	**0.80**	**1.19**	**1.79**	**1.20**
AT1G74450	Protein of unknown function (DUF793)	0.41	**1.09**	**1.16**	**1.06**	**1.10**
AT3G04000	NAD(P)-binding Rossmann-fold superfamily protein	0.06	**0.95**	**1.16**	**1.53**	**1.23**
AT5G54500	FQR1__flavodoxin-like quinone reductase 1	0.47	**1.12**	**1.14**	**1.50**	**1.79**
AT1G30700	FAD-binding Berberine family protein	0.48	**1.26**	**1.06**	**1.56**	**2.28**
AT1G78660	ATGGH1_GGH1__gamma-glutamyl hydrolase 1	0.36	**1.98**	0.95	**1.96**	**1.27**
AT2G15530	RING/U-box superfamily protein	0.56	**0.81**	0.89	**1.71**	**2.15**
AT1G78680	ATGGH2_GGH2__gamma-glutamyl hydrolase 2	-0.03	**1.24**	0.77	**1.53**	**1.00**
AT4G20860	FAD-binding Berberine family protein	0.51	**0.91**	0.61	**1.45**	**1.79**
AT3G46080	C2H2-type zinc finger family protein	0.27	**1.03**	0.95	**1.39**	**1.72**
AT1G21670	unknown protein.	0.16	**0.97**	0.12	**1.20**	**1.79**
AT1G62320	ERD (early-responsive to dehydration stress) family protein	0.50	**0.98**	0.90	**0.94**	**0.85**
AT3G21520	AtDMP1_DMP1__DUF679 domain membrane protein 1	0.07	**1.10**	0.70	**0.92**	**0.97**
AT3G50440	ATMES10_MES10__methyl esterase 10	0.04	**0.96**	0.82	0.18	**1.12**
AT5G12960	Putative glycosyl hydrolase of unknown function (DUF1680)	0.01	**1.12**	0.88	0.66	0.53
AT1G34630	FUNCTIONS IN: molecular_function unknown; INVOLVED IN: biological_process unknown; LOCATED IN: cellular_component unknown; EXPRESSED IN: 25 plant structures; EXPRESSED DURING: 15 growth stages; BEST *Arabidopsis thaliana* protein match is: Mitochondrial import inner membrane translocase subunit Tim17/Tim22/Tim23 family protein (TAIR:AT5G51150.1)	-0.19	**1.06**	0.52	0.42	0.36
AT4G17280	Auxin-responsive family protein	0.00	**0.89**	0.49	0.05	0.11
AT1G78340	**ATGSTU22_GSTU22__glutathione S-transferase TAU 22**	0.04	0.56	**1.62**	**1.75**	**1.69**
AT1G17170	**ATGSTU24_GST_GSTU24__glutathione S-transferase TAU 24**	0.06	0.39	**1.57**	**2.00**	**2.05**
AT3G51660	Tautomerase/MIF superfamily protein	0.10	0.75	**1.47**	**1.80**	**2.27**
AT5G36270	**pseudogene of dehydroascorbate reductase**	0.00	0.55	**1.38**	**1.56**	**1.74**
AT4G15480	**UGT84A1__UDP-Glycosyltransferase superfamily protein**	0.18	0.47	**1.27**	**1.02**	**1.40**
AT1G78380	**ATGSTU19_GST8_GSTU19__glutathione S-transferase TAU 19**	0.10	0.69	**1.23**	**1.45**	**1.49**
AT1G05680	**UGT74E2__Uridine diphosphate glycosyltransferase 74E2**	0.14	-0.05	**1.01**	**1.80**	**0.83**
AT1G75270	**DHAR2__dehydroascorbate reductase 2**	0.36	0.78	**1.09**	**1.60**	**1.49**
AT1G75030	ATLP-3_TLP-3__thaumatin-like protein 3	0.19	0.59	**1.13**	**1.45**	**1.35**

AGI identifier	Gene annotation	30 min	2h	4h	8h	24h
AT3G13520	AGP12_ATAGP12__arabinogalactan protein 12	0.17	0.57	**1.08**	**1.39**	**0.88**
AT1G64900	**CYP89_CYP89A2__cytochrome P450, family 89, subfamily A, polypeptide 2**	-0.03	0.33	**1.08**	**1.16**	**1.19**
AT2G29500	HSP20-like chaperones superfamily protein	0.16	0.29	**1.15**	**1.11**	**1.53**
AT4G13180	NAD(P)-binding Rossmann-fold superfamily protein	0.28	0.29	**1.03**	**1.07**	**1.39**
AT2G12190	**Cytochrome P450 superfamily protein**	-0.04	0.43	**1.04**	**0.97**	**0.96**
AT2G48140	EDA4__Bifunctional inhibitor/lipid-transfer protein/seed storage 2S albumin superfamily protein	0.02	0.74	**1.20**	**0.73**	0.40
AT1G23490	ARF1_ATARF_ATARF1_ATARFA1A__ADP-ribosylation factor 1	0.48	0.76	**1.04**	0.64	**1.32**
AT3G09270	**ATGSTU8_GSTU8__glutathione S-transferase TAU 8**	-0.12	0.41	**1.15**	0.26	**1.09**
AT3G49570	LSU3__response to low sulfur 3	0.17	0.24	**1.04**	0.68	0.65
AT5G38020	S-adenosyl-L-methionine-dependent methyltransferases superfamily protein	0.13	0.06	**1.15**	-0.35	-0.11
AT1G14120	2-oxoglutarate (2OG) and Fe(II)-dependent oxygenase superfamily protein	0.08	0.22	**1.08**	-0.05	-0.21
AT3G25830	ATTPS-CIN_TPS-CIN_TPS-CIN__terpene synthase-like sequence-1,8-cineole	-0.04	0.45	**1.19**	0.06	-0.22
AT1G58370	**ATXYN1_RXF12__glycosyl hydrolase family 10 protein / carbohydrate-binding domain-containing protein**	0.17	0.64	**1.13**	0.08	**-0.86**
AT3G28210	PMZ_SAP12__zinc finger (AN1-like) family protein	0.36	0.52	0.98	**1.60**	**2.09**
AT3G54420	ATCHITIV_ATEP3_CHIV_EP3__homolog of carrot EP3-3 chitinase	-0.06	0.24	0.52	**0.98**	**2.05**
AT2G23110	Late embryogenesis abundant protein, group 6	0.45	0.78	0.51	**1.87**	**2.04**
AT5G54206	0	0.17	0.15	0.29	**1.41**	**2.04**
AT3G44190	FAD/NAD(P)-binding oxidoreductase family protein	0.03	0.21	0.95	**2.05**	**2.01**
AT2G41380	S-adenosyl-L-methionine-dependent methyltransferases superfamily protein	-0.07	0.04	0.47	**0.87**	**1.99**
AT2G01180	ATLPP1_ATPAP1_LPP1_PAP1__phosphatidic acid phosphatase 1	0.20	0.33	0.95	**1.44**	**1.97**
AT2G18680	unknown protein	0.19	0.78	0.19	**0.75**	**1.97**
AT5G22140	FAD/NAD(P)-binding oxidoreductase family protein	0.30	0.02	0.76	**2.15**	**1.97**
AT4G11600	ATGPX6_GPX6_LSC803_PHGPX__glutathione peroxidase 6	0.12	0.34	0.69	**1.03**	**1.95**
AT2G05380	GRP3S__glycine-rich protein 3 short isoform	0.25	0.23	-0.09	**1.00**	**1.85**
AT2G21620	RD2__Adenine nucleotide alpha hydrolases-like superfamily protein	-0.01	0.75	0.94	**1.28**	**1.82**
AT5G03630	ATMDAR2__Pyridine nucleotide-disulphide oxidoreductase family protein	0.03	-0.05	0.96	**0.75**	**1.80**
AT2G05530	Glycine-rich protein family	-0.04	-0.19	0.22	**0.85**	**1.73**

AGI identifier	Gene annotation	30 min	2h	4h	8h	24h
AT5G55750	hydroxyproline-rich glycoprotein family protein	0.01	-0.24	0.29	**0.95**	**1.62**
AT1G65280	DNAJ heat shock N-terminal domain-containing protein	0.02	-0.02	0.30	**0.89**	**1.56**
AT5G64250	Aldolase-type TIM barrel family protein	-0.01	0.35	0.59	**1.62**	**1.55**
AT5G48400	ATGLR1.2_GLR1.2__Glutamate receptor family protein	-0.07	0.29	0.52	**0.77**	**1.54**
AT1G66580	RPL10C_SAG24__senescence associated gene 24	0.32	0.45	0.63	**1.26**	**1.44**
AT1G33590	Leucine-rich repeat (LRR) family protein	0.06	0.38	0.48	**0.73**	**1.43**
AT5G27760	Hypoxia-responsive family protein	0.14	0.47	0.83	**1.19**	**1.43**
AT3G14620	**CYP72A8__cytochrome P450, family 72, subfamily A, polypeptide 8**	-0.05	0.41	-0.13	**0.86**	**1.40**
AT4G34131	**UGT73B3__UDP-glucosyl transferase 73B3**	0.33	0.38	0.89	**1.31**	**1.38**
AT4G23190	AT-RLK3_CRK11__cysteine-rich RLK (RECEPTOR-like protein kinase) 11	0.21	0.07	0.14	**0.80**	**1.38**
AT1G75280	NmrA-like negative transcriptional regulator family protein	0.15	0.62	0.86	**1.56**	**1.37**
AT5G16970	AER_AT-AER__alkenal reductase	-0.22	0.02	0.18	**1.15**	**1.28**
AT1G22710	ATSUC2_SUC2_SUT1__sucrose-proton symporter 2	-0.25	0.71	0.30	**0.87**	**1.27**
AT4G24160	alpha/beta-Hydrolases superfamily protein	-0.01	0.40	0.59	**1.52**	**1.25**
AT5G61820	unknown protein	0.11	0.05	0.72	**0.96**	**1.25**
AT5G42300	UBL5__ubiquitin-like protein 5	0.08	0.21	0.64	**0.81**	**1.23**
AT4G20830	FAD-binding Berberine family protein	0.14	0.55	0.52	**0.87**	**1.20**
AT3G22370	AOX1A_ATAOX1A_AtHSR3_HSR3__alternative oxidase 1A	-0.03	0.32	0.59	**0.99**	**1.18**
AT3G10500	anac053_NAC053__NAC domain containing protein 53	0.12	0.77	0.66	**1.48**	**1.16**
AT2G23680	Cold acclimation protein WCOR413 family	0.10	0.21	0.77	**0.88**	**1.12**
AT3G04120	GAPC_GAPC-1_GAPC1__glyceraldehyde-3-phosphate dehydrogenase C subunit 1	0.25	0.60	0.86	**1.09**	**1.11**
AT5G51830	pfkB-like carbohydrate kinase family protein	0.03	-0.13	0.42	**1.07**	**1.10**
AT1G72490	unknown protein	-0.09	0.20	0.02	**1.25**	**1.10**
AT5G17000	Zinc-binding dehydrogenase family protein	0.09	0.03	0.69	**1.02**	**1.09**
AT1G09400	FMN-linked oxidoreductases superfamily protein	-0.08	0.04	0.34	**0.74**	**1.08**
AT2G36460	Aldolase superfamily protein	0.12	0.45	0.48	**0.72**	**1.08**
AT1G67600	Acid phosphatase/vanadium-dependent haloperoxidase-related protein	0.01	0.45	0.50	**1.25**	**1.07**
AT3G26200	**CYP71B22__cytochrome P450, family 71, subfamily B, polypeptide 22**	0.19	0.72	0.66	**1.07**	**1.07**
AT5G39090	**HXXXD-type acyl-transferase family protein**	0.16	0.55	0.45	**0.82**	**1.05**
AT5G50210	OLD5_QS_SUFE3__quinolinate synthase	0.00	-0.12	0.26	**0.75**	**1.02**
AT1G77120	ADH_ADH1_ATADH_ATADH1__alcohol dehydrogenase 1	-0.18	0.54	0.25	**1.30**	**1.02**
AT2G36950	Heavy metal transport/detoxification superfamily protein	0.21	0.45	-0.10	**1.26**	**1.01**
AT3G27380	SDH2-1__succinate dehydrogenase 2-1	0.09	0.35	0.33	**0.99**	**0.95**

AGI identifier	Gene annotation	30 min	2h	4h	8h	24h
AT2G29460	**ATGSTU4_GST22_GSTU4__glutathione S-transferase tau 4**	0.12	0.52	1.00	**1.37**	**0.95**
AT1G64930	**CYP89A7__cytochrome P450, family 87, subfamily A, polypeptide 7**	0.20	0.36	0.92	**0.85**	**0.94**
AT2G45550	**CYP76C4__cytochrome P450, family 76, subfamily C, polypeptide 4**	-0.01	0.11	-0.15	**0.91**	**0.89**
AT1G76530	Auxin efflux carrier family protein	0.06	0.13	0.30	**0.90**	**0.88**
AT3G45180	Ubiquitin-like superfamily protein	0.06	0.30	0.45	**0.86**	**0.87**
AT1G14130	2-oxoglutarate (2OG) and Fe(II)-dependent oxygenase superfamily protein	-0.04	0.07	0.60	**1.04**	**0.86**
AT4G34120	CBSX2_CDCP1_LEJ1__Cystathionine beta-synthase (CBS) family protein	0.11	0.43	0.46	**0.77**	**0.86**
AT4G33420	Peroxidase superfamily protein	0.14	0.55	-0.20	**0.74**	**0.85**
AT4G03320	AtTic20-IV_Tic20-IV__translocon at the inner envelope membrane of chloroplasts 20-IV	0.15	0.22	0.69	**1.00**	**0.82**
AT2G07671	ATP synthase subunit C family protein	-0.03	0.32	0.30	**0.86**	**0.82**
AT2G24500	FZF__Zinc finger protein 622	0.11	0.45	0.35	**1.13**	**0.76**
AT2G29470	**ATGSTU3_GST21_GSTU3__glutathione S-transferase tau 3**	0.12	0.40	0.77	**1.14**	**0.76**
AT2G44460	BGLU28__beta glucosidase 28	-0.15	-0.03	0.11	**0.74**	**0.70**
AT1G05670	**Pentatricopeptide repeat (PPR-like) superfamily protein**	0.20	0.02	0.71	**1.30**	**0.69**
AT2G33150	KAT2_PED1_PKT3__peroxisomal 3-ketoacyl-CoA thiolase 3	-0.25	0.67	-0.42	**0.84**	**0.68**
AT1G76070	unknown protein	0.06	0.19	0.24	**0.90**	**0.68**
AT3G51130	unknown protein	-0.16	-0.14	-0.10	**0.83**	**0.67**
AT3G59140	**ABCC10_ATMRP14_MRP14__multidrug resistance-associated protein 14**	-0.15	0.01	0.19	**0.76**	**0.67**
AT1G76520	Auxin efflux carrier family protein	-0.04	0.11	0.35	**0.87**	**0.66**
AT5G07870	HXXXD-type acyl-transferase family protein	0.17	-0.04	0.28	**1.20**	0.65
AT2G36770	**UDP-Glycosyltransferase superfamily protein**	-0.02	0.19	0.11	**1.65**	0.64
AT1G61790	Oligosaccharyltransferase complex/magnesium transporter family protein	-0.21	-0.01	-0.13	**0.74**	0.64
AT1G71520	Integrase-type DNA-binding superfamily protein	0.11	0.57	0.73	**1.47**	0.62
AT2G07811	0	-0.03	0.18	0.01	**1.01**	0.60
AT3G28910	ATMYB30_MYB30__myb domain protein 30	-0.26	-0.03	-0.16	**0.89**	0.59
AT2G12557	unknown protein	0.04	0.20	0.40	**0.81**	0.59
AT2G29940	**ABCG31_ATPDR3_PDR3__pleiotropic drug resistance 3**	-0.06	0.30	0.22	**0.96**	0.58
AT1G27190	Leucine-rich repeat protein kinase family protein	0.14	0.07	0.41	**1.96**	0.57
AT1G18510	TET16__tetraspanin 16	0.15	0.42	0.41	**1.26**	0.56
AT1G22500	AtATL15_ATL15__RING/U-box superfamily protein	0.03	0.03	-0.56	**0.88**	0.55
AT2G38250	Homeodomain-like superfamily protein	-0.17	0.44	0.40	**0.71**	0.54

AGI identifier	Gene annotation	30 min	2h	4h	8h	24h
AT4G17840	unknown protein	-0.28	0.10	-0.62	**0.99**	0.52
AT5G15640	Mitochondrial substrate carrier family protein	-0.11	0.29	0.29	**1.19**	0.49
AT2G34355	Major facilitator superfamily protein	0.04	0.26	0.24	**1.07**	0.48
AT1G66570	ATSUC7_SUC7__sucrose-proton symporter 7	-0.16	0.28	0.08	**0.73**	0.46
AT5G62720	Integral membrane HPP family protein	0.14	0.42	-0.34	**0.91**	0.46
AT1G68410	Protein phosphatase 2C family protein	-0.15	0.50	-0.32	**0.96**	0.40
AT1G23890	NHL domain-containing protein	-0.08	0.35	0.61	**1.26**	0.40
AT1G55850	**ATCSLE1_CSLE1__cellulose synthase like E1**	-0.09	0.17	-0.25	**1.17**	0.36
AT5G54640	ATHTA1_HTA1_RAT5__Histone superfamily protein	0.11	0.42	0.42	**0.94**	0.36
AT1G15415	The protein encoded by this gene was identified as a part of pollen proteome by mass spec analysis. It has weak homology to LEA (late embryo abundant) proteins.	0.00	0.03	0.28	**0.74**	0.32
AT1G05100	Encodes protein phosphatase 2A (PP2A) B'gamma subunit. Targeted to nucleus and cytosol. MAPKKK18__mitogen-activated protein kinase kinase kinase 18	0.14	0.70	0.26	**0.99**	0.32
AT4G29670	ACHT2__atypical CYS HIS rich thioredoxin 2	-0.21	0.17	0.03	**0.80**	0.30
AT1G53580	ETHE1_GLX2-3_GLY3__glyoxalase II 3	-0.14	0.39	-0.06	**1.07**	0.29
AT1G71530	Protein kinase superfamily protein	0.06	0.31	0.34	**0.70**	0.27
AT5G64890	PROPEP2__elicitor peptide 2 precursor	0.31	0.04	0.21	**1.07**	0.27
AT1G05575	unknown protein	0.09	0.45	0.57	**1.21**	0.26
AT5G59570	BOA__Homeodomain-like superfamily protein	0.00	0.40	0.24	**1.32**	0.16
AT3G14000	ATBRXL2_BRX-LIKE2__DZC (Disease resistance/zinc finger/chromosome condensation-like region) domain containing protein	-0.05	0.13	-0.01	**0.91**	0.12
AT3G22530	unknown protein	-0.01	0.09	0.05	**0.72**	0.09
AT2G34070	TBL37__TRICHOME BIREFRINGENCE-LIKE 37	-0.19	0.09	0.13	**0.99**	0.03
AT4G00750	S-adenosyl-L-methionine-dependent methyltransferases superfamily protein	0.08	0.02	-0.08	**0.95**	0.00
AT3G14770	AtSWEET2_SWEET2__Nodulin MtN3 family protein	0.05	0.47	-0.48	**1.02**	-0.15
AT2G43445	F-box and associated interaction domains-containing protein	-0.05	0.07	0.19	**0.73**	-0.39
AT1G66100	Plant thionin	-0.20	-0.03	0.44	**0.82**	**-1.11**
AT1G65290	mtACP2__mitochondrial acyl carrier protein 2	0.13	0.06	0.13	0.34	**2.63**
AT4G37990	ATCAD8_CAD-B2_ELI3_ELI3-2__elicitor-activated gene 3-2	0.07	0.30	0.34	0.00	**2.43**
AT5G25260	SPFH/Band 7/PHB domain-containing membrane-associated protein family	-0.10	-0.06	0.30	0.04	**2.07**
AT2G18690	unknown protein	0.11	0.70	0.54	0.66	**1.98**

AGI identifier	Gene annotation	30 min	2h	4h	8h	24h
AT4G12490	Bifunctional inhibitor/lipid-transfer protein/seed storage 2S albumin superfamily protein	0.22	0.07	0.66	0.28	**1.90**
AT1G14870	AtPCR2_PCR2__PLANT CADMIUM RESISTANCE 2	-0.03	0.51	0.03	0.48	**1.76**
AT2G23150	ATNRAMP3_NRAMP3__natural resistance-associated macrophage protein 3	-0.17	-0.16	0.01	0.59	**1.69**
AT2G17740	Cysteine/Histidine-rich C1 domain family protein	-0.03	-0.15	0.66	0.20	**1.67**
AT1G66090	Disease resistance protein (TIR-NBS class)	0.36	0.29	0.66	0.55	**1.67**
AT5G06320	NHL3__NDR1/HIN1-like 3	-0.28	0.11	-0.08	0.31	**1.60**
AT2G29350	SAG13__senescence-associated gene 13	-0.17	0.17	0.82	0.59	**1.55**
AT1G13330	AHP2__*Arabidopsis* Hop2 homolog	0.00	-0.09	0.69	0.36	**1.55**
AT5G13320	GDG1_GH3.12_PBS3_WIN3__Auxin-responsive GH3 family protein	-0.10	-0.25	0.11	-0.07	**1.54**
AT5G17380	Thiamine pyrophosphate dependent pyruvate decarboxylase family protein	0.04	0.03	0.35	0.65	**1.48**
AT2G20142	Toll-Interleukin-Resistance (TIR) domain family protein	0.06	0.05	0.21	0.23	**1.47**
AT4G26200	ACS7_ATACS7__1-amino-cyclopropane-1-carboxylate synthase 7	0.22	-0.01	0.18	0.26	**1.44**
AT1G74710	ATICS1_EDS16_ICS1_SID2__ADC synthase superfamily protein	0.05	-0.19	0.14	-0.09	**1.41**
AT4G11890	Protein kinase superfamily protein	0.10	0.19	-0.04	0.56	**1.38**
AT5G25250	SPFH/Band 7/PHB domain-containing membrane-associated protein family	0.07	0.00	0.28	0.40	**1.38**
AT1G26380	FAD-binding Berberine family protein	0.24	0.24	0.34	0.43	**1.38**
AT5G39670	Calcium-binding EF-hand family protein	-0.17	-0.07	0.12	0.05	**1.38**
AT4G14365	XBAT34__XB3 ortholog 4 in *Arabidopsis thaliana*	-0.10	-0.35	0.17	-0.05	**1.36**
AT1G26630	ATELF5A-2_ELF5A-2_FBR12__Eukaryotic translation initiation factor 5A-1 (eIF-5A 1) protein	0.04	-0.12	0.51	0.26	**1.36**
AT5G14780	FDH__formate dehydrogenase	-0.17	-0.60	-0.79	0.05	**1.33**
AT2G32190	unknown protein	0.11	0.18	0.45	0.53	**1.33**
AT5G19440	NAD(P)-binding Rossmann-fold superfamily protein	-0.11	-0.07	0.33	0.66	**1.28**
AT3G49530	ANAC062_NAC062_NTL6__NAC domain containing protein 62	0.09	0.35	0.29	0.48	**1.28**
AT1G32960	ATSBT3.3_SBT3.3__Subtilase family protein	0.11	0.06	0.20	0.47	**1.27**
AT5G19550	AAT2_ASP2__aspartate aminotransferase 2	0.04	0.09	0.16	0.19	**1.26**
AT5G47120	ATBI-1_ATBI1_BI-1_BI1__BAX inhibitor 1	0.09	0.37	0.44	0.20	**1.21**
AT5G62630	HIPL2__hipl2 protein precursor	0.14	0.07	0.43	0.52	**1.21**
AT4G12480	EARLI1_pEARLI 1__Bifunctional inhibitor/lipid-transfer protein/seed storage 2S albumin superfamily protein	-0.03	0.13	0.02	-0.15	**1.19**
AT4G02380	AtLEA5_SAG21__senescence-associated gene 21	0.19	0.22	-0.18	0.59	**1.17**
AT2G31865	PARG2__poly(ADP-ribose) glycohydrolase 2	-0.04	-0.22	0.33	0.31	**1.17**

AGI identifier	Gene annotation	30 min	2h	4h	8h	24h
AT2G39200	ATMLO12_MLO12__Seven transmembrane MLO family protein	-0.16	-0.44	-0.20	-0.18	**1.17**
AT5G01540	LECRKA4.1__lectin receptor kinase a4.1	-0.05	-0.19	0.19	-0.16	**1.17**
AT5G47130	Bax inhibitor-1 family protein	-0.12	0.19	0.21	0.26	**1.16**
AT5G02490	AtHsp70-2_Hsp70-2__Heat shock protein 70 (Hsp 70) family protein	0.00	-0.23	0.19	-0.11	**1.16**
AT5G54710	Ankyrin repeat family protein	-0.11	-0.16	0.51	-0.10	**1.15**
AT2G23810	TET8__tetraspanin8	-0.22	0.08	-0.11	0.45	**1.15**
AT3G51670	SEC14 cytosolic factor family protein / phosphoglyceride transfer family protein	-0.05	0.32	0.64	0.18	**1.15**
AT1G68570	Major facilitator superfamily protein	0.19	0.61	0.54	0.48	**1.14**
AT5G52640	ATHS83_AtHsp90-1_ATHSP90.1_HSP81-1_HSP81.1_HSP83_HSP90.1__heat shock protein 90.1	-0.06	0.01	0.53	0.50	**1.13**
AT1G11610	**CYP71A18__cytochrome P450, family 71, subfamily A, polypeptide 18**	0.03	0.09	0.43	0.47	**1.12**
AT1G36622	unknown protein	-0.11	0.07	0.65	0.62	**1.12**
AT3G13950	unknown protein	0.01	-0.03	-0.01	0.37	**1.12**
AT2G41100	ATCAL4_TCH3__Calcium-binding EF hand family protein	-0.06	-0.48	-0.93	-0.42	**1.10**
AT2G43590	Chitinase family protein	0.14	-0.01	0.24	0.48	**1.09**
AT4G14630	GLP9__germin-like protein 9	-0.19	0.07	-0.39	0.06	**1.09**
AT4G12720	AtNUDT7_GFG1_NUDT7__MutT/nudix family protein	-0.10	-0.16	-0.18	0.16	**1.07**
AT1G32940	ATSBT3.5_SBT3.5__Subtilase family protein	-0.02	0.03	0.51	0.35	**1.06**
AT5G18480	PGSIP6__plant glycogenin-like starch initiation protein 6	-0.17	0.21	-0.15	0.53	**1.05**
AT1G70490	ARFA1D_ATARFA1D__Ras-related small GTP-binding family protein	0.14	0.22	0.18	0.11	**1.04**
AT5G20400	2-oxoglutarate (2OG) and Fe(II)-dependent oxygenase superfamily protein	-0.12	-0.08	0.19	0.22	**1.03**
AT2G15240	UNC-50 family protein	0.00	-0.02	0.03	0.11	**1.02**
AT3G26210	**CYP71B23__cytochrome P450, family 71, subfamily B, polypeptide 23**	0.24	0.03	0.37	0.21	**1.01**
AT5G51770	Protein kinase superfamily protein	0.17	0.45	0.27	0.27	**1.00**
AT5G52810	NAD(P)-binding Rossmann-fold superfamily protein	0.04	0.00	0.80	0.33	**1.00**
AT3G59700	ATHLECRK_HLECRK_LECRK1__lectin-receptor kinase	0.01	-0.12	0.33	0.34	**0.99**
AT5G14930	SAG101__senescence-associated gene 101	0.00	-0.14	-0.21	-0.15	**0.98**
AT4G23700	ATCHX17_CHX17__cation/H+ exchanger 17	0.14	0.40	0.28	0.38	**0.97**
AT1G77510	ATPDI6_ATPDIL1-2_PDI6_PDIL1-2__PDI-like 1-2	0.17	0.06	0.43	-0.45	**0.96**
AT3G20510	Transmembrane proteins 14C	0.00	0.38	0.59	0.20	**0.96**
AT2G16430	ATPAP10_PAP10__purple acid phosphatase 10	0.13	-0.11	0.31	-0.20	**0.96**
AT4G01770	RGXT1_rhamnogalacturonan xylosyltransferase 1	0.06	0.23	0.60	0.07	**0.95**
AT2G37110	PLAC8 family protein	0.01	-0.03	-0.27	0.26	**0.94**

AGI identifier	Gene annotation	30 min	2h	4h	8h	24h
AT1G21750	ATPDI5_ATPDIL1-1_PDI5_PDIL1-1__PDI-like 1-1	0.12	-0.12	0.21	-0.50	**0.93**
AT3G47480	Calcium-binding EF-hand family protein	-0.04	-0.08	0.11	-0.08	**0.93**
AT2G44350	ATCS_CSY4__Citrate synthase family protein	0.18	0.02	0.30	-0.14	**0.91**
AT5G57710	Double Clp-N motif-containing P-loop nucleoside triphosphate hydrolases superfamily protein	0.01	-0.02	0.49	0.52	**0.91**
AT1G59860	HSP20-like chaperones superfamily protein	0.40	0.54	0.79	0.67	**0.91**
AT1G60680	NAD(P)-linked oxidoreductase superfamily protein	-0.15	-0.02	0.06	0.57	**0.91**
AT5G54960	PDC2__pyruvate decarboxylase-2	0.05	0.19	0.33	0.32	**0.90**
AT5G06860	ATPGIP1_PGIP1__polygalacturonase inhibiting protein 1	-0.11	-0.11	-0.58	0.21	**0.90**
AT1G27080	NRT1.6__nitrate transporter 1.6	-0.02	-0.20	-0.38	-0.13	**0.88**
AT3G56260	unknown protein	0.08	0.23	0.62	0.47	**0.88**
AT3G29360	UGD2__UDP-glucose 6-dehydrogenase family protein	-0.07	0.07	0.38	-0.16	**0.87**
AT3G57670	NTT_WIP2__C2H2-type zinc finger family protein	0.10	-0.06	0.03	0.46	**0.85**
AT1G11910	APA1_ATAPA1__aspartic proteinase A1	-0.08	-0.07	-0.06	-0.21	**0.84**
AT5G45350	proline-rich family protein	-0.23	-0.30	-0.24	0.15	**0.84**
AT1G80330	ATGA3OX4_GA3OX4__gibberellin 3-oxidase 4	-0.02	-0.09	0.35	0.48	**0.83**
AT5G51040	unknown protein	-0.04	-0.09	0.31	0.33	**0.83**
AT1G61800	ATGPT2_GPT2__glucose-6-phosphate/phosphate translocator 2	-0.24	0.09	-0.34	0.50	**0.83**
AT2G37760	AKR4C8__NAD(P)-linked oxidoreductase superfamily protein	-0.08	0.05	0.58	0.63	**0.82**
AT1G19220	ARF11_ARF19_IAA22__auxin response factor 19	0.09	0.19	0.63	0.18	**0.82**
AT4G25900	Galactose mutarotase-like superfamily protein	-0.05	0.07	-0.01	0.11	**0.82**
AT1G65845	unknown protein	-0.18	-0.51	0.00	-0.27	**0.81**
AT3G62260	Protein phosphatase 2C family protein	-0.14	0.27	0.32	0.40	**0.81**
AT4G29040	RPT2a__regulatory particle AAA-ATPase 2A	0.11	-0.08	0.17	0.51	**0.79**
AT3G62600	ATERDJ3B_ERDJ3B__DNAJ heat shock family protein	0.03	-0.16	0.54	-0.13	**0.79**
AT3G52430	ATPAD4_PAD4__alpha/beta-Hydrolases superfamily protein	-0.17	-0.61	-0.33	-0.21	**0.79**
AT5G63680	Pyruvate kinase family protein	0.20	0.36	0.64	0.15	**0.79**
AT2G37940	AtIPCS2_ERH1__*Arabidopsis* Inositol phosphorylceramide synthase 2	0.00	0.29	0.38	0.52	**0.79**
AT1G62570	FMO GS-OX4__flavin-monooxygenase glucosinolate S-oxygenase 4	0.05	0.69	0.97	0.68	**0.78**
AT1G23880	NHL domain-containing protein	-0.33	0.11	0.11	0.66	**0.78**
AT2G33380	AtCLO3_CLO-3_CLO3_RD20__Caleosin-related family protein	-0.31	-0.01	0.03	0.09	**0.77**
AT2G05840	PAA2__20S proteasome subunit PAA2	0.07	0.06	0.47	0.44	**0.77**

AGI identifier	Gene annotation	30 min	2h	4h	8h	24h
AT2G46400	ATWRKY46_WRKY46__WRKY DNA-binding protein 46	-0.19	-0.20	0.27	0.15	**0.76**
AT3G50930	BCS1__cytochrome BC1 synthesis	0.06	-0.14	0.34	-0.08	**0.76**
AT4G21120	AAT1_CAT1__amino acid transporter 1	-0.13	-0.13	-0.21	0.45	**0.76**
AT4G36640	Sec14p-like phosphatidylinositol transfer family protein	0.02	-0.01	0.85	0.56	**0.75**
AT1G14540	Peroxidase superfamily protein	0.06	0.10	-0.15	0.17	**0.75**
AT1G66160	ATCMPG1_CMPG1__CYS, MET, PRO, and GLY protein 1	0.04	0.21	0.29	0.58	**0.75**
AT4G15760	MO1__monooxygenase 1	-0.19	0.27	-0.31	0.67	**0.75**
AT2G46390	SDH8__unknown protein	0.07	0.22	0.60	0.20	**0.73**
AT3G24170	ATGR1_GR1__glutathione-disulfide reductase	-0.15	0.19	0.62	0.50	**0.73**
AT5G01750	Protein of unknown function (DUF567)	0.16	0.06	-0.56	0.20	**0.72**
AT5G61790	ATCNX1_CNX1__calnexin 1	0.20	-0.02	0.42	-0.34	**0.72**
AT1G60710	ATB2__NAD(P)-linked oxidoreductase superfamily protein	-0.03	0.04	0.19	0.58	**0.72**
AT3G51260	PAD1__20S proteasome alpha subunit PAD1	0.03	-0.01	0.21	0.30	**0.71**
AT4G09750	NAD(P)-binding Rossmann-fold superfamily protein	-0.12	0.08	0.58	0.37	**0.71**
AT3G18250	Putative membrane lipoprotein	0.13	-0.12	-0.12	0.13	**0.71**
AT5G56030	AtHsp90.2_ERD8_HSP81-2_HSP81.2_HSP90.2__heat shock protein 81-2	0.07	0.08	0.42	-0.14	**0.70**
AT3G56400	ATWRKY70_WRKY70__WRKY DNA-binding protein 70	-0.18	-0.08	0.23	-0.10	**0.70**
AT2G28930	APK1B_PK1B__protein kinase 1B	-0.06	0.36	0.24	0.13	**0.70**
AT5G26030	ATFC-I_FC-I_FC1__ferrochelatase 1	-0.40	0.05	0.26	0.64	**0.69**
AT1G29310	SecY protein transport family protein	0.04	0.12	0.22	0.06	**0.68**
AT2G31660	EMA1_SAD2_URM9__ARM repeat superfamily protein	0.00	0.74	-0.40	0.55	**0.68**
AT5G38530	TSBtype2__tryptophan synthase beta type 2	0.08	0.09	0.50	0.18	**0.68**
AT5G36960	unknown protein	0.18	-0.11	0.22	0.56	**0.68**
AT5G23540	Mov34/MPN/PAD-1 family protein	0.04	-0.04	0.25	0.60	**0.68**
AT1G07135	glycine-rich protein	-0.27	-0.07	0.07	0.26	**0.66**
AT3G50685	unknown protein	-0.06	0.18	-0.28	-0.31	**-0.66**
AT5G13120	ATCYP20-2_CYP20-2_PnsI5__cyclophilin 20-2	0.11	-0.14	-0.08	-0.34	**-0.67**
AT4G14130	XTH15_XTR7__xyloglucan endotransglucosylase/hydrolase 15	0.10	-0.14	-0.83	-0.34	**-0.67**
AT3G48930	EMB1080__Nucleic acid-binding, OB-fold-like protein	0.09	0.03	-0.23	-0.34	**-0.68**
AT1G80050	APT2_ATAPT2_PHT1.1__adenine phosphoribosyl transferase 2	0.03	-0.26	-0.54	-0.58	**-0.70**
AT4G24770	ATRBP31_ATRBP33_CP31_RBP31__31-kDa RNA binding protein	0.20	0.05	-0.36	-0.17	**-0.70**
AT4G14320	Zinc-binding ribosomal protein family protein	0.33	0.09	-0.33	-0.29	**-0.70**

AGI identifier	Gene annotation	30 min	2h	4h	8h	24h
AT4G38690	PLC-like phosphodiesterases superfamily protein	-0.14	0.12	-0.54	-0.39	**-0.71**
AT4G27090	Ribosomal protein L14	-0.03	0.02	-0.06	-0.28	**-0.71**
AT2G05990	ENR1_MOD1__NAD(P)-binding Rossmann-fold superfamily protein	0.25	0.12	-0.18	-0.46	**-0.72**
AT5G04430	BTR1_BTR1L_BTR1S__binding to TOMV RNA 1L (long form)	0.07	-0.15	-0.09	-0.19	**-0.72**
AT1G60950	ATFD2_FED A__2Fe-2S ferredoxin-like superfamily protein	-0.07	-0.12	-0.24	-0.65	**-0.72**
AT2G40890	**CYP98A3__cytochrome P450, family 98, subfamily A, polypeptide 3**	0.05	-0.66	-0.92	-0.44	**-0.74**
AT4G34290	SWIB/MDM2 domain superfamily protein	0.18	0.04	-0.25	-0.57	**-0.74**
AT3G56910	PSRP5__plastid-specific 50S ribosomal protein 5	0.13	0.14	-0.13	-0.32	**-0.75**
AT4G34670	Ribosomal protein S3Ae	0.22	0.12	-0.14	-0.40	**-0.76**
AT3G23390	Zinc-binding ribosomal protein family protein	0.03	0.06	-0.18	-0.26	**-0.77**
AT5G62670	AHA11_HA11__H(+)-ATPase 11	0.05	-0.07	-0.08	-0.52	**-0.77**
AT2G45470	AGP8_FLA8__FASCICLIN-like arabinogalactan protein 8	-0.06	0.08	-0.48	-0.55	**-0.77**
AT4G24930	thylakoid lumenal 17.9 kDa protein, chloroplast	0.10	-0.02	0.00	-0.50	**-0.78**
AT3G02560	Ribosomal protein S7e family protein	0.06	-0.05	0.23	-0.31	**-0.80**
AT3G62530	ARM repeat superfamily protein	0.03	0.07	0.04	-0.32	**-0.81**
AT3G16690	AtSWEET16_SWEET16__Nodulin MtN3 family protein	-0.20	0.08	0.14	-0.18	**-0.81**
AT1G22640	ATMYB3_MYB3__myb domain protein 3	0.20	-0.47	-0.67	-0.58	**-0.83**
AT1G18290	unknown protein	-0.03	-0.28	-0.82	-0.09	**-0.83**
AT4G34620	SSR16__small subunit ribosomal protein 16	0.07	0.10	-0.26	-0.33	**-0.85**
AT3G20820	Leucine-rich repeat (LRR) family protein	0.01	-0.07	-0.80	-0.60	**-0.86**
AT3G11170	AtFAD7_FAD7_FADD__fatty acid desaturase 7	0.03	-0.12	-0.30	-0.63	**-0.87**
AT3G01480	ATCYP38_CYP38__cyclophilin 38	0.07	0.01	-0.76	-0.54	**-0.88**
AT3G15850	ADS3_FAD5_FADB_JB67_fatty acid desaturase 5	-0.21	-0.01	-0.68	-0.06	**-0.91**
AT3G16440	ATMLP-300B_MEE36_MLP-300B__myrosinase-binding protein-like protein-300B	-0.24	0.21	-0.37	-0.38	**-0.91**
AT3G16420	JAL30_PBP1__PYK10-binding protein 1	-0.04	0.07	0.01	-0.64	**-1.02**
AT5G58260	NdhN__oxidoreductases, acting on NADH or NADPH, quinone or similar compound as acceptor	0.04	-0.01	-0.14	-0.58	**-1.05**
AT1G54000	GLL22__GDSL-like Lipase/Acylhydrolase superfamily protein	0.03	-0.28	-0.77	-0.55	**-1.06**
AT1G12090	ELP__extensin-like protein	-0.06	-0.04	-0.52	-0.33	**-1.08**
AT3G45140	ATLOX2_LOX2__lipoxygenase 2	-0.12	0.51	0.51	-0.24	**-1.11**
AT4G16980	arabinogalactan-protein family	0.07	-0.10	-0.84	-0.54	**-1.14**
AT3G02380	ATCOL2_COL2__CONSTANS-like 2	-0.11	-0.60	-0.41	0.04	**-1.15**

AGI identifier	Gene annotation	30 min	2h	4h	8h	24h
AT4G13870	ATWEX_ATWRNEXO_WEX_WRNEXO__Werner syndrome-like exonuclease	-0.02	0.10	0.61	-0.34	**-1.19**
AT5G24420	PGL5__6-phosphogluconolactonase 5	0.00	0.05	-0.32	-0.02	**-1.20**
AT5G51720	2 iron, 2 sulfur cluster binding	-0.06	-0.25	-0.17	-0.38	**-1.24**
AT3G28270	Protein of unknown function (DUF677)	-0.26	0.46	0.25	-0.57	**-1.26**
AT4G35100	PIP2;7_PIP3_PIP3A_SIMIP__plasma membrane intrinsic protein 3	0.01	0.10	-0.81	-0.67	**-1.26**
AT3G16450	JAL33__Mannose-binding lectin superfamily protein	0.00	0.28	-0.51	-0.67	**-1.30**
AT1G17190	**ATGSTU26_GSTU26__glutathione S-transferase tau 26**	-0.01	-0.19	0.32	-0.31	**-1.41**
AT2G25510	unknown protein	-0.09	0.23	0.11	-0.40	**-1.52**
AT5G36910	THI2.2__thionin 2.2	-0.16	0.04	-0.38	0.21	**-1.73**
AT1G69500	**CYP704B1__cytochrome P450, family 704, subfamily B, polypeptide 1**	-0.14	-0.53	-0.28	**-0.71**	**0.71**
AT5G26570	ATGWD3_OK1_PWD__catalytics;carbohydrate kinases;phosphoglucan, water dikinases	0.17	0.05	-0.06	**-0.75**	0.34
AT5G07340	Calreticulin family protein	0.08	-0.18	-0.16	**-0.96**	0.26
AT1G69520	S-adenosyl-L-methionine-dependent methyltransferases superfamily protein	-0.06	0.13	0.12	**-0.69**	0.13
AT1G19100	Histidine kinase-, DNA gyrase B-, and HSP90-like ATPase family protein	-0.02	-0.25	-0.38	**-0.69**	0.12
AT5G58900	Homeodomain-like transcriptional regulator	-0.06	-0.40	-0.22	**-0.72**	0.11
AT1G01960	EDA10__SEC7-like guanine nucleotide exchange family protein	0.23	0.05	-0.37	**-0.96**	0.06
AT3G23300	S-adenosyl-L-methionine-dependent methyltransferases superfamily protein	0.05	-0.23	-0.14	**-0.72**	0.05
AT1G66200	ATGSR2_GLN1;2_GSR2__glutamine synthase clone F11	0.02	-0.41	-0.26	**-1.18**	-0.04
AT2G07050	CAS1__cycloartenol synthase 1	0.28	0.05	-0.39	**-0.96**	-0.08
AT3G13470	Cpn60beta2__TCP-1/cpn60 chaperonin family protein	0.16	-0.06	0.36	**-0.74**	-0.08
AT5G55930	ATOPT1_OPT1__oligopeptide transporter 1	0.08	-0.61	-0.72	**-1.07**	-0.09
AT5G63420	emb2746__RNA-metabolising metallo-beta-lactamase family protein	0.12	-0.13	-0.15	**-0.74**	-0.11
AT3G50740	**UGT72E1__UDP-glucosyl transferase 72E1**	0.00	-0.38	-0.02	**-0.88**	-0.18
AT1G04430	S-adenosyl-L-methionine-dependent methyltransferases superfamily protein	-0.02	-0.25	-0.13	**-0.78**	-0.21
AT5G49910	cpHsc70-2_HSC70-7__chloroplast heat shock protein 70-2	0.10	-0.13	0.09	**-0.71**	-0.24
AT5G17230	PSY__PHYTOENE SYNTHASE	0.11	-0.16	-0.08	**-0.86**	-0.27
AT1G72090	Methylthiotransferase	0.03	0.05	0.00	**-0.74**	-0.27
AT3G54600	Class I glutamine amidotransferase-like superfamily protein	0.18	-0.12	0.04	**-0.77**	-0.27
AT1G18810	phytochrome kinase substrate-related	0.05	-0.64	-0.89	**-1.27**	-0.29
AT5G55230	ATMAP65-1_MAP65-1_MAP65-1__microtubule-associated proteins 65-1	0.11	-0.16	-0.25	**-1.06**	-0.30
AT2G25000	ATWRKY60_WRKY60__WRKY DNA-binding protein 60	-0.04	-0.29	-0.13	**-0.93**	-0.32

AGI identifier	Gene annotation	30 min	2h	4h	8h	24h
AT1G55490	CPN60B_Cpn60beta1_LEN1__chaperonin 60 beta	0.03	0.03	-0.10	**-0.79**	-0.38
AT5G09870	**CESA5__cellulose synthase 5**	0.11	-0.09	0.08	**-0.76**	-0.39
AT4G12310	**CYP706A5__cytochrome P450, family 706, subfamily A, polypeptide 5**	-0.33	-0.08	-0.33	**-0.88**	-0.39
AT5G33320	ARAPPT_CUE1_PPT__Glucose-6-phosphate/phosphate translocator-related	0.10	-0.15	0.05	**-0.87**	-0.39
AT1G70280	NHL domain-containing protein	0.04	0.00	-0.32	**-0.90**	-0.39
AT3G57050	CBL__cystathionine beta-lyase	0.11	-0.07	-0.24	**-0.77**	-0.41
AT5G44580	unknown protein	0.01	-0.32	-0.33	**-0.81**	-0.44
AT1G29050	TBL38__TRICHOME BIREFRINGENCE-LIKE 38	-0.04	-0.06	-0.03	**-0.77**	-0.44
AT5G45930	CHL I2_CHLI-2_CHLI2__magnesium chelatase i2	-0.06	-0.13	-0.15	**-0.88**	-0.46
AT1G76160	sks5__SKU5 similar 5	0.09	-0.26	-0.75	**-1.08**	-0.46
AT3G04940	ATCYSD1_CYSD1__cysteine synthase D1	0.00	-0.05	-0.50	**-0.70**	-0.48
AT1G29280	ATWRKY65_WRKY65__WRKY DNA-binding protein 65	0.02	0.07	-0.09	**-0.95**	-0.51
AT4G18480	CH-42_CH42_CHL11_CHLI-1_CHLI1__P-loop containing nucleoside triphosphate hydrolases superfamily protein	0.15	-0.16	0.00	**-0.73**	-0.54
AT4G39350	**ATCESA2_ATH-A_CESA2__cellulose synthase A2**	0.12	-0.19	-0.25	**-1.10**	-0.54
AT4G16830	Hyaluronan / mRNA binding family	0.01	-0.02	-0.42	**-0.82**	-0.54
AT1G21570	Unknown protein	-0.07	-0.70	-0.14	**-1.57**	-0.55
AT3G23940	dehydratase family	0.02	0.07	-0.12	**-0.87**	-0.55
AT5G50375	CPI1__cyclopropyl isomerase	0.03	-0.35	-0.19	**-0.76**	-0.55
AT4G37800	XTH7__xyloglucan endotransglucosylase/hydrolase 7	0.07	0.07	-0.35	**-0.69**	-0.56
AT5G22640	emb1211__MORN (Membrane Occupation and Recognition Nexus) repeat-containing protein	0.24	0.03	-0.37	**-0.90**	-0.56
AT5G10560	Glycosyl hydrolase family protein	0.03	-0.22	-0.53	**-1.00**	-0.56
AT1G72930	TIR__toll/interleukin-1 receptor-like	-0.12	-0.33	-0.10	**-1.33**	-0.57
AT1G07280	Tetratricopeptide repeat (TPR)-like superfamily protein	-0.09	-0.35	-0.59	**-0.92**	-0.58
AT3G06650	ACLB-1__ATP-citrate lyase B-1	0.26	-0.09	-0.24	**-0.73**	-0.59
AT4G12420	SKU5__Cupredoxin superfamily protein	0.10	-0.11	-0.93	**-1.07**	-0.60
AT4G29060	emb2726__elongation factor Ts family protein	-0.03	0.04	-0.24	**-1.07**	-0.60
AT1G64740	TUA1__alpha-1 tubulin	0.09	-0.15	-0.06	**-0.83**	-0.61
AT1G16350	Aldolase-type TIM barrel family protein	0.07	-0.31	-0.33	**-0.74**	-0.61
AT3G47070	LOCATED IN: thylakoid, chloroplast thylakoid membrane, chloroplast, chloroplast envelope; EXPRESSED IN: 22 plant structures; EXPRESSED DURING: 13 growth stages; CONTAINS InterPro DOMAIN/s: Thylakoid soluble phosphoprotein TSP9 (InterPro:IPR021584 (source: NCBI BLink).	0.09	-0.05	-0.46	**-0.76**	-0.62

AGI identifier	Gene annotation	30 min	2h	4h	8h	24h
AT1G06550	ATP-dependent caseinolytic (Clp) protease/crotonase family protein	0.17	-0.16	0.19	**-0.77**	-0.62
AT5G15410	ATCNGC2_CNGC2_DND1__Cyclic nucleotide-regulated ion channel family protein	0.08	-0.16	-0.63	**-0.78**	-0.63
AT5G46580	pentatricopeptide (PPR) repeat-containing protein	-0.10	-0.01	-0.02	**-0.93**	-0.64
AT3G26060	ATPRX Q_PRXQ__Thioredoxin superfamily protein	0.16	-0.07	-0.16	**-0.79**	**-0.67**
AT5G45490	P-loop containing nucleoside triphosphate hydrolases superfamily protein	0.04	-0.24	-0.42	**-0.89**	**-0.68**
AT5G11420	Protein of unknown function, DUF642	-0.08	-0.31	-0.89	**-0.79**	**-0.71**
AT1G80830	ATNRAMP1_NRAMP1_PMIT1__natural resistance-associated macrophage protein 1	-0.02	-0.46	-0.93	**-0.99**	**-0.75**
AT4G23820	Pectin lyase-like superfamily protein	0.25	-0.11	-0.74	**-0.74**	**-0.76**
AT3G49670	BAM2__Leucine-rich receptor-like protein kinase family protein	0.01	0.02	-0.33	**-0.93**	**-0.76**
AT3G60320	Protein of unknown function (DUF630 and DUF632)	0.03	-0.18	-0.72	**-1.10**	**-0.77**
AT4G38160	pde191__Mitochondrial transcription termination factor family protein	0.27	-0.10	-0.90	**-0.92**	**-0.79**
AT3G17170	RFC3__Translation elongation factor EF1B/ribosomal protein S6 family protein	0.02	0.23	-0.31	**-0.72**	**-0.79**
AT3G09260	BGLU23_LEB_PSR3.1_PYK10__Glycosyl hydrolase superfamily protein	0.08	0.24	0.27	**-0.85**	**-0.81**
AT5G04230	ATPAL3_PAL3__phenyl alanine ammonia-lyase 3	-0.05	-0.48	-0.59	**-0.88**	**-0.81**
AT2G37180	PIP2;3_PIP2C_RD28__Aquaporin-like superfamily protein	-0.16	-0.10	-0.82	**-0.87**	**-0.82**
AT3G54580	Proline-rich extensin-like family protein	-0.15	0.35	-0.61	**-0.91**	**-0.82**
AT4G33010	AtGLDP1_GLDP1__glycine decarboxylase P-protein 1	0.11	0.03	-0.54	**-0.97**	**-0.83**
AT5G65010	ASN2__asparagine synthetase 2	-0.03	0.07	-0.15	**-0.97**	**-0.84**
AT3G06350	EMB3004_MEE32__dehydroquinate dehydratase, putative / shikimate dehydrogenase, putative	-0.11	-0.25	-0.62	**-1.03**	**-0.85**
AT2G39730	RCA__rubisco activase	0.13	-0.01	-0.78	**-0.71**	**-0.88**
AT5G54770	THI1_THI4_TZ__thiazole biosynthetic enzyme, chloroplast (ARA6) (THI1) (THI4)	0.09	-0.07	-0.11	**-0.75**	**-0.89**
AT5G39210	CRR7__chlororespiratory reduction 7	-0.09	0.14	-0.58	**-1.27**	**-0.89**
AT5G51550	EXL3__EXORDIUM like 3	0.08	-0.27	-0.91	**-0.94**	**-0.90**
AT1G47890	AtRLP7_RLP7__receptor like protein 7	-0.15	-0.41	-0.59	**-0.70**	**-0.92**
AT3G45700	Major facilitator superfamily protein	-0.28	-0.42	0.27	**-0.91**	**-0.93**
AT1G29560	Zinc finger C-x8-C-x5-C-x3-H type family protein	0.15	-0.38	-0.45	**-1.00**	**-0.93**
AT5G03300	ADK2__adenosine kinase 2	0.16	-0.30	0.03	**-0.99**	**-0.94**
AT2G44160	MTHFR2_methylenetetrahydrofolate reductase 2	0.20	-0.28	-0.52	**-1.28**	**-0.95**
AT3G29200	ATCM1_CM1__chorismate mutase 1	-0.11	-0.42	-0.39	**-0.95**	**-0.96**

AGI identifier	Gene annotation	30 min	2h	4h	8h	24h
AT5G38430	Ribulose bisphosphate carboxylase (small chain) family protein	0.05	-0.15	-0.30	**-0.74**	**-0.98**
AT5G26260	TRAF-like family protein	0.04	-0.18	0.14	**-0.78**	**-0.99**
AT5G17920	ATCIMS_ATMETS_ATMS1__Cobalamin-independent synthase family protein	0.13	-0.26	-0.41	**-1.06**	**-0.99**
AT4G23550	ATWRKY29_WRKY29__WRKY family transcription factor	-0.19	-0.38	-0.73	**-0.76**	**-1.01**
AT4G14890	FdC2__2Fe-2S ferredoxin-like superfamily protein	-0.10	-0.19	-0.48	**-0.97**	**-1.01**
AT1G29600	Zinc finger C-x8-C-x5-C-x3-H type family protein	-0.10	-0.15	-0.19	**-1.22**	**-1.02**
AT3G16390	NSP3__nitrile specifier protein 3	0.06	0.20	0.30	**-1.03**	**-1.02**
AT4G17810	C2H2 and C2HC zinc fingers superfamily protein	0.11	-0.18	-0.89	**-0.78**	**-1.03**
AT5G01015	unknown protein	0.00	-0.36	-0.60	**-0.78**	**-1.03**
AT3G59970	MTHFR1_methylenetetrahydrofolate reductase 1	0.02	-0.54	-0.40	**-1.30**	**-1.06**
AT3G20370	TRAF-like family protein	0.07	-0.20	0.35	**-0.94**	**-1.06**
AT3G55630	ATDFD_DFD_FPGS3__DHFS-FPGS homolog D	-0.05	-0.19	-0.23	**-0.86**	**-1.06**
AT5G38980	unknown protein	-0.15	-0.03	-0.30	**-0.96**	**-1.09**
AT5G47950	HXXXD-type acyl-transferase family protein	-0.17	-0.54	-0.15	**-0.96**	**-1.11**
AT1G51940	protein kinase family protein / peptidoglycan-binding LysM domain-containing protein	-0.32	-0.08	0.11	**-0.87**	**-1.13**
AT1G11860	Glycine cleavage T-protein family	0.00	-0.16	-0.32	**-1.17**	**-1.14**
AT3G19820	CBB1_DIM_DIM1_DWF1_EVE1__cell elongation protein / DWARF1 / DIMINUTO (DIM)	0.07	-0.11	-0.45	**-1.27**	**-1.15**
AT5G24760	GroES-like zinc-binding dehydrogenase family protein	-0.04	-0.50	-0.34	**-1.08**	**-1.19**
AT4G22210	LCR85__low-molecular-weight cysteine-rich 85	-0.16	-0.27	-0.69	**-1.56**	**-1.27**
AT4G38840	SAUR-like auxin-responsive protein family	-0.04	-0.42	-0.57	**-0.84**	**-1.31**
AT3G16460	JAL34__Mannose-binding lectin superfamily protein	-0.11	0.14	-0.51	**-0.89**	**-1.53**
AT4G15390	HXXXD-type acyl-transferase family protein	0.08	-0.44	-0.70	**-1.39**	**-1.54**
AT4G12545	Bifunctional inhibitor/lipid-transfer protein/seed storage 2S albumin superfamily protein	-0.03	0.28	-0.70	**-1.20**	**-1.66**
AT3G03780	ATMS2_MS2__methionine synthase 2	0.15	-0.55	-0.50	**-1.66**	**-2.22**
AT5G48430	Eukaryotic aspartyl protease family protein	-0.21	-0.77	**-1.12**	0.67	**1.47**
AT3G10985	ATWI-12_SAG20_WI12__senescence associated gene 20	0.12	0.04	**-1.07**	-0.17	**0.74**
AT1G73260	ATKTI1_KTI1__kunitz trypsin inhibitor 1	-0.05	0.20	**-1.74**	-0.39	0.23
AT1G12780	ATUGE1_UGE1__UDP-D-glucose/UDP-D-galactose 4-epimerase 1	-0.25	-0.10	**-1.06**	0.46	-0.09

AGI identifier	Gene annotation	30 min	2h	4h	8h	24h
AT3G16150	ASPGB1__N-terminal nucleophile aminohydrolases (Ntn hydrolases) superfamily protein	-0.04	-0.57	**-1.48**	0.23	-0.36
AT3G53460	CP29__chloroplast RNA-binding protein 29	-0.19	-0.27	**-1.04**	-0.50	-0.56
AT1G66180	Eukaryotic aspartyl protease family protein	-0.33	-0.48	**-1.07**	-0.40	**-0.68**
AT5G26280	TRAF-like family protein	0.17	-0.29	**-1.02**	-0.16	**-0.86**
AT4G36850	PQ-loop repeat family protein / transmembrane family protein	-0.13	-0.17	**-1.17**	0.30	**-0.95**
AT2G27385	Pollen Ole e 1 allergen and extensin family protein	-0.01	-0.10	**-1.40**	-0.57	**-1.00**
AT1G64370	unknown protein	-0.15	-0.22	**-1.01**	**-0.77**	-0.16
AT2G45960	ATHH2_PIP1;2_PIP1B_TMP-A__plasma membrane intrinsic protein 1B	-0.17	-0.11	**-1.14**	**-0.77**	-0.37
AT5G01210	HXXXD-type acyl-transferase family protein	0.05	-0.78	**-1.65**	**-1.37**	-0.38
AT1G65930	cICDH__cytosolic NADP+-dependent isocitrate dehydrogenase	-0.03	-0.29	**-1.13**	**-0.96**	-0.56
AT4G14040	EDA38_SBP2__selenium-binding protein 2	0.21	-0.31	**-1.01**	**-0.70**	-0.60
AT1G05240	Peroxidase superfamily protein	0.08	0.19	**-1.07**	**-1.48**	**-0.91**
AT1G43160	RAP2.6__related to AP2 6	0.02	-0.57	**-1.57**	**-1.16**	**-0.99**
AT1G69100	Eukaryotic aspartyl protease family protein	0.13	-0.04	**-1.06**	**-1.21**	**-1.03**
AT5G25460	Protein of unknown function, DUF642	-0.03	-0.55	**-1.30**	**-1.72**	**-1.41**
AT5G49730	ATFRO6_FRO6_FRO6_ferric reduction oxidase 6	-0.05	-0.27	**-1.35**	**-0.79**	**-1.46**
AT4G23400	PIP1;5_PIP1D__plasma membrane intrinsic protein 1;5	-0.29	-0.16	**-1.06**	**-0.99**	**-1.50**
AT1G08630	THA1__threonine aldolase 1	0.06	-0.54	**-1.81**	**-0.92**	**-1.62**
AT4G29905	unknown protein	0.00	0.29	**-1.16**	**-0.76**	**-1.83**
AT2G36690	2-oxoglutarate (2OG) and Fe(II)-dependent oxygenase superfamily protein	0.09	**-1.13**	-0.18	-0.61	0.31
AT1G48320	Thioesterase superfamily protein	-0.16	**-0.80**	-0.78	**-0.93**	-0.52
AT5G26290	TRAF-like family protein	-0.15	**-0.87**	-0.71	**-1.50**	**-1.36**
AT5G48930	HCT__hydroxycinnamoyl-CoA shikimate/quinate hydroxycinnamoyl transferase	-0.20	**-1.17**	**-1.11**	**-1.50**	**-1.18**
AT3G19450	ATCAD4_CAD_CAD-C_CAD4__GroES-like zinc-binding alcohol dehydrogenase family protein	0.03	**-0.82**	**-1.22**	**-1.74**	**-1.74**
AT1G26810	**GALT1__galactosyltransferase1**	-0.13	**-1.16**	**-1.71**	**-1.65**	**-1.79**

Supplemental Table IV: Biological pathways with significant genes over-represented (P-values < 0.05), indicated in bold face. Genes lists for each time point used correspond to diffentially expressed genes selected after ANOVA analysis.
Normed Frequency is calculated as follows: (Number_in_Classinput_set/Number_Classifiedinput_set)/(Number_in_Classreference_set (25k)/Number_Classifiedreference_set). DEG: Differentially expressed gene.
The 3rd column of the normalized value table represents the p-value of the hypergeometric distribution, which was calculated as follows: p = BC(M,x) * BC(N-M, n-x) / BC(N,n). BC is the binomial coefficient, calculated as follows: BC(n,k) = n! / (k! * [n-k]!). In the above equations, x is the number of input genes with the selected classification, n is the total number of input genes, M is the number of genes with the selected classification in the database (GO/MapMan), and N is the total number of genes in this database. The MapMan data used by Classification SuperViewer is updated to Ath_AGI_LOCUS_TAIR10_Aug2012.txt. [most recent version as of 4 June 2013].

MAPMAN based classification	DEG 2 h down			DEG 4 h down			DEG 8 h down			DEG 24 h down		
	Normed frequency	± bootstrap StdDev	p-value	Normed frequency	± bootstrap StdDev	p-value	Normed frequency	± bootstrap StdDev	p-value	Normed frequency	± bootstrap StdDev	p-value
amino acid metabolism (Input set freq.: 0.06; 0)	-	-	-	**9.94**	***6.496***	**0.016**	**11.74**	***3.492***	**2.71E-05**	**7.86**	***3.05***	**2.96E-05**
C1-metabolism (Input set freq.: 0.03; 0)	-	-	-	-	-	-	**27.77**	***13.538***	**1.29E-05**	**29.21**	***14.576***	**1.06E-05**
cell wall (Input set freq.: 0.04; 0.01)	-	-	-	2.35	*1.58*	0.281	**2.53**	***0.856***	**0.034**	**2.66**	***1.191***	**0.029**
Co-factor and vitamine metabolism (Input set freq.: 0; 0)	-	-	-	-	-	-	**6.85**	***4.24***	**0.031**	3.6	*3.168*	0.211
DNA (Input set freq.: 0; 0.09)	-	-	-	-	-	-	**0.08**	***0.074***	**9.14E-05**	**0.09**	***0.086***	**1.56E-04**
hormone metabolism (Input set freq.: 0.06; 0.01)	-	-	-	-	-	-	**3.07**	***1.191***	**0.01**	**3.78**	***1.295***	**2.09E-03**
lipid metabolism (Input set freq.: 0.03; 0.01)	13.05	-	0.072	-	-	-	1.94	*1.062*	0.132	**2.72**	***1.415***	**0.044**
metal handling (Input set freq.: 0; 0)	-	-	-	**31.14**	***17.149***	**1.85E-03**	**6.69**	***4.07***	**0.033**	3.52	*2.31*	0.215
misc (Input set freq.: 0.07; 0.04)	3.52	*3.184*	0.223	0.81	*0.687*	0.366	1.04	*0.375*	0.164	**1.65**	***0.551***	**0.049**
not assigned (Input set freq.: 0.22; 0.35)	0.47	*0.399*	0.242	0.76	*0.265*	0.117	**0.56**	***0.104***	**9.78E-05**	**0.64**	***0.111***	**1.26E-03**
protein (Input set freq.: 0.11; 0.14)	1.15	*0.911*	0.397	0.8	*0.457*	0.217	**0.28**	***0.125***	**1.78E-04**	0.78	*0.19*	0.072
PS (Input set freq.: 0.05; 0)	-	-	-	-	-	-	**6.74**	***2.684***	**8.17E-04**	**8.51**	***3.302***	**7.24E-05**
secondary metabolism (Input set freq.: 0.05; 0.01)	**25.22**	***14.944***	**2.48E-03**	**8.73**	***4.084***	**4.40E-03**	**5.62**	***1.7***	**2.97E-05**	**3.94**	***1.665***	**3.46E-03**
signalling (Input set freq.: 0; 0.04)	-	-	-	-	-	-	0.81	*0.395*	0.181	**0.21**	***0.175***	**0.041**
TCA / org transformation (Input set freq.: 0.01; 0)	-	-	-	16.35	*11.594*	0.058	**7.03**	***5.297***	**0.03**	-	-	-
tetrapyrrole synthesis (Input set freq.: 0.01; 0)	-	-	-	-	-	-	**11.57**	***6.227***	**0.012**	-	-	-
transport (Input set freq.: 0.05; 0.03)	-	-	-	2.53	*1.763*	0.143	**2.17**	***0.805***	**0.02**	1.71	*0.676*	0.077

MAPMAN based classification	DEG 30 min up			DEG 2 h up			DEG 4 h up			DEG 8 h up			DEG 24 h up		
	Normed frequency	± bootstrap StdDev	p-value	Normed frequency	± bootstrap StdDev	p-value	Normed frequency	± bootstrap StdDev	p-value	Normed frequency	± bootstrap StdDev	p-value	Normed frequency	± bootstrap S	p-value
DNA (Input set freq.: 0; 0.09)	0.76	*0.557*	0.366	0.26	*0.207*	0.077	**0.21**	***0.143***	**0.036**	**0.07**	***0.052***	**5.04E-06**	**0.04**	***0.028***	**9.72E-10**
fermentation (Input set freq.: 0.01; 0)	-	-	-	-	-	-	-	-	-	15.68	*12.201*	0.06	**29.38**	***15.091***	**1.29E-04**
glycolysis (Input set freq.: 0.01; 0)	**30.38**	***31.597***	**0.032**	10.37	*12.411*	0.088	8.34	*6.131*	0.107	**8.34**	***4.696***	**5.21E-03**	**6.94**	***3.017***	**2.41E-03**
hormone metabolism (Input set freq.: 0.04; 0.01)	-	-	-	1.51	*1.272*	0.345	2.43	*1.516*	0.149	2.02	*0.937*	0.064	**2.78**	***0.781***	**1.55E-03**
misc (Input set freq.: 0.17; 0.04)	-	-	-	**3.09**	***1.262***	**9.19E-03**	**6.21**	***1.269***	**7.03E-09**	**4.14**	***0.62***	**2.39E-11**	**3.62**	***0.531***	**3.29E-13**
not assigned (Input set freq.: 0.21; 0.35)	1.22	*0.423*	0.177	0.97	*0.225*	0.129	**0.61**	***0.148***	**0.015**	**0.68**	***0.112***	**1.04E-03**	**0.6**	***0.072***	**7.37E-07**
protein (Input set freq.: 0.11; 0.14)	0.49	*0.368*	0.267	0.67	*0.325*	0.138	**0.27**	***0.17***	**0.013**	**0.54**	***0.144***	**5.24E-03**	**0.79**	***0.143***	**0.031**
redox (Input set freq.: 0.02; 0)	-	-	-	-	-	-	**6.27**	***3.542***	**0.037**	**5.22**	***2.279***	**2.40E-03**	**4.57**	***1.606***	**7.64E-04**
RNA (Input set freq.: 0.04; 0.09)	1.57	*0.64*	0.239	0.8	*0.428*	0.215	0.43	*0.295*	0.099	**0.64**	***0.212***	**0.047**	**0.45**	***0.134***	**1.31E-03**
stress (Input set freq.: 0.09; 0.03)	-	-	-	2	*1.059*	0.126	2.14	*1.023*	0.077	**2.32**	***0.597***	**2.66E-03**	**2.68**	***0.552***	**8.68E-06**
transport (Input set freq.: 0.06; 0.03)	2.35	*2.307*	0.285	2.4	*1.324*	0.093	1.93	*1.027*	0.133	**2.79**	***0.814***	**5.82E-04**	**2.14**	***0.515***	**2.14E-03**

Supplemental Table V: The 467 genes found to be differentially expressed in all the comparisons between phenanthrene-treated and control plants (hybridizations 5-9), selected after ANOVA analysis. Expression changes in bolt correspond to genes differentially expressed at the significant threshold of Bonferroni p-value<0.05. AGI and gene annotation in bold face correspond to gene involved in the "xenome". Our list of genes was compare to diffentially expressed genes identified in the plant response aluminum (60), atrazine (33), BOA (benzoxazolin-2(3H)-one) (61), cadmium (62), PCB (Polychlorinated biphenyl) (63), phenol (64) selenium (65) and TNT (trinitrotoluene) (66). Our list was also compare to genes differentially regulated by anoxia, hypoxia, and O2 deprivation in the seedlings/shoots of *Arabidopsis* microarray datasets (Picciariello et al., 2012). *: log2 ratios

AGI identifier	Bincode identifier	MAPMAN classification	Gene annotation	Our study					DEG in common with other xenobiotic transcriptomes	Weisman et al., 2010	Jin *et al.*, 2011	Van Hoewyk *et al.*, 2008		Ramel *et al.*, 2007		Baerson *et al.*, 2005	Goodwin and Sutter, 2009	Xu *et al.*, 2012	Landa *et al.*, 2010		Herbette *et al.*, 2006		Pucciariello et al., 2012
				Phenanthrene Seedlings						Phenanthrene Seedlings	PCB ?	Selenium		Atrazine Mannitol	Atrazine Sucrose	BOA	Aluminium	Phénol	Trinitrotoluene		Cadmium		Anoxia-hypoxia
				30 min*	2h*	4h*	8h*	24h*	Number in common	109	146	Leaves 32	Roots 52	Seedlings 113	119	45	14	16	Leaves 15	Roots 2	Leaves 134	Roots 182	3
AT1G05670	**17.8.1**	**hormone metabolism.salicylic acid.synthesis-degradation**	**Pentatricopeptide repeat (PPR-like) superfamily protein**	ns	ns	ns	**1.30**	**0.69**							X								
AT1G05680	**17.8.1**	**hormone metabolism.salicylic acid.synthesis-degradation**	**UGT74E2__UDP-glycosyltransferase 74E2**	ns	ns	**1.01**	**1.80**	**0.83**	X		X	X	X			X							
AT1G11610	**26.10**	**misc.cytochrome P450**	**CYP71A18__cytochrome P450, family 71, subfamily A, polypeptide 18**	ns	ns	ns	ns	**1.12**															
AT1G17170	**26.9**	**misc.glutathione S transferases**	**ATGSTU24_GST_GSTU24__glutathione S-transferase TAU 24**	ns	ns	**1.57**	**2.00**	**2.05**	X	up		X				X							
AT1G17190	**26.9**	**misc.glutathione S transferases**	**ATGSTU26_GSTU26__glutathione S-transferase tau 26**	ns	ns	ns	ns	**-1.41**	X													X	
AT1G26810	**29.7.12**	**protein.glycosylation.beta-1,3-galactosyltransferase(beta-1,3-GalT)**	**GALACTOSYLTRANSFERASE1**	ns	**-1.16**	**-1.71**	**-1.65**	**-1.79**															
AT1G27120	**26.2**	**misc.UDP glucosyl and glucoronyl transferases**	**Galactosyltransferase family protein**	ns	**0.91**	**2.00**	**2.30**	**2.45**															
AT1G55850	**10.2.1**	**cell wall.cellulose synthesis.cellulose synthase**	**ATCSLE1_CSLE1__cellulose synthase like E1**	ns	ns	ns	**1.17**	ns	X			X				X							
AT1G58370	**10.6.2**	**cell wall.degradation.mannan-xylose-arabinose-fucose**	**ATXYN1_RXF12__glycosyl hydrolase family 10 protein / carbohydrate-binding domain-containing protein**	ns	ns	**1.13**	ns	**-0.86**	X		X	X											
AT1G64900	**26.10**	**misc.cytochrome P450**	**CYP89_CYP89A2__cytochrome P450, family 89, subfamily A, polypeptide 2**	ns	ns	**1.08**	**1.16**	**1.19**	X		X	X											
AT1G64930	**26.10**	**misc.cytochrome P450**	**CYP89A7__cytochrome P450, family 87, subfamily A, polypeptide 7**	ns	ns	ns	**0.85**	**0.94**															
AT1G69500	**26.10**	**misc.cytochrome P450**	**CYP704B1__cytochrome P450, family 704, subfamily B, polypeptide 1**	ns	ns	ns	**-0.71**	**0.71**															
AT1G75270	**21.2.1**	**redox.ascorbate and glutathione.ascorbate**	**DHAR2__dehydroascorbate reductase 2**	ns	ns	**1.09**	**1.60**	**1.49**	X	up				X								X	
AT1G78340	**26.9**	**misc.glutathione S transferases**	**ATGSTU22_GSTU22__glutathione S-transferase TAU 22**	ns	ns	**1.62**	**1.75**	**1.69**	X	up	X					X		X					
AT1G78380	**26.9**	**misc.glutathione S transferases**	**ATGSTU19_GST8_GSTU19__glutathione S-transferase TAU 19**	ns	ns	**1.23**	**1.45**	**1.49**	X	up												X	
AT2G12190	**26.10**	**misc.cytochrome P450**	**Cytochrome P450 superfamily protein**	ns	ns	**1.04**	**0.97**	**0.96**	X		X												
AT2G29460	**26.9**	**misc.glutathione S transferases**	**ATGSTU4_GST22_GSTU4__glutathione S-transferase tau 4**	ns	ns	ns	**1.37**	**0.95**	X	up		X	X										
AT2G29470	**26.9**	**misc.glutathione S transferases**	**ATGSTU3_GST21_GSTU3__glutathione S-transferase tau 3**	ns	ns	ns	**1.14**	**0.76**															
AT2G29940	**34.16**	**transport.ABC transporters and multidrug resistance systems**	**ATPDR3_PDR3__pleiotropic drug resistance 3**	ns	ns	ns	**0.96**	ns	X						X							X	
AT2G36770	**26.2**	**misc.UDP glucosyl and glucoronyl transferases**	**UDP-Glycosyltransferase superfamily protein**	ns	ns	ns	**1.65**	ns															
AT2G40890	**26.10**	**misc.cytochrome P450**	**CYP98A3__cytochrome P450, family 98, subfamily A, polypeptide 3**	ns	ns	ns	ns	**-0.74**	X					X								X	
AT2G45550	**26.10**	**misc.cytochrome P450**	**CYP76C4__cytochrome P450, family 76, subfamily C, polypeptide 4**	ns	ns	ns	**0.91**	**0.89**	X					X	X							X	
AT3G09270	**26.9**	**misc.glutathione S transferases**	**ATGSTU8_GSTU8__glutathione S-transferase TAU 8**	ns	ns	**1.15**	ns	**1.09**	X	up	X			X		X						X	
AT3G14620	**26.10**	**misc.cytochrome P450**	**CYP72A8__cytochrome P450, family 72, subfamily A, polypeptide 8**	ns	ns	ns	**0.86**	**1.40**	X	up		X				X							
AT3G21560	**26.2**	**misc.UDP glucosyl and glucoronyl transferases**	**UGT84A2__UDP-Glycosyltransferase superfamily protein**	ns	**1.48**	**2.21**	**1.60**	**1.93**	X	up	X										X		
AT3G26200	**26.10**	**misc.cytochrome P450**	**CYP71B22__cytochrome P450, family 71, subfamily B, polypeptide 22**	ns	ns	ns	ns	**1.07**	X		X										X	X	
AT3G26210	**26.10**	**misc.cytochrome P450**	**CYP71B23__cytochrome P450, family 71, subfamily B, polypeptide 23**	ns	ns	ns	ns	**1.01**	X	up						X					X		
AT3G50740	**16.2.1**	**secondary metabolism.phenylpropanoids.lignin biosynthesis**	**UGT72E1__UDP-glucosyl transferase 72E1**	ns	ns	ns	**-0.88**	ns	X	up				X	X							X	
AT3G59140	**34.16**	**transport.ABC transporters and multidrug resistance systems**	**ATMRP14_MRP14__multidrug resistance-associated protein 14**	ns	ns	ns	**0.76**	**0.67**	X		X	X				X							
AT4G12310	**16.8.3**	**secondary metabolism.flavonoids.dihydroflavonols**	**CYP706A5__cytochrome P450, family 706, subfamily A, polypeptide 5**	ns	ns	ns	**-0.88**	ns	X		X												
AT4G15480	**26.2**	**misc.UDP glucosyl and glucoronyl transferases**	**UGT84A1__UDP-Glycosyltransferase superfamily protein**	ns	ns	**1.27**	**1.02**	**1.40**	X		X												
AT4G34131	**26.2**	**misc.UDP glucosyl and glucoronyl transferases**	**UGT73B3__UDP-glucosyl transferase 73B3**	ns	ns	ns	**1.31**	**1.38**															
AT4G39350	**10.2.1**	**cell wall.cellulose synthesis.cellulose synthase**	**ATCESA2_ATH-A_CESA2__cellulose synthase A2**	ns	ns	ns	**-1.10**	ns															
AT5G09870	**10.2.1**	**cell wall.cellulose synthesis.cellulose synthase**	**CESA5__cellulose synthase 5**	ns	ns	ns	**-0.76**	ns	X						X							X	
AT5G36270	**21.2.1**	**redox.ascorbate and glutathione.ascorbate**	**pseudogene of dehydroascorbate reductase**	ns	ns	**1.38**	**1.56**	**1.74**	X				X										

AGI identifier	Bincode identifier	MAPMAN classification	Gene annotation	Our study					DEG in common with other xenobiotic transcritpomes	Weisman et al., 2010	Jin *et al.*, 2011	Van Hoewyk *et al.*, 2008		Ramel *et al.*, 2007		Baerson *et al.*, 2005	Goodwin and Sutter, 2009	Xu *et al.*, 2012	Landa *et al.*, 2010		Herbette *et al.*, 2006		Pucciariello et al., 2012
				Phenanthrene Seedlings						Phenanthrene Seedlings	PCB ?	Selenium		Atrazine Mannitol	Atrazine Sucrose	BOA	Aluminium	Phénol	Trinitrotoluene		Cadmium		Anoxia-hypoxia
				30 min*	2h*	4h*	8h*	24h*	Number in commmon	109	146	Leaves 32	Roots 52	Seedlings 113	119	45	14	16	Leaves 15	Roots 2	Leaves 134	Roots 182	3
AT5G39090	**16.8.1.21**	**secondary metabolism.flavonoids.anthocyanins.anthocyanin 5-aromatic acyltransferase**	**HXXXD-type acyl-transferase family protein**	ns	ns	ns	**0.82**	**1.05**	X			X									X	X	
AT1G60950	1.1.5.2	PS.lightreaction.other electron carrier (ox/red).ferredoxin	ATFD2_FED A__2Fe-2S ferredoxin-like superfamily protein	ns	ns	ns	ns	**-0.72**	X	down	X										X	X	
AT5G58260	1.1.6	PS.lightreaction.NADH DH	oxidoreductases, acting on NADH or NADPH, quinone or similar compound as acceptor	ns	ns	ns	ns	**-1.05**	X	down	X										X		
AT4G33010	1.2.4.1	PS.photorespiration.glycine cleavage.P subunit	AtGLDP1_GLDP1__glycine decarboxylase P-protein 1	ns	ns	ns	**-0.97**	**-0.83**	X	down	X												
AT1G11860	1.2.4.2	PS.photorespiration.glycine cleavage.T subunit	Glycine cleavage T-protein family	ns	ns	ns	**-1.17**	**-1.14**	X	down	X										X	X	
AT2G39730	1.3.13	PS.calvin cyle.rubisco interacting	RCA__rubisco activase	ns	ns	ns	**-0.71**	**-0.88**	X	down	X			X	X						X	X	
AT4G16980	10.5.1	cell wall.cell wall proteins.AGPs	arabinogalactan-protein family	ns	ns	ns	ns	**-1.14**	X	down	X							X			X	X	
AT2G45470	10.5.1	cell wall.cell wall proteins.AGPs	AGP8_FLA8__FASCICLIN-like arabinogalactan protein 8	ns	ns	ns	ns	**-0.77**	X	down				X	X						X	X	
AT4G23820	10.6.3	cell wall.degradation.pectate lyases and polygalacturonases	Pectin lyase-like superfamily protein	ns	ns	ns	**-0.74**	**-0.76**	X	down	X			X							X		
AT5G06860	10.6.3	cell wall.degradation.pectate lyases and polygalacturonases	ATPGIP1_PGIP1__polygalacturonase inhibiting protein 1	ns	ns	ns	ns	**0.90**	X	up				X		X			X		X	X	
AT4G37800	10.7	cell wall.modification	XTH7__xyloglucan endotransglucosylase/hydrolase 7	ns	ns	ns	**-0.69**	ns	X	down			X	X	X							X	
AT3G15850	11.2.1	lipid metabolism.FA desaturation.desaturase	ADS3_FAD5_FADB_JB67__fatty acid desaturase 5	ns	ns	ns	ns	**-0.91**	X	down				X	X								
AT5G54500	11.8	lipid metabolism."exotics" (steroids, squalene etc)	FQR1__flavodoxin-like quinone reductase 1	ns	**1.12**	**1.14**	**1.50**	**1.79**	X	up						X						
AT4G38690	11.9.3	lipid metabolism.lipid degradation.lysophospholipases	PLC-like phosphodiesterases superfamily protein	ns	ns	ns	ns	**-0.71**	X	down	X		X										
AT1G68620	11.9.3.2	lipid metabolism.lipid degradation.lysophospholipases.carboxylesterase	alpha/beta-Hydrolases superfamily protein	**0.93**	**2.18**	**1.68**	**2.77**	**2.70**	X	up	X		X	X	X	X				X		X		
AT5G19550	13.1.1.2.1	amino acid metabolism.synthesis.central amino acid metabolism.aspartate.aspartate aminotransferase	AAT2_ASP2__aspartate aminotransferase 2	ns	ns	ns	ns	**1.26**	X	up				X	X		X				X		X
AT5G65010	13.1.3.1.1	amino acid metabolism.synthesis.aspartate family.asparagine.asparagine synthetase	ASN2__asparagine synthetase 2	ns	ns	ns	**-0.97**	**-0.84**	X	down	X			X	X								
AT2G33150	13.2.4.1	amino acid metabolism.degradation.branched-chain group.shared	KAT2_PED1_PKT3__peroxisomal 3-ketoacyl-CoA thiolase 3	ns	ns	ns	**0.84**	**0.68**	X	up	X			X	X								
AT1G62570	16.5.1.1.1.10	secondary metabolism.sulfur-containing.glucosinolates.synthesis.aliphatic.flavin-containing monooxygenase	FMO GS-OX4__flavin-monooxygenase glucosinolate S-oxygenase 4	ns	ns	ns	ns	**0.78**	X	up					X						X		
AT3G45140	17.7.1.2	hormone metabolism.jasmonate.synthesis-degradation.lipoxygenase	ATLOX2_LOX2__lipoxygenase 2	ns	ns	ns	ns	**-1.11**	X	up	X			X	X								
AT5G45930	19.10	tetrapyrrole synthesis.magnesium chelatase	CHL I2_CHLI-2_CHLI2__magnesium chelatase i2	ns	ns	ns	**-0.88**	ns	X	down				X	X							X	
AT1G66100	20.1	stress.biotic	Plant thionin	ns	ns	ns	**0.82**	**-1.11**	X	down					X						X		
AT2G43590	20.1	stress.biotic	Chitinase family protein	ns	ns	ns	ns	**1.09**	X	up	X					X							
AT1G75040	20.1	stress.biotic	PR-5_PR5__pathogenesis-related gene 5	ns	**1.32**	**1.50**	**1.71**	**1.75**	X	up	X	X									X	X	
AT1G73260	20.1.7.6.1	stress.biotic.PR-proteins.proteinase inhibitors.trypsin inhibitor	ATKTI1_KTI1__kunitz trypsin inhibitor 1	ns	ns	**-1.74**	ns	ns	X	up					X						X	X	
AT3G62600	20.2.1	stress.abiotic.heat	ATERDJ3B_ERDJ3B__DNAJ heat shock family protein	ns	ns	ns	ns	**0.79**	X	up				X	X						X	X	
AT1G18980	20.2.99	stress.abiotic.unspecified	RmlC-like cupins superfamily protein	ns	**1.16**	**1.55**	**1.57**	**1.59**	X	up												X	
AT2G21620	20.2.99	stress.abiotic.unspecified	RD2__Adenine nucleotide alpha hydrolases-like superfamily protein	ns	ns	ns	**1.28**	**1.82**	X	up					X		X				X		
AT1G21750	21.1	redox.thioredoxin	ATPDI5_ATPDIL1-1_PDI5_PDIL1-1__PDI-like 1-1	ns	ns	ns	ns	**0.93**	X	up				X	X						X		
AT1G77510	21.1	redox.thioredoxin	ATPDI6_ATPDIL1-2_PDI6_PDIL1-2__PDI-like 1-2	ns	ns	ns	ns	**0.96**	X	up	X												
AT3G24170	21.2.2	redox.ascorbate and glutathione.glutathione	ATGR1_GR1__glutathione-disulfide reductase	ns	ns	ns	ns	**0.73**	X	up	X						X					X	
AT3G55630	25.8	C1-metabolism.tetrahydrofolate synthase	ATDFD_DFD__DHFS-FPGS homolog D	ns	ns	ns	**-0.86**	**-1.06**	X	down	X			X	X						X		
AT5G64250	26.1	misc.misc2	Aldolase-type TIM barrel family protein	ns	ns	ns	**1.62**	**1.55**	X	up						X							
AT5G19440	26.11.1	misc.alcohol dehydrogenases	NAD(P)-binding Rossmann-fold superfamily protein	ns	ns	ns	ns	**1.28**	X	up												X	
AT1G12090	26.21	misc.protease inhibitor/seed storage/lipid transfer protein (LTP) family protein	ELP__extensin-like protein	ns	ns	ns	ns	**-1.08**	X	down							X				X	X	
AT4G12480	26.21	misc.protease inhibitor/seed storage/lipid transfer protein (LTP) family protein	pEARLI 1__Bifunctional inhibitor/lipid-transfer protein/seed storage 2S albumin superfamily protein	ns	ns	ns	ns	**1.19**	X	up		X				X							
AT4G12490	26.21	misc.protease inhibitor/seed storage/lipid transfer protein (LTP) family protein	Bifunctional inhibitor/lipid-transfer protein/seed storage 2S albumin superfamily protein	ns	ns	ns	ns	**1.90**	X	up	X					X	X						
AT3G22600	26.21	misc.protease inhibitor/seed storage/lipid transfer protein (LTP) family protein	Bifunctional inhibitor/lipid-transfer protein/seed storage 2S albumin superfamily protein	ns	**1.68**	**1.96**	**1.36**	**1.96**	X	up	X												
AT2G48140	26.21	misc.protease inhibitor/seed storage/lipid transfer protein (LTP) family protein	EDA4__Bifunctional inhibitor/lipid-transfer protein/seed storage 2S albumin superfamily protein	ns	ns	**1.20**	**0.73**	ns	X	up												X	
AT3G04000	26.22	misc.short chain dehydrogenase/reductase (SDR)	NAD(P)-binding Rossmann-fold superfamily protein	ns	**0.95**	**1.16**	**1.53**	**1.23**	X	up		X				X							
AT4G13180	26.22	misc.short chain dehydrogenase/reductase (SDR)	NAD(P)-binding Rossmann-fold superfamily protein	ns	ns	**1.03**	**1.07**	**1.39**	X	up					X	X					X	X	
AT4G14890	26.30	misc. other Ferredoxins and Rieske domain	2Fe-2S ferredoxin-like superfamily protein	ns	ns	ns	**-0.97**	**-1.01**	X	down												X	
AT5G16970	26.7	misc.oxidases - copper, flavone etc.	AER_AT-AER__alkenal reductase	ns	ns	ns	**1.15**	**1.28**	X	up	X	X				X							
AT2G29350	26.8	misc.nitrilases, *nitrile lyases, berberine bridge enzymes, reticuline oxidases, troponine reductases	SAG13__senescence-associated gene 13	ns	ns	ns	ns	**1.55**	X	up	X			X	X	X					X		
AT4G20860	26.8	misc.nitrilases, *nitrile lyases, berberine bridge enzymes, reticuline oxidases, troponine reductases	FAD-binding Berberine family protein	ns	**0.91**	ns	**1.45**	**1.79**	X	up	X		X	X		X							
AT1G30700	26.8	misc.nitrilases, *nitrile lyases, berberine bridge enzymes, reticuline oxidases, troponine reductases	FAD-binding Berberine family protein	ns	**1.26**	**1.06**	**1.56**	**2.28**	X	up				X	X	X						X	
AT5G59820	27.3.11	RNA.regulation of transcription.C2H2 zinc finger family	RHL41_ZAT12__C2H2-type zinc finger family protein	**1.19**	**1.63**	**2.14**	**2.70**	**2.50**	X	up			X		X							X	
AT1G22640	27.3.25	RNA.regulation of transcription.MYB domain transcription factor family	ATMYB3_MYB3__myb domain protein 3	ns	ns	ns	ns	**-0.83**	X	down												X	
AT4G38620	27.3.25	RNA.regulation of transcription.MYB domain transcription factor family	ATMYB4_MYB4__myb domain protein 4	**3.51**	**2.19**	**2.30**	**2.18**	**1.94**	X	up						X							
AT4G24770	27.4	RNA.RNA binding	ATRBP31_ATRBP33_CP31_RBP31__31-kDa RNA binding protein	ns	ns	ns	ns	**-0.70**	X	down												X	

AGI identifier	Bincode identifier	MAPMAN classification	Gene annotation	Our study					DEG in common with other xenobiotic transcriptomes	Weisman et al., 2010	Jin *et al.*, 2011	Van Hoewyk *et al.*, 2008		Ramel *et al.*, 2007		Baerson *et al.*, 2005	Goodwin and Sutter, 2009	Xu *et al.*, 2012	Landa *et al.*, 2010		Herbette *et al.*, 2006		Pucciariello et al., 2012
				Phenanthrene						Phenanthrene	PCB	Selenium		Atrazine Mannitol	Atrazine Sucrose	BOA	Aluminium	Phénol	Trinitrotoluene		Cadmium		Anoxia-hypoxia
				Seedlings						Seedlings	?	Leaves	Roots	Seedlings					Leaves	Roots	Leaves	Roots	
				30 min*	2h*	4h*	8h*	24h*	Number in commmon	109	146	32	52	113	119	45	14	16	15	2	134	182	3
AT3G56910	29.2.1.1.1.2.85	protein.synthesis.ribosomal protein.prokaryotic.chloroplast.50S subunit.PSRP5	PSRP5__plastid-specific 50S ribosomal protein 5	ns	ns	ns	ns	**-0.75**	X	down											X		
AT1G66580	29.2.1.2.2.10	protein.synthesis.ribosomal protein.eukaryotic.60S subunit.L10	RPL10C_SAG24__senescence associated gene 24	ns	ns	ns	**1.26**	**1.44**	X	up					X						X	X	
AT4G29060	29.2.4	protein.synthesis.elongation	emb2726__elongation factor Ts family protein	ns	ns	ns	**-1.07**	ns	X	down	X										X		
AT1G78660	29.5	protein.degradation	ATGGH1_GGH1__gamma-glutamyl hydrolase 1	ns	**1.98**	ns	**1.96**	**1.27**	X	up				X								X	
AT1G32960	29.5.1	protein.degradation.subtilases	ATSBT3.3_SBT3.3__Subtilase family protein	ns	ns	ns	ns	**1.27**	X	up						X							
AT5G42300	29.5.11.1	protein.degradation.ubiquitin.ubiquitin	UBL5__ubiquitin-like protein 5	ns	ns	ns	**0.81**	**1.23**	X	up													
AT1G63840	29.5.11.4.2	protein.degradation.ubiquitin.E3.RING	RING/U-box superfamily protein	**0.83**	**1.80**	**1.64**	**2.10**	**2.16**	X	up													
AT3G01480	29.6	protein.folding	ATCYP38_CYP38__cyclophilin 38	ns	ns	ns	ns	**-0.88**	X	down											X		
AT4G25900	3.5	minor CHO metabolism.others	Galactose mutarotase-like superfamily protein	ns	ns	ns	ns	**0.82**	X	up											X	X	
AT2G37760	3.5	minor CHO metabolism.others	NAD(P)-linked oxidoreductase superfamily protein	ns	ns	ns	ns	**0.82**	X	up		X				X							
AT3G22840	30.11	signalling.light	ELIP_ELIP1__Chlorophyll A-B binding family protein	**0.89**	**1.40**	**2.19**	**1.70**	**2.38**	X	up	X		X				X				X	X	
AT1G51940	30.2.21	signalling.receptor kinases.lysine motif	protein kinase family protein / peptidoglycan-binding LysM domain-containing protein	ns	ns	ns	**-0.87**	**-1.13**	X	down	X			X	X				X			X	
AT5G61790	30.3	signalling.calcium	ATCNX1_CNX1__calnexin 1	ns	ns	ns	ns	**0.72**	X	up				X	X						X	X	
AT2G33380	30.3	signalling.calcium	CLO-3_RD20__Caleosin-related family protein	ns	ns	ns	ns	**0.77**	X	up	X	X									X		
AT2G41100	30.3	signalling.calcium	ATCAL4_TCH3__Calcium-binding EF hand family protein	ns	ns	ns	ns	**1.10**	X	down			X						X				
AT4G14365	31.1	cell.organisation	XBAT34__XB3 ortholog 4 in Arabidopsis thaliana	ns	ns	ns	ns	**1.36**	X	up			X			X					X	X	
AT4G02380	33.2	development.late embryogenesis abundant	AtLEA5_SAG21__senescence-associated gene 21	ns	ns	ns	ns	**1.17**	X	up	X			X	X						X		
AT3G10500	33.99	development.unspecified	anac053_NAC053__NAC domain containing protein 53	ns	ns	ns	**1.48**	**1.16**	X	up						X					X		
AT2G41380	33.99	development.unspecified	S-adenosyl-L-methionine-dependent methyltransferases superfamily protein	ns	ns	ns	**0.87**	**1.99**	X	up						X					X	X	
AT5G22640	33.99	development.unspecified	emb1211__MORN (Membrane Occupation and Recognition Nexus) repeat-containing protein	ns	ns	ns	**-0.90**	ns	X	down													
AT4G23700	34.12	transport.metal	ATCHX17_CHX17__cation/H+ exchanger 17	ns	ns	ns	ns	**0.97**	X	up			X			X						X	
AT1G68570	34.13	transport.peptides and oligopeptides	Major facilitator superfamily protein	ns	ns	ns	ns	**1.14**	X	up	X	X		X	X	X						X	
AT4G23400	34.19.1	transport.Major Intrinsic Proteins.PIP	PIP1;5_PIP1D__plasma membrane intrinsic protein 1;5	ns	ns	**-1.06**	**-0.99**	**-1.50**	X	down	X			X	X						X	X	
AT2G36950	34.99	transport.misc	Heavy metal transport/detoxification superfamily protein	ns	ns	ns	**1.26**	**1.01**	X	up				X						X		X	
AT4G25640	34.99	transport.misc	ATDTX35_DTX35_FFT__detoxifying efflux carrier 35	ns	**1.66**	**1.40**	**1.98**	**2.11**	X	up	X			X	X								
AT3G20820	35.1	not assigned.no ontology	Leucine-rich repeat (LRR) family protein	ns	ns	ns	ns	**-0.86**	X	down							X				X		
AT3G50440	35.1	not assigned.no ontology	ATMES10_MES10__methyl esterase 10	ns	**0.96**	ns	ns	**1.12**	X	up	X												
AT5G27760	35.1	not assigned.no ontology	Hypoxia-responsive family protein	ns	ns	ns	**1.19**	**1.43**	X	up	X										X	X	
AT1G21670	35.1	not assigned.no ontology	unknown protein	ns	**0.97**	ns	**1.20**	**1.79**	X	up						X							
AT2G05380	35.1.40	not assigned.no ontology.glycine rich proteins	GRP3S__glycine-rich protein 3 short isoform	ns	ns	ns	**1.00**	**1.85**	X	up													
AT2G25510	35.2	not assigned.unknown	unknown protein	ns	ns	ns	ns	**-1.52**	X	up				X	X				X		X	X	
AT5G51720	35.2	not assigned.unknown	2 iron, 2 sulfur cluster binding	ns	ns	ns	ns	**-1.24**	X	down				X	X						X		
AT5G39210	35.2	not assigned.unknown	CRR7__chlororespiratory reduction 7	ns	ns	ns	**-1.27**	**-0.89**	X	down	X										X		
AT5G11420	35.2	not assigned.unknown	Protein of unknown function, DUF642	ns	ns	ns	**-0.79**	**-0.71**	X	down	X			X							X	X	
AT3G50685	35.2	not assigned.unknown	unknown protein	ns	ns	ns	ns	**-0.66**	X	down											X		
AT3G18250	35.2	not assigned.unknown	Putative membrane lipoprotein	ns	ns	ns	ns	**0.71**	X	up					X	X					X	X	
AT5G51040	35.2	not assigned.unknown	unknown protein	ns	ns	ns	ns	**0.83**	X	up													
AT5G62630	35.2	not assigned.unknown	HIPL2__hipl2 protein precursor	ns	ns	ns	ns	**1.21**	X	up						X						X	
AT5G61820	35.2	not assigned.unknown	unknown protein	ns	ns	ns	**0.96**	**1.25**	X	up	X	X		X	X	X							
AT2G18690	35.2	not assigned.unknown	unknown protein	ns	ns	ns	ns	**1.98**	X	up			X			X						X	
AT2G16900	35.2	not assigned.unknown	Arabidopsis phospholipase-like protein (PEARLI 4) family	**0.98**	**1.68**	**1.67**	**1.61**	**2.16**	X	up					X						X	X	
AT5G48540	35.2	not assigned.unknown	receptor-like protein kinase-related family protein	**1.42**	**2.44**	**3.27**	**3.48**	**3.51**	X	up						X					X		
AT1G07280	35.2	not assigned.unknown	Tetratricopeptide repeat (TPR)-like superfamily protein	ns	ns	ns	**-0.92**	ns	X	down	X												
AT3G47070	35.2	not assigned.unknown	unknown protein	ns	ns	ns	**-0.76**	ns	X	down					X						X	X	
AT5G63680	4.1.15	glycolysis.cytosolic branch.pyruvate kinase (PK)	Pyruvate kinase family protein	ns	ns	ns	ns	**0.79**	X	up											X	X	
AT3G04120	4.1.9	glycolysis.cytosolic branch.glyceraldehyde 3-phosphate dehydrogenase (GAP-DH)	GAPC_GAPC-1_GAPC1__glyceraldehyde-3-phosphate dehydrogenase C subunit 1	ns	ns	ns	ns	**1.09**	**1.11**	X	up				X									
AT5G56630	4.3.5	glycolysis.unclear/dually targeted.phosphofructokinase (PFK)	PFK7__phosphofructokinase 7	**0.91**	**1.59**	**2.41**	**1.54**	**2.53**	X	up	X				X		X				X		
AT5G17380	5.2	fermentation.PDC	Thiamine pyrophosphate dependent pyruvate decarboxylase family protein	ns	ns	ns	ns	**1.48**	X	up											X	X	
AT1G77120	5.3	fermentation.ADH	ADH_ADH1_ATADH_ATADH1__alcohol dehydrogenase 1	ns	ns	ns	**1.30**	**1.02**	X	up	X	X	X	X			X					X	X
AT2G44350	8.1.2	TCA / org. transformation.TCA.CS	ATCS_CSY4__Citrate synthase family protein	ns	ns	ns	ns	**0.91**	X	up				X									

AGI identifier	Bincode identifier	MAPMAN classification	Gene annotation	Our study					DEG in common with other xenobiotic transcriptpomes	Weisman et al., 2010	Jin *et al.*, 2011	Van Hoewyk *et al.*, 2008		Ramel *et al.*, 2007		Baerson *et al.*, 2005	Goodwin and Sutter, 2009	Xu *et al.*, 2012	Landa *et al.*, 2010		Herbette *et al.*, 2006		Pucciariello et al., 2012
				Phenanthrene Seedlings						Phenanthrene Seedlings	PCB ?	Selenium		Atrazine Mannitol Seedlings	Atrazine Sucrose Seedlings	BOA	Aluminium	Phénol	Trinitrotoluene		Cadmium		Anoxia-hypoxia
				30 min*	2h*	4h*	8h*	24h*	Number in commmon	109	146	Leaves 32	Roots 52	113	119	45	14	16	Leaves 15	Roots 2	Leaves 134	Roots 182	3
AT4G14040	15	metal handling	EDA38_SBP2__selenium-binding protein 2	ns	ns	**-1.01**	**-0.70**	ns	X				X								X		
AT1G55490	1.3.13	PS.calvin cyle.rubisco interacting	CPN60B_LEN1__chaperonin 60 beta	ns	ns	ns	**-0.79**	ns	X					X	X						X		
AT5G38430	1.3.2	PS.calvin cyle.rubisco small subunit	Ribulose bisphosphate carboxylase (small chain) family protein	ns	ns	ns	**-0.74**	**-0.98**	X										X				
AT1G12780	10.1.2	cell wall.precursor synthesis.UGE	ATUGE1_UGE1__UDP-D-glucose/UDP-D-galactose 4-epimerase 1	ns	ns	**-1.06**	ns	ns	X		X			X	X				X				
AT3G29360	10.1.4	cell wall.precursor synthesis.UGD	UDP-glucose 6-dehydrogenase family protein	ns	ns	ns	ns	**0.87**															
AT4G01770	10.4.3.6	cell wall.pectin synthesis.rhamnogalacturonan II.Xylose Transferase with Fucose Acceptor	RGXT1__rhamnogalacturonan xylosyltransferase 1	ns	ns	ns	ns	**0.95**															
AT3G13520	10.5.1	cell wall.cell wall proteins.AGPs	AGP12_ATAGP12__arabinogalactan protein 12	ns	ns	**1.08**	**1.39**	**0.88**	X		X								X		X		
AT5G10560	10.6.2	cell wall.degradation.mannan-xylose-arabinose-fucose	Glycosyl hydrolase family protein	ns	ns	ns	**-1.00**	ns	X					X	X							X	
AT4G14130	10.7	cell wall.modification	XTH15_XTR7__xyloglucan endotransglucosylase/hydrolase 15	ns	ns	ns	ns	**-0.67**	X		X						X						
AT1G65290	11.1.12	lipid metabolism.FA synthesis and FA elongation.ACP protein	mtACP2__mitochondrial acyl carrier protein 2	ns	ns	ns	ns	**2.63**	X					X	X								
AT2G05990	11.1.6	lipid metabolism.FA synthesis and FA elongation.enoyl ACP reductase	ENR1_MOD1__NAD(P)-binding Rossmann-fold superfamily protein	ns	ns	ns	ns	**-0.72**	X					X	X							X	
AT3G11170	11.2.3	lipid metabolism.FA desaturation.omega 3 desaturase	FAD7_FADD__fatty acid desaturase 7	ns	ns	ns	ns	**-0.87**	X				X										
AT1G06550	11.9.4.3	lipid metabolism.lipid degradation.beta-oxidation.enoyl CoA hydratase	ATP-dependent caseinolytic (Clp) protease/crotonase family protein	ns	ns	ns	**-0.77**	ns	X					X	X							X	
AT1G48320	11.9.4.5	lipid metabolism.lipid degradation.beta-oxidation.acyl-CoA thioesterase	Thioesterase superfamily protein	ns	ns	ns	**-0.93**	ns	X												X		
AT1G66200	12.2.2	N-metabolism.ammonia metabolism.glutamine synthase	ATGSR2_GSR2__glutamine synthase clone F11	ns	ns	ns	**-1.18**	ns															
AT5G17920	13.1.3.4	amino acid metabolism.synthesis.aspartate family.methionine	ATCIMS_ATMETS_ATMS1__Cobalamin-independent synthase family protein	ns	ns	ns	**-1.06**	**-0.99**	X					X	X								
AT1G69520	13.1.3.4.12	amino acid metabolism.synthesis.aspartate family.methionine.homocysteine S-methyltransferase	S-adenosyl-L-methionine-dependent methyltransferases superfamily protein	ns	ns	ns	**-0.69**	ns	X		X												
AT3G57050	13.1.3.4.2	amino acid metabolism.synthesis.aspartate family.methionine.cystathionine beta-lyase	CBL__cystathionine beta-lyase	ns	ns	ns	**-0.77**	ns															
AT3G03780	13.1.3.4.3	amino acid metabolism.synthesis.aspartate family.methionine.methionine synthase	ATMS2_MS2__methionine synthase 2	ns	ns	ns	**-1.66**	**-2.22**	X		X			X	X						X	X	
AT3G04940	13.1.5.3.1	amino acid metabolism.synthesis.serine-glycine-cysteine group.cysteine.OASTL	ATCYSD1_CYSD1__cysteine synthase D1	ns	ns	ns	**-0.70**	ns															
AT3G06350	13.1.6.1.10	amino acid metabolism.synthesis.aromatic aa.chorismate.dehydroquinate/shikimate dehydrogenase	EMB3004_MEE32__dehydroquinate dehydratase, putative / shikimate dehydrogenase, putative	ns	ns	ns	**-1.03**	**-0.85**															
AT3G29200	13.1.6.2.1	amino acid metabolism.synthesis.aromatic aa.phenylalanine and tyrosine.chorismate mutase	ATCM1_CM1__chorismate mutase 1	ns	ns	ns	**-0.95**	**-0.96**															
AT5G38530	13.1.6.5.5	amino acid metabolism.synthesis.aromatic aa.tryptophan.tryptophan synthase	TSBtype2__tryptophan synthase beta type 2	ns	ns	ns	ns	**0.68**	X			X		X									
AT3G16150	13.2.3.1.1	amino acid metabolism.degradation.aspartate family.asparagine.L-asparaginase	N-terminal nucleophile aminohydrolases (Ntn hydrolases) superfamily protein	ns	ns	**-1.48**	ns	ns	X			X		X	X							X	
AT1G08630	13.2.5.2	amino acid metabolism.degradation.serine-glycine-cysteine group.glycine	THA1__threonine aldolase 1	ns	ns	**-1.81**	**-0.92**	**-1.62**	X		X			X	X								
AT5G49730	15.1	metal handling.acquisition	ATFRO6_FRO6_FRO6__ferric reduction oxidase 6	ns	ns	**-1.35**	**-0.79**	**-1.46**	X		X				X						X		
AT5G17230	16.1.4.1	secondary metabolism.isoprenoids.carotenoids.phytoene synthase	PSY__PHYTOENE SYNTHASE	ns	ns	ns	**-0.86**	ns	X		X												
AT3G25830	16.1.5	secondary metabolism.isoprenoids.terpenoids	ATTPS-CIN_TPS-CIN_TPS-CIN__terpene synthase-like sequence-1,8-cineole	ns	ns	**1.19**	ns	ns															
AT5G01210	16.2	secondary metabolism.phenylpropanoids	HXXXD-type acyl-transferase family protein	ns	ns	**-1.65**	**-1.37**	ns	X		X										X	X	
AT5G47950	16.2	secondary metabolism.phenylpropanoids	HXXXD-type acyl-transferase family protein	ns	ns	ns	**-0.96**	**-1.11**	X													X	
AT5G07870	16.2	secondary metabolism.phenylpropanoids	HXXXD-type acyl-transferase family protein	ns	ns	ns	**1.20**	ns															
AT5G04230	16.2.1.1	secondary metabolism.phenylpropanoids.lignin biosynthesis.PAL	ATPAL3_PAL3__phenyl alanine ammonia-lyase 3	ns	ns	ns	**-0.88**	**-0.81**						X									
AT3G19450	16.2.1.10	secondary metabolism.phenylpropanoids.lignin biosynthesis.CAD	ATCAD4_CAD_CAD-C_CAD4__GroES-like zinc-binding alcohol dehydrogenase family protein	ns	ns	**-1.22**	**-1.74**	**-1.74**	X		X											X	
AT4G37990	16.2.1.10	secondary metabolism.phenylpropanoids.lignin biosynthesis.CAD	ATCAD8_CAD-B2_ELI3_ELI3-2__elicitor-activated gene 3-2	ns	ns	ns	ns	**2.43**															
AT5G48930	16.2.1.4	secondary metabolism.phenylpropanoids.lignin biosynthesis.HCT	HCT__hydroxycinnamoyl-CoA shikimate/quinate hydroxycinnamoyl transferase	ns	**-1.17**	**-1.11**	**-1.50**	**-1.18**	X					X								X	
AT1G74010	16.4.1	secondary metabolism.N misc.alkaloid-like	Calcium-dependent phosphotriesterase superfamily protein	ns	**1.39**	**1.68**	**1.32**	**2.50**	X												X	X	
AT3G16390	16.5.1.3.2	secondary metabolism.sulfur-containing.glucosinolates.degradation.nitrilespecifier protein	NSP3__nitrile specifier protein 3	ns	ns	ns	**-1.03**	**-1.02**															
AT1G75280	16.8.5	secondary metabolism.flavonoids.isoflavonols	NmrA-like negative transcriptional regulator family protein	ns	ns	ns	**1.56**	**1.37**	X				X	X	X							X	
AT5G52810	16.99	secondary metabolism.unspecified	NAD(P)-binding Rossmann-fold superfamily protein	ns	ns	ns	ns	**1.00**	X		X			X							X	X	
AT4G17280	17.2.3	hormone metabolism.auxin.induced-regulated-responsive-activated	Auxin-responsive family protein	ns	**0.89**	ns	ns	ns	X									X				X	
AT4G38840	17.2.3	hormone metabolism.auxin.induced-regulated-responsive-activated	SAUR-like auxin-responsive protein family	ns	ns	ns	**-0.84**	**-1.31**	X						X			X			X		
AT1G60710	17.2.3	hormone metabolism.auxin.induced-regulated-responsive-activated	ATB2__NAD(P)-linked oxidoreductase superfamily protein	ns	ns	ns	ns	**0.72**	X													X	
AT1G60680	17.2.3	hormone metabolism.auxin.induced-regulated-responsive-activated	NAD(P)-linked oxidoreductase superfamily protein	ns	ns	ns	ns	**0.91**	X													X	
AT5G13320	17.2.3	hormone metabolism.auxin.induced-regulated-responsive-activated	GDG1_GH3.12_PBS3_WIN3__Auxin-responsive GH3 family protein	ns	ns	ns	ns	**1.54**	X		X										X	X	
AT3G19820	17.3.1.2.8	hormone metabolism.brassinosteroid.synthesis-degradation.sterols.DWF1	CBB1_DIM_DIM1_DWF1_EVE1__cell elongation protein / DWARF1 / DIMINUTO (DIM)	ns	ns	ns	**-1.27**	**-1.15**	X		X											X	
AT2G07050	17.3.1.2.99	hormone metabolism.brassinosteroid.synthesis-degradation.sterols.other	CAS1__cycloartenol synthase 1	ns	ns	ns	**-0.96**	ns															
AT5G50375	17.3.1.2.99	hormone metabolism.brassinosteroid.synthesis-degradation.sterols.other	CPI1__cyclopropyl isomerase	ns	ns	ns	**-0.76**	ns	X					X	X							X	
AT5G20400	17.5.1	hormone metabolism.ethylene.synthesis-degradation	2-oxoglutarate (2OG) and Fe(II)-dependent oxygenase superfamily protein	ns	ns	ns	ns	**1.03**	X			X											

AGI identifier	Bincode identifier	MAPMAN classification	Gene annotation	Our study					DEG in common with other xenobiotic transcriptomes	Weisman et al., 2010	Jin *et al.*, 2011	Van Hoewyk *et al.*, 2008		Ramel *et al.*, 2007		Baerson *et al.*, 2005	Goodwin and Sutter, 2009	Xu *et al.*, 2012	Landa *et al.*, 2010		Herbette *et al.*, 2006		Pucciariello et al., 2012
				Phenanthrene						Phenanthrene	PCB	Selenium		Atrazine Mannitol	Atrazine Sucrose	BOA	Aluminium	Phénol	Trinitrotoluene		Cadmium		Anoxia-hypoxia
				Seedlings						Seedlings	?	Leaves	Roots	Seedlings					Leaves	Roots	Leaves	Roots	
				30 min*	2h*	4h*	8h*	24h*	Number in commmon	109	146	32	52	113	119	45	14	16	15	2	134	182	3
AT4G26200	17.5.1.1	hormone metabolism.ethylene.synthesis-degradation.1-aminocyclopropane-1-carboxylate synthase	ACS7_ATACS7__1-amino-cyclopropane-1-carboxylate synthase 7	ns	ns	ns	ns	**1.44**	X		X	X										X	
AT1G80330	17.6.1.12	hormone metabolism.gibberelin.synthesis-degradation.GA3 oxidase	ATGA3OX4_GA3OX4__gibberellin 3-oxidase 4	ns	ns	ns	ns	**0.83**																
AT1G09400	17.7.1.5	hormone metabolism.jasmonate.synthesis-degradation.12-Oxo-PDA-reductase	FMN-linked oxidoreductases superfamily protein	ns	ns	ns	**0.74**	**1.08**	X		X												X	
AT5G54206	17.7.1.5	hormone metabolism.jasmonate.synthesis-degradation.12-Oxo-PDA-reductase	pseudogene	ns	ns	ns	**1.41**	**2.04**	X						X								X	
AT3G16460	17.7.3	hormone metabolism.jasmonate.induced-regulated-responsive-activated	Mannose-binding lectin superfamily protein	ns	ns	ns	**-0.89**	**-1.53**	X					X									X	
AT3G16450	17.7.3	hormone metabolism.jasmonate.induced-regulated-responsive-activated	Mannose-binding lectin superfamily protein	ns	ns	ns	ns	**-1.30**	X		X			X									X	
AT3G16440	17.7.3	hormone metabolism.jasmonate.induced-regulated-responsive-activated	ATMLP-300B_MEE36_MLP-300B__myrosinase-binding protein-like protein-300B	ns	ns	ns	ns	**-0.91**	X														X	
AT5G38020	17.8.1	hormone metabolism.salicylic acid.synthesis-degradation	S-adenosyl-L-methionine-dependent methyltransferases superfamily protein	ns	ns	**1.15**	ns	ns	X			X												
AT5G54770	18.2	Co-factor and vitamine metabolism.thiamine	THI1_THI4_TZ__thiazole biosynthetic enzyme, chloroplast (ARA6) (THI1) (THI4)	ns	ns	ns	**-0.75**	**-0.89**	X								X							
AT1G74710	18.5.2.1	Co-factor and vitamine metabolism.folate & vitamine K.vitamine K.isochorismate synthase	ATICS1_EDS16_ICS1_SID2__ADC synthase superfamily protein	ns	ns	ns	ns	**1.41**	X		X						X				X	X		
AT1G72090	18.7	Co-factor and vitamine metabolism.iron-sulphur clusters	Methylthiotransferase	ns	ns	ns	**-0.74**	ns																
AT5G50210	18.7	Co-factor and vitamine metabolism.iron-sulphur clusters	OLD5_QS_SUFE3__quinolinate synthase	ns	ns	ns	**0.75**	**1.02**							X									
AT4G18480	19.10	tetrapyrrole synthesis.magnesium chelatase	CH-42_CH42_CHL11_CHLI-1_CHLI1__P-loop containing nucleoside triphosphate hydrolases superfamily protein	ns	ns	ns	**-0.73**	ns	X					X	X						X			
AT5G26030	19.20	tetrapyrrole synthesis.ferrochelatase	ATFC-I_FC-I_FC1__ferrochelatase 1	ns	ns	ns	ns	**0.69**	X				X									X		
AT5G51830	2.2.1.1	major CHO metabolism.degradation.sucrose.fructokinase	pfkB-like carbohydrate kinase family protein	ns	ns	ns	**1.07**	**1.10**	X						X						X	X		
AT5G26570	2.2.2.3	major CHO metabolism.degradation.starch.glucan water dikinase	ATGWD3_OK1_PWD__catalytics;carbohydrate kinases;phosphoglucan, water dikinases	ns	ns	ns	**-0.75**	ns																
AT1G75030	20.1	stress.biotic	ATLP-3_TLP-3__thaumatin-like protein 3	ns	ns	**1.13**	**1.45**	**1.35**																
AT3G54420	20.1	stress.biotic	ATCHITIV_ATEP3_CHIV_EP3__homolog of carrot EP3-3 chitinase	ns	ns	ns	**0.98**	**2.05**	X														X	
AT3G52430	20.1	stress.biotic	ATPAD4_PAD4__alpha/beta-Hydrolases superfamily protein	ns	ns	ns	ns	**0.79**	X		X												X	
AT5G47130	20.1	stress.biotic	Bax inhibitor-1 family protein	ns	ns	ns	ns	**1.16**	X		X												X	
AT5G47120	20.1	stress.biotic	ATBI-1_ATBI1_BI-1_BI1__BAX inhibitor 1	ns	ns	ns	ns	**1.21**	X														X	
AT5G06320	20.1	stress.biotic	NHL3__NDR1/HIN1-like 3	ns	ns	ns	ns	**1.60**	X				X						X		X	X		
AT1G72930	20.1.2	stress.biotic.receptors	TIR__toll/interleukin-1 receptor-like	ns	ns	ns	**-1.33**	ns	X				X								X	X		
AT5G36910	20.1.2	stress.biotic.receptors	THI2.2__thionin 2.2	ns	ns	ns	ns	**-1.73**	X		X												X	
AT2G20142	20.1.2	stress.biotic.receptors	Toll-Interleukin-Resistance (TIR) domain family protein	ns	ns	ns	ns	**1.47**	X		X												X	
AT5G64890	20.1.3	stress.biotic.signalling	PROPEP2__elicitor peptide 2 precursor	ns	ns	ns	**1.07**	ns	X		X													
AT2G39200	20.1.3.1	stress.biotic.signalling.MLO-like	ATMLO12_MLO12__Seven transmembrane MLO family protein	ns	ns	ns	ns	**1.17**	X							X								
AT4G22210	20.1.7	stress.biotic.PR-proteins	LCR85 (Low-molecular-weight cysteine-rich 85)	ns	ns	ns	**-1.56**	**-1.27**																
AT5G45490	20.1.7	stress.biotic.PR-proteins	P-loop containing nucleoside triphosphate hydrolases superfamily protein	ns	ns	ns	**-0.89**	**-0.68**	X												X	X		
AT1G47890	20.1.7	stress.biotic.PR-proteins	AtRLP7_RLP7__receptor like protein 7	ns	ns	ns	**-0.70**	**-0.92**	X		X													
AT1G33590	20.1.7	stress.biotic.PR-proteins	Leucine-rich repeat (LRR) family protein	ns	ns	ns	**0.73**	**1.43**	X		X		X											
AT1G66090	20.1.7	stress.biotic.PR-proteins	Disease resistance protein (TIR-NBS class)	ns	ns	ns	ns	**1.67**	X						X			X	X				X	
AT2G29500	20.2.1	stress.abiotic.heat	HSP20-like chaperones superfamily protein	ns	ns	**1.15**	**1.11**	**1.53**	X				X										X	
AT5G49910	20.2.1	stress.abiotic.heat	cpHsc70-2_CPHSC70-2EAT SHOCK PROTEIN 70-2_HSC70-7__chloroplast heat shock protein 70-2	ns	ns	ns	**-0.71**	ns	X		X				X						X			
AT3G22530	20.2.1	stress.abiotic.heat	unknown protein	ns	ns	ns	**0.72**	ns																
AT1G65280	20.2.1	stress.abiotic.heat	DNAJ heat shock N-terminal domain-containing protein	ns	ns	ns	**0.89**	**1.56**																
AT5G56030	20.2.1	stress.abiotic.heat	AtHsp90.2_ERD8_HSP81-2_HSP90.2__heat shock protein 81-2	ns	ns	ns	ns	**0.70**	X		X			X										
AT1G59860	20.2.1	stress.abiotic.heat	HSP20-like chaperones superfamily protein	ns	ns	ns	ns	**0.91**	X		X		X	X	X		X						X	
AT5G57710	20.2.1	stress.abiotic.heat	Double Clp-N motif-containing P-loop nucleoside triphosphate hydrolases superfamily protein	ns	ns	ns	ns	**0.91**	X												X	X		
AT5G52640	20.2.1	stress.abiotic.heat	ATHS83_AtHsp90-1_ATHSP90.1_HSP81-1_HSP81.1_HSP83_HSP90.1__heat shock protein 90.1	ns	ns	ns	ns	**1.13**	X				X	X	X						X	X		
AT1G62320	20.2.3	stress.abiotic.drought/salt	ERD (early-responsive to dehydration stress) family protein	ns	**0.98**	ns	**0.94**	**0.85**																
AT1G04430	20.2.3	stress.abiotic.drought/salt	S-adenosyl-L-methionine-dependent methyltransferases superfamily protein	ns	ns	ns	**-0.78**	ns	X		X			X	X									
AT3G23300	20.2.3	stress.abiotic.drought/salt	S-adenosyl-L-methionine-dependent methyltransferases superfamily protein	ns	ns	ns	**-0.72**	ns	X					X	X									
AT4G00750	20.2.3	stress.abiotic.drought/salt	S-adenosyl-L-methionine-dependent methyltransferases superfamily protein	ns	ns	ns	**0.95**	ns						X										
AT3G10985	20.2.4	stress.abiotic.touch/wounding	ATWI-12_SAG20_WI12__senescence associated gene 20	ns	ns	**-1.07**	ns	**0.74**	X						X						X	X		
AT4G14630	20.2.99	stress.abiotic.unspecified	GLP9__germin-like protein 9	ns	ns	ns	ns	**1.09**	X		X													
AT4G29670	21.1	redox.thioredoxin	ACHT2__atypical CYS HIS rich thioredoxin 2	ns	ns	ns	**0.80**	ns	X				X											
AT5G03630	**21.2.1**	**redox.ascorbate and glutathione.ascorbate**	**ATMDAR2__Pyridine nucleotide-disulphide oxidoreductase family protein**	ns	ns	ns	**0.75**	**1.80**	X					X							X			
AT4G11600	**21.2.2**	**redox.ascorbate and glutathione.glutathione**	**ATGPX6_GPX6_LSC803_PHGPX__glutathione peroxidase 6**	ns	ns	ns	**1.03**	**1.95**																

AGI identifier	Bincode identifier	MAPMAN classification	Gene annotation	Our study					DEG in common with other xenobiotic transcriptomes	Weisman et al., 2010	Jin *et al.*, 2011	Van Hoewyk *et al.*, 2008		Ramel *et al.*, 2007		Baerson *et al.*, 2005	Goodwin and Sutter, 2009	Xu *et al.*, 2012	Landa *et al.*, 2010		Herbette *et al.*, 2006		Pucciariello et al., 2012
				Phenanthrene						Phenanthrene	PCB	Selenium		Atrazine Mannitol	Atrazine Sucrose	BOA	Aluminium	Phénol	Trinitrotoluene		Cadmium		Anoxia-hypoxia
				Seedlings						Seedlings	?	Leaves	Roots	Seedlings					Leaves	Roots	Leaves	Roots	
				30 min*	2h*	4h*	8h*	24h*	Number in common	109	146	32	52	113	119	45	14	16	15	2	134	182	3
AT3G26060	21.5	redox.peroxiredoxin	ATPRX Q__Thioredoxin superfamily protein	ns	ns	ns	**-0.79**	**-0.67**	X												X		
AT1G16350	23.1.2.30	nucleotide metabolism.synthesis.purine.IMP dehydrogenase	Aldolase-type TIM barrel family protein	ns	ns	ns	**-0.74**	ns	X					X	X							X	
AT1G80050	23.3.1.1	nucleotide metabolism.salvage.phosphoribosyltransferases.aprt	APT2_ATAPT2_PHT1.1__adenine phosphoribosyl transferase 2	ns	ns	ns	ns	**-0.70**	X												X	X	
AT5G03300	23.3.2.1	nucleotide metabolism.salvage.nucleoside kinases.adenosine kinase	ADK2__adenosine kinase 2	ns	ns	ns	**-0.99**	**-0.94**	X					X	X							X	
AT4G12720	23.3.3	nucleotide metabolism.salvage.NUDIX hydrolases	AtNUDT7_ATNUDX7_GFG1_NUDT7_ _MutT/nudix family protein	ns	ns	ns	ns	**1.07**	X				X		X						X	X	
AT1G53580	24.1	Biodegradation of Xenobiotics.hydroxyacylglutathione hydrolase	ETHE1_GLX2-3_GLY3__glyoxalase II 3	ns	ns	ns	**1.07**	ns	X					X	X								
AT5G14780	25.10	C1-metabolism.formate dehydrogenase	FDH__formate dehydrogenase	ns	ns	ns	ns	**1.33**	X													X	
AT3G59970	25.6	C1-metabolism.methylenetetrahydrofolate reductase	MTHFR1__methylenetetrahydrofolate reductase 1	ns	ns	ns	**-1.30**	**-1.06**	X					X	X						X	X	
AT2G44160	25.6	C1-metabolism.methylenetetrahydrofolate reductase	MTHFR2__methylenetetrahydrofolate reductase 2	ns	ns	ns	**-1.28**	**-0.95**															
AT5G24760	26.11.1	misc.alcohol dehydrogenases	GroES-like zinc-binding dehydrogenase family protein	ns	ns	ns	**-1.08**	**-1.19**	X					X								X	
AT1G05240	26.12	misc.peroxidases	Peroxidase superfamily protein	ns	ns	**-1.07**	**-1.48**	**-0.91**	X													X	
AT4G33420	26.12	misc.peroxidases	Peroxidase superfamily protein	ns	ns	ns	**0.74**	**0.85**															
AT2G01180	26.13	misc.acid and other phosphatases	ATLPP1_ATPAP1_LPP1_PAP1__phosphatidic acid phosphatase 1	ns	ns	ns	**1.44**	**1.97**	X										X				
AT2G16430	26.13	misc.acid and other phosphatases	ATPAP10_PAP10__purple acid phosphatase 10	ns	ns	ns	ns	**0.96**	X		X			X	X							X	
AT1G54000	26.16	misc.myrosinases-lectin-jacalin	GDSL-like Lipase/Acylhydrolase superfamily protein	ns	ns	ns	ns	**-1.06**	X		X			X									
AT3G16420	26.16	misc.myrosinases-lectin-jacalin	JAL30_PBP1__PYK10-binding protein 1	ns	ns	ns	ns	**-1.02**	X		X												
AT4G12545	26.21	misc.protease inhibitor/seed storage/lipid transfer protein (LTP) family protein	Bifunctional inhibitor/lipid-transfer protein/seed storage 2S albumin superfamily protein	ns	ns	ns	**-1.20**	**-1.66**															
AT4G09750	26.22	misc.short chain dehydrogenase/reductase (SDR)	NAD(P)-binding Rossmann-fold superfamily protein	ns	ns	ns	ns	**0.71**	X		X										X		
AT3G09260	26.3	misc.gluco-, galacto- and mannosidases	BGLU23_LEB_PSR3.1_PYK10__Glycosyl hydrolase superfamily protein	ns	ns	ns	**-0.85**	**-0.81**	X		X												
AT2G44460	26.3	misc.gluco-, galacto- and mannosidases	BGLU28__beta glucosidase 28	ns	ns	ns	**0.74**	**0.70**	X		X	X	X		X								
AT2G36690	26.7	misc.oxidases - copper, flavone etc.	2-oxoglutarate (2OG) and Fe(II)-dependent oxygenase superfamily protein	ns	**-1.13**	ns	ns	ns	X		X											X	X
AT1G14120	26.7	misc.oxidases - copper, flavone etc.	2-oxoglutarate (2OG) and Fe(II)-dependent oxygenase superfamily protein	ns	ns	**1.08**	ns	ns	X		X			X				X					
AT5G17000	26.7	misc.oxidases - copper, flavone etc.	Zinc-binding dehydrogenase family	ns	ns	ns	**1.02**	**1.09**	X		X												
AT1G14130	26.7	misc.oxidases - copper, flavone etc.	2-oxoglutarate (2OG) and Fe(II)-dependent oxygenase superfamily protein	ns	ns	ns	**1.04**	**0.86**	X							X							
AT4G15760	26.7	misc.oxidases - copper, flavone etc.	Encodes a protein with similarity to monooxygenases that are known to degrade salicylic acid (SA).	ns	ns	ns	ns	**0.75**	X		X			X	X								
AT4G20830	26.8	misc.nitrilases, *nitrile lyases, berberine bridge enzymes, reticuline oxidases, troponine reductases	FAD-binding Berberine family protein	ns	ns	ns	**0.87**	**1.20**	X						X	X						X	
AT1G26380	26.8	misc.nitrilases, *nitrile lyases, berberine bridge enzymes, reticuline oxidases, troponine reductases	FAD-binding Berberine family protein	ns	ns	ns	ns	**1.38**	X		X	X											
AT1G14540	**26.9**	**misc.glutathione S transferases**	**Peroxidase superfamily protein**	ns	ns	ns	ns	**0.75**	X													X	
AT1G29600	27.3.11	RNA.regulation of transcription.C2H2 zinc finger family	Zinc finger C-x8-C-x5-C-x3-H type family protein	ns	ns	ns	**-1.22**	**-1.02**															
AT4G17810	27.3.11	RNA.regulation of transcription.C2H2 zinc finger family	C2H2 and C2HC zinc fingers superfamily protein	ns	ns	ns	**-0.78**	**-1.03**															
AT2G24500	27.3.11	RNA.regulation of transcription.C2H2 zinc finger family	FZF__Zinc finger protein 622	ns	ns	ns	**1.13**	**0.76**															
AT3G28210	27.3.11	RNA.regulation of transcription.C2H2 zinc finger family	PMZ_SAP12__zinc finger (AN1-like) family protein	ns	ns	ns	**1.60**	**2.09**	X				X		X						X	X	
AT3G57670	27.3.11	RNA.regulation of transcription.C2H2 zinc finger family	NTT_WIP2__C2H2-type zinc finger family protein	ns	ns	ns	ns	**0.85**															
AT3G46080	27.3.11	RNA.regulation of transcription.C2H2 zinc finger family	C2H2-type zinc finger family protein	ns	**1.03**	ns	**1.39**	**1.72**															
AT5G59570	27.3.20	RNA.regulation of transcription.G2-like transcription factor family, GARP	Homeodomain-like superfamily protein	ns	ns	ns	**1.32**	ns	X		X												
AT3G28910	27.3.25	RNA.regulation of transcription.MYB domain transcription factor family	ATMYB30_MYB30__myb domain protein 30	ns	ns	ns	**0.89**	ns	X													X	
AT5G58900	27.3.26	RNA.regulation of transcription.MYB-related transcription factor family	Homeodomain-like transcriptional regulator	ns	ns	ns	**-0.72**	ns	X						X							X	
AT1G71520	27.3.3	RNA.regulation of transcription.AP2/EREBP, APETALA2/Ethylene-responsive element binding protein family	encodes a member of the DREB subfamily A-5 of ERF/AP2 transcription factor family	ns	ns	ns	**1.47**	ns															
AT1G43160	27.3.3	RNA.regulation of transcription.AP2/EREBP, APETALA2/Ethylene-responsive element binding protein family	RAP2.6__related to AP2 6	ns	ns	**-1.57**	**-1.16**	**-0.99**	X		X												
AT2G38250	27.3.30	RNA.regulation of transcription.Trihelix, Triple-Helix transcription factor family	Homeodomain-like superfamily protein	ns	ns	ns	**0.71**	ns	X									X					
AT1G29280	27.3.32	RNA.regulation of transcription.WRKY domain transcription factor family	ATWRKY65_WRKY65__WRKY DNA-binding protein 65	ns	ns	ns	**-0.95**	ns															
AT2G25000	27.3.32	RNA.regulation of transcription.WRKY domain transcription factor family	ATWRKY60_WRKY60__WRKY DNA-binding protein 60	ns	ns	ns	**-0.93**	ns	X		X			X	X								
AT4G23550	27.3.32	RNA.regulation of transcription.WRKY domain transcription factor family	WRKY29 (WRKY DNA-binding protein 29); transcription factor	ns	ns	ns	**-0.76**	**-1.01**	X												X	X	
AT3G56400	27.3.32	RNA.regulation of transcription.WRKY domain transcription factor family	ATWRKY70_WRKY70__WRKY DNA-binding protein 70	ns	ns	ns	ns	**0.70**	X													X	
AT2G46400	27.3.32	RNA.regulation of transcription.WRKY domain transcription factor family	ATWRKY46_WRKY46__WRKY DNA-binding protein 46	ns	ns	ns	ns	**0.76**	X				X									X	
AT1G19220	27.3.4	RNA.regulation of transcription.ARF, Auxin Response Factor family	ARF11_ARF19_IAA22__auxin response factor 19	ns	ns	ns	ns	**0.82**															
AT1G66160	27.3.64	RNA.regulation of transcription.PHOR1	ATCMPG1_CMPG1__CYS, MET, PRO, and GLY protein 1	ns	ns	ns	ns	**0.75**	X				X						X				
AT1G21570	27.3.99	RNA.regulation of transcription.unclassified	zinc finger (CCCH-type) family protein	ns	ns	ns	**-1.57**	ns															
AT4G38160	27.3.99	RNA.regulation of transcription.unclassified	pde191__Mitochondrial transcription termination factor family protein	ns	ns	ns	**-0.92**	**-0.79**	X												X	X	
AT3G53460	27.3.99	RNA.regulation of transcription.unclassified	CP29__chloroplast RNA-binding protein 29	ns	ns	**-1.04**	ns	ns	X		X												
AT4G16830	27.4	RNA.RNA binding	Hyaluronan / mRNA binding family	ns	ns	ns	**-0.82**	ns	X		X												
AT5G04430	27.4	RNA.RNA binding	BTR1_BTR1L_BTR1S__binding to TOMV RNA 1L (long form)	ns	ns	ns	ns	**-0.72**															

AGI identifier	Bincode identifier	MAPMAN classification	Gene annotation	Our study					DEG in common with other xenobiotic transcriptomes	Weisman et al., 2010	Jin *et al.*, 2011	Van Hoewyk *et al.*, 2008		Ramel *et al.*, 2007		Baerson *et al.*, 2005	Goodwin and Sutter, 2009	Xu *et al.*, 2012	Landa *et al.*, 2010		Herbette *et al.*, 2006		Pucciariello et al., 2012
				Phenanthrene						Phenanthrene	PCB	Selenium		Atrazine Mannitol	Atrazine Sucrose	BOA	Aluminium	Phénol	Trinitrotoluene		Cadmium		Anoxia-hypoxia
				Seedlings						Seedlings	?	Leaves	Roots	Seedlings					Leaves	Roots	Leaves	Roots	
				30 min*	2h*	4h*	8h*	24h*	Number in commmon	109	146	32	52	113	119	45	14	16	15	2	134	182	3
AT5G46580	28.1	DNA.synthesis/chromatin structure	pentatricopeptide (PPR) repeat-containing protein	ns	ns	ns	**-0.93**	ns	X						X						X		
AT5G54640	28.1.3	DNA.synthesis/chromatin structure.histone	ATHTA1_HTA1_RAT5__Histone superfamily protein	ns	ns	ns	**0.94**	ns															
AT4G15248	28.99	DNA.unspecified	B-box type zinc finger family protein	**1.39**	**1.75**	**1.04**	ns	**1.63**	X		X												
AT4G13870	28.99	DNA.unspecified	WRNEXO (WERNER SYNDROME-LIKE EXONUCLEASE); 3p-5p exonuclease/ nucleic acid binding, glycine-rich RNA-binding protein, putative	ns	ns	ns	ns	**-1.19**															
AT2G07811	29.2.1.1.2.1.3	protein.synthesis.ribosomal protein.prokaryotic.mitochondrion.30S subunit.S3	unknown protein	ns	ns	ns	**1.01**	ns															
AT4G34620	29.2.1.1.3.1.16	protein.synthesis.ribosomal protein.prokaryotic.unknown organellar.30S subunit.S16	SSR16__small subunit ribosomal protein 16	ns	ns	ns	ns	**-0.85**	X													X	
AT3G17170	29.2.1.1.3.1.6	protein.synthesis.ribosomal protein.prokaryotic.unknown organellar.30S subunit.S6	RFC3__Translation elongation factor EF1B/ribosomal protein S6 family protein	ns	ns	ns	**-0.72**	**-0.79**	X		X			X	X						X	X	
AT3G48930	29.2.1.2.1.11	protein.synthesis.ribosomal protein.eukaryotic.40S subunit.S11	EMB1080__Nucleic acid-binding, OB-fold-like protein	ns	ns	ns	ns	**-0.68**	X					X	X						X		
AT4G34670	29.2.1.2.1.53	protein.synthesis.ribosomal protein.eukaryotic.40S subunit.S3A	Ribosomal protein S3Ae	ns	ns	ns	ns	**-0.76**	X													X	
AT3G02560	29.2.1.2.1.7	protein.synthesis.ribosomal protein.eukaryotic.40S subunit.S7	Ribosomal protein S7e family protein	ns	ns	ns	ns	**-0.80**															
AT4G27090	29.2.1.2.2.14	protein.synthesis.ribosomal protein.eukaryotic.60S subunit.L14	Ribosomal protein L14	ns	ns	ns	ns	**-0.71**															
AT3G23390	29.2.1.2.2.536	protein.synthesis.ribosomal protein.eukaryotic.60S subunit.L36A	Zinc-binding ribosomal protein family protein	ns	ns	ns	ns	**-0.77**	X		X			X	X							X	
AT4G14320	29.2.1.2.2.536	protein.synthesis.ribosomal protein.eukaryotic.60S subunit.L36A	Zinc-binding ribosomal protein family protein	ns	ns	ns	ns	**-0.70**	X													X	
AT1G26630	29.2.3	protein.synthesis.initiation	ATELF5A-2_ELF5A-2_FBR12__Eukaryotic translation initiation factor 5A-1 (eIF-5A 1) protein	ns	ns	ns	ns	**1.36**						X									
AT2G31660	29.3.1	protein.targeting.nucleus	SAD2_URM9__ARM repeat superfamily protein	ns	ns	ns	ns	**0.68**															
AT4G03320	29.3.3	protein.targeting.chloroplast	tic20-IV__translocon at the inner envelope membrane of chloroplasts 20-IV	ns	ns	ns	**1.00**	**0.82**															
AT1G23490	29.3.4.99	protein.targeting.secretory pathway.unspecified	ARF1_ATARF_ATARF1_ATARFA1A__ADP-ribosylation factor 1	ns	ns	**1.04**	ns	**1.32**															
AT1G71530	29.4	protein.postranslational modification	Protein kinase superfamily protein	ns	ns	ns	**0.70**	ns	X						X							X	
AT1G68410	29.4	protein.postranslational modification	Protein phosphatase 2C family protein	ns	ns	ns	**0.96**	ns							X								
AT3G62260	29.4	protein.postranslational modification	Protein phosphatase 2C family protein	ns	ns	ns	ns	**0.81**	X				X		X			X	X			X	
AT1G70490	29.4	protein.postranslational modification	ARFA1D_ATARFA1D__Ras-related small GTP-binding family protein	ns	ns	ns	ns	**1.04**						X									
AT4G11890	29.4.1	protein.postranslational modification.kinase	Protein kinase superfamily protein	ns	ns	ns	ns	**1.38**	X			X			X						X	X	
AT2G28930	29.4.1.57	protein.postranslational modification.kinase.receptor like cytoplasmatic kinase VII	APK1B_PK1B__protein kinase 1B	ns	ns	ns	ns	**0.70**	X		X												
AT5G51770	29.4.1.61	protein.postranslational modification.kinase.receptor like cytoplasmatic kinase X	Protein kinase superfamily protein	ns	ns	ns	ns	**1.00**	X												X		
AT1G78680	29.5	protein.degradation	ATGGH2_GGH2__gamma-glutamyl hydrolase 2	ns	**1.24**	ns	**1.53**	**1.00**	X		X				X							X	
AT3G51260	29.5	protein.degradation	PAD1__20S proteasome alpha subunit PAD1	ns	ns	ns	ns	**0.71**						X									
AT2G31865	29.5	protein.degradation	poly(ADP-ribose) glycohydrolase 2 (PARG2)	ns	ns	ns	ns	**1.17**	X						X						X	X	
AT1G32940	29.5.1	protein.degradation.subtilases	ATSBT3.5_SBT3.5__Subtilase family protein	ns	ns	ns	ns	**1.06**	X							X							
AT3G45180	29.5.11.1	protein.degradation.ubiquitin.ubiquitin	ubiquitin family protein	ns	ns	ns	**0.86**	**0.87**															
AT5G23540	29.5.11.20	protein.degradation.ubiquitin.proteasom	Mov34/MPN/PAD-1 family protein	ns	ns	ns	ns	**0.68**															
AT2G05840	29.5.11.20	protein.degradation.ubiquitin.proteasom	PAA2__20S proteasome subunit PAA2	ns	ns	ns	ns	**0.77**						X									
AT4G29040	29.5.11.20	protein.degradation.ubiquitin.proteasom	RPT2a__regulatory particle AAA-ATPase 2A	ns	ns	ns	ns	**0.79**						X									
AT2G15530	29.5.11.4.2	protein.degradation.ubiquitin.E3.RING	RING/U-box superfamily protein	ns	**0.81**	ns	**1.71**	**2.15**															
AT1G22500	29.5.11.4.2	protein.degradation.ubiquitin.E3.RING	RING/U-box superfamily protein	ns	ns	ns	**0.88**	ns	X		X												
AT1G66180	29.5.4	protein.degradation.aspartate protease	Eukaryotic aspartyl protease family protein	ns	ns	**-1.07**	ns	**-0.68**															
AT1G69100	29.5.4	protein.degradation.aspartate protease	Eukaryotic aspartyl protease family protein	ns	ns	**-1.06**	**-1.21**	**-1.03**	X												X		
AT1G11910	29.5.4	protein.degradation.aspartate protease	APA1_ATAPA1__aspartic proteinase A1	ns	ns	ns	ns	**0.84**															
AT3G50930	29.5.9	protein.degradation.AAA type	BCS1__cytochrome BC1 synthesis	ns	ns	ns	ns	**0.76**	X				X	X							X	X	
AT3G13470	29.6	protein.folding	TCP-1/cpn60 chaperonin family protein	ns	ns	ns	**-0.74**	ns	X					X	X						X		
AT5G02490	29.6	protein.folding	Heat shock protein 70 (Hsp 70) family protein	ns	ns	ns	ns	**1.16**	X				X					X			X	X	
AT5G48400	30.1.1	signalling.in sugar and nutrient physiology	ATGLR1.2_GLR1.2__Glutamate receptor family protein	ns	ns	ns	**0.77**	**1.54**	X		X												
AT1G18810	30.11	signalling.light	phytochrome kinase substrate-related	ns	ns	ns	**-1.27**	ns	X		X												
AT1G27190	30.2.10	signalling.receptor kinases.leucine rich repeat X	Leucine-rich repeat protein kinase family protein	ns	ns	ns	**1.96**	ns															
AT4G23190	30.2.17	signalling.receptor kinases.DUF 26	AT-RLK3_CRK11__cysteine-rich RLK (RECEPTOR-like protein kinase) 11	ns	ns	ns	**0.80**	**1.38**	X		X											X	X	
AT3G59700	30.2.19	signalling.receptor kinases.legume-lectin	ATHLECRK_HLECRK_LECRK1__lectin-receptor kinase	ns	ns	ns	ns	**0.99**	X													X	X	
AT5G01540	30.2.99	signalling.receptor kinases.misc	LECRKA4.1__lectin receptor kinase a4.1	ns	ns	ns	ns	**1.17**															
AT5G07340	30.3	signalling.calcium	Calreticulin family protein	ns	ns	ns	**-0.96**	ns	X		X			X	X								
AT3G47480	30.3	signalling.calcium	Calcium-binding EF-hand family protein	ns	ns	ns	ns	**0.93**	X		X	X	X		X						X	X	
AT5G39670	30.3	signalling.calcium	Calcium-binding EF-hand family protein	ns	ns	ns	ns	**1.38**	X				X								X	X	
AT1G01960	30.5	signalling.G-proteins	EDA10__SEC7-like guanine nucleotide exchange family protein	ns	ns	ns	**-0.96**	ns															

AGI identifier	Bincode identifier	MAPMAN classification	Gene annotation	Our study					DEG in common with other xenobiotic transcritpomes	Weisman et al., 2010	Jin *et al.*, 2011	Van Hoewyk *et al.*, 2008		Ramel *et al.*, 2007		Baerson *et al.*, 2005	Goodwin and Sutter, 2009	Xu *et al.*, 2012	Landa *et al.*, 2010		Herbette *et al.*, 2006		Pucciariello et al., 2012
				Phenanthrene Seedlings						Phenanthrene Seedlings	PCB ?	Selenium		Atrazine Mannitol Seedlings	Atrazine Sucrose Seedlings	BOA	Aluminium	Phénol	Trinitrotoluene		Cadmium		Anoxia-hypoxia
				30 min*	2h*	4h*	8h*	24h*	Number in commmon	109	146	Leaves 32	Roots 52	113	119	45	14	16	Leaves 15	Roots 2	Leaves 134	Roots 182	3
AT1G05100	30.6	signalling.MAP kinases	MAPKKK18__mitogen-activated protein kinase kinase kinase 18	ns	ns	ns	**0.99**	ns	X		X												
AT5G55230	31.1	cell.organisation	ATMAP65-1_MAP65-1_MAP65-1__microtubule-associated proteins 65-1	ns	ns	ns	**-1.06**	ns	X					X	X							X	
AT1G64740	31.1	cell.organisation	TUA1__alpha-1 tubulin	ns	ns	ns	**-0.83**	ns	X					X	X							X	
AT5G54710	31.1	cell.organisation	Ankyrin repeat family protein	ns	ns	ns	ns	**1.15**															
AT1G13330	31.1	cell.organisation	AHP2__Arabidopsis Hop2 homolog	ns	ns	ns	ns	**1.55**	X						X						X	X	
AT5G13120	31.3.1	cell.cycle.peptidylprolyl isomerase	ATCYP20-2_CYP20-2__cyclophilin 20-2	ns	ns	ns	ns	**-0.67**	X					X	X							X	
AT3G49670	33.99	development.unspecified	BAM2__Leucine-rich receptor-like protein kinase family protein	ns	ns	ns	**-0.93**	**-0.76**	X			X		X							X	X	
AT2G35980	33.99	development.unspecified	ATNHL10_NHL10_YLS9__Late embryogenesis abundant (LEA) hydroxyproline-rich glycoprotein family	ns	**1.72**	**1.96**	**1.81**	**2.34**	X							X	X				X	X	
AT4G12420	33.99	development.unspecified	SKU5__Cupredoxin superfamily protein	ns	ns	ns	**-1.07**	ns	X		X										X	X	
AT5G63420	33.99	development.unspecified	emb2746__RNA-metabolising metallo-beta-lactamase family protein	ns	ns	ns	**-0.74**	ns	X												X		
AT3G14770	33.99	development.unspecified	Nodulin MtN3 family protein	ns	ns	ns	**1.02**	ns	X					X	X								
AT2G34355	33.99	development.unspecified	nodulin-related	ns	ns	ns	**1.07**	ns	X		X												
AT3G02380	33.99	development.unspecified	ATCOL2_COL2__CONSTANS-like 2	ns	ns	ns	ns	**-1.15**	X		X								X				
AT3G16690	33.99	development.unspecified	Nodulin MtN3 family protein	ns	ns	ns	ns	**-0.81**															
AT5G14930	33.99	development.unspecified	SAG101__senescence-associated gene 101	ns	ns	ns	ns	**0.98**	X													X	
AT2G23810	33.99	development.unspecified	TET8__tetraspanin8	ns	ns	ns	ns	**1.15**	X												X	X	
AT3G49530	33.99	development.unspecified	ANAC062_NAC062_NTL6__NAC domain containing protein 62	ns	ns	ns	ns	**1.28**	X				X								X	X	
AT5G62670	34.1	transport.p- and v-ATPases	AHA11_HA11__H(+)-ATPase 11	ns	ns	ns	ns	**-0.77**	X													X	
AT2G07671	34.1.1.2	transport.p- and v-ATPases.H+-transporting two-sector ATPase.subunit C	ATP synthase subunit C family protein	ns	ns	ns	**0.86**	**0.82**	X		X				X							X	
AT1G80830	34.12	transport.metal	ATNRAMP1_NRAMP1_PMIT1__natural resistance-associated macrophage protein 1	ns	ns	ns	**-0.99**	**-0.75**	X		X												
AT2G23150	34.12	transport.metal	ATNRAMP3_NRAMP3__natural resistance-associated macrophage protein 3	ns	ns	ns	ns	**1.69**	X												X	X	
AT5G55930	34.13	transport.peptides and oligopeptides	ATOPT1_OPT1__oligopeptide transporter 1	ns	ns	ns	**-1.07**	ns	X		X			X							X		
AT3G45700	34.13	transport.peptides and oligopeptides	Major facilitator superfamily protein	ns	ns	ns	**-0.91**	**-0.93**	X				X										
AT1G27080	34.13	transport.peptides and oligopeptides	NRT1.6__nitrate transporter 1.6	ns	ns	ns	ns	**0.88**															
AT2G45960	34.19.1	transport.Major Intrinsic Proteins.PIP	ATHH2_PIP1;2_PIP1B_TMP-A__plasma membrane intrinsic protein 1B	ns	ns	**-1.14**	**-0.77**	ns	X		X										X	X	
AT2G37180	34.19.1	transport.Major Intrinsic Proteins.PIP	PIP2;3_PIP2C_RD28__Aquaporin-like superfamily protein	ns	ns	ns	**-0.87**	**-0.82**	X		X						X					X	
AT4G35100	34.19.1	transport.Major Intrinsic Proteins.PIP	PIP2;7_PIP3_PIP3A_SIMIP__plasma membrane intrinsic protein 3	ns	ns	ns	ns	**-1.26**	X		X										X	X	
AT1G66570	34.2.1	transporter.sugars.sucrose	ATSUC7_SUC7__sucrose-proton symporter 7	ns	ns	ns	**0.73**	ns	X		X												
AT1G22710	34.2.1	transporter.sugars.sucrose	ATSUC2_SUC2_SUT1__sucrose-proton symporter 2	ns	ns	ns	**0.87**	**1.27**															
AT5G15410	34.22	transport.cyclic nucleotide or calcium regulated channels	ATCNGC2_CNGC2_DND1__Cyclic nucleotide-regulated ion channel family protein	ns	ns	ns	**-0.78**	ns															
AT2G36590	34.3	transport.amino acids	ATPROT3_ProT3__proline transporter 3	**0.79**	**1.42**	**1.93**	**1.80**	**2.24**	X											X			
AT1G61790	34.3	transport.amino acids	Oligosaccharyltransferase complex/magnesium transporter family protein	ns	ns	ns	**0.74**	ns	X													X	
AT4G21120	34.3	transport.amino acids	AAT1_CAT1__amino acid transporter 1	ns	ns	ns	ns	**0.76**															
AT5G33320	34.8	transport.metabolite transporters at the envelope membrane	ARAPPT_CUE1_PPT__Glucose-6-phosphate/phosphate translocator-related	ns	ns	ns	**-0.87**	ns															
AT1G61800	34.8	transport.metabolite transporters at the envelope membrane	ATGPT2_GPT2__glucose-6-phosphate/phosphate translocator 2	ns	ns	ns	ns	**0.83**															
AT5G15640	34.9	transport.metabolite transporters at the mitochondrial membrane	Mitochondrial substrate carrier family protein	ns	ns	ns	**1.19**	ns	X													X	
AT2G17500	34.99	transport.misc	Auxin efflux carrier family protein	ns	**0.80**	**1.19**	**1.79**	**1.20**	X					X	X								
AT1G76520	34.99	transport.misc	Auxin efflux carrier family protein	ns	ns	ns	**0.87**	**0.66**	X							X							
AT1G76530	34.99	transport.misc	Auxin efflux carrier family protein	ns	ns	ns	**0.90**	**0.88**	X		X	X										X	
AT1G29310	34.99	transport.misc	SecY protein transport family protein	ns	ns	ns	ns	**0.68**															
AT4G36640	34.99	transport.misc	Sec14p-like phosphatidylinositol transfer family protein	ns	ns	ns	ns	**0.75**	X												X		
AT3G51670	34.99	transport.misc	SEC14 cytosolic factor family protein / phosphoglyceride transfer family protein	ns	ns	ns	ns	**1.15**	X					X	X						X		
AT1G19100	35.1	not assigned.no ontology	Histidine kinase-, DNA gyrase B-, and HSP90-like ATPase family protein	ns	ns	ns	**-0.69**	ns															
AT5G26290	35.1	not assigned.no ontology	TRAF-like family protein	ns	**-0.87**	ns	**-1.50**	**-1.36**															
AT4G36850	35.1	not assigned.no ontology	PQ-loop repeat family protein / transmembrane family protein	ns	ns	**-1.17**	ns	**-0.95**	X		X			X	X								
AT5G48430	35.1	not assigned.no ontology	Eukaryotic aspartyl protease family protein	ns	ns	**-1.12**	ns	**1.47**	X					X								X	
AT5G26280	35.1	not assigned.no ontology	TRAF-like family protein	ns	ns	**-1.02**	ns	**-0.86**															
AT3G51660	35.1	not assigned.no ontology	Tautomerase/MIF superfamily protein	ns	ns	**1.47**	**1.80**	**2.27**	X					X					X		X	X	
AT4G15390	35.1	not assigned.no ontology	HXXXD-type acyl-transferase family protein	ns	ns	ns	**-1.39**	**-1.54**	X		X					X							
AT1G76160	35.1	not assigned.no ontology	sks5__SKU5 similar 5	ns	ns	ns	**-1.08**	ns	X		X			X	X								

AGI identifier	Bincode identifier	MAPMAN classification	Gene annotation	Our study					DEG in common with other xenobiotic transcritpomes	Weisman et al., 2010	Jin *et al.*, 2011	Van Hoewyk *et al.*, 2008		Ramel *et al.*, 2007		Baerson *et al.*, 2005	Goodwin and Sutter, 2009	Xu *et al.*, 2012	Landa *et al.*, 2010		Herbette *et al.*, 2006		Pucciariello et al., 2012
				Phenanthrene Seedlings						Phenanthrene Seedlings	PCB ?	Selenium		Atrazine Mannitol	Atrazine Sucrose	BOA	Aluminium	Phénol	Trinitrotoluene		Cadmium		Anoxia-hypoxia
												Leaves	Roots	Seedlings					Leaves	Roots	Leaves	Roots	
				30 min*	2h*	4h*	8h*	24h*	Number in commmon	109	146	32	52	113	119	45	14	16	15	2	134	182	3
AT5G51550	35.1	not assigned.no ontology	EXL3__EXORDIUM like 3	ns	ns	ns	**-0.94**	**-0.90**	X		X											X	
AT3G20370	35.1	not assigned.no ontology	TRAF-like family protein	ns	ns	ns	**-0.94**	**-1.06**	X					X	X			X				X	
AT1G70280	35.1	not assigned.no ontology	NHL domain-containing protein	ns	ns	ns	**-0.90**	ns	X					X	X						X		
AT3G23940	35.1	not assigned.no ontology	dehydratase family	ns	ns	ns	**-0.87**	ns	X					X	X						X		
AT5G26260	35.1	not assigned.no ontology	TRAF-like family protein	ns	ns	ns	**-0.78**	**-0.99**															
AT3G54600	35.1	not assigned.no ontology	Class I glutamine amidotransferase-like superfamily protein	ns	ns	ns	**-0.77**	ns	X		X			X	X								
AT2G43445	35.1	not assigned.no ontology	unknown protein	ns	ns	ns	**0.73**	ns	X		X												
AT4G34120	35.1	not assigned.no ontology	CDCP1_LEJ1__Cystathionine beta-synthase (CBS) family protein	ns	ns	ns	**0.77**	**0.86**															
AT2G23680	35.1	not assigned.no ontology	Cold acclimation protein WCOR413 family	ns	ns	ns	**0.88**	**1.12**	X		X										X	X	
AT5G62720	35.1	not assigned.no ontology	Integral membrane HPP family protein	ns	ns	ns	**0.91**	ns	X				X					X			X		
AT1G23890	35.1	not assigned.no ontology	NHL domain-containing protein	ns	ns	ns	**1.26**	ns															
AT4G24160	35.1	not assigned.no ontology	alpha/beta-Hydrolases superfamily protein	ns	ns	ns	**1.52**	**1.25**	X						X	X							
AT3G44190	35.1	not assigned.no ontology	FAD/NAD(P)-binding oxidoreductase family protein	ns	ns	ns	**2.05**	**2.01**	X						X			X				X	
AT5G22140	35.1	not assigned.no ontology	FAD/NAD(P)-binding oxidoreductase family protein	ns	ns	ns	**2.15**	**1.97**	X		X												
AT3G28270	35.1	not assigned.no ontology	Protein of unknown function (DUF677)	ns	ns	ns	ns	**-1.26**	X		X	X						X			X		
AT4G24930	35.1	not assigned.no ontology	thylakoid lumenal 17.9 kDa protein, chloroplast	ns	ns	ns	ns	**-0.78**	X												X		
AT4G34290	35.1	not assigned.no ontology	SWIB/MDM2 domain superfamily protein	ns	ns	ns	ns	**-0.74**	X					X							X	X	
AT1G23880	35.1	not assigned.no ontology	NHL domain-containing protein	ns	ns	ns	ns	**0.78**															
AT2G15240	35.1	not assigned.no ontology	UNC-50 family protein	ns	ns	ns	ns	**1.02**															
AT5G18480	35.1	not assigned.no ontology	plant glycogenin-like starch initiation protein 6 (PGSIP6)	ns	ns	ns	ns	**1.05**	X													X	
AT1G36622	35.1	not assigned.no ontology	unknown protein	ns	ns	ns	ns	**1.12**	X		X										X		
AT1G14870	35.1	not assigned.no ontology	PCR2__PLANT CADMIUM RESISTANCE 2	ns	ns	ns	ns	**1.76**															
AT1G70800	35.1.19	not assigned.no ontology.C2 domain-containing protein	ENHANCED BENDING 1	**0.64**	**1.23**	**1.91**	**1.97**	**1.19**															
AT2G17740	35.1.26	not assigned.no ontology.DC1 domain containing protein	Cysteine/Histidine-rich C1 domain family protein	ns	ns	ns	ns	**1.67**	X		X					X		X					
AT3G62530	35.1.3	not assigned.no ontology.armadillo/beta-catenin repeat family protein	ARM repeat superfamily protein	ns	ns	ns	ns	**-0.81**	X					X	X						X		
AT2G05530	35.1.40	not assigned.no ontology.glycine rich proteins	Glycine-rich protein family	ns	ns	ns	**0.85**	**1.73**															
AT1G07135	35.1.40	not assigned.no ontology.glycine rich proteins	glycine-rich protein	ns	ns	ns	ns	**0.66**	X				X		X							X	
AT5G55750	35.1.41	not assigned.no ontology.hydroxyproline rich proteins	hydroxyproline-rich glycoprotein family protein	ns	ns	ns	**0.95**	**1.62**															
AT3G54580	35.1.42	not assigned.no ontology.proline rich family	Proline-rich extensin-like family protein	ns	ns	ns	**-0.91**	**-0.82**	X				X									X	
AT5G45350	35.1.42	not assigned.no ontology.proline rich family	proline-rich family protein	ns	ns	ns	ns	**0.84**	X		X		X									X	
AT1G67600	35.2	not assigned.unknown	Acid phosphatase/vanadium-dependent haloperoxidase-related protein	ns	ns	ns	**1.25**	**1.07**	X		X												
AT4G27657	35.2	not assigned.unknown	unknown protein	**0.70**	**1.26**	**1.10**	**1.75**	**0.74**	X				X	X									
AT4G39670	35.2	not assigned.unknown	Glycolipid transfer protein (GLTP) family protein	**0.73**	**1.26**	**1.01**	**1.42**	**2.13**	X				X		X			X				X	
AT2G47950	35.2	not assigned.unknown	unknown protein	**1.49**	**2.27**	**2.27**	**2.65**	**1.91**	X		X		X					X			X	X	
AT1G34630	35.2	not assigned.unknown	unknown protein	ns	**1.06**	ns	ns	ns	X		X			X	X								
AT1G74450	35.2	not assigned.unknown	Protein of unknown function (DUF793)	ns	**1.09**	**1.16**	**1.06**	**1.10**	X		X		X								X	X	
AT3G21520	35.2	not assigned.unknown	AtDMP1_DMP1__DUF679 domain membrane protein 1	ns	**1.10**	ns	**0.92**	**0.97**	X		X		X								X	X	
AT5G12960	35.2	not assigned.unknown	Putative glycosyl hydrolase of unknown function (DUF1680)	ns	**1.12**	ns	ns	ns															
AT1G76980	35.2	not assigned.unknown	unknown protein	ns	**1.15**	**1.67**	**1.78**	**1.85**	X		X										X	X	
AT3G04300	35.2	not assigned.unknown	RmlC-like cupins superfamily protein;	ns	**1.25**	**1.73**	**2.08**	**2.25**															
AT2G27385	35.2	not assigned.unknown	Pollen Ole e 1 allergen and extensin family protein	ns	ns	**-1.40**	ns	**-1.00**	X						X						X		
AT5G25460	35.2	not assigned.unknown	Protein of unknown function, DUF642	ns	ns	**-1.30**	**-1.72**	**-1.41**	X		X										X	X	
AT4G29905	35.2	not assigned.unknown	unknown protein	ns	ns	**-1.16**	**-0.76**	**-1.83**	X						X						X	X	
AT1G64370	35.2	not assigned.unknown	unknown protein	ns	ns	**-1.01**	**-0.77**	ns	X				X										
AT3G49570	35.2	not assigned.unknown	unknown protein	ns	ns	**1.04**	ns	ns	X		X												
AT3G60320	35.2	not assigned.unknown	Protein of unknown function (DUF630 and DUF632)	ns	ns	ns	**-1.10**	**-0.77**	X		X												
AT1G29560	35.2	not assigned.unknown	Zinc finger C-x8-C-x5-C-x3-H type family protein	ns	ns	ns	**-1.00**	**-0.93**															
AT5G38980	35.2	not assigned.unknown	unknown protein	ns	ns	ns	**-0.96**	**-1.09**	X													X	
AT5G44580	35.2	not assigned.unknown	unknown protein	ns	ns	ns	**-0.81**	ns	X													X	
AT5G01015	35.2	not assigned.unknown	unknown protein	ns	ns	ns	**-0.78**	**-1.03**	X												X		

AGI identifier	Bincode identifier	MAPMAN classification	Gene annotation	Our study					DEG in common with other xenobiotic transcritpomes	Weisman et al., 2010	Jin *et al.*, 2011	Van Hoewyk *et al.*, 2008		Ramel *et al.*, 2007		Baerson *et al.*, 2005	Goodwin and Sutter, 2009	Xu *et al.*, 2012	Landa *et al.*, 2010		Herbette *et al.*, 2006		Pucciariello et al., 2012
				Phenanthrene						Phenanthrene	PCB	Selenium		Atrazine Mannitol	Atrazine Sucrose	BOA	Aluminium	Phénol	Trinitrotoluene		Cadmium		Anoxia-hypoxia
				Seedlings						Seedlings	?	Leaves	Roots	Seedlings					Leaves	Roots	Leaves	Roots	
				30 min*	2h*	4h*	8h*	24h*	Number in commmon	109	146	32	52	113	119	45	14	16	15	2	134	182	3
AT1G29050	35.2	not assigned.unknown	TBL38__TRICHOME BIREFRINGENCE-LIKE 38	ns	ns	ns	**-0.77**	ns	X													X	
AT1G15415	35.2	not assigned.unknown	part of pollen proteome	ns	ns	ns	**0.74**	ns	X		X				X								
AT2G18680	35.2	not assigned.unknown	unknown protein	ns	ns	ns	**0.75**	**1.97**															
AT2G12557	35.2	not assigned.unknown	unknown protein	ns	ns	ns	**0.81**	ns															
AT3G51130	35.2	not assigned.unknown	unknown protein	ns	ns	ns	**0.83**	**0.67**	X					X	X								
AT1G76070	35.2	not assigned.unknown	unknown protein	ns	ns	ns	**0.90**	**0.68**	X						X						X	X	
AT3G14000	35.2	not assigned.unknown	ATBRXL2_BRX-LIKE2__DZC (Disease resistance/zinc finger/chromosome condensation-like region) domain containing protein	ns	ns	ns	**0.91**	ns							X								
AT4G17840	35.2	not assigned.unknown	unknown protein	ns	ns	ns	**0.99**	ns	X		X			X	X								
AT2G34070	35.2	not assigned.unknown	TBL37__TRICHOME BIREFRINGENCE-LIKE 37	ns	ns	ns	**0.99**	ns	X		X			X									
AT1G05575	35.2	not assigned.unknown	unknown protein	ns	ns	ns	**1.21**	ns	X				X										
AT1G72490	35.2	not assigned.unknown	unknown protein	ns	ns	ns	**1.25**	**1.10**															
AT1G18510	35.2	not assigned.unknown	TET16__tetraspanin 16	ns	ns	ns	**1.26**	ns															
AT2G23110	35.2	not assigned.unknown	Late embryogenesis abundant protein, group 6	ns	ns	ns	**1.87**	**2.04**						X									
AT1G18290	35.2	not assigned.unknown	unknown protein	ns	ns	ns	ns	**-0.83**	X				X	X	X						X		
AT5G36960	35.2	not assigned.unknown	unknown protein	ns	ns	ns	ns	**0.68**															
AT5G01750	35.2	not assigned.unknown	Protein of unknown function (DUF567)	ns	ns	ns	ns	**0.72**	X													X	
AT2G46390	35.2	not assigned.unknown	unknown protein	ns	ns	ns	ns	**0.73**															
AT2G37940	35.2	not assigned.unknown	AtIPCS2__Arabidopsis Inositol phosphorylceramide synthase 2	ns	ns	ns	ns	**0.79**	X												X		
AT1G65845	35.2	not assigned.unknown	unknown protein	ns	ns	ns	ns	**0.81**															
AT3G56260	35.2	not assigned.unknown	unknown protein	ns	ns	ns	ns	**0.88**	X		X			X	X								
AT2G37110	35.2	not assigned.unknown	PLAC8 family protein	ns	ns	ns	ns	**0.94**	X												X	X	
AT3G20510	35.2	not assigned.unknown	Transmembrane proteins 14C	ns	ns	ns	ns	**0.96**	X					X							X	X	
AT3G13950	35.2	not assigned.unknown	unknown protein	ns	ns	ns	ns	**1.12**	X		X				X						X	X	
AT2G32190	35.2	not assigned.unknown	unknown protein	ns	ns	ns	ns	**1.33**	X				X										
AT5G25250	35.2	not assigned.unknown	SPFH/Band 7/PHB domain-containing membrane-associated protein family	ns	ns	ns	ns	**1.38**	X					X	X						X	X	
AT5G25260	35.2	not assigned.unknown	SPFH/Band 7/PHB domain-containing membrane-associated protein family	ns	ns	ns	ns	**2.07**	X		X												
AT2G36460	4.1.11	glycolysis.cytosolic branch.aldolase	Aldolase superfamily protein	ns	ns	ns	**0.72**	**1.08**	X													X	
AT5G54960	5.2	fermentation.PDC	PDC2__pyruvate decarboxylase-2	ns	ns	ns	ns	**0.90**	X		X		X								X		
AT5G24420	7.1.2	OPP.oxidative PP.6-phosphogluconolactonase	PGL5__6-phosphogluconolactonase 5	ns	ns	ns	ns	**-1.20**	X		X	X									X	X	
AT1G65930	8.1.4	TCA / org. transformation.TCA.IDH	cICDH__cytosolic NADP+-dependent isocitrate dehydrogenase	ns	ns	**-1.13**	**-0.96**	ns															
AT3G27380	8.1.7	TCA / org. transformation.TCA.succinate dehydrogenase	SDH2-1__succinate dehydrogenase 2-1	ns	ns	ns	**0.99**	**0.95**	X												X		
AT3G06650	8.2.11	TCA / org. transformation.other organic acid transformaitons.atp-citrate lyase	ACLB-1__ATP-citrate lyase B-1	ns	ns	ns	**-0.73**	ns															
AT3G22370	9.4	mitochondrial electron transport / ATP synthesis.alternative oxidase	AOX1A_ATAOX1A__alternative oxidase 1A	ns	ns	ns	**0.99**	**1.18**	X			X											

Supplemental Table VI: Primers used for quantitative RT-PCR.

Primer name	Sequence (5' → 3')	Targets
3G16390_L1	GACCCACTCCTCGTAGTTTCC	AT3G16390
3G16390_R1	CGAACAATGAAACCACGTCTT	
3G24170_L2	CCCACAAACCCAAACCTAAGA	AT3G24170
3G24170_R2	CAAATCCTTTATTGGGACACG	
3G48990_L1	TCTCCGTTTCTGGAAAATTCA	AT3G48990
3G48990_R1	GGTGTTAGGGAAGGTGAGAGC	
4G13615_L2	AGAAAGCGGCTAAGAAAGCTG	
4G13615_R2	TGCTCAAAAGACAAACCAAATG	AT4G13615
4G37930_L1	AAGGATTTCGTGTCAGCAATG	AT4G37930
4G37930_R1	CCAATTGTTGGGAACTGCTTA	
4G38970_L2	CAAAGAAACCAAAGGCAGAGA	AT4G38970
4G38970_R2	AGAAGGCTGACGGAAGAGAAC	
5G11670_L2	AGTTTGCAGAGAGCAGCATGT	AT5G11670
5G11670_R2	CAAACAACAAACAAACAAACAAAA	
5G17380_L1	ATATTGTGGAAACACCCGATG	AT5G17380
5G17380_R1	GCACCAGCAAAAGGATCAATA	
5G21090_L2	GAGAACAACCCGAGATTGGA	
5G21090_R2	CCCCCAATTCTTCATTTTCAG	AT5G21090
5G24490_L2	GTGCTGAGGAAGATGCTGAGA	AT5G24490
5G24490_R2	TGAAACCTTTCATGTGCCTTC	
5G43700_L2	AAAGGTTTAGGTTGTGGTGGTC	AT5G43700
5G43700_R2	AAACATCTCTCCCCAAGAACC	
5G47990_L1	CCAGTGGTAAGGACGTTCAAA	AT5G47990
5G47990_R1	CTCAGGGTCTTCCCAGAAATC	
5G48000_L1	AGACGTTCATGGTGTTTGGAG	AT5G48000
5G48000_R1	ATTCTTGGGCCAATGAGAAAT	
5G48010_L1	CATGAGAACTGTGATGCTCCA	AT5G48010
5G48010_R1	TGTGACATGGTTAAGGGAGGA	
5G56630_L2	GGAGCTGTCGATATTCCTCCT	AT5G56630
5G56630_R2	GCATCGGTTACAGAACCCTCT	

Acknoledgments

This work was supported in part by Axson-Coatings (France) firm and the French government (CIFRE n°1017/2009). The authors thank Marie Laure Martin Magniette for statistical analysis performed on microarray data, Marie-Noëlle Soler for help with microscopy, Nathalie Marnet for making target analysis of metabolites.

Authors' contributions

The grant was written and obtained by AE. RB and AE conceived the study and designed experiments. ASD, EB and DB performed the experiments. RB coordinated the microarray analysis at the Unité de Recherche en Génomique Végétale (URGV) using the Complete *Arabidopsis* Transcriptome MicroArray (CATMA), ASD and LT performed microarray experiments. MLMM carried out statistical analysis for microarray data and GR ANOVA analysis. ASD and RB carried out analysis and interpretation of experimental data including bioinformatics analyses. The manuscript was written by RB, AE and ASD and read and revised by all other authors.

Literature cited

Abramoff MD, Magalhães PJ, Ram SJ (2004) Image processing with ImageJ. Biophotonics Int **11**: 36–42

Alena Torres Netto EC (2005) Photosynthetic pigments, nitrogen, chlorophyll a fluorescence and SPAD-502 readings in coffee leaves. Sci Hortic 199–209

Alkio M, Tabuchi TM, Wang X, Colón-Carmona A (2005) Stress responses to polycyclic aromatic hydrocarbons in Arabidopsis include growth inhibition and hypersensitive response-like symptoms. J Exp Bot **56**: 2983–2994

Alkorta I, Garbisu C (2001) Phytoremediation of organic contaminants in soils. Bioresour Technol **79**: 273–276

Andersson BE, Henrysson T (1996) Accumulation and degradation of dead-end metabolites during treatment of soil contaminated with polycyclic aromatic hydrocarbons with five strains of white-rot fungi. Appl Microbiol Biotechnol **46**: 647–652

Andersson BE, Lundstedt S, Tornberg K, Schnürer Y, Öberg LG, Mattiasson B (2003) Incomplete degradation of polycyclic aromatic hydrocarbons in soil inoculated with wood-rotting fungi and their effect on the indigenous soil bacteria. Environ Toxicol Chem **22**: 1238–1243

Armstrong B, Hutchinson E, Unwin J, Fletcher T (2004) Lung Cancer Risk after Exposure to Polycyclic Aromatic Hydrocarbons: A Review and Meta-Analysis. Environ Health Perspect **112**: 970–978

Ashraf M, Foolad MR (2007) Roles of glycine betaine and proline in improving plant abiotic stress resistance. Environ Exp Bot **59**: 206–216

Atagana HI (2004) Bioremediation of creosote-contaminated soil in South Africa by landfarming. J Appl Microbiol **96**: 510–520

Bae J-W, Park Y-H (2006) Homogeneous versus heterogeneous probes for microbial ecological microarrays. Trends Biotechnol **24**: 318–323

Baerson SR, Sánchez-Moreiras A, Pedrol-Bonjoch N, Schulz M, Kagan IA, Agarwal AK, Reigosa MJ, Duke SO (2005) Detoxification and Transcriptome Response in Arabidopsis Seedlings Exposed to the Allelochemical Benzoxazolin-2(3H)-one. J Biol Chem **280**: 21867–21881

Bak S, Beisson F, Bishop G, Hamberger B, Höfer R, Paquette S, Werck-Reichhart D (2011) Cytochromes P450. Arab Book e0144

Balabanič D, Rupnik M, Klemenčič AK (2011) Negative impact of endocrine-disrupting compounds on human reproductive health. Reprod Fertil Dev **23**: 403–416

Bhargava A, Carmona FF, Bhargava M, Srivastava S (2012) Approaches for enhanced phytoextraction of heavy metals. J Environ Manage **105**: 103–120

Bilgin DD, Zavala JA, Zhu J, Clough SJ, Ort DR, DeLUCIA EH (2010) Biotic stress globally down regulates photosynthesis genes. Plant Cell Environ **33**: 1597–1613

Bizub D, Wood AW, Skalka AM (1986) Mutagenesis of the Ha-ras oncogene in mouse skin tumors induced by polycyclic aromatic hydrocarbons. Proc Natl Acad Sci **83**: 6048–6052

Boyes DC, Zayed AM, Ascenzi R, McCaskill AJ, Hoffman NE, Davis KR, Görlach J (2001) Growth stage-based phenotypic analysis of Arabidopsis: a model for high throughput functional genomics in plants. Plant Cell **13**: 1499–1510

Callén MS, López JM, Iturmendi A, Mastral AM (2012) Nature and sources of particle associated polycyclic aromatic hydrocarbons (PAH) in the atmospheric environment of an urban area. Environ Pollut Barking Essex 1987. doi: 10.1016/j.envpol.2012.11.009

Carillo P, Grazia M, Pontecorvo G, Fuggi A, Woodrow P (2011) Salinity Stress and Salt Tolerance. Abiotic Stress Plants - Mech. Adapt.

Cheema SA, Imran Khan M, Shen C, Tang X, Farooq M, Chen L, Zhang C, Chen Y (2010) Degradation of phenanthrene and pyrene in spiked soils by single and combined plants cultivation. J Hazard Mater **177**: 384–389

Chitwood DH, Guo M, Nogueira FTS, Timmermans MCP (2007) Establishing leaf polarity: the role of small RNAs and positional signals in the shoot apex. Dev Camb Engl **134**: 813–823

Choi YE, Harada E, Wada M, Tsuboi H, Morita Y, Kusano T, Sano H (2001) Detoxification of cadmium in tobacco plants: formation and active excretion of crystals containing cadmium and calcium through trichomes. Planta **213**: 45–50

Couée I, Sulmon C, Gouesbet G, Amrani AE (2006) Involvement of soluble sugars in reactive oxygen species balance and responses to oxidative stress in plants. J Exp Bot **57**: 449–459

Crowe ML, Serizet C, Thareau V, Aubourg S, Rouze P, Hilson P, Beynon J, Weisbeek P, van Hummelen P, Reymond P, et al (2003) CATMA: a complete Arabidopsis GST database. Nucleic Acids Res **31**: 156–158

Deng WL, Preston G, Collmer A, Chang CJ, Huang HC (1998) Characterization of the hrpC and hrpRS operons of Pseudomonas syringae pathovars syringae, tomato, and glycinea and analysis of the ability of hrpF, hrpG, hrcC, hrpT, and hrpV mutants to elicit the hypersensitive response and disease in plants. J Bacteriol **180**: 4523–4531

Domínguez-Solís JR, López-Martín MC, Ager FJ, Ynsa MD, Romero LC, Gotor C (2004) Increased cysteine availability is essential for cadmium tolerance and accumulation in Arabidopsis thaliana. Plant Biotechnol J **2**: 469–476

Edwards R, BrazieHicks M, Dixon DP, Cummins I (2005) Chemical Manipulation of Antioxidant Defences in Plants. *In* J. A. Callow, ed, Adv. Bot. Res. Academic Press, pp 1–32

Ellis MH, Dennis ES, Peacock WJ (1999) Arabidopsis roots and shoots have different mechanisms for hypoxic stress tolerance. Plant Physiol **119**: 57–64

Furuno S, Foss S, Wild E, Jones KC, Semple KT, Harms H, Wick LY (2012) Mycelia Promote Active Transport and Spatial Dispersion of Polycyclic Aromatic Hydrocarbons. Environ Sci Technol **46**: 5463–5470

Furuno S, Päzolt K, Rabe C, Neu TR, Harms H, Wick LY (2010) Fungal mycelia allow chemotactic dispersal of polycyclic aromatic hydrocarbon-degrading bacteria in water-unsaturated systems. Environ Microbiol **12**: 1391–1398

Gagnot S, Tamby J-P, Martin-Magniette M-L, Bitton F, Taconnat L, Balzergue S, Aubourg S, Renou J-P, Lecharny A, Brunaud V (2008) CATdb: a public access to Arabidopsis transcriptome data from the URGV-CATMA platform. Nucleic Acids Res **36**: D986–D990

Galili G (1995) Regulation of Lysine and Threonine Synthesis. Plant Cell **7**: 899–906

Gammon MD, Santella RM (2008) PAH, genetic susceptibility and breast cancer risk: an update from the Long Island Breast Cancer Study Project. Eur J Cancer Oxf Engl 1990 **44**: 636–640

Gan S, Lau EV, Ng HK (2009) Remediation of soils contaminated with polycyclic aromatic hydrocarbons (PAHs). J Hazard Mater **172**: 532–549

Ge Y, Dudoit S, Speed TP (2003) Resampling-based multiple testing for microarray data analysis. Test **12**: 1–77

Göhre V, Jones AME, Sklenář J, Robatzek S, Weber APM (2012) Molecular crosstalk between PAMP-triggered immunity and photosynthesis. Mol Plant-Microbe Interactions MPMI **25**: 1083–1092

Guo W-J, Bundithya W, Goldsbrough PB (2003) Characterization of the Arabidopsis metallothionein gene family: tissue-specific expression and induction during senescence and in response to copper. New Phytol **159**: 369–381

Gutiérrez-Alcalá G, Gotor C, Meyer AJ, Fricker M, Vega JM, Romero LC (2000) Glutathione biosynthesis in Arabidopsis trichome cells. Proc Natl Acad Sci **97**: 11108–11113

Haritash AK, Kaushik CP (2009) Biodegradation aspects of Polycyclic Aromatic Hydrocarbons (PAHs): A review. J Hazard Mater **169**: 1–15

Herbette S, Taconnat L, Hugouvieux V, Piette L, Magniette M-LM, Cuine S, Auroy P, Richaud P, Forestier C, Bourguignon J, et al (2006) Genome-wide transcriptome profiling of the early cadmium response of Arabidopsis roots and shoots. Biochimie **88**: 1751–1765

Hilson P, Allemeersch J, Altmann T, Aubourg S, Avon A, Beynon J, Bhalerao RP, Bitton F, Caboche M, Cannoot B, et al (2004) Versatile Gene-Specific Sequence Tags for Arabidopsis Functional Genomics: Transcript Profiling and Reverse Genetics Applications. Genome Res **14**: 2176–2189

Van Hoewyk D, Takahashi H, Inoue E, Hess A, Tamaoki M, Pilon-Smits EAH (2008) Transcriptome analyses give insights into selenium-stress responses and selenium tolerance mechanisms in Arabidopsis. Physiol Plant **132**: 236–253

Jin X-F, Shuai J-J, Peng R-H, Zhu B, Fu X-Y, Tian Y-S, Zhao W, Han H-J, Chen C, Xu J, et al (2011) Identification of candidate genes involved in responses of Arabidopsis to polychlorinated biphenyls based on microarray analysis. Plant Growth Regul **65**: 127–135

Katsoyiannis A, Sweetman AJ, Jones KC (2011) PAH molecular diagnostic ratios applied to atmospheric sources: a critical evaluation using two decades of source inventory and air concentration data from the UK. Environ Sci Technol **45**: 8897–8906

Keunen E, Peshev D, Vangronsveld J, VAN DEN Ende W, Cuypers A (2013) Plant sugars are crucial players in the oxidative challenge during abiotic stress: extending the traditional concept. Plant Cell Environ. doi: 10.1111/pce.12061

Kim MG, Geng X, Lee SY, Mackey D (2009a) The Pseudomonas syringae type III effector AvrRpm1 induces significant defenses by activating the Arabidopsis nucleotide-binding leucine-rich repeat protein RPS2. Plant J Cell Mol Biol **57**: 645–653

Kolb M, Harms H (2000) Metabolism of fluoranthene in different plant cell cultures and intact plants. Environ Toxicol Chem **19**: 1304–1310

Kvesitadze E, Sadunishvili T, Kvesitadze G (2009) Mechanisms of Organic Contaminants Uptake and Degradation in Plants. World Acad Sci Eng Technol **55**: 458

Landa P, Storchova H, Hodek J, Vankova R, Podlipna R, Marsik P, Ovesna J, Vanek T (2010) Transferases and transporters mediate the detoxification and capacity to tolerate trinitrotoluene in Arabidopsis. Funct Integr Genomics **10**: 547–559

Larcher W (2003) Physiological Plant Ecology: Ecophysiology and Stress Physiology of Functional Groups. Springer

Lichtenthaler H, Wellburn A (1983) Determinations of total carotenoids and chlorophylls a and b of leaf extracts indifferent solvents. Biochem Soc Trans **603**: 591–592

Liu H, Weisman D, Ye Y, Cui B, Huang Y, Colón-Carmona A, Wang Z (2009) An oxidative stress response to polycyclic aromatic hydrocarbon exposure is rapid and complex in Arabidopsis thaliana. Plant Sci **176**: 375 – 382

Luch A (2005) The carcinogenic effects of polycyclic aromatic hydrocarbons. Imperial College Press, Hackensack, NJ

Lurin C, Andrés C, Aubourg S, Bellaoui M, Bitton F, Bruyère C, Caboche M, Debast C, Gualberto J, Hoffmann B, et al (2004) Genome-wide analysis of Arabidopsis pentatricopeptide repeat proteins reveals their essential role in organelle biogenesis. Plant Cell **16**: 2089–2103

Mitsch WJ (2012) What is ecological engineering? Ecol Eng **45**: 5–12

Panz K, Miksch K (2012) Phytoremediation of explosives (TNT, RDX, HMX) by wild-type and transgenic plants. J Environ Manage **113**: 85–92

Paul MJ, Pellny TK (2003) Carbon metabolite feedback regulation of leaf photosynthesis and development. J Exp Bot **54**: 539–547

Provart T. and Z (2003) A Browser-based Functional Classification SuperViewer for Arabidopsis Genomics. Curr Comput Mol Biol 271–272

Pucciariello C, Parlanti S, Banti V, Novi G, Perata P (2012) Reactive oxygen species-driven transcription in Arabidopsis under oxygen deprivation. Plant Physiol **159**: 184–196

Ramel F, Sulmon C, Bogard M, Couée I, Gouesbet G (2009) Differential patterns of reactive oxygen species and antioxidative mechanisms during atrazine injury and sucrose-induced tolerance in Arabidopsis thaliana plantlets. BMC Plant Biol **9**: 28

Ramel F, Sulmon C, Cabello-Hurtado F, Taconnat L, Martin-Magniette M-L, Renou J-P, Amrani AE, Couée I, Gouesbet G (2007) Genome-wide interacting effects of sucrose and herbicide-mediated stress in Arabidopsis thaliana: novel insights into atrazine toxicity and sucrose-induced tolerance. BMC Genomics **8**: 450

Ramel F, Sulmon C, Serra A-A, Gouesbet G, Couée I (2012) Xenobiotic sensing and signalling in higher plants. J Exp Bot **63**: 3999–4014

Rozen S, Skaletsky H (2000) Primer3 on the WWW for general users and for biologist programmers. Methods Mol Biol Clifton NJ **132**: 365–386

Rylott EL, Budarina MV, Barker A, Lorenz A, Strand SE, Bruce NC (2011) Engineering plants for the phytoremediation of RDX in the presence of the co-contaminating explosive TNT. New Phytol **192**: 405–413

Sandermann Jr. H (1992) Plant metabolism of xenobiotics. Trends Biochem Sci **17**: 82–84

Sandermann Jr. H, Scheel D, Trenck T v. d. (1984) Use of plant cell cultures to study the metabolism of environmental chemicals. Ecotoxicol Environ Saf **8**: 167–182

Sarret G, Harada E, Choi Y-E, Isaure M-P, Geoffroy N, Fakra S, Marcus MA, Birschwilks M, Clemens S, Manceau A (2006) Trichomes of Tobacco Excrete Zinc as Zinc-Substituted Calcium Carbonate and Other Zinc-Containing Compounds. Plant Physiol **141**: 1021–1034

Sattler SE, Mene-Saffrane L, Farmer EE, Krischke M, Mueller MJ, DellaPenna D (2006) Nonenzymatic Lipid Peroxidation Reprograms Gene Expression and Activates Defense Markers in Arabidopsis Tocopherol-Deficient Mutants. Plant Cell **18**: 3706–3720

Schamfuß S, Neu TR, van der Meer JR, Tecon R, Harms H, Wick LY (2013b) Impact of Mycelia on the Accessibility of Fluorene to PAH-Degrading Bacteria. Environ Sci Technol **47**: 6908–6915

Schreiber R, Altenburger R, Paschke A, Küster E (2008) How to deal with lipophilic and volatile organic substances in microtiter plate assays. Environ Toxicol Chem SETAC **27**: 1676–1682

Shim D, Kim S, Choi Y-I, Song W-Y, Park J, Youk ES, Jeong S-C, Martinoia E, Noh E-W, Lee Y (2013) Transgenic poplar trees expressing yeast cadmium factor 1 exhibit the characteristics necessary for the phytoremediation of mine tailing soil. Chemosphere **90**: 1478–1486

Sitaras IE, Bakeas EB, Siskos PA (2004) Gas/particle partitioning of seven volatile polycyclic aromatic hydrocarbons in a heavy traffic urban area. Sci Total Environ **327**: 249–264

Skipsey M, Knight KM, Brazier-Hicks M, Dixon DP, Steel PG, Edwards R (2011) Xenobiotic Responsiveness of Arabidopsis thaliana to a Chemical Series Derived from a Herbicide Safener. J Biol Chem **286**: 32268–32276

Ana Sofia Duque AMDA (2013) Abiotic Stress Responses in Plants: Unraveling the Complexity of Genes and Networks to Survive. doi: 10.5772/52779

Sulmon C, Gouesbet G, Binet F, Martin-Laurent F, El Amrani A, Couée I (2007a) Sucrose amendment enhances phytoaccumulation of the herbicide atrazine in Arabidopsis thaliana. Environ Pollut **145**: 507–515

Sulmon C, Gouesbet G, Couée I, Amrani AE (2004) Sugar-induced tolerance to atrazine in Arabidopsis seedlings: interacting effects of atrazine and soluble sugars on psbA mRNA and D1 protein levels. Plant Sci **167**: 913–923

Sulmon C, Gouesbet G, El Amrani A, Couee I (2007b) Involvement of the ethylene-signalling pathway in sugar-induced tolerance to the herbicide atrazine in Arabidopsis thaliana seedlings. J Plant Physiol **164**: 1083–1092

team RDC (2013) R: a language and environment for statistical computing. R foundation for statistical computing, Vienna, Austria

Verslues PE, Zhu J-K (2005) Before and beyond ABA: upstream sensing and internal signals that determine ABA accumulation and response under abiotic stress. Biochem Soc Trans **33**: 375–379

Wang P, Song C-P (2008) Guard-cell signalling for hydrogen peroxide and abscisic acid. New Phytol **178**: 703–718

Weisman D, Alkio M, Colón-Carmona A (2010b) Transcriptional responses to polycyclic aromatic hydrocarbon-induced stress in Arabidopsis thaliana reveal the involvement of hormone and defense signaling pathways. BMC Plant Biol **10**: 59

Wu J, Omokawa H, Hatzios KK (1996) GlutathioneS-Transferase Activity in Unsafened and Fenclorim-Safened Rice (Oryza sativa). Pestic Biochem Physiol **54**: 220–229

Xu J, Su Z-H, Chen C, Han H-J, Zhu B, Fu X-Y, Zhao W, Jin X-F, Wu A-Z, Yao Q-H (2012) Stress responses to phenol in Arabidopsis and transcriptional changes revealed by microarray analysis. Planta **235**: 399–410

Zhan X-H, Ma H-L, Zhou L-X, Liang J-R, Jiang T-H, Xu G-H (2010) Accumulation of phenanthrene by roots of intact wheat (Triticum acstivnm L.) seedlings: passive or active uptake? BMC Plant Biol **10**: 52

Zrenner R, Stitt M, Sonnewald U, Boldt R (2006) Pyrimidine and purine biosynthesis and degradation in plants. Annu Rev Plant Biol **57**: 805–836

Zurbriggen MD, Carrillo N, Hajirezaei M-R (2010) ROS signaling in the hypersensitive response. Plant Signal Behav **5**: 393–396

Chapitre 3 : **Etude des mécanismes moléculaires et métabolique de protection de saccharose en condition de stress provoqué par le phénanthrène**

Préambule

Dans le chapitre précédant, nous avons vu que le phénanthrène causait rapidement des dommages sévères aux cellules, ce qui se traduit par des modifications transcriptionnelles et métaboliques.

Dans cette partie du manuscrit, nous avons utilisé les propriétés du saccharose, qui est une molécule aux fonctions multiples. Il est à la fois un métabolite important, une molécule signal et il a aussi des fonctions de protection face aux stress abiotiques. L'objectif de cette partie de mon travail a été de voir si le saccharose a un effet protecteur face à l'effet nocif du phénanthrène, et quelles sont éventuellement les processus cellulaires qui sont à l'origine de cette tolérance induite.

Dans un premier temps, une étude à long terme sur l'impact du saccharose sur le développement d'*Arabidopsis thaliana* en présence de phénanthrène a permis de montrer l'effet protecteur du saccharose. Une étude de l'effet du saccharose au niveau du métabolome et du transcriptome a montré que, même en condition de stress abiotique, les plantes, ici Arabidopsis, sont capables de prélever le sucre de leur milieu de culture et de le métaboliser rapidement après quelques heures, compensant ainsi les effets du phénanthrène sur leur métabolisme primaire.

D'autre part, de nombreuses études, notamment celles de Ramel et al. (2004 et 2006), ont mis en évidence le rôle protecteur du saccharose face aux dérivés actifs de l'oxygène (ROS). Il est donc intéressant de voir comment le saccharose régule le système antioxydant en condition de stress causé par le phénanthrène. De plus, afin de mieux cerner cet effet protecteur, une étude des gènes liés à la réponse à un stress est importante.

Enfin, le modèle de détoxification dit du « green-liver » semble pouvoir se transposer pour la détoxification des HAPs. Il est donc important d'étudier l'action du saccharose sur ces gènes de détoxification.

Title: Sucrose mitigated phenanthrene-induced stress and reconfigured wide genes transcription and metabolome profiles in *Arabidopsis thaliana*

Authors:

Anne-Sophie Dumas[1]

Richard Berthomé[2]

Emilie Jardet[3]

Abdelhak El Amrani[1]

Institutions:

[1]Université de Rennes1, CNRS UMR 6553, Ecosystèmes-Biodiversité-Evolution, 35042 Rennes cedex, France.

[2]INRA, UMR 1165, Unité de Recherche en Génomique Végétale (URGV), CNRS, ERL 8196, UEVE, 91057, Evry cedex, France.

[3]Université de Rennes 1, Géosciences Rennes, UMR6118, Campus de Beaulieu, 35042 Rennes cedex

Key words: transcriptomic, Arabidopsis, stress, phenanthrene, sucrose

Corresponding author**:** Abdelhak El Amrani (abdelhak.elamrani@uni-rennes1.fr)

Abstract:

Plants have developed strategies to adapt quickly to environmental changes. However, the regulation of these adaptive responses and coordination of signals involved remains poorly understood for many abiotic stresses. Indeed, signalling molecules play a central role in the perception of environmental stimuli and may participate in adaption of the plants behaviour to environmental cues. Sucrose is the major transport carbohydrate in higher plants, in addition to its metabolic role, recent investigations suggested that sucrose impact the plasticity of plant development by controlling gene expression. It was also suggested to play a role as scavenger and signalling molecule. In this paper we showed that sucrose mitigate phenanthrene-induced plant response. Indeed, sucrose allowed growth and chlorophyll accumulation in the presence of high phenanthrene concentrations, whereas *Arabidopsis* development was blocked and seedlings were unable to accumulate chlorophyll without sucrose. To decipher the earlier molecular changes that seem to be involved in sucrose tolerance to phenanthrene, wide transcriptional genes analysis and targeted metabolic profiling were carried out. We showed that sucrose induced plant response was associated with a deep reconfiguration of both genes expression and metabolites accumulation. Results suggest that sucrose, through its different functions, allowed the plant to sustain the primary metabolism and to overcome the phenanthrene-induced injuries.

1. Introduction

Higher plants are sessile organisms; they have to regulate their physiology and genes expression to adapt to biotic and abiotic stresses. Environmental pollution constitutes a new world wide ecological problem and may affect plant development.

Among the main pollutants, Polycyclic Aromatic Hydrocarbons (PAHs) are ubiquitous organic pollutant found in all the compartments of the environment. They are mainly considered as byproducts of anthropogenic activities with the incomplete combustion of petroleum products for example. This pollutant represents a great hazard for human health, creating the necessity to remediate contaminated environment.

Traditional clean-up techniques like incineration or physical-chemical processes represent a high cost and could also impact the environment. Indeed, development of green technologies using natural capacity of leaving organisms to store and degrade pollutants led to the creation of biological remediation techniques such as bioremediation and phytoremediation. A model of plant detoxification system, inspired by the detoxification system of the mammalian liver, was proposed by Sandermann (1992) and named the “green liver model”. In other hand, Edwards et al. (2005) defined the xenome as the whole expressed genome involved in the detection, signaling, transformation and transport of xenobiotics. While little is known about the sensing and transport mechanisms, the “green liver” is a molecular model of the transformation and transport. Several multigenic enzymes families are involved in these processes: cytochrome P450 (CYP) for the activation step, Glutathione-S-transferase (GST) and UDP-glucuronosyltransferase(UGT) for the conjugation step and ATP-binding cassette transporter (ABC transporter) for the compartmentalization step.

Phytoremediation is the utilization of plants and their associated micro-organisms to decontaminate a polluted environment. It is of high interest to get a better understanding on how plants cope with the presence of organic pollutants s in their environment. In-vitro studies, using the model plant *Arabidopsis thaliana*, revealed that phenanthrene, used as a model molecule of PAHs, cause several damages in plants. After a long-term (14 to 30 days) phenanthrene treatment, *Arabidopsis* presents a decrease in shoots development, roots length, chlorophyll content in a dose dependent way (Alkio et al., 2005; Liu et al., 2009).

Phenanthrene induced, like several abiotic stresses, an accumulation of reactive oxygen species (ROS). It also increased the activity of several anti-oxidant enzymes like the superoxide dismutase (SOD), the peroxide dismutase (POD) and the ascorbate peroxidase (APX) (Liu et al., 2009). These biochemical data corroborated with a transcriptomic analysis carried out in phenanthrene containing medium (Weisman et al., 2010a) which revealed that phenanthrene induced significant change in genes expression involved ROS scavenging pathways.

Sucrose is considered as the major form of transport and the main product of photosynthesis. It plays a pivotal role in plants responses to abiotic stresses, and acts not only as a metabolite, but has also signaling properties (Koch, 2004; Rosa et al., 2009; Wind et al., 2010). Several studies (Price et al., 2004; Thum et al., 2004) showed that sugars modulate a broad range of genes involved in central cellular processes: carbohydrate and nitrogen metabolism, signal transduction, metabolites transport and stress responses. In addition disaccharides such as sucrose, raffinose family polysaccharides (RFO) and fructans are water-soluble carbohydrates known to be involved in plant stress response (Valluru and Ende, 2008; Rosa et al., 2009).

It has been shown that under different abiotic stresses, soluble sugars accumulate in response to the oxidative stress. They are potentially involved in the modulation of oxidative stress and might interact with ROS signaling pathway (Bolouri-Moghaddam et al., 2010). Soluble sugars have a central position in the cellular redox balance system: they are at the junction of photosynthesis, mitochondrial respiration and the beta-oxidation of fatty acids, pathways that lead to ROS production (Couée et al., 2006).

An emerging concept suggested that sugars act as antioxidants (Ende and Valluru, 2009; Keunen et al., 2013). In vitro studies have shown that the *in-vivo* antioxidant capacity of soluble sugars have been underestimated: among other sugars, sucrose have been suggested to function as an antioxidant (Ende and Valluru, 2009; Bolouri-Moghaddam et al., 2010; Keunen et al., 2013).

Sucrose has been shown to increase tolerance to a variety of abiotic stress such anoxia (Loreti et al., 2005), herbice induced stress. Indeed, plants grown on sucrose showed increased tolerance to the herbicide (Sulmon et al., 2006; Ramel et al., 2007; Ramel et al.,

2009). Hence, Sucrose enhances protection against reactive oxygen species (ROS) through the activation of specific ROS scavenging systems.

The aim of this work was to examine if sucrose play a protective effect when *Arabidopsis* was challenged with phenanthrene stressed condition, and to elucidate the early molecular events involved in the presence of exogenous sucrose. Transcriptional profiling and targeted metabolomic approaches were used to decipher the main signaling and metabolic pathways involved in sucrose induced tolerance to phenanthrene injury.

2. Material and methods

2.1. Plant material and growth conditions

Seeds of *Arabidopsis thaliana,* ecotype Columbia-0 (Col-0) were used in all experiments. Seeds were surface sterilized and sown on Petri dishes containing half-strength Murashige and Skoog (1962) medium, supplemented with sugar (sucrose, glucose or mannitol), phenanthrene and dimethylsulfoxide (DMSO).

As phenanthrene solubility in water is low, a stock solution of phenanthrene in DMSO was prepared at the concentration of 700mM and used to adapt the final concentration in the culture medium. DMSO was added in the same amount in all the conditions of each experiment. So that phenanthrene dose was the only parameter changing.

Petri dishes were placed at 4°C during 48h in order to break dormancy and to homogenize germination. Plants were grown at 22°C under a 16h-light period at approximately 5000lux.

2.2. Measurement of plant growth and development

For root measurement and determination of the fresh weight, plants were grown on MS/2 solid medium supplemented with 88mM of sugar (mannitol, sucrose or glucose), phenanthrene and DMSO. Phenanthrene was added from a 700mM stock solution of phenanthrene in DMSO (as a solvent). DMSO was added in order to have the same amount of the solvent in all conditions.

Fresh weight was determined after 22 days of growth for plants grown on MS/ supplemented with mannitol or sucrose at 88mM and with 0, 50, 100, 200 and 500µM of phenanthrene or with DMSO alone. Plantlets were grown on circle dishes horizontally for a better development and aerial parts were separated and harvested. For the two biological replicates, for each condition, 6 samples with 3 plantlets were harvested.

For a better observation of the primary root, plants were cultivated on Petri dishes vertically. Roots were measured after 14 days of growth on digital photographs using ImageJ v 1.45s software (Abramoff et al., 2004). For each condition, 30 independent plants were measured.

Results represent the mean with the standard error (SE). Statistical analyses were carried on using the Wilcoxon test by R software (team RDC, 2013).

2.3. Fluorescence microscopy

Microscopic observations were performed at the Imagif platform, in the Cellular Biology Pole (CNRS, Gif-sur-Yvette, France).

Arabidopsis plantlets used in this experiment were grown on half-strength MS medium for 15 days, then transferred on half-strength MS medium supplemented with sucrose at 88mM containing 200µM of phenanthrene (prepared from a 700mM solution of phenanthrene in DMSO) or the same volume of DMSO. In order to facilitate the transfer, plants were grown vertically. A sterile and transparent plastic film was added to protect the shoot, so only roots are in contact with the contaminated medium.

After 5 days of phenanthrene treatment, leaves and roots were observed with a Zeiss LSM510 META microscope under UV-light (excitation 364nm and acquisition with 32

channels between 362nm and 704nm). Data were acquired using Zen2008 software developed by Zeiss (Germany).

2.4. Phenanthrene quantification

Plants used for phenanthrene quantification were grown for 15 days on MS/2 then transferred in liquid medium supplemented with 0mM or 88mM of sucrose and containing 200µM of phenanthrene.

After 24h of incubation, plants were harvested and rinsed with water, absolute ethanol and then water. 3 samples of 20 plantlets pooled were taken. Plants samples were dried then pounded and weighted.

Phenanthrene was extracted from plants tissues by an accelerated solvent extractor (ASE 200, Dionex) with dichloromethane at 100°C and under a pressure of 100bar. Extracts were dried under a gentle flux of nitrogen, and finally weight for quantification using internal standard. One microliter of the extract was injected onto a Shimadzu QP2010+MS gas chromatograph/mass spectrometer (Shimadzu, Tokyo, Japan). The injector used was in splitless mode and maintained at a temperature of 310°C. The chromatographic separation was performed on a fused silica SLB-5 ms capillary column (from Supelco, length = 60 m, diameter = 0.25 mm, film thickness = 0.25µm) under the following temperature program: 70°C (held for 1 min) to 130 at 15°C/min, then 130 to 300°C (held for 15 min) at 3°C/min. The helium flow was maintained at 1mL/min. The chromatograph was coupled to the mass spectrometer by a transfer line heated to 250°C. The analyses were performed in SIM mode (selective ion monitoring). Quantification was based on the internal standard phenanthrene-d10, which was added to the sample post-extraction and prior to the analysis by GC-MS.

2.5. Targeted analysis of metabolites

Analysis of metabolites levels were performed by the CORSAIRE platform (Biogenouest, INRA UMR 1359, Le Rheu, France).

Arabidopsis plants used for this analysis were grown on half-strength MS medium for 15 days, then transferred on liquid half-strength MS medium supplemented with 0 or 88mM of sucrose and containing 200µM of phenanthrene (prepared from a 700mM solution of phenanthrene in DMSO) or the same volume of DMSO.

After 24 hours of incubation, plants were harvested, frost in liquid nitrogen, lyophilized and ground. A total of 10mg of dry plant material was extracted in 500µL of extraction solvent and 250µL of chloroform. The extraction solvent is composed of 5% of methanol and 95% of beta amino benzoic acid (10mM) – adonitol (20mM) concentrated solution. Samples were shaken 10 min at room temperature then 500µL of ultra pure water were added. All samples were vortexed for 30s then centrifugated for 5 min at 12000g at 15°C. The entire liquid phase is transferred to a new tube. For amino acids analysis, 50µL of the extract was dried under vacuum and 50µL of water were added. Samples are derivated using the AccQTag method (Waters) and analyzed by Ultra Performance Liquid Chromatography (UPLC, Waters). For sugars, organic acids, alcohol and ammonium quantification, 50µL of the extract supplemented with 50µL of internal standard are dried under vacuum. 50µL of methoxamine in pyridine (concentration 20mg/mL) were added to the dried samples which are incubated 90min at 30°C. 50µL of MSTFA (N-Methyl-N-(trimethylsilyl)trifluoroacetamide) are added to each sample which are incubated for 30min at 37°C and than analyzed by GC-MS.

2.6. Transcriptome studies

Transcriptome analysis was carried out at the Research Unit in Plant Genomics (INRA, Evry, France), using the CATMA version 5 microarrayscontaining 31776 specific gene tags corresponding to 22,089 genes from *Arabidopsis* (Crowe et al., 2003; Hilson et al., 2004).

Arabidopsis thaliana ecotype Columbia (Col 0) was grown *in-vitro* for 15 days on solid half-strength Murashige and Skoog (MS) medium. Plantlets at stage 1.04 (Boyes et al., 2001)

were then transferred on liquid half-strength MS medium containing 0.2mM of phenanthrene (prepared from a 700mM solution of phenanthrene in DMSO) or the same amount of phenanthrene and 3% sucrose. Total RNA extractions of two independent replicates were performed using the Qiagen RNAeasy plant minikit according to the manufacturer's instructions. Each biological replicates content phenanthrene-treated and phenanthrene plus sucrose treated plants. Each sample corresponding to 30 plants pooled were harvested after 30 min, 2h and 8h of incubation. For all comparisons performed, the experiment was done using the dye-switch technique. Lurin et al. (2004) described the protocol used for the labelling of antisense amplified mRNA with Cy3-dUTP and Cy5-dUTP (Perkins-Elmer-NEN Life science products), the hybridization to the slides and the scanning.

2.7. Statistical Analysis of microarray data

The Bioinformatic and Predictive Genomics group at the Research Unit in Plants Genomics (Evry, France), with whom the experiments were designed, developed specific statistics to analyse CATMA hybridations. For each array, the raw data include the logarithm of median feature pixel intensity (in log base 2) at wavelengths of 635 nm (red) and 532 nm (green). No background was subtracted. The normalization method used was described by (Lurin et al., 2004). Differentially expressed genes were determined by performing a paired t-test on the log ratios averaged on the dye switch. A trimmed variance was calculated from spots that did not display extreme variance. The raw P values were adjusted by the Bonferroni method, which controls the family-wise error rate (with a type I error equal to 5%). We also adjusted the raw P values to control a false discovery rate using Benjamini-Yetkutieli at a level of 1%. Nonetheless, in the CATMA analysis pipeline, family-wise error rate proved to be the best solution to balance the estimated number of false positives and false negatives (Ge et al., 2003). As described by Gagnot et al. (2008), when the Bonferroni P value was lower than 0.05, the gene was declared differentially expressed.

2.8. Biological pathways enrichment

Biological pathways significantly over-represented in the list of differentially expressed genes were identified with the classification superviewer tool of the university of Toronto website (http://bar.utoronto.ca/ntools/cgi-bin/ntools_classification_superviewer.cgi) using MAPMAN classification (Provart T., 2003a) as a source.

2.9. Microarrays data validation by quantitative Real-Time PCR (qRT-PCR)

The qRT-PCR validation was carried on 15 genes being found differentially expressed in the microarrays experiments.

Primers were designed using the online software Primers3 ((Rozen and Skaletsky, 2000), http://frodo.wi.mit.edu/, optimal temperature 60°C, Supplemental Table I).

The primer pairs were first tested on a dilution series of genomic DNA (5, 0.5, 0.05, and 0.005ng) to generate a standard curve and assess their PCR efficiency, which ranged between 90% and 110%. RT was performed on 1µg of total RNA with oligo(dT) primer (18-mer) and the SuperScript II RNase H- reverse transcriptase according to the manufacturer's instructions (Invitrogen). In every run, at least three replicates PCRs were done for each cDNAs. For each gene investigated using qPCR, a dilution series covering 3 orders of magnitude (1, 1/10 and 1/100) of the cDNA stock solution was prepared. Three replicates of each of the three standards were used in qPCR experiment together with three no-template controls. qPCR was performed in 5□L, with 0.5 □L of RT reaction (1/100 dilution), 900 nM final concentration of each primer pair, and 2,5µL of MESA GREEN qPCR MasterMix Plus for SYBR® Assay (Eurogentec)). Corresponding minus-RT controls were performed with each primer pair. All reactions were performed with the CFX384 Touch™ Real-Time PCR Detection System (Bio-Rad) as follows: 95°C for 5 min; 40x95°C for 10 s and 60°C for 30 s ; and a dissociation step to discriminate primer dimers from the PCR product. Using CFX Manager™ Software version 3.0 provided by the manufacturer, the optimal cycle threshold (Ct) was determined from the dilution series, with the raw expression data derived. Six housekeeping genes were assessed in this experiment, and the two best control genes, consistently expressed, were selected to calculate the average normalization factor: AT4G13615 and

AT5G21090 for each sample pair. Normalized (Norm) ΔCt for each differentially expressed gene was calculated as following: Norm ΔCt = - (rawΔCt - Norm factor). Microarray data from this article were deposited at Gene Expression Omnibus (http://www.ncbi.nlm.nih.gov/geo/), accession no. GSE48181) and at CATdb (http://urgv.evry.inra.fr/CATdb/; Project: AU10-04_phytoremediation) according to the "Minimum Information About a Microarray Experiment" standards.

3. Results and discussion

3.1. Sucrose induced tolerance to phenanthrene injury

Sucrose was shown to protect the plant against abiotic stresses such anoxia and herbice injury (Sulmon et al., 2004; Loreti et al., 2005). However no data were available about its effect on stresses induced by organic pollutants such as PAHs. In this work, we studied the incidence of sucrose implementation on plant response to phenanthrene exposition.

Arabidopsis plants were grown on media containing 3% w/v of sucrose (=88mM), then compared to control plants grown in the same culture medium supplemented with 88mM of mannitol, used as previously described as an osmoticum (Borsani et al., 2001; Sulmon et al., 2004). In these conditions, plants were submitted to a phenanthrene treatment at different concentrations ranging from 0µM to 400µM. Shoots fresh weight was measured as marker of development to assess sucrose effects. Control plants, grown on mannitol supplemented medium, showed a significant reduction of growth development even at low phenanthrene concentration (50 µm) (Fig.1 and Fig.2), and reduction of the number and leaves surface. 70% of plants failed to accumulate chlorophyll (Fig.1). In parallel, when phenanthrene increased up to 100 µm, 100% of plants showed high toxicity symptoms (chlorosis) and are unable to initiate first leaves are unable to initiate first leaves development and chlorophyll synthesis. On the contrary, plants growing on sucrose supplemented media showed a significantly highest fresh weight compared to plants grown on mannitol-supplemented media whatever the phenanthrene concentration applied, and even at high phenanthrene

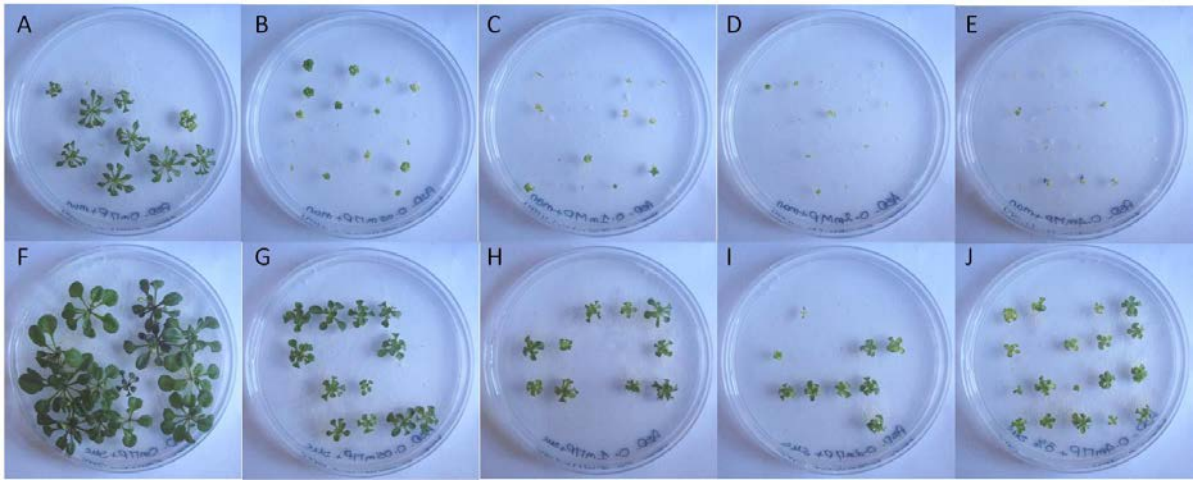

Figure 1: Sucrose mitigated phenanthrene induced stress.
22 days old plantlets were grown on half MS medium. Phenanthrene was supplemented at 0µM (A, F), 50µM (B, G), 100µM (C, H), 200µM (D, I) and 400µM (E, J). Control plants (A to E) were grown on medium supplemented with mannitol as an osmoticum, plants from pictures F to J grown on sucrose supplemented media.

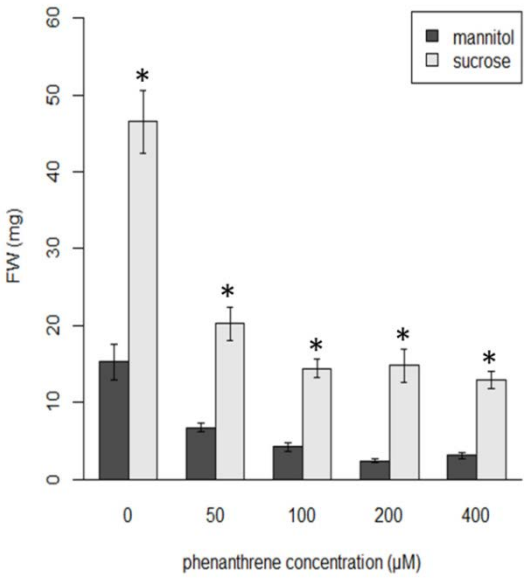

Figure 2: Fresh weight of 22-day-old plants following a phenanthrene treatment (0µM, 50µM, 100µM, 200µM and 400µM) in a growth medium supplemented with sucrose or mannitol (used as osmoticum). * statistical difference between sucrose and mannitol treatments (p-value≤0.05).

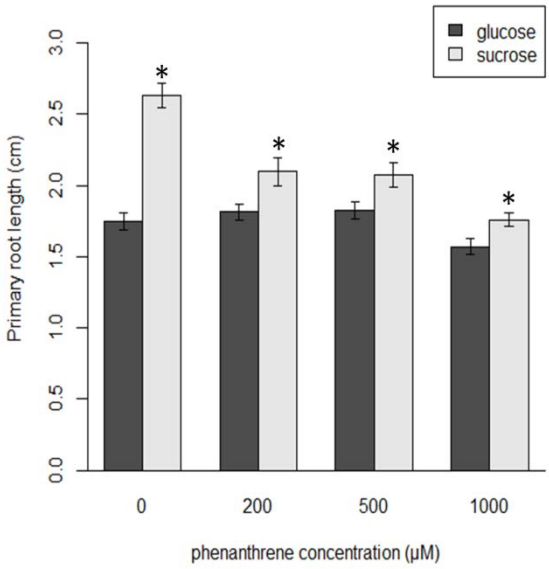

Figure 3: Primary root length of 14-day-old plantlets after a phenanthrene treatment (grown on 0µM, 200µM, 500µM and 1000µM respectively) in a growth-medium supplemented with 88mM of sucrose or glucose. * statistical difference between sucrose and glucose treatments (p-value≤0.05).

concentration (400 µm) plants maintained growth and developed leaves and chlorophyll biosynthesis.

In order to assess the specific sucrose effect, to evaluate to what extend sucrose protects plants against high doses of phenanthrene and to better understand the role of sucrose in plant development under a phenanthrene-induced stress, a comparison has been carried out with plants grown on media supplement with glucose. Both molecules were exogenously added to the growing medium at identical concentration (88mM) under high content of phenanthrene ranging from 200µM to 1000µM. In this experiment, we used primary root elongation as marker, since this later was highly sensitive to abiotic stresses (Fig. 3) (Pasternak et al., 2005). Statistical analysis of results obtained revealed that sucrose showed a pronounced effect in high phenanthrene supplemented medium, even if glucose mitigated the phenanthrene inhibition of the primary roots this protection was at a lesser extent. This observation corroborates with several already published data about the specific effect of sucrose. Moreover, figure 2 showed that in the presence of exogenous sucrose, no significant differences were observed in the fresh weigh between 200µM and 400µM doses. These results suggested that, even for lethal doses of phenanthrene, sucrose protected plants against the toxic effects of this molecule.

Solfanelli *et al*, (2006) carried out transcriptome analysis and showed that sucrose exhibited specific induction of the anthocyanin biosynthetic pathway. In other hand, emerging ideas suggested that sucrose impacts also plant tolerance to environmental stress. Loreti et al (2010) showed exogenous sucrose greatly enhances anoxia tolerance of *Arabidopsis* seedlings but glucose did not substitute for sucrose in this process. Sucrose exhibited similar effect when *Arabidopsis* was challenged with atrazine. In these conditions sucrose induced the ROS scavenging system and allowed plant development and growth (Sulmon et al., 2006; Ramel et al., 2007).

Hence, Barker et al. (2000) proposed that sucrose transporter SUT2 act as a sucrose sensor, but this assumption, has not been demonstrated yet. Since the elucidation of sucrose-specific signaling pathway is difficult to study as sucrose is readily hydrolyzed into hexoses. However, functional genomics and omics approaches should give new insight to

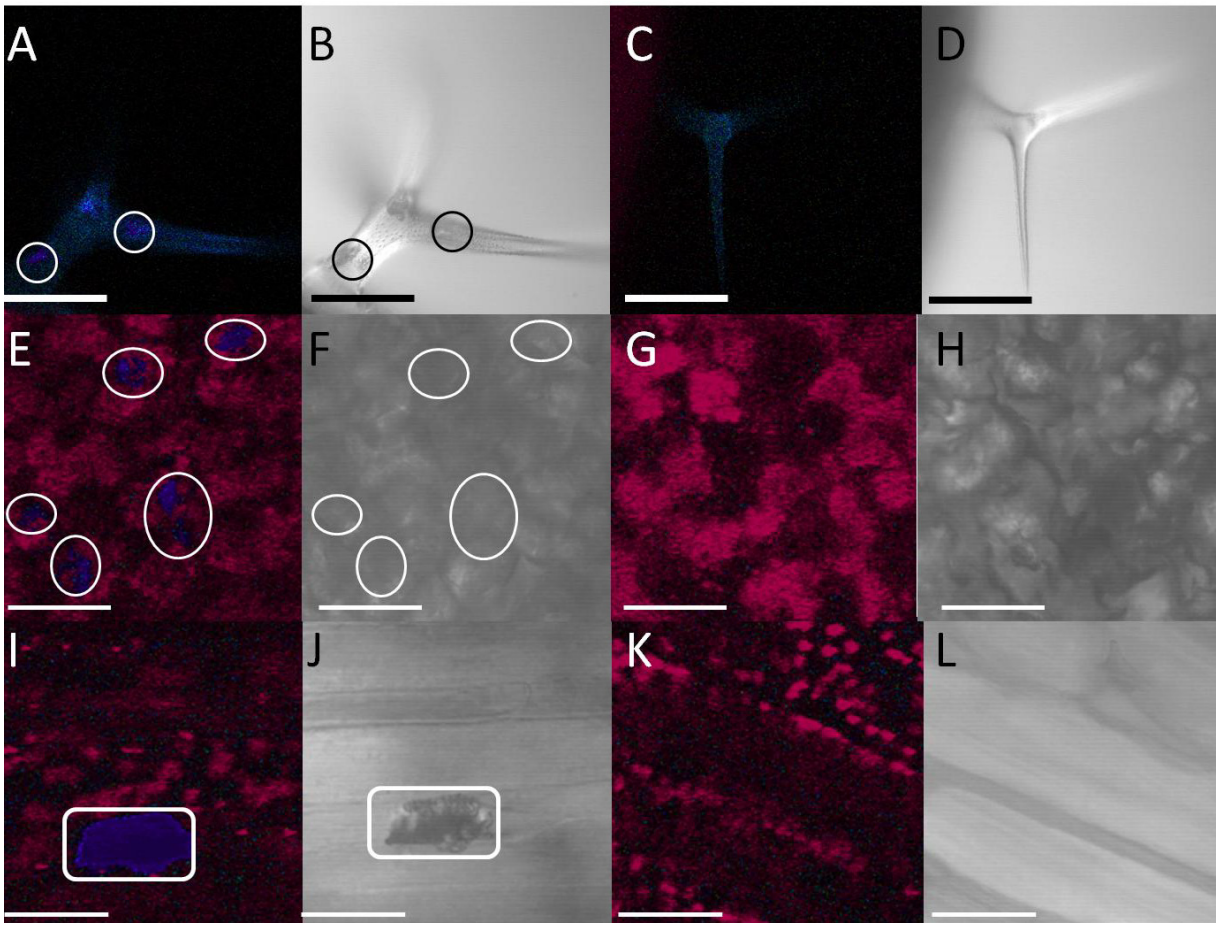

<u>Figure 4</u>: Cellular and histological localization of free phenanthrene.
Plants were treated for 6 days with 0.2mM of phenanthrene + sucrose (A, B, E, F, I, J and M) or DMSO + sucrose as control (C, D, G, H, K and L). Pictures A to D are an observation of the trichomes, E to H of the underside of the leaves and I to L of the vein from the underside of the leaf. 2 consecutives photos (A-B, C-D …) represent the same area. A, C, E, G, I, K and M are observations made under UV light and B, D, F, H, J and L with transmission. Circles show the localization of phenanthrene. Bar scales represent 100µm for pictures A to D and 50µM for pictures E to L.

understand how this important molecule controls plant development and tolerance to environmental constraints.

3.2. Cellular and histological localization of phenanthrene under protective sucrose condition

It is of high interest to understand how sucrose modulates the phenanthrene accumulation in plant cells and tissues. In this paper, we used fluorescence properties of free phenanthrene under UV light (Dabestani and Ivanov, 1999) for *in-planta* histological localization. Indeed, after an excitation at 564nm, a specific signal was emitted between 450-500nm, corresponding to phenanthrene fluorescence.

In sucrose supplemented medium, confocal microscopy analysis showed accumulation of free phenanthrene in the trichome (Fig.4A) and in the abaxial leaf surface (Fig.4E). In addition, sucrose allows the accumulation in vascular tissues (Fig. 4I). This last result was different from those published in Dumas et *al*. (paper in preparation, 2013). Which showed that when plants were grown on sucrose free medium the phenanthrene accumulated only in trichome and abaxial cells of *Arabidopsis* leaves.

These results corroborates data published by Alkio et al. (2005), where plant treated with phenanthrene during 21 days on a sucrose containing medium showed local necrosis similar to hypersensitive responses. Authors also found that the frequency and size of these lesions were dose-dependent on the phenanthrene concentration in the medium.

These results suggested that sucrose triggered discrete changes in the cellular and tissular transport and/or accumulation of the free phenanthrene, as this later was also localized in vascular tissues.

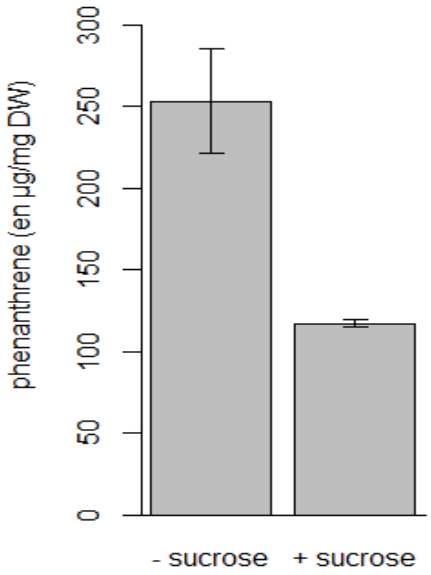

<u>Figure 5:</u> Phenanthrene concentration of 16-day-old plantlets incubated for 24h with 200µM of phenanthrene, supplemented with or without sucrose in the growth medium.

In order to quantify phenanthrene accumulation in plant tissues, 16 days old plantlets were transferred to liquid medium containing phenanthrene alone (control) or phenanthrene plus sucrose. After 24h of incubation, phenanthrene quantification was carried out. Surprisingly, plants grown on sucrose supplemented medium accumulated 50% less phenanthrene compared to plants grown on a sugar free medium (Fig. 5). This observation suggested that sucrose induced either new gene-network involved in phenanthrene metabolization, transport or likely a complete degradation, which were silenced when phenanthrene was present alone.

All these data taken together suggested that sucrose reconfigure cellular and molecular processes involved in storage, metabolization and/or tolerance strategy in phenanthrene-induced stress condition.

In several other organisms such bacteria and fungus, genes such as P-450 have been demonstrated to be involved in complete phenanthrene degradation (Bezalel et al., 1997; Syed et al., 2010). However, until today, data demonstrating that plants are able to degrade phenanthrene are still missing. Meanwhile, genome sequencing programs revealed a myriad of genes coding for proteins that could be involved in detoxification of xenobiotics, such phenanthrene. These processes involved several genes family known to be involved in the xenome, described firstly in animals and suggested to function similarly in plants (Sandermann Jr., 1992). In this work, in order to understand molecular and metabolic changes involved in sucrose induced tolerance, “-omics” approaches were used.

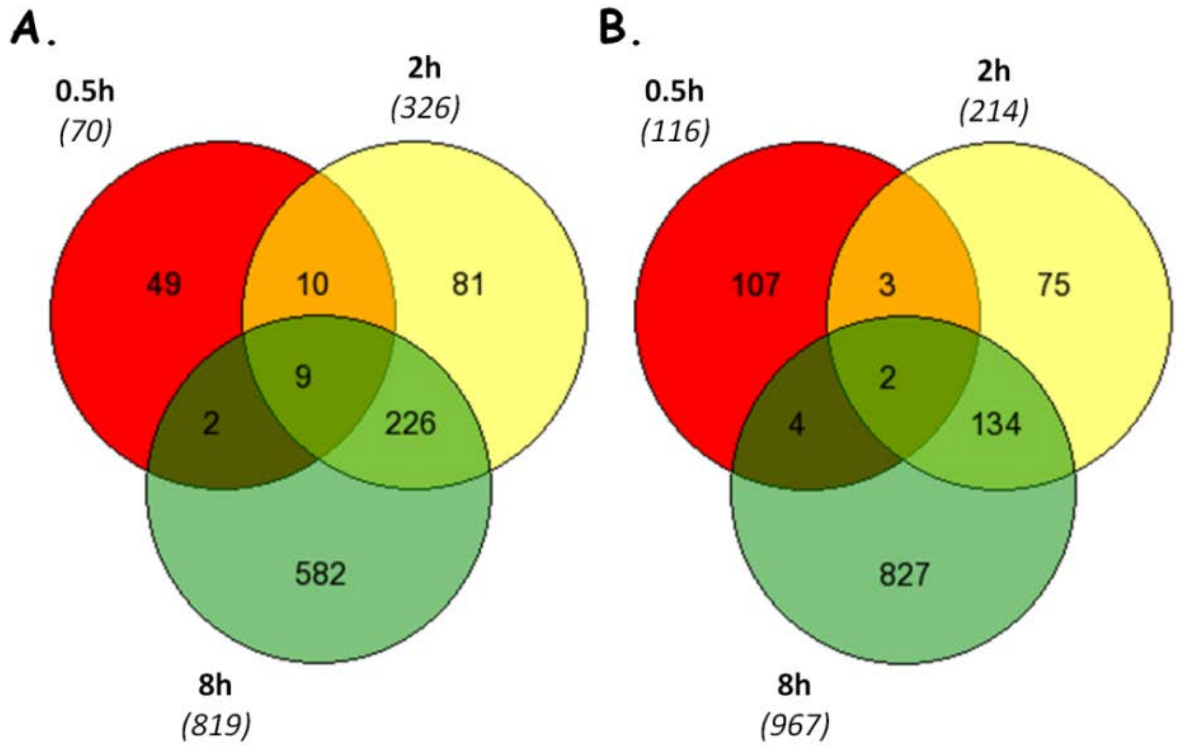

<u>Figure 6</u>: Number of down- (A.) and up-(B.) regulated genes at 0.5h, 2h and 8h
Venn diagrams were generated using the online application Gene List Venn Diagram (http://simbioinf.com/mcbc/applications/genevenn/genevenn.htm, (Pirooznia et al., 2007))

3.3. Sucrose reconfigured transcriptomic and metabolomic profile under phenanthrene-induced stress

3.3.1. Early Arabidopsis transcriptional responses to sucrose under phenanthrene-induced stress

Transcriptional analysis was carried out at the 2.04 developmental stage (Boyes et al., 2001). Plantlets were grown on solid medium for 15 days, and then were transferred respectively into liquid medium supplemented with 200µM of phenanthrene or with 200µM of phenanthrene in protective condition (88mM of sucrose). During the incubation, liquid medium was agitated in order to avoid any oxygen deprivation.

Transcriptional analysis was performed using CATMA microarrays (version 5) and two independent biological replicates were carried out. The experimental design was performed to study sucrose effect on transcriptional response of plants incubated with phenanthrene- during 0.5h, 2h and 8h, respectively. We will refer this experiment as the "sucrose experiment" (Supplemental table II). In other hand, the microarray experiment previously performed to study the plant response to phenanthrene alone (Dumas et al., 2014, in preparation) will be referred as the "phenanthrene experiment".

Overall, 2088 differentially expressed genes (DEG) were found in all the kinetic points of the experiment (Supplemental table III).

Hence, list of DEG at each kinetic point were compared with Venn diagrams (Fig. 6 A and B). Indeed, 186, 540 and 1786 DEG were found at 0.5h, 2h and 8h respectively. While at 0.5h and 8h, most of DEG were up regulated (respectively 70 down/116 up and 819 down /967 up), DEG found at 2h treatment, where mainly down-regulated (326 down/214 up). It might be argued that 2h constitute a transition point where a change of transcriptional regulation occurred. Meanwhile, few genes were found to be common, 7 genes (*AT1G31817*, *AT1G54740*, *AT1G70290*, *AT2G20670*, *AT2G31810*, *AT4G21870* and

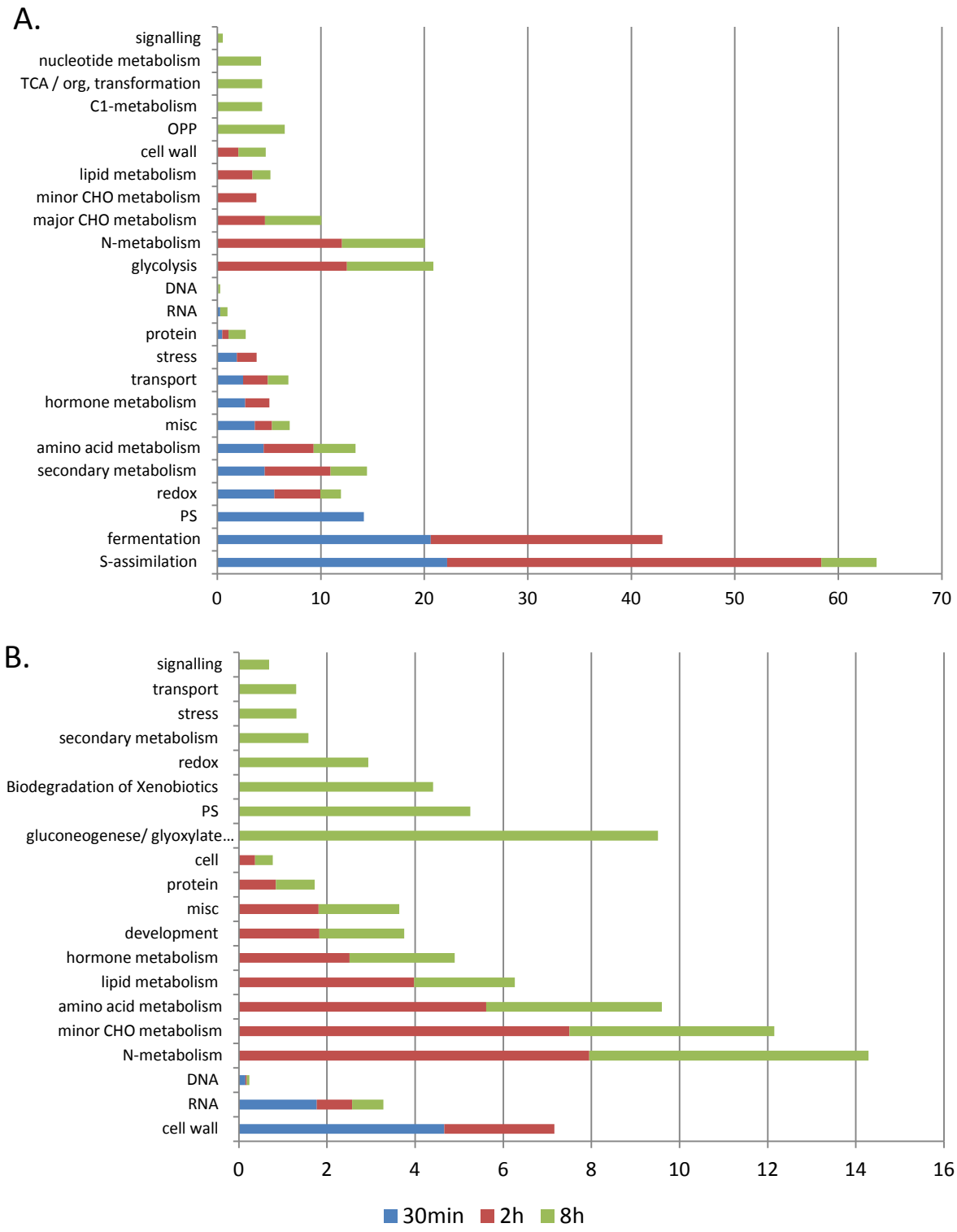

Figure 7: Biological pathways with significant over-representation of up- (A) and down-regulated (B) genes (P-values<0.05) after 0.5h, 2h and 8h of treatment with sucrose unde phenanthrene-induced stress. Functional enrichment is shown for differentially expressed genes analyzed using the classification superviewer tool from the Bio-Array Resource for Plant Biology (Provart T., 2003b) (http://www.bar.utoronto.ca/ntools/cgi-bin/ntools_classification_superviewer.cgi) using the MapMan classification as the source. PS, Photosynthesis. Misc, miscellaneous.

AT5G61590) are down-regulated at each point of the kinetic. The ascorbate peroxidase 1 (APX1, *AT1G07890*) and the cytochrome P450 83A1 (CYP83A1, *AT4G13770*) are up-regulated at all kinetic points of the experiment.

In parallel, the classification superviewer tool from the Bio-Array Resource for Plant Biology (Provart T., 2003a) using the MapMan classification (Thimm et al., 2004) (Fig. 7) were used to identify the most affected pathways by sucrose under phenanthrene-induced stress. We found that as early as 0.5h, sucrose induced up regulation of 50% of the analyzed pathways, and most of them are involved in the energy production (fermentation, photosynthesis) and stress tolerance (redox, stress, misc) . However, only few pathways (12.5%) involved in cell development (cell wall, RNA and DNA) were significantly down regulated. These data strongly suggested that, in phenanthrene-induced stress conditions, sucrose induced rapid transcriptional changes to maintain high energy production in order to face phenanthrene deleterious effects. These evidences suggested that sucrose or its derivates (glucose, fructose…) act very rapidly as a signaling molecule to induce very rapid changes to adapt transcriptional activity to unbalance phenanthrene-induced stress. Surprisingly, photosynthesis was found to be induced also very early in these conditions. This observation showed a discrepancy with published data since available carbon source induce inhibition of photosynthesis as shown by Roitsch (1999) and Paul and Foyer (2001). It is interesting to notice that these changes were obtained under long sucrose treatment, as we found, after 8 hours of sucrose treatment, that the transcriptional activity of genes involved in photosynthesis was down regulated. This repression of photosynthesis after 8 hours of treatment is characteristic of the late sucrose effect as previously described (Roitsch, 1999; Rolland et al., 2002). All these data taken together indicated that sucrose might trigger directly or indirectly different responses, rapid response (as a signaling molecule) and late response (as metabolic molecule).

In other hand, pathways significantly induced during late stages of sucrose treatment (8h) involves a strong regulation of primary metabolism with the activation of the oxidative pentose phosphate pathway (OPP), the tricarboxilic acid (TCA) pathway and the C1-metabolism and the inhibition of gluconeogenese/glyoxylate cycle pathway and

photosynthesis. Most of these pathways are known to be regulated by sucrose (Coruzzi and Zhou, 2001; Price et al., 2004; Thum et al., 2004; Rosa et al., 2009). Meanwhile, sucrose was also described to play an important role in the antioxidant system (Couée et al., 2006; Ende and Peshev, 2013). This action of sucrose is observable through the strong regulation of the redox system at 8h.

Strikingly, fermentation was up-regulated after at 0.5h and 2 hours of the kinetic points. This phenomenon was also observed after 24h treatment of phenanthrene alone (see Dumas et *al*., 2014). We argued that fermentation do not seems to be associated to our experimental condition as plants during incubation were shaken to avoid any oxygen deprivation. In other hand, to exclude this possibility, we compared our gene lists to genes differentially regulated by anoxia, hypoxia, and O_2 deprivation in the seedlings/shoots of *Arabidopsis* microarray datasets (55) and showed that only 3 genes are found in common (see Dumas et *al*. (2014), in preparation).

3.3.2. Targeted metabolomic changes under phenanthrene in unprotected and protected conditions

During higher plants evolution, sucrose was selected as the major form of transport of carbohydrates. It has been shown that its variation induced a close regulation of many cell processes including the primary metabolism (Roitsch, 1999; Farrar et al., 2000; Rosa et al., 2009; Wind et al., 2010). Indeed, our transcriptional analysis showed that primary metabolism was affected by sucrose since 2h of treatment. Indeed, glycolysis and TCA were found to be induced contrary to gluconeogenese/glyoxylate cycle pathways were inhibited after 8h of treatment. In order to get insight into these transcriptional changed, we carried out a targeted metabolomic analysis. Targeted metabolomic analysis was performed on plants at the stage 2.04 (Boyes et al., 2001). 15 days old plantlets were grown on solid basal medium, and then transferred into liquid medium. Comparison was carried out on plants incubated during 24h in the presence of either 200µM of phenanthrene or 200µm of phenanthrene and 3% of sucrose. This comparison allowed the analysis of the effect of sucrose under phenanthrene-induced stress at the metabolomic level.

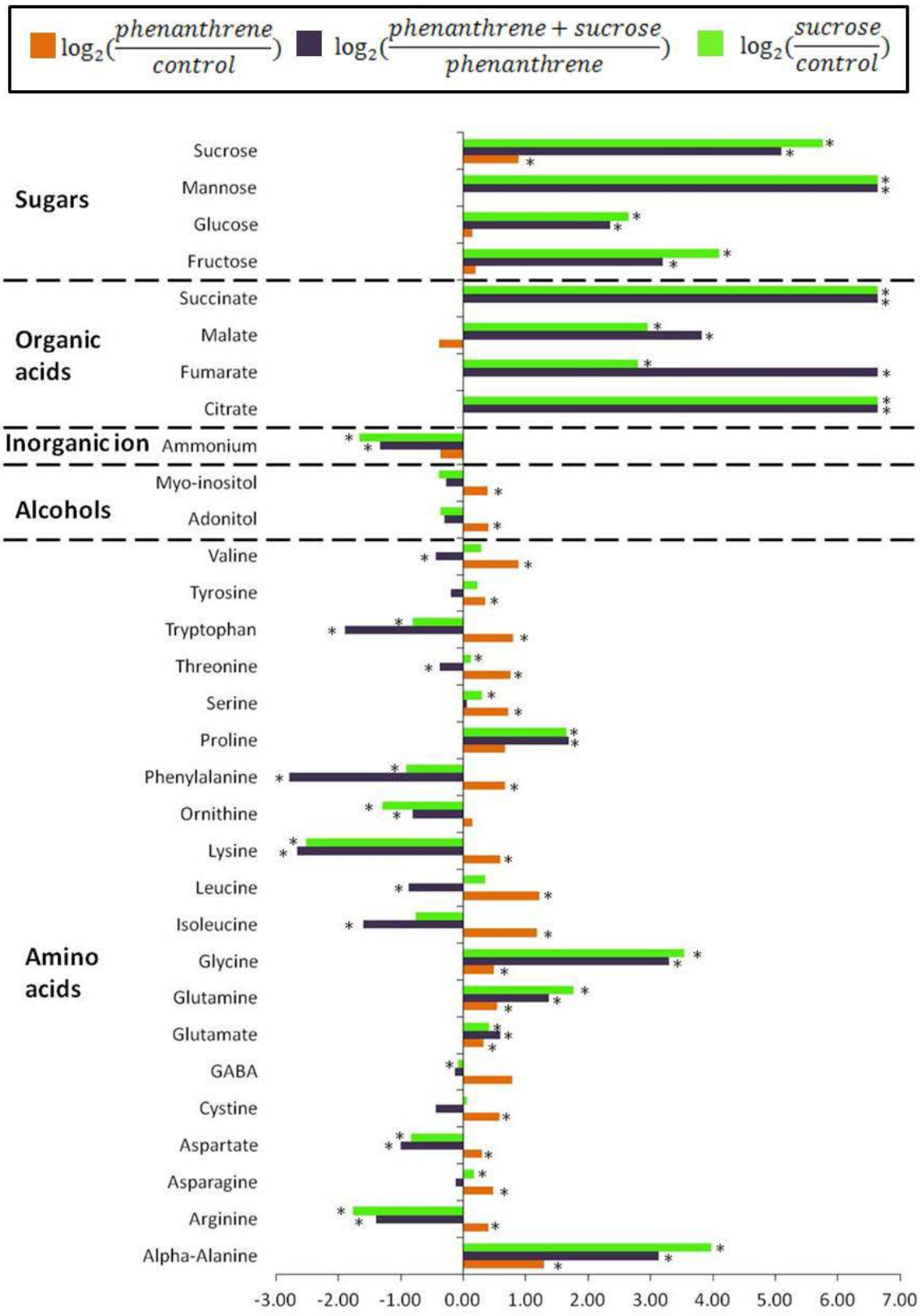

<u>Figure 8</u>: Logarithmic ratios of average metabolites content in whole plants according to the treatment applied.

Selected metabolites (with *) are statistically different between both conditions of the ratio (t-Test, p-value≤0.05). Complete data are available in supplemental table IV.

Figure 8 showed sucrose effects on metabolites ratio in control (green) and stressed condition (purple). Sucrose induced deep reconfiguration of several metabolites levels in both conditions. 20 metabolites levels were affected by sucrose in non-stressed conditions and 24 in phenanthrene-induced stress conditions. 8 metabolites are affected in only one condition (stressed or control). Sucrose strongly induced the accumulation of sugars and organic acids after 24h of incubation, which are intermediates of the TCA cycle. All together, these results revealed a strong regulation of the primary metabolism. Metabolomic and transcriptomic changes induced by sucrose under phenanthrene-induced-stress revealed a strong activation of primary metabolism suggesting that plants absorb and metabolize through glycolysis and TCA the exogenous sucrose (Fig 8). In parallel, exogenous sucrose induced a reduction of ammonium levels in both condition. Amino acids content is also strongly regulated by sucrose. These changes of nitrogen compounds revealed the impact of the addition of a carbon source on nitrogen metabolism and showed the importance of the balance between nitrogen and carbon (Coruzzi and Zhou, 2001).

Additionally, figure 8 showed comparison of metabolites ratios of plants grown in unprotected condition, ($\log_2 \frac{phenanthrene}{control}$), where phenanthrene induced significant changes of 20 metabolites levels, while 24 metabolites were impacted by sucrose under phenanthrene induced stress, ($\log_2 \frac{sucrose+phenanthrene}{phenanthrene}$). As it was previously observed, phenanthrene alone induced a slight accumulation of sucrose. However, in protective conditions, we observed accumulation of not only sucrose but also several other sugars (mannose, maltose, glucose, gentiobiose and fructose). In protective conditions, the accumulation of soluble sugars was highly increased. This result corroborates with the protective effect of the soluble sugars observed in our precedent results and showed in different abiotic stress conditions, such as anoxia (Loreti et al., 2005) and atrazine (Sulmon et al., 2004). Similarly, several studies revealed that abiotic stresses induced the accumulation of sugars (Dubey and Singh, 1999; Gill et al., 2003; Lloyd and Zakhleniuk, 2004). Recently, it was suggested by several authors that sugars, like sucrose, fructans and raffinose family oligosaccharides (RFOs), may contribute directly or indirectly to antioxidative mechanisms (Valluru and Ende, 2008; Bolouri-Moghaddam et al., 2010; Ende and Peshev, 2013; Keunen et al., 2013; Peshev et al., 2013). In other hand, after 24h of incubation in phenanthrene-

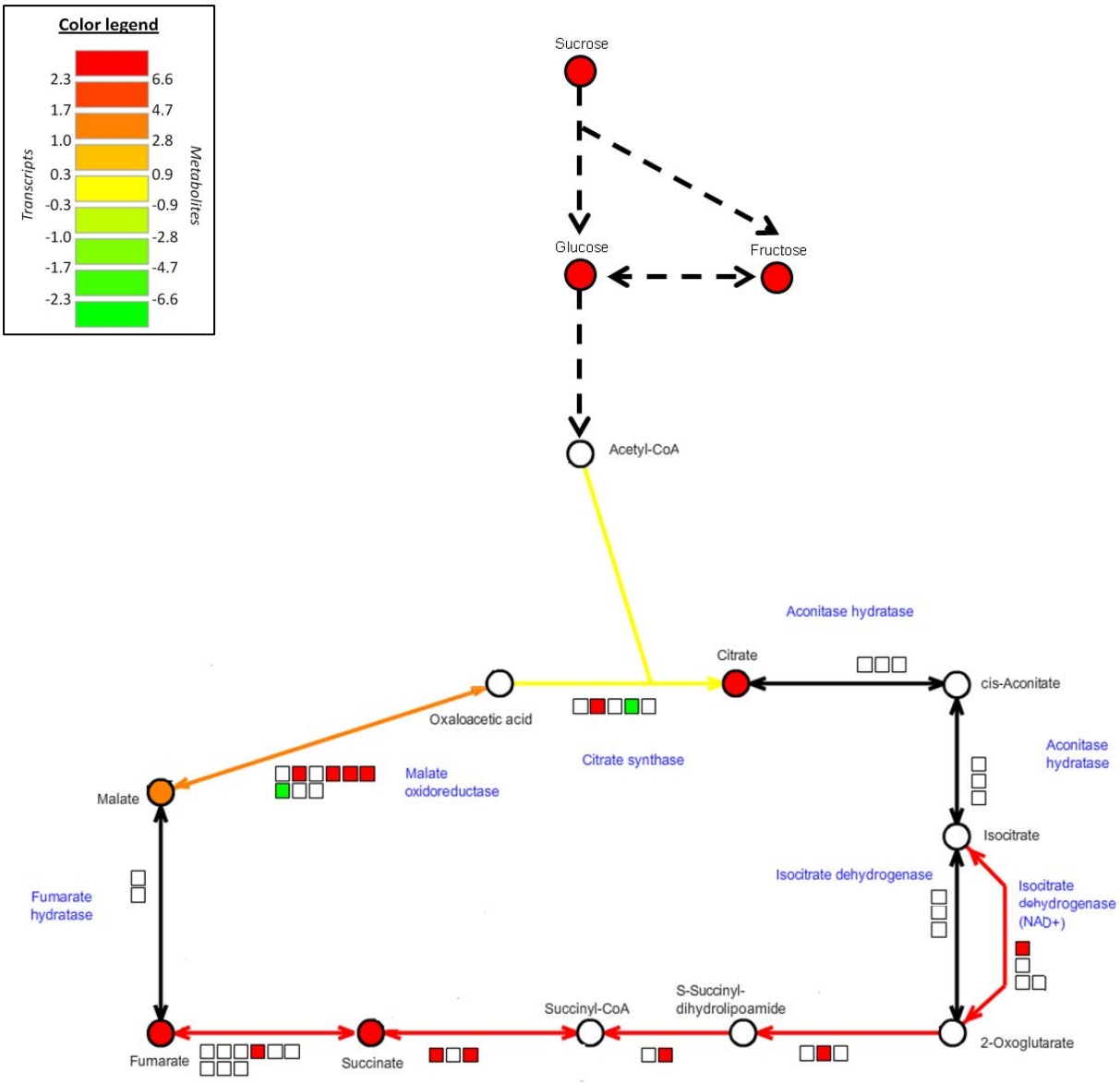

Figure 9: Citric acid cycle and glycolysis representation.

Circles showed the metabolomic data from the experiment phenanthrene vs phenanthrene+sucrose (Raw data are in table 1). Squares represented differentially expressed genes from the transcriptomic experiment for an incubation time of 8h. Modified from diagrams acquired with the online software KaPPaView 4 (Tokimatsu et al., 2005)

induced stress condition, sucrose allowed the accumulation of organic acid such succinate, malate, fumarate and citrate. These data corroborate with the transcriptional activity observed at late stage of treatment; as major carbohydrate pathways were strongly up-regulated such glycolysis and TCA. Genes, involved in sucrose and starch degradation, were also shown to be significantly induced, possibly leading to the accumulation of glucose and fructose observed in the metabolomic analysis (Fig. 8). Figure 9 summarizes and links transcriptomic and metabolomic data, showing a strong regulation of sugar metabolization and the formation of organic acids.

Most of amino acids monitored in our experiment (18 among 25) increased significantly in non-protective conditions ($\log_2 \frac{phenanthrene}{control}$)). Rai (2002) stated that plants subjected to stress (water, heavy metals, cold, salt…) tended to accumulate amino acids. This author discussed the roles of amino acids that are not only precursors for protein synthesis but also act at different levels (enzyme synthesis and activity regulation, gene expression, redox homeostasis, osmolyte…). This observation may also explain a proteolytic activity related to stressed conditions. Contrary, the comparison of phenanthrene effect in protective against stressed conditions ($\log_2 \frac{sucrose+phenanthrene}{phenanthrene}$) revealed that sucrose induced a deep reconfiguration of metabolites levels as among the 25 amino acids analyzed, 5 amino acids increased (proline, glycine, glutamine, glutamate and alpha-alanine) while 14 amino acids showed significant reduction (Fig. 8).

Transcription activity of genes involved in nitrogen metabolism is strongly affected by sucrose after 2h and 8h of treatment. Moreover, amino acid and protein metabolism are also strongly regulated at these kinetic pints (Fig. 7). Through these pathways, glutamate and glutamine synthesis is stimulated which is consistent with the accumulation of alpha-alanine, glutamine, glutamate and proline (Fig. 8). Proline is known to be accumulated in numerous stress response such as water, heavy metals, cold, salt (Rai, 2002; Szabados and Savouré, 2010). Proline like sucrose is known to be a multi-functional metabolite involved not only in primary metabolism but also in signaling and in the redox balance (Szabados and Savouré, 2010). It was also found that external application of proline had a protective effect under abiotic stress (salt and drought) (Ashraf and Foolad, 2007). Sucrose induced a more

important accumulation of glutamate and glutamine that are precursors of proline synthesis. While most amino acids analyzed (Fig. 8) are accumulated in response to a phenanthrene-induced stress, amino acids contain seems to decrease when sucrose is added, suggesting that through the sucrose protective effects, plants are less impacted by the phenanthrene in their environment and their stress response is quite limited.

In conclusion, data obtained from the "phenanthrene experiment" revealed that phenanthrene strongly affected primary metabolism, as photosynthesis and respiration were dramatically down regulated. Meanwhile, soluble sugars and amino acids levels increased. This physiological unbalance revealed a carbohydrate starvation as cell metabolism was unable to face energetic demand. These metabolic unbalance was associated with chlorotic phenotype and inhibition of plant development. However, in protective conditions, sucrose allowed to maintain metabolic pathways involved in cell building structures (cell wall, amino acids and nucleotide synthesis, S assimilation) and energy production (fermentation, glycolysis and TCA cycle) (Fig. 7). It may be argued that sucrose, at the later stage, compensates the negative effect of phenanthrene as it is used as metabolic molecule to face energy demand.

3.3.3. Transcriptional profile of genes involved in stress was reconfigured by exogenous sucrose

Several published data showed that phenanthrene induced oxidative stress (Alkio et al., 2005; Liu et al., 2009; Weisman et al., 2010a). In parallel it might also induce a myriad of other genes involved in stress. It is of high interest to study how these specific genes family are regulated in the presence of sucrose.

Results obtained from pathways enrichment analysis in "sucrose experiment" (Fig. 7) revealed that up-regulated genes belonging to the stress response pathways were over-represented only in the early stages. In contrast, at the late stage, they were down regulated (Fig. 7B). A close analysis of the DEG involved in these two stages revealed that they constitute two distinct clusters, suggesting the involvement of different control mechanisms.

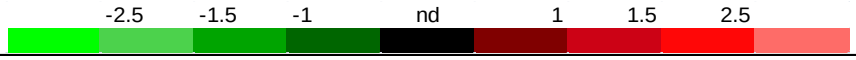

AGI	GO	"Sucrose experiment" (Suc+ phen /phen) 30min	2h	8h	"Phenanthrene experiment" (phenanthrene / control) 30 min	2h	8h
AT3G05890	RCI2B__Low temperature and salt responsive protein family	-1.01		-0.99			
AT4G21870	HSP20-like chaperones superfamily protein	-0.74	-1.31	-1.75			
AT1G80920	J8__Chaperone DnaJ-domain superfamily protein		-2.95	-1.98			
AT1G75380	ATBBD1_BBD1__bifunctional nuclease in basal defense response 1		-1.88	-1.14			
AT2G24550	unknown protein		-1.61	-0.96			
AT3G50480	HR4 (HOMOLOG OF RPW8 4)		-1.21	-1.25		1.80	2.35
AT2G41430	CID1_ERD15_LSR1__dehydration-induced protein (ERD15)		-1.18	-0.99			
AT3G59930	Encodes a defensin-like (DEFL) family protein.		-1.16	-2.13		1.79	2.04
AT1G58190	AtRLP9_RLP9__receptor like protein 9		-1.10	-1.38			
AT4G28240	Wound-responsive family protein		-1.03	-1.00			-0.63
AT1G19660	Wound-responsive family protein		-0.81	-1.86			
AT1G04430	S-adenosyl-L-methionine-dependent methyltransferases superfamily protein		-0.77	0.93			-0.78
AT5G43570	PR (pathogenesis-related) peptide that belongs to the PR-6 proteinase inhibitor family.			-1.88			
AT2G38870	Serine protease inhibitor, potato inhibitor I-type family protein		x	-1.75			
AT4G11650	ATOSM34_OSM34__osmotin 34			-1.55		0.93	
AT4G36040	Chaperone DnaJ-domain superfamily protein			-1.55		0.69	
AT3G50970	LTI30_XERO2__dehydrin family protein			-1.42		0.92	1.16
AT2G02180	TOM3__tobamovirus multiplication protein 3			-1.36			0.78
AT1G56280	ATDI19_DI19__drought-induced 19			-1.29			
AT1G01170	Protein of unknown function (DUF1138)			-1.25			
AT2G21970	SEP2__stress enhanced protein 2			-1.09			
AT2G43510	ATTI1_TI1__trypsin inhibitor protein 1			-1.07			
AT5G44420	LCR77_PDF1.2_PDF1.2A__plant defensin 1.2			-1.06			
AT1G75830	LCR67_PDF1.1__low-molecular-weight cysteine-rich 67			-1.06			
AT5G18140	Chaperone DnaJ-domain superfamily protein			-1.05	1.13	1.12	1.27
AT3G10985	ATWI-12_SAG20_WI12__senescence associated gene 20			-1.00			
AT4G00750	S-adenosyl-L-methionine-dependent methyltransferases superfamily protein			-0.98			0.95
AT1G34047	Encodes a defensin-like (DEFL) family protein.			-0.93			0.82
AT2G43520	ATTI2_TI2__trypsin inhibitor protein 2			-0.91			
AT3G05880	RCI2A__Low temperature and salt responsive protein family			-0.86			
AT1G17860	Kunitz family trypsin and protease inhibitor protein			-0.86			1.10
AT3G22530	unknown protein			-0.84			0.72
AT3G62190	Chaperone DnaJ-domain superfamily protein	x		-0.83			
AT3G01520	Adenine nucleotide alpha hydrolases-like superfamily protein			-0.82			
AT1G24020	MLP423__MLP-like protein 423			-0.78			
AT3G25760	AOC1_ERD12__allene oxide cyclase 1			-0.78			
AT5G64890	PROPEP2__elicitor peptide 2 precursor			-0.75			1.07
AT3G06340	DNAJ heat shock N-terminal domain-containing protein			-0.75			
AT4G21320	HSA32 (HEAT-STRESS-ASSOCIATED 32)			-0.74			
AT5G56010	AtHsp90-3_AtHsp90.3_HSP81-3_Hsp81.3__heat shock protein 81-3		0.76				
AT5G51440	HSP20-like chaperones superfamily protein		0.79				0.90
AT4G36020	CSDP1__cold shock domain protein 1		0.79	0.97			
AT3G54420	ATCHITIV_ATEP3_CHIV_EP3__homolog of carrot EP3-3 chitinase		0.85				0.98
AT5G53760	ATMLO11_MLO11__Seven transmembrane MLO family protein		0.88				
AT2G42540	COR15_COR15A__cold-regulated 15a		0.90	0.90			0.79
AT1G07400	HSP20-like chaperones superfamily protein		0.92				1.18
AT5G56030	AtHsp90.2_ERD8_HSP81-2_HSP90.2__heat shock protein 81-2		0.98	0.98			
AT3G14200	Chaperone DnaJ-domain superfamily protein		1.01				0.77
AT3G09440	Heat shock protein 70 (Hsp 70) family protein		1.06	x			
AT3G12580	ATHSP70_HSP70__heat shock protein 70		1.11				0.77
AT5G25610	ATRD22_RD22__BURP domain-containing protein		1.12	1.25			
AT4G36010	Pathogenesis-related thaumatin superfamily protein		1.34	0.81			1.24
AT2G43620	Chitinase family protein		1.45	1.86			
AT5G36910	THI2.2__thionin 2.2	0.68					
AT3G01420	ALPHA-DOX1_DIOX1_DOX1_PADOX-1__Peroxidase superfamily protein	0.68					
AT3G50950	ZAR1__HOPZ-ACTIVATED RESISTANCE 1	0.71					
AT1G18700	DNAJ heat shock N-terminal domain-containing protein	0.79					0.77
AT3G26450	Polyketide cyclase/dehydrase and lipid transport superfamily protein	0.80					
AT5G42020	BIP_BIP2__Heat shock protein 70 (Hsp 70) family protein	0.93	x				
AT1G76180	ERD14__Dehydrin family protein	0.97		-1.27			
AT1G13930	Involved in response to salt stress. Knockout mutants are hypersensitive to salt stress.	0.98					

Figure 10: List of differentially expressed genes belonging to the stress response pathway in the "sucrose experiment". In parallel, data extracted from the "phenanthrene experiment" were also shown (right) (Dumas et al (2014) in preparation). A negative ratio indicates that the gene is decreased and a positive ratio indicates that the gene is increased in expression in the indicative point of the kinetic, respectively. Ratios in black boxes were not found to be statistically significant after Bonferroni correction (P >0.05)

It is interesting to notice that, in the presence of sucrose, genes involved in stress responses are mostly down-regulated (68%) after 8h of treatment in comparison to phenanthrene-induced stress condition (Fig. 10). These results suggested that sucrose mitigated phenanthrene-induced stress at the transcriptional level, particularly at the late stage. Indeed, more analysis are needed to investigate if these transcriptional regulations are sucrose specific responses or might be induced by other metabolic molecules such glucose or fructose. Additionally, sucrose is also known to induce changes in the redox scavenging system (Ramel et al., 2007; Bolouri-Moghaddam et al., 2010; Ende and Peshev, 2013).

Published data obtained trough long phenanthrene exposition in sucrose supplemented medium revealed strong activity of antioxidant enzymes such as ascorbate peroxidases (APX) and catalases (CAT) (Liu et al., 2009). In other hand, transcriptomic analysis of 21-day-old plantlets grown phenanthrene and sucrose supplemented medium also revealed a strong stimulation of the redox scavenging system (Weisman et al., 2010a). In our experiment ("sucrose experiment"), the redox pathway is significantly over-represented over the whole experiment (Fig 7A). Redox genes up-regulated in the early stages (0.5h) are all involved in the ascorbate and glutathione redox system. Liu et al. (2009) showed that phenanthrene-induced an increase in the activity of ascorbate peroxidase and that *APX1* (*AT1G07890*) mRNA levels which increased after 48h of treatment. In our experiment, this gene is up-regulated all over the kinetic while, in the "phenanthrene experiment", it was up-regulated only after 24h of treatment (Fig. 11). This antioxidant enzyme seems to play a key role in the abiotic stress tolerance. In other hand, among the 26 genes of the redox pathway differentially expressed at 8h, 11 are up-regulated and 15 are down-regulated. They are mainly belonging to the ascorbate and glutathione redox system (8/26) and to the thioredoxin system (11/26). Indeed, both systems are described as major antioxidant systems in plants (Vieira Dos Santos and Rey, 2006; Foyer and Noctor, 2011). These observations suggested a strong regulation of oxidative scavenging system occurred at the late stage in the presence of exogenous sucrose.

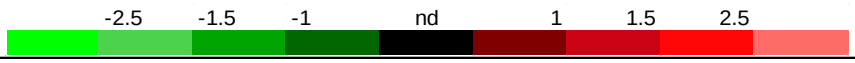

AGI identifier	GO	"Sucrose experiment" suc+phen/phen			"Phenanthrene experiment" phen/control		
		30min	2h	8h	30 min	2h	8h
AT1G03850	Glutaredoxin family protein		-1.83	-1.53			
AT5G06690	WCRKC1__WCRKC thioredoxin 1		-1.24	-1.51			
AT1G11530	ATCXXS1_CXXS1__C-terminal cysteine residue is changed to a serine 1		-0.86	-1.46			
AT5G63030	Thioredoxin superfamily protein			-1.07			
AT3G62930	Thioredoxin superfamily protein			-1.06			
AT1G76080	ATCDSP32_CDSP32__chloroplastic drought-induced stress protein of 32 kD			-1.03			
AT4G35090	CAT2__catalase 2			-0.98			
AT5G28840	GME__GDP-D-mannose 3',5'-epimerase			-0.95			-0.68
AT4G25570	ACYB-2__Cytochrome b561/ferric reductase transmembrane protein family			-0.94			
AT5G16400	ATF2_TRXF2__thioredoxin F2			-0.92			
AT5G51010	Rubredoxin-like superfamily protein			-0.88			
AT4G31870	ATGPX7_GPX7__glutathione peroxidase 7			-0.81			
AT1G07700	Thioredoxin superfamily protein			-0.77			
AT5G61440	ACHT5__atypical CYS HIS rich thioredoxin 5			-0.75			
AT1G12520	ATCCS_CCS__copper chaperone for SOD1			-0.72			
AT3G54960	ATPDI1_ATPDIL1-3_PDI1_PDIL1-3__PDI-like 1-3			0.81			
AT5G60640	ATPDI2_ATPDIL1-4_PDI2_PDIL1-4__PDI-like 1-4			0.85			-0.73
AT1G06830	Glutaredoxin family protein			0.90			
AT2G32720	ATCB5-B_B5 #4_CB5-B__cytochrome B5 isoform B			0.93			-1.04
AT3G10520	AHB2_ARATH GLB2 ATGLB2_GLB2_HB2_NSHB2__haemoglobin 2			0.94			
AT1G77510	ATPDI6_ATPDIL1-2_PDI6_PDIL1-2__PDI-like 1-2			1.08			
AT1G21750	ATPDI5_ATPDIL1-1_PDI5_PDIL1-1__PDI-like 1-1			1.13			
AT2G46650	ATCB5-C_B5 #1_CB5-C__cytochrome B5 isoform C		0.74	0.99			
AT5G03630	ATMDAR2__Pyridine nucleotide-disulphide oxidoreductase family protein		0.77	0.76			0.75
AT1G19570	ATDHAR1_DHAR1_DHAR5__dehydroascorbate reductase		0.79	1.06			
AT1G19550	Glutathione S-transferase family protein		0.82				1.05
AT4G26850	VTC2__mannose-1-phosphate guanylyltransferase (GDP)s		1.15				
AT4G23100	ATECS1_CAD2_GSH1_GSHA_PAD2_RML1__glutamate-cysteine ligase	0.67					
AT2G25080	ATGPX1_GPX1__glutathione peroxidase 1	0.67					
AT4G11600	ATGPX6_GPX6_LSC803_PHGPX__glutathione peroxidase 6	0.82	x				1.03
AT1G07890	APX1_ATAPX01_ATAPX1_CS1_MEE6 _ascorbate peroxidase 1	1.18	1.10	0.90			

Figure 11: List of differentially expressed genes of the redox pathway in the "sucrose experiment".In parallel, data extracted from the "phenanthrene experiment" were also shown (right) (Dumas et al (2013) submitted paper). A negative ratio indicates that the gene is decreased and a positive ratio indicates that the gene is increased in expression in the indicative point of the kinetic, respectively. Ratios in black boxes were not found to be statistically significant after Bonferroni correction (P >0.05)

3.3.4. *The xenome expression was reconfigured by exogenous sucrose*

Transport and detoxification encoding genes of the xenome are belonging to several multigenic enzymes families involved in a three-step process: the first step is an activation of the xenobiotic performed by the cytochrome P450 (CYP), the second step is a conjugation of the xenobiotic with a glutathione performed by glutathione-S-transferases (GST) or a conjugation of the activated xenobiotic with UDP-glucose catalyzed by the UDP-glucuronosyltransferase (UGT), additional malonylation may occurred using a malonyltransferases. Finally, the last step consist in the compartmentalization through the transport of the conjugated xenobiotic by the ATP-binding cassette transporters (ABC transporters) (Edwards et al., 2005; Edwards et al., 2011b). Hence, we hypothesized that sucrose might induce also xenome transcription changes to reduce phenanthrene toxicity or even metabolization. In order to understand how sucrose mitigates phenanthrene-induced stress at the transcriptional xenome expression, all differentially expressed genes family belonging to the xenome were identified and compared with phenanthrene-induced stress condition. This approach might bring new insight into sucrose role in plant tolerance to phenanthrene-induced stress.

The complete set of differentially expressed xenome genes in the presence of sucrose is listed in figure 12. This list was confronted to results previously obtained in the “phenanthrene experiment”.

50 genes belonging to the xenome set are differentially expressed in the “sucrose experiment”. The most noticeable modifications of the xenome genes, induced by sucrose, occurred at the late stage, as 46 genes among the 50 xenome DEG are differentially expressed after 8h of treatment, while only 3 are up-regulated after 0.5h of treatment. All xenome genes differentially expressed in the “sucrose experiment” also appeared to be differentially expressed in at least one other “xenobiotic experiment” and, by consequences, are in the xenome list established in our previous work on phenanthrene effect.

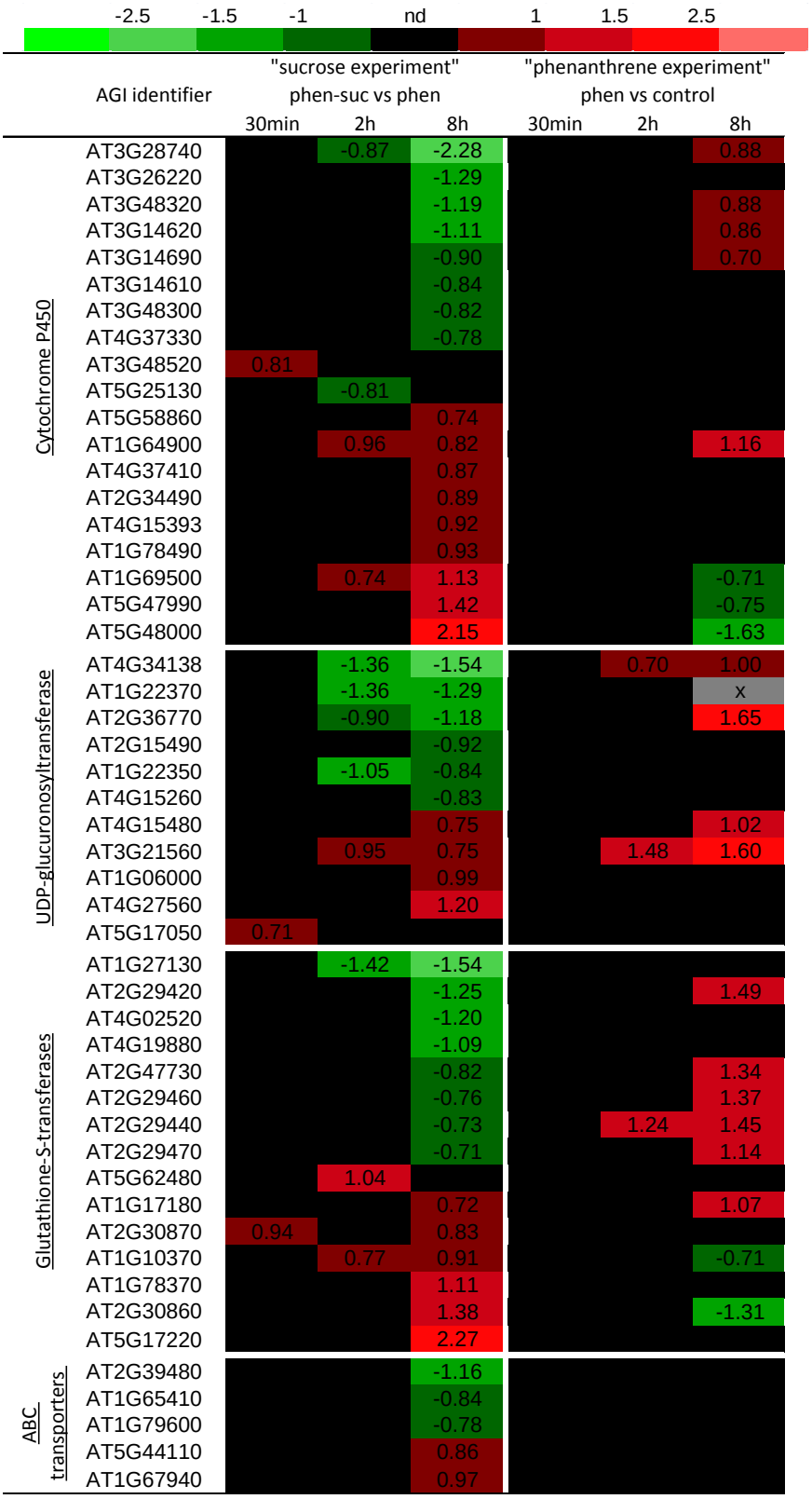

Figure 12: List of differentially expressed xenome genes in the "sucrose experiment".In parallel, data extracted from the "phenanthrene experiment" were also shown (right) (Dumas et al (2014) in preparation). A negative ratio indicates that the gene is decreased and a positive ratio indicates that the gene is increased in expression in the indicative point of the kinetic, respectively. Ratios in black boxes were not found to be statistically significant after Bonferroni correction (P >0.05).

The transcriptional reconfiguration of the xenome, in the presence of sucrose suggests significant changes in the potential phenanthrene conjugation or metabolization. These observations were corroborated by fluorescence microscopy and GC-MS quantification. Since plants accumulated less free phenanthrene in the presence of exogenous sucrose. The signaling and metabolic mechanisms involved in sucrose induced tolerance is still unknown, however, our results and accumulated data suggested that sucrose play a pivotal role in environmental adaptation.

4. Conclusion

In this work, we showed that, whereas phenanthrene alone induced a sever inhibition of plant growth and chlorophyll accumulation, exogenous sucrose allowed to maintain plant development even at high phenanthrene concentration. This protective effect was associated with discrete changes in tissues accumulation of this pollutant. In parallel, quantification by GC-MS showed that treated plants with exogenous sucrose reduced plant phenanthrene content; this observation was associated with tolerant phenotype. Indicating either the induction of cellular processes involved in phenanthrene tolerance or the occurrence of biochemical changes this molecule, such as conjugation or association with cell wall polymers as it was suggested for phenolic xenobiotics (Taguchi et al., 2010; Matsui et al., 2011). Thus we hypothesized that sucrose, induced either new gene-network involved in phenanthrene tolerance such oxidative stress scavenging system, metabolization, transport or likely a complete degradation. In order to verify this hypothesis wide-genome transcriptional and targeted metabolomic approaches were used to decipher early molecular processes involved in sucrose induce tolerance. 2088 genes were found to be differentially expressed in the presence of exogenous sucrose during the first 8h which allowed the identification of significant over represented metabolic pathways.

Indeed, as early as 0.5 h, at the transcriptional level, sucrose allowed maintaining the activity of photosynthesis, energy supply and biosyntheses of protein genes. In contrary to

phenanthrene-induced injury where cellular homeostasis was unbalanced as respiration and photosynthesis were inhibited, whereas amino acids and soluble sugars increased which indicated the incapacity of cells to overcame phenanthrene toxicity and likely a sugar starvation symptoms. Surprisingly fermentation was also significantly induced. However, the metabolic switch from respiration to fermentation is dictated by oxygen availability. Pyruvate decarboxylase and alcohol dehydrogenase are dedicated to ethanolic fermentation and are induced under oxygen deprivation. Tadege and Kuhlemeier (1997) showed that similar situation have been occurred in rapid developing pollen tube, and a flux through ethanolic fermentation pathway could already be detected very early in pollen development. This flux was primarily controlled not by oxygen availability, but rather by sugar supply. It was suggested that at a high rate of sugar metabolism, respiration and fermentation took place concurrently. These authors proposed that aerobic fermentation provides a shunt from pyruvate to acetyl-CoA to accommodate the increased demand for energy and biosynthetic intermediates. Additionally, aerobic fermentation was discussed in the context of stress-signal transduction; as this metabolic pathway was induce under abiotic stress such as cold, deshydratation and ozone exposure, produce considerable amounts of acetaldehyde and ethanol at ambient or even at elevated oxygen concentration(Tadege et al., 1999). Our results give additional data indicating that aerobic fermentation may play a pivotal role in sugar metabolism under abiotic stress conditions. But the functional significance is still to be elucidated.

Tolerance and metabolization of organic pollutants in higher plants alter a myriad of genes family. We showed in this word that exogenous sucrose reconfigured most genes involved in oxidative stress and the xenome. Thus, the P-450 which are involved in the metabolization of organic pollutants in fungus and animal, showed in the presence of sucrose many transcriptional changes, as 19 genes have been differentially regulated. The identification of mutants corresponding to the induced genes have been isolated and their characterization is under investigation. In other hand, metabolization of organic pollutant involves a variety of biochemical pathways. The family 1 Glycosyltransferase (UGT) has emerged as an important group of bio-conjugating enzymes that are involved in the detoxification of xenobiotic (Cole and Edwards, 2000), as they catalyze the O-, S- and N-glyco-conjugation of a range of pollutants using NDP-activated sugar donors (Schröder *et al*.,

2001). In Arabidopsis, a UGT termed UGT72B1 catalyse the conjugation 3,4-dichloroaniline (DCA) with glucose, was identified by Loutre et al. 2003. *UGT72B1* knockout *Arabidopsis* mutant where the UGT72B1 was selectively disrupted by transposon mutagenesis, and over-expression approaches (Brazier-Hicks et al.2007) revealed the identification of competing patways (i) the N-glucosylation produced soluble conjugates which are addressed to extrea celullar space and (ii) insoluble and bound residue mainly attached to cell wall. Thus, when N-glycolsylation activity was suppressed *in planta*, the DCA was directed into lignin fraction. Meanwhile, Matsui et al. (2011) showed that peroxidase have been involved in the removal of organic pollutants, such phenolic compounds, by the cross-linking them to cell wall polysaccharides or proteins at the expense of reduction of hydrogen peroxide. According to these data, we may hypothesize that metabolic pathways involved in pollutants detoxification may be unbalanced depending of environment, nutritional status or signaling stimuli. Our analyses showed that sucrose induced seven genes coding UDP-Glycosil-transferases and nine peroxidases respectively (Supplemental table V). Functional analysis of these genes such knockout strategy, protein expression, will give new insight to understand how sucrose induces tolerance to abiotic stresses.

Supplemental Table I: Primers used for quantitative RT-PCR

Primers name	Sequence (5' → 3')	Targets
1G07890_L1	CTCTGCTGGAACTTTCGATTG	AT1G07890
1G07890_R1	ATGGGGTCCAACAACCTAAGA	
1G07890_L2	TTCGGAACAATGAGGTTTGAC	
1G07890_R2	TCAGCAAAAGAGATGGTAGGG	
1G15380_L1	GAAGAAGGAGGGATCCAAGTG	AT1G15380
1G15380_R1	TTTCTCCTACGAGGGGGACTA	
1G15380_L2	AGAAGAAGCTGGAGGAAATGG	
1G15380_R2	GCTATCGCAGTTGCAAATCTC	
1G30530_L1	GAAGGTTGGAGTGATGATGGA	AT1G30530
1G30530_R1	AGCTTCTTGGCATTAGCCTTC	
1G30530_L2	TCAGTGTTGGAGAGTGTGTCG	
1G30530_R2	TCCATCATCACTCCAACCTTC	
1G44750_L1	TCGCTCTTCTCAAACGTCATT	AT1G44750
1G44750_R1	CGATCAGCATTGCCATAATCT	
1G44750_L2	CATCGACGTATTCGCTCATTT	
1G44750_R2	CGGAGTTGAGAATCAAAGCAG	
1G53310_L1	GCGACCACACATTTCTAAGGA	AT1G53310
1G53310_R1	TGTAGACCAGCAGCAATACCC	
1G53310_L2	CAAAACACCGGTTAAGCTACAA	
1G53310_R2	AATCAACATTTTGACGGTGGA	
2G30870_L1	CTGAGTATCTCGCGATTCAGG	AT2G30870
2G30870_R1	GACTGGGATTTTACCGAAAGG	
2G30870_L2	TGTTGTGACATTGGTGGAGAA	
2G30870_R2	AAAGAGGGAAAATCGGAACCT	
3G03250_L1	TGCTCTTTGAATTTTCCCAAA	AT3G03250
3G03250_R1	CCATCAGTTTCCAAGCAAAGA	
3G03250_L2	AAAGATCACAAGTGGCACAGC	
3G03250_R2	TGGGAAAATTCAAAGAGCAAA	
3G13450_L1	GGATGCAATCAGATCCACTGT	AT3G13450
3G13450_R1	GTCTGAACCACCAGCATCAAT	
3G13450_L2	GCATTGTACACATGATTCTCTGTC	
3G13450_R2	CAAAGATGGAGAGTTTCAAGATCA	
3G52930_L1	CTAAGCTTGGTGATGGAGCAG	AT3G52930
3G52930_R1	TCCAGGAAGATGACAAACGTC	
3G52930_L2	GAGTTCTTCCCGGTATCAAGG	
3G52930_R2	ACGAGCACCAGCTTCGTAGTA	
3G54470_L1	ATTACACGGAGGGAGGAGAAA	AT3G54470
3G54470_R1	CCAAACAAAAGAATCATCAACG	
3G54470_L2	CGTTTTATTGAAATCGCCAAG	
3G54470_R2	TGTTGTTAGTAAATGAACGATGAGG	
4G03950_L1	TTGCCTCAATCATCATCTTCC	AT4G03950
4G03950_R1	GCATTCCTAGACAAAGAACAAGC	
4G03950_L2	CCAAACCCTCTTAAACATGTCA	

4G03950_R2	AGGTTCAAGCATTCCTAGACAAA	
Primers name	Sequence (5' → 3')	Targets
4G13770_L1	GTGGCCACCTTTAAGCATGTA	AT4G13770
4G13770_R1	CGAGTTCGTGAAGGTCAACAT	
4G13770_L2	TCCCATATTGTGGCTTTCTTG	
4G13770_R2	CGGGCTTGACTCTCTTAGGAT	
4G33030_L1	TGATGGAACTTGGACTTGAGC	AT4G33030
4G33030_R1	AGGCATGATTTGTTTCGTGTC	
4G33030_L2	TTGGGCTAGACGTGAAAAAGA	
4G33030_R2	AGGCTCAAGTCCAAGTTCCAT	
4G39940_L1	AACACACAGGAGACGACGAGT	AT4G39940
4G39940_R1	ATTGGGTTGATTTTTCCGACT	
4G39940_L2	ACGTCAGATGGCTGAGAACAT	
4G39940_R2	ACCGAATCAGGGAGAACAATC	
5G03300_L1	GCATTTGTGGGAGGATTTATG	AT5G03300
5G03300_R1	GTTAAAGTCGGGCTTCTCAGG	
5G03300_L2	GATTGAGGAATGCGTGAAGG	
5G03300_R2	AAACTGAGGGTAACCCAATTGTT	
5G08570_L1	CTCGAGAGTCTTGCATCATCC	AT5G08570
5G08570_R1	AGCCACGAGATTAGCAGTTGA	
5G08570_L2	GCAAATGCTGTTCTTGATGGT	
5G08570_R2	CGGCTTCAATGCAGATCTTAG	
5G14180_L1	AGATAGCCTGGCTGATGTGAA	AT5G14180
5G14180_R1	TTTGGCAGTAACACCCATGAT	
5G14180_L2	CATACAACATATCGGCGATCC	
5G14180_R2	TGGTCAAGGAGAAACTCAACG	

Supplemental Table II: Transcriptome data obtained for each kinetic point (30min, 2h and 8h) performed. Differentially regulated genes, in bold face, were selected by statistical analysis based on the Bonferroni method using a P value cut-off of 0.05.
(cf. electronic data)

Supplemental Table III: Genes found to be differentially expressed in all the comparisons between phenanthrene-treated and phenanthrene+sucrose treated plants. *Arabidopsis* annotation from TAIR, called TAIR10 (most recent versions as of 21 September 2012). Expression changes are given as log2. Expression changes in bolt correspond to genes differentially expressed at the significant threshold of Bonferroni p-value<0.05.

AGI identifier	Gene annotation	30 min	2h	8h
AT1E11140	EUGENE prediction	-0.03	-0.02	**-0.88**
AT1E21870	EUGENE prediction	-0.17	0.74	**0.99**
AT1E29130	EUGENE prediction	-0.06	**-1.66**	**-1.99**
AT1E61070	EUGENE prediction	-0.28	**-1.65**	**-2.02**
AT1E70680	EUGENE prediction	-0.04	0.23	**0.86**
AT1G01140	CIPK9_PKS6_SnRK3.12__CBL-interacting protein kinase 9	**0.89**	-0.16	x
AT1G01170	Protein of unknown function (DUF1138)	-0.11	-0.40	**-1.25**
AT1G01470	LEA14_LSR3__Late embryogenesis abundant protein	0.44	x	**-0.83**
AT1G01490	Heavy metal transport/detoxification superfamily protein	0.00	-0.51	**-0.84**
AT1G01640	BTB/POZ domain-containing protein	0.45	0.09	**0.80**
AT1G02080	transcription regulators	**-0.68**	-0.04	0.19
AT1G02305	Cysteine proteinases superfamily protein	-0.01	-0.18	**-0.96**
AT1G02400	ATGA2OX4_ATGA2OX6_DTA1_GA2OX6__gibberellin 2-oxidase 6	**0.81**	0.07	-0.03
AT1G02660	alpha/beta-Hydrolases superfamily protein	-0.01	**-0.96**	**-1.36**
AT1G02816	Protein of unknown function, DUF538	x	-0.56	**-1.06**
AT1G03090	MCCA__methylcrotonyl-CoA carboxylase alpha chain, mitochondrial / 3-methylcrotonyl-CoA carboxylase 1 (MCCA)	-0.14	**-1.01**	**-1.61**
AT1G03220	Eukaryotic aspartyl protease family protein	0.26	-0.70	**-1.33**
AT1G03230	Eukaryotic aspartyl protease family protein	0.14	-0.44	**-0.80**
AT1G03610	Protein of unknown function (DUF789)	-0.03	**-1.05**	-0.68
AT1G03850	Glutaredoxin family protein	-0.20	**-1.83**	**-1.53**
AT1G03870	FLA9__FASCICLIN-like arabinoogalactan 9	-0.51	**-1.10**	0.52
AT1G04170	EIF2 GAMMA__eukaryotic translation initiation factor 2 gamma subunit	-0.45	0.45	**1.28**
AT1G04190	Tetratricopeptide repeat (TPR)-like superfamily protein	-0.20	0.34	**0.95**
AT1G04270	RPS15__cytosolic ribosomal protein S15	-0.09	0.38	**0.95**
AT1G04350	2-oxoglutarate (2OG) and Fe(II)-dependent oxygenase superfamily protein	-0.15	-0.08	**-0.93**
AT1G04400	AT-PHH1_ATCRY2_CRY2_FHA_PHH1 _cryptochrome 2	-0.06	**-1.02**	**-0.85**
AT1G04430	S-adenosyl-L-methionine-dependent methyltransferases superfamily protein	-0.44	**-0.77**	**0.93**
AT1G04680	Pectin lyase-like superfamily protein	-0.16	-0.12	**1.08**
AT1G04710	KAT1_PKT4__peroxisomal 3-ketoacyl-CoA thiolase 4	-0.01	-0.32	**-0.88**
AT1G04820	TOR2_TUA4__tubulin alpha-4 chain	-0.35	-0.16	**1.21**
AT1G05010	ACO4_EAT1_EFE__ethylene-forming enzyme	**1.54**	0.23	0.40
AT1G05170	Galactosyltransferase family protein	-0.04	**1.10**	0.23
AT1G05240	Peroxidase superfamily protein	0.31	-0.08	**1.68**
AT1G05250	Peroxidase superfamily protein	0.30	0.06	**0.82**
AT1G05300	ZIP5__zinc transporter 5 precursor	0.06	0.34	**0.87**
AT1G05340	unknown protein	-0.05	-0.70	**-1.66**

AGI identifier	Gene annotation	30 min	2h	8h
AT1G05560	UGT1_UGT75B1__UDP-glucosyltransferase 75B1	-0.05	-0.55	**-0.93**
AT1G05575	unknown protein	0.48	0.18	**-1.41**
AT1G05670	Pentatricopeptide repeat (PPR-like) superfamily protein	0.25	-0.01	**-0.72**
AT1G05680	UGT74E2__UDP-glycosyltransferase 74E2	0.01	-0.24	**-0.93**
AT1G05890	ARI5_ATARI5__RING/U-box superfamily protein	-0.36	-0.46	**-0.74**
AT1G06000	UDP-Glycosyltransferase superfamily protein	0.15	0.71	**0.99**
AT1G06400	ARA-2_ARA2_ATRAB11E_ATRABA1A__Ras-related small GTP-binding family protein	-0.26	**-0.90**	x
AT1G06550	ATP-dependent caseinolytic (Clp) protease/crotonase family protein	-0.21	0.07	**0.91**
AT1G06570	HPD_PDS1__phytoene desaturation 1	0.40	-0.59	**-1.89**
AT1G06700	Protein kinase superfamily protein	0.35	-0.70	**-1.52**
AT1G06720	P-loop containing nucleoside triphosphate hydrolases superfamily protein	x	0.14	**0.79**
AT1G06830	Glutaredoxin family protein	-0.20	-0.19	**0.90**
AT1G07040	unknown protein	-0.32	-0.19	**-1.17**
AT1G07070	Ribosomal protein L35Ae family protein	-0.16	0.67	**1.01**
AT1G07135	glycine-rich protein	-0.58	-0.35	**-0.83**
AT1G07370	ATPCNA1_PCNA1__proliferating cellular nuclear antigen 1	-0.28	0.48	**0.95**
AT1G07400	HSP20-like chaperones superfamily protein	0.20	**0.92**	-0.29
AT1G07700	Thioredoxin superfamily protein	0.02	-0.04	**-0.77**
AT1G07890	APX1_ATAPX01_ATAPX1_CS1_MEE6__ascorbate peroxidase 1	**1.18**	**1.10**	**0.90**
AT1G07930	GTP binding Elongation factor Tu family protein	-0.23	0.28	**0.85**
AT1G08090	ACH1_ATNRT2.1_ATNRT2:1_LIN1_NRT2_NRT2.1_NRT2:1_NRT2;1AT__nitrate transporter 2:1	0.18	0.03	**1.05**
AT1G08360	Ribosomal protein L1p/L10e family	-0.15	0.41	**0.83**
AT1G08550	AVDE1_NPQ1__non-photochemical quenching 1	-0.02	-0.66	**-0.85**
AT1G08630	THA1__threonine aldolase 1	0.29	**-0.78**	**-2.09**
AT1G08650	ATPPCK1_PPCK1__phosphoenolpyruvate carboxylase kinase 1	0.03	**1.28**	**0.95**
AT1G08920	ESL1__ERD (early response to dehydration) six-like 1	-0.37	0.08	**-0.94**
AT1G08980	AMI1_ATAMI1_ATTOC64-I_TOC64-I__amidase 1	0.30	-0.31	**-0.77**
AT1G09070	(AT)SRC2_SRC2__soybean gene regulated by cold-2	0.37	-0.63	**-1.32**
AT1G09310	Protein of unknown function, DUF538	0.55	**0.86**	**0.95**
AT1G09340	CRB_CSP41B__chloroplast RNA binding	-0.02	-0.09	**-0.72**
AT1G09400	FMN-linked oxidoreductases superfamily protein	0.18	-0.32	**-0.79**
AT1G09430	ACLA-3__ATP-citrate lyase A-3	0.09	-0.31	**-0.87**
AT1G09480	NAD(P)-binding Rossmann-fold superfamily protein	0.29	0.01	**-1.02**
AT1G09500	NAD(P)-binding Rossmann-fold superfamily protein	-0.06	-0.44	**-1.56**
AT1G09590	Translation protein SH3-like family protein	-0.02	0.50	**0.97**
AT1G09690	Translation protein SH3-like family protein	-0.03	0.38	**0.92**
AT1G09830	Glycinamide ribonucleotide (GAR) synthetase	-0.19	0.43	**0.87**
AT1G10020	Protein of unknown function (DUF1005)	**-0.78**	**-0.95**	-0.41
AT1G10070	ATBCAT-2_BCAT-2__branched-chain amino acid transaminase 2	0.16	**-1.26**	**-2.69**
AT1G10140	Uncharacterised conserved protein UCP031279	-0.19	**-0.87**	**-1.16**

AGI identifier	Gene annotation	30 min	2h	8h
AT1G10150	Carbohydrate-binding protein	-0.46	**-1.75**	**-1.21**
AT1G10370	ATGSTU17_ERD9_GST30_GST30B__Glutathione S-transferase family protein	0.14	**0.77**	**0.91**
AT1G11530	ATCXXS1_CXXS1__C-terminal cysteine residue is changed to a serine 1	0.21	**-0.86**	**-1.46**
AT1G11700	Protein of unknown function, DUF584	**0.68**	-0.13	0.13
AT1G11840	ATGLX1_GLX1__glyoxalase I homolog	x	0.32	**1.37**
AT1G12110	ATNRT1_B-1_CHL1_CHL1-1_NRT1_NRT1.1__nitrate transporter 1.1	0.56	**0.94**	x
AT1G12250	Pentapeptide repeat-containing protein	0.01	-0.48	**-1.40**
AT1G12440	A20/AN1-like zinc finger family protein	-0.15	**-1.03**	**-1.27**
AT1G12520	ATCCS_CCS__copper chaperone for SOD1	-0.03	-0.27	**-0.72**
AT1G12560	ATEXP7_ATEXPA7_ATHEXP ALPHA 1.26_EXP7_EXPA7__expansin A7	0.29	0.26	**0.96**
AT1G12780	ATUGE1_UGE1__UDP-D-glucose/UDP-D-galactose 4-epimerase 1	0.36	**-0.84**	**-1.85**
AT1G12900	GAPA-2__glyceraldehyde 3-phosphate dehydrogenase A subunit 2	-0.06	-0.07	**-0.72**
AT1G13245	ROTUNDIFOLIA like 17 (RTFL17)	-0.39	**-1.06**	**-0.90**
AT1G13260	EDF4_RAV1__related to ABI3/VP1 1	-0.15	**-1.09**	**-0.91**
AT1G13440	GAPC-2_GAPC2__glyceraldehyde-3-phosphate dehydrogenase C2	-0.07	0.47	**0.87**
AT1G13930	Involved in response to salt stress. Knockout mutants are hypersensitive to salt stress.	**0.98**	0.20	0.00
AT1G14120	2-oxoglutarate (2OG) and Fe(II)-dependent oxygenase superfamily protein	-0.10	0.24	**0.76**
AT1G14200	RING/U-box superfamily protein	0.01	-0.37	**-0.79**
AT1G14290	SBH2__sphingoid base hydroxylase 2	-0.32	**-0.91**	-0.43
AT1G14610	TWN2_VALRS__valyl-tRNA synthetase / valine--tRNA ligase (VALRS)	-0.28	0.18	**0.82**
AT1G14620	DECOY__decoy	-0.28	0.30	**1.08**
AT1G14870	PCR2__PLANT CADMIUM RESISTANCE 2	0.08	-0.54	**-1.00**
AT1G14880	PCR1__PLANT CADMIUM RESISTANCE 1	-0.07	-0.28	**-0.78**
AT1G14980	CPN10__chaperonin 10	-0.21	0.54	**1.07**
AT1G15040	Class I glutamine amidotransferase-like superfamily protein	-0.07	**-1.17**	**-2.01**
AT1G15250	Zinc-binding ribosomal protein family protein	-0.22	0.64	**0.94**
AT1G15380	Lactoylglutathione lyase / glyoxalase I family protein	-0.26	**-1.38**	**-2.30**
AT1G15440	ATPWP2_PWP2__periodic tryptophan protein 2	-0.11	0.61	**0.73**
AT1G15670	Galactose oxidase/kelch repeat superfamily protein	0.18	**-0.87**	-0.69
AT1G15740	Leucine-rich repeat family protein	-0.14	**-1.00**	**-1.06**
AT1G15820	CP24_LHCB6__light harvesting complex photosystem II subunit 6	**0.79**	0.31	-0.36
AT1G15980	NDF1_NDH48__NDH-dependent cyclic electron flow 1	0.21	-0.32	**-1.18**
AT1G16240	ATSYP51_SYP51__syntaxin of plants 51	-0.22	**-0.75**	-0.69
AT1G16390	ATOCT3__organic cation/carnitine transporter 3	-0.28	**-0.80**	-0.06
AT1G16410	BUS1_CYP79F1_SPS1__cytochrome p450 79f1	-0.05	0.46	**1.24**
AT1G16530	ASL9_LBD3__ASYMMETRIC LEAVES 2-like 9	0.13	0.26	**0.92**
AT1G16720	HCF173__high chlorophyll fluorescence phenotype 173	0.47	**-0.82**	**-1.30**

AGI identifier	Gene annotation	30 min	2h	8h
AT1G16880	uridylyltransferase-related	0.51	0.15	**-0.97**
AT1G17100	SOUL heme-binding family protein	0.20	0.65	**-0.74**
AT1G17147	VQ motif-containing protein	0.21	-0.66	**-1.71**
AT1G17180	ATGSTU25_GSTU25__glutathione S-transferase TAU 25	0.15	0.59	**0.72**
AT1G17420	LOX3__lipoxygenase 3	0.04	**0.79**	0.38
AT1G17560	HLL__Ribosomal protein L14p/L23e family protein	x	0.01	**1.06**
AT1G17720	ATB BETA__Protein phosphatase 2A, regulatory subunit PR55	**-0.68**	-0.01	x
AT1G17860	Kunitz family trypsin and protease inhibitor protein	0.39	0.04	**-0.86**
AT1G17880	ATBTF3_BTF3__basic transcription factor 3	-0.14	0.44	**0.96**
AT1G18020	FMN-linked oxidoreductases superfamily protein	-0.62	**-0.90**	**-1.37**
AT1G18060	unknown protein	0.03	-0.02	**-0.78**
AT1G18080	ATARCA_RACK1A_RACK1A_AT__Transducin/WD40 repeat-like superfamily protein	0.17	0.63	**0.89**
AT1G18290	unknown protein	-0.14	-0.63	**-0.78**
AT1G18320	Mitochondrial import inner membrane translocase subunit Tim17/Tim22/Tim23 family protein	-0.06	0.36	**1.14**
AT1G18510	TET16__tetraspanin 16	-0.14	-0.26	**-0.76**
AT1G18540	Ribosomal protein L6 family protein	0.32	0.68	**1.04**
AT1G18700	DNAJ heat shock N-terminal domain-containing protein	**0.79**	-0.12	-0.63
AT1G18800	NRP2__NAP1-related protein 2	-0.16	0.25	**0.83**
AT1G19400	Erythronate-4-phosphate dehydrogenase family protein	-0.27	**-0.77**	**-1.10**
AT1G19450	Major facilitator superfamily protein	-0.41	0.09	**1.08**
AT1G19520	NFD5__pentatricopeptide (PPR) repeat-containing protein	-0.46	0.27	**1.08**
AT1G19530	unknown protein	-0.29	**-2.21**	**-2.48**
AT1G19550	Glutathione S-transferase family protein	0.38	**0.82**	0.53
AT1G19570	ATDHAR1_DHAR1_DHAR5__dehydroascorbate reductase	0.35	**0.79**	**1.06**
AT1G19660	Wound-responsive family protein	-0.01	**-0.81**	**-1.86**
AT1G19770	ATPUP14_PUP14__purine permease 14	-0.29	**-1.29**	**-1.25**
AT1G19800	TGD1__trigalactosyldiacylglycerol 1	-0.17	0.16	**0.72**
AT1G20340	DRT112_PETE2__Cupredoxin superfamily protein	0.29	0.11	**-0.74**
AT1G20530	Protein of unknown function (DUF630 and DUF632)	0.11	0.71	**1.91**
AT1G20650	Protein kinase superfamily protein	**0.73**	-0.70	-0.68
AT1G20720	RAD3-like DNA-binding helicase protein	-0.32	0.25	**0.96**
AT1G20860	PHT1;8__phosphate transporter 1;8	0.38	0.10	**1.17**
AT1G20870	HSP20-like chaperones superfamily protein	0.00	-0.67	**-2.15**
AT1G20925	Auxin efflux carrier family protein	-0.14	**-1.73**	**-2.05**
AT1G20940	F-box family protein	x	**-1.75**	**-3.27**
AT1G20950	Phosphofructokinase family protein	0.21	-0.36	**-0.77**
AT1G21000	PLATZ transcription factor family protein	0.12	-0.61	**-0.88**
AT1G21080	DNAJ heat shock N-terminal domain-containing protein	0.17	0.07	**0.90**
AT1G21090	Cupredoxin superfamily protein	-0.32	0.32	**1.24**
AT1G21190	Small nuclear ribonucleoprotein family protein	-0.14	-0.06	**0.91**
AT1G21320	nucleotide binding;nucleic acid binding	0.12	0.46	**1.11**
AT1G21480	Exostosin family protein	-0.04	-0.41	**-1.17**
AT1G21525	unknown protein	-0.05	0.45	**0.93**
AT1G21570	zinc finger (CCCH-type) family protein	-0.01	0.07	**0.71**

AGI identifier	Gene annotation	30 min	2h	8h
AT1G21680	DPP6 N-terminal domain-like protein	0.08	-0.62	**-1.46**
AT1G21750	ATPDI5_ATPDIL1-1_PDI5_PDIL1-1__PDI-like 1-1	0.16	0.28	**1.13**
AT1G21780	BTB/POZ domain-containing protein	0.18	0.03	**-0.76**
AT1G21910	Integrase-type DNA-binding superfamily protein	**-1.16**	**-1.04**	-0.19
AT1G21920	Histone H3 K4-specific methyltransferase SET7/9 family protein	-0.08	**-0.79**	-0.63
AT1G22070	TGA3__TGA1A-related gene 3	0.02	**1.05**	**1.16**
AT1G22190	Integrase-type DNA-binding superfamily protein	**-0.74**	**-0.85**	-0.39
AT1G22270	Trm112p-like protein	0.03	**0.74**	**0.75**
AT1G22350	putative UDP-glucose glucosyltransferase	-0.03	**-1.05**	**-0.84**
AT1G22370	AtUGT85A5_UGT85A5__UDP-glucosyl transferase 85A5	0.14	**-1.36**	**-1.29**
AT1G22400	ATUGT85A1_UGT85A1__UDP-Glycosyltransferase superfamily protein	-0.39	**-0.97**	**-0.74**
AT1G22500	RING/U-box superfamily protein	0.20	-0.34	**-1.13**
AT1G22530	PATL2__PATELLIN 2	0.39	**-1.09**	-0.45
AT1G22630	unknown protein	-0.34	**-0.96**	**-1.22**
AT1G22950	2-oxoglutarate (2OG) and Fe(II)-dependent oxygenase superfamily protein	-0.14	-0.03	**0.74**
AT1G23200	Plant invertase/pectin methylesterase inhibitor superfamily	0.65	**1.63**	**1.99**
AT1G23280	MAK16 protein-related	-0.08	0.42	**0.99**
AT1G23350	Plant invertase/pectin methylesterase inhibitor superfamily protein	-0.06	**-1.14**	**-1.29**
AT1G23750	Nucleic acid-binding, OB-fold-like protein	0.29	-0.25	**-0.82**
AT1G23790	Plant protein of unknown function (DUF936)	**0.88**	x	-0.08
AT1G24020	MLP423__MLP-like protein 423	0.06	-0.04	**-0.78**
AT1G24290	AAA-type ATPase family protein	-0.09	**1.07**	**1.32**
AT1G24440	RING/U-box superfamily protein	0.02	-0.64	**-0.88**
AT1G24510	TCP-1/cpn60 chaperonin family protein	x	0.01	**0.78**
AT1G25097	unknown protein	**-0.97**	-0.36	-0.39
AT1G25260	Ribosomal protein L10 family protein	-0.10	0.43	**0.71**
AT1G25275	unknown protein	0.38	**-0.96**	**-1.03**
AT1G25400	unknown protein	-0.45	**-1.61**	**-1.32**
AT1G26500	Pentatricopeptide repeat (PPR) superfamily protein	-0.20	**0.85**	0.62
AT1G26630	ATELF5A-2_ELF5A-2_FBR12__Eukaryotic translation initiation factor 5A-1 (eIF-5A 1) protein	0.60	0.37	**0.77**
AT1G26761	Arabinanase/levansucrase/invertase	-0.11	**-1.00**	**-1.37**
AT1G27030	unknown protein	-0.04	-0.05	**0.92**
AT1G27130	ATGSTU13_GST12_GSTU13__glutathione S-transferase tau 13	-0.03	**-1.42**	**-1.54**
AT1G27190	Leucine-rich repeat protein kinase family protein	-0.12	-0.21	**-1.63**
AT1G27470	Transducin family protein / WD-40 repeat family protein	-0.12	0.45	**0.73**
AT1G27760	ATSAT32_SAT32__interferon-related developmental regulator family protein / IFRD protein family	0.27	**0.91**	0.67
AT1G27950	LTPG1__glycosylphosphatidylinositol-anchored lipid protein transfer 1	0.58	0.50	**1.12**
AT1G28100	unknown protein	-0.03	-0.73	**-0.76**
AT1G28110	SCPL45__serine carboxypeptidase-like 45	-0.15	**-0.85**	-0.57

AGI identifier	Gene annotation	30 min	2h	8h
AT1G28150	unknown protein	-0.15	-0.40	**-0.82**
AT1G28290	AGP31__arabinogalactan protein 31	-0.30	-0.04	**1.01**
AT1G28330	DRM1_DYL1__dormancy-associated protein-like 1	-0.26	**-2.53**	**-2.19**
AT1G28340	AtRLP4_RLP4__receptor like protein 4	-0.21	0.09	**0.87**
AT1G28400	unknown protein	-0.06	0.16	**0.90**
AT1G29070	Ribosomal protein L34	0.03	0.58	**0.96**
AT1G29280	ATWRKY65_WRKY65__WRKY DNA-binding protein 65	-0.13	0.26	**1.13**
AT1G29400	AML5_ML5__MEI2-like protein 5	-0.34	**-0.80**	**-0.80**
AT1G29630	5'-3' exonuclease family protein	-0.15	0.58	**1.19**
AT1G29670	GDSL-like Lipase/Acylhydrolase superfamily protein	**1.17**	-0.07	0.28
AT1G29724	protein binding	-0.03	0.02	**0.90**
AT1G29970	RPL18AA__60S ribosomal protein L18A-1	-0.04	-0.11	**0.96**
AT1G29980	Protein of unknown function, DUF642	0.24	-0.08	**-1.01**
AT1G30280	Chaperone DnaJ-domain superfamily protein	-0.59	**-0.83**	-0.01
AT1G30510	ATRFNR2_RFNR2__root FNR 2	0.50	0.60	**1.09**
AT1G30530	UGT78D1__UDP-glucosyl transferase 78D1	-0.08	**0.75**	**1.48**
AT1G30580	GTP binding	-0.33	0.21	**0.87**
AT1G30700	FAD-binding Berberine family protein	0.41	-0.18	**-0.91**
AT1G30720	FAD-binding Berberine family protein	0.28	-0.39	**-0.90**
AT1G30730	FAD-binding Berberine family protein	0.23	**-0.93**	**-1.01**
AT1G30820	CTP synthase family protein	-0.25	**-1.95**	**-1.12**
AT1G30870	Peroxidase superfamily protein	0.34	-0.06	**0.79**
AT1G31180	ATIMD3_IMD3_IPMDH1_isopropylmalate dehydrogenase 3	**0.88**	0.57	**1.24**
AT1G31817	NFD3__Ribosomal L18p/L5e family protein	**-0.68**	**-1.22**	**-0.98**
AT1G31930	XLG3__extra-large GTP-binding protein 3	-0.28	0.37	**1.86**
AT1G31940	unknown protein	-0.33	0.07	**1.15**
AT1G32100	ATPRR1_PRR1__pinoresinol reductase 1	**0.74**	0.10	-0.17
AT1G32320	ATMKK10_MKK10__MAP kinase kinase 10	0.30	0.04	**-0.86**
AT1G32375	F-box/RNI-like/FBD-like domains-containing protein	0.10	0.59	**1.06**
AT1G32400	TOM2A__tobamovirus multiplication 2A	0.12	0.46	**0.91**
AT1G32860	Glycosyl hydrolase superfamily protein	0.05	0.22	**0.92**
AT1G32900	UDP-Glycosyltransferase superfamily protein	-0.07	**1.75**	**2.36**
AT1G32928	unknown protein	0.07	-0.64	**-0.97**
AT1G33050	unknown protein	0.06	-0.71	**-0.95**
AT1G33110	MATE efflux family protein	-0.25	0.15	**-0.79**
AT1G33140	PGY2__Ribosomal protein L6 family	-0.02	0.21	**0.74**
AT1G33760	Integrase-type DNA-binding superfamily protein	**-0.79**	-0.04	-0.07
AT1G33800	Protein of unknown function (DUF579)	0.09	0.63	**0.74**
AT1G34000	OHP2__one-helix protein 2	-0.02	-0.47	**-0.97**
AT1G34042	unknown protein	**-0.74**	0.05	-0.18
AT1G34047	Encodes a defensin-like (DEFL) family protein.	0.12	-0.31	**-0.93**
AT1G34130	STT3B__staurosporin and temperature sensitive 3-like b	-0.29	0.36	**0.79**
AT1G34355	ATPS1_PS1__forkhead-associated (FHA) domain-containing protein	0.06	-0.34	**-0.73**
AT1G34440	unknown protein	-0.34	-0.08	**-0.92**
AT1G34460	CYC3_CYCB1;5__CYCLIN B1;5	-0.01	-0.16	**-0.90**
AT1G34630	unknown protein	-0.10	**0.97**	0.20

AGI identifier	Gene annotation	30 min	2h	8h
AT1G34680	pseudogene, ribosomal maturase	**-0.89**	0.17	0.03
AT1G35140	EXL7_PHI-1__Phosphate-responsive 1 family protein	-0.21	**-1.89**	**-2.18**
AT1G35160	14-3-3PHI_GF14 PHI_GRF4__GF14 protein phi chain	-0.19	-0.29	**-1.10**
AT1G35350	EXS (ERD1/XPR1/SYG1) family protein	-0.51	**-0.75**	-0.46
AT1G35490	bZIP family transcription factor	0.39	0.27	**0.93**
AT1G35510	O-fucosyltransferase family protein	0.15	**-0.79**	**-1.22**
AT1G35550	elongation factor Tu C-terminal domain-containing protein	x	0.18	**0.86**
AT1G36230	unknown protein	-0.33	0.10	**0.98**
AT1G37130	ATNR2_B29_CHL3_NIA2_NIA2-1_NR_NR2__nitrate reductase 2	0.16	-0.62	**-1.25**
AT1G41830	SKS6_SKS6__SKU5-similar 6	-0.05	0.17	**1.18**
AT1G42440	unknown protein	-0.04	0.58	**1.28**
AT1G43160	RAP2.6__related to AP2 6	-0.02	-0.70	**-0.94**
AT1G43170	ARP1_emb2207_RP1_RPL3A__ribosomal protein 1	-0.58	0.20	**1.17**
AT1G43670	Inositol monophosphatase family protein	0.46	-0.14	**-1.11**
AT1G43710	emb1075__Pyridoxal phosphate (PLP)-dependent transferases superfamily protein	-0.10	0.68	**0.83**
AT1G43790	TED6__tracheary element differentiation-related 6	**0.99**	0.15	0.12
AT1G44350	ILL6__IAA-leucine resistant (ILR)-like gene 6	-0.02	0.27	**-0.95**
AT1G44750	ATPUP11_PUP11__purine permease 11	0.13	**1.13**	**1.49**
AT1G44960	SNARE associated Golgi protein family	0.07	**-1.03**	-0.59
AT1G45063	copper ion binding;electron carriers	-0.17	0.65	**1.11**
AT1G45201	TRIACYLGLYCEROL LIPASE-LIKE 1	0.09	0.61	**1.74**
AT1G45688	unknown protein	0.12	0.02	**0.83**
AT1G47128	RD21_RD21A__Granulin repeat cysteine protease family protein	0.05	-0.38	**-0.75**
AT1G47240	ATNRAMP2_NRAMP2__NRAMP metal ion transporter 2	0.20	**-0.81**	**-1.08**
AT1G47490	ATRBP47C_RBP47C__RNA-binding protein 47C	-0.14	0.34	**0.81**
AT1G47720	OSB1__Primosome PriB/single-strand DNA-binding	0.29	0.15	**-0.82**
AT1G47750	PEX11A__peroxin 11A	-0.05	-0.31	**-0.96**
AT1G48300	unknown protein	-0.04	-0.39	**-0.97**
AT1G48570	zinc finger (Ran-binding) family protein	0.03	0.34	**0.89**
AT1G48600	AtPMEAMT_PMEAMT__S-adenosyl-L-methionine-dependent methyltransferases superfamily protein	0.03	0.32	**1.33**
AT1G48760	delta-ADR__delta-adaptin	0.26	0.32	**0.95**
AT1G48830	Ribosomal protein S7e family protein	0.13	0.24	**0.82**
AT1G48850	EMB1144__chorismate synthase, putative / 5-enolpyruvylshikimate-3-phosphate phospholyase, putative	-0.06	0.51	**0.79**
AT1G48920	ATNUC-L1_NUC-L1_PARL1__nucleolin like 1	-0.15	0.69	**1.00**
AT1G49360	F-box family protein	-0.18	0.25	**0.84**
AT1G49570	Peroxidase superfamily protein	-0.38	0.45	**0.83**
AT1G49630	ATPREP2_PREP2__presequence protease 2	**0.72**	-0.34	-0.30
AT1G49780	PUB26__plant U-box 26	0.41	-0.09	**1.05**
AT1G49880	Erv1/Alr family protein	-0.03	-0.54	**-0.86**
AT1G49980	DNA/RNA polymerases superfamily protein	-0.37	0.38	**0.79**
AT1G50280	Phototropic-responsive NPH3 family protein	0.14	-0.34	**-0.71**

AGI identifier	Gene annotation	30 min	2h	8h
AT1G50640	ATERF3_ERF3_ethylene responsive element binding factor 3	-0.08	-0.06	**-0.83**
AT1G50920	Nucleolar GTP-binding protein	-0.21	0.30	**0.76**
AT1G51402	unknown protein	0.25	-0.40	**-0.98**
AT1G51630	O-fucosyltransferase family protein	-0.03	0.21	**0.78**
AT1G51980	Insulinase (Peptidase family M16) protein	0.19	0.69	**0.94**
AT1G52060	Mannose-binding lectin superfamily protein	**0.98**	-0.04	**0.90**
AT1G52220	unknown protein	**0.74**	-0.34	-0.40
AT1G52380	NUP50 (Nucleoporin 50 kDa) protein	-0.20	0.14	**1.01**
AT1G52580	ATRBL5_RBL5__RHOMBOID-like protein 5	0.31	-0.10	**-1.10**
AT1G52620	Pentatricopeptide repeat (PPR) superfamily protein	**0.84**	0.15	0.38
AT1G52730	Transducin family protein / WD-40 repeat family protein	-0.15	**-0.89**	**-1.33**
AT1G52970	DD11__downregulated in DIF1 11	-0.27	0.43	**0.80**
AT1G53010	RING/U-box superfamily protein	-0.02	0.46	**0.74**
AT1G53040	Protein of unknown function (DUF616)	0.03	**-1.08**	**-1.15**
AT1G53240	mMDH1__Lactate/malate dehydrogenase family protein	-0.23	0.56	**0.85**
AT1G53310	ATPEPC1_ATPPC1_PEPC1_PPC1__phosphoenolpyruvate carboxylase 1	0.15	**0.75**	**1.45**
AT1G53320	AtTLP7_TLP7__tubby like protein 7	0.18	-0.07	**-0.72**
AT1G53380	Plant protein of unknown function (DUF641)	-0.26	-0.04	**0.75**
AT1G53480	MTO 1 RESPONDING DOWN 1	-0.11	0.13	**0.74**
AT1G53500	ATMUM4_ATRHM2_MUM4_RHM2__NAD-dependent epimerase/dehydratase family protein	-0.08	0.31	**0.87**
AT1G53560	Ribosomal protein L18ae family	0.35	-0.16	**-0.97**
AT1G53580	ETHE1_GLX2-3_GLY3__glyoxalase II 3	0.42	-0.19	**-1.17**
AT1G53645	hydroxyproline-rich glycoprotein family protein	-0.36	0.17	**0.96**
AT1G53670	ATMSRB1_MSRB1__methionine sulfoxide reductase B 1	0.13	0.05	**-0.87**
AT1G53890	Protein of unknown function (DUF567)	-0.08	**-0.82**	x
AT1G54000	GDSL-like Lipase/Acylhydrolase superfamily protein	0.27	0.27	**1.07**
AT1G54010	GDSL-like Lipase/Acylhydrolase superfamily protein	0.09	0.41	**0.91**
AT1G54030	MVP1__GDSL-like Lipase/Acylhydrolase superfamily protein	0.03	0.29	**1.11**
AT1G54100	ALDH7B4__aldehyde dehydrogenase 7B4	0.48	-0.31	**-1.24**
AT1G54210	APG12_ATATG12_ATG12A__Ubiquitin-like superfamily protein	-0.09	**-0.75**	**-1.19**
AT1G54270	EIF4A-2__eif4a-2	**0.66**	0.71	0.39
AT1G54630	ACP3__acyl carrier protein 3	-0.28	0.15	**0.89**
AT1G54740	Protein of unknown function (DUF3049)	**-0.76**	**-2.16**	**-0.87**
AT1G54780	TLP18.3__thylakoid lumen 18.3 kDa protein	0.01	-0.03	**-1.14**
AT1G55050	unknown protein	-0.07	**-1.12**	**-1.19**
AT1G55090	carbon-nitrogen hydrolase family protein	**-0.68**	-0.13	-0.50
AT1G55180	PLDALPHA4_PLDEPSILON__phospholipase D alpha 4	x	0.40	**1.28**
AT1G55190	PRA1.F2_PRA7__PRA1 (Prenylated rab acceptor) family protein	0.03	0.31	**0.76**
AT1G55210	Disease resistance-responsive (dirigent-like protein) family protein	0.19	0.72	**0.94**
AT1G55510	BCDH BETA1__branched-chain alpha-keto acid decarboxylase E1 beta subunit	0.30	**-0.79**	**-1.95**

AGI identifier	Gene annotation	30 min	2h	8h
AT1G55850	ATCSLE1_CSLE1__cellulose synthase like E1	0.09	-0.29	**-1.09**
AT1G55890	Tetratricopeptide repeat (TPR)-like superfamily protein	-0.24	0.44	**0.80**
AT1G55900	emb1860_TIM50__Haloacid dehalogenase-like hydrolase (HAD) superfamily protein	0.16	0.48	**0.83**
AT1G55910	ZIP11__zinc transporter 11 precursor	0.51	**0.86**	0.11
AT1G56000	FAD/NAD(P)-binding oxidoreductase family protein	-0.07	-0.54	**-0.96**
AT1G56010	anac021_ANAC022_NAC1_NAC domain containing protein 1	-0.05	-0.26	**-0.80**
AT1G56070	LOS1__Ribosomal protein S5/Elongation factor G/III/V family protein	-0.30	0.45	**0.81**
AT1G56110	NOP56__homolog of nucleolar protein NOP56	-0.43	0.65	**1.32**
AT1G56200	emb1303__embryo defective 1303	-0.24	-0.56	**-0.90**
AT1G56220	Dormancy/auxin associated family protein	0.31	**-1.08**	**-1.54**
AT1G56280	ATDI19_DI19__drought-induced 19	0.20	-0.37	**-1.29**
AT1G56330	ATSAR1_ATSAR1B_ATSARA1B_SAR1_SAR1B__secretion-associated RAS 1B	0.13	0.12	**0.93**
AT1G56580	SVB__Protein of unknown function, DUF538	-0.02	0.62	**0.96**
AT1G56650	ATMYB75_MYB75_PAP1_SIAA1__production of anthocyanin pigment 1	-0.03	0.62	**1.27**
AT1G56700	Peptidase C15, pyroglutamyl peptidase I-like	-0.25	-0.57	**-1.27**
AT1G57590	Pectinacetylesterase family protein	-0.05	**0.86**	**0.75**
AT1G57770	FAD/NAD(P)-binding oxidoreductase family protein	0.05	-0.46	**-0.80**
AT1G57990	ATPUP18_PUP18__purine permease 18	0.27	**-0.90**	-0.67
AT1G58180	ATBCA6_BCA6__beta carbonic anhydrase 6	-0.53	**-1.53**	**-1.68**
AT1G58190	AtRLP9_RLP9__receptor like protein 9	0.18	**-1.10**	**-1.38**
AT1G58210	EMB1674__kinase interacting family protein	0.20	0.19	**1.79**
AT1G58235	unknown protein	0.00	0.09	**-0.83**
AT1G58430	RXF26__GDSL-like Lipase/Acylhydrolase family protein	-0.08	0.11	**0.87**
AT1G59840	CCB4__cofactor assembly of complex C	-0.19	-0.08	**0.97**
AT1G60140	ATTPS10_TPS10_TPS10__trehalose phosphate synthase	-0.12	**-1.08**	**-0.88**
AT1G60750	NAD(P)-linked oxidoreductase superfamily protein	-0.02	0.06	**-0.74**
AT1G60770	Tetratricopeptide repeat (TPR)-like superfamily protein	0.06	0.42	**1.00**
AT1G60940	SNRK2-10_SNRK2.10_SRK2B__SNF1-related protein kinase 2.10	0.08	-0.42	**-0.71**
AT1G61580	ARP2_RPL3B__R-protein L3 B	-0.43	0.30	**1.36**
AT1G61630	ATENT7_ENT7__equilibrative nucleoside transporter 7	0.49	0.26	**-0.77**
AT1G61670	Lung seven transmembrane receptor family protein	-0.35	-0.30	**-0.75**
AT1G61820	BGLU46__beta glucosidase 46	-0.12	-0.64	**-0.76**
AT1G61900	unknown protein	-0.12	**-0.88**	-0.67
AT1G62130	AAA-type ATPase family protein	-0.08	**0.77**	**1.16**
AT1G62310	transcription factor jumonji (jmjC) domain-containing protein	x	-0.17	**-0.73**
AT1G62422	unknown protein	0.02	**0.90**	**1.03**
AT1G62660	Glycosyl hydrolases family 32 protein	0.39	-0.65	**-0.73**
AT1G62690	unknown protein	**0.83**	-0.08	**-0.75**

AGI identifier	Gene annotation	30 min	2h	8h
AT1G62960	ACS10__ACC synthase 10	-0.06	-0.11	**-0.98**
AT1G63660	GMP synthase (glutamine-hydrolyzing), putative / glutamine amidotransferase, putative	-0.15	0.31	**0.93**
AT1G64090	RTNLB3__Reticulan like protein B3	-0.02	0.23	**0.73**
AT1G64170	ATCHX16_CHX16__cation/H+ exchanger 16	0.11	0.33	**0.75**
AT1G64190	6-phosphogluconate dehydrogenase family protein	-0.13	0.52	**0.85**
AT1G64230	UBC28__ubiquitin-conjugating enzyme 28	0.17	-0.61	**-1.08**
AT1G64350	SEH1H__Transducin/WD40 repeat-like superfamily protein	-0.03	0.28	**0.77**
AT1G64355	unknown protein	0.59	-0.03	**-1.25**
AT1G64385	unknown protein	0.02	**1.08**	**0.87**
AT1G64640	AtENODL8_ENODL8__early nodulin-like protein 8	**0.90**	0.35	0.49
AT1G64740	TUA1__alpha-1 tubulin	-0.07	0.28	**1.02**
AT1G64760	O-Glycosyl hydrolases family 17 protein	-0.22	0.00	**0.78**
AT1G64900	CYP89_CYP89A2__cytochrome P450, family 89, subfamily A, polypeptide 2	0.33	**0.96**	**0.82**
AT1G65040	HOMOLOG OF YEAST HRD1	0.04	**0.95**	**1.31**
AT1G65130	Ubiquitin carboxyl-terminal hydrolase-related protein	0.08	**-1.04**	**-1.81**
AT1G65250	Protein kinase superfamily protein	0.20	-0.12	**-0.71**
AT1G65260	PTAC4_VIPP1__plastid transcriptionally active 4	-0.05	-0.42	**-0.72**
AT1G65410	ATNAP11_NAP11_TGD3__non-intrinsic ABC protein 11	0.23	-0.52	**-0.84**
AT1G65510	unknown protein	0.51	-0.32	**-0.95**
AT1G65840	ATPAO4_PAO4__polyamine oxidase 4	-0.03	**0.76**	**1.54**
AT1G65845	unknown protein	0.15	-0.28	**-0.91**
AT1G65960	GAD2__glutamate decarboxylase 2	**0.75**	0.07	0.39
AT1G66150	TMK1__transmembrane kinase 1	-0.08	**-0.90**	-0.34
AT1G66180	Eukaryotic aspartyl protease family protein	-0.26	-0.50	**-0.76**
AT1G66200	ATGSR2_GSR2__glutamine synthase clone F11	-0.01	-0.18	**1.59**
AT1G66330	senescence-associated family protein	**0.71**	-0.61	**-0.79**
AT1G66390	ATMYB90_MYB90_PAP2__myb domain protein 90	0.15	0.74	**1.48**
AT1G66430	pfkB-like carbohydrate kinase family protein	-0.26	0.15	**0.81**
AT1G66530	Arginyl-tRNA synthetase, class Ic	-0.30	-0.66	**-0.81**
AT1G66670	CLPP3_NCLPP3__CLP protease proteolytic subunit 3	-0.15	-0.06	**-0.83**
AT1G66760	MATE efflux family protein	0.29	0.02	**-1.36**
AT1G66940	protein kinase-related	-0.54	0.15	**0.77**
AT1G67020	unknown protein	-0.06	0.28	**-0.72**
AT1G67070	DIN9_PMI2__Mannose-6-phosphate isomerase, type I	0.27	-0.52	**-0.95**
AT1G67300	Major facilitator superfamily protein	0.09	**0.98**	0.38
AT1G67350	unknown protein	0.16	0.39	**0.93**
AT1G67440	emb1688__Minichromosome maintenance (MCM2/3/5) family protein	0.06	-0.19	**-1.28**
AT1G67500	ATREV3_REV3__recovery protein 3	-0.51	x	**-1.76**
AT1G67530	ARM repeat superfamily protein	0.09	-0.56	**-1.10**
AT1G67570	Protein of unknown function (DUF3537)	0.00	**-0.99**	0.02

AGI identifier	Gene annotation	30 min	2h	8h
AT1G67800	Copine (Calcium-dependent phospholipid-binding protein) family	-0.21	**-1.24**	**-1.21**
AT1G67860	unknown protein	-0.03	**0.82**	**1.92**
AT1G67870	glycine-rich protein	0.10	-0.64	**-1.13**
AT1G67920	unknown protein	0.10	**0.76**	0.66
AT1G67940	ATNAP3_AtSTAR1_NAP3_NAP3_non-intrinsic ABC protein 3	0.12	0.21	**0.97**
AT1G67980	CCOAMT__caffeoyl-CoA 3-O-methyltransferase	-0.20	-0.10	**-1.40**
AT1G68010	ATHPR1_HPR__hydroxypyruvate reductase	0.13	-0.28	**-1.25**
AT1G68420	Class II aaRS and biotin synthetases superfamily protein	0.06	0.05	**0.72**
AT1G68440	unknown protein	-0.32	**-1.19**	**-1.16**
AT1G68550	Integrase-type DNA-binding superfamily protein	x	0.71	**0.81**
AT1G68560	ATXYL1_TRG1_XYL1__alpha-xylosidase 1	-0.10	0.24	**0.84**
AT1G68620	alpha/beta-Hydrolases superfamily protein	x	0.13	**-1.29**
AT1G69070	unknown protein	**-0.68**	0.35	0.59
AT1G69170	Squamosa promoter-binding protein-like (SBP domain) transcription factor family protein	-0.61	-0.31	**-1.00**
AT1G69430	unknown protein	-0.09	-0.22	**-0.77**
AT1G69440	AGO7_ZIP__Argonaute family protein	0.12	-0.54	**-0.99**
AT1G69500	CYP704B1__cytochrome P450, family 704, subfamily B, polypeptide 1	0.12	**0.74**	**1.13**
AT1G69526	S-adenosyl-L-methionine-dependent methyltransferases superfamily protein	0.03	**-0.91**	**-1.40**
AT1G69570	Dof-type zinc finger DNA-binding family protein	-0.19	0.14	**0.73**
AT1G69600	ATHB29_ZFHD1__zinc finger homeodomain 1	0.00	0.53	**1.03**
AT1G69620	RPL34__ribosomal protein L34	-0.29	0.08	**0.78**
AT1G69740	HEMB1__Aldolase superfamily protein	**0.70**	-0.02	x
AT1G69860	Major facilitator superfamily protein	-0.09	**-0.85**	-0.58
AT1G69890	Protein of unknown function (DUF569)	0.21	0.25	**0.72**
AT1G70130	Concanavalin A-like lectin protein kinase family protein	-0.18	-0.06	**0.79**
AT1G70230	TBL27__TRICHOME BIREFRINGENCE-LIKE 27	-0.16	**0.86**	**0.86**
AT1G70290	ATTPS8_ATTPSC_TPS8__trehalose-6-phosphatase synthase S8	**-0.72**	**-1.96**	**-1.28**
AT1G70420	Protein of unknown function (DUF1645)	0.16	-0.56	**-0.77**
AT1G70490	ARFA1D_ATARFA1D__Ras-related small GTP-binding family protein	-0.11	0.18	**0.77**
AT1G70530	CRK3__cysteine-rich RLK (RECEPTOR-like protein kinase) 3	0.05	-0.70	**-0.81**
AT1G70660	MMZ2_UEV1B__MMS ZWEI homologue 2	x	-0.50	**-0.97**
AT1G70700	JAZ9_TIFY7__TIFY domain/Divergent CCT motif family protein	x	0.24	**-1.38**
AT1G70770	Protein of unknown function DUF2359, transmembrane	0.17	0.30	**0.94**
AT1G70820	phosphoglucomutase, putative / glucose phosphomutase, putative	x	**-0.85**	**-1.09**
AT1G70900	unknown protein	0.03	0.55	**0.85**
AT1G70980	SYNC3__Class II aminoacyl-tRNA and biotin synthetases superfamily protein	-0.30	0.31	**0.80**
AT1G71030	ATMYBL2_MYBL2__MYB-like 2	-0.39	**-2.33**	**-1.91**
AT1G71500	Rieske (2Fe-2S) domain-containing protein	-0.18	-0.30	**-1.19**

AGI identifier	Gene annotation	30 min	2h	8h
AT1G71520	encodes a member of the DREB subfamily A-5 of ERF/AP2 transcription factor family	0.29	0.00	**-1.28**
AT1G71695	Peroxidase superfamily protein	**0.87**	0.07	0.04
AT1G71980	Protease-associated (PA) RING/U-box zinc finger family protein	-0.11	-0.68	**-0.81**
AT1G72040	P-loop containing nucleoside triphosphate hydrolases superfamily protein	-0.15	0.36	**0.90**
AT1G72060	serine-type endopeptidase inhibitors	0.10	-0.64	**-1.76**
AT1G72090	Methylthiotransferase	-0.41	0.27	**0.84**
AT1G72150	PATL1__PATELLIN 1	**0.73**	**-1.11**	**-1.44**
AT1G72340	NagB/RpiA/CoA transferase-like superfamily protein	0.24	0.06	**0.75**
AT1G72450	JAZ6_TIFY11B__jasmonate-zim-domain protein 6	-0.36	**0.76**	0.23
AT1G72490	unknown protein	0.02	-0.16	**-0.84**
AT1G72520	PLAT/LH2 domain-containing lipoxygenase family protein	0.01	**0.81**	0.18
AT1G72680	ATCAD1_CAD1__cinnamyl-alcohol dehydrogenase	0.22	**-0.97**	**-1.33**
AT1G72730	DEA(D/H)-box RNA helicase family protein	-0.22	0.28	**0.97**
AT1G72800	RNA-binding (RRM/RBD/RNP motifs) family protein	-0.22	**0.94**	0.17
AT1G73010	ATPS2_PS2__phosphate starvation-induced gene 2	0.08	**1.15**	0.70
AT1G73120	unknown protein	0.13	-0.38	**-0.87**
AT1G73220	1-Oct_AtOCT1__organic cation/carnitine transporter1	-0.38	0.44	**0.80**
AT1G73490	RNA-binding (RRM/RBD/RNP motifs) family protein	**-0.68**	0.39	0.38
AT1G73500	ATMKK9_MKK9__MAP kinase kinase 9	-0.32	-0.51	**-0.96**
AT1G73600	S-adenosyl-L-methionine-dependent methyltransferases superfamily protein	-0.21	**0.78**	**1.36**
AT1G73620	Pathogenesis-related thaumatin superfamily protein	0.08	0.30	**0.79**
AT1G73650	Protein of unknown function (DUF1295)	0.03	-0.19	**-0.72**
AT1G73655	FKBP-like peptidyl-prolyl cis-trans isomerase family protein	0.20	-0.36	**-0.78**
AT1G73885	unknown protein	0.07	0.03	**-1.01**
AT1G73920	alpha/beta-Hydrolases superfamily protein	-0.27	**-1.10**	**-1.29**
AT1G73940	unknown protein	-0.11	0.32	**0.88**
AT1G74010	Calcium-dependent phosphotriesterase superfamily protein	0.13	0.51	**0.98**
AT1G74030	ENO1__enolase 1	-0.12	0.18	**1.56**
AT1G74100	ATSOT16_ATST5A_CORI-7_SOT16__sulfotransferase 16	0.08	**1.11**	**0.86**
AT1G74260	PUR4__purine biosynthesis 4	-0.44	0.38	**0.95**
AT1G74270	Ribosomal protein L35Ae family protein	0.00	0.40	**0.90**
AT1G74460	GDSL-like Lipase/Acylhydrolase superfamily protein	0.20	0.38	**1.13**
AT1G74560	NRP1__NAP1-related protein 1	-0.06	0.26	**1.00**
AT1G74840	Homeodomain-like superfamily protein	0.09	**-0.91**	-0.42
AT1G74900	OTP43__Pentatricopeptide repeat (PPR) superfamily protein	-0.14	**-0.87**	**-0.79**
AT1G75040	PR-5_PR5__pathogenesis-related gene 5	0.08	**0.80**	**0.83**
AT1G75220	Major facilitator superfamily protein	-0.31	**-1.30**	**-1.38**
AT1G75290	NAD(P)-binding Rossmann-fold superfamily protein	-0.04	0.16	**-0.72**
AT1G75380	ATBBD1_BBD1__bifunctional nuclease in basal defense response 1	-0.26	**-1.88**	**-1.14**
AT1G75500	WAT1__Walls Are Thin 1	0.12	0.11	**0.76**
AT1G75670	DNA-directed RNA polymerases	0.09	**0.75**	**0.83**

AGI identifier	Gene annotation	30 min	2h	8h
AT1G75690	DnaJ/Hsp40 cysteine-rich domain superfamily protein	-0.10	-0.15	**-1.13**
AT1G75750	GASA1__GAST1 protein homolog 1	0.24	**-0.93**	**-1.58**
AT1G75830	LCR67_PDF1.1__low-molecular-weight cysteine-rich 67	-0.26	-0.29	**-1.06**
AT1G76070	unknown protein	0.19	-0.14	**-0.83**
AT1G76080	ATCDSP32_CDSP32__chloroplastic drought-induced stress protein of 32 kD	0.07	-0.41	**-1.03**
AT1G76150	ATECH2_ECH2__enoyl-CoA hydratase 2	0.27	-0.38	**-0.74**
AT1G76160	sks5__SKU5 similar 5	-0.28	**-0.85**	0.56
AT1G76180	ERD14__Dehydrin family protein	**0.97**	-0.05	**-1.27**
AT1G76400	Ribophorin I	-0.01	0.54	**0.74**
AT1G76490	HMG1_HMGR1__hydroxy methylglutaryl CoA reductase 1	-0.13	-0.48	**-0.79**
AT1G76590	PLATZ transcription factor family protein	-0.14	**-1.06**	**-1.09**
AT1G76600	unknown protein	-0.21	**-0.98**	**-1.37**
AT1G76670	Nucleotide-sugar transporter family protein	-0.02	-0.10	**0.90**
AT1G76680	ATOPR1_OPR1__12-oxophytodienoate reductase 1	0.03	-0.57	**-0.97**
AT1G76720	eukaryotic translation initiation factor 2 (eIF-2) family protein	**-0.68**	0.10	-0.04
AT1G76790	O-methyltransferase family protein	-0.13	0.38	**1.57**
AT1G76825	obsolete and replaced by AT1G76820 on 2009-04-27	**-1.44**	0.33	-0.19
AT1G76960	unknown protein	0.40	**0.82**	**1.17**
AT1G76980	unknown protein	0.43	**0.74**	-0.36
AT1G77210	AtSTP14_STP14__sugar transporter 14	-0.15	**-1.36**	**-1.46**
AT1G77510	ATPDI6_ATPDIL1-2_PDI6_PDIL1-2__PDI-like 1-2	-0.02	0.42	**1.08**
AT1G77750	Ribosomal protein S13/S18 family	0.08	0.22	**0.83**
AT1G77760	GNR1_NIA1_NR1__nitrate reductase 1	-0.29	-0.14	**-1.30**
AT1G77940	Ribosomal protein L7Ae/L30e/S12e/Gadd45 family protein	-0.14	0.49	**0.72**
AT1G78290	SNRK2-8_SNRK2.8_SRK2C__Protein kinase superfamily protein	-0.08	**-0.76**	-0.26
AT1G78370	ATGSTU20_GSTU20__glutathione S-transferase TAU 20	0.05	0.53	**1.11**
AT1G78460	SOUL heme-binding family protein	0.18	-0.63	**-1.23**
AT1G78490	CYP708A3__cytochrome P450, family 708, subfamily A, polypeptide 3	-0.36	0.26	**0.93**
AT1G78570	ATRHM1_RHM1_ROL1__rhamnose biosynthesis 1	0.13	0.69	**1.61**
AT1G78680	ATGGH2_GGH2__gamma-glutamyl hydrolase 2	0.21	**0.96**	0.42
AT1G78820	D-mannose binding lectin protein with Apple-like carbohydrate-binding domain	0.08	**-1.19**	**-1.47**
AT1G78830	Curculin-like (mannose-binding) lectin family protein	0.02	**-1.60**	**-1.59**
AT1G79040	PSBR__photosystem II subunit R	0.08	-0.05	**-0.79**
AT1G79150	binding	-0.05	0.36	**1.23**
AT1G79245	pseudogene	**-1.04**	0.14	-0.03
AT1G79390	unknown protein	0.25	0.31	**1.02**
AT1G79470	Aldolase-type TIM barrel family protein	-0.22	0.50	**1.33**
AT1G79530	GAPCP-1__glyceraldehyde-3-phosphate dehydrogenase of plastid 1	-0.07	0.24	**1.52**
AT1G79550	PGK__phosphoglycerate kinase	0.06	0.59	**1.05**
AT1G79600	Protein kinase superfamily protein	0.31	-0.20	**-0.78**
AT1G79920	Heat shock protein 70 (Hsp 70) family protein	-0.46	0.47	**0.81**
AT1G79930	HSP91__heat shock protein 91	-0.11	0.21	**0.78**

AGI identifier	Gene annotation	30 min	2h	8h
AT1G80070	EMB14_EMB177_EMB33_SUS2__Pre-mRNA-processing-splicing factor	**-0.84**	0.07	0.46
AT1G80130	Tetratricopeptide repeat (TPR)-like superfamily protein	-0.02	0.47	**1.06**
AT1G80160	Lactoylglutathione lyase / glyoxalase I family protein	-0.06	-0.45	**-1.57**
AT1G80180	unknown protein	0.49	-0.71	**-1.22**
AT1G80280	alpha/beta-Hydrolases superfamily protein	**-0.70**	0.20	0.05
AT1G80380	P-loop containing nucleoside triphosphate hydrolases superfamily protein	**0.70**	**-0.78**	**-1.59**
AT1G80440	Galactose oxidase/kelch repeat superfamily protein	-0.14	**-2.70**	**-2.51**
AT1G80460	GLI1_NHO1__Actin-like ATPase superfamily protein	0.19	-0.58	**-0.75**
AT1G80530	Major facilitator superfamily protein	0.10	0.69	**1.24**
AT1G80560	ATIMD2_IMD2__isopropylmalate dehydrogenase 2	-0.11	0.22	**0.72**
AT1G80750	Ribosomal protein L30/L7 family protein	0.11	**0.83**	**1.00**
AT1G80800	pseudogene	**-0.72**	-0.10	-0.25
AT1G80920	J8__Chaperone DnaJ-domain superfamily protein	-0.60	**-2.95**	**-1.98**
AT2E04300	EUGENE prediction	-0.08	0.62	**1.01**
AT2E05040	EUGENE prediction	**-1.14**	0.47	-0.37
AT2E07670	EUGENE prediction	-0.17	-0.15	**-0.98**
AT2E07770	EUGENE prediction	0.05	-0.10	**-0.77**
AT2G01140	Aldolase superfamily protein	0.15	0.35	**1.07**
AT2G01250	Ribosomal protein L30/L7 family protein	-0.18	0.30	**0.90**
AT2G01490	phytanoyl-CoA dioxygenase (PhyH) family protein	0.16	-0.15	**-0.74**
AT2G01540	Calcium-dependent lipid-binding (CaLB domain) family protein	-0.02	-0.14	**-0.77**
AT2G01620	MEE11__RNI-like superfamily protein	0.16	0.11	**-0.77**
AT2G01850	ATXTH27_EXGT-A3_XTH27__endoxyloglucan transferase A3	-0.47	**-1.38**	-0.49
AT2G01860	EMB975__Tetratricopeptide repeat (TPR)-like superfamily protein	0.11	-0.62	**-0.83**
AT2G02010	GAD4__glutamate decarboxylase 4	**0.67**	0.16	0.58
AT2G02180	TOM3__tobamovirus multiplication protein 3	0.25	-0.73	**-1.36**
AT2G02710	PLP_PLPA_PLPB_PLPC__PAS/LOV protein B	0.09	**-1.93**	**-1.67**
AT2G02750	Pentatricopeptide repeat (PPR) superfamily protein	-0.09	0.32	**0.92**
AT2G02800	APK2B__protein kinase 2B	-0.24	-0.13	**-0.76**
AT2G02950	PKS1__phytochrome kinase substrate 1	-0.04	**-0.77**	-0.42
AT2G02990	ATRNS1_RNS1__ribonuclease 1	-0.13	**1.00**	**1.43**
AT2G03090	ATEXP15_ATEXPA15_ATHEXP ALPHA 1.3_EXP15_EXPA15__expansin A15	-0.34	0.56	**2.23**
AT2G03480	QUL2__QUASIMODO2 LIKE 2	-0.21	0.19	**0.82**
AT2G03505	glycosyl hydrolase family protein 17	0.12	0.11	**0.71**
AT2G03730	ACR5__ACT domain repeat 5	-0.12	**-0.81**	-0.25
AT2G03760	AtSOT1_AtSOT12_ATST1_RAR047_SOT12_ST_ST1__sulphotransferase 12	0.03	0.28	**1.06**
AT2G04030	AtHsp90.5_CR88_EMB1956_Hsp88.1_HSP90.5__Chaperone protein htpG family protein	-0.60	0.30	**0.79**
AT2G04050	MATE efflux family protein	-0.02	0.20	**0.89**
AT2G04160	AIR3__Subtilisin-like serine endopeptidase family protein	0.05	0.43	**1.13**

AGI identifier	Gene annotation	30 min	2h	8h
AT2G04390	Ribosomal S17 family protein	0.13	0.61	**0.92**
AT2G04690	Pyridoxamine 5'-phosphate oxidase family protein	0.11	-0.55	**-0.72**
AT2G04780	FLA7__FASCICLIN-like arabinoogalactan 7	0.11	0.23	**1.12**
AT2G04795	unknown protein	-0.04	**-0.98**	x
AT2G05140	phosphoribosylaminoimidazole carboxylase family protein / AIR carboxylase family protein	0.05	0.14	**1.07**
AT2G05220	Ribosomal S17 family protein	-0.27	0.54	**0.81**
AT2G05380	GRP3S__glycine-rich protein 3 short isoform	0.36	-0.42	**-1.09**
AT2G05510	Glycine-rich protein family	-0.12	-0.37	**-0.73**
AT2G05520	ATGRP-3_ATGRP3_GRP-3_GRP3__glycine-rich protein 3	**1.22**	-0.72	**-1.26**
AT2G05530	Glycine-rich protein family	**0.68**	-0.67	**-1.14**
AT2G05540	Glycine-rich protein family	0.16	**-1.96**	**-2.66**
AT2G05620	PGR5__proton gradient regulation 5	0.25	0.09	**-0.96**
AT2G05920	Subtilase family protein	-0.56	0.17	**1.33**
AT2G05990	ENR1_MOD1__NAD(P)-binding Rossmann-fold superfamily protein	-0.33	0.35	**0.90**
AT2G06025	GCN5-related N-acetyltransferase (GNAT) family protein	-0.12	**-0.96**	**-0.96**
AT2G06050	DDE1_OPR3__oxophytodienoate-reductase 3	**0.72**	0.61	x
AT2G06850	EXGT-A1_EXT_XTH4__xyloglucan endotransglucosylase/hydrolase 4	-0.40	**-1.32**	-0.20
AT2G07600	pseudogene	x	x	**-1.82**
AT2G07688	pseudogene	-0.17	x	**-0.73**
AT2G07689	NADH-ubiquinone oxidoreductase, putative	**-1.28**	-0.11	-0.05
AT2G07732	Ribulose bisphosphate carboxylase large chain, catalytic domain	**-0.67**	x	-0.28
AT2G12462	unknown protein	0.13	-0.02	**0.76**
AT2G13360	AGT_AGT1_SGAT__alanine:glyoxylate aminotransferase	-0.36	-0.47	**-2.17**
AT2G13820	Bifunctional inhibitor/lipid-transfer protein/seed storage 2S albumin superfamily protein	0.14	0.51	**1.30**
AT2G14080	Disease resistance protein (TIR-NBS-LRR class) family	**-0.73**	**-0.77**	-0.52
AT2G14750	AKN1_APK_APK1_ATAKN1__APS kinase	-0.30	**0.82**	**0.79**
AT2G14820	NAKED PINS IN YUC MUTANTS 2, NPY2	0.64	-0.18	**-0.77**
AT2G14860	Peroxisomal membrane 22 kDa (Mpv17/PMP22) family protein	0.07	**0.86**	0.69
AT2G14890	AGP9__arabinogalactan protein 9	-0.10	0.04	**1.25**
AT2G14910	unknown protein	0.18	-0.12	**-0.89**
AT2G15020	unknown protein	**0.69**	-0.29	-0.12
AT2G15050	LTP_LTP7__lipid transfer protein	0.42	**0.77**	0.55
AT2G15090	KCS8__3-ketoacyl-CoA synthase 8	-0.21	**-0.75**	0.24
AT2G15490	UGT73B4__UDP-glycosyltransferase 73B4	0.22	-0.17	**-0.92**
AT2G15620	ATHNIR_NIR_NIR1__nitrite reductase 1	-0.08	**1.01**	**1.34**
AT2G15695	Protein of unknown function DUF829, transmembrane 53	-0.03	-0.36	**-1.05**
AT2G15890	MEE14__maternal effect embryo arrest 14	0.29	**-1.74**	**-1.51**
AT2G15960	unknown protein	-0.37	**-2.69**	**-2.44**
AT2G16280	KCS9__3-ketoacyl-CoA synthase 9	0.45	**-0.80**	-0.12
AT2G16340	unknown protein	0.29	0.07	**0.71**
AT2G16430	ATPAP10_PAP10__purple acid phosphatase 10	0.10	**0.78**	**1.24**
AT2G16586	unknown protein	-0.35	-0.28	**-0.73**

AGI identifier	Gene annotation	30 min	2h	8h
AT2G16600	ROC3__rotamase CYP 3	-0.01	0.23	**0.77**
AT2G16660	Major facilitator superfamily protein	0.31	**0.77**	**1.54**
AT2G17033	pentatricopeptide (PPR) repeat-containing protein	-0.01	-0.52	**-0.83**
AT2G17230	EXL5__EXORDIUM like 5	**-0.83**	-0.15	x
AT2G17250	EMB2762__CCAAT-binding factor	0.03	0.32	**0.71**
AT2G17350	unknown protein	0.23	-0.15	**-0.72**
AT2G17360	Ribosomal protein S4 (RPS4A) family protein	0.03	0.46	**1.07**
AT2G17450	RHA3A__RING-H2 finger A3A	0.22	-0.51	**-0.88**
AT2G17500	Auxin efflux carrier family protein	0.29	0.18	**-0.85**
AT2G17630	Pyridoxal phosphate (PLP)-dependent transferases superfamily protein	-0.02	0.37	**1.27**
AT2G17670	Tetratricopeptide repeat (TPR)-like superfamily protein	0.05	0.37	**0.84**
AT2G17720	2-oxoglutarate (2OG) and Fe(II)-dependent oxygenase superfamily protein	0.38	0.34	**0.72**
AT2G17880	Chaperone DnaJ-domain superfamily protein	-0.25	**-1.10**	x
AT2G18110	Translation elongation factor EF1B/ribosomal protein S6 family protein	-0.01	0.40	**0.76**
AT2G18290	APC10__anaphase promoting complex 10	0.12	-0.45	**-0.94**
AT2G18420	Gibberellin-regulated family protein	0.18	-0.59	**-1.74**
AT2G18690	unknown protein	0.25	-0.04	**-0.71**
AT2G18700	ATTPS11_ATTPSB_TPS11_TPS11__trehalose phosphatase/synthase 11	-0.54	**-2.44**	**-1.75**
AT2G18900	Transducin family protein / WD-40 repeat family protein	-0.39	0.63	**1.42**
AT2G18960	AHA1_HA1_OST2_PMA__H(+)-ATPase 1	-0.22	0.37	**0.92**
AT2G19350	Eukaryotic protein of unknown function (DUF872)	0.07	-0.35	**-0.78**
AT2G19385	zinc ion binding	-0.07	0.27	**0.79**
AT2G19480	NAP1;2_NFA02_NFA2__nucleosome assembly protein 1;2	0.14	0.24	**0.87**
AT2G19520	ACG1_ATMSI4_FVE_MSI4_NFC04_NFC4__Transducin family protein / WD-40 repeat family protein	-0.38	0.17	**0.72**
AT2G19540	Transducin family protein / WD-40 repeat family protein	0.08	0.53	**1.12**
AT2G19620	N-MYC downregulated-like 3 (NDL3)	**-0.73**	-0.34	0.35
AT2G19670	*ARABIDOPSIS THALIANA* PROTEIN ARGININE METHYLTRANSFERASE 1A	-0.13	0.35	**0.77**
AT2G19730	Ribosomal L28e protein family	-0.06	0.33	**0.71**
AT2G19750	Ribosomal protein S30 family protein	0.18	0.72	**1.10**
AT2G19800	MIOX2__myo-inositol oxygenase 2	-0.10	**-2.51**	**-1.33**
AT2G19860	ATHXK2 (HEXOKINASE 2)	0.14	0.45	**0.93**
AT2G20060	Ribosomal protein L4/L1 family	-0.12	0.10	**0.75**
AT2G20230	Tetraspanin family protein	0.06	-0.35	**-0.76**
AT2G20260	PSAE-2__photosystem I subunit E-2	**0.93**	0.14	-0.28
AT2G20420	ATP citrate lyase (ACL) family protein	-0.13	0.15	**0.78**
AT2G20450	Ribosomal protein L14	-0.28	0.61	**1.15**
AT2G20490	NOP10	-0.22	0.57	**1.17**
AT2G20610	ALF1_HLS3_RTY_RTY1_SUR1__Tyrosine transaminase family protein	-0.13	0.61	**0.71**
AT2G20670	Protein of unknown function (DUF506)	**-0.89**	**-1.86**	**-1.65**
AT2G20740	Tetraspanin family protein	0.03	-0.22	**-0.97**

AGI identifier	Gene annotation	30 min	2h	8h
AT2G20920	Protein of unknown function (DUF3353)	-0.10	-0.25	**-1.00**
AT2G21045	Rhodanese/Cell cycle control phosphatase superfamily protein	0.38	-0.19	**0.72**
AT2G21050	LAX2__like AUXIN RESISTANT 2	0.42	0.47	**1.00**
AT2G21300	ATP binding microtubule motor family protein	-0.26	0.17	**0.72**
AT2G21320	B-box zinc finger family protein	0.13	**0.75**	-0.08
AT2G21390	Coatomer, alpha subunit	-0.26	0.00	**0.74**
AT2G21580	Ribosomal protein S25 family protein	-0.21	0.67	**1.03**
AT2G21640	Encodes a protein of unknown function that is a marker for oxidative stress response.	-0.15	0.02	**1.30**
AT2G21660	ATGRP7_CCR2_GR-RBP7_GRP7__cold, circadian rhythm, and rna binding 2	-0.04	0.40	**0.93**
AT2G21960	unknown protein	0.06	-0.05	**-1.01**
AT2G21970	SEP2__stress enhanced protein 2	0.35	-0.46	**-1.09**
AT2G22170	Lipase/lipooxygenase, PLAT/LH2 family protein	0.00	-0.24	**0.92**
AT2G22400	S-adenosyl-L-methionine-dependent methyltransferases superfamily protein	-0.31	0.39	**0.81**
AT2G22500	ATPUMP5_DIC1_UCP5__uncoupling protein 5	**0.69**	**0.93**	0.46
AT2G22510	hydroxyproline-rich glycoprotein family protein	0.04	0.37	**0.83**
AT2G22900	Galactosyl transferase GMA12/MNN10 family protein	0.09	0.20	**0.80**
AT2G23110	Late embryogenesis abundant protein, group 6	-0.03	-0.70	**-1.53**
AT2G23120	Late embryogenesis abundant protein, group 6	0.59	-0.38	**-0.96**
AT2G23810	TET8__tetraspanin8	-0.56	**-0.76**	-0.65
AT2G24100	unknown protein	-0.07	-0.49	**-0.78**
AT2G24170	Endomembrane protein 70 protein family	-0.14	0.23	**1.03**
AT2G24550	unknown protein	-0.13	**-1.61**	**-0.96**
AT2G24590	RNA recognition motif and CCHC-type zinc finger domains containing protein	-0.09	0.42	**0.87**
AT2G24730	60S ribosomal protein L4/L1 (RPL4C), pseudogene	0.10	0.48	**1.25**
AT2G24762	AtGDU4_GDU4__glutamine dumper 4	-0.03	0.26	**0.94**
AT2G25080	ATGPX1_GPX1__glutathione peroxidase 1	**0.67**	-0.07	-0.61
AT2G25090	CIPK16_SnRK3.18__CBL-interacting protein kinase 16	-0.01	-0.42	**-0.80**
AT2G25200	Plant protein of unknown function (DUF868)	-0.47	-0.69	**-0.74**
AT2G25210	Ribosomal protein L39 family protein	-0.02	0.37	**0.96**
AT2G25450	2-oxoglutarate (2OG) and Fe(II)-dependent oxygenase superfamily protein	-0.17	**-1.25**	x
AT2G25540	CESA10__cellulose synthase 10	-0.33	-0.20	**0.74**
AT2G25625	unknown protein	0.33	0.49	**1.17**
AT2G25735	unknown protein	0.09	-0.48	**-0.82**
AT2G25900	ATCTH_ATTZF1__Zinc finger C-x8-C-x5-C-x3-H type family protein	-0.17	**-1.21**	**-0.93**
AT2G26250	FDH_KCS10__3-ketoacyl-CoA synthase 10	**0.73**	0.20	0.07
AT2G26340	unknown protein	-0.33	-0.20	**-0.74**
AT2G26500	cytochrome b6f complex subunit (petM), putative	0.09	-0.10	**-1.01**
AT2G26530	AR781__Protein of unknown function (DUF1645)	0.27	0.04	**-0.78**
AT2G26560	PLA IIA_PLA2A_PLP2_PLP2__phospholipase A 2A	0.25	-0.63	**-0.78**
AT2G26670	ATHO1_GUN2_HO1_HY1_HY6_TED4__Plant haem oxygenase (decyclizing) family protein	0.19	-0.30	**-0.85**

AGI identifier	Gene annotation	30 min	2h	8h
AT2G26740	ATSEH_SEH__soluble epoxide hydrolase	-0.13	0.05	**-0.83**
AT2G26975	unknown protein	0.28	-0.20	**-0.96**
AT2G27040	AGO4_OCP11__Argonaute family protein	-0.40	0.31	**0.72**
AT2G27050	AtEIL1_EIL1__ETHYLENE-INSENSITIVE3-like 1	0.59	-0.58	**-0.77**
AT2G27290	Protein of unknown function (DUF1279)	-0.13	-0.18	**-0.78**
AT2G27402	unknown protein	0.29	0.05	**1.43**
AT2G27420	Cysteine proteinases superfamily protein	0.36	**0.76**	0.00
AT2G27510	ATFD3_FD3__ferredoxin 3	-0.03	0.74	**1.11**
AT2G27530	PGY1__Ribosomal protein L1p/L10e family	0.36	0.55	**1.18**
AT2G27550	ATC__centroradialis	0.04	0.66	**1.67**
AT2G27710	60S acidic ribosomal protein family	-0.37	0.32	**0.87**
AT2G27830	unknown protein	-0.26	**-1.26**	**-1.52**
AT2G27840	HDA13_HDT04_HDT4__histone deacetylase-related / HD-related	-0.10	**0.96**	**1.28**
AT2G28000	CH-CPN60A_CPN60A_SLP__chaperonin-60alpha	0.30	0.63	**0.80**
AT2G28110	FRA8_IRX7__Exostosin family protein	0.03	-0.37	**-0.86**
AT2G28120	Major facilitator superfamily protein	0.08	**-1.03**	**-1.12**
AT2G28315	Nucleotide/sugar transporter family protein	0.04	-0.06	**0.76**
AT2G28460	Cysteine/Histidine-rich C1 domain family protein	**-0.66**	-0.41	0.09
AT2G28510	Dof-type zinc finger DNA-binding family protein	0.09	0.58	**1.02**
AT2G28600	P-loop containing nucleoside triphosphate hydrolases superfamily protein	0.08	0.37	**0.80**
AT2G28820	pseudogene	**-1.30**	0.28	-0.44
AT2G28900	ATOEP16-1_ATOEP16-L_OEP16_OEP16-1__outer plastid envelope protein 16-1	-0.02	**1.12**	**2.09**
AT2G28950	ATEXP6_ATEXPA6_ATHEXP ALPHA 1.8_EXPA6__expansin A6	0.15	0.19	**0.99**
AT2G29310	NAD(P)-binding Rossmann-fold superfamily protein	0.20	**-0.90**	**-1.18**
AT2G29340	NAD-dependent epimerase/dehydratase family protein	0.51	-0.37	**-1.37**
AT2G29420	ATGSTU7_GST25_GSTU7__glutathione S-transferase tau 7	0.33	-0.21	**-1.25**
AT2G29440	ATGSTU6_GST24_GSTU6__glutathione S-transferase tau 6	0.02	0.18	**-0.73**
AT2G29460	ATGSTU4_GST22_GSTU4__glutathione S-transferase tau 4	0.05	0.10	**-0.76**
AT2G29470	ATGSTU3_GST21_GSTU3__glutathione S-transferase tau 3	0.09	0.08	**-0.71**
AT2G29530	TIM10__Tim10/DDP family zinc finger protein	-0.52	0.45	**1.03**
AT2G29670	Tetratricopeptide repeat (TPR)-like superfamily protein	0.29	**0.82**	**1.42**
AT2G29720	CTF2B__FAD/NAD(P)-binding oxidoreductase family protein	0.29	0.06	**-0.98**
AT2G30040	MAPKKK14__mitogen-activated protein kinase kinase kinase 14	-0.02	**-0.78**	**-0.74**
AT2G30490	ATC4H_C4H_CYP73A5_REF3__cinnamate-4-hydroxylase	0.03	0.17	**0.96**
AT2G30520	RPT2__Phototropic-responsive NPH3 family protein	0.37	**-0.90**	**-1.09**
AT2G30600	BTB/POZ domain-containing protein	-0.16	**-0.88**	**-1.08**
AT2G30790	PSBP-2__photosystem II subunit P-2	-0.32	0.30	**0.89**
AT2G30830	2-oxoglutarate (2OG) and Fe(II)-dependent oxygenase superfamily protein	-0.47	0.20	**1.20**
AT2G30860	ATGSTF7_ATGSTF9_GLUTTR_GSTF9__glutathione S-transferase PHI 9	-0.10	0.46	**1.38**

AGI identifier	Gene annotation	30 min	2h	8h
AT2G30870	ATGSTF10_ATGSTF4_ERD13_GSTF10__glutathione S-transferase PHI 10	**0.94**	0.60	**0.83**
AT2G31010	Protein kinase superfamily protein	0.04	-0.12	**-0.85**
AT2G31140	unknown protein	-0.03	0.28	**0.73**
AT2G31370	Basic-leucine zipper (bZIP) transcription factor family protein	-0.02	0.30	**1.16**
AT2G31430	Plant invertase/pectin methylesterase inhibitor superfamily protein	0.40	0.24	**0.73**
AT2G31460	Domain of unknown function (DUF313)	0.61	x	**-1.04**
AT2G31560	unknown protein	-0.09	0.30	**0.76**
AT2G31610	Ribosomal protein S3 family protein	0.21	**0.75**	**1.55**
AT2G31660	SAD2_URM9__ARM repeat superfamily protein	-0.05	**-1.00**	**-1.50**
AT2G31780	ARI11_ATARI11__RING/U-box superfamily protein	**0.66**	0.34	**-0.86**
AT2G31810	ACT domain-containing small subunit of acetolactate synthase protein	**-0.83**	**-1.55**	**-1.17**
AT2G31860	pseudogene	0.21	-0.22	**-1.02**
AT2G31945	unknown protein	0.04	**-1.02**	**-1.88**
AT2G32060	Ribosomal protein L7Ae/L30e/S12e/Gadd45 family protein	-0.25	0.63	**1.17**
AT2G32150	Haloacid dehalogenase-like hydrolase (HAD) superfamily protein	-0.24	**-1.69**	**-1.26**
AT2G32220	Ribosomal L27e protein family	0.02	0.66	**1.01**
AT2G32690	ATGRP23_GRP23__glycine-rich protein 23	**0.90**	-0.55	0.30
AT2G32720	ATCB5-B_B5 #4_CB5-B__cytochrome B5 isoform B	-0.09	0.25	**0.93**
AT2G32800	AP4.3A__protein kinase family protein	0.06	**-0.82**	**-0.71**
AT2G32990	AtGH9B8_GH9B8__glycosyl hydrolase 9B8	0.20	0.33	**0.85**
AT2G33150	KAT2_PED1_PKT3__peroxisomal 3-ketoacyl-CoA thiolase 3	0.45	-0.22	**-0.94**
AT2G33210	HSP60-2__heat shock protein 60-2	-0.19	0.21	**1.43**
AT2G33250	unknown protein	-0.30	-0.35	**-0.87**
AT2G33830	Dormancy/auxin associated family protein	0.24	**-2.39**	**-2.08**
AT2G33840	Tyrosyl-tRNA synthetase, class Ib, bacterial/mitochondrial	0.11	0.25	**0.78**
AT2G33850	unknown protein	0.12	-0.01	**0.83**
AT2G34357	ARM repeat superfamily protein	-0.21	0.27	**0.77**
AT2G34410	REDUCED WALL ACETYLATION 3	0.01	-0.26	**-0.97**
AT2G34430	LHB1B1_LHCB1.4__light-harvesting chlorophyll-protein complex II subunit B1	0.23	-0.38	**-1.07**
AT2G34480	Ribosomal protein L18ae/LX family protein	-0.37	0.32	**1.02**
AT2G34490	CYP710A2__cytochrome P450, family 710, subfamily A, polypeptide 2	-0.05	0.72	**0.89**
AT2G34570	MEE21__PIN domain-like family protein	-0.14	0.51	**0.71**
AT2G34750	RNA polymerase I specific transcription initiation factor RRN3 protein	-0.35	0.14	**0.80**
AT2G34770	ATFAH1_FAH1__fatty acid hydroxylase 1	-0.21	**-0.87**	-0.16
AT2G34890	CTP synthase family protein	0.06	**-1.22**	-0.54
AT2G35040	AICARFT/IMPCHase bienzyme family protein	0.12	0.28	**1.06**
AT2G35120	Single hybrid motif superfamily protein	-0.09	0.23	**0.72**
AT2G35190	ATNPSN11_NPSN11_NSPN11__novel plant snare 11	-0.12	-0.15	**0.76**
AT2G35860	FLA16__FASCICLIN-like arabinogalactan protein 16 precursor	-0.19	0.40	**1.37**

AGI identifier	Gene annotation	30 min	2h	8h
AT2G36070	ATTIM44-2_TIM44-2__translocase inner membrane subunit 44-2	-0.06	0.32	**0.93**
AT2G36170	Ubiquitin supergroup;Ribosomal protein L40e	-0.04	0.50	**0.72**
AT2G36230	APG10_HISN3__Aldolase-type TIM barrel family protein	x	0.16	**0.71**
AT2G36310	URH1__uridine-ribohydrolase 1	-0.09	**-1.27**	**-0.81**
AT2G36320	A20/AN1-like zinc finger family protein	0.10	**-1.39**	**-1.43**
AT2G36390	BE3_SBE2.1__starch branching enzyme 2.1	-0.38	0.48	**0.81**
AT2G36530	ENO2_LOS2__Enolase	-0.15	0.73	**1.50**
AT2G36570	Leucine-rich repeat protein kinase family protein	-0.11	0.28	**0.78**
AT2G36590	ATPROT3_ProT3__proline transporter 3	-0.05	**1.60**	**1.41**
AT2G36620	RPL24A__ribosomal protein L24	-0.19	0.38	**1.15**
AT2G36770	UDP-Glycosyltransferase superfamily protein	0.18	**-0.90**	**-1.18**
AT2G36830	GAMMA-TIP_GAMMA-TIP1_TIP1;1__gamma tonoplast intrinsic protein	**0.82**	0.24	-0.55
AT2G36835	unknown protein	-0.11	-0.15	**-0.94**
AT2G36870	XTH32__xyloglucan endotransglucosylase/hydrolase 32	0.40	0.67	**1.10**
AT2G36880	MAT3__methionine adenosyltransferase 3	0.18	**0.92**	**1.32**
AT2G36895	unknown protein	-0.09	-0.42	**-0.96**
AT2G36950	Heavy metal transport/detoxification superfamily protein	0.16	-0.58	**-1.40**
AT2G37040	ATPAL1_PAL1__PHE ammonia lyase 1	**0.91**	0.38	0.59
AT2G37130	Peroxidase superfamily protein	x	-0.09	**-0.93**
AT2G37190	Ribosomal protein L11 family protein	0.46	0.39	**1.00**
AT2G37250	ADK_ATPADK1__adenosine kinase	x	0.59	**1.14**
AT2G37270	ATRPS5B_RPS5B__ribosomal protein 5B	-0.02	0.60	**0.91**
AT2G37400	Tetratricopeptide repeat (TPR)-like superfamily protein	-0.01	0.28	**0.73**
AT2G37540	NAD(P)-binding Rossmann-fold superfamily protein	-0.01	-0.55	**-0.77**
AT2G37550	AGD7_ASP1__ARF-GAP domain 7	0.12	-0.15	**0.71**
AT2G37600	Ribosomal protein L36e family protein	-0.08	0.29	**0.74**
AT2G37710	RLK__receptor lectin kinase	0.31	**0.80**	**0.95**
AT2G37750	unknown protein	0.07	**-0.98**	**-1.91**
AT2G37770	NAD(P)-linked oxidoreductase superfamily protein	0.00	**1.10**	0.64
AT2G37830	pseudogene	**0.66**	-0.03	x
AT2G37970	SOUL-1__SOUL heme-binding family protein	0.47	-0.26	**-1.20**
AT2G37990	ribosome biogenesis regulatory protein (RRS1) family protein	0.08	0.49	**0.86**
AT2G38170	ATCAX1_CAX1_RCI4__cation exchanger 1	-0.09	**1.44**	**1.12**
AT2G38210	PDX1L4__putative PDX1-like protein 4	0.05	0.20	**-0.85**
AT2G38240	2-oxoglutarate (2OG) and Fe(II)-dependent oxygenase superfamily protein	-0.16	**-0.90**	x
AT2G38360	PRA1.B4__prenylated RAB acceptor 1.B4	-0.17	0.50	**0.84**
AT2G38400	AGT3__alanine:glyoxylate aminotransferase 3	-0.22	**-1.11**	**-1.78**
AT2G38540	ATLTP1_LP1_LTP1__lipid transfer protein 1	0.41	**1.08**	**1.29**
AT2G38550	Transmembrane proteins 14C	-0.23	0.26	**0.92**
AT2G38700	ATMVD1_MVD1_mevalonate diphosphate decarboxylase 1	-0.01	0.11	**1.07**
AT2G38740	Haloacid dehalogenase-like hydrolase (HAD) superfamily protein	0.03	0.47	**0.71**
AT2G38750	ANNAT4__annexin 4	0.14	**1.04**	**1.12**

AGI identifier	Gene annotation	30 min	2h	8h
AT2G38820	Protein of unknown function (DUF506)	-0.07	**-1.00**	x
AT2G38870	Serine protease inhibitor, potato inhibitor I-type family protein	0.41	x	**-1.75**
AT2G38940	ATPT2_PHT1;4__phosphate transporter 1;4	0.14	**1.64**	**1.95**
AT2G39000	Acyl-CoA N-acyltransferases (NAT) superfamily protein	0.01	-0.63	**-1.27**
AT2G39130	Transmembrane amino acid transporter family protein	0.13	0.40	**0.82**
AT2G39310	JAL22__jacalin-related lectin 22	0.17	-0.20	**0.90**
AT2G39390	Ribosomal L29 family protein	-0.10	0.57	**0.87**
AT2G39400	alpha/beta-Hydrolases superfamily protein	0.28	**-1.71**	**-1.77**
AT2G39450	ATMTP11_MTP11__Cation efflux family protein	0.03	0.06	**-0.76**
AT2G39460	ATRPL23A_RPL23A_RPL23AA__ribosomal protein L23AA	0.42	0.66	**1.17**
AT2G39480	PGP6__P-glycoprotein 6	-0.18	-0.26	**-1.16**
AT2G39570	ACT domain-containing protein	-0.48	**-2.66**	**-2.01**
AT2G39580	unknown protein	**-0.90**	-0.47	-0.24
AT2G39700	ATEXPA4 (*ARABIDOPSIS THALIANA* EXPANSIN A4)	0.12	0.32	**1.11**
AT2G39730	RCA__rubisco activase	0.10	0.20	**-1.14**
AT2G39795	Mitochondrial glycoprotein family protein	-0.01	0.33	**0.74**
AT2G39820	Translation initiation factor IF6	-0.02	0.42	**0.78**
AT2G39870	unknown protein	**-0.67**	-0.05	0.13
AT2G39900	GATA type zinc finger transcription factor family protein	-0.24	0.30	**0.85**
AT2G40000	ATHSPRO2_HSPRO2__ortholog of sugar beet HS1 PRO-1 2	**0.74**	**-2.11**	**-1.12**
AT2G40010	Ribosomal protein L10 family protein	0.43	0.45	**0.80**
AT2G40360	Transducin family protein / WD-40 repeat family protein	-0.05	0.57	**1.07**
AT2G40420	Transmembrane amino acid transporter family protein	-0.04	-0.28	**-1.35**
AT2G40475	unknown protein	0.20	0.72	**1.04**
AT2G40590	Ribosomal protein S26e family protein	0.08	0.56	**0.93**
AT2G40840	DPE2__disproportionating enzyme 2	0.06	0.71	**1.53**
AT2G41090	Calcium-binding EF-hand family protein	-0.16	0.40	**0.98**
AT2G41100	ATCAL4_TCH3__Calcium-binding EF hand family protein	0.03	-0.63	**-0.81**
AT2G41220	GLU2__glutamate synthase 2	-0.35	0.25	**1.27**
AT2G41250	Haloacid dehalogenase-like hydrolase (HAD) superfamily protein	0.03	**-1.41**	-0.52
AT2G41420	proline-rich family protein	-0.29	**-0.77**	-0.62
AT2G41430	CID1_ERD15_LSR1__dehydration-induced protein (ERD15)	-0.25	**-1.18**	**-0.99**
AT2G41475	unknown protein	0.25	0.07	**0.94**
AT2G41650	unknown protein	-0.51	0.47	**1.23**
AT2G41800	Protein of unknown function, DUF642	-0.09	0.60	**1.22**
AT2G41840	Ribosomal protein S5 family protein	-0.09	0.47	**1.00**
AT2G42170	actin, putative	0.44	-0.47	**-0.89**
AT2G42395	unknown protein	0.11	0.06	**0.80**
AT2G42540	COR15_COR15A__cold-regulated 15a	0.14	**0.90**	**0.90**
AT2G42590	GF14 MU_GRF9__general regulatory factor 9	0.02	-0.29	**-0.89**
AT2G42600	ATPPC2_PPC2__phosphoenolpyruvate carboxylase 2	0.17	0.62	**0.81**
AT2G42740	RPL16A__ribosomal protein large subunit 16A	-0.24	0.44	**1.03**
AT2G42890	AML2_ML2__MEI2-like 2	-0.14	-0.36	**-0.96**
AT2G43020	ATPAO2_PAO2__polyamine oxidase 2	-0.13	0.53	**0.81**
AT2G43290	calmodulin-like MSS3.	0.63	0.47	**0.75**

AGI identifier	Gene annotation	30 min	2h	8h
AT2G43330	ATINT1_INT1__inositol transporter 1	-0.15	**-0.79**	-0.31
AT2G43360	BIO2_BIOB__Radical SAM superfamily protein	0.18	0.37	**0.93**
AT2G43460	Ribosomal L38e protein family	0.01	0.52	**0.96**
AT2G43510	ATTI1_TI1__trypsin inhibitor protein 1	-0.30	-0.22	**-1.07**
AT2G43520	ATTI2_TI2__trypsin inhibitor protein 2	-0.07	-0.29	**-0.91**
AT2G43620	Chitinase family protein	0.23	**1.45**	**1.86**
AT2G43650	EMB2777__Sas10/U3 ribonucleoprotein (Utp) family protein	-0.21	0.45	**0.77**
AT2G43820	ATSAGT1_GT_SAGT1_SGT1_UGT74F2__UDP-glucosyltransferase 74F2	0.14	**-0.92**	x
AT2G44060	Late embryogenesis abundant protein, group 2	**0.71**	-0.05	0.09
AT2G44140	Peptidase family C54 protein	0.05	-0.56	**-0.95**
AT2G44160	MTHFR2__methylenetetrahydrofolate reductase 2	-0.18	-0.04	**0.87**
AT2G44350	ATCS_CSY4__Citrate synthase family protein	x	0.19	**0.74**
AT2G44380	Cysteine/Histidine-rich C1 domain family protein	0.17	**-0.97**	**-0.86**
AT2G44500	O-fucosyltransferase family protein	**-0.89**	-0.56	0.03
AT2G44670	Protein of unknown function (DUF581)	0.01	**0.94**	x
AT2G44790	UCC2__uclacyanin 2	**0.68**	-0.19	**-1.35**
AT2G44860	Ribosomal protein L24e family protein	-0.03	0.59	**0.74**
AT2G44920	Tetratricopeptide repeat (TPR)-like superfamily protein	0.09	x	**-0.79**
AT2G44940	Integrase-type DNA-binding superfamily protein	-0.16	**0.81**	0.32
AT2G45170	ATATG8E_ATG8E__AUTOPHAGY 8E	-0.21	**-1.58**	**-1.06**
AT2G45470	AGP8_FLA8__FASCICLIN-like arabinogalactan protein 8	0.00	0.08	**0.71**
AT2G45710	Zinc-binding ribosomal protein family protein	x	0.59	**0.82**
AT2G45820	Remorin family protein	**0.88**	-0.33	x
AT2G45960	ATHH2_PIP1;2_PIP1B_TMP-A__plasma membrane intrinsic protein 1B	0.32	-0.21	**-1.16**
AT2G46220	Uncharacterized conserved protein (DUF2358)	0.30	-0.64	**-2.04**
AT2G46420	Plant protein 1589 of unknown function	-0.06	**0.80**	**1.17**
AT2G46600	Calcium-binding EF-hand family protein	0.03	**0.80**	-0.01
AT2G46650	ATCB5-C_B5 #1_CB5-C__cytochrome B5 isoform C	0.10	**0.74**	**0.99**
AT2G46740	D-arabinono-1,4-lactone oxidase family protein	0.15	-0.34	**-0.75**
AT2G46750	D-arabinono-1,4-lactone oxidase family protein	0.12	-0.24	**-0.99**
AT2G47110	UBQ6__ubiquitin 6	-0.09	0.46	**0.99**
AT2G47270	sequence-specific DNA binding transcription factors;transcription regulators	-0.27	**-0.95**	**-1.50**
AT2G47400	CP12-1__CP12 domain-containing protein 1	0.05	-0.12	**-0.86**
AT2G47440	Tetratricopeptide repeat (TPR)-like superfamily protein	**-0.73**	0.04	x
AT2G47450	CAO_CPSRP43__chloroplast signal recognition particle component (CAO)	0.09	-0.44	**-0.93**
AT2G47480	Protein of unknown function (DUF3511)	-0.10	0.26	**0.97**
AT2G47610	Ribosomal protein L7Ae/L30e/S12e/Gadd45 family protein	-0.37	0.34	**1.03**
AT2G47650	UXS4__UDP-xylose synthase 4	-0.03	0.10	**0.75**
AT2G47730	ATGSTF5_ATGSTF8_GST6_GSTF8__glutathione S-transferase phi 8	0.23	0.05	**-0.82**
AT2G48020	Major facilitator superfamily protein	-0.31	-0.61	**-1.19**
AT3E56080	EUGENE prediction	0.01	-0.05	**-0.83**

AGI identifier	Gene annotation	30 min	2h	8h
AT3G01190	Peroxidase superfamily protein	**0.69**	-0.11	**1.12**
AT3G01280	ATVDAC1_VDAC1__voltage dependent anion channel 1	-0.01	0.31	**0.86**
AT3G01290	SPFH/Band 7/PHB domain-containing membrane-associated protein family	**0.77**	**-0.93**	**-1.96**
AT3G01420	ALPHA-DOX1_DIOX1_DOX1_PADOX-1__Peroxidase superfamily protein	**0.68**	0.35	-0.31
AT3G01520	Adenine nucleotide alpha hydrolases-like superfamily protein	0.01	-0.38	**-0.82**
AT3G01770	ATBET10_BET10__bromodomain and extraterminal domain protein 10	-0.21	-0.42	**-0.80**
AT3G01820	P-loop containing nucleoside triphosphate hydrolases superfamily protein	-0.01	**0.89**	0.66
AT3G01850	Aldolase-type TIM barrel family protein	0.01	-0.19	**-1.02**
AT3G01930	Major facilitator superfamily protein	0.38	-0.35	**-1.14**
AT3G01970	ATWRKY45_WRKY45__WRKY DNA-binding protein 45	-0.08	0.01	**-1.21**
AT3G02020	AK3__aspartate kinase 3	-0.02	0.31	**0.78**
AT3G02040	SRG3__senescence-related gene 3	0.19	**1.24**	0.58
AT3G02140	AFP4_TMAC2__AFP2 (ABI five-binding protein 2) family protein	-0.23	-0.37	**-0.76**
AT3G02230	ATRGP1_RGP1__reversibly glycosylated polypeptide 1	0.06	**0.85**	**2.27**
AT3G02340	RING/U-box superfamily protein	-0.03	-0.37	**-0.74**
AT3G02390	unknown protein	-0.15	**-1.17**	**-0.82**
AT3G02470	SAMDC__S-adenosylmethionine decarboxylase	**0.80**	-0.35	x
AT3G02530	TCP-1/cpn60 chaperonin family protein	-0.31	0.20	**1.00**
AT3G02630	Plant stearoyl-acyl-carrier-protein desaturase family protein	0.03	0.30	**0.79**
AT3G02650	Tetratricopeptide repeat (TPR)-like superfamily protein	0.30	0.10	**0.93**
AT3G02700	NC domain-containing protein-related	-0.13	-0.57	**-0.85**
AT3G02870	VTC4__Inositol monophosphatase family protein	-0.05	0.55	**0.97**
AT3G02885	GASA5__GAST1 protein homolog 5	0.03	-0.19	**0.80**
AT3G02910	AIG2-like (avirulence induced gene) family protein	-0.17	**1.10**	**1.46**
AT3G03060	P-loop containing nucleoside triphosphate hydrolases superfamily protein	-0.17	0.55	**1.51**
AT3G03150	unknown protein	0.35	-0.39	**-1.41**
AT3G03250	AtUGP1_UGP_UGP1__UDP-GLUCOSE PYROPHOSPHORYLASE 1	0.06	**0.81**	**1.89**
AT3G03780	ATMS2_MS2__methionine synthase 2	-0.01	**0.92**	**2.30**
AT3G03920	H/ACA ribonucleoprotein complex, subunit Gar1/Naf1 protein	-0.21	0.38	**1.14**
AT3G03960	TCP-1/cpn60 chaperonin family protein	-0.14	0.46	**1.13**
AT3G03990	alpha/beta-Hydrolases superfamily protein	0.00	**-1.21**	**-1.88**
AT3G04290	ATLTL1_LTL1__Li-tolerant lipase 1	-0.19	0.25	**1.32**
AT3G04400	emb2171__Ribosomal protein L14p/L23e family protein	-0.15	0.19	**0.79**
AT3G04730	IAA16__indoleacetic acid-induced protein 16	0.54	-0.59	**-0.81**
AT3G04770	RPSAb__40s ribosomal protein SA B	-0.35	**0.85**	**1.12**
AT3G04840	Ribosomal protein S3Ae	-0.18	0.44	**1.42**
AT3G04920	Ribosomal protein S24e family protein	-0.39	0.20	**0.84**
AT3G05060	NOP56-like pre RNA processing ribonucleoprotein	0.08	0.66	**1.24**

AGI identifier	Gene annotation	30 min	2h	8h
AT3G05590	RPL18__ribosomal protein L18	-0.50	0.39	**0.94**
AT3G05880	RCI2A__Low temperature and salt responsive protein family	-0.41	-0.53	**-0.86**
AT3G05890	RCI2B__Low temperature and salt responsive protein family	**-1.01**	0.03	**-0.99**
AT3G05910	Pectinacetylesterase family protein	-0.08	-0.04	**1.45**
AT3G06070	unknown protein	-0.37	**-0.96**	-0.41
AT3G06080	TBL10__Plant protein of unknown function (DUF828)	0.05	**-0.89**	-0.66
AT3G06340	DNAJ heat shock N-terminal domain-containing protein	0.00	-0.36	**-0.75**
AT3G06380	ATTLP9_TLP9__tubby-like protein 9	-0.14	**-1.04**	**-1.32**
AT3G06420	ATG8H__Ubiquitin-like superfamily protein	-0.01	**-0.85**	**-1.47**
AT3G06483	ATPDHK_PDK__pyruvate dehydrogenase kinase	-0.13	-0.52	**-0.94**
AT3G06530	ARM repeat superfamily protein	-0.53	0.41	**0.97**
AT3G06550	unknown protein	0.37	0.16	**1.01**
AT3G06700	Ribosomal L29e protein family	-0.10	0.44	**0.87**
AT3G06850	BCE2_DIN3_LTA1__2-oxoacid dehydrogenases acyltransferase family protein	0.00	**-1.56**	**-1.81**
AT3G06890	unknown protein	-0.02	0.43	**0.98**
AT3G06930	ATPRMT4B_PRMT4B__protein arginine methyltransferase 4B	-0.20	0.30	**0.79**
AT3G07030	pseudogene	0.19	0.17	**0.72**
AT3G07050	GTP-binding family protein	-0.06	0.32	**0.78**
AT3G07110	Ribosomal protein L13 family protein	-0.17	0.57	**0.82**
AT3G07310	Protein of unknown function (DUF760)	-0.03	**-1.33**	-0.64
AT3G07320	O-Glycosyl hydrolases family 17 protein	-0.07	0.23	**0.73**
AT3G07350	Protein of unknown function (DUF506)	-0.06	-0.64	**-1.05**
AT3G07370	ATCHIP_CHIP__carboxyl terminus of HSC70-interacting protein	-0.37	-0.48	**-0.81**
AT3G07380	Domain of unknown function (DUF23)	0.15	0.25	**1.10**
AT3G07390	AIR12__auxin-responsive family protein	0.19	**1.26**	**1.74**
AT3G07560	APM2_PEX13__peroxin 13	-0.47	-0.32	**-1.17**
AT3G07650	COL9__CONSTANS-like 9	-0.16	-0.13	**-1.07**
AT3G07770	AtHsp90-6_AtHsp90.6_Hsp89.1__HEAT SHOCK PROTEIN 89.1	-0.35	0.54	**1.57**
AT3G08020	PHD finger family protein	-0.27	-0.18	**-1.02**
AT3G08580	AAC1__ADP/ATP carrier 1	-0.15	0.61	**1.35**
AT3G08590	Phosphoglycerate mutase, 2,3-bisphosphoglycerate-independent	-0.08	0.61	**1.45**
AT3G08630	Protein of unknown function (DUF3411)	-0.14	0.32	**1.29**
AT3G08640	Protein of unknown function (DUF3411)	0.01	**0.98**	**1.23**
AT3G08770	LTP6__lipid transfer protein 6	-0.22	0.35	**1.32**
AT3G08850	ATRAPTOR1B_RAPTOR1_RAPTOR1B__HEAT repeat ;WD domain, G-beta repeat protein protein	**-0.74**	-0.18	x
AT3G09200	Ribosomal protein L10 family protein	-0.22	0.25	**0.85**
AT3G09260	BGLU23_LEB_PSR3.1_PYK10__Glycosyl hydrolase superfamily protein	0.43	0.07	**1.29**
AT3G09350	Fes1A	-0.11	**0.91**	-0.31

AGI identifier	Gene annotation	30 min	2h	8h
AT3G09440	Heat shock protein 70 (Hsp 70) family protein	0.19	**1.06**	x
AT3G09500	Ribosomal L29 family protein	0.14	0.33	**0.85**
AT3G09630	Ribosomal protein L4/L1 family	-0.33	0.35	**0.95**
AT3G09820	ADK1_ATADK1__adenosine kinase 1	-0.11	0.23	**1.60**
AT3G09860	unknown protein	0.08	-0.17	**-0.74**
AT3G10020	unknown protein	0.10	**-2.14**	**-2.40**
AT3G10113	myb family transcription factor	-0.47	**-1.36**	**-1.53**
AT3G10120	unknown protein	-0.10	-0.34	**-0.81**
AT3G10230	LYC__lycopene cyclase	0.47	-0.23	**-0.90**
AT3G10250	Plant protein 1589 of unknown function	0.00	-0.05	**-0.71**
AT3G10450	SCPL7__serine carboxypeptidase-like 7	-0.13	-0.17	**-0.94**
AT3G10520	AHB2_ARATH GLB2_ATGLB2_GLB2_HB2_NSHB2_ haemoglobin 2	-0.10	0.43	**0.94**
AT3G10610	Ribosomal S17 family protein	-0.33	0.48	**1.00**
AT3G10690	GYRA__DNA GYRASE A	-0.22	0.12	**0.87**
AT3G10770	Single-stranded nucleic acid binding R3H protein	-0.09	-0.24	**-0.86**
AT3G10985	ATWI-12_SAG20_WI12__senescence associated gene 20	0.18	-0.47	**-1.00**
AT3G11230	Yippee family putative zinc-binding protein	-0.39	-0.31	**-0.79**
AT3G11250	Ribosomal protein L10 family protein	-0.04	0.27	**0.81**
AT3G11510	Ribosomal protein S11 family protein	-0.22	0.39	**0.85**
AT3G11560	LETM1-like protein	-0.03	-0.10	**-0.89**
AT3G12150	unknown protein	-0.28	**-1.31**	**-1.02**
AT3G12240	SCPL15__serine carboxypeptidase-like 15	x	-0.23	**-0.80**
AT3G12345	unknown protein	0.00	-0.34	**-1.23**
AT3G12370	Ribosomal protein L10 family protein	0.12	0.41	**0.74**
AT3G12390	Nascent polypeptide-associated complex (NAC), alpha subunit family protein	-0.08	0.32	**0.86**
AT3G12580	ATHSP70_HSP70__heat shock protein 70	-0.03	**1.11**	0.58
AT3G12610	DRT100__Leucine-rich repeat (LRR) family protein	0.01	0.35	**0.73**
AT3G12780	PGK1__phosphoglycerate kinase 1	**0.86**	0.24	0.06
AT3G13110	ATSERAT2;2_SAT-1_SAT-A_SAT-M_SAT3_SERAT2;2__serine acetyltransferase 2;2	0.22	**0.98**	0.66
AT3G13230	RNA-binding KH domain-containing protein	0.22	**0.93**	**1.06**
AT3G13450	DIN4__Transketolase family protein	-0.09	**-1.09**	**-2.34**
AT3G13470	TCP-1/cpn60 chaperonin family protein	-0.27	0.51	**0.95**
AT3G13610	2-oxoglutarate (2OG) and Fe(II)-dependent oxygenase superfamily protein	0.51	0.18	**0.83**
AT3G13750	BGAL1_BGAL1__beta galactosidase 1	0.61	**-1.15**	**-0.83**
AT3G13940	DNA binding;DNA-directed RNA polymerases	0.20	0.65	**1.22**
AT3G14100	RNA-binding (RRM/RBD/RNP motifs) family protein	**0.67**	-0.02	-0.05
AT3G14200	Chaperone DnaJ-domain superfamily protein	0.04	**1.01**	0.51
AT3G14210	ESM1__epithiospecifier modifier 1	-0.05	**1.62**	**1.49**
AT3G14415	Aldolase-type TIM barrel family protein	-0.14	-0.19	**-1.42**
AT3G14420	Aldolase-type TIM barrel family protein	-0.04	-0.06	**-1.01**
AT3G14610	CYP72A7__cytochrome P450, family 72, subfamily A, polypeptide 7	-0.05	-0.12	**-0.84**
AT3G14620	CYP72A8__cytochrome P450, family 72, subfamily A, polypeptide 8	0.07	-0.25	**-1.11**

AGI identifier	Gene annotation	30 min	2h	8h
AT3G14690	CYP72A15__cytochrome P450, family 72, subfamily A, polypeptide 15	-0.08	-0.08	**-0.90**
AT3G14770	Nodulin MtN3 family protein	-0.07	**-1.14**	**-1.59**
AT3G14870	unknown protein	0.26	**-0.77**	-0.01
AT3G14940	ATPPC3_PPC3__phosphoenolpyruvate carboxylase 3	0.13	0.30	**2.25**
AT3G14990	Class I glutamine amidotransferase-like superfamily protein	-0.01	**-0.74**	**-1.43**
AT3G15000	cobalt ion binding	-0.18	0.25	**0.90**
AT3G15020	mMDH2__Lactate/malate dehydrogenase family protein	-0.10	0.36	**0.97**
AT3G15350	Core-2/I-branching beta-1,6-N-acetylglucosaminyltransferase family protein	-0.19	0.53	**0.82**
AT3G15353	ATMT3_MT3__metallothionein 3	-0.15	x	**-1.03**
AT3G15356	Legume lectin family protein	0.33	-0.72	**-1.02**
AT3G15450	Aluminium induced protein with YGL and LRDR motifs	-0.16	**-3.69**	**-2.61**
AT3G15500	ANAC055_ATNAC3_NAC055_NAC3__NAC domain containing protein 3	0.06	**-0.83**	**-1.46**
AT3G15580	APG8H_ATG8I__Ubiquitin-like superfamily protein	0.12	-0.22	**-0.78**
AT3G15630	unknown protein	-0.23	**-2.51**	**-1.80**
AT3G15650	alpha/beta-Hydrolases superfamily protein	-0.35	**0.82**	x
AT3G15770	unknown protein	-0.10	**-1.09**	**-1.18**
AT3G15840	PIFI__post-illumination chlorophyll fluorescence increase	0.10	-0.39	**-0.87**
AT3G15950	NAI2__DNA topoisomerase-related	0.48	-0.04	**1.13**
AT3G15990	SULTR3;4__sulfate transporter 3;4	-0.09	**0.98**	**0.71**
AT3G16050	A37_ATPDX1.2_PDX1.2__pyridoxine biosynthesis 1.2	-0.08	**0.77**	**0.72**
AT3G16080	Zinc-binding ribosomal protein family protein	-0.36	0.47	**0.95**
AT3G16190	Isochorismatase family protein	0.04	-0.05	**-0.84**
AT3G16240	AQP1_ATTIP2;1_DELTA-TIP_DELTA-TIP1_TIP2;1__delta tonoplast integral protein	**0.72**	-0.16	x
AT3G16400	ATMLP-470_ATNSP1_NSP1__nitrile specifier protein 1	**0.86**	-0.37	0.46
AT3G16410	NSP4__nitrile specifier protein 4	x	0.10	**0.72**
AT3G16470	JR1__Mannose-binding lectin superfamily protein	-0.04	0.18	**0.94**
AT3G16770	ATEBP_EBP_ERF72_RAP2.3__ethylene-responsive element binding protein	0.08	-0.46	**-1.50**
AT3G16780	Ribosomal protein L19e family protein	-0.26	0.43	**0.99**
AT3G16810	APUM24_PUM24__pumilio 24	-0.11	0.59	**1.14**
AT3G17040	HCF107__high chlorophyll fluorescent 107	-0.01	-0.08	**-0.73**
AT3G17390	MAT4_MTO3_SAMS3__S-adenosylmethionine synthetase family protein	-0.15	0.15	**1.53**
AT3G17430	Nucleotide-sugar transporter family protein	-0.18	0.05	**0.79**
AT3G17440	ATNPSN13_NPSN13__novel plant snare 13	-0.49	**-0.93**	**-0.71**
AT3G17465	RPL3P__ribosomal protein L3 plastid	-0.19	0.19	**0.90**
AT3G17510	CIPK1_SnRK3.16__CBL-interacting protein kinase 1	-0.14	-0.69	**-1.10**
AT3G17770	Dihydroxyacetone kinase	-0.33	-0.59	**-1.02**
AT3G17790	ATACP5_ATPAP17_PAP17__purple acid phosphatase 17	0.46	**1.76**	**1.16**
AT3G17800	Protein of unknown function (DUF760)	**1.04**	0.34	-0.30
AT3G17810	PYD1__pyrimidine 1	0.07	-0.13	**-0.80**
AT3G18000	NMT1_PEAMT_XPL1__S-adenosyl-L-methionine-dependent methyltransferases superfamily protein	-0.33	0.29	**0.97**

AGI identifier	Gene annotation	30 min	2h	8h
AT3G18130	RACK1C_AT__receptor for activated C kinase 1C	-0.35	**0.84**	**1.46**
AT3G18190	TCP-1/cpn60 chaperonin family protein	-0.20	0.39	**1.35**
AT3G18600	P-loop containing nucleoside triphosphate hydrolases superfamily protein	-0.16	0.64	**1.47**
AT3G18760	Translation elongation factor EF1B/ribosomal protein S6 family protein	-0.03	0.11	**0.79**
AT3G18773	zinc finger (C3HC4-type RING finger) family protein	-0.02	**-0.81**	**-0.73**
AT3G18780	ACT2_DER1_ENL2_LSR2__actin 2	-0.24	-0.65	**-0.74**
AT3G18830	ATPLT5_ATPMT5_PMT5__polyol/monosaccharide transporter 5	0.20	**0.84**	0.40
AT3G19030	unknown protein	-0.06	-0.44	**-1.27**
AT3G19160	ATIPT8_IPT8_IPT8_PGA22__ATP/ADP isopentenyltransferases	-0.43	0.37	**1.07**
AT3G19290	ABF4_AREB2__ABRE binding factor 4	-0.02	-0.67	**-0.74**
AT3G19390	Granulin repeat cysteine protease family protein	0.17	**-0.97**	**-1.20**
AT3G19615	unknown protein	-0.16	-0.05	**-0.84**
AT3G19680	Protein of unknown function (DUF1005)	**-1.11**	**-0.81**	-0.10
AT3G19710	BCAT4__branched-chain aminotransferase4	0.21	0.07	**1.35**
AT3G19720	ARC5_DRP5B__P-loop containing nucleoside triphosphate hydrolases superfamily protein	0.03	0.21	**1.08**
AT3G19800	Protein of unknown function (DUF177)	0.13	-0.14	**-0.71**
AT3G19820	CBB1_DIM_DIM1_DWF1_EVE1__cell elongation protein / DWARF1 / DIMINUTO (DIM)	0.00	-0.17	**1.04**
AT3G19930	ATSTP4_STP4__sugar transporter 4	0.20	**-0.87**	**-1.05**
AT3G20000	TOM40__translocase of the outer mitochondrial membrane 40	-0.21	0.43	**0.95**
AT3G20050	ATTCP-1_TCP-1__T-complex protein 1 alpha subunit	-0.28	0.27	**1.39**
AT3G20060	UBC19__ubiquitin-conjugating enzyme19	0.31	-0.49	**-0.87**
AT3G20200	Protein kinase protein with adenine nucleotide alpha hydrolases-like domain	-0.14	-0.11	**0.77**
AT3G20330	PYRB__PYRIMIDINE B	-0.11	0.44	**0.90**
AT3G20340	unknown protein	-0.12	**-0.94**	**-1.80**
AT3G20370	TRAF-like family protein	0.08	0.16	**1.48**
AT3G20390	endoribonuclease L-PSP family protein	-0.59	0.13	**0.78**
AT3G20500	ATPAP18_PAP18__purple acid phosphatase 18	**0.87**	0.21	-0.02
AT3G20660	4-Oct_AtOCT4__organic cation/carnitine transporter4	0.06	-0.44	**-1.09**
AT3G21190	O-fucosyltransferase family protein	0.18	0.42	**1.10**
AT3G21260	GLTP3__Glycolipid transfer protein (GLTP) family protein	-0.16	0.05	**-0.99**
AT3G21520	AtDMP1_DMP1__DUF679 domain membrane protein 1	-0.01	0.29	**-1.07**
AT3G21560	UGT84A2__UDP-Glycosyltransferase superfamily protein	0.21	**0.95**	**0.75**
AT3G21670	Major facilitator superfamily protein	0.50	**0.95**	-0.30
AT3G21710	unknown protein	0.24	-0.38	**-0.90**
AT3G21770	Peroxidase superfamily protein	0.18	0.12	**1.33**
AT3G21890	B-box type zinc finger family protein	0.49	**0.76**	-0.01
AT3G22120	CWLP__cell wall-plasma membrane linker protein	**0.72**	-0.15	-0.63
AT3G22200	GABA-T_HER1_POP2__Pyridoxal phosphate (PLP)-dependent transferases superfamily protein	-0.17	-0.50	**-0.84**
AT3G22210	unknown protein	0.00	-0.40	**-0.94**

AGI identifier	Gene annotation	30 min	2h	8h
AT3G22440	FRIGIDA-like protein	0.14	-0.26	**-0.77**
AT3G22460	OASA2__O-acetylserine (thiol) lyase (OAS-TL) isoform A2	-0.44	-0.45	**-0.92**
AT3G22530	unknown protein	-0.14	-0.16	**-0.84**
AT3G22660	rRNA processing protein-related	0.20	0.57	**0.98**
AT3G22850	Aluminium induced protein with YGL and LRDR motifs	-0.14	-0.13	**0.79**
AT3G23000	ATSR2_ATSRPK1_CIPK7_PKS7_SnRK3.10__CBL-interacting protein kinase 7	0.35	0.65	**0.81**
AT3G23080	Polyketide cyclase/dehydrase and lipid transport superfamily protein	0.26	**-0.77**	**-1.02**
AT3G23300	S-adenosyl-L-methionine-dependent methyltransferases superfamily protein	-0.05	0.08	**0.98**
AT3G23450	unknown protein	**0.70**	-0.29	x
AT3G23550	MATE efflux family protein	-0.01	-0.69	**-0.88**
AT3G23620	Ribosomal RNA processing Brix domain protein	-0.37	0.47	**0.73**
AT3G23700	Nucleic acid-binding proteins superfamily	0.09	-0.61	**-1.12**
AT3G23810	ATSAHH2_SAHH2__S-adenosyl-l-homocysteine (SAH) hydrolase 2	0.16	0.50	**1.81**
AT3G23830	GR-RBP4_GRP4__glycine-rich RNA-binding protein 4	-0.61	0.51	**1.56**
AT3G23940	dehydratase family	-0.40	0.33	**1.21**
AT3G23990	HSP60_HSP60-3B__heat shock protein 60	-0.18	0.47	**1.29**
AT3G24300	AMT1;3_ATAMT1;3__ammonium transporter 1;3	0.24	0.41	**1.25**
AT3G24420	alpha/beta-Hydrolases superfamily protein	0.44	-0.30	**-1.50**
AT3G24480	Leucine-rich repeat (LRR) family protein	-0.06	-0.32	**0.76**
AT3G24503	ALDH1A_ALDH2C4_REF1__aldehyde dehydrogenase 2C4	0.43	**0.89**	**0.79**
AT3G24600	unknown protein	0.22	0.28	**0.76**
AT3G24927	pseudogene	-0.21	-0.32	**-0.99**
AT3G25110	AtFaTA_FaTA__fatA acyl-ACP thioesterase	-0.06	0.45	**0.78**
AT3G25190	Vacuolar iron transporter (VIT) family protein	-0.03	-0.14	**-1.53**
AT3G25700	Eukaryotic aspartyl protease family protein	0.08	0.43	**0.77**
AT3G25760	AOC1_ERD12__allene oxide cyclase 1	0.30	0.62	**-0.78**
AT3G25780	AOC3__allene oxide cyclase 3	0.08	**0.86**	0.34
AT3G26030	ATB' DELTA__serine/threonine protein phosphatase 2A 55 kDa regulatory subunit B prime delta	0.55	**-0.90**	**-0.99**
AT3G26220	CYP71B3__cytochrome P450, family 71, subfamily B, polypeptide 3	0.05	-0.52	**-1.29**
AT3G26410	methyltransferases;nucleic acid binding	-0.05	0.24	**0.73**
AT3G26450	Polyketide cyclase/dehydrase and lipid transport superfamily protein	**0.80**	0.60	0.70
AT3G26520	GAMMA-TIP2_SITIP_TIP1;2_TIP2__tonoplast intrinsic protein 2	0.22	-0.16	**-1.06**
AT3G26580	Tetratricopeptide repeat (TPR)-like superfamily protein	-0.15	-0.41	**-0.73**
AT3G26650	GAPA_GAPA-1__glyceraldehyde 3-phosphate dehydrogenase A subunit	0.09	-0.06	**-0.80**
AT3G26690	ATNUDT13_ATNUDX13_NUDX13__nudix hydrolase homolog 13	-0.37	-0.65	**-1.01**
AT3G26740	CCL__CCR-like	-0.06	**-1.67**	**-1.60**
AT3G27110	Peptidase family M48 family protein	0.16	-0.16	**-0.98**
AT3G27160	GHS1__Ribosomal protein S21 family protein	-0.18	-0.29	**-0.73**

AGI identifier	Gene annotation	30 min	2h	8h
AT3G27280	ATPHB4_PHB4__prohibitin 4	-0.16	0.45	**1.15**
AT3G27570	Sucrase/ferredoxin-like family protein	-0.10	**0.86**	**1.32**
AT3G27690	LHCB2_LHCB2.3_LHCB2.4__photosystem II light harvesting complex gene 2.3	**1.12**	-0.54	-0.06
AT3G27740	CARA__carbamoyl phosphate synthetase A	-0.14	0.35	**0.88**
AT3G27770	unknown protein	-0.16	**-0.96**	**-1.56**
AT3G27850	RPL12-C__ribosomal protein L12-C	**0.77**	0.48	0.01
AT3G28200	Peroxidase superfamily protein	-0.65	0.07	**0.88**
AT3G28740	CYP81D1__Cytochrome P450 superfamily protein	0.07	**-0.87**	**-2.28**
AT3G28900	Ribosomal protein L34e superfamily protein	-0.40	0.34	**0.84**
AT3G29035	ANAC059_ATNAC3_NAC3__NAC domain containing protein 3	-0.07	-0.52	**-0.89**
AT3G29240	Protein of unknown function (DUF179)	0.16	**-1.45**	**-1.80**
AT3G29250	NAD(P)-binding Rossmann-fold superfamily protein	0.45	-0.18	**1.13**
AT3G29330	unknown protein	-0.26	0.18	**0.78**
AT3G29360	UDP-glucose 6-dehydrogenase family protein	-0.24	0.05	**1.01**
AT3G30390	Transmembrane amino acid transporter family protein	x	-0.33	**-0.72**
AT3G30775	AT-POX_ATPDH_ATPOX_ERD5_PRO1_PRODH_ Methylenetetrahydrofolate reductase family protein	0.55	**-2.18**	**-2.34**
AT3G32990	pseudogene	**-1.32**	0.20	-0.19
AT3G43230	RING/FYVE/PHD-type zinc finger family protein	-0.08	-0.44	**-0.73**
AT3G43810	CAM7__calmodulin 7	-0.02	0.04	**0.82**
AT3G43850	unknown protein	-0.15	-0.57	**-0.74**
AT3G43980	Ribosomal protein S14p/S29e family protein	-0.08	0.33	**0.75**
AT3G44190	FAD/NAD(P)-binding oxidoreductase family protein	0.33	-0.04	**-1.22**
AT3G44300	AtNIT2_NIT2__nitrilase 2	0.15	-0.43	**-1.63**
AT3G44450	unknown protein	0.16	**0.85**	0.53
AT3G44550	FAR5__fatty acid reductase 5	0.02	0.23	**1.02**
AT3G44590	60S acidic ribosomal protein family	-0.23	0.51	**0.97**
AT3G44750	ATHD2A_HD2A_HDA3_HDT1__histone deacetylase 3	-0.04	0.60	**1.69**
AT3G44755	unknown protein	-0.08	-0.57	**-1.01**
AT3G44860	FAMT__farnesoic acid carboxyl-O-methyltransferase	0.07	**1.06**	x
AT3G44870	S-adenosyl-L-methionine-dependent methyltransferases superfamily protein	0.42	**1.36**	-0.13
AT3G44880	ACD1_LLS1_PAO__Pheophorbide a oxygenase family protein with Rieske [2Fe-2S] domain	0.39	-0.04	**-0.84**
AT3G44990	ATXTR8_XTH31_XTR8__xyloglucan endo-transglycosylase-related 8	0.30	0.63	**2.04**
AT3G45300	ATIVD_IVD_IVDH__isovaleryl-CoA-dehydrogenase	0.56	**-0.93**	x
AT3G45650	NAXT1__nitrate excretion transporter1	0.03	0.19	**0.75**
AT3G45700	Major facilitator superfamily protein	0.19	-0.01	**0.79**
AT3G45730	unknown protein	-0.15	**-1.44**	**-1.90**
AT3G45970	ATEXLA1_ATEXPL1_ATHEXP BETA 2.1_EXLA1_EXPL1__expansin-like A1	**-0.68**	**-1.29**	**-0.90**
AT3G46080	C2H2-type zinc finger family protein	-0.16	-0.72	**-0.98**
AT3G46450	SEC14 cytosolic factor family protein / phosphoglyceride transfer family protein	-0.02	0.37	**0.74**

AGI identifier	Gene annotation	30 min	2h	8h
AT3G46540	ENTH/VHS family protein	0.14	0.65	**1.01**
AT3G46560	emb2474_TIM9__Tim10/DDP family zinc finger protein	0.25	0.62	**1.20**
AT3G46600	GRAS family transcription factor	0.17	-0.41	**-0.76**
AT3G46970	ATPHS2_PHS2__alpha-glucan phosphorylase 2	0.26	x	**1.10**
AT3G47070	unknown protein	-0.02	-0.10	**-1.25**
AT3G47160	RING/U-box superfamily protein	-0.09	**-1.37**	x
AT3G47340	ASN1_AT-ASN1_DIN6__glutamine-dependent asparagine synthase 1	0.11	**-2.07**	**-2.59**
AT3G47370	Ribosomal protein S10p/S20e family protein	-0.02	**0.76**	**1.07**
AT3G47420	ATPS3_PS3__phosphate starvation-induced gene 3	0.36	**0.92**	**0.99**
AT3G47470	CAB4_LHCA4__light-harvesting chlorophyll-protein complex I subunit A4	-0.20	-0.41	**-1.33**
AT3G47520	MDH__malate dehydrogenase	-0.27	0.63	**0.92**
AT3G47540	Chitinase family protein	0.02	0.26	**0.74**
AT3G47800	Galactose mutarotase-like superfamily protein	0.31	**-1.00**	**-2.12**
AT3G47960	Major facilitator superfamily protein	-0.12	**1.05**	**0.96**
AT3G48000	ALDH2_ALDH2A_ALDH2B4__aldehyde dehydrogenase 2B4	**0.76**	0.14	x
AT3G48250	Pentatricopeptide repeat (PPR) superfamily protein	0.15	0.27	**0.72**
AT3G48300	CYP71A23 (cytochrome P450, family 71, subfamily A, polypeptide 23); oxygen binding	-0.14	-0.36	**-0.82**
AT3G48320	CYP71A21 (cytochrome P450, family 71, subfamily A, polypeptide 21); oxygen binding	0.25	-0.60	**-1.19**
AT3G48360	ATBT2_BT2__BTB and TAZ domain protein 2	-0.40	**-2.47**	**-1.66**
AT3G48390	MA3 domain-containing protein	-0.13	-0.59	**-0.78**
AT3G48520	CYP94B3__cytochrome P450, family 94, subfamily B, polypeptide 3	**0.81**	0.19	-0.17
AT3G48530	KING1__SNF1-related protein kinase regulatory subunit gamma 1	0.19	**-0.80**	**-1.33**
AT3G48930	EMB1080__Nucleic acid-binding, OB-fold-like protein	0.01	0.43	**0.84**
AT3G48960	Ribosomal protein L13e family protein	0.31	0.62	**1.16**
AT3G48990	AMP-dependent synthetase and ligase family protein	0.61	0.02	**-1.19**
AT3G49010	ATBBC1_BBC1_RSU2__breast basic conserved 1	0.13	0.59	**0.89**
AT3G49040	FBD, F-box and Leucine Rich Repeat domains containing protein	0.01	0.40	**0.73**
AT3G49070	Protein of unknown function (DUF677)	0.39	0.07	**-1.10**
AT3G49160	pyruvate kinase family protein	0.10	**-0.86**	-0.68
AT3G49220	Plant invertase/pectin methylesterase inhibitor superfamily	-0.16	**0.78**	**1.00**
AT3G49320	Metal-dependent protein hydrolase	-0.05	0.05	**0.93**
AT3G49590	Autophagy-related protein 13	-0.06	-0.40	**-0.90**
AT3G49620	DIN11__2-oxoglutarate (2OG) and Fe(II)-dependent oxygenase superfamily protein	-0.21	-0.10	**-1.37**
AT3G49670	BAM2__Leucine-rich receptor-like protein kinase family protein	-0.46	**0.75**	**0.90**
AT3G49720	unknown protein	0.12	-0.10	**0.92**
AT3G49780	ATPSK3 (FORMER SYMBOL)_ATPSK4_PSK4__phytosulfokine 4 precursor	-0.17	x	**-1.19**
AT3G49790	Carbohydrate-binding protein	0.00	**-0.89**	**-1.26**
AT3G50130	Plant protein of unknown function (DUF247)	0.06	0.26	**0.72**

AGI identifier	Gene annotation	30 min	2h	8h
AT3G50210	2-oxoglutarate (2OG) and Fe(II)-dependent oxygenase superfamily protein	0.11	0.02	**-0.85**
AT3G50260	ATERF#011_CEJ1_DEAR1__cooperatively regulated by ethylene and jasmonate 1	x	**-0.84**	**-1.54**
AT3G50340	unknown protein	0.06	**0.78**	**0.79**
AT3G50480	HR4 (HOMOLOG OF RPW8 4)	-0.10	**-1.21**	**-1.25**
AT3G50560	NAD(P)-binding Rossmann-fold superfamily protein	0.10	**-1.97**	-0.70
AT3G50610	unknown protein	-0.09	0.12	**0.77**
AT3G50660	CLM_CYP90B1_DWF4_PSC1_SAV1_SNP2__Cytochrome P450 superfamily protein	0.05	0.05	**0.74**
AT3G50740	UGT72E1__UDP-glucosyl transferase 72E1	0.28	0.34	**1.21**
AT3G50820	OEC33_PSBO-2_PSBO2__photosystem II subunit O-2	**1.42**	0.10	-0.21
AT3G50830	ATCOR413-PM2_COR413-PM2__cold-regulated 413-plasma membrane 2	-0.25	-0.61	**-0.72**
AT3G50950	ZAR1__HOPZ-ACTIVATED RESISTANCE 1	**0.71**	-0.33	-0.40
AT3G50970	LTI30_XERO2__dehydrin family protein	0.29	-0.21	**-1.42**
AT3G51000	alpha/beta-Hydrolases superfamily protein	x	-0.19	**-1.07**
AT3G51130	unknown protein	0.27	-0.59	**-1.08**
AT3G51240	F3'H_F3H_TT6__flavanone 3-hydroxylase	0.19	**0.97**	**2.11**
AT3G51370	Protein phosphatase 2C family protein	-0.13	-0.69	**-0.91**
AT3G51600	LTP5__lipid transfer protein 5	**0.72**	-0.17	-0.32
AT3G51730	saposin B domain-containing protein	0.36	-0.61	**-1.81**
AT3G51800	ATEBP1_ATG2_EBP1__metallopeptidase M24 family protein	-0.15	0.45	**1.09**
AT3G51840	ACX4_ATG6_ATSCX__acyl-CoA oxidase 4	-0.03	**-1.01**	**-2.15**
AT3G51910	AT-HSFA7A_HSFA7A__heat shock transcription factor A7A	-0.31	**-1.63**	**-1.35**
AT3G52060	Core-2/I-branching beta-1,6-N-acetylglucosaminyltransferase family protein	0.22	-0.73	**-0.80**
AT3G52105	unknown protein	0.00	-0.48	**-0.79**
AT3G52170	DNA binding	0.00	0.28	**0.85**
AT3G52180	ATPTPKIS1_ATSEX4_DSP4_SEX4__dual specificity protein phosphatase (DsPTP1) family protein	-0.15	0.57	**1.74**
AT3G52190	PHF1__phosphate transporter traffic facilitator1	-0.03	0.64	**1.36**
AT3G52340	ATSPP2_SPP2__sucrose-6F-phosphate phosphohydrolase 2	-0.19	0.69	**1.34**
AT3G52370	FLA15__FASCICLIN-like arabinogalactan protein 15 precursor	x	0.56	**1.46**
AT3G52470	Late embryogenesis abundant (LEA) hydroxyproline-rich glycoprotein family	0.02	**0.76**	0.69
AT3G52600	AtcwINV2_CWINV2__cell wall invertase 2	0.18	0.20	**0.84**
AT3G52840	BGAL2__beta-galactosidase 2	0.03	**-0.83**	-0.59
AT3G52930	Aldolase superfamily protein	0.07	**0.89**	**1.99**
AT3G52940	ELL1_FK_HYD2__Ergosterol biosynthesis ERG4/ERG24 family	-0.04	-0.10	**0.86**
AT3G52990	Pyruvate kinase family protein	-0.04	0.50	**0.90**
AT3G53020	RPL24_RPL24B_STV1__Ribosomal protein L24e family protein	-0.50	0.37	**0.71**
AT3G53260	ATPAL2_PAL2__phenylalanine ammonia-lyase 2	**0.79**	0.10	0.33
AT3G53420	PIP2_PIP2;1_PIP2A__plasma membrane intrinsic protein 2A	0.25	-0.31	**-0.89**

AGI identifier	Gene annotation	30 min	2h	8h
AT3G53800	Fes1B	-0.12	-0.68	**-0.74**
AT3G53870	Ribosomal protein S3 family protein	-0.18	0.46	**0.98**
AT3G54400	Eukaryotic aspartyl protease family protein	-0.27	**1.13**	**1.47**
AT3G54420	ATCHITIV_ATEP3_CHIV_EP3__homolog of carrot EP3-3 chitinase	0.34	**0.85**	0.26
AT3G54470	uridine 5p-monophosphate synthase / UMP synthase (PYRE-F) (UMPS)	-0.17	0.48	**1.49**
AT3G54500	unknown protein	**-0.93**	-0.56	-0.65
AT3G54580	Proline-rich extensin-like family protein	0.31	0.04	**1.29**
AT3G54590	ATHRGP1_HRGP1__hydroxyproline-rich glycoprotein	0.23	-0.09	**1.39**
AT3G54600	Class I glutamine amidotransferase-like superfamily protein	-0.10	0.41	**0.93**
AT3G54640	TRP3_TSA1__tryptophan synthase alpha chain	0.05	0.67	**1.27**
AT3G54680	proteophosphoglycan-related	-0.18	0.21	**0.92**
AT3G54810	BME3_BME3-ZF_GATA8__Plant-specific GATA-type zinc finger transcription factor family protein	**-0.66**	0.34	0.67
AT3G54880	unknown protein	-0.41	**-1.54**	x
AT3G54890	LHCA1__photosystem I light harvesting complex gene 1	0.47	0.25	**-0.80**
AT3G54900	ATGRXCP_CXIP1__CAX interacting protein 1	**0.66**	0.27	0.00
AT3G54960	ATPDI1_ATPDIL1-3_PDI1_PDIL1-3__PDI-like 1-3	-0.06	0.31	**0.81**
AT3G55010	ATPURM_PUR5__phosphoribosylformylglycinamidine cyclo-ligase, chloroplast / phosphoribosyl-aminoimidazole synthetase / AIR synthase (PUR5)	-0.04	0.46	**1.39**
AT3G55120	A11_CFI_TT5__Chalcone-flavanone isomerase family protein	0.16	**0.81**	**1.40**
AT3G55280	RPL23AB__ribosomal protein L23AB	-0.35	0.69	**1.07**
AT3G55330	PPL1__PsbP-like protein 1	-0.50	-0.38	**-1.04**
AT3G55340	PHIP1, PHRAGMOPLASTIN INTERACTING PROTEIN 1	0.05	**0.88**	**1.24**
AT3G55360	ATTSC13_CER10_ECR_TSC13__3-oxo-5-alpha-steroid 4-dehydrogenase family protein	0.21	**0.75**	**0.75**
AT3G55440	ATCTIMC_CYTOTPI_TPI__triosephosphate isomerase	0.04	0.20	**0.76**
AT3G55605	Mitochondrial glycoprotein family protein	0.09	0.41	**0.79**
AT3G55610	P5CS2__delta 1-pyrroline-5-carboxylate synthase 2	x	-0.59	**-0.75**
AT3G55620	emb1624__Translation initiation factor IF6	-0.09	0.40	**0.77**
AT3G55760	unknown protein	0.03	0.61	**0.79**
AT3G55970	ATJRG21_JRG21__jasmonate-regulated gene 21	0.10	0.07	**-0.75**
AT3G56070	ROC2__rotamase cyclophilin 2	0.17	**0.91**	**1.29**
AT3G56310	Melibiase family protein	0.61	0.10	**-0.79**
AT3G56360	unknown protein	-0.10	-0.50	**-1.24**
AT3G57010	Calcium-dependent phosphotriesterase superfamily protein	0.02	**1.33**	**1.11**
AT3G57150	AtCBF5_AtNAP57_CBF5_NAP57__homologue of NAP57	-0.27	0.60	**1.07**
AT3G57490	Ribosomal protein S5 family protein	-0.01	0.60	**1.05**
AT3G57520	AtSIP2_SIP2__seed imbibition 2	-0.20	**-1.63**	**-1.48**
AT3G57610	ADSS__adenylosuccinate synthase	-0.37	0.37	**1.04**
AT3G57660	NRPA1__nuclear RNA polymerase A1	-0.07	0.48	**1.13**
AT3G58610	ketol-acid reductoisomerase	0.26	0.47	**0.93**
AT3G58660	Ribosomal protein L1p/L10e family	-0.07	0.48	**0.85**
AT3G58700	Ribosomal L5P family protein	0.00	0.54	**1.00**

AGI identifier	Gene annotation	30 min	2h	8h
AT3G58750	CSY2__citrate synthase 2	0.00	-0.46	**-0.85**
AT3G58990	IPMI1__isopropylmalate isomerase 1	0.09	**1.08**	**1.64**
AT3G59220	ATPIRIN1_PRN_PRN1__pirin	-0.08	**0.93**	**0.75**
AT3G59260	pirin, putative	0.29	**0.91**	**0.79**
AT3G59340	Eukaryotic protein of unknown function (DUF914)	0.13	-0.17	**0.75**
AT3G59350	Protein kinase superfamily protein	-0.49	**-1.27**	**-0.85**
AT3G59540	Ribosomal L38e protein family	-0.05	0.52	**0.93**
AT3G59670	unknown protein	-0.04	0.46	**0.97**
AT3G59890	Dihydrodipicolinate reductase, bacterial/plant	-0.08	0.26	**0.92**
AT3G59930	Encodes a defensin-like (DEFL) family protein.	0.45	**-1.16**	**-2.13**
AT3G59940	Galactose oxidase/kelch repeat superfamily protein	-0.08	**-1.66**	**-1.77**
AT3G59970	MTHFR1__methylenetetrahydrofolate reductase 1	0.03	-0.01	**0.89**
AT3G60130	BGLU16__beta glucosidase 16	-0.01	**-0.91**	**-1.16**
AT3G60140	BGLU30_DIN2_SRG2__Glycosyl hydrolase superfamily protein	-0.04	**-0.86**	**-2.02**
AT3G60245	Zinc-binding ribosomal protein family protein	-0.36	0.37	**1.09**
AT3G60300	RWD domain-containing protein	-0.09	-0.67	**-1.19**
AT3G61010	Ferritin/ribonucleotide reductase-like family protein	**-0.72**	-0.15	-0.01
AT3G61060	AtPP2-A13_PP2-A13__phloem protein 2-A13	0.20	**-2.14**	**-2.13**
AT3G61240	DEA(D/H)-box RNA helicase family protein	-0.45	0.29	**0.76**
AT3G61260	Remorin family protein	0.45	**-0.76**	**-0.78**
AT3G61470	LHCA2__photosystem I light harvesting complex gene 2	0.46	0.20	**-0.77**
AT3G61560	reticulon family protein (RTNLB6)	-0.02	0.47	**0.71**
AT3G61820	Eukaryotic aspartyl protease family protein	-0.04	**1.02**	**1.75**
AT3G62190	Chaperone DnaJ-domain superfamily protein	x	-0.15	**-0.83**
AT3G62360	Carbohydrate-binding-like fold	-0.20	0.07	**0.77**
AT3G62410	CP12-2__CP12 domain-containing protein 2	0.45	-0.28	**-1.20**
AT3G62420	ATBZIP53_BZIP53__basic region/leucine zipper motif 53	**-0.80**	**-1.13**	**-0.97**
AT3G62460	Putative endonuclease or glycosyl hydrolase	-0.17	0.61	**1.02**
AT3G62550	Adenine nucleotide alpha hydrolases-like superfamily protein	-0.02	**-1.20**	**-1.56**
AT3G62650	unknown protein	0.04	-0.38	**-0.93**
AT3G62720	ATXT1_XT1_XXT1__xylosyltransferase 1	-0.48	**-0.77**	-0.09
AT3G62870	Ribosomal protein L7Ae/L30e/S12e/Gadd45 family protein	-0.12	0.43	**1.00**
AT3G62930	Thioredoxin superfamily protein	-0.12	-0.40	**-1.06**
AT4G00100	ATRPS13A_PFL2_RPS13_RPS13A__ribosomal protein S13A	-0.17	0.50	**1.00**
AT4G00430	PIP1;4_PIP1E_TMP-C__plasma membrane intrinsic protein 1;4	0.37	**0.87**	**0.82**
AT4G00570	NAD-ME2__NAD-dependent malic enzyme 2	-0.09	0.13	**0.93**
AT4G00600	Amino acid dehydrogenase family protein	-0.10	0.04	**0.77**
AT4G00620	Amino acid dehydrogenase family protein	-0.12	0.18	**0.76**
AT4G00630	ATKEA2_KEA2__K+ efflux antiporter 2	-0.18	0.40	**0.85**
AT4G00750	S-adenosyl-L-methionine-dependent methyltransferases superfamily protein	0.03	-0.35	**-0.98**
AT4G00752	UBX domain-containing protein	-0.22	-0.25	**-0.87**
AT4G00810	60S acidic ribosomal protein family	-0.22	0.17	**0.81**
AT4G01030	pentatricopeptide (PPR) repeat-containing protein	0.05	**-0.85**	**-0.92**

AGI identifier	Gene annotation	30 min	2h	8h
AT4G01080	TBL26__TRICHOME BIREFRINGENCE-LIKE 26	0.00	**1.63**	**1.06**
AT4G01100	ADNT1__adenine nucleotide transporter 1	-0.32	-0.21	**0.81**
AT4G01265	raffinose synthase family protein	0.16	**-0.82**	**-0.94**
AT4G01770	RGXT1__rhamnogalacturonan xylosyltransferase 1	0.34	0.34	**0.73**
AT4G01870	tolB protein-related	0.53	0.11	**-0.97**
AT4G02220	zinc finger (MYND type) family protein / programmed cell death 2 C-terminal domain-containing protein	-0.02	0.18	**0.71**
AT4G02230	Ribosomal protein L19e family protein	-0.12	0.05	**0.87**
AT4G02405	unknown protein	0.05	0.38	**0.82**
AT4G02440	EID1__F-box family protein	-0.32	-0.62	**-0.75**
AT4G02520	ATGSTF2_ATPM24_ATPM24.1_GST2_GSTF2__glutathione S-transferase PHI 2	0.04	0.31	**-1.20**
AT4G02930	GTP binding Elongation factor Tu family protein	-0.05	0.22	**0.84**
AT4G02940	oxidoreductase, 2OG-Fe(II) oxygenase family protein	0.17	**0.97**	0.38
AT4G03280	PETC_PGR1__photosynthetic electron transfer C	0.03	-0.14	**-0.87**
AT4G03510	ATRMA1_RMA1__RING membrane-anchor 1	-0.09	**-1.29**	x
AT4G03540	Uncharacterised protein family (UPF0497)	0.05	**1.04**	0.27
AT4G03950	Nucleotide/sugar transporter family protein	0.17	**1.00**	**2.21**
AT4G04020	FIB__fibrillin	0.48	**0.98**	**0.71**
AT4G04330	Chaperonin-like RbcX protein	-0.06	-0.39	**-0.90**
AT4G04610	APR_APR1_ATAPR1_PRH19__APS reductase 1	**0.68**	**0.85**	0.09
AT4G04640	ATPC1__ATPase, F1 complex, gamma subunit protein	**0.78**	0.28	-0.43
AT4G04745	unknown protein	-0.01	0.11	**0.90**
AT4G04760	Major facilitator superfamily protein	0.12	0.06	**0.86**
AT4G04940	Transducin family protein / WD-40 repeat family protein	-0.22	0.26	**0.71**
AT4G04990	Protein of unknown function (DUF761)	0.28	-0.40	**-0.79**
AT4G05310	Ubiquitin-like superfamily protein	0.19	-0.13	**-1.18**
AT4G05420	DDB1A__damaged DNA binding protein 1A	-0.18	0.34	**0.74**
AT4G05450	ATMFDX1_MFDX1__mitochondrial ferredoxin 1	-0.09	0.67	**0.99**
AT4G06746	RAP2.9 (related to AP2 9); transcription factor	0.25	-0.47	**-0.99**
AT4G08210	Pentatricopeptide repeat (PPR-like) superfamily protein	0.17	0.66	**1.44**
AT4G08920	ATCRY1_BLU1_CRY1_HY4_OOP2__cryptochrome 1	-0.37	**-1.25**	**-0.87**
AT4G08950	EXO__Phosphate-responsive 1 family protein	**-1.32**	**-1.15**	x
AT4G09020	ATISA3_ISA3__isoamylase 3	-0.10	0.15	**0.75**
AT4G09320	NDPK1__Nucleoside diphosphate kinase family protein	-0.08	0.42	**1.12**
AT4G10110	RNA-binding (RRM/RBD/RNP motifs) family protein	0.07	**1.17**	**1.40**
AT4G10160	RING/U-box superfamily protein	0.16	**-0.74**	**-0.93**
AT4G10390	Protein kinase superfamily protein	0.13	0.57	**0.84**
AT4G10480	Nascent polypeptide-associated complex (NAC), alpha subunit family protein	0.43	0.31	**0.80**
AT4G10770	ATOPT7_OPT7__oligopeptide transporter 7	**-0.69**	0.35	**0.75**
AT4G11130	RDR2_SMD1__RNA-dependent RNA polymerase 2	0.10	-0.50	**-0.83**
AT4G11175	Nucleic acid-binding, OB-fold-like protein	**0.69**	0.18	x
AT4G11360	RHA1B__RING-H2 finger A1B	0.03	-0.46	**-0.76**
AT4G11430	hydroxyproline-rich glycoprotein family protein	0.16	0.06	**0.84**
AT4G11570	Haloacid dehalogenase-like hydrolase (HAD) superfamily protein	x	-0.38	**-0.91**

AGI identifier	Gene annotation	30 min	2h	8h
AT4G11600	ATGPX6_GPX6_LSC803_PHGPX__glutathione peroxidase 6	**0.82**	x	-0.13
AT4G11650	ATOSM34_OSM34__osmotin 34	0.55	0.09	**-1.55**
AT4G12030	BASS5_BAT5__bile acid transporter 5	-0.13	0.61	**1.22**
AT4G12420	SKU5__Cupredoxin superfamily protein	-0.51	**-1.14**	0.15
AT4G12490	Bifunctional inhibitor/lipid-transfer protein/seed storage 2S albumin superfamily protein	0.02	0.24	**0.82**
AT4G12500	Bifunctional inhibitor/lipid-transfer protein/seed storage 2S albumin superfamily protein	0.08	0.22	**0.82**
AT4G12560	PR1 (Constitutive Expresser of PR Genes 1, also known as CPR30)	-0.28	**-0.80**	**-0.80**
AT4G12600	Ribosomal protein L7Ae/L30e/S12e/Gadd45 family protein	-0.30	0.58	**1.09**
AT4G12650	Endomembrane protein 70 protein family	-0.07	0.08	**1.03**
AT4G12730	FLA2__FASCICLIN-like arabinogalactan 2	-0.28	-0.40	**0.90**
AT4G12880	AtENODL19_ENODL19__early nodulin-like protein 19	**0.70**	0.13	0.30
AT4G13170	Ribosomal protein L13 family protein	-0.01	0.40	**1.02**
AT4G13180	NAD(P)-binding Rossmann-fold superfamily protein	**0.80**	0.64	-0.05
AT4G13250	NYC1__NAD(P)-binding Rossmann-fold superfamily protein	0.10	-0.16	**-0.89**
AT4G13410	ATCSLA15_CSLA15__Nucleotide-diphospho-sugar transferases superfamily protein	-0.18	**0.85**	0.07
AT4G13430	ATLEUC1_IIL1__isopropyl malate isomerase large subunit 1	-0.03	0.22	**1.11**
AT4G13530	unknown protein	0.39	-0.47	**-1.31**
AT4G13770	CYP83A1_REF2__cytochrome P450, family 83, subfamily A, polypeptide 1	**1.14**	**0.93**	**1.92**
AT4G13840	HXXXD-type acyl-transferase family protein	0.24	0.04	**0.73**
AT4G13940	ATSAHH1_EMB1395_HOG1_MEE58_SAHH1__S-adenosyl-L-homocysteine hydrolase	-0.27	0.24	**1.20**
AT4G14040	EDA38_SBP2__selenium-binding protein 2	-0.13	-0.24	**-0.78**
AT4G14130	XTH15_XTR7__xyloglucan endotransglucosylase/hydrolase 15	**-0.75**	**-0.87**	-0.27
AT4G14270	Protein containing PAM2 motif which mediates interaction with the PABC domain of polyadenyl binding proteins.	-0.37	**-1.24**	**-0.89**
AT4G14320	Zinc-binding ribosomal protein family protein	-0.34	0.23	**0.80**
AT4G14410	bHLH104__basic helix-loop-helix (bHLH) DNA-binding superfamily protein	0.08	-0.10	**-0.72**
AT4G14430	ATECI2_ECHIB_ECI2_IBR10_PEC12__indole-3-butyric acid response 10	0.02	-0.34	**-0.79**
AT4G14440	ATECI3_ECI3_HCD1__3-hydroxyacyl-CoA dehydratase 1	0.51	**0.87**	0.60
AT4G14880	ATCYS-3A_CYTACS1_OASA1_OLD3__O-acetylserine (thiol) lyase (OAS-TL) isoform A1	**0.82**	-0.06	-0.40
AT4G14960	TUA6__Tubulin/FtsZ family protein	-0.20	0.02	**0.87**
AT4G15210	AT-BETA-AMY_ATBETA-AMY_BAM5_BMY1_RAM1__beta-amylase 5	0.09	0.55	**0.73**
AT4G15248	B-box type zinc finger family protein	**0.82**	0.26	-0.14
AT4G15260	UDP-Glycosyltransferase superfamily protein	-0.03	-0.20	**-0.83**
AT4G15390	HXXXD-type acyl-transferase family protein	0.43	-0.37	**1.44**
AT4G15393	CYP702A5 (cytochrome P450, family 702, subfamily A, polypeptide 5); heme binding / iron ion binding / monooxygenase	-0.11	-0.12	**0.92**

AGI identifier	Gene annotation	30 min	2h	8h
AT4G15480	UGT84A1__UDP-Glycosyltransferase superfamily protein	0.44	0.62	**0.75**
AT4G15530	PPDK__pyruvate orthophosphate dikinase	0.33	-0.46	**-1.94**
AT4G15550	IAGLU__indole-3-acetate beta-D-glucosyltransferase	0.07	-0.16	**-1.18**
AT4G15610	Uncharacterised protein family (UPF0497)	-0.05	-0.41	**-1.21**
AT4G15640	unknown protein	-0.10	0.36	**1.25**
AT4G15760	Encodes a protein with similarity to monooxygenases that are known to degrade salicylic acid (SA).	**0.66**	-0.61	**-0.86**
AT4G15765	FAD/NAD(P)-binding oxidoreductase family protein	-0.10	-0.34	**-0.90**
AT4G15770	RNA binding	0.16	0.62	**0.84**
AT4G16141	unknown protein	**-0.88**	0.21	0.63
AT4G16146	cAMP-regulated phosphoprotein 19-related protein	-0.12	0.28	**0.95**
AT4G16190	Papain family cysteine protease	0.57	0.21	**-1.47**
AT4G16340	SPK1__guanyl-nucleotide exchange factors;GTPase binding;GTP binding	-0.53	-0.01	**0.74**
AT4G16400	unknown protein	0.16	0.08	**-0.85**
AT4G16520	ATG8F__Ubiquitin-like superfamily protein	-0.33	**-1.13**	**-1.75**
AT4G16563	Eukaryotic aspartyl protease family protein	**-1.19**	**-1.25**	-0.46
AT4G16590	ATCSLA01_ATCSLA1_CSLA01_CSLA01__cellulose synthase-like A01	0.08	**1.26**	**0.74**
AT4G16660	heat shock protein 70 (Hsp 70) family protein	0.01	0.20	**1.00**
AT4G16690	ATMES16_MES16__methyl esterase 16	0.31	-0.56	**-0.97**
AT4G16720	Ribosomal protein L23/L15e family protein	-0.14	0.49	**0.95**
AT4G16840	unknown protein	0.13	-0.10	**-0.78**
AT4G17090	BAM3_BMY8_CT-BMY__chloroplast beta-amylase	0.02	0.05	**1.45**
AT4G17245	RING/U-box superfamily protein	0.10	**-0.94**	**-1.26**
AT4G17280	Auxin-responsive family protein	0.09	**0.84**	0.10
AT4G17340	DELTA-TIP2_TIP2;2__tonoplast intrinsic protein 2;2	**0.66**	0.09	-0.06
AT4G17390	Ribosomal protein L23/L15e family protein	-0.20	0.25	**0.93**
AT4G17460	HAT1__Homeobox-leucine zipper protein 4 (HB-4) / HD-ZIP protein	**-0.95**	-0.29	-0.29
AT4G17470	alpha/beta-Hydrolases superfamily protein	-0.01	0.19	**0.73**
AT4G17500	ATERF-1_ERF-1__ethylene responsive element binding factor 1	-0.02	-0.53	**-1.40**
AT4G17520	Hyaluronan / mRNA binding family	-0.26	0.52	**0.97**
AT4G17770	ATTPS5_TPS5_TPS5__trehalose phosphatase/synthase 5	-0.02	0.51	**1.35**
AT4G17840	unknown protein	0.39	-0.31	**-1.35**
AT4G18010	5PTASE2_AT5PTASE2_IP5PII__myo-inositol polyphosphate 5-phosphatase 2	-0.46	-0.37	**-0.90**
AT4G18030	S-adenosyl-L-methionine-dependent methyltransferases superfamily protein	0.52	-0.04	**1.34**
AT4G18100	Ribosomal protein L32e	0.17	0.56	**0.84**
AT4G18230	unknown protein	-0.17	-0.70	**-0.84**
AT4G18330	Translation elongation factor EF1A/initiation factor IF2gamma family protein	0.16	0.38	**1.03**
AT4G18700	ATWL4_CIPK12_SnRK3.9_WL4__CBL-interacting protein kinase 12	-0.41	0.42	**1.08**
AT4G18730	RPL16B__ribosomal protein L16B	-0.14	0.32	**0.94**

AGI identifier	Gene annotation	30 min	2h	8h
AT4G18905	Transducin family protein / WD-40 repeat family protein	-0.19	0.35	**0.79**
AT4G19160	unknown protein	-0.40	**-1.48**	**-1.25**
AT4G19170	CCD4_NCED4__nine-cis-epoxycarotenoid dioxygenase 4	0.31	**-0.90**	-0.38
AT4G19200	proline-rich family protein	0.36	-0.31	**-1.08**
AT4G19410	Pectinacetylesterase family protein	0.02	-0.50	**-1.12**
AT4G19530	disease resistance protein (TIR-NBS-LRR class) family	-0.57	**-1.19**	-0.25
AT4G19690	ATIRT1_IRT1__iron-regulated transporter 1	0.60	0.18	**1.46**
AT4G19860	alpha/beta-Hydrolases superfamily protein	-0.01	**-1.01**	**-0.99**
AT4G19880	Glutathione S-transferase family protein	0.14	-0.71	**-1.09**
AT4G20070	AAH_ATAAH__allantoate amidohydrolase	-0.09	-0.41	**-0.99**
AT4G20380	LSD1 zinc finger family protein	-0.08	**-0.80**	-0.70
AT4G20390	Uncharacterised protein family (UPF0497)	0.23	0.17	**0.76**
AT4G20860	FAD-binding Berberine family protein	**0.81**	-0.32	**-1.18**
AT4G21150	HAP6__ribophorin II (RPN2) family protein	-0.12	0.16	**0.73**
AT4G21280	PSBQ_PSBQ-1_PSBQA__photosystem II subunit QA	0.64	-0.08	**-0.84**
AT4G21320	HSA32 (HEAT-STRESS-ASSOCIATED 32)	0.15	-0.05	**-0.74**
AT4G21810	DER2.1__DERLIN-2.1	0.40	-0.55	**-1.05**
AT4G21870	HSP20-like chaperones superfamily protein	**-0.74**	**-1.31**	**-1.75**
AT4G21910	MATE efflux family protein	-0.32	0.41	**0.91**
AT4G21960	PRXR1__Peroxidase superfamily protein	0.17	0.11	**1.03**
AT4G22210	LCR85 (Low-molecular-weight cysteine-rich 85)	0.08	-0.26	**0.76**
AT4G22220	ATISU1_ISU1__SufE/NifU family protein	**0.69**	0.25	-0.02
AT4G22610	Bifunctional inhibitor/lipid-transfer protein/seed storage 2S albumin superfamily protein	0.07	-0.08	**0.91**
AT4G22750	DHHC-type zinc finger family protein	0.04	-0.16	**-0.73**
AT4G22870	2-oxoglutarate (2OG) and Fe(II)-dependent oxygenase superfamily protein	0.01	0.03	**1.01**
AT4G22880	ANS_LDOX_TDS4_TT18__leucoanthocyanidin dioxygenase	-0.17	0.10	**0.79**
AT4G22920	ATNYE1_NYE1__non-yellowing 1	0.14	-0.29	**-0.79**
AT4G23100	ATECS1_CAD2_GSH1_GSHA_PAD2_RML1__glutamate-cysteine ligase	**0.67**	0.09	-0.33
AT4G23450	RING/U-box superfamily protein	-0.33	0.09	**-0.77**
AT4G23470	PLAC8 family protein	-0.07	-0.26	**-1.00**
AT4G23600	CORI3_JR2__Tyrosine transaminase family protein	-0.08	**0.87**	**1.12**
AT4G23890	unknown protein	0.19	0.11	**-0.88**
AT4G24120	ATYSL1_YSL1__YELLOW STRIPE like 1	-0.05	0.14	**0.75**
AT4G24160	alpha/beta-Hydrolases superfamily protein	0.17	-0.31	**-0.97**
AT4G24190	AtHsp90-7_AtHsp90.7_HSP90.7_SHD__Chaperone protein htpG family protein	0.05	0.00	**1.04**
AT4G24230	ACBP3 (ACYL-COA-BINDING DOMAIN 3)	0.19	**-1.31**	**-1.90**
AT4G24620	PGI_PGI1__phosphoglucose isomerase 1	0.03	0.29	**0.96**
AT4G24780	Pectin lyase-like superfamily protein	-0.07	-0.05	**1.77**
AT4G24830	arginosuccinate synthase family	0.17	**0.78**	**1.41**
AT4G25050	ACP4__acyl carrier protein 4	-0.30	-0.24	**-1.06**
AT4G25080	CHLM__magnesium-protoporphyrin IX methyltransferase	0.17	-0.49	**-1.25**
AT4G25170	Uncharacterised conserved protein (UCP012943)	0.25	-0.30	**-1.75**
AT4G25340	ATFKBP53_FKBP53__FK506 BINDING PROTEIN 53	-0.46	0.48	**1.10**

AGI identifier	Gene annotation	30 min	2h	8h
AT4G25480	ATCBF3_CBF3_DREB1A__dehydration response element B1A	**0.66**	0.52	0.47
AT4G25570	ACYB-2__Cytochrome b561/ferric reductase transmembrane protein family	0.05	0.00	**-0.94**
AT4G25620	hydroxyproline-rich glycoprotein family protein	x	**-0.83**	-0.64
AT4G25630	ATFIB2_FIB2__fibrillarin 2	-0.39	**1.15**	**1.97**
AT4G25690	unknown protein	-0.32	-0.58	**-1.12**
AT4G25730	FtsJ-like methyltransferase family protein	-0.49	0.61	**1.23**
AT4G25810	XTH23_XTR6_xyloglucan endotransglycosylase 6	**-0.94**	**-1.38**	-0.46
AT4G25890	60S acidic ribosomal protein family	-0.26	0.33	**1.12**
AT4G26110	ATNAP1;1_NAP1;1__nucleosome assembly protein1;1	-0.35	0.17	**0.76**
AT4G26210	Mitochondrial ATP synthase subunit G protein	-0.22	0.40	**0.84**
AT4G26530	Aldolase superfamily protein	0.20	-0.25	**-1.25**
AT4G26850	VTC2__mannose-1-phosphate guanylyltransferase (GDP)s;GDP-galactose:mannose-1-phosphate guanylyltransferases;GDP-galactose:glucose-1-phosphate guanylyltransferases;GDP-galactose:myoinositol-1-phosphate guanylyltransferases;glucose-1-phosphate guanylyltransferase	0.18	**1.15**	0.14
AT4G26950	Protein of unknown function, DUF584	x	**0.76**	0.60
AT4G27270	Quinone reductase family protein	0.15	0.06	**-0.81**
AT4G27280	Calcium-binding EF-hand family protein	**-0.96**	-0.19	-0.23
AT4G27410	ANAC072_RD26__NAC (No Apical Meristem) domain transcriptional regulator superfamily protein	0.12	**-0.99**	**-1.42**
AT4G27450	Aluminium induced protein with YGL and LRDR motifs	-0.33	**-2.07**	**-1.88**
AT4G27520	AtENODL2_ENODL2__early nodulin-like protein 2	0.42	**0.95**	0.63
AT4G27560	UDP-Glycosyltransferase superfamily protein	-0.13	0.67	**1.20**
AT4G27570	UDP-Glycosyltransferase superfamily protein	0.09	0.53	**1.30**
AT4G27585	SPFH/Band 7/PHB domain-containing membrane-associated protein family	0.16	0.13	**0.73**
AT4G27600	NARA5__pfkB-like carbohydrate kinase family protein	-0.33	-0.49	**-0.88**
AT4G27640	ARM repeat superfamily protein	x	0.24	**0.76**
AT4G27745	unknown protein	-0.02	**-0.80**	**-1.22**
AT4G27900	CCT motif family protein	-0.13	**1.14**	0.62
AT4G27940	ATMTM1_MTM1__manganese tracking factor for mitochondrial SOD2	-0.07	0.60	**0.79**
AT4G28030	Acyl-CoA N-acyltransferases (NAT) superfamily protein	-0.06	-0.06	**-0.94**
AT4G28040	Nodulin MtN21 /EamA-like transporter family protein	-0.11	-0.17	**-1.51**
AT4G28240	Wound-responsive family protein	-0.23	**-1.03**	**-1.00**
AT4G28250	ATEXPB3_ATHEXP BETA 1.6_EXPB3__expansin B3	-0.08	0.05	**2.06**
AT4G28300	Protein of unknown function (DUF1421)	0.00	-0.42	**-0.72**
AT4G28360	Ribosomal protein L22p/L17e family protein	-0.13	0.28	**1.06**
AT4G28450	nucleotide binding;protein binding	-0.20	0.43	**0.93**
AT4G28510	ATPHB1_PHB1__prohibitin 1	-0.15	-0.03	**0.95**
AT4G29030	Putative membrane lipoprotein	-0.06	0.03	**0.94**
AT4G29230	anac075_NAC075__NAC domain containing protein 75	0.20	0.09	**0.75**
AT4G29270	HAD superfamily, subfamily IIIB acid phosphatase	0.18	-0.13	**0.92**

AGI identifier	Gene annotation	30 min	2h	8h
AT4G29410	Ribosomal L28e protein family	-0.25	0.54	**0.90**
AT4G29510	ATPRMT11_ATPRMT1B_PRMT11_PRMT1B__arginine methyltransferase 11	-0.32	0.43	**0.92**
AT4G29680	Alkaline-phosphatase-like family protein	-0.08	0.28	**0.92**
AT4G29700	Alkaline-phosphatase-like family protein	0.08	0.42	**0.90**
AT4G29905	unknown protein	-0.35	**-1.75**	**-1.14**
AT4G29930	basic helix-loop-helix (bHLH) DNA-binding superfamily protein	0.09	**0.81**	0.01
AT4G30150	unknown protein	-0.10	0.21	**0.73**
AT4G30190	AHA2_HA2_PMA2__H(+)-ATPase 2	0.05	0.56	**1.73**
AT4G30270	MERI-5_MERI5B_SEN4_XTH24__xyloglucan endotransglucosylase/hydrolase 24	-0.07	**-1.34**	x
AT4G30280	ATXTH18_XTH18__xyloglucan endotransglucosylase/hydrolase 18	-0.46	**-1.02**	-0.15
AT4G30530	Class I glutamine amidotransferase-like superfamily protein	0.17	**1.19**	**0.95**
AT4G30650	Low temperature and salt responsive protein family	-0.22	0.68	**1.60**
AT4G30660	Low temperature and salt responsive protein family	-0.09	0.55	**1.06**
AT4G30800	Nucleic acid-binding, OB-fold-like protein	0.18	0.38	**1.06**
AT4G30810	scpl29__serine carboxypeptidase-like 29	0.30	0.11	**0.94**
AT4G30930	NFD1__Ribosomal protein L21	-0.06	0.12	**0.71**
AT4G30993	Calcineurin-like metallo-phosphoesterase superfamily protein	0.28	-0.27	**-1.08**
AT4G31500	ATR4_CYP83B1_RED1_RNT1_SUR2__cytochrome P450, family 83, subfamily B, polypeptide 1	0.04	**1.13**	**1.40**
AT4G31700	RPS6_RPS6A__ribosomal protein S6	-0.19	0.48	**1.06**
AT4G31790	Tetrapyrrole (Corrin/Porphyrin) Methylases	0.25	0.48	**0.82**
AT4G31810	ATP-dependent caseinolytic (Clp) protease/crotonase family protein	-0.15	0.39	**1.19**
AT4G31850	PGR3__proton gradient regulation 3	-0.29	-0.12	**-0.80**
AT4G31870	ATGPX7_GPX7__glutathione peroxidase 7	0.28	-0.27	**-0.81**
AT4G31910	HXXXD-type acyl-transferase family protein	-0.05	0.05	**0.89**
AT4G31985	Ribosomal protein L39 family protein	-0.08	0.32	**0.95**
AT4G32060	calcium-binding EF hand family protein	-0.50	**-0.99**	-0.63
AT4G32400	ATBT1_EMB104_EMB42_SHS1__Mitochondrial substrate carrier family protein	0.07	0.29	**0.73**
AT4G32410	AtCESA1_CESA1_RSW1__cellulose synthase 1	-0.56	-0.33	**0.88**
AT4G32480	unknown protein	-0.63	**-1.41**	**-1.20**
AT4G32520	AtSHMT3_SHM3__serine hydroxymethyltransferase 3	-0.15	0.36	**0.81**
AT4G32850	nPAP_PAP(IV)__nuclear poly(a) polymerase	**-0.68**	-0.19	-0.17
AT4G32870	Polyketide cyclase/dehydrase and lipid transport superfamily protein	0.08	-0.56	**-1.60**
AT4G32940	GAMMA-VPE_GAMMAVPE__gamma vacuolar processing enzyme	0.26	-0.41	**-0.98**
AT4G33030	SQD1__sulfoquinovosyldiacylglycerol 1	0.14	**1.02**	**1.61**
AT4G33070	Thiamine pyrophosphate dependent pyruvate decarboxylase family protein	0.13	**1.29**	**0.75**
AT4G33110	S-adenosyl-L-methionine-dependent methyltransferases superfamily protein	0.45	-0.12	**-0.80**

AGI identifier	Gene annotation	30 min	2h	8h
AT4G33420	Peroxidase superfamily protein	-0.24	-0.57	**-0.76**
AT4G33540	metallo-beta-lactamase family protein	-0.10	0.21	**-0.72**
AT4G33610	glycine-rich protein	**0.68**	x	x
AT4G33680	AGD2__Pyridoxal phosphate (PLP)-dependent transferases superfamily protein	0.36	0.24	**0.93**
AT4G33905	Peroxisomal membrane 22 kDa (Mpv17/PMP22) family protein	-0.04	**0.89**	0.56
AT4G33940	RING/U-box superfamily protein	-0.42	-0.70	**-0.96**
AT4G33980	unknown protein	x	0.01	**-1.20**
AT4G34030	MCCB__3-methylcrotonyl-CoA carboxylase	0.36	**-0.94**	x
AT4G34050	CCoAOMT1__S-adenosyl-L-methionine-dependent methyltransferases superfamily protein	0.62	**0.84**	**1.23**
AT4G34138	UGT73B1__UDP-glucosyl transferase 73B1	-0.03	**-1.36**	**-1.54**
AT4G34250	KCS16__3-ketoacyl-CoA synthase 16	-0.17	**-0.81**	-0.18
AT4G34350	CLB6_HDR_ISPH__4-hydroxy-3-methylbut-2-enyl diphosphate reductase	-0.08	-0.08	**-0.71**
AT4G34555	Ribosomal protein S25 family protein	-0.13	0.46	**0.86**
AT4G34588	CPuORF2__conserved peptide upstream open reading frame 2	-0.48	**0.81**	**1.73**
AT4G34670	Ribosomal protein S3Ae	-0.40	0.10	**0.74**
AT4G34850	LAP5__Chalcone and stilbene synthase family protein	-0.09	0.14	**0.78**
AT4G34870	ATCYP1_ROC5__rotamase cyclophilin 5	-0.21	0.51	**1.05**
AT4G34920	PLC-like phosphodiesterases superfamily protein	x	**-0.96**	**-1.17**
AT4G34950	Major facilitator superfamily protein	0.04	**1.57**	**1.83**
AT4G35090	CAT2__catalase 2	0.12	0.21	**-0.98**
AT4G35160	O-methyltransferase family protein	-0.10	0.41	**1.00**
AT4G35300	TMT2__tonoplast monosaccharide transporter2	-0.03	0.41	**0.72**
AT4G35630	PSAT__phosphoserine aminotransferase	0.65	**1.12**	**1.58**
AT4G35650	IDH-III__isocitrate dehydrogenase III	0.40	0.39	**0.75**
AT4G35750	SEC14 cytosolic factor family protein / phosphoglyceride transfer family protein	0.34	**-0.83**	**-1.40**
AT4G35770	ATSEN1_DIN1_SEN1_SEN1__Rhodanese/Cell cycle control phosphatase superfamily protein	-0.10	**-1.64**	**-2.67**
AT4G35860	ATGB2_ATRAB2C_ATRABB1B_GB2__GTP-binding 2	-0.08	-0.47	**-0.90**
AT4G36010	Pathogenesis-related thaumatin superfamily protein	0.25	**1.34**	**0.81**
AT4G36020	CSDP1__cold shock domain protein 1	0.11	**0.79**	**0.97**
AT4G36040	Chaperone DnaJ-domain superfamily protein	0.05	-0.50	**-1.55**
AT4G36050	endonuclease/exonuclease/phosphatase family protein	0.02	-0.31	**-0.72**
AT4G36130	Ribosomal protein L2 family	-0.10	0.53	**0.89**
AT4G36400	FAD-linked oxidases family protein	0.34	-0.18	**-0.78**
AT4G36410	UBC17__ubiquitin-conjugating enzyme 17	x	**-0.85**	-0.17
AT4G36530	alpha/beta-Hydrolases superfamily protein	-0.10	-0.22	**-0.87**
AT4G36580	AAA-type ATPase family protein	0.11	0.48	**1.17**
AT4G36660	Protein of unknown function (DUF1195)	0.25	0.29	**0.90**
AT4G36670	Major facilitator superfamily protein	-0.11	**-2.31**	**-1.61**
AT4G36680	Tetratricopeptide repeat (TPR)-like superfamily protein	-0.17	0.32	**0.82**
AT4G36830	HOS3-1__GNS1/SUR4 membrane protein family	-0.10	0.35	**0.94**

AGI identifier	Gene annotation	30 min	2h	8h
AT4G36850	PQ-loop repeat family protein / transmembrane family protein	0.29	**-1.27**	**-1.71**
AT4G37060	AtPLAIVB_PLA IVB_PLP5__PATATIN-like protein 5	0.12	-0.19	**-0.79**
AT4G37200	HCF164__Thioredoxin superfamily protein	x	0.00	**-0.76**
AT4G37220	Cold acclimation protein WCOR413 family	x	-0.48	**-1.75**
AT4G37260	ATMYB73_MYB73__myb domain protein 73	-0.54	**-1.09**	-0.34
AT4G37295	unknown protein	0.07	0.47	**0.81**
AT4G37330	CYP81D4__cytochrome P450, family 81, subfamily D, polypeptide 4	0.32	-0.16	**-0.78**
AT4G37410	CYP81F4__cytochrome P450, family 81, subfamily F, polypeptide 4	0.26	0.35	**0.87**
AT4G37450	AGP18_ATAGP18__arabinogalactan protein 18	0.09	-0.26	**0.99**
AT4G37520	Peroxidase superfamily protein	-0.02	**-1.07**	**-1.63**
AT4G37530	Peroxidase superfamily protein	-0.13	**-0.74**	**-0.89**
AT4G37910	mtHsc70-1__mitochondrial heat shock protein 70-1	-0.44	0.57	**1.62**
AT4G37925	NDH-M (SUBUNIT NDH-M OF NAD(P)H:PLASTOQUINONE DEHYDROGENASE COMPLEX)	0.14	-0.51	**-0.79**
AT4G38060	unknown protein	-0.17	-0.37	**-0.71**
AT4G38080	hydroxyproline-rich glycoprotein family protein	0.64	x	**1.01**
AT4G38100	unknown protein	-0.22	**0.89**	0.68
AT4G38400	ATEXLA2_ATEXPL2_ATHEXP BETA 2.2_EXLA2_EXPL2__expansin-like A2	**-0.69**	-0.29	-0.20
AT4G38470	ACT-like protein tyrosine kinase family protein	-0.60	**-2.68**	**-2.39**
AT4G38510	ATPase, V1 complex, subunit B protein	-0.04	0.13	**0.86**
AT4G38630	ATMCB1_MBP1_MCB1_RPN10__regulatory particle non-ATPase 10	0.49	0.47	**0.76**
AT4G38660	Pathogenesis-related thaumatin superfamily protein	0.15	0.34	**0.77**
AT4G38740	ROC1__rotamase CYP 1	-0.15	0.62	**0.98**
AT4G38770	ATPRP4_PRP4__proline-rich protein 4	**0.91**	0.12	x
AT4G38810	Calcium-binding EF-hand family protein	0.19	-0.64	**-1.61**
AT4G38970	FBA2__fructose-bisphosphate aldolase 2	**1.18**	0.24	0.00
AT4G39070	B-box zinc finger family protein	0.07	-0.31	**-0.89**
AT4G39090	RD19_RD19A__Papain family cysteine protease	0.24	**-0.99**	**-1.38**
AT4G39200	Ribosomal protein S25 family protein	-0.34	0.21	**0.73**
AT4G39210	APL3__Glucose-1-phosphate adenylyltransferase family protein	-0.29	**0.87**	**2.16**
AT4G39260	ATGRP8_CCR1_GR-RBP8_GRP8__cold, circadian rhythm, and RNA binding 1	0.18	0.45	**0.95**
AT4G39280	phenylalanyl-tRNA synthetase, putative / phenylalanine--tRNA ligase, putative	-0.37	0.20	**0.89**
AT4G39300	unknown protein	0.15	0.47	**0.98**
AT4G39330	ATCAD9_CAD9__cinnamyl alcohol dehydrogenase 9	-0.05	**1.04**	0.55
AT4G39350	ATCESA2_ATH-A_CESA2__cellulose synthase A2	-0.47	-0.02	**0.88**
AT4G39390	ATNST-KT1_NST-K1__nucleotide sugar transporter-KT 1	0.08	0.12	**0.72**
AT4G39660	AGT2__alanine:glyoxylate aminotransferase 2	-0.10	-0.42	**-0.84**
AT4G39675	unknown protein	-0.18	-0.53	**-1.15**
AT4G39730	Lipase/lipooxygenase, PLAT/LH2 family protein	0.25	0.74	**1.12**
AT4G39780	Integrase-type DNA-binding superfamily protein	0.22	-0.38	**-1.09**

AGI identifier	Gene annotation	30 min	2h	8h
AT4G39800	ATIPS1_ATMIPS1_MI-1-P SYNTHASE_MIPS1__myo-inositol-1-phosphate synthase 1	0.12	**1.16**	**1.16**
AT4G39940	AKN2_APK2__APS-kinase 2	0.11	**1.43**	**1.92**
AT4G39950	CYP79B2__cytochrome P450, family 79, subfamily B, polypeptide 2	-0.02	**1.01**	**1.37**
AT4G39980	DHS1__3-deoxy-D-arabino-heptulosonate 7-phosphate synthase 1	-0.16	**0.85**	x
AT5G01015	unknown protein	-0.53	**-0.80**	-0.39
AT5G01220	SQD2__sulfoquinovosyldiacylglycerol 2	0.37	**1.18**	**0.88**
AT5G01500	TAAC__thylakoid ATP/ADP carrier	-0.01	0.35	**1.09**
AT5G01610	Protein of unknown function, DUF538	-0.04	-0.52	**-0.92**
AT5G01715	pseudogene	-0.16	**0.98**	-0.02
AT5G02050	Mitochondrial glycoprotein family protein	-0.11	0.49	**1.28**
AT5G02090	unknown protein	0.21	-0.66	**-1.17**
AT5G02130	NDP1__Tetratricopeptide repeat (TPR)-like superfamily protein	-0.07	0.07	**-1.06**
AT5G02160	unknown protein	0.22	-0.09	**-0.72**
AT5G02240	NAD(P)-binding Rossmann-fold superfamily protein	-0.25	0.18	**0.75**
AT5G02490	Heat shock protein 70 (Hsp 70) family protein	-0.32	0.72	**0.82**
AT5G02500	AT-HSC70-1_HSC70_HSC70-1_HSP70-1__heat shock cognate protein 70-1	-0.21	0.40	**0.72**
AT5G02610	Ribosomal L29 family protein	0.01	0.39	**0.93**
AT5G02870	Ribosomal protein L4/L1 family	-0.08	0.44	**1.08**
AT5G02960	Ribosomal protein S12/S23 family protein	-0.38	0.28	**0.97**
AT5G03040	iqd2__IQ-domain 2	0.17	**-0.78**	0.06
AT5G03210	unknown protein	x	**1.23**	**0.80**
AT5G03240	UBQ3__polyubiquitin 3	0.01	-0.33	**-0.82**
AT5G03300	ADK2__adenosine kinase 2	-0.17	0.35	**1.53**
AT5G03380	Heavy metal transport/detoxification superfamily protein	**0.90**	-0.20	0.18
AT5G03520	ATRAB-E1D_ATRAB8C_ATRABE1D_RAB-E1D_RAB8C__RAB GTPase homolog 8C	-0.18	**-0.81**	-0.21
AT5G03610	GDSL-like Lipase/Acylhydrolase superfamily protein	0.18	0.43	**0.74**
AT5G03630	ATMDAR2__Pyridine nucleotide-disulphide oxidoreductase family protein	0.23	**0.77**	**0.76**
AT5G03650	SBE2.2__starch branching enzyme 2.2	-0.13	0.25	**1.01**
AT5G03740	HD2C_HDT3__histone deacetylase 2C	-0.14	0.64	**0.76**
AT5G04040	SDP1__Patatin-like phospholipase family protein	-0.22	-0.59	**-0.88**
AT5G04160	Nucleotide-sugar transporter family protein	0.00	0.11	**1.02**
AT5G04840	bZIP protein	-0.04	0.25	**0.71**
AT5G04950	ATNAS1_NAS1__nicotianamine synthase 1	0.65	**1.06**	**1.36**
AT5G05010	clathrin adaptor complexes medium subunit family protein	0.33	0.11	**0.73**
AT5G05100	Single-stranded nucleic acid binding R3H protein	0.04	-0.46	**-1.07**
AT5G05270	Chalcone-flavanone isomerase family protein	-0.10	0.60	**1.61**
AT5G05410	DREB2_DREB2A__DRE-binding protein 2A	0.40	-0.61	**-1.68**
AT5G05440	PYL5_RCAR8__Polyketide cyclase/dehydrase and lipid transport superfamily protein	-0.05	**-0.94**	**-0.98**
AT5G05500	Pollen Ole e 1 allergen and extensin family protein	0.26	0.31	**0.95**

AGI identifier	Gene annotation	30 min	2h	8h
AT5G05590	PAI2 (PHOSPHORIBOSYLANTHRANILATE ISOMERASE 2); phosphoribosylanthranilate isomerase, PAI1 (PHOSPHORIBOSYLANTHRANILATE ISOMERASE 1); phosphoribosylanthranilate isomerase	0.07	0.31	**0.85**
AT5G06110	DnaJ domain ;Myb-like DNA-binding domain	0.01	**0.85**	**0.72**
AT5G06300	Putative lysine decarboxylase family protein	-0.39	-0.62	**-0.95**
AT5G06370	NC domain-containing protein-related	-0.02	-0.21	**-0.78**
AT5G06550	unknown protein	0.15	0.26	**0.90**
AT5G06690	WCRKC1__WCRKC thioredoxin 1	0.02	**-1.24**	**-1.51**
AT5G06760	LEA4-5__Late Embryogenesis Abundant 4-5	0.07	**0.99**	-0.02
AT5G06860	ATPGIP1_PGIP1__polygalacturonase inhibiting protein 1	0.07	-0.57	**-1.02**
AT5G06870	ATPGIP2_PGIP2__polygalacturonase inhibiting protein 2	-0.02	-0.42	**-0.71**
AT5G07030	Eukaryotic aspartyl protease family protein	0.05	0.07	**0.88**
AT5G07080	HXXXD-type acyl-transferase family protein	0.27	**-0.76**	-0.53
AT5G07090	Ribosomal protein S4 (RPS4A) family protein	-0.16	0.18	**0.94**
AT5G07340	Calreticulin family protein	-0.19	0.05	**0.83**
AT5G07440	GDH2__glutamate dehydrogenase 2	x	**-2.08**	**-2.09**
AT5G07510	ATGRP-4_ATGRP14_GRP-4_GRP14__glycine-rich protein 14	**0.71**	-0.71	-0.67
AT5G07860	HXXXD-type acyl-transferase family protein	-0.02	-0.28	**-0.99**
AT5G07870	HXXXD-type acyl-transferase family protein	-0.10	-0.31	**-1.24**
AT5G07990	CYP75B1_D501_TT7__Cytochrome P450 superfamily protein	-0.14	0.18	**1.69**
AT5G08180	Ribosomal protein L7Ae/L30e/S12e/Gadd45 family protein	-0.43	0.54	**0.83**
AT5G08260	scpl35__serine carboxypeptidase-like 35	-0.02	0.10	**1.24**
AT5G08500	Transmembrane CLPTM1 family protein	**-0.66**	0.19	0.21
AT5G08570	Pyruvate kinase family protein	0.08	**0.94**	**1.25**
AT5G08620	ATRH25_STRS2__DEA(D/H)-box RNA helicase family protein	-0.49	0.20	**0.81**
AT5G08640	ATFLS1_FLS_FLS1__flavonol synthase 1	-0.10	**0.76**	**1.50**
AT5G09440	EXL4__EXORDIUM like 4	-0.19	**-0.93**	**-0.76**
AT5G09510	Ribosomal protein S19 family protein	-0.18	0.25	**0.84**
AT5G09590	heat shock protein 70 (Hsc70-5); nuclear	0.10	0.72	**1.13**
AT5G09660	PMDH2__peroxisomal NAD-malate dehydrogenase 2	0.19	-0.11	**-1.21**
AT5G09810	ACT7__actin 7	-0.21	-0.01	**0.98**
AT5G09870	CESA5__cellulose synthase 5	-0.49	0.17	**1.20**
AT5G09880	Splicing factor, CC1-like	**-0.85**	-0.16	0.01
AT5G10380	ATRING1_RING1__RING/U-box superfamily protein	0.22	**0.76**	-0.30
AT5G10450	14-3-3lambda_AFT1_GRF6__G-box regulating factor 6	0.17	-0.51	**-1.44**
AT5G10540	Zincin-like metalloproteases family protein	**-0.74**	-0.18	0.21
AT5G10580	Protein of unknown function, DUF599	0.03	0.15	**0.91**
AT5G10695	unknown protein	-0.07	**-0.92**	**-0.98**
AT5G10830	S-adenosyl-L-methionine-dependent methyltransferases superfamily protein	0.06	0.00	**0.74**
AT5G10860	Cystathionine beta-synthase (CBS) family protein	-0.17	**-0.92**	**-1.54**
AT5G10920	L-Aspartase-like family protein	-0.15	0.36	**1.16**
AT5G11110	ATSPS2F_KNS2_SPS1_SPS2F__sucrose phosphate synthase 2F	-0.22	**1.50**	**0.72**

AGI identifier	Gene annotation	30 min	2h	8h
AT5G11170	DEAD/DEAH box RNA helicase family protein	-0.44	0.02	**0.80**
AT5G11240	Transducin family protein / WD-40 repeat family protein	0.09	0.13	**0.90**
AT5G11520	ASP3_YLS4__aspartate aminotransferase 3	0.17	-0.31	**-0.99**
AT5G11740	AGP15_ATAGP15__arabinogalactan protein 15	-0.24	0.21	**0.95**
AT5G11880	Pyridoxal-dependent decarboxylase family protein	0.29	0.25	**0.73**
AT5G12410	THUMP domain-containing protein	-0.30	0.08	**0.75**
AT5G12470	Protein of unknown function (DUF3411)	-0.12	0.68	**1.42**
AT5G13000	ATGSL12_gsl12_GSL12__glucan synthase-like 12	-0.29	0.14	**0.85**
AT5G13080	ATWRKY75_WRKY75__WRKY DNA-binding protein 75	0.27	**-0.76**	**-1.72**
AT5G13170	SAG29__senescence-associated gene 29	0.22	**1.24**	**0.72**
AT5G13190	GSH-INDUCED LITAF DOMAIN PROTEIN	**-0.70**	-0.01	-0.13
AT5G13200	GRAM domain family protein	**0.66**	x	0.24
AT5G13400	Major facilitator superfamily protein	-0.06	0.29	**1.14**
AT5G13420	Aldolase-type TIM barrel family protein	0.25	0.35	**1.12**
AT5G13490	AAC2__ADP/ATP carrier 2	x	0.66	**1.05**
AT5G13570	ATDCP2_DCP2_TDT__decapping 2	-0.17	-0.40	**-0.74**
AT5G13710	CPH_SMT1__sterol methyltransferase 1	-0.19	**-0.88**	-0.61
AT5G13720	Uncharacterised protein family (UPF0114)	-0.01	-0.18	**-1.10**
AT5G13750	ZIFL1__zinc induced facilitator-like 1	0.09	**0.88**	-0.24
AT5G13770	Pentatricopeptide repeat (PPR-like) superfamily protein	0.40	-0.49	**-0.87**
AT5G13930	ATCHS_CHS_TT4__Chalcone and stilbene synthase family protein	-0.02	**0.84**	**1.85**
AT5G14040	PHT3;1__phosphate transporter 3;1	0.49	0.46	**0.75**
AT5G14120	Major facilitator superfamily protein	x	**-1.65**	**-2.06**
AT5G14180	MPL1__Myzus persicae-induced lipase 1	x	**-1.21**	**-2.45**
AT5G14200	ATIMD1_IMD1__isopropylmalate dehydrogenase 1	0.06	0.44	**1.70**
AT5G14470	GHMP kinase family protein	-0.05	-0.46	**-1.35**
AT5G14580	polyribonucleotide nucleotidyltransferase, putative	-0.23	0.11	**1.30**
AT5G14640	ATSK13_SK13__shaggy-like kinase 13	0.03	0.60	**1.24**
AT5G14780	FDH__formate dehydrogenase	**0.67**	-0.02	**-1.88**
AT5G14910	Heavy metal transport/detoxification superfamily protein	-0.12	-0.36	**-1.00**
AT5G15090	ATVDAC3_VDAC3__voltage dependent anion channel 3	-0.05	0.63	**1.52**
AT5G15200	Ribosomal protein S4	-0.18	0.13	**0.71**
AT5G15350	AtENODL17_ENODL17__early nodulin-like protein 17	-0.27	**-1.26**	-0.01
AT5G15450	APG6_CLPB-P_CLPB3__casein lytic proteinase B3	0.05	0.35	**0.76**
AT5G15490	UDP-glucose 6-dehydrogenase family protein	0.09	0.35	**1.54**
AT5G15550	Transducin family protein / WD-40 repeat family protein	-0.05	0.38	**0.73**
AT5G15650	ATRGP2_RGP2__reversibly glycosylated polypeptide 2	-0.03	0.01	**0.81**
AT5G15850	ATCOL1_COL1__CONSTANS-like 1	0.42	-0.23	**-0.88**
AT5G15960	KIN1__stress-responsive protein (KIN1) / stress-induced protein (KIN1)	-0.18	0.25	**0.87**
AT5G16110	unknown protein	-0.39	**-1.55**	**-1.37**
AT5G16130	Ribosomal protein S7e family protein	-0.06	0.48	**1.05**
AT5G16360	NC domain-containing protein	x	-0.32	**-0.72**
AT5G16370	AAE5__acyl activating enzyme 5	0.01	**-1.61**	**-1.58**
AT5G16400	ATF2_TRXF2__thioredoxin F2	-0.03	-0.46	**-0.92**

AGI identifier	Gene annotation	30 min	2h	8h
AT5G16570	GLN1;4__glutamine synthetase 1;4	0.21	0.71	**1.70**
AT5G16660	unknown protein	0.11	-0.28	**-0.98**
AT5G16970	AER_AT-AER__alkenal reductase	**0.79**	0.06	**-1.28**
AT5G17010	Major facilitator superfamily protein	-0.04	0.15	**0.77**
AT5G17020	ATCRM1_ATXPO1_HIT2_XPO1_XPO1A__exportin 1A	**-0.73**	-0.09	0.28
AT5G17050	UGT78D2__UDP-glucosyl transferase 78D2	**0.71**	0.37	0.01
AT5G17220	ATGSTF12_GST26_GSTF12_TT19__glutathione S-transferase phi 12	0.01	0.28	**2.27**
AT5G17280	unknown protein	0.41	-0.42	**-0.89**
AT5G17300	RVE1__Homeodomain-like superfamily protein	-0.16	**-1.00**	-0.27
AT5G17310	AtUGP2_UGP2__UDP-glucose pyrophosphorylase 2	0.04	0.14	**0.86**
AT5G17400	ER-ANT1__endoplasmic reticulum-adenine nucleotide transporter 1	-0.17	-0.36	**-0.90**
AT5G17920	ATCIMS_ATMETS_ATMS1__Cobalamin-independent synthase family protein	-0.05	0.23	**1.30**
AT5G17990	pat1_TRP1__tryptophan biosynthesis 1	0.49	0.14	**0.72**
AT5G18140	Chaperone DnaJ-domain superfamily protein	0.08	-0.65	**-1.05**
AT5G18170	GDH1__glutamate dehydrogenase 1	-0.09	**-1.02**	**-1.48**
AT5G18180	H/ACA ribonucleoprotein complex, subunit Gar1/Naf1 protein	-0.18	0.45	**0.91**
AT5G18470	Curculin-like (mannose-binding) lectin family protein	0.54	**1.06**	0.39
AT5G18490	Plant protein of unknown function (DUF946)	0.34	-0.34	**-0.78**
AT5G18600	Thioredoxin superfamily protein	-0.49	**-1.65**	x
AT5G18630	alpha/beta-Hydrolases superfamily protein	-0.30	**-1.26**	**-1.41**
AT5G18650	CHY-type/CTCHY-type/RING-type Zinc finger protein	-0.17	**-1.05**	**-1.14**
AT5G18670	BAM9_BMY3__beta-amylase 3	-0.37	**-2.19**	**-0.94**
AT5G18840	Major facilitator superfamily protein	0.09	-0.28	**1.00**
AT5G19110	Eukaryotic aspartyl protease family protein	-0.47	-0.03	**1.14**
AT5G19120	Eukaryotic aspartyl protease family protein	0.11	**-2.31**	**-2.09**
AT5G19230	unknown protein	**0.84**	x	-0.06
AT5G19240	Glycoprotein membrane precursor GPI-anchored	**0.78**	0.55	0.16
AT5G19510	Translation elongation factor EF1B/ribosomal protein S6 family protein	-0.10	0.40	**0.97**
AT5G19550	AAT2_ASP2__aspartate aminotransferase 2	0.09	0.26	**0.75**
AT5G19690	STT3A__staurosporin and temperature sensitive 3-like A	-0.33	-0.09	**0.86**
AT5G19855	Chaperonin-like RbcX protein	0.18	-0.20	**-1.06**
AT5G20160	Ribosomal protein L7Ae/L30e/S12e/Gadd45 family protein	-0.20	0.63	**1.13**
AT5G20190	unknown protein	0.48	**1.50**	**1.03**
AT5G20230	ATBCB_BCB_BCB_SAG14__blue-copper-binding protein	0.08	**-0.76**	**-1.99**
AT5G20250	DIN10__Raffinose synthase family protein	-0.21	**-3.14**	**-2.34**
AT5G20280	ATSPS1F_SPS1F__sucrose phosphate synthase 1F	-0.55	0.43	**1.72**
AT5G20290	Ribosomal protein S8e family protein	-0.40	0.27	**0.90**
AT5G20320	ATDCL4_DCL4__dicer-like 4	-0.05	-0.56	**-1.13**
AT5G20520	WAV2__alpha/beta-Hydrolases superfamily protein	0.24	-0.42	**-0.92**
AT5G20900	JAZ12_TIFY3B__jasmonate-zim-domain protein 12	**0.67**	-0.02	x
AT5G21020	unknown protein	0.27	-0.26	**-0.99**
AT5G21170	AKINBETA1__5'-AMP-activated protein kinase beta-2 subunit protein	0.17	**-0.79**	-0.30

AGI identifier	Gene annotation	30 min	2h	8h
AT5G21940	unknown protein	-0.59	**-1.80**	x
AT5G22100	RNA cyclase family protein	-0.04	0.65	**0.83**
AT5G22140	FAD/NAD(P)-binding oxidoreductase family protein	0.19	0.26	**-0.96**
AT5G22270	unknown protein	0.17	-0.61	**-0.78**
AT5G22440	Ribosomal protein L1p/L10e family	-0.29	0.63	**1.20**
AT5G22650	ATHD2_ATHD2B_HD2_HD2B_HDA4_HDT02_HDT2__histone deacetylase 2B	0.16	**0.96**	**1.55**
AT5G22660	F-box family protein	-0.11	**0.75**	**1.28**
AT5G22740	ATCSLA02_ATCSLA2_CSLA02_CSLA2__cellulose synthase-like A02	-0.27	0.34	**1.23**
AT5G22920	CHY-type/CTCHY-type/RING-type Zinc finger protein	-0.63	**-2.55**	**-1.82**
AT5G23010	IMS3_MAM1__methylthioalkylmalate synthase 1	0.14	0.28	**0.94**
AT5G23020	IMS2_MAM-L_MAM3__2-isopropylmalate synthase 2	-0.10	-0.03	**1.87**
AT5G23220	NIC3__nicotinamidase 3	0.30	**1.63**	**1.00**
AT5G23250	Succinyl-CoA ligase, alpha subunit	-0.03	0.31	**0.83**
AT5G23340	RNI-like superfamily protein	0.16	-0.47	**-1.06**
AT5G23530	AtCXE18_CXE18__carboxyesterase 18	0.13	0.45	**0.83**
AT5G23660	MTN3__homolog of Medicago truncatula MTN3	0.03	-0.21	**-0.97**
AT5G23730	Transducin family protein / WD-40 repeat family protein	**0.73**	-0.47	**-0.71**
AT5G23740	RPS11-BETA__ribosomal protein S11-beta	-0.10	0.42	**0.97**
AT5G23830	MD-2-related lipid recognition domain-containing protein	-0.06	-0.12	**1.59**
AT5G23840	MD-2-related lipid recognition domain-containing protein	0.08	0.04	**0.78**
AT5G23900	Ribosomal protein L13e family protein	-0.21	0.28	**0.76**
AT5G24120	ATSIG5_SIG5_SIGE__sigma factor E	0.23	-0.26	**-0.84**
AT5G24160	SQE6__squalene monoxygenase 6	-0.19	-0.05	**-1.36**
AT5G24165	unknown protein	0.05	-0.40	**-0.83**
AT5G24490	30S ribosomal protein, putative	0.27	**-1.28**	**-1.82**
AT5G24610	unknown protein	-0.32	-0.38	**-0.77**
AT5G24655	LSU4__response to low sulfur 4	-0.19	**0.79**	**0.80**
AT5G24660	LSU2__response to low sulfur 2	-0.03	**1.42**	**0.93**
AT5G24760	GroES-like zinc-binding dehydrogenase family protein	-0.13	-0.07	**1.01**
AT5G24810	ABC1 family protein	-0.15	x	**-1.08**
AT5G25100	Endomembrane protein 70 protein family	-0.15	-0.23	**0.78**
AT5G25130	CYP71B12__cytochrome P450, family 71, subfamily B, polypeptide 12	-0.22	**-0.81**	-0.11
AT5G25210	unknown protein	-0.09	**-0.82**	-0.42
AT5G25280	serine-rich protein-related	-0.13	-0.59	**-0.73**
AT5G25610	ATRD22_RD22__BURP domain-containing protein	0.43	**1.12**	**1.25**
AT5G25630	Tetratricopeptide repeat (TPR)-like superfamily protein	-0.49	**-0.99**	**-0.75**
AT5G25757	unknown protein	0.04	0.71	**0.90**
AT5G25770	alpha/beta-Hydrolases superfamily protein	-0.12	-0.36	**-0.73**
AT5G25780	ATEIF3B-2_EIF3B_EIF3B-2__eukaryotic translation initiation factor 3B-2	-0.28	0.44	**0.83**
AT5G25900	ATKO1_CYP701A3_GA3__GA requiring 3	0.01	-0.21	**-0.78**
AT5G26260	TRAF-like family protein	0.12	-0.25	**1.59**
AT5G26667	uridine 5'-monophosphate (UMP)/cytidine 5'-monophosphate (CMP) kinase.	0.42	0.05	**0.86**

AGI identifier	Gene annotation	30 min	2h	8h
AT5G26740	Protein of unknown function (DUF300)	x	**-1.07**	**-0.73**
AT5G26820	ATIREG3_IREG3_IREG3_MAR1_RTS3__iron-regulated protein 3	-0.55	-0.53	**-0.81**
AT5G26830	Threonyl-tRNA synthetase	-0.38	0.20	**0.80**
AT5G26860	LON1_LON_ARA_ARA__lon protease 1	-0.01	0.07	**0.77**
AT5G27120	NOP56-like pre RNA processing ribonucleoprotein	-0.08	0.50	**1.43**
AT5G27280	Zim17-type zinc finger protein	x	-0.09	**-0.98**
AT5G27290	unknown protein	-0.19	-0.44	**-0.77**
AT5G27330	Prefoldin chaperone subunit family protein	-0.13	0.29	**1.13**
AT5G27350	SFP1__Major facilitator superfamily protein	-0.05	-0.69	**-1.19**
AT5G27770	Ribosomal L22e protein family	0.02	0.13	**0.83**
AT5G27850	Ribosomal protein L18e/L15 superfamily protein	**-0.70**	0.36	**0.88**
AT5G27860	unknown protein	**-0.85**	-0.16	-0.63
AT5G28050	Cytidine/deoxycytidylate deaminase family protein	-0.08	**-1.20**	**-1.79**
AT5G28510	BGLU24__beta glucosidase 24	**0.94**	0.07	0.47
AT5G28770	AtbZIP63_BZO2H3__bZIP transcription factor family protein	-0.31	**-2.38**	**-1.84**
AT5G28840	GME__GDP-D-mannose 3',5'-epimerase	-0.18	-0.57	**-0.95**
AT5G33290	XGD1__xylogalacturonan deficient 1	-0.11	**0.81**	0.53
AT5G33320	ARAPPT_CUE1_PPT__Glucose-6-phosphate/phosphate translocator-related	-0.39	0.29	**1.12**
AT5G33370	GDSL-like Lipase/Acylhydrolase superfamily protein	0.44	0.28	**1.06**
AT5G35525	unknown protein	x	-0.53	**-1.17**
AT5G35530	Ribosomal protein S3 family protein	-0.19	0.30	**0.98**
AT5G35630	ATGSL1_GLN2_GS2__glutamine synthetase 2	**1.18**	0.32	0.03
AT5G36910	THI2.2__thionin 2.2	**0.68**	0.03	0.17
AT5G37170	O-methyltransferase family protein	0.11	0.23	**0.87**
AT5G37260	CIR1_RVE2__Homeodomain-like superfamily protein	0.06	-0.69	**-1.23**
AT5G37600	ATGLN1;1_ATGSR1_GLN1;1_GSR 1__glutamine synthase clone R1	0.17	**0.91**	**1.51**
AT5G37690	SGNH hydrolase-type esterase superfamily protein	0.44	0.23	**1.41**
AT5G38020	S-adenosyl-L-methionine-dependent methyltransferases superfamily protein	0.13	0.08	**1.79**
AT5G38060	unknown protein	-0.13	-0.25	**-1.01**
AT5G38520	alpha/beta-Hydrolases superfamily protein	0.27	-0.12	**-0.75**
AT5G39080	HXXXD-type acyl-transferase family protein	-0.38	**-0.78**	**-0.92**
AT5G39320	UDP-glucose 6-dehydrogenase family protein	0.17	0.11	**1.24**
AT5G39530	unknown protein	-0.20	-0.46	**-0.88**
AT5G39580	Peroxidase superfamily protein	0.30	**-1.56**	**-0.95**
AT5G39590	TLD-domain containing nucleolar protein	0.06	-0.41	**-0.75**
AT5G39610	ANAC092_ATNAC2_ATNAC6_NAC2_NAC6_ORE1__NAC domain containing protein 6	0.04	-0.45	**-0.80**
AT5G39690	ANAC093_NAC093__NAC domain containing protein 93	0.35	-0.24	**-0.76**
AT5G39740	OLI7_RPL5B__ribosomal protein L5 B	-0.11	0.28	**0.85**
AT5G39785	Protein of unknown function (DUF1666)	-0.63	**-2.70**	**-2.18**
AT5G39850	Ribosomal protein S4	-0.08	0.44	**1.25**
AT5G40390	SIP1__Raffinose synthase family protein	0.21	**0.78**	0.66
AT5G40480	EMB3012__embryo defective 3012	-0.59	0.10	**1.13**

AGI identifier	Gene annotation	30 min	2h	8h
AT5G40670	PQ-loop repeat family protein / transmembrane family protein	0.10	-0.07	**-0.75**
AT5G40760	G6PD6__glucose-6-phosphate dehydrogenase 6	0.07	0.46	**1.05**
AT5G40770	ATPHB3_PHB3__prohibitin 3	0.14	0.59	**0.90**
AT5G40850	UPM1__urophorphyrin methylase 1	0.37	**1.23**	0.49
AT5G40890	ATCLC-A_ATCLCA_CLC-A_CLC-A_CLCA__chloride channel A	-0.08	**-0.98**	**-1.00**
AT5G41080	PLC-like phosphodiesterases superfamily protein	-0.54	**-1.91**	**-2.08**
AT5G41340	ATUBC4_UBC4__ubiquitin conjugating enzyme 4	-0.23	-0.69	**-0.76**
AT5G41400	RING/U-box superfamily protein	0.30	**0.88**	0.51
AT5G41600	BTI3_RTNLB4__VIRB2-interacting protein 3	-0.20	0.08	**0.72**
AT5G41670	6-phosphogluconate dehydrogenase family protein	-0.14	**1.65**	**1.90**
AT5G42020	BIP_BIP2__Heat shock protein 70 (Hsp 70) family protein	**0.93**	x	0.67
AT5G42060	DEK, chromatin associated protein	0.00	0.32	**0.73**
AT5G42090	Lung seven transmembrane receptor family protein	**0.71**	0.19	x
AT5G42100	ATBG_PAP_ATBG_PPAP_BG_PPAP__beta-1,3-glucanase_putative	**-0.76**	-0.22	0.60
AT5G42110	unknown protein	-0.43	0.15	**0.73**
AT5G42445	pseudogene	-0.22	0.02	**0.71**
AT5G42650	AOS_CYP74A_DDE2__allene oxide synthase	0.25	**1.15**	**1.18**
AT5G42800	DFR_M318_TT3__dihydroflavonol 4-reductase	0.00	0.18	**0.79**
AT5G43060	Granulin repeat cysteine protease family protein	0.43	-0.42	**-0.79**
AT5G43150	unknown protein	0.04	0.41	**0.75**
AT5G43260	chaperone protein dnaJ-related	-0.09	-0.30	**-0.98**
AT5G43370	APT1_PHT1;2_PHT2__phosphate transporter 2	0.43	0.21	**1.01**
AT5G43430	ETFBETA__electron transfer flavoprotein beta	-0.16	-0.39	**-0.87**
AT5G43520	Cysteine/Histidine-rich C1 domain family protein	0.17	**-0.88**	**-0.80**
AT5G43570	PR (pathogenesis-related) peptide that belongs to the PR-6 proteinase inhibitor family.	-0.37	-0.72	**-1.88**
AT5G43580	Serine protease inhibitor, potato inhibitor I-type family protein	-0.18	-0.62	**-0.91**
AT5G43830	Aluminium induced protein with YGL and LRDR motifs	-0.13	**-0.91**	**-0.76**
AT5G44020	HAD superfamily, subfamily IIIB acid phosphatase	0.49	**-0.91**	**-0.92**
AT5G44110	ATNAP2_ATPOP1_POP1__P-loop containing nucleoside triphosphate hydrolases superfamily protein	0.12	0.38	**0.86**
AT5G44420	LCR77_PDF1.2_PDF1.2A__plant defensin 1.2	-0.15	-0.34	**-1.06**
AT5G44550	Uncharacterised protein family (UPF0497)	0.46	0.26	**1.05**
AT5G44585	unknown protein	0.11	-0.19	**-1.07**
AT5G44720	Molybdenum cofactor sulfurase family protein	-0.13	0.46	**0.91**
AT5G45800	MEE62__Leucine-rich repeat protein kinase family protein	0.08	0.03	**0.71**
AT5G45950	GDSL-like Lipase/Acylhydrolase superfamily protein	0.35	0.26	**0.75**
AT5G46110	APE2_TPT__Glucose-6-phosphate/phosphate translocator-related	**0.81**	-0.07	-0.35
AT5G46180	DELTA-OAT__ornithine-delta-aminotransferase	0.27	-0.43	**-0.85**
AT5G46250	RNA-binding protein	0.45	-0.28	**-0.74**
AT5G46290	KAS I_KAS1__3-ketoacyl-acyl carrier protein synthase I	0.06	0.37	**0.75**
AT5G47030	ATPase, F1 complex, delta/epsilon subunit	0.40	0.56	**0.76**
AT5G47060	Protein of unknown function (DUF581)	0.09	**1.24**	0.62

AGI identifier	Gene annotation	30 min	2h	8h
AT5G47220	ATERF-2_ATERF2_ERF2__ethylene responsive element binding factor 2	-0.05	0.13	**-0.71**
AT5G47500	Pectin lyase-like superfamily protein	**-0.69**	0.09	0.56
AT5G47550	Cystatin/monellin superfamily protein	0.22	-0.03	**-0.72**
AT5G47560	ATSDAT_ATTDT_TDT__tonoplast dicarboxylate transporter	0.28	-0.50	**-1.60**
AT5G47980	HXXXD-type acyl-transferase family protein	0.18	0.30	**0.75**
AT5G47990	CYP705A5_THAD_THAD1__cytochrome P450, family 705, subfamily A, polypeptide 5	0.25	0.34	**1.42**
AT5G48000	CYP708 A2_CYP708A2_THAH_THAH1__cytochrome P450, family 708, subfamily A, polypeptide 2	0.12	0.28	**2.15**
AT5G48010	THAS_THAS1__thalianol synthase 1	0.14	0.58	**2.33**
AT5G48030	GFA2__gametophytic factor 2	-0.20	0.08	**0.85**
AT5G48180	NSP5__nitrile specifier protein 5	-0.01	-0.24	**-1.04**
AT5G48485	DIR1__Bifunctional inhibitor/lipid-transfer protein/seed storage 2S albumin superfamily protein	-0.22	-0.61	**-0.81**
AT5G48490	Bifunctional inhibitor/lipid-transfer protein/seed storage 2S albumin superfamily protein	**-0.67**	**-1.10**	-0.12
AT5G48540	receptor-like protein kinase-related family protein	**0.74**	**0.80**	-0.13
AT5G48545	HISTIDINE TRIAD NUCLEOTIDE-BINDING 3	-0.18	-0.57	**-0.72**
AT5G48760	Ribosomal protein L13 family protein	-0.20	0.49	**0.74**
AT5G48930	HCT__hydroxycinnamoyl-CoA shikimate/quinate hydroxycinnamoyl transferase	0.11	**0.86**	0.69
AT5G49330	ATMYB111_MYB111_PFG3__myb domain protein 111	0.07	0.10	**0.92**
AT5G49360	ATBXL1_BXL1__beta-xylosidase 1	0.41	**-2.29**	**-2.77**
AT5G49450	AtbZIP1_bZIP1__basic leucine-zipper 1	-0.58	**-2.65**	**-2.36**
AT5G49480	ATCP1_CP1__Ca2+-binding protein 1	0.26	**1.17**	-0.01
AT5G49720	ATGH9A1_DEC_GH9A1_IRX2_KOR_KOR1_RSW2_TSD1__glycosyl hydrolase 9A1	**0.67**	-0.58	-0.16
AT5G49730	ATFRO6_FRO6_FRO6__ferric reduction oxidase 6	-0.15	**-0.95**	-0.14
AT5G49810	MMT__methionine S-methyltransferase	-0.08	0.29	**0.86**
AT5G50370	Adenylate kinase family protein	0.08	0.65	**0.84**
AT5G50670	Squamosa promoter-binding protein-like (SBP domain) transcription factor family protein	**-0.77**	-0.09	-0.02
AT5G51010	Rubredoxin-like superfamily protein	-0.27	-0.09	**-0.88**
AT5G51020	CRL__crumpled leaf	0.18	0.05	**-0.78**
AT5G51070	CLPD_ERD1_SAG15__Clp ATPase	-0.02	0.17	**-0.71**
AT5G51110	Transcriptional coactivator/pterin dehydratase	-0.13	0.04	**-0.82**
AT5G51440	HSP20-like chaperones superfamily protein	0.04	**0.79**	0.62
AT5G51750	ATSBT1.3_SBT1.3__subtilase 1.3	-0.06	0.20	**0.81**
AT5G51890	Peroxidase superfamily protein	**0.72**	0.35	0.65
AT5G51970	GroES-like zinc-binding alcohol dehydrogenase family protein	0.06	**-0.96**	**-1.76**
AT5G52190	Sugar isomerase (SIS) family protein	0.02	-0.08	**-0.83**
AT5G52470	ATFBR1_ATFIB1_FBR1_FIB1_SKIP7__fibrillarin 1	-0.22	0.41	**1.08**
AT5G52780	Protein of unknown function (DUF3464)	0.01	-0.35	**-1.11**
AT5G52820	WD-40 repeat family protein / notchless protein, putative	0.00	0.49	**0.72**
AT5G52840	NADH-ubiquinone oxidoreductase-related	-0.10	0.10	**0.85**
AT5G53070	Ribosomal protein L9/RNase H1	0.00	0.18	**0.79**

AGI identifier	Gene annotation	30 min	2h	8h
AT5G53140	Protein phosphatase 2C family protein	-0.32	0.32	**0.90**
AT5G53160	PYL8_RCAR3__regulatory components of ABA receptor 3	-0.34	**-1.07**	**-1.17**
AT5G53290	CRF3__cytokinin response factor 3	0.08	**0.85**	**1.10**
AT5G53420	CCT motif family protein	-0.25	**1.57**	**0.99**
AT5G53460	GLT1__NADH-dependent glutamate synthase 1	-0.50	0.23	**0.82**
AT5G53490	Tetratricopeptide repeat (TPR)-like superfamily protein	-0.17	**-0.78**	**-1.54**
AT5G53750	unknown protein	0.49	**1.09**	**1.09**
AT5G53760	ATMLO11_MLO11__Seven transmembrane MLO family protein	-0.21	**0.88**	0.47
AT5G53970	Tyrosine transaminase family protein	0.34	-0.50	**-1.82**
AT5G54060	UF3GT__UDP-glucose:flavonoid 3-o-glucosyltransferase	0.11	-0.06	**0.92**
AT5G54080	HGO__homogentisate 1,2-dioxygenase	0.07	**-1.22**	**-2.02**
AT5G54090	DNA mismatch repair protein MutS, type 2	-0.11	**-0.91**	-0.29
AT5G54100	SPFH/Band 7/PHB domain-containing membrane-associated protein family	-0.14	0.07	**1.25**
AT5G54160	ATOMT1_OMT1__O-methyltransferase 1	**0.82**	0.20	x
AT5G54170	Polyketide cyclase/dehydrase and lipid transport superfamily protein	-0.20	-0.71	**-1.00**
AT5G54206	pseudogene	0.43	-0.38	**-1.21**
AT5G54270	LHCB3_LHCB3*1__light-harvesting chlorophyll B-binding protein 3	**1.11**	0.34	0.08
AT5G54370	Late embryogenesis abundant (LEA) protein-related	0.63	0.20	**1.16**
AT5G54490	PBP1__pinoid-binding protein 1	**-0.90**	-0.28	-0.50
AT5G54540	Uncharacterised conserved protein (UCP012943)	**0.69**	-0.32	**-0.92**
AT5G54580	RNA-binding (RRM/RBD/RNP motifs) family protein	-0.13	0.35	**0.72**
AT5G54710	Ankyrin repeat family protein	0.02	0.26	**1.00**
AT5G54800	ATGPT1_GPT1__glucose 6-phosphate/phosphate translocator 1	0.26	0.37	**1.04**
AT5G55050	GDSL-like Lipase/Acylhydrolase superfamily protein	0.19	0.49	**1.02**
AT5G55070	Dihydrolipoamide succinyltransferase	-0.07	0.74	**1.13**
AT5G55230	ATMAP65-1_MAP65-1_MAP65-1__microtubule-associated proteins 65-1	-0.10	-0.36	**0.76**
AT5G55280	ATFTSZ1-1_CPFTSZ_FTSZ1-1__homolog of bacterial cytokinesis Z-ring protein FTSZ 1-1	-0.02	0.46	**0.92**
AT5G55450	Bifunctional inhibitor/lipid-transfer protein/seed storage 2S albumin superfamily protein	-0.10	0.47	**1.26**
AT5G55480	SVL1__SHV3-like 1	-0.10	-0.05	**0.88**
AT5G55620	unknown protein	**0.71**	0.70	0.49
AT5G55680	glycine-rich protein	0.35	**0.98**	x
AT5G55700	BAM4_BMY6__beta-amylase 4	-0.13	-0.54	**-0.83**
AT5G55750	hydroxyproline-rich glycoprotein family protein	**0.90**	-0.71	**-1.13**
AT5G55970	RING/U-box superfamily protein	x	**-1.02**	**-1.32**
AT5G56010	AtHsp90-3_AtHsp90.3_HSP81-3_Hsp81.3__heat shock protein 81-3	-0.24	**0.76**	0.65
AT5G56030	AtHsp90.2_ERD8_HSP81-2_HSP90.2__heat shock protein 81-2	-0.07	**0.98**	**0.98**
AT5G56100	glycine-rich protein / oleosin	-0.30	-0.63	**-1.58**
AT5G56360	PSL4__calmodulin-binding protein	-0.26	-0.10	**0.71**

AT5G56630	PFK7__phosphofructokinase 7	0.07	**1.27**	**1.69**
AT5G56670	Ribosomal protein S30 family protein	0.26	0.54	**1.06**
AT5G56680	EMB2755_SYNC1_SYNC1 ARATH__Class II aminoacyl-tRNA and biotin synthetases superfamily protein	-0.32	0.53	**0.98**
AT5G56710	Ribosomal protein L31e family protein	-0.35	0.29	**0.76**
AGI identifier	Gene annotation	30 min	2h	8h
AT5G56750	NDL1__N-MYC downregulated-like 1	-0.51	**-1.04**	**-1.50**
AT5G56870	BGAL4__beta-galactosidase 4	-0.03	**-1.22**	**-2.04**
AT5G57035	U-box domain-containing protein kinase family protein	0.14	-0.01	**-0.88**
AT5G57560	TCH4_XTH22__Xyloglucan endotransglucosylase/hydrolase family protein	x	**-1.89**	-0.64
AT5G57630	CIPK21_SnRK3.4__CBL-interacting protein kinase 21	0.38	-0.40	**-0.71**
AT5G57660	ATCOL5_COL5__CONSTANS-like 5	0.20	-0.49	**-1.04**
AT5G57887	unknown protein	-0.01	**-1.24**	**-1.19**
AT5G57900	SKIP1__SKP1 interacting partner 1	0.12	-0.61	**-0.94**
AT5G57910	unknown protein	-0.05	-0.26	**-0.87**
AT5G58200	Calcineurin-like metallo-phosphoesterase superfamily protein	-0.59	-0.12	**-0.79**
AT5G58350	WNK4_ZIK2__with no lysine (K) kinase 4	0.20	-0.35	**-0.87**
AT5G58375	Methyltransferase-related protein	0.25	-0.01	**-0.83**
AT5G58420	Ribosomal protein S4 (RPS4A) family protein	-0.18	0.49	**0.80**
AT5G58640	Selenoprotein, Rdx type	-0.03	**-1.07**	**-1.81**
AT5G58800	Quinone reductase family protein	0.13	0.00	**-0.77**
AT5G58860	CYP86A1 (cytochrome P450, family 86, subfamily A, polypeptide 1); oxygen binding	0.14	-0.11	**0.74**
AT5G58900	Homeodomain-like transcriptional regulator	-0.21	0.59	**0.81**
AT5G59090	ATSBT4.12_SBT4.12__subtilase 4.12	0.08	0.06	**0.71**
AT5G59240	Ribosomal protein S8e family protein	0.06	0.23	**0.78**
AT5G59330	Bifunctional inhibitor/lipid-transfer protein/seed storage 2S albumin superfamily protein	0.06	**0.90**	0.43
AT5G59400	unknown protein	-0.02	-0.07	**-0.74**
AT5G59570	Homeodomain-like superfamily protein	-0.09	-0.38	**-1.43**
AT5G59820	RHL41_ZAT12__C2H2-type zinc finger family protein	0.42	-0.33	**-1.06**
AT5G59850	Ribosomal protein S8 family protein	-0.34	0.51	**1.00**
AT5G59870	HTA6__histone H2A 6	-0.37	0.24	**0.86**
AT5G59960	unknown protein	-0.06	**-0.97**	**-1.23**
AT5G60360	AALP_ALP_SAG2__aleurain-like protease	0.22	-0.15	**-0.83**
AT5G60390	GTP binding Elongation factor Tu family protein	-0.17	0.36	**1.27**
AT5G60640	ATPDI2_ATPDIL1-4_PDI2_PDIL1-4__PDI-like 1-4	-0.13	0.00	**0.85**
AT5G60670	Ribosomal protein L11 family protein	-0.02	0.56	**0.95**
AT5G60680	Protein of unknown function, DUF584	-0.18	**-1.03**	**-0.85**
AT5G60780	ATNRT2.3 (*Arabidopsis thaliana* high affinity nitrate transporter 2.3); nitrate transporter	0.06	-0.02	**1.11**
AT5G60890	ATMYB34_ATR1_MYB34__myb domain protein 34	0.02	**1.21**	**1.32**
AT5G61020	ECT3__evolutionarily conserved C-terminal region 3	-0.29	0.44	**0.82**
AT5G61160	AACT1__anthocyanin 5-aromatic acyltransferase 1	-0.03	0.12	**0.86**
AT5G61170	Ribosomal protein S19e family protein	-0.21	0.64	**0.91**
AT5G61330	rRNA processing protein-related	-0.04	0.35	**0.88**
AT5G61440	ACHT5__atypical CYS HIS rich thioredoxin 5	-0.14	-0.72	**-0.75**

AGI identifier	Gene annotation	30 min	2h	8h
AT5G61520	Major facilitator superfamily protein	0.00	0.66	**0.92**
AT5G61590	Integrase-type DNA-binding superfamily protein	**-1.18**	**-2.02**	**-1.68**
AT5G61600	ERF104__ethylene response factor 104	**-0.83**	-0.61	**-0.91**
AT5G61790	ATCNX1_CNX1__calnexin 1	-0.11	0.22	**0.87**
AT5G61960	AML1_ML1__MEI2-like protein 1	**-0.79**	0.44	0.52
AT5G62020	AT-HSFB2A_HSFB2A__heat shock transcription factor B2A	-0.33	-0.14	**-0.76**
AT5G62190	PRH75__DEAD box RNA helicase (PRH75)	-0.18	0.23	**0.74**
AT5G62220	ATGT18_GT18__glycosyltransferase 18	0.06	**1.04**	**0.85**
AT5G62440	Protein of unknown function (DUF3223)	0.06	0.67	**0.83**
AT5G62480	ATGSTU9_GST14_GST14B_GSTU9__glutathione S-transferase tau 9	0.15	**1.04**	0.52
AT5G62540	UBC3__ubiquitin-conjugating enzyme 3	-0.16	-0.22	**-0.74**
AT5G62680	Major facilitator superfamily protein	**0.83**	0.34	0.20
AT5G63030	Thioredoxin superfamily protein	-0.08	-0.26	**-1.07**
AT5G63070	Ribosomal protein S19 family protein	0.03	0.28	**0.80**
AT5G63085	unknown protein	-0.24	0.29	**0.79**
AT5G63160	BT1 (BTB and TAZ domain protein 1); protein binding / transcription regulator	-0.09	**-1.47**	**-1.73**
AT5G63190	MA3 domain-containing protein	0.31	-0.53	**-1.05**
AT5G63620	GroES-like zinc-binding alcohol dehydrogenase family protein	-0.11	-0.68	**-1.08**
AT5G63680	Pyruvate kinase family protein	-0.04	0.22	**0.83**
AT5G63790	ANAC102_NAC102__NAC domain containing protein 102	0.41	-0.50	**-0.97**
AT5G63840	PSL5_RSW3__Glycosyl hydrolases family 31 protein	0.17	-0.08	**-0.84**
AT5G63980	ALX8_ATSAL1_FRY1_HOS2_RON1_SAL1__Inositol monophosphatase family protein	0.43	**0.86**	**0.77**
AT5G64040	PSAN__photosystem I reaction center subunit PSI-N, chloroplast, putative / PSI-N, putative (PSAN)	0.26	-0.39	**-1.70**
AT5G64100	Peroxidase superfamily protein	**0.89**	-0.72	**-1.44**
AT5G64120	Peroxidase superfamily protein	-0.37	0.04	**1.23**
AT5G64140	RPS28__ribosomal protein S28	-0.20	0.43	**0.75**
AT5G64200	ATSC35_SC35__ortholog of human splicing factor SC35	0.43	-0.23	**-0.74**
AT5G64250	Aldolase-type TIM barrel family protein	0.21	-0.30	**-1.50**
AT5G64560	ATMGT9_MGT9_MRS2-2__magnesium transporter 9	0.11	0.12	**1.05**
AT5G64640	Plant invertase/pectin methylesterase inhibitor superfamily	-0.09	0.26	**1.01**
AT5G64820	unknown protein	**0.81**	-0.23	**-0.83**
AT5G64890	PROPEP2__elicitor peptide 2 precursor	-0.02	-0.29	**-0.75**
AT5G65020	ANNAT2__annexin 2	0.42	0.06	**0.78**
AT5G65110	ACX2_ATACX2__acyl-CoA oxidase 2	0.11	**-0.89**	**-1.26**
AT5G65300	unknown protein	**0.88**	0.19	-0.05
AT5G65390	AGP7__arabinogalactan protein 7	-0.42	-0.06	**0.82**
AT5G66540	unknown protein	0.06	-0.65	**-1.23**
AT5G66570	MSP-1_OE33_OEE1_OEE33_PSBO-1_PSBO1__PS II oxygen-evolving complex 1	**1.34**	0.08	-0.50
AT5G66720	Protein phosphatase 2C family protein	0.09	-0.27	**-0.73**
AT5G67210	Protein of unknown function (DUF579)	0.00	0.57	**0.77**
AT5G67240	SDN3__small RNA degrading nuclease 3	-0.03	0.57	**0.76**

AGI identifier	Gene annotation	30 min	2h	8h
AT5G67300	ATMYB44_ATMYBR1_MYB44_MYBR1__myb domain protein r1	0.27	**0.77**	0.25
AT5G67360	ARA12__Subtilase family protein	0.23	**0.79**	**1.33**
AT5G67420	ASL39_LBD37__LOB domain-containing protein 37	-0.18	-0.34	**-0.75**
AT5G67480	ATBT4_BT4_BTB and TAZ domain protein 4	-0.53	**-1.00**	-0.17

Supplemental table IV: Complete data from the metabolomic analysis. Numbers in bold are ratios with a statistical (t-Test, p-value≤0.05) difference between both conditions.

	Log_2 (phenanthrene/ control)	Log_2 (sucrose + phenanthrene/ phenanthrene)	Log_2 (sucrose/ control)
Adonitol	**0.40**	-0.31	-0.37
Alpha-Alanine	**1.29**	**3.14**	**3.98**
Ammonium	-0.37	**-1.34**	**-1.66**
Arginine	**0.40**	**-1.40**	**-1.76**
Asparagine	**0.48**	-0.12	**0.17**
Aspartate	**0.29**	**-1.00**	**-0.83**
Beta-Alanine	-3.35	0.25	-3.54
Cellobiose	0.00	0.00	0.00
Citrate	0.00	**6.64**	**6.64**
Cystine	**0.58**	-0.44	0.06
Fructose	0.20	**3.20**	**4.11**
Fumarate	0.00	**6.64**	**2.80**
GABA	0.79	-0.14	**-0.08**
Galactinol	0.00	0.00	0.00
Galactose	0.00	0.00	0.00
Gentiobiose	0.00	0.00	0.00
Glucose	0.14	**2.35**	**2.65**
Glutamate	**0.33**	**0.60**	**0.41**
Glutamine	**0.54**	**1.37**	**1.77**
Glycerate	0.00	0.00	0.00
Glycine	**0.49**	**3.30**	**3.53**
Histidine	0.28	0.07	0.39
Hydroxyproline	0.00	0.00	0.00
Isoleucine	**1.18**	**-1.60**	-0.76
Leucine	**1.22**	**-0.88**	0.35
Lysine	**0.59**	**-2.66**	**-2.52**
Malate	-0.39	**3.83**	**2.95**
Maltose	0.00	0.00	0.00
Mannitol	0.00	0.00	0.00
Mannose	0.00	**6.64**	**6.64**
Melibiose	0.00	0.00	0.00
Methionine	0.52	-0.17	-0.77
Methylcysteine	-0.85	-0.39	-1.13
Myo-inositol	**0.39**	-0.28	-0.39
Ornithine	0.15	**-0.81**	**-1.29**
Phenylalanine	**0.67**	**-2.79**	**-0.91**
Proline	0.67	**1.68**	**1.66**
Quinate	0.00	0.00	0.00
Serine	**0.72**	0.05	**0.30**
Sorbitol	0.00	0.00	0.00
Succinate	0.00	**6.64**	**6.64**
Sucrose	**0.88**	**5.09**	**5.76**
Threonine	**0.75**	**-0.38**	**0.12**
Trehalose	0.00	0.00	0.00
Tryptophan	**0.80**	**-1.89**	**-0.81**
Tyrosine	**0.35**	-0.19	0.22
Valine	**0.89**	**-0.44**	0.29

Supplemental table V: List of UDP-Glycosil-transferases and peroxidases differentially expressed in at leat one condition. Expression changes are given as log2. Expression changes in bolt correspond to genes differentially expressed at the significant threshold of Bonferroni p-value<0.05.

	AGI identifiers	30min	2h	8h
Peroxidases	AT4G37520	-0.02	**-1.07**	**-1.63**
	AT5G64100	**0.89**	-0.72	**-1.44**
	AT5G39580	0.30	**-1.56**	**-0.95**
	AT2G37130	x	-0.09	**-0.93**
	AT4G37530	-0.13	**-0.74**	**-0.89**
	AT4G33420	-0.24	-0.57	**-0.76**
	AT1G71695	**0.87**	0.07	0.04
	AT5G51890	**0.72**	0.35	0.65
	AT1G30870	0.34	-0.06	**0.79**
	AT1G05250	0.30	0.06	**0.82**
	AT1G49570	-0.38	0.45	**0.83**
	AT3G28200	-0.65	0.07	**0.88**
	AT4G21960	0.17	0.11	**1.03**
	AT3G01190	**0.69**	-0.11	**1.12**
	AT5G64120	-0.37	0.04	**1.23**
	AT3G21770	0.18	0.12	**1.33**
	AT1G05240	0.31	-0.08	**1.68**
UDP-Glycosil-transferases	AT4G34138	-0.03	**-1.36**	**-1.54**
	AT1G22370	0.14	**-1.36**	**-1.29**
	AT4G15550	0.07	-0.16	**-1.18**
	AT2G36770	0.18	**-0.90**	**-1.18**
	AT1G21480	-0.04	-0.41	**-1.17**
	AT2G15490	0.22	-0.17	**-0.92**
	AT1G22350	-0.03	**-1.05**	**-0.84**
	AT4G15260	-0.03	-0.20	**-0.83**
	AT3G62720	-0.48	**-0.77**	-0.09
	AT5G17050	**0.71**	0.37	0.01
	AT4G15480	0.44	0.62	**0.75**
	AT3G21560	0.21	**0.95**	**0.75**
	AT2G22900	0.09	0.20	**0.80**
	AT3G15350	-0.19	0.53	**0.82**
	AT5G62220	0.06	**1.04**	**0.85**
	AT1G06000	0.15	0.71	**0.99**
	AT4G27560	-0.13	0.67	**1.20**
	AT2G43820	0.14	**-0.92**	x

Acknowledgment

This work was funded by the Axson-Coatings firm and the French government (CIFRE n°1017/2009). Authors would like to thank Nathalie Marnet for targeted metabolomic analysis and Marie-Noëlle Soler for observation and imaging of the fluorescence microscopy.

Bibliography

Abramoff MD, Magalhães PJ, Ram SJ (2004) Image processing with ImageJ. Biophotonics Int **11**: 36–42

Alkio M, Tabuchi TM, Wang X, Colón-Carmona A (2005) Stress responses to polycyclic aromatic hydrocarbons in *Arabidopsis* include growth inhibition and hypersensitive response-like symptoms. J Exp Bot **56**: 2983–2994

Ashraf M, Foolad MR (2007) Roles of glycine betaine and proline in improving plant abiotic stress resistance. Environ Exp Bot **59**: 206–216

Barker L, Kühn C, Weise A, Schulz A, Gebhardt C, Hirner B, Hellmann H, Schulze W, Ward JM, Frommer WB (2000) SUT2, a Putative Sucrose Sensor in Sieve Elements. Plant Cell Online **12**: 1153–1164

Bezalel L, Hadar Y, Cerniglia CE (1997) Enzymatic Mechanisms Involved in Phenanthrene Degradation by the White Rot Fungus Pleurotus ostreatus. Appl Environ Microbiol **63**: 2495–2501

Bolouri-Moghaddam MR, Le Roy K, Xiang L, Rolland F, Van den Ende W (2010) Sugar signalling and antioxidant network connections in plant cells. FEBS J **277**: 2022–2037

Borsani O, Valpuesta V, Botella MA (2001) Evidence for a Role of Salicylic Acid in the Oxidative Damage Generated by NaCl and Osmotic Stress in *Arabidopsis* Seedlings. Plant Physiol **126**: 1024–1030

Boyes DC, Zayed AM, Ascenzi R, McCaskill AJ, Hoffman NE, Davis KR, Görlach J (2001) Growth stage-based phenotypic analysis of Arabidopsis: a model for high throughput functional genomics in plants. Plant Cell **13**: 1499–1510

Coruzzi GM, Zhou L (2001) Carbon and nitrogen sensing and signaling in plants: emerging "matrix effects."Curr Opin Plant Biol **4**: 247 – 253

Couée I, Sulmon C, Gouesbet G, Amrani AE (2006) Involvement of soluble sugars in reactive oxygen species balance and responses to oxidative stress in plants. J Exp Bot **57**: 449–459

Crowe ML, Serizet C, Thareau V, Aubourg S, Rouze P, Hilson P, Beynon J, Weisbeek P, van Hummelen P, Reymond P, et al (2003) CATMA: a complete *Arabidopsis* GST database. Nucleic Acids Res **31**: 156–158

Dabestani R, Ivanov IN (1999) A Compilation of Physical, Spectroscopic and Photophysical Properties of Polycyclic Aromatic Hydrocarbons. Photochem Photobiol **70**: 10–34

Dubey RS, Singh AK (1999) Salinity Induces Accumulation of Soluble Sugars and Alters the Activity of Sugar Metabolising Enzymes in Rice Plants. Biol Plant **42**: 233–239

Edwards R, Brazier-Hicks M, Dixon DP, Cummins I (2005) Chemical Manipulation of Antioxidant Defences in Plants. *In* J. A. Callow, ed, Adv. Bot. Res. Academic Press, pp 1–32

Edwards R, Dixon DP, Cummins I, Brazier-Hicks M, Skipsey M (2011) New Perspectives on the Metabolism and Detoxification of Synthetic Compounds in Plants. *In* P Schröder, CD Collins, eds, Org. Xenobiotics Plants. Springer Netherlands, pp 125–148

Ende WV den, Peshev D (2013) Sugars as Antioxidants in Plants. *In* N Tuteja, SS Gill, eds, Crop Improv. Adverse Cond. Springer New York, pp 285–307

Ende WV den, Valluru R (2009) Sucrose, sucrosyl oligosaccharides, and oxidative stress: scavenging and salvaging? J Exp Bot **60**: 9–18

Farrar J, Pollock C, Gallagher J (2000) Sucrose and the integration of metabolism in vascular plants. Plant Sci **154**: 1–11

Foyer CH, Noctor G (2011) Ascorbate and Glutathione: The Heart of the Redox Hub. Plant Physiol **155**: 2–18

Gagnot S, Tamby J-P, Martin-Magniette M-L, Bitton F, Taconnat L, Balzergue S, Aubourg S, Renou J-P, Lecharny A, Brunaud V (2008) CATdb: a public access to *Arabidopsis* transcriptome data from the URGV-CATMA platform. Nucleic Acids Res **36**: D986–D990

Ge Y, Dudoit S, Speed TP (2003) Resampling-based multiple testing for microarray data analysis. Test **12**: 1–77

Gill PK, Sharma AD, Singh P, Bhullar SS (2003) Changes in germination, growth and soluble sugar contents of Sorghum bicolor (L.) Moench seeds under various abiotic stresses. Plant Growth Regul **40**: 157–162

Hilson P, Allemeersch J, Altmann T, Aubourg S, Avon A, Beynon J, Bhalerao RP, Bitton F, Caboche M, Cannoot B, et al (2004) Versatile Gene-Specific Sequence Tags for *Arabidopsis* Functional Genomics: Transcript Profiling and Reverse Genetics Applications. Genome Res **14**: 2176–2189

Keunen E, Peshev D, Vangronsveld J, VAN DEN Ende W, Cuypers A (2013) Plant sugars are crucial players in the oxidative challenge during abiotic stress: extending the traditional concept. Plant Cell Environ. doi: 10.1111/pce.12061

Koch K (2004) Sucrose metabolism: regulatory mechanisms and pivotal roles in sugar sensing and plant development. Curr Opin Plant Biol **7**: 235 – 246

Liu H, Weisman D, Ye Y, Cui B, Huang Y, Colón-Carmona A, Wang Z (2009) An oxidative stress response to polycyclic aromatic hydrocarbon exposure is rapid and complex in *Arabidopsis thaliana*. Plant Sci **176**: 375 – 382

Lloyd JC, Zakhleniuk OV (2004) Responses of primary and secondary metabolism to sugar accumulation revealed by microarray expression analysis of the *Arabidopsis* mutant, pho3. J Exp Bot **55**: 1221–1230

Loreti E, Poggi A, Novi G, Alpi A, Perata P (2005) A Genome-Wide Analysis of the Effects of Sucrose on Gene Expression in *Arabidopsis* Seedlings under Anoxia. Plant Physiol **137**: 1130–1138

Lurin C, Andrés C, Aubourg S, Bellaoui M, Bitton F, Bruyère C, Caboche M, Debast C, Gualberto J, Hoffmann B, et al (2004) Genome-wide analysis of *Arabidopsis* pentatricopeptide repeat proteins reveals their essential role in organelle biogenesis. Plant Cell **16**: 2089–2103

Matsui T, Nomura Y, Takano M, Imai S, Nakayama H, Miyasaka H, Okuhata H, Tanaka S, Matsuura H, Harada K, et al (2011) Molecular Cloning and Partial Characterization of a Peroxidase Gene Expressed in the Roots of <I>Portulaca oleracea</I> cv., One Potentially Useful in the Remediation of Phenolic Pollutants. Biosci Biotechnol Biochem **75**: 882–890

Murashige T, Skoog F (1962) A Revised Medium for Rapid Growth and Bio Assays with Tobacco Tissue Cultures. Physiol Plant **15**: 473–497

Pasternak T, Rudas V, Potters G, Jansen MAK (2005) Morphogenic effects of abiotic stress: reorientation of growth in *Arabidopsis thaliana* seedlings. Environ Exp Bot **53**: 299–314

Paul MJ, Foyer CH (2001) Sink regulation of photosynthesis. J Exp Bot **52**: 1383–1400

Peshev D, Vergauwen R, Moglia A, Hideg É, Ende WV den (2013) Towards understanding vacuolar antioxidant mechanisms: a role for fructans? J Exp Bot ers377

Price J, Laxmi A, Martin SKS, Jang J-C (2004) Global Transcription Profiling Reveals Multiple Sugar Signal Transduction Mechanisms in Arabidopsis. Plant Cell Online **16**: 2128–2150

Provart T. and Z (2003) A Browser-based Functional Classification SuperViewer for *Arabidopsis* Genomics. Curr Comput Mol Biol 271–272

Rai VK (2002) Role of Amino Acids in Plant Responses to Stresses. Biol Plant **45**: 481–487

Ramel F, Sulmon C, Bogard M, Couée I, Gouesbet G (2009) Differential patterns of reactive oxygen species and antioxidative mechanisms during atrazine injury and sucrose-induced tolerance in *Arabidopsis thaliana* plantlets. BMC Plant Biol **9**: 28

Ramel F, Sulmon C, Cabello-Hurtado F, Taconnat L, Martin-Magniette M-L, Renou J-P, Amrani AE, Couée I, Gouesbet G (2007) Genome-wide interacting effects of sucrose and herbicide-mediated stress in *Arabidopsis thaliana*: novel insights into atrazine toxicity and sucrose-induced tolerance. BMC Genomics **8**: 450

Roitsch T (1999) Source-sink regulation by sugar and stress. Curr Opin Plant Biol **2**: 198–206

Rolland F, Moore B, Sheen J (2002) Sugar Sensing and Signaling in Plants. Plant Cell **14**: s185–s205

Rosa M, Prado C, Podazza G, Interdonato R, Gonzalez JA, Hilal M, Prado FE (2009) Soluble sugars: Metabolism, sensing and abiotic stress: A complex network in the life of plants. Signal Behav **4**: 288–393

Rozen S, Skaletsky H (2000) Primer3 on the WWW for general users and for biologist programmers. Methods Mol Biol Clifton NJ **132**: 365–386

Sandermann Jr. H (1992) Plant metabolism of xenobiotics. Trends Biochem Sci **17**: 82–84

Solfanelli C, Poggi A, Loreti E, Alpi A, Perata P (2006) Sucrose-Specific Induction of the Anthocyanin Biosynthetic Pathway in Arabidopsis. Plant Physiol **140**: 637–646

Sulmon C, Gouesbet G, Amrani AE, Couée I (2006) Sugar-induced tolerance to the herbicide atrazine in *Arabidopsis* seedlings involves activation of oxidative and xenobiotic stress responses. Plant Cell Reports **25**: 489–498

Sulmon C, Gouesbet G, Couée I, Amrani AE (2004) Sugar-induced tolerance to atrazine in *Arabidopsis* seedlings: interacting effects of atrazine and soluble sugars on psbA mRNA and D1 protein levels. Plant Sci **167**: 913–923

Syed K, Doddapaneni H, Subramanian V, Lam YW, Yadav JS (2010) Genome-to-function characterization of novel fungal P450 monooxygenases oxidizing polycyclic aromatic hydrocarbons (PAHs). Biochem Biophys Res Commun **399**: 492–497

Szabados L, Savouré A (2010) Proline: a multifunctional amino acid. Trends Plant Sci **15**: 89–97

Tadege M, Dupuis I, Kuhlemeier C (1999) Ethanolic fermentation: new functions for an old pathway. Trends Plant Sci **4**: 320–325

Taguchi G, Ubukata T, Nozue H, Kobayashi Y, Takahi M, Yamamoto H, Hayashida N (2010) Malonylation is a key reaction in the metabolism of xenobiotic phenolic glucosides in *Arabidopsis* and tobacco. Plant J **63**: 1031–1041

team RDC (2013) R: a language and environment for statistical computing. R foundation for statistical computing, Vienna, Austria

Thimm O, Bläsing O, Gibon Y, Nagel A, Meyer S, Krüger P, Selbig J, Müller LA, Rhee SY, Stitt M (2004) MAPMAN: a user-driven tool to display genomics data sets onto diagrams of metabolic pathways and other biological processes. Plant J Cell Mol Biol **37**: 914–939

Thum KE, Shin MJ, Palenchar PM, Kouranov A, Coruzzi GM (2004) Genome-wide investigation of light and carbon signaling interactions in Arabidopsis. Genome Biol **5**: R10

Valluru R, Ende WV den (2008) Plant fructans in stress environments: emerging concepts and future prospects. J Exp Bot **59**: 2905–2916

Vieira Dos Santos C, Rey P (2006) Plant thioredoxins are key actors in the oxidative stress response. Trends Plant Sci **11**: 329–334

Weisman D, Alkio M, Colón-Carmona A (2010) Transcriptional responses to polycyclic aromatic hydrocarbon-induced stress in *Arabidopsis thaliana* reveal the involvement of hormone and defense signaling pathways. BMC Plant Biol **10**: 59

Wind J, Smeekens S, Hanson J (2010) Sucrose: Metabolite and signaling molecule. Phytochemistry **71**: 1610–1614

Chapitre 4 : **Approche expérimentale pour l'amélioration de la phytoremédiation naturelle des HAPs: mise en place et conception d'un site pilote.**

1. Introduction

L'entreprise Axson-Coatings (anciennement Bs Coatings, membre du groupe Axson) est une entreprise française qui produit des revêtements industriels (protections anticorrosion, isolants thermiques…) qui peuvent être et ont longtemps été synthétisés à partir de produits pétroliers. Au début de son activité, dans les années 1940-1950, dans un contexte d'absence de réglementation, les déchets étaient enfouis dans des trous sur un terrain vague à proximité des bâtiments de production, comme cela était couramment fait à cette époque. Ceci a généré un site fortement contaminé avec un niveau de pollution très hétérogène (Figure supplémentaire S1).

Dans le contexte réglementaire actuel, l'entreprise a pris la décision de remédier à ce problème. Des analyses de sol ont été réalisées au début des années 2000 afin d'évaluer l'ampleur de cette pollution. Elles ont montré que seuls les hydrocarbures aromatiques polycycliques (HAPs) sont retrouvés dans le sol répartis de manière très hétérogène sur l'ensemble du site. Les zones où les déchets ont été enfouis sont fortement contaminées par rapport au reste du site dans lequel les produits ont été diffusés par la suite, créant un effet de pépites (Figure supplémentaire S1).

Des études préliminaires ont été réalisées afin d'évaluer les coûts de dépollution du site avec des méthodes de traitement *ex-situ* « classiques ». En raison du coût important de ces techniques, malgré leur efficacité avérée et leur rapidité, les dirigeants d'Axson-Coatings ont décidé d'étudier, en collaboration avec l'Université de Rennes 1, la faisabilité de l'utilisation d'un système de dépollution naturelle basé sur la capacité des végétaux à décontaminer leur environnement : la phytoremédiation.

Les études préliminaires au laboratoire, *in-vitro*, ont permis de montrer que même si les HAPs affectent le développement des plantes, l'apport de saccharose dans le milieu de culture permet de limiter les effets négatifs des HAPs (inhibition de la croissance des racines et des parties aériennes, chloroses…) et de maintenir le développement des plantes lorsque ces dernières poussent sur des milieux contenant de fortes concentrations de HAPs. De par cette collaboration, un site pilote de phytoremédiation a été mis en place afin de (i) identifier les espèces végétales présentant la meilleure capacité d'adaptation et de décontamination des zones fortement polluées et (ii) voir si un apport de saccharose permet d'améliorer la phytoremédiation des HAPs et la décontamination des sols *in-situ*.

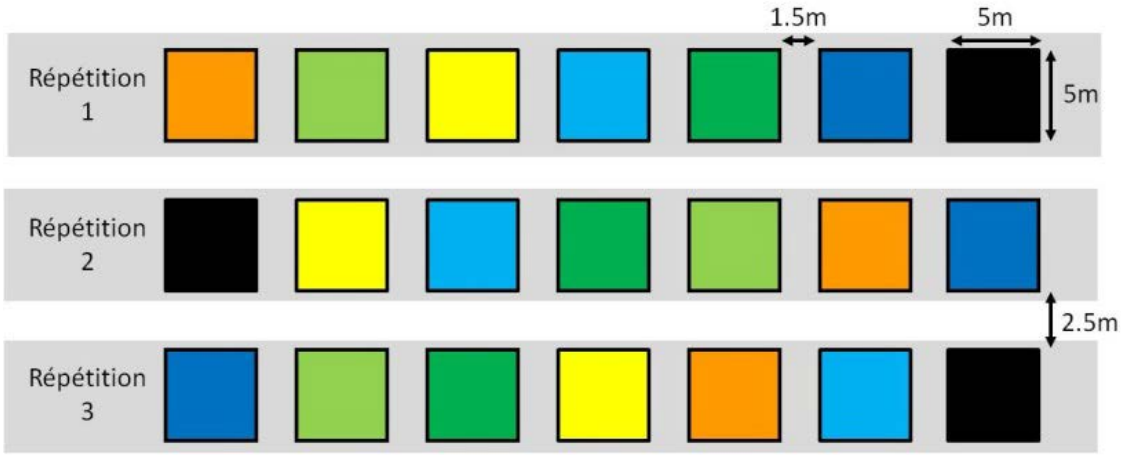

	Apport de terre végétale		
	+		-
	Apport de sucrose		
Plantation	+	-	-
Aucune			
Plantes ligneuses			
Plantes herbacées			

<u>Figure 1</u> : Plan expérimental du site pilote

2. Matériel et méthodes

2.1. Mise en place du système expérimental

2.1.1. Préparation de la parcelle

Le terrain pollué correspond à une surface totale de plus de 1 hectare. Nous avons choisi, après avoir défini le plan expérimental, de travailler sur une parcelle de 1000m² représentative du site.

Pout obtenir des conclusions objectives et significatives malgré la grande variabilité due à la répartition hétérogène de la pollution, il est nécessaire de faire plusieurs répétitions dans lesquelles les différentes conditions sont réparties aléatoirement. Toutefois, pour des raisons pratiques de circulation avec les engins de terrassement, les parcelles laissées intactes, qui serviront de témoin (en noir sur la figure 1), ont été placées aux extrémités de chaque répétition.

Pour les autres parcelles (en couleur sur la figure 1), la couche superficielle d'environ 20 cm de remblai, constituée de blocs de pierres, apportés après l'enfouissement des déchets, a été enlevée et remplacée par de la terre végétale. Cet apport a deux objectifs : (i) il doit permettre aux plantes de mieux s'installer, et (ii) il apporte de nouveaux consortiums bactériens et fongiques (Huang et al., 2004; Escalante-Espinosa et al., 2005). En effet, de nombreux travaux ont montrés que l'apport de matière organique (compost, terre végétale…) permet de stimuler l'élimination des HAPs du sol (Ghanem et al., 2013; Wang et al., 2012b; Wang et al., 2012a).

2.1.2. Mise en place des plantes

Plusieurs espèces végétales ont été utilisées. Le choix des espèces végétales s'est effectué selon plusieurs critères. Dans un premier temps, nous avons voulu comparer deux types de plantes différents.

(i) Des plantes ligneuses à enracinement profond : le saule, une plante connue pour sa capacité épuratrice notamment des eaux usées, est également un genre fréquemment utilisé pour la phytoremédiation des sols pollués par les HAPs (Vervaeke et al., 2003; Euliss et al., 2008). De plus, deux espèces de saule étaient déjà présentes sur le site : *Salix fragilis* et *Salix caprea*. *Buddleja davidii* a aussi été choisi comme plante ligneuse à enracinement profond car cette espèce était présente naturellement sur le site et se développait bien et rapidement, ce qui en faisait un bon candidat pour la phytoremédiation des HAPs.

(ii) Une plante herbacée, le miscanthus a été choisi pour d'une part sa capacité à produire une forte biomasse en une saison végétative et d'autre part le potentiel de cette plante pour la phytoremédiation des HAPs (Gawronski and Gawronska, 2007).

Pour chaque parcelle « plantes ligneuses », 6 saules (*Salix fragilis*) et 6 arbres aux papillons (*Buddleja davidii*) ont été plantés. Les parcelles « plantes herbacées » ont reçu des rhizomes de *Miscanthus* × *giganteus*. Les végétaux ont été plantés à la saison adéquate : fin décembre 2010 pour les arbres et fin mars 2011 pour le miscanthus. Un système d'arrosage automatique au goutte-à-goutte a été installé afin d'irriguer de façon continue et la plus homogène possible l'ensemble des parcelles du site pilote.

2.2. Apports en saccharose et entretien du site

Les parcelles traitées ont reçu 3kg de saccharose tous les quinze jours. Nous avons choisi d'apporter le saccharose directement sous forme de poudre comme cela est fait pour les apports d'engrais agricoles, après avoir vérifié qu'en deux semaines l'ensemble du saccharose apporté a été bien dissous par l'arrosage et l'humidité naturelle (plus particulièrement en période sèche).

La dose a été établie en se référant aux doses appliquées *in-vitro* et aux besoins en eau d'un arbre. On estime à 8L le besoin en eau moyen d'un arbre à chaque arrosage pour les conditions de sol, précipitations, ensoleillement du site pilote. Sachant que la solution nutritive utilisée *in-vitro* contient 30g/L de saccharose, un arrosage de 8L avec cette solution

apporterait une quantité de 250g de saccharose par arbre soit 3kg pour l'ensemble de la parcelle. La même dose a ensuite été appliquée sur l'ensemble des parcelles ayant reçu un apport de saccharose.

Enfin nous avons pris la décision de ne pas appliquer de désherbant pour éviter toute interférence avec les analyses ultérieures. En effet, même si certains herbicides permettent de cibles les adventices, des études ont montré que les plantes sont capables de les accumuler. D'autre part, le saccharose permet d'augmenter l'accumulation de l'atrazine dans les plantes (Sulmon et al., 2007a), ce qui pourrait avoir un effet croisé avec les HAPs. Les parties aériennes de miscanthus ont été coupées à la fin de la première saison végétative quand les feuilles sont devenues sèches et ont été utilisées comme paillis afin de limiter le développement des adventices, ce qui est couramment fait dans la culture du miscanthus (Chambre d'Agriculture de Picardie, 2010).

2.3. Suivi du site pilote

Lors de chaque traitement, l'ensemble des parcelles est photographié successivement au cours des saisons afin de suivre le développement des plantes qui ont été mises en place ainsi que des autres végétaux qui se sont développés naturellement.

Les photographies ont été analysées avec le logiciel 'ImageJ' (Abramoff et al., 2004) afin d'évaluer globalement l'intensité de la chlorophylle, mesure ce qui permet d'évaluer le développement de la végétation au cours du temps (Richardson et al., 2001).

De plus, à la fin de l'expérimentation, un relevé du nombre d'arbres vivants a été effectué pour chacune des parcelles, nous permettant ainsi de calculer un taux de survie pour chaque espèce d'arbres (saules et *Buddleja*) qui est exprimé en pourcentage ($taux = \frac{nombre\ d'arbres\ vivants}{nombre\ d'arbres\ plantés}$). Le taux de survie minimum correspond au taux de survie le plus faible des 3 répétitions d'une condition donnée alors que le taux de survie maximum correspond au taux de survie le plus élevé des 3 répétitions.

2.4. Echantillonnage et dosages des HAPs

Les échantillons de sols ont été prélevés sur une profondeur de 30cm sur 5 points de chaque parcelle, mélangés et envoyés à analyser. Les 5 points de prélèvements ont été choisis aléatoirement et regroupés afin d'obtenir un échantillon le plus représentatif de l'état global de la parcelle et de limiter la variabilité qu'il peut y avoir au sein même d'une parcelle. Les échantillons de sols ainsi obtenus ont directement été envoyés au laboratoire d'analyse qui a effectué la préparation (séchage, broyage, tamisage) des échantillons. Le prélèvement des échantillons de sol et de végétaux ont été effectués en fin de saison végétative. L'ensemble des échantillons a été prélevé le même jour.

A la fin de la deuxième saison végétative (début octobre 2012), pour chaque parcelle plantée, l'ensemble de la végétation (saules, miscanthus, *Buddleja*) a été coupé, broyé grossièrement, mélangé avant de prélever 250g de matière fraiche qui sera lyophilisée pour éviter tout risque de moisissures et pourrissements lors de la période de transport.

Afin de déterminer la quantité des HAPs qui a été enlevée des sols et de déterminer la quantité absorbée par les plantes, des dosages des 16 HAPs (Partie 1, Tableau 1) listés comme prioritaires par l'agence de l'environnement américaine (Wilson and Jones, 1993) ont été réalisés par le laboratoire CARSO (Lyon, France). Pour les sols, le dosage est effectué par chromatographie en phase liquide à haute performance (HPLC), après une extraction par des solvants (Accelerated Solvant Extraction, ASE), en suivant le protocole normalisé NF X33-012. Pour les végétaux, le dosage est effectué par chromatographie en phase gazeuse couplée à de la spectrométrie de masse GC-MS.

2.5. Analyses statistiques

L'intégralité des analyses statistiques a été réalisé en utilisant le test de Wilcoxon avec le logiciel R (team RDC, 2013). Etant donnée la forte variabilité existant sur le site pilote, les données ont été considérées statistiquement significatives quand la p-value était inférieure à 0,1.

3. Résultats-discussion

3.1. Suivi du développement de la végétation sur le site pilote

Chaque parcelle a été photographiée tous les mois, entre décembre 2010 et octobre 2012, afin de suivre le développement de la végétation. Ces données montrent que, malgré un sol fortement pollué, où ne poussaient que quelques espèces herbacées clairsemées caractéristiques des friches industrielles (Figure supplémentaire 1), l'ensemble des espèces se sont bien installées. L'apport de terre végétale a probablement aidé les plantes à se développer et a permis d'implanter d'autres espèces (orties et chardons) qui n'étaient pas naturellement présentes sur le site. De plus, on peut noter que des plantes se sont développées sur les parcelles pour lesquelles seul un arrosage a été effectué (parcelles « contrôles ») soulignant ainsi l'importance de l'apport en eau pour favoriser le développement des plantes dans ces conditions sur ce site.

La figure 2 montre l'évolution des différentes conditions testées sur une parcelle représentative au cours des saisons. Nous avons, par ailleurs, cherché à quantifier le développement des plantes en utilisant des marqueurs mesurables et surtout non-destructifs. Une approche très grossière a tout d'abord été utilisée de manière à évaluer l'évolution des plantes à travers la quantification de la chlorophylle par le biais d'analyse d'images numériques. Cette mesure prend en compte aussi bien les espèces que nous avons installées que les espèces qui se sont installées de manière spontanée. L'ensemble des photos a été pris au même moment de la journée, selon le même angle.

A partir des photographies prises tout au long de l'expérimentation (Figure supplémentaire S2), une analyse de l'intensité de la chlorophylle (couleur verte) a été effectuée, grâce au logiciel de traitement d'image 'ImageJ'.

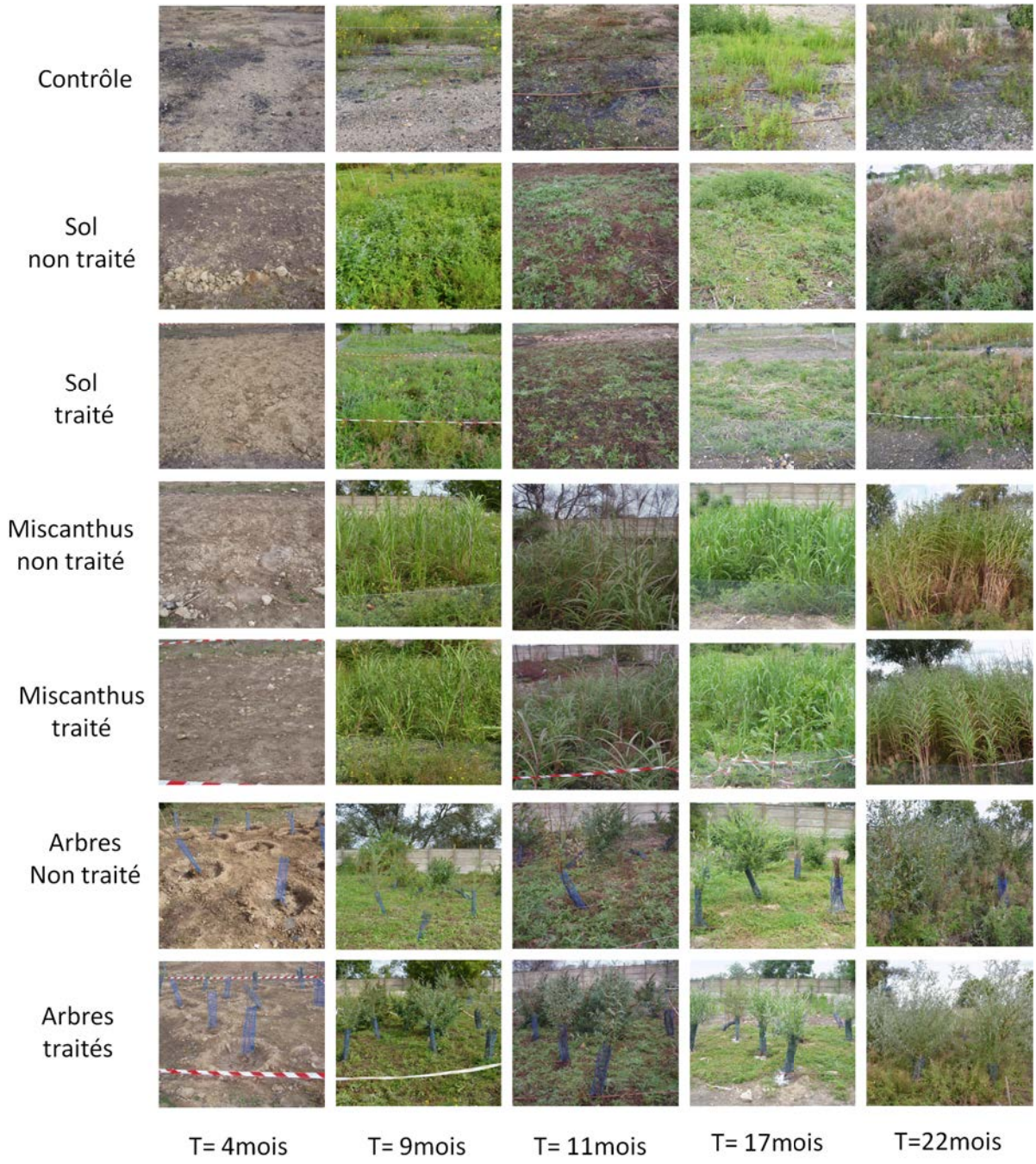

<u>Figure 2</u> : Suivi du développement de la végétation sur une parcelle représentative de chaque condition

Les temps indiqués représentent les pics saisonniers pour lesquels le développement de la végétation est à son maximum (en été T=9mois et T=17mois) ou à son minimum (T=4 mois qui est aussi le point de départ de l'ensemble de l'expérimentation et T=11 mois) puis à au moment des prélèvements (T=22mois).

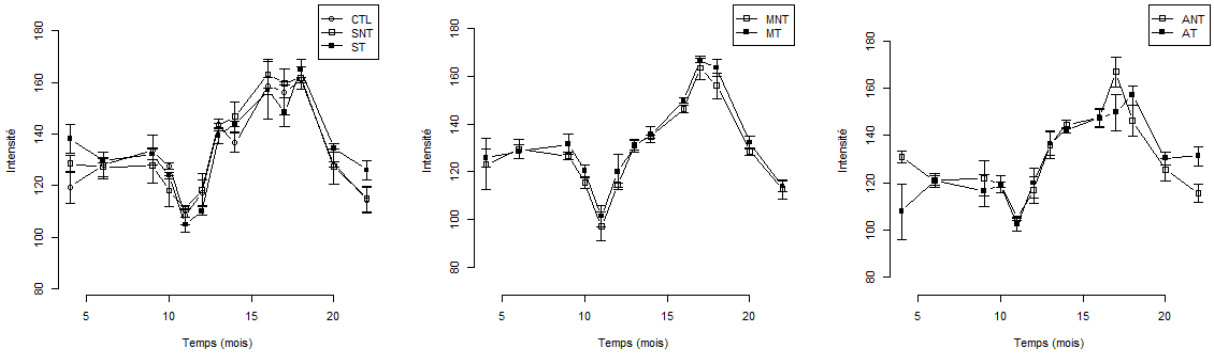

<u>Figure 3</u> : Evolution de l'intensité du vert des photographies prises au cours de l'expérimentation (en annexe 1) pour les différentes conditions étudiées.

CTL, contrôle ; SNT, sol nu non traité ; ST, sol nu traité ; MNT, herbacées (miscanthus) non traitées ; MT, herbacées (miscanthus) traitées ; ANT, ligneuses (arbres) non traitées ; AT, ligneuses (arbres) traitées.

La figure 3 retrace l'évolution de ce paramètre au cours du temps. Les pics correspondent aux mois d'été et les creux à ceux d'hiver. En effet, comme on peut l'observer sur la figure S2, la coloration verte due à la chlorophylle des plantes est beaucoup plus intense en été quand la végétation est à son maximum de croissance alors qu'en hiver, les feuilles ont jaunies ou sont tombées d'où la diminution de l'intensité de la couleur verte. La variation saisonnière de ce paramètre montre bien que c'est un indicateur de la variation de la teneur chlorophylle et de développement des parties aériennes (en particuliers des feuilles). De plus, cet indicateur est non destructif et nous permet donc de suivre l'évolution de l'ensemble des plantes au cours du temps. Cette quantification très globale n'a pas permis de dégager des différences significatives entre les différentes conditions de traitement en saccharose. Ce résultat montre que l'apport de saccharose n'a pas rendu les plantes plus « vertes » c'est-à-dire plus riches en chlorophylles. D'autre part, l'absence de différence observée entre les sols plantés et non plantés montrent que le seul apport de terre végétale et surtout l'irrigation ont permis le développement de la végétation sur les parcelles.

Par ailleurs, un taux de survie (Figure 4) a pu être calculé pour les deux espèces ligneuses, étant donné que 6 arbres de chaque espèce ont été plantés dans chaque parcelle. Ce taux est un critère permettant d'évaluer la viabilité des espèces et leur capacité d'adaptation aux conditions aussi bien climatiques et pédologiques du site qu'à la forte

teneur en HAPs. Cependant, aucune différence n'est observable entre les taux moyens de chaque condition, ces résultats pouvant être expliqués par l'hétérogénéité du site.

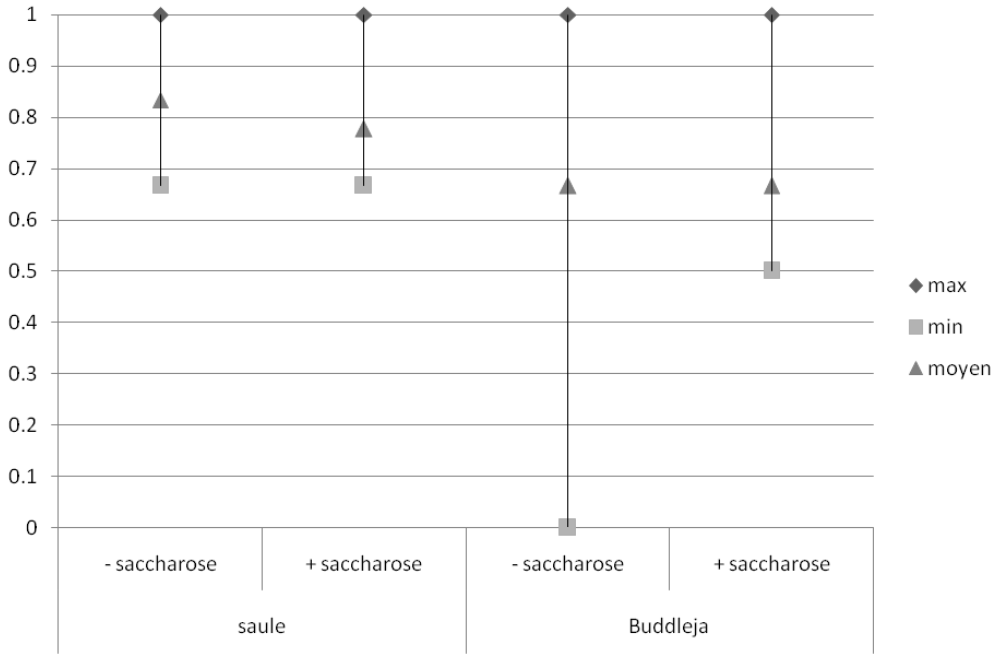

<u>Figure 4</u> : Taux de survie des plantes ligneuses.

Max, représente le taux de survie le plus élevé des 3 répétitions ; min, le taux de survie le plus faible des 3 répétitions ; moyen, le taux de survie moyen des 3 répétitions.

Cependant, le taux de survie minimal représente le taux de survie pour la parcelle la plus affectée avec le plus d'arbres morts. Les résultats obtenus montrent que *Buddleja* est l'espèce la plus fortement affectée par les HAPs avec un taux de survie nul pour les parcelles non-traitées et de 0,5 pour les traitées alors que pour le saule ce taux est de près de 0,7 sur parcelle traitée, ce qui montrerait l'effet potentiel du saccharose même sur le terrain. De plus, il est important de noter que, dans le cas du *Buddleja*, la parcelle la plus affectée est une parcelle non-traitée alors qu'aucune différence n'est observable pour le saule.

D'autre part, nous avons observé que le miscanthus ne présentait pas une répartition homogène sur certaines parcelles. Ceci serait probablement dû à un manque d'arrosage. L'arrosage par goutte-à-goutte se faisant de la gauche vers la droite du plan expérimental (Figure 1) et les parcelles les plus touchées étant à droite, il se peut que, malgré les précautions prises, ces parcelles-là aient reçu une quantité d'eau insuffisante. De plus, pour les deux espèces ligneuses (*Buddleja* et saule), les parcelles pour lesquelles le taux de survie

(Figure 4) est le plus faible se situent elles aussi vers la droite du site pilote. L'installation d'une irrigation par aspersion serait probablement plus adaptée à la culture du miscanthus (surtout pour de grandes surfaces), étant donné que c'est ce type d'arrosage qui est utilisé pour l'irrigation du maïs. D'autre part, l'utilisation d'un paillis, comme par exemple les résidus de la première coupe de miscanthus, permet de conserver l'humidité dans le sol et d'optimiser au mieux l'arrosage au goutte-à-goutte.

De manière générale, la végétation s'est bien développée et surtout de nouvelles espèces, autres que celles installées, se sont implantées.

De plus, la mise en place des parcelles de phytoremédiation a permis l'introduction d'insectes, arachnides et vers. Un inventaire non-exhaustif effectué au cours de la première saison végétative, après 6 mois d'expérimentation, a permis d'identifier une quarantaine d'espèces végétales qui se développent spontanément sur le site (Figure S2). Parmi ces espèces, on retrouve le saule fragile et *Buddleja* qui ont été utilisés pour l'expérimentation. Certaines espèces telles que le bouillon blanc, le millepertuis ou bien le sureau sont présentes de façon abondante sur le site. La terre végétale a probablement apporté, en plus des micro-organismes et des vers, de nouvelles espèces notamment des chardons qui se développent uniquement dans les zones où se trouve cette terre.

3.2. Estimation des capacités de stockage des HAPs par les 3 espèces végétales

La méthode de dosage des HAPs utilisée ne prend en compte que les HAPs libres. Par conséquent, la fraction dosée ne représente probablement pas l'intégralité des HAPs stockés dans la plante. Il est possible que les cellules végétales, comme c'est le cas pour les bactéries, les champignons et les cellules animales, métabolisent les xénobiotiques, ou bien les conjuguent avec des molécules simples comme les sucres ou le glutathion afin de les rendre moins toxiques. Ce processus a été démontré au moins pour les polluants phénoliques chez Arabidopsis. En effet une fois absorbé par les cellules végétales, ces derniers sont glycosylés par une glucosyltransferase (Brazier-Hicks et al., 2007) ou bien associé aux parois via probablement des peroxydases comme l'ont suggéré Matsui et al. 2011.

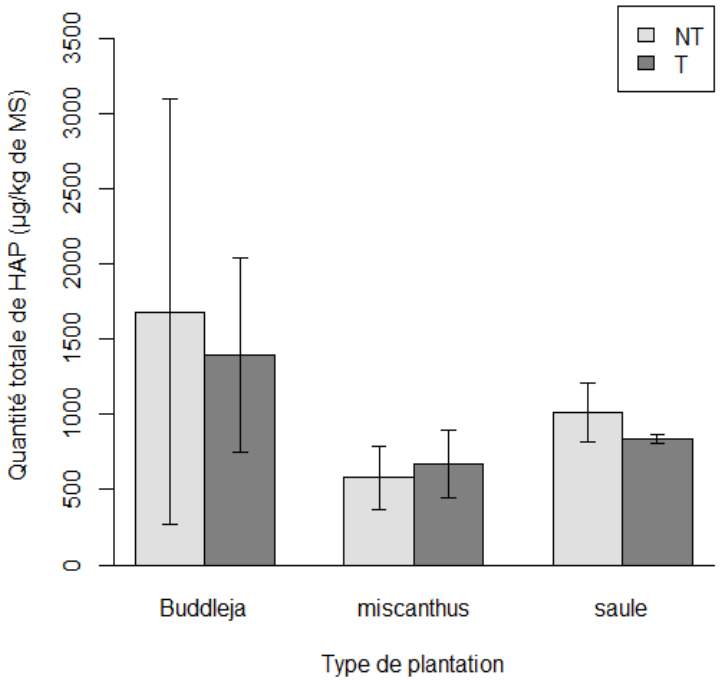

<u>Figure 5</u>: Quantité totale des 16 HAPs dosés dans les plantes pour l'ensemble des conditions étudiées.

NT représente les parcelles n'ayant pas reçu un apport de saccharose ; T représente les parcelles ayant reçu un apport de saccharose.

Les HAPs détectés dans les plantes sont donc probablement ceux qui n'ont pas été transformés et pourraient représenter uniquement la partie directement absorbée et accumulée dans la cellule de la plante sans transformation. D'autre part, les HAPs peuvent être retrouvés dans les parties racinaires (racines et rhizomes) mais, généralement, en quantité moins importantes que dans les parties aériennes (Wang et al., 2012c).

Les HAPs ont été dosés uniquement dans les parties aériennes des plantes afin de permettre la repousse des plantes et la poursuite de l'expérimentation sur plusieurs années. Les plantes ont absorbé entre 500 et 1700µg de HAPs totaux par kilogramme de matière sèche analysée. Nos données montrent cependant une grande variabilité de la teneur des HAPs accumulés par les trois espèces, ce qui pourrait refléter l'hétérogénéité de la pollution du site pilote, la présence d'effet pépites mais aussi que les trois espèces n'ont pas la même capacité d'absorption. On peut remarquer que les arbres ont tendance à absorber plus de HAPs que le miscanthus, probablement grâce à leur enracinement beaucoup plus profond qui leur donne une plus grande surface de contact et leur permet d'accéder à des zones plus fortement polluées.

Même si aucune différence statistiquement significative n'est observée entre les trois espèces étudiées, une tendance se dessine montrant que les arbres semblent absorber plus de HAPs que l'espèce herbacée (Figure 5).

Il est intéressant de noter que le *Buddleja,* qui est la plante qui paraît accumuler le plus de HAPs libres, est l'espèce qui présente le plus faible taux de survie. Cette observation semble indiquer que la stratégie de gestion des HAPs par les trois espèces végétales est différente.

Quant à l'effet du saccharose, une tendance se dessine sans être pour autant significative. En effet, le saccharose semble permettre aux miscanthus d'absorber plus de HAPs, mais cette tendance n'apparaît pas pour les deux autres espèces. Le miscanthus a un système racinaire superficiel qui lui permettrait d'absorber le saccharose apporté en surface plus rapidement avant qu'il soit lessivé. De plus, cette espèce est capable de stocker le saccharose dans ses rhizomes directement ou sous forme d'amidon (Lebas, 2012). Malgré ce

résultat très contrasté, on peut noter que les espèces installées sur le site pilote sont capables d'absorber les HAPs et de les stocker.

Toutefois, la fraction de HAPs libres stockée par les plantes ne représente que 1 à 3% de la quantité totale de HAPs enlevée des sols, ce qui montre que la phytoaccumulation des polluants non-transformés n'est pas le processus principal de la phytoremédiation. Dans la part des HAPs enlevés du sol, il y a ceux qui ont été potentiellement transformés voire même complètement dégradés par les plantes. Pour avoir une idée claire sur l'implication des plantes dans les processus de remédiation des HAPs des sols pollués, il serait important de quantifier la partie conjuguée ou métabolisée en procédant à des expérimentations basées sur un marquage au carbone 13, afin d'effectuer un suivi des produits marqués dans la plante. Cette approche compléterait les analyses des HAPs libres dans la biomasse végétale.

Le benzo[b]fluoranthène et le dibenz[a,h]anthracène ne sont pas détectés dans l'ensemble des échantillons. Ce sont deux HMW HAPs, les moins hydrosolubles (Partie 1, Tableau 1) et donc les moins mobiles dans le sol et les moins disponibles pour les plantes. Les valeurs correspondant aux HAPs non détectés ont été majorées au niveau du seuil de détection car, étant donné qu'ils sont présents dans le sol, il est fort possible qu'ils soient dans les plantes en très faibles quantités.

D'autre part, l'acénaphtylène qui n'est pas détecté dans les échantillons de sol est présent dans les plantes, ce qui montre que ce HAP est bien présent dans le sol en très faible quantité. L'acénaphtylène est un HAP à 3 cycles, de faible poids moléculaire et avec une solubilité dans l'eau plutôt élevée pour un HAP (Partie 1, Tableau 1) ce qui le rend facilement disponible pour les plantes. D'autre part, la technique d'analyse utilisée pour les dosages des HAPs dans les végétaux a un seuil de détection beaucoup plus bas que la technique utilisée pour les dosages dans les sols. L'absorption de l'acénaphtylène par les plantes montre que les végétaux sont capables d'éliminer les composés présents de façon résiduelle dans le sol, ce qui peut rendre leur utilisation intéressante pour une « finition » en complément d'autres techniques de dépollution.

En plus des analyses des résultats des HAPs totaux, nous avons réalisé un suivi de chaque molécule séparément. La figure 6 représente la quantité de chaque HAP détecté dans les parties aériennes des trois espèces végétales plantées sur le site pilote.

Malgré le fort écart-type lié à la forte hétérogénéité de la pollution dans le site pilote, on remarque que, globalement la gestion des HAPs, pris un à un, est relativement variable d'une plante à l'autre et d'un traitement à l'autre. Cependant, au moins pour les HAPs les plus fortement accumulés (phénanthrène, fluoranthène et pyrène), les quantités libres dans les espèces ligneuses, à enracinement profond, sont plus importantes dans les plantes contrôles que dans les plantes traitées. Le Buddleja des parcelles non-traitées semblent être la condition pour laquelle la plante stocke le plus de HAPs. Si on met ce résultat en parallèle avec le fait que cette espèce présente une forte mortalité, on peut émettre l'hypothèse que c'est l'absorption des HAPs qui a provoqué la mort de cette espèce. On peut aussi envisager l'idée que le saccharose augmente la tolérance de cette espèce aux HAPs ou bien que le saccharose modifie la population bactérienne au niveau de la rhizosphère, favorisant ainsi la dégradation des polluants et limitant les dégâts qu'ils peuvent causer sur les plantes. Cette hypothèse devrait être validée sur un site pilote pour lequel la pollution est répartie de façon homogène.

Pour une plante à enracinement peu profond comme le miscanthus, cette hypothèse ne semble pas être valide puis qu'elle semble accumuler d'avantage d'HAPs libres dans les plantes traitées que les plantes contrôles, ce qui suggérerait que le miscanthus aurait une gestion cellulaire différente, probablement une compartimentation de ces polluants dans les vacuoles, pour réduire leur toxicité, qui serait liée à une induction de transporteurs non-spécifiques comme c'est la cas pour le blé qui est, comme le miscanthus, une Poacée (Zhan et al., 2010; Zhan et al., 2012). Les résultats d'accumulation des HAPs totaux soutiennent cette hypothèse (Fig. 5). Le miscanthus et les deux espèces d'arbres n'ont pas le même fonctionnement métabolique, en effet, la première espèce est une plante en C4 alors que les deux arbres sont des plantes en C3. Les données bibliographiques disponibles ne montrent pas que les plantes en C4 telles que le miscanthus ont une gestion différente des xénobiotiques de celle des plantes en C3. Vavrek et Campbell (2002) ont essayé de comparer l'efficacité de plantes en C3 et en C4 pour la bioremédiation de produits pétroliers mais ils

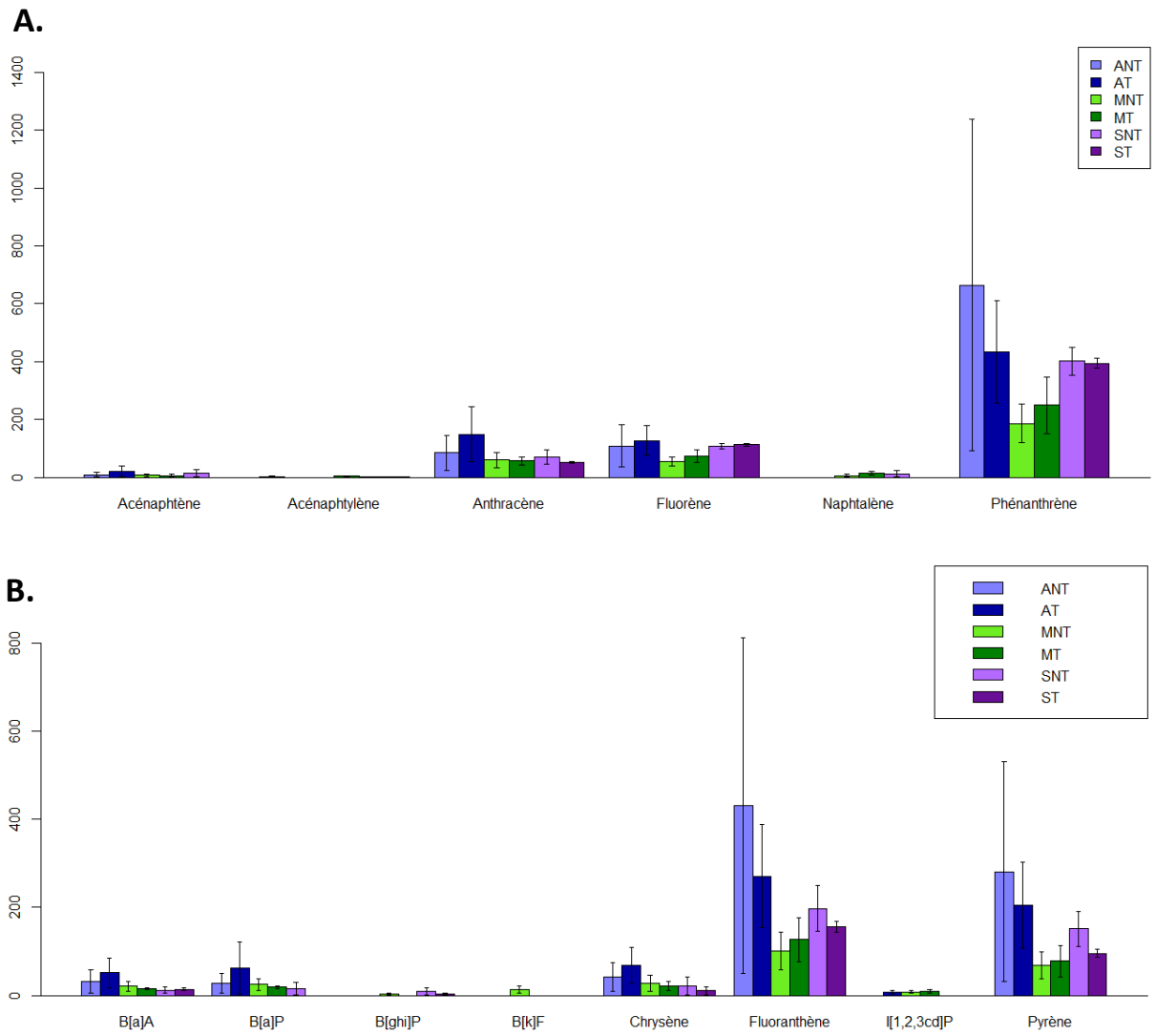

<u>Figure 6</u> : Répartition des HAPs détectés dans les plantes pour les LMW HAPs (A) et les HMW HAPs (B).

ANT, Buddleja non traités ; AT, Buddleja traités ; MNT, Miscanthus non traités ; MT, Miscanthus traités ; SNT, Saules non traités ; ST, Saules traités.

B[a]A, Benzo[a]Anthracène ; B[a]P, Benzo[a]Pyrène ; B[ghi]P, Benzo[ghi]Périylène, B[k]F, Benzo[k]Fluoranthène ; I[1,2,3cd]P, Indéno[1,2,3cd]Pyrène.

n'ont pas pu mettre en évidence de différence entre ces deux types de plantes, probablement car l'effet « taille des plantes » était prédominant.

On ne peut cependant pas exclure que des voies de métabolisation pourrait être fonctionnelles et différentes entre ces espèces, chose que nous n'avons pas eu la possibilité de vérifier dans ce travail.

3.3. Les HAPs restant dans les sols après 21 mois de traitement

Les dosages de HAPs ont été réalisés sur les 30 premiers centimètres de sol. Afin de représenter une valeur moyenne de la quantité de HAPs de la parcelle, nous avons effectué 5 prélèvements que nous avons regroupés et mélangés avant d'effectuer le dosage. La détoxification naturelle et passive des sols (par atténuation naturelle, volatilisation) n'est pas prise en compte dans nos calculs étant donné que le sol « contrôle » subit lui aussi la même évolution que ceux des parcelles traitées. Pour les échantillons provenant des parcelles ayant reçu un apport de terre végétale, nous avons tenu compte de la dilution d'un facteur 3 qui a été faite lors du prélèvement. En effet, en prélevant les 30 premiers centimètres de sol, nous avons prélevé la couche de 15-20 cm de terre végétale non-polluée qui a été apportée et qui représente les deux tiers de la terre prélevée.

Les résultats présentent une grande hétérogénéité qui n'est pas surprenante étant donnée l'histoire du site. En effet, les zones qui ont été polluées sont locales et donc la teneur en HAPs n'est pas homogène sur l'ensemble des parcelles, d'où l'importance de la randomisation des trois répétitions au cours de cette expérimentation. Dans toutes les conditions, la quantité d'acénaphtylène dans le sol étant en dessous du seuil de détection, la valeur de ce HAP a été majorée au niveau du seuil de détection donné par le laboratoire. Ce HAP, qui est un des plus hydrosolubles, aurait également pu être lessivé et par conséquent se retrouver dans des couches plus profondes ou bien tout simplement ne pas être un déchet de la fabrication des revêtements de la société Axson. Etant donné que ce HAP est présent dans les plantes, cela montre qu'il est présent dans le sol mais dans une quantité inférieure au seuil de détection de la méthode de dosage utilisée. On retrouve ce HAP dans les trois espèces du site pilote que ce soit dans les parcelles traitées et non-traitées.

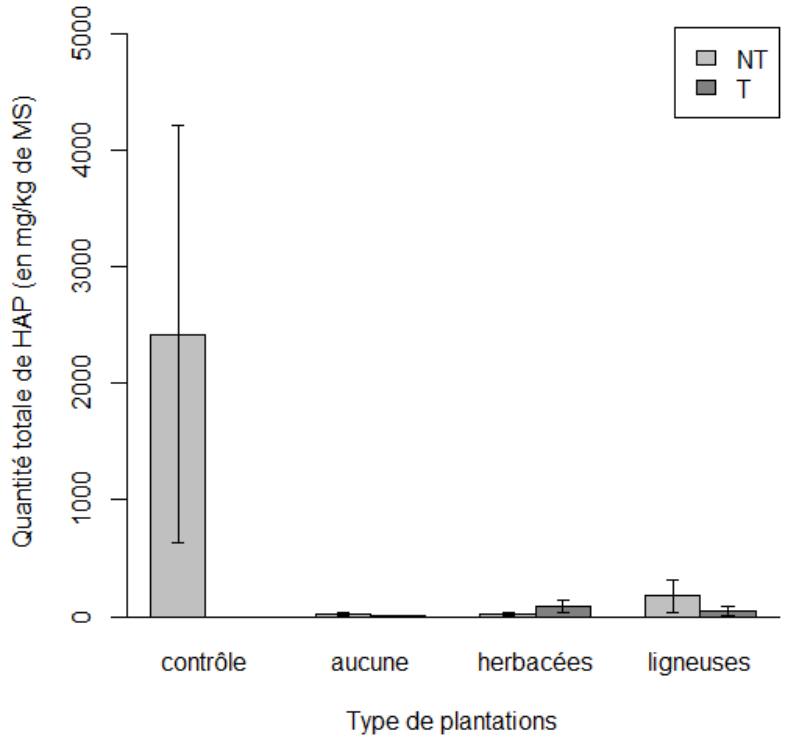

<u>Figure 7</u> : Quantité totale des 16 HAPs dosés dans les sols pour l'ensemble des conditions étudiées.

NT représente les parcelles n'ayant pas reçu un apport de saccharose ; T représente les parcelles ayant reçu un apport de saccharose

La quantité totale des 16 HAPs dosés dans les sols diminue de plus de 90% sur cette profondeur entre les différents traitements (apport de saccharose et type de plantation) et les parcelles contrôles (Figure 7). Aucun effet significatif n'a été détecté entre les parcelles ayant reçu un apport de saccharose et celles qui n'en ont pas eu et entre les parcelles plantées et les parcelles non plantées. L'ajout de terre végétale, lors de la mise en place du site pilote, a probablement fortement contribué à la diminution importante de la quantité totale de HAPs dans le sol, quel que soit le type de plantation (plantes herbacées, ligneuses ou aucune). Cette forte diminution des HAPs dans le sol pourrait être expliquée par l'apport de consortiums bactériens et fongiques qui sont naturellement associés au sol végétal et à l'oxygénation du sol après prélèvement du remblai, qui constitue la couche superficielle du sol pilote. En effet, il existe des techniques de dépollution, connues sous le terme de 'landfarming' (Al-Awadhi et al., 1996; Atagana, 2004; Hansen et al., 2004; Maila and Cloete, 2004), qui consistent à composter les terres polluées. Ces techniques sont efficaces, du moins pour les couches superficielles, prises en compte dans cette étude. Ce même résultat, lié à la préparation du sol, a aussi été observé par Techer et al., (2012) lors de leurs essais de phytoremédiation des HAPs en pots. L'effet stimulateur de l'introduction de plantes sur la diminution des HAPs dans le sol est largement décrit (Pradhan et al., 1998; Liste and Alexander, 2000b; Euliss et al., 2008; Técher et al., 2012). Par contre, dans l'ensemble de ces études, les sols plantés ont une diminution de leur teneur en HAPs beaucoup plus importante que les sols non-plantés. L'ensemble de ces études ont été effectuées en conditions semi-contrôlées (en serre, avec des échantillons de sols contaminés) à échelle réduite (petit volume de sol), ce qui pourrait expliquer pourquoi en l'espace de quelques mois (2-13 mois selon l'étude), on observe un effet des plantes. Vervaeke et al. (2003) et Euliss et al. (2008) ont conduit un essai en plein champ et n'ont pas pu mettre en évidence l'effet stimulateur de plantes après plus d'un an d'expérimentation.

Une autre hypothèse expliquant le fait que la quantité de HAPs restant semble supérieure dans les sols plantés que les sols non-plantés est le mécanisme de phytostabilisation. D'ailleurs, la part des HAPs stockée sans transformation par les plantes est très faible ce qui montre que la phytoaccumulation n'est pas le processus principal de la phytoremédiation des HAPs. En effet, dans ce cas, les plantes piègent les molécules au

niveau de leurs racines. Ce processus est plutôt typique de la phytoremédiation des métaux (Pulford and Watson, 2003) et n'a pas été décrit pour les HAPs.

Encore une fois, les résultats présentent un écart-type très élevé à cause l'hétérogénéité du site. En effet, de part son histoire, le site présente une pollution hétérogène sous forme de « pépites », zones dans lesquelles la teneur en HAPs est très élevées. La mise en place du site pilote a été faite de sorte que cette hétérogénéité soit minimisée. Cependant, le nombre de répétitions effectuées s'est avéré insuffisant pour contrebalancer l'hétérogénéité de la répartition de la pollution. De plus, il n'est pas certain qu'au sein d'une même parcelle la pollution soit homogène. C'est pour cela que les prélèvements de sols ont été réalisés à plusieurs endroits de façon aléatoire. Afin d'améliorer les résultats obtenus et d'éviter d'obtenir une telle hétérogénéité dans les mesures effectuées, il paraît nécessaire de multiplier le nombre de répétitions mais aussi d'augmenter le nombre d'échantillons de sol prélevés. *A posteriori*, une homogénéisation du site suite à l'apport de terre végétale par un labour profond et fragmentation du sol (herse etc.) aurait permis une meilleure répartition des polluants sur ce site expérimental.

En ce qui concerne les HAPs qui n'ont pu être détecté dans nos analyses, ni dans les sols, ni dans les plantes, ces résultats peuvent être expliqués par plusieurs processus: leur volatilisation au niveau des feuilles des plantes ou du sol, leur transformation ou même la dégradation par les plantes et/ou les micro-organismes du sol ou leur lessivage et leur non accessibilité par les racines. Des études réalisées, en parallèle par la société Sol-Environnement ont permis de révéler la présence naturelle de bactéries du genre Pseudomonas, capables de dégrader les HAPs, sur le site. L'oxygénation et la richesse de la terre végétale ajoutée au sol du site expérimental a pu favoriser leur croissance et leur activité. D'ailleurs, de nombreux micro-organismes, agissant seuls ou en consortium et vivant dans des sites pollués par les HAPs, ont déjà été identifiés et sont caractérisés par leur capacité à dégrader les HAPs (Cerniglia, 1992; Mrozik et al., 2003; Haritash and Kaushik, 2009).

<u>Tableau 1</u> : Quantité des HAPs (en ppm) pour chaque condition testée.
Chaque résultat représente la moyenne des 3 répétitions.

	Contrôle non traité		Sol nu non traité		Sol nu traité		Miscanthus non traité		Miscanthus traité		Arbres non traité		Arbres traité	
	Teneur en HAP (ppm)	***SD***	**Teneur en HAP (ppm)**	***SD***	**Teneur en HAP (ppm)**	***SD***	**Teneur en HAP (ppm)**	***SD***	**Teneur en HAP (ppm)**	***SD***	**Teneur en HAP (ppm)**	***SD***	**Teneur en HAP (ppm)**	***SD***
Acénaphtylène	0.15	*0.00*	0.16	*0.00*	0.15	*0.00*	0.15	*0.00*	0.15	*0.00*	0.15	*0.00*	0.15	*0.00*
Fluoranthène	276.40	*210.15*	0.66	*0.46*	0.29	*0.05*	0.57	*0.09*	2.24	*1.28*	5.33	*4.19*	2.11	*1.77*
Benzo[b]fluoranthène	247.89	*172.46*	0.95	*0.75*	0.31	*0.07*	0.59	*0.05*	4.10	*2.54*	8.05	*5.90*	2.30	*1.78*
Benzo[k]fluoranthène	90.20	*59.69*	0.40	*0.24*	0.15	*0.00*	0.22	*0.03*	1.62	*1.05*	2.67	*1.89*	0.81	*0.57*
Benzo[a]pyrène	217.31	*148.95*	0.79	*0.61*	0.25	*0.05*	0.49	*0.07*	3.94	*2.69*	6.71	*4.95*	1.83	*1.39*
Benzo[ghi]Pérylène	160.89	*99.86*	0.74	*0.58*	0.21	*0.03*	0.31	*0.07*	3.47	*2.28*	6.10	*4.40*	1.58	*1.13*
Indéno[1,2,3cd]pyrène	241.55	*154.79*	1.00	*0.84*	0.15	*0.00*	0.15	*0.00*	3.96	*2.25*	6.39	*4.92*	1.80	*1.31*
Anthracène	217.48	*198.43*	0.25	*0.04*	0.15	*0.00*	2.55	*2.37*	0.38	*0.14*	3.36	*3.10*	0.55	*0.40*
Acénaphtène	19.86	*15.85*	0.16	*0.00*	0.15	*0.00*	0.15	*0.00*	0.20	*0.05*	0.40	*0.25*	0.18	*0.03*
Chrysène	228.58	*157.92*	0.67	*0.49*	0.27	*0.06*	0.52	*0.11*	2.80	*1.80*	5.30	*4.15*	1.71	*1.36*
Dibenzo[a,h]anthracène	41.73	*35.20*	0.16	*0.00*	0.15	*0.00*	0.15	*0.00*	0.97	*0.54*	1.09	*0.94*	0.33	*0.18*
Fluorène	35.78	*31.21*	0.16	*0.00*	0.15	*0.00*	0.29	*0.14*	0.23	*0.08*	0.56	*0.41*	0.26	*0.11*
Naphtalène	6.33	*4.10*	0.16	*0.00*	0.15	*0.00*	0.15	*0.00*	0.20	*0.05*	0.30	*0.15*	0.10	*0.05*
Pyrène	186.01	*136.35*	0.60	*0.43*	0.22	*0.04*	0.47	*0.11*	2.25	*1.39*	4.50	*3.42*	1.76	*1.45*
Phénanthrène	295.40	*251.49*	0.54	*0.22*	0.44	*0.06*	1.31	*0.79*	1.34	*0.64*	4.46	*3.67*	1.52	*1.15*
Benzo[a]anthracène	157.39	*110.92*	0.43	*0.27*	0.17	*0.01*	0.30	*0.07*	1.79	*1.14*	3.22	*2.50*	1.15	*0.91*
total HAPs	2422.94	*1786.53*	7.79	*4.88*	3.37	*0.27*	8.38	*3.49*	29.63	*17.84*	58.60	*44.82*	18.14	*13.48*

D'autres part, plusieurs études ont montré que, dans le cadre de la phytoremédiation des HAPs, la rhizodégradation, qui combine l'action des plantes et des micro-organismes associés au système racinaire, est un des processus moteur de la détoxification des sols (Muratova et al., 2003; Kuiper et al., 2004; Abhilash et al., 2012).

Pour chacun des HAPs analysés, la quantité dans le sol des parcelles « contrôle » est significativement plus élevée que dans les autres conditions (Tableau 1). Ce résultat n'est pas dû au simple remplacement des 20 premiers centimètres constitué initialement par des gravats, par une épaisseur équivalente en terre végétale puisque les valeurs trouvées ont été corrigées en introduisant le facteur de dilution correspondant à la quantité de sol végétal rajouté ($quantité\ du\ HAP = valeur\ mesurée \times 3$). D'autre part, une attention particulière a été portée sur les méthodes de prélèvement des sols sur le terrain. La figure 8 donne la quantité de chacun des 16 HAPs dosés dans les sols pour chaque condition testée. Ce résultat montre que l'ensemble des traitements effectués (apport de terre végétale, plantations, amendements en saccharose) a permis de faire diminuer significativement la teneur des sols en HAPs.

La grande variabilité des résultats, qui traduit encore une fois très probablement l'hétérogénéité de la pollution sur le site se retrouve aussi lors de l'analyse des HAPs individuellement. La nature des HAPs dans les sols varie en fonction du traitement (type de plantation et apport en saccharose) appliqué. La comparaison du sol nu traité et non-traité nous permet d'évaluer l'effet du saccharose. Pour chaque HAP analysé, la quantité résiduelle dans le sol non traité est plus importante que dans le sol traité: l'apport de saccharose semble donc produire un effet sur le sol permettant une évolution différente des HAPs dans le sol. Le même type de réponse est observé pour les parcelles plantées avec des arbres, de façon plus marquée surtout pour les HMW HAPs. Ce résultat pourrait être dû à plusieurs facteurs :

- un développement plus important des micro-organismes dégradant les HAPs,
- une activité de ces micro-organismes favorisée par l'apport d'une nouvelle source d'énergie.

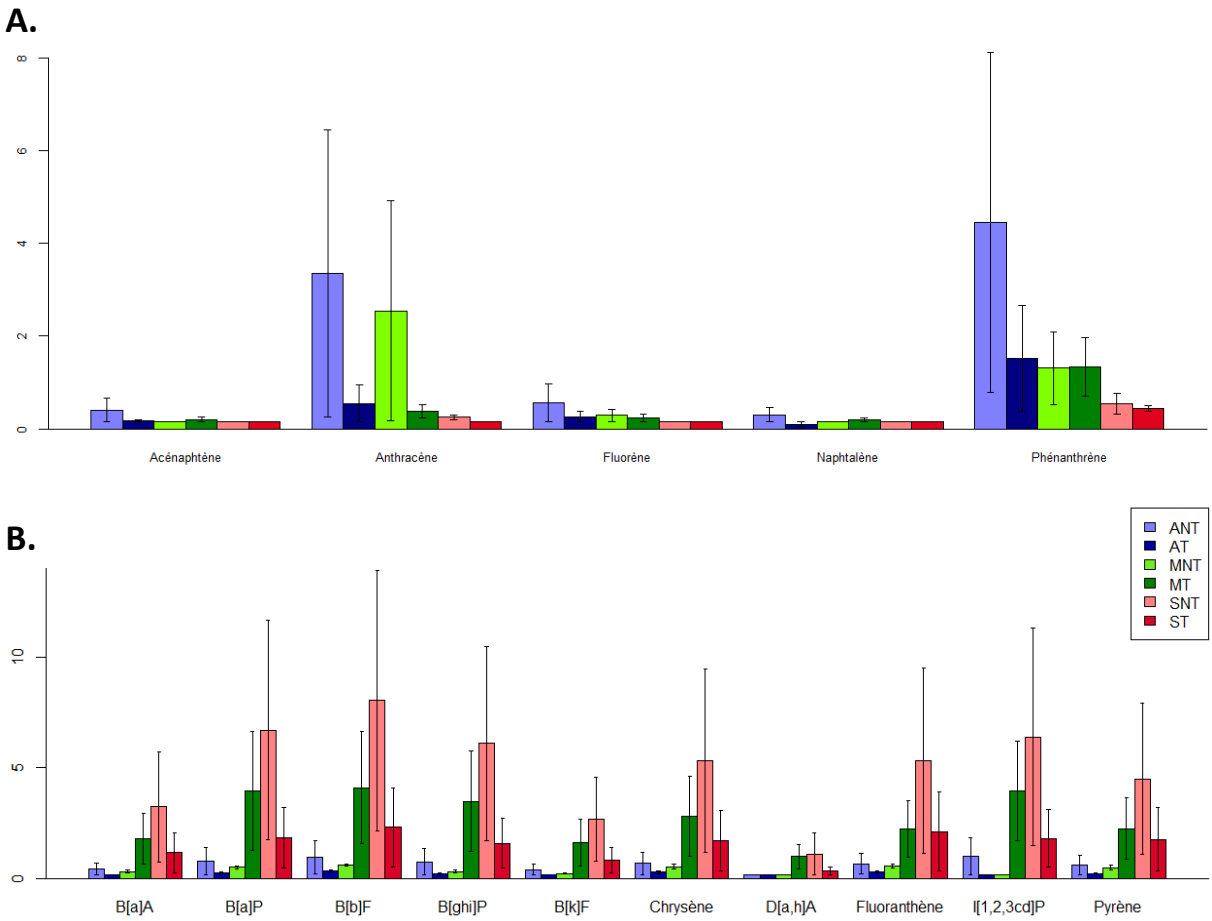

<u>Figure 8</u> : Quantité de chaque HAP (en mg/kg de MS) détecté dans les sols en distinguant les LMW HAPs (A) et les HMW HAPs (B).

ANT, Arbres non traités ; AT, Arbres traités ; MNT, Miscanthus non traités ; MT, Miscanthus traités ; SNT, Sols non traités ; ST, Sols traités. B[a]A, Benzo[a]Anthracène ; B[a]P, Benzo[a]Pyrène ; B[b]F, Benzo[b]Fluoranthène ; B[ghi]P, Benzo[ghi]Périylène ; B[k]F, Benzo[k]Fluoranthène ; D[a,h]A, Dibenzo[a,h]Anthracène ; I[1,2,3cd]P, Indéno[1,2,3cd]Pyrène.

- une meilleure interaction entre plantes et microorganismes particulièrement au niveau de la rhizosphère,
- à un meilleur développement des plantes et par conséquent une meilleure métabolisation des HAPs.

Par contre, pour le miscanthus, l'effet du saccharose diffère selon le type de HAPs : pour les LMW HAPs (Fig. 8A), le saccharose semble stimuler la disparition de ces HAPs alors que, pour les HMW HAPs (Fig. 8B), le saccharose aurait l'effet inverse et limiterait la disparition de ces HAPs du sol. Des études *in-vitro* ont montré que les exsudats racinaires du miscanthus étaient utilisés comme source d'énergie et de carbone pour le développement de la biomasse bactérienne, induisant ainsi une activité bactérienne plus importante pour la dégradation du phénanthrène et du pyrène. Une analyse de la composition des exsudats racinaires de miscanthus a permis de montrer que ce sont des molécules de la famille des flavonoïdes qui sont responsables de la biostimulation bactérienne (Técher et al., 2011). D'autre part, il est connu que le saccharose est un régulateur de la voie de biosynthèse des flavonoïdes chez les plantes (Solfanelli et al., 2006). L'apport de saccharose aurait donc pu entrainer une production de flavonoïdes qui ont été exsudés par les racines dans la rhizosphère entrainant ainsi la stimulation de l'activité bactérienne au sein des parcelles de miscanthus traitées. De plus, les LMW HAPs sont en général bien plus hydrosolubles que les HMW HAPs, ce qui les rend plus disponibles pour les bactéries qui les dégradent. Les premiers essais de biodégradation des HAPs *in-situ* ont montré que les HMW HAPs sont moins bien dégradés que les LMW HAPs (Wilson and Jones, 1993). Cette différence aurait probablement pu être exacerbée par l'apport de saccharose, en favorisant de façon directe ou indirecte (par les exsudats racinaires du miscanthus) le développement des populations bactériennes dégradant les LMW HAPs qui concurrenceraient les microorganismes dégradant les HMW PAHs.

4. Conclusion et perspectives

Le système mis en place lors de cette expérimentation se montre très efficace sur les couches superficielles du sol. En effet, la quantité totale des HAPs diminue largement par rapport à une parcelle non traitée (parcelles « contrôle » du site pilote).

Les dosages des HAPs dans les plantes ont permis de montrer que la phytoaccumulation des HAPs non-transformés semble être un processus mineur de la phytoremédiation des HAPs. Les plantes ne semblent pas absorber l'ensemble des 16 HAPs avec une efficacité équivalente mais sont capables d'absorber certains des LMW et des HMW HAPs.

La différence observée entre les espèces végétales se fait surtout sur la variété des HAPs absorbés et aussi sur la tolérance à ces derniers. Le miscanthus qui absorbe le plus large panel de HAPs est la plante qui a présenté le plus de difficulté à s'implanter. Le *Buddleja* semble être plus sensible car une parcelle entière n'a pas survécu après la première année et cette plante parait absorber légèrement plus de HAPs libres que les autres espèces. Enfin, le saule s'est plus facilement implanté mais semble être un peu moins performant dans sa capacité à absorber/utiliser les HAPs.

Il serait, à ce point de l'étude, intéressant de suivre l'évolution de ces végétaux sur plusieurs années. En effet, on estime que le miscanthus atteint son optimum de production de biomasse après 3 ans de culture et que les arbres ont besoin de plusieurs années afin de bien s'implanter dans le sol. Toutefois, cette expérimentation sur presque 2 ans a permis de montrer les difficultés de mise en place et de gestion d'un site de phytoremédiation.

Les plantes ont aussi permis de révéler la présence d'un HAP qui n'était pas détecté dans le sol car il était probablement en trop faible quantité. Nos résultats montrent le rôle de bio-accumulateur des végétaux, puisqu'ils ont permis de mettre en évidence la présence de molécules indétectables dans le sol, du moins avec les techniques de dosage que nous avons utilisées. Aussi, mêmes si des pollutions ne sont pas détectables dans le sol, elles peuvent se retrouver dans les végétaux qui sont cultivés dans ces sols, soulignant ainsi le rôle important de la qualité des sols agricoles et surtout des agences pour la sécurité alimentaire.

L'apport de terre végétale seule a permis de diminuer fortement la quantité de HAPs dans le sol, ce qui montre l'intérêt de cet apport non seulement pour favoriser l'implantation des végétaux, mais aussi pour apporter de nouveaux micro-organismes dans le sol pollué et oxygéner ce dernier.

L'apport de saccharose a favorisé la diminution des HAPs, notamment les HMW HAPs pour les sols non-plantés et les sols plantés d'arbres, ce qui montre le potentiel de cette technique surtout pour stimuler la bioremédiation de ces HAPs les plus récalcitrants. Toutefois, des études supplémentaires sur le devenir du saccharose dans le sol, l'impact de cet apport sur les micro-organismes et sur la gestion des apports (quantité, forme, fréquence…) paraissent nécessaires afin de comprendre et d'optimiser le système. L'installation d'un tel système de dépollution demande une vigilance constante afin de limiter le stress subit par les végétaux. D'autre part, la répartition de la pollution de façon ponctuelle rend difficiles les comparaisons entre les parcelles. Afin de mieux identifier les performances de chaque condition expérimentale, il serait pertinent de poursuivre l'expérimentation sur plusieurs années, d'analyser les couches de sol les plus profondes, la structure des systèmes racinaires pour chaque espèce végétale et d'étudier les populations microbiennes retrouvées dans chaque condition.

De ces résultats, il ressort que le saccharose modifie le comportement des plantes et probablement des micro-organismes du sol. Suivant le type de plantation (arbres, herbacées ou aucune plantation), l'effet du saccharose est différent, ce qui suggère qu'il existe un effet combiné pour ces deux paramètres : un effet du saccharose, du types de plantations et une interaction entre ces deux paramètres. L'effet entre les espèces végétales peut être de métabolisme primaire entre les plantes en C3 (les arbres) et les plantes en C4 (le miscanthus). Cependant, probablement à cause de l'hétérogénéité du site, il n'a pas été possible de vérifier statistiquement cet effet combiné des deux paramètres (plantation et apport de saccharose). D'autre part, malgré la grande variabilité, globalement, il semble que le miscanthus soit la plante qui a permis de mieux dépolluer le sol. En effet, quelque soit le HAP, sa teneur dans les sols plantés de miscanthus est moins élevée que dans les sols plantés d'arbres.

De nombreuses questions restent en suspens afin de bien déterminer le rôle de chaque paramètre de notre étude : (i) quelle est la quantité de HAPs qui a été métabolisée ou dégradée par les plantes, ii) quel(s) est(sont) le(s) mécanisme(s) prépondérant(s) impliqué(s) dans la gestion des HAPs par les plantes (stabilisation, accumulation sous des formes insolubles, volatilisation) ,(ii) quels rôles jouent les micro-organismes dans nos conditions et quelle est la part des HAPs éliminés par ces dernier dans le sol.

Afin de comprendre comment les plantes gèrent les HAPs, il est nécessaire d'approfondir les données *in-vitro* car, pour le moment, aucun modèle n'a été décrit pour les plantes. Pour l'étude des micro-organismes du sol et de leur rôle, il pourrait être judicieux de faire des analyses de métagénomiques qui permettent d'identifier les différentes populations présentes dans le sol mais aussi de suivre la dynamique de cette population.

A.

B.

C.

<u>Figure Supplémentaire 1</u> : Photographies du site avant la mise en place des parcelles expérimentales. (A.) Galette de produit pétrolier à la surface, photographie prise en juin 2010. (B) Zone fortement contaminée appelée « pépite » (entourée en rouge), photographie prise en juin 2010. (C) Vue d'ensemble du site pilote, photographie prise en décembre 2010.

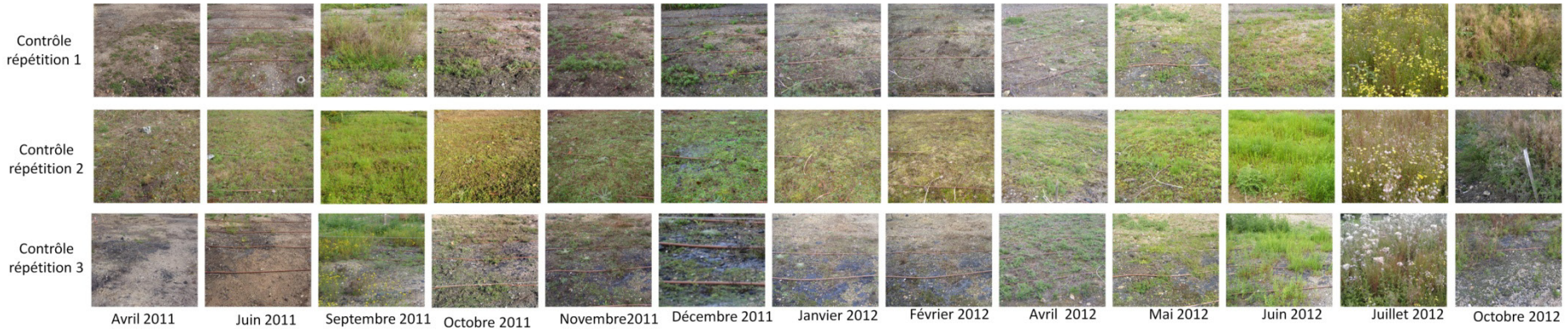

Figure Ssupplémentaire 2 : Evolution des parcelles au cours de la durée l'expérimentation pour les parcelles contrôles

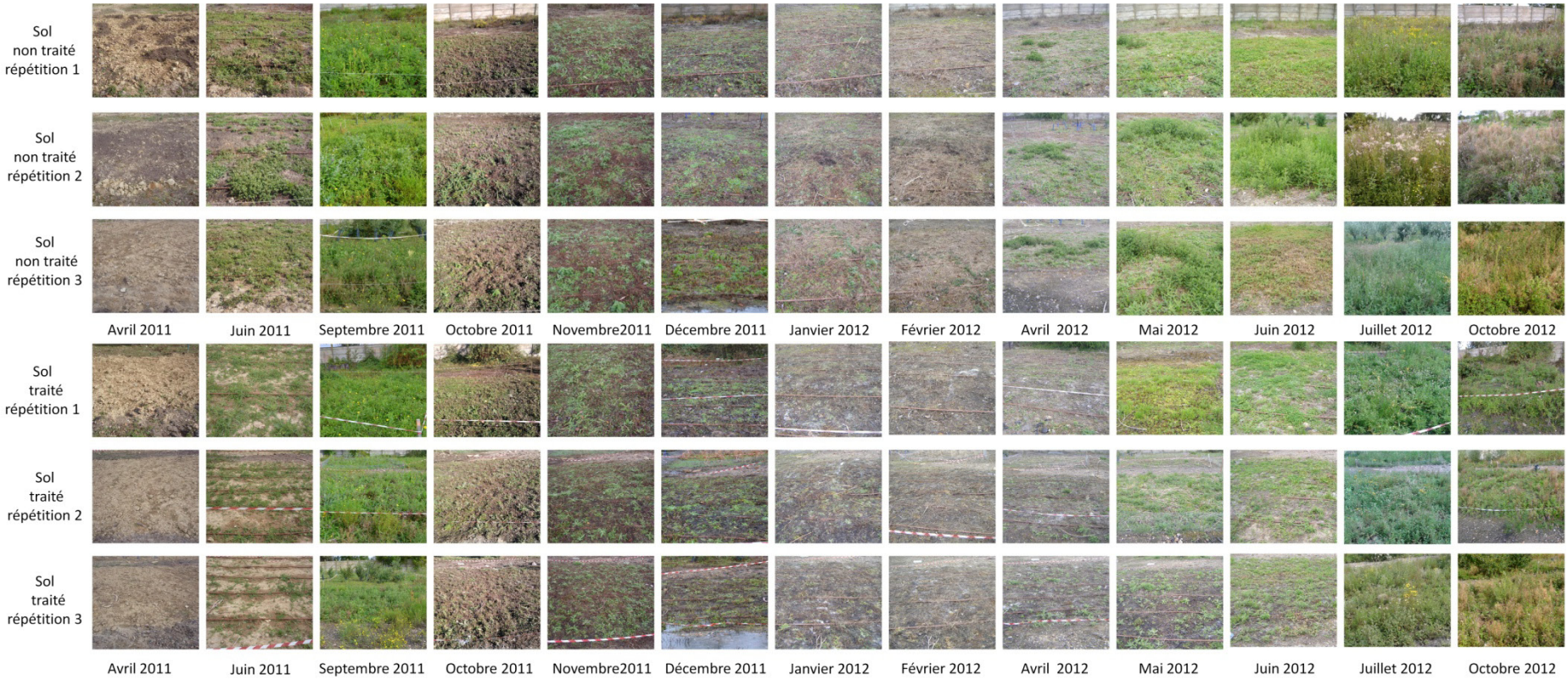

Figure Supplémentaire 2 (suite) : Evolution des parcelles au cours de la durée l'expérimentation pour les parcelles non-plantées avec et sans apport de saccharose

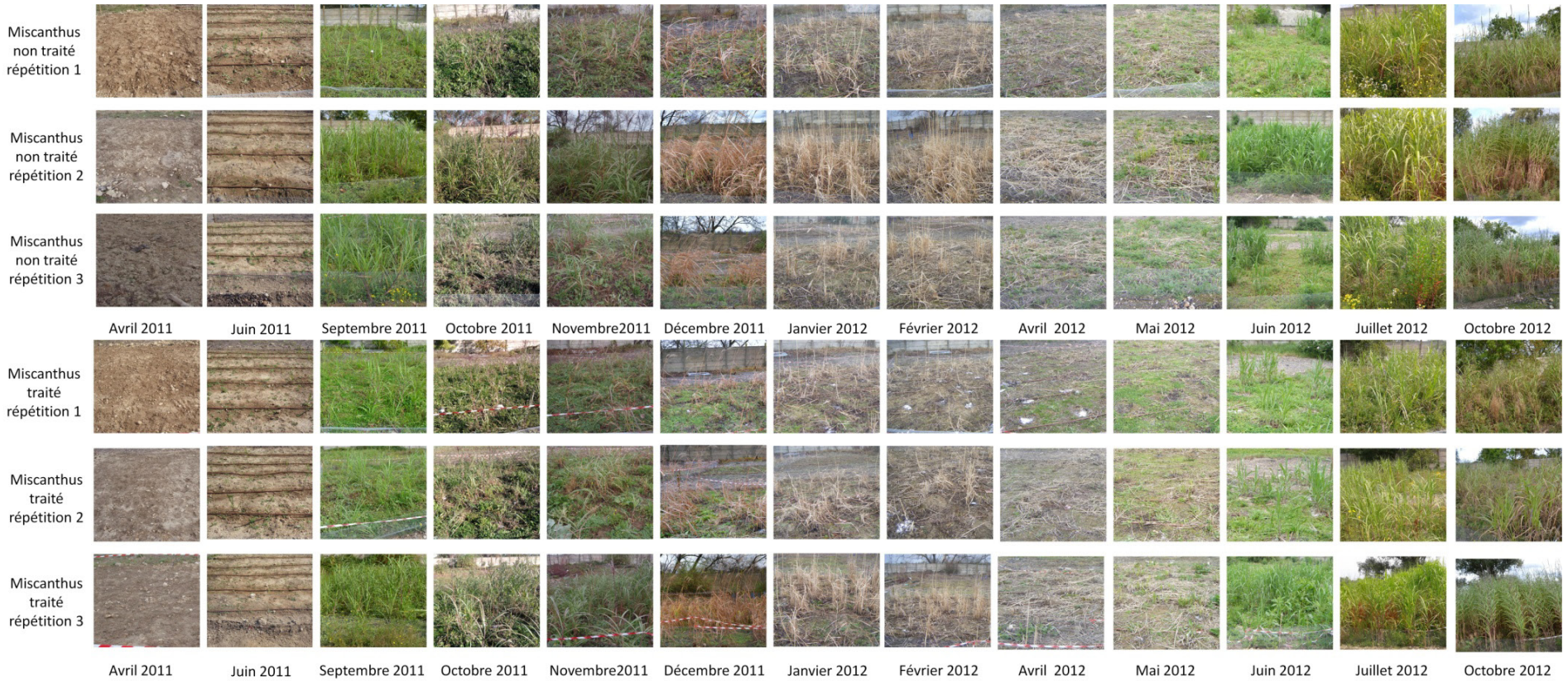

Figure Supplémentaire 2 (suite) : Evolution des parcelles au cours de la durée l'expérimentation pour les parcelles plantées avec du miscanthus qui ont reçu ou pas un traitement par apport de saccharose

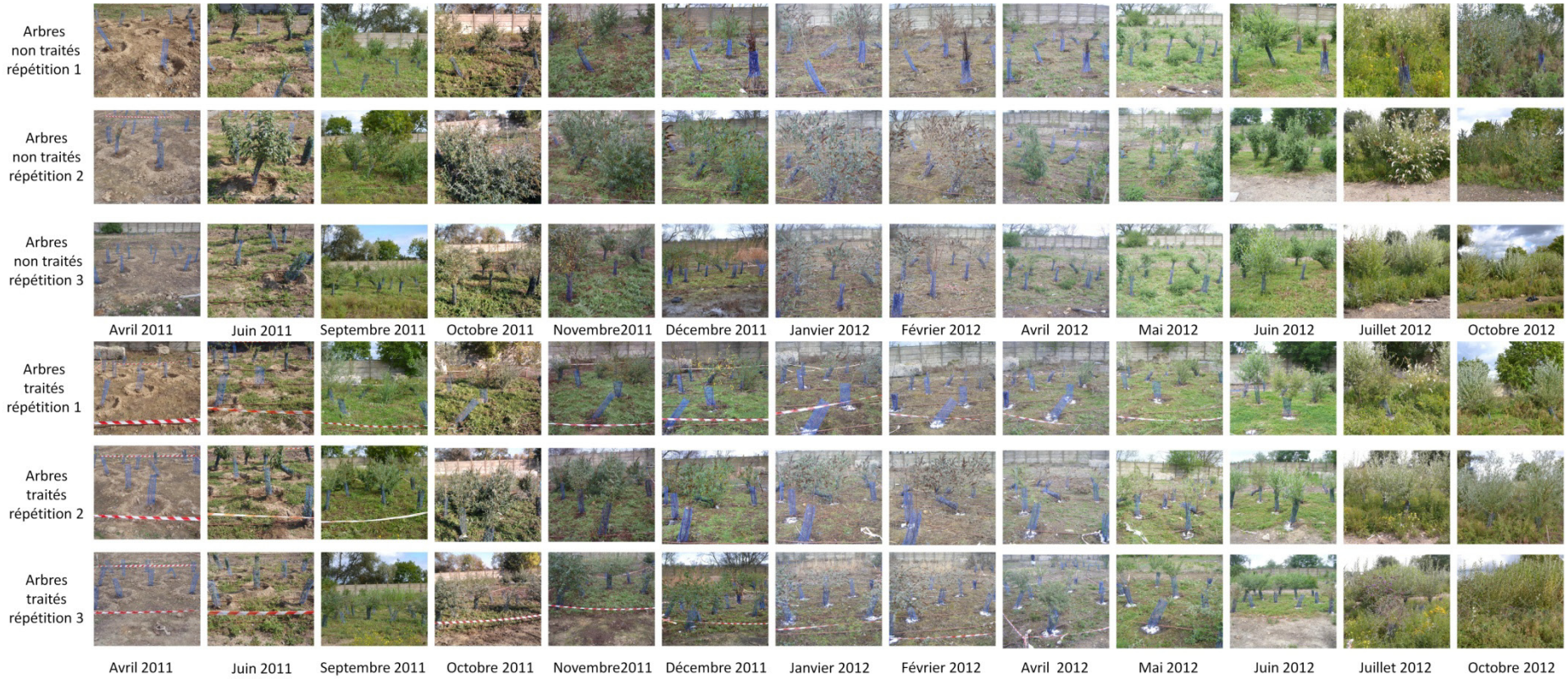

Figure Supplémentaire 2 (suite) : Evolution des parcelles au cours de la durée l'expérimentation pour les parcelles plantées avec des arbres (Buddleja et saules) qui ont reçu ou pas un traitement par apport de saccharose

Figure Supplémentaire 3 : Planche des espèces identifiées sur le site pilote lors du 6ème mois d'expérimentation

	Nom	**Nom commun**	**Famille**
1	*Cornus sanguinea*	Cornouiller sanguin	Cornacées
2	*Circium arvense*	Chardon des vignes	Astéracées
3	*Hypericum perforatum*	Millepertuis	Hypericacées
4	*Verbascum nigrum*	Molène noire	Scrophulariacées
5	*Resda lutea*	Réséda jaune	Résédacées
6	*Sambucus ebulus*	Sureau hièlbe	Caprifoliacées
7	*Carex sp*	Carex sp	Cyperacées
8	nd	nd	Astéracées

	Nom	**Nom commun**	**Famille**
9	*Crataegus monogyna*	Aubépine	Rosacées
10	*Acer pseudoplatanus*	Erable sycomore	Acéracées
11	*Rosa canina*	Rosier des chiens	Rosacées
12	*Geranium molle*	Géranium à feuilles molles	Géraniacées
13	*Juglans regia*	Noyer commun	Juglandacées
14	*Acer campestre*	Erable champêtre	Acéracées
15	*Rumex crispus*	Parelle crépu	Polygonacées

Figure Supplémentaire 3 (Suite) : Planche des espèces identifiées sur le site pilote lors du 6ème mois d'expérimentation

	Nom	Nom commun	Famille
16	*Anagallis arvensis*	Mouron rouge	Primulacées
17	*Plantago lanceolata*	Plantain lancéolé	Plantaginacées
18	*Renonculus repens*	Renoncule rampante	Renonculacées
19	*Calystegia*	Liseron	Convolvulacées
20	*Veronica persica*	Véronique de Perse	Scrofulariacées
21	nd	Fenouil/ carotte/ armoise	Apiacées
22	*Epilobium ciliatum*	Epilobe	Onagracées
23	*Persicaria maculosa*	Renouée/persicaire	Polygonacées

	Nom	Nom commun	Famille
24	*Rubus fructicosa*	Ronce	Rosacées
25	*Circium palustre*	Cirse des marais	Astéracées
26	*Dipsacus fullonum*	Cardère	Caprifiolacées
27	*Chenopodium*	nd	Chénopodiacées
28	*Betulus pendula*	Bouleau	Bétulacées
29	nd	nd	Poacées
30	*Juncus effusus*	Jonc épars	Juncacées
31	*Salix caprea*	Saule marsault	Salicacées

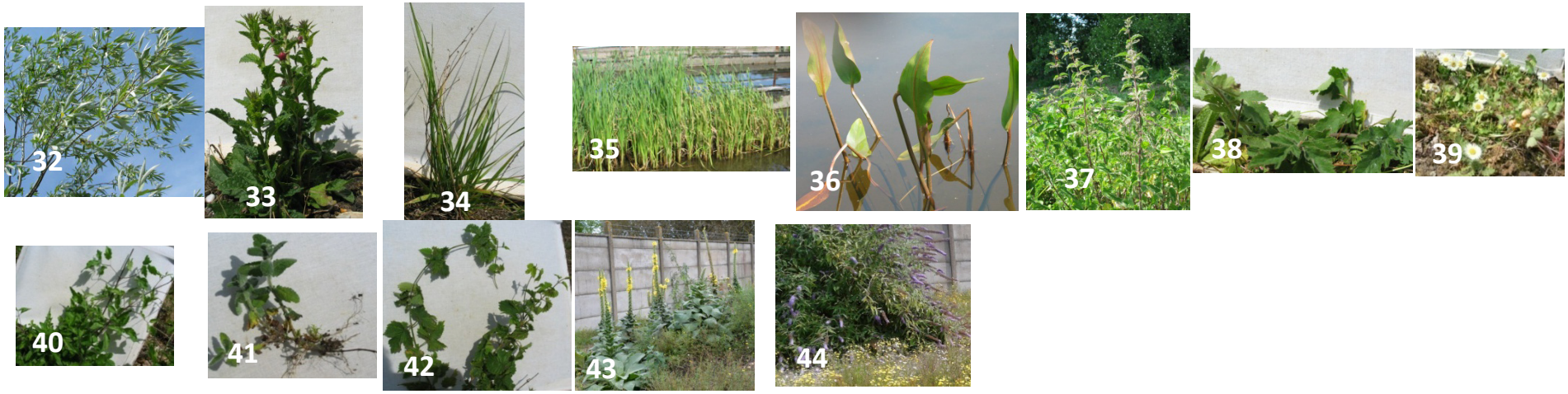

Figure Supplémentaire 3 (Suite) : Planche des espèces identifiées sur le site pilote lors du 6ème mois d'expérimentation

	Nom	**Nom commun**	**Famille**
32	*Salix fragilis*	Saule fragile	Salicacées
33	nd	nd	nd
34	*Carex sp*	Carex sp	Cypéracées
35	*Typha angustifolia*	Jonc massette	Juncacées
36	*Persicaria amphibia ou Polyganum amphibium*	Renouée amphibie	Polygonacées
37	*Urtica dioica*	Ortie	Urticacées
38	*Heracleum sphondylium*	Berce	Apiacées

	Nom	**Nom commun**	**Famille**
39	*Bellis perennis*	Pâquerette	Astéracées
40	*Clematis vitalbas*	Clématite sauvage	Renonculacées
41	*Mentha pulegium*	Menthe pouillot	Lamiacées
42	*Humulus lupulus*	Houblon	Cannabinacées
43	*Verbascum thapsus*	Bouillon-blanc	Scrofulariacée
44	*Buddleja Davidii*	Arbres aux papillons ou *Buddleja* de David	Scrofulariacée

Chapitre 5 : Conclusion générale et perspectives

Jusqu'à présent les études *in-vitro* des effets des hydrocarbures aromatiques polycycliques (HAPs) sur le développement des plantes ont été réalisées pour des expositions longues (plusieurs semaines) (Alkio et al., 2005; Liu et al., 2009; Weisman et al., 2010a). Ces études permettent de comprendre les effets du phénanthrène à long terme sur les plantes mais ces effets sont modulés par le vieillissement d'*Arabidopsis* qui est, à ce stade-là, en fin de cycle de croissance. Des travaux plus récents ont mis en évidence la rapidité avec laquelle la plante est capable d'absorber et de modifier sa façon de transporter ce polluant (Zhan et al., 2010; Zhan et al., 2012), soulignant ainsi l'importance des premiers moments de contact entre la plante et le polluant. Il a donc semblé important de comprendre comment la plante était affectée à court terme (en l'espace de quelques heures).

D'autre part, bien que de nombreuses études aient mis en évidence le rôle protecteur des sucres solubles notamment du saccharose en condition de stress abiotique (Sulmon et al., 2004; Sulmon et al., 2007a; Rosa et al., 2009), l'ensemble des études sur les effets du phénanthrène sur *Arabidopsis thaliana* a été réalisé avec des milieux de cultures contenant du saccharose. Ces études ont donc montré un effet du phénanthrène modulé par celui du saccharose. En ayant travaillé avec des milieux sans sucre, l'effet protecteur des sucres en condition de stress abiotique, notamment sur la régulation des gènes de stress oxydant, a été éliminé. Ceci a permis de comprendre le réel impact des HAPs (dans notre cas, le phénanthrène) sur le développement des plantes, et le contrôle transcriptionnel et métabolique.

Les résultats que nous avons obtenus montrent que la réponse de la plante au niveau de l'expression des gènes se décompose en 3 phases : (i) une phase de perception et signalisation qui débute à 30 minutes d'incubation, (ii) une phase intermédiaire de tentative de détoxification entre 4h et 8h de traitement et enfin (iii) une phase tardive durant laquelle on observe un déficit en carbone et une inhibition de la photosynthèse après 8 à 24h de traitement. Le fonctionnement général de la plante est complètement affecté dés 8h et, à partir de 24h, le métabolisme de la plante paraît être complètement désorganisé.

Ces expérimentations ont permis de montrer que l'effet du phénanthrène sur *Arabidopsis thaliana* est très rapide et très drastique. D'autre part, à travers ces expositions

courtes au phénanthrène en absence de sucre dans le milieu de culture, nous avons pu mettre en évidence que le phénanthrène n'est pas seulement responsable d'un stress oxydant mais que ce xénobiotique affecte aussi des fonctions plus essentielles du métabolisme primaire.

Il a paru intéressant à ce stade de voir si l'apport de saccharose permet de compenser ces dommages causés par le phénanthrène.

D'un point de vue physiologique, les plantes sont moins affectées par le phénanthrène en présence de saccharose. Cet effet se retrouve aussi avec le glucose mais à un niveau moindre.

Le saccharose semble temporiser les effets du phénanthrène au niveau métabolique. Il est pris en charge et métabolisé compensant donc l'inhibition de l'activité photosynthétique. D'autre part, le saccharose pris en charge par la plante a aussi une activité régulatrice du métabolisme primaire. L'ajout du saccharose dans le milieu de culture semble limiter les dommages causés par le phénanthrène au niveau du métabolisme primaire.

En condition de stress causé par le phénanthrène, le saccharose semble moduler les gènes de réponse à un stress et stimuler de manière spécifique un groupe de gène du système antioxydant. Des études d'activités d'enzymes antioxydantes, après une exposition à court terme et dans un milieu avec ou sans sucre, permettraient de mieux cerner comment le système antioxydant est gérer dans les deux conditions. D'autre part, en réalisant l'expérience pour différents temps d'incubation comme cela a été réalisé pour l'analyse de l'effet du phénanthrène sur le transcriptome, il serait intéressant de cibler au bout de combien de temps le système antioxydant se met en place.

Cet effet protecteur du saccharose a aussi pu être observé, partiellement, sur le site pilote de phytoremédiation. En effet, les parcelles de Buddleja ayant reçu du saccharose paraissent plus résistantes et ont montré moins de symptômes de toxicité. D'autre part, l'apport de saccharose aurait permis aux plantes de mieux éliminer les HAPs, en particulier les HMW HAPs plus récalcitrants.

D'autre part, le système de détoxification des xénobiotiques décrit par Sandermann (1992) et complété par Edwards (2011) semble pouvoir être transposable aux HAPs. En effet, les familles de gènes impliquées dans ce processus sont fortement exprimées durant la phase intermédiaire pour des temps d'incubation allant de 4 à 8 heures. Ce système de détoxification parait fortement modifié par l'ajout de saccharose. En effet, l'expression de nombreux gènes impliqués dans le « green-liver » est complètement modifiée. Le saccharose semble inhiber fortement des gènes qui étaient stimulés par l'apport de phénanthrène et stimule d'autres gènes qui ne sont pas différentiellement exprimés en présence de phénanthrène. Cela suggère un système de détoxification différent lorsque le saccharose est ajouté au milieu de culture.

Grâce à l'analyse transcriptomique, des gènes potentiellement impliqués dans la détoxification des HAPs ont été identifiés. Des études supplémentaires sur l'activité des enzymes codées par ces gènes permettraient d'identifier celles qui joueraient un rôle direct dans la métabolisation de ces molécules. Un criblage à l'aide d'écotypes d'*Arabidopsis* mutés sur les gènes listés comme appartenant au xénome et étant impliqué dans la réponse aux HAPs permettrait d'identifier les gènes qui confèrent une tolérance aux HAPs. En effet un criblage des cytochromes P450 potentiellement impliqués dans la détoxification des HAPs a été lancé. Une liste de gènes a été identifiée à partir des données de nos analyses transcriptomiques mais aussi des données de Weisman. Cette étude nous permettra d'identifier les écotypes mutés sensibles, et donc de cibler les CYP impliqués directement ou indirectement dans la gestion du phénanthrène. Le mutant transparent testa 7 (tt7) muté au niveau du CYP75B1 présente un phénotype sensible en présence de phénanthrène en comparaison avec des plantes contrôles. Des essais in-vitro n'ont pas pu mettre en évidence une activité hydroxylation de cette enzyme vis-à-vis du phénanthrène. Ces résultats montrent que ce cytochrome semble plutôt exercer une action indirecte.

La spectrométrie par résonnance magnétique nucléaire (RMN) est une stratégie qui permettrait de mieux comprendre comment les plantes métabolisent/ transforment/ conjuguent les HAPs. Cette méthode est utilisée aussi bien pour l'identification de métabolites que pour faire des profils métabolomiques et des dosages de métabolites (Ratcliffe and Shachar-Hill, 2001). Mieux comprendre les processus de détoxification chez les plantes permettrait d'identifier les plantes les plus efficaces pour la phytoremédiation. Afin

de localiser le phénanthrène et ses dérivés dans les cellules végétales nous avons utilisé la technique de NanoSIMS (Multi-isotope imaging mass spectrometry) qui allie la spectrométrie de masse à de l'imagerie permettant ainsi l'identification d'isotopes tels que le carbone 13. Pour cette expérimentation, des plantules d'*Arabidopsis thaliana* ont été incubés dans du phénanthrène C13. L'analyse par NanoSIMS n'a pas permis d'identifier le signal correspondant aux carbones 13 introduits. Ceci est peut-être dû à (i) la technique de préparation des échantillons pas inclusion dans la résine qui aurait éliminé le phénanthrène libre ou (ii) un marquage insuffisant, en dessous du seuil de détection de l'appareil.

D'autre part, l'utilisation de plantes génétiquement modifiées (PGM) est une approche très intéressante d'un point de vue de la stratégie d'amélioration de la phytoremédiation. Des essais de PGM ont été réalisés en insérant un gène fongique de GST chez le tabac, améliorant ainsi l'efficacité de la plante à éliminer le naphtalène (Dixit et al., 2011). Les transporteurs actifs du phénanthrène chez le blé ont été identifiés (Zhan et al., 2010; Zhan et al., 2012). La surexpression des gènes codant pour ces protéines pourrait permettre de les multiplier et donc de stimuler l'absorption du phénanthrène par les plantes. Toutefois cette stratégie reste au stade expérimental suite à la mise en place du principe de précaution interdisant toute exploitation de PGM en condition naturelle en France. De plus, les PGM sont très mal perçues par la population européenne et plus particulièrement française. Toutefois aux Etats-Unis, en Asie et en Amérique du Sud, les PGM sont cultivées ce qui rend leur utilisation possible pour la phytoremédiation.

Enfin, la mise en place du site pilote de phytoremédiation a permis de mettre en évidence l'efficacité d'un tel système et aussi l'importance des pratiques agricoles (aération du sol, apport de terre saine) dans la diminution des taux de HAPs. Toutefois, ce travail de terrain a montré aussi la difficulté de gérer un tel site à cause la répartition hétérogène de la pollution. Toutefois ce site est représentatif des conditions de pollution des sols industriels suite à un déversement de produit ou à une gestion ancienne des déchets.

L'étude du site pilote a permis de montrer le potentiel de la phytoremédiation. En deux ans, la teneur de HAPs a bien diminué sur les 30 premiers centimètres. Il serait intéressant de faire des études complémentaires afin de voir quel système de plantation est le plus efficace sur des profondeurs plus importantes. Parmi les 3 espèces étudiées, chacune

présente des avantages et des inconvénients rendant le choix de l'espèce difficile. Afin d'obtenir le meilleur résultat, il paraît important de poursuivre l'expérimentation sur 5-10 ans afin que les plantes atteignent leur maximum de potentiel de croissance (après 3 ans pour le miscanthus, après 5 ans pour le saule par exemple) et donc soient les plus efficaces possibles dans l'élimination des HAPs du sol. De plus les conditions environnementales (arrosage, type de sol, climat…) sont déterminantes à la fois pour le choix de l'espèce et pour la mise en place du site de phytoremédiation.

Le rôle des microorganismes du sol dans la phytoremédiation du sol n'est pas à négliger. Les parcelles non-plantées ayant reçu un apport de terre végétale et donc une nouvelle population microbienne ont montré une forte diminution de leur teneur en HAPs. Il serait aussi donc intéressant d'évaluer la population microbienne du sol afin de voir comment l'apport de terre végétale mais aussi les différentes espèces végétales modifient la composition de cette population.

D'autre part, le saccharose est aussi une source de carbone pour les microorganismes et l'apport de cette molécule a probablement modifié la composition microbienne du sol en favorisant le développement ou l'activité de certaines souches.

De plus, il me parait important avant de généraliser l'application du saccharose comme amendement favorisant la phytoremédiation des HAPs d'étudier son devenir dans le sol afin d'ajuster la dose appliquée et de voir son impact sur la qualité du sol. Cependant, afin de rester dans le cadre du développement durable, il serait intéressant de voir si le même effet protecteur est obtenu en épandant des déchets issus de l'industrie sucrière comme de la mélasse ou des pulpes de betterave, permettant ainsi de valoriser les déchets de l'industrie sucrière et de ne plus utiliser des sucres raffinés destinés à l'alimentation humaine.

Bibliographie

Abhilash PC, Powell JR, Singh HB, Singh BK (2012) Plant–microbe interactions: novel applications for exploitation in multipurpose remediation technologies. Trends Biotechnol **30**: 416–420

Abramoff MD, Magalhães PJ, Ram SJ (2004) Image processing with ImageJ. Biophotonics Int **11**: 36–42

ADEME (2011) Taux d'utilisation et couts des différentes techniques et filières de traitement des sols et des eaux souterraines polluées en France-Données 2008.

Al-Awadhi N, Al-Daher R, EINawawy A, Salba MT (1996) Bioremediation of oil-contaminated soil in Kuwait. I. landfarming to remediate oil-contaminated soil. J Soil Contam **5**: 243–260

Alena Torres Netto EC (2005) Photosynthetic pigments, nitrogen, chlorophyll a fluorescence and SPAD-502 readings in coffee leaves. Sci Hortic 199–209

Alkio M, Tabuchi TM, Wang X, Colón-Carmona A (2005) Stress responses to polycyclic aromatic hydrocarbons in *Arabidopsis* include growth inhibition and hypersensitive response-like symptoms. J Exp Bot **56**: 2983–2994

Alkorta I, Garbisu C (2001) Phytoremediation of organic contaminants in soils. Bioresour Technol **79**: 273–276

Andersson BE, Henrysson T (1996) Accumulation and degradation of dead-end metabolites during treatment of soil contaminated with polycyclic aromatic hydrocarbons with five strains of white-rot fungi. Appl Microbiol Biotechnol **46**: 647–652

Andersson BE, Lundstedt S, Tornberg K, Schnürer Y, Öberg LG, Mattiasson B (2003) Incomplete degradation of polycyclic aromatic hydrocarbons in soil inoculated with wood-rotting fungi and their effect on the indigenous soil bacteria. Environ Toxicol Chem **22**: 1238–1243

Antizar-Ladislao, B., Lopez-Real, J. and Beck, A. (2004) Bioremediation of Polycyclic Aromatic Hydrocarbon (PAH)-Contaminated Waste Using Composting Approaches. *Critical Reviews in Environmental Science and Technology*, **34**, 249–289.

Armstrong B, Hutchinson E, Unwin J, Fletcher T (2004) Lung Cancer Risk after Exposure to Polycyclic Aromatic Hydrocarbons: A Review and Meta-Analysis. Environ Health Perspect **112**: 970–978

Ashraf M, Foolad MR (2007) Roles of glycine betaine and proline in improving plant abiotic stress resistance. Environ Exp Bot **59**: 206–216

Atagana HI (2004) Bioremediation of creosote-contaminated soil in South Africa by landfarming. J Appl Microbiol **96**: 510–520

Bae J-W, Park Y-H (2006) Homogeneous versus heterogeneous probes for microbial ecological microarrays. Trends Biotechnol **24**: 318–323

Baerson SR, Sánchez-Moreiras A, Pedrol-Bonjoch N, Schulz M, Kagan IA, Agarwal AK, Reigosa MJ, Duke SO (2005) Detoxification and Transcriptome Response in *Arabidopsis* Seedlings Exposed to the Allelochemical Benzoxazolin-2(3H)-one. J Biol Chem **280**: 21867–21881

Bak S, Beisson F, Bishop G, Hamberger B, Höfer R, Paquette S, Werck-Reichhart D (2011) Cytochromes P450. Arab Book e0144

Balabanič D, Rupnik M, Klemenčič AK (2011) Negative impact of endocrine-disrupting compounds on human reproductive health. Reprod Fertil Dev **23**: 403–416

Banks MK, Kulakow P, Schwab AP, Chen Z, Rathbone K (2003) Degradation of crude oil in the rhizosphere of Sorghum bicolor. Int J Phytoremediation **5**: 225–234

Barker L, Kühn C, Weise A, Schulz A, Gebhardt C, Hirner B, Hellmann H, Schulze W, Ward JM, Frommer WB (2000) SUT2, a Putative Sucrose Sensor in Sieve Elements. Plant Cell Online **12**: 1153–1164

Bezalel L, Hadar Y, Cerniglia CE (1996a) Mineralization of Polycyclic Aromatic Hydrocarbons by the White Rot Fungus Pleurotus ostreatus. Appl Environ Microbiol **62**: 292–295

Bezalel L, Hadar Y, Cerniglia CE (1997) Enzymatic Mechanisms Involved in Phenanthrene Degradation by the White Rot Fungus Pleurotus ostreatus. Appl Environ Microbiol **63**: 2495–2501

Bezalel L, Hadar Y, Fu PP, Freeman JP, Cerniglia CE (1996b) Metabolism of phenanthrene by the white rot fungus Pleurotus ostreatus. Appl Environ Microbiol **62**: 2547–2553

Bhargava A, Carmona FF, Bhargava M, Srivastava S (2012) Approaches for enhanced phytoextraction of heavy metals. J Environ Manage **105**: 103–120

Bilgin DD, Zavala JA, Zhu J, Clough SJ, Ort DR, DeLUCIA EH (2010) Biotic stress globally downregulates photosynthesis genes. Plant Cell Environ **33**: 1597–1613

Bizub D, Wood AW, Skalka AM (1986) Mutagenesis of the Ha-ras oncogene in mouse skin tumors induced by polycyclic aromatic hydrocarbons. Proc Natl Acad Sci **83**: 6048–6052

Bjoerseth A (1983) Handbook of polycyclic aromatic hydrocarbons. Marcel Dekker,New York, NY

Boffetta P, Jourenkova N, Gustavsson P (1997) Cancer risk from occupational and environmental exposure to polycyclic aromatic hydrocarbons. Cancer Causes Control **8**: 444–472

Bolouri-Moghaddam MR, Le Roy K, Xiang L, Rolland F, Van den Ende W (2010) Sugar signalling and antioxidant network connections in plant cells. FEBS J **277**: 2022–2037

Bonassi S, Mfrlo F, Pearce N, Puntoni R (1989) Bladder cancer and occupational exposure to polycyclic aromatic hydrocarbons. Int J Cancer **44**: 648–651

Boonchan S, Britz ML, Stanley GA (2000) Degradation and Mineralization of High-Molecular-Weight Polycyclic Aromatic Hydrocarbons by Defined Fungal-Bacterial Cocultures. Appl Environ Microbiol **66**: 1007–1019

Borsani O, Valpuesta V, Botella MA (2001) Evidence for a Role of Salicylic Acid in the Oxidative Damage Generated by NaCl and Osmotic Stress in *Arabidopsis* Seedlings. Plant Physiol **126**: 1024–1030

Boyes DC, Zayed AM, Ascenzi R, McCaskill AJ, Hoffman NE, Davis KR, Görlach J (2001) Growth stage-based phenotypic analysis of Arabidopsis: a model for high throughput functional genomics in plants. Plant Cell **13**: 1499–1510

Brazier-Hicks M, Offen WA, Gershater MC, Revett TJ, Lim E-K, Bowles DJ, Davies GJ, Edwards R (2007) Characterization and engineering of the bifunctional N- and O-glucosyltransferase involved in xenobiotic metabolism in plants. Proc Natl Acad Sci **104**: 20238–20243

Brennerova MV, Josefiova J, Brenner V, Pieper DH, Junca H (2009) Metagenomics reveals diversity and abundance of meta-cleavage pathways in microbial communities from soil highly contaminated with jet fuel under air-sparging bioremediation. Environ Microbiol **11**: 2216–2227

Callén MS, López JM, Iturmendi A, Mastral AM (2012) Nature and sources of particle associated polycyclic aromatic hydrocarbons (PAH) in the atmospheric environment of an urban area. Environ Pollut Barking Essex 1987. doi: 10.1016/j.envpol.2012.11.009

Carillo P, Grazia M, Pontecorvo G, Fuggi A, Woodrow P (2011) Salinity Stress and Salt Tolerance. Abiotic Stress Plants - Mech. Adapt.

Cerniglia CE (1997) Fungal metabolism of polycyclic aromatic hydrocarbons: past, present and future applications in bioremediation. J Ind Microbiol Biotechnol **19**: 324–333

Cerniglia CE (1992) Biodegradation of polycyclic aromatic hydrocarbons. Biodegradation **3**: 351–368

Cerniglia CE, Baalen CV, Gibson DT (1980) Metabolism of Naphthalene by the Cyanobacterium Oscillatoria sp., Strain JCM. J Gen Microbiol **116**: 485–494

Chambre d'Agriculture de Picardie (2010) Fiche technique du miscanthus. http://www.chambres-agriculture-picardie.fr/no_cache/productions/energie-biomasse/cultures-biomasse/miscanthus.html?access=tlbxaaofywzjsdi&print=1

Cheema SA, Imran Khan M, Shen C, Tang X, Farooq M, Chen L, Zhang C, Chen Y (2010) Degradation of phenanthrene and pyrene in spiked soils by single and combined plants cultivation. J Hazard Mater **177**: 384–389

Cheng CL, Acedo GN, Cristinsin M, Conkling MA (1992) Sucrose mimics the light induction of *Arabidopsis* nitrate reductase gene transcription. Proc Natl Acad Sci **89**: 1861–1864

Chiou TJ, Bush DR (1998) Sucrose is a signal molecule in assimilate partitioning. Proc Natl Acad Sci U S A **95**: 4784–4788

Chitwood DH, Guo M, Nogueira FTS, Timmermans MCP (2007) Establishing leaf polarity: the role of small RNAs and positional signals in the shoot apex. Dev Camb Engl **134**: 813–823

Choi YE, Harada E, Wada M, Tsuboi H, Morita Y, Kusano T, Sano H (2001) Detoxification of cadmium in tobacco plants: formation and active excretion of crystals containing cadmium and calcium through trichomes. Planta **213**: 45–50

Choudhury S, Panda P, Sahoo L, Panda SK (2013) Reactive oxygen species signaling in plants under abiotic stress. Plant Signal. Behav. 8:

Clavel J, Mandereau L, Limasset J-C, Hémon D, Cordier S (1994) Occupational Exposure to Polycyclic Aromatic Hydrocarbons and the Risk of Bladder Cancer: A French Case-Control Study. Int J Epidemiol **23**: 1145–1153

Coleman J, Blake-Kalff M, Davies E (1997) Detoxification of xenobiotics by plants: chemical modification and vacuolar compartmentation. Trends Plant Sci **2**: 144–151

Coruzzi GM, Zhou L (2001) Carbon and nitrogen sensing and signaling in plants: emerging "matrix effects."Curr Opin Plant Biol **4**: 247 – 253

Couée I, Sulmon C, Gouesbet G, Amrani AE (2006) Involvement of soluble sugars in reactive oxygen species balance and responses to oxidative stress in plants. J Exp Bot **57**: 449–459

Cowdrey AE (1975) Pioneering Environmental Law: The Army Corps of Engineers and the Refuse Act. Pac Hist Rev **44**: 331–349

Crowe ML, Serizet C, Thareau V, Aubourg S, Rouze P, Hilson P, Beynon J, Weisbeek P, van Hummelen P, Reymond P, et al (2003) CATMA: a complete *Arabidopsis* GST database. Nucleic Acids Res **31**: 156–158

Cunningham SD, Berti WR, Huang JW (1995) Phytoremediation of contaminated soils. Trends Biotechnol **13**: 393–397

Dabestani R, Ivanov IN (1999) A Compilation of Physical, Spectroscopic and Photophysical Properties of Polycyclic Aromatic Hydrocarbons. Photochem Photobiol **70**: 10–34

Dai C, Tian L, Zhao Y, Chen Y, Xie H (2010) Degradation of phenanthrene by the endophytic fungus Ceratobasidum stevensii found in Bischofia polycarpa. Biodegradation **21**: 245–255

Dejmek J, Solanský I, Benes I, Lenícek J, Srám RJ (2000) The impact of polycyclic aromatic hydrocarbons and fine particles on pregnancy outcome. Environ Health Perspect **108**: 1159–1164

Deng WL, Preston G, Collmer A, Chang CJ, Huang HC (1998) Characterization of the hrpC and hrpRS operons of Pseudomonas syringae pathovars syringae, tomato, and

glycinea and analysis of the ability of hrpF, hrpG, hrcC, hrpT, and hrpV mutants to elicit the hypersensitive response and disease in plants. J Bacteriol **180**: 4523–4531

Derudi M, Venturini G, Lombardi G, Nano G, Rota R (2007) Biodegradation combined with ozone for the remediation of contaminated soils. Eur J Soil Biol **43**: 297–303

Desai C, Pathak H, Madamwar D (2010) Advances in molecular and "-omics" technologies to gauge microbial communities and bioremediation at xenobiotic/anthropogen contaminated sites. Bioresour Technol **101**: 1558–1569

Dixit P, Mukherjee PK, Sherkhane PD, Kale SP, Eapen S (2011) Enhanced tolerance and remediation of anthracene by transgenic tobacco plants expressing a fungal glutathione transferase gene. J Hazard Mater **192**: 270–276

Dixon DP, Edwards R (2010) Glutathione Transferases. Arab Book Am Soc Plant Biol. doi: 10.1199/tab.0131

Domínguez-Solís JR, López-Martín MC, Ager FJ, Ynsa MD, Romero LC, Gotor C (2004) Increased cysteine availability is essential for cadmium tolerance and accumulation in *Arabidopsis thaliana*. Plant Biotechnol J **2**: 469–476

Doty SL (2008) Enhancing phytoremediation through the use of transgenics and endophytes. New Phytol **179**: 318–333

Dubey RS, Singh AK (1999) Salinity Induces Accumulation of Soluble Sugars and Alters the Activity of Sugar Metabolising Enzymes in Rice Plants. Biol Plant **42**: 233–239

Edema CU, Idu TE, Edema MO (2011) Remediation of soil contaminated with polycyclic aromatic hydrocarbons from crude oil. Afr J Biotechnol **10**: 1146–1149

Edwards R, Brazier-Hicks M, Dixon DP, Cummins I (2005) Chemical Manipulation of Antioxidant Defences in Plants. *In* J. A. Callow, ed, Adv. Bot. Res. Academic Press, pp 1–32

Edwards R, Dixon DP, Cummins I, Brazier-Hicks M, Skipsey M (2011a) New Perspectives on the Metabolism and Detoxification of Synthetic Compounds in Plants. *In* P Schröder, CD Collins, eds, Org. Xenobiotics Plants. Springer Netherlands, pp 125–148

Edwards R, Dixon DP, Cummins I, Brazier-Hicks M, Skipsey M (2011b) New Perspectives on the Metabolism and Detoxification of Synthetic Compounds in Plants. *In* P Schröder, CD Collins, eds, Org. Xenobiotics Plants. Springer Netherlands, pp 125–148

EEA (2011a) Overview of economic activities causing soil contamination in some WCE and SEE countries (pct. of investigated sites) — European Environment Agency (EEA). http://www.eea.europa.eu/data-and-maps/figures/overview-of-economic-activities-causing-soil-contamination-in-some-wce-and-see-countries-pct-of-investigated-sites

EEA (2011b) Overview of contaminants affecting soil and groundwater in Europe — European Environment Agency (EEA). http://www.eea.europa.eu/data-and-maps/figures/overview-of-contaminants-affecting-soil-and-groundwater-in-europe

Ellis MH, Dennis ES, Peacock WJ (1999) *Arabidopsis* roots and shoots have different mechanisms for hypoxic stress tolerance. Plant Physiol **119**: 57–64

Ende WV den, Peshev D (2013) Sugars as Antioxidants in Plants. *In* N Tuteja, SS Gill, eds, Crop Improv. Adverse Cond. Springer New York, pp 285–307

Ende WV den, Valluru R (2009) Sucrose, sucrosyl oligosaccharides, and oxidative stress: scavenging and salvaging? J Exp Bot **60**: 9–18

EPA (1996) Superfund today- Focus on cleanup cost.

Escalante-Espinosa E, Gallegos-Martínez ME, Favela-Torres E, Gutiérrez-Rojas M (2005) Improvement of the hydrocarbon phytoremediation rate by Cyperus laxus Lam. inoculated with a microbial consortium in a model system. Chemosphere **59**: 405–413

Euliss K, Ho C, Schwab AP, Rock S, Banks MK (2008) Greenhouse and field assessment of phytoremediation for petroleum contaminants in a riparian zone. Bioresour Technol **99**: 1961–1971

Farrar J, Pollock C, Gallagher J (2000) Sucrose and the integration of metabolism in vascular plants. Plant Sci **154**: 1–11

Ford C, Wilson J (1981) Changes in Levels of Solutes During Osmotic Adjustment to Water Stress in Leaves of Four Tropical Pasture Species. Funct Plant Biol **8**: 77–91

Foyer CH, Noctor G (2005) Oxidant and antioxidant signalling in plants: a re-evaluation of the concept of oxidative stress in a physiological context. Plant Cell Environ **28**: 1056–1071

Foyer CH, Noctor G (2011) Ascorbate and Glutathione: The Heart of the Redox Hub. Plant Physiol **155**: 2–18

FRTR (2002) Remediation Technologies Screening Matrix and Reference Guide, Version 4.0. US Army and EPA, USA

Furuno S, Foss S, Wild E, Jones KC, Semple KT, Harms H, Wick LY (2012) Mycelia Promote Active Transport and Spatial Dispersion of Polycyclic Aromatic Hydrocarbons. Environ Sci Technol **46**: 5463–5470

Furuno S, Päzolt K, Rabe C, Neu TR, Harms H, Wick LY (2010) Fungal mycelia allow chemotactic dispersal of polycyclic aromatic hydrocarbon-degrading bacteria in water-unsaturated systems. Environ Microbiol **12**: 1391–1398

Gagnot S, Tamby J-P, Martin-Magniette M-L, Bitton F, Taconnat L, Balzergue S, Aubourg S, Renou J-P, Lecharny A, Brunaud V (2008) CATdb: a public access to *Arabidopsis* transcriptome data from the URGV-CATMA platform. Nucleic Acids Res **36**: D986–D990

Galili G (1995) Regulation of Lysine and Threonine Synthesis. Plant Cell **7**: 899–906

Gammon MD, Santella RM (2008) PAH, genetic susceptibility and breast cancer risk: an update from the Long Island Breast Cancer Study Project. Eur J Cancer Oxf Engl 1990 **44**: 636–640

Gan S, Lau EV, Ng HK (2009) Remediation of soils contaminated with polycyclic aromatic hydrocarbons (PAHs). J Hazard Mater **172**: 532–549

Gawronski S, Gawronska H (2007) PLANT TAXONOMY FOR PHYTOREMEDIATION. *In* N Marmiroli, B Samotokin, M Marmiroli, eds, Adv. Sci. Technol. Biol. Decontam. Sites Affect. Chem. Radiol. Nucl. Agents. Springer Netherlands, pp 79–88

Ge Y, Dudoit S, Speed TP (2003) Resampling-based multiple testing for microarray data analysis. Test **12**: 1–77

Gerhardt KE, Huang X-D, Glick BR, Greenberg BM (2009) Phytoremediation and rhizoremediation of organic soil contaminants: Potential and challenges. Plant Sci **176**: 20–30

Germaine KJ, Keogh E, Ryan D, Dowling DN (2009) Bacterial endophyte-mediated naphthalene phytoprotection and phytoremediation. FEMS Microbiol Lett **296**: 226–234

Ghanem A, D'Orazio V, Senesi N (2013) Effects of Compost Addition on Pyrene Removal from Soil Cultivated with Three Selected Plant Species. CLEAN – Soil Air Water n/a–n/a

Ghosh M, Singh SP (2005) A Review on Phytoremediation of Heavy Metals and Utilization of It's by Products. Appl Ecol Environ Res **3**: 1–18

Giddings B, Hopwood B, O'Brien G (2002) Environment, economy and society: fitting them together into sustainable development. Sustain Dev **10**: 187–196

Gill PK, Sharma AD, Singh P, Bhullar SS (2003) Changes in germination, growth and soluble sugar contents of Sorghum bicolor (L.) Moench seeds under various abiotic stresses. Plant Growth Regul **40**: 157–162

Göhre V, Jones AME, Sklenář J, Robatzek S, Weber APM (2012) Molecular crosstalk between PAMP-triggered immunity and photosynthesis. Mol Plant-Microbe Interactions MPMI **25**: 1083–1092

Gonzali S, Loreti E, Solfanelli C, Novi G, Alpi A, Perata P (2006) Identification of sugar-modulated genes and evidence for in vivo sugar sensing in Arabidopsis. J Plant Res **119**: 115–123

Goodwin S, Sutter T (2009) Microarray analysis of <i>Arabidopsis</i> genome response to aluminum stress. Biol Plant **53**: 85–99

Guazzaroni M-E, Herbst F-A, Lores I, Tamames J, Peláez AI, López-Cortés N, Alcaide M, Del Pozo MV, Vieites JM, von Bergen M, et al (2013) Metaproteogenomic insights beyond bacterial response to naphthalene exposure and bio-stimulation. ISME J **7**: 122–136

Guo W-J, Bundithya W, Goldsbrough PB (2003) Characterization of the *Arabidopsis* metallothionein gene family: tissue-specific expression and induction during senescence and in response to copper. New Phytol **159**: 369–381

Gupta AK, Kaur N (2005) Sugar signalling and gene expression in relation to carbohydrate metabolism under abiotic stresses in plants. J Biosci **30**: 761–776

Gutiérrez-Alcalá G, Gotor C, Meyer AJ, Fricker M, Vega JM, Romero LC (2000) Glutathione biosynthesis in *Arabidopsis* trichome cells. Proc Natl Acad Sci **97**: 11108–11113

Guy CL, Huber JLA, Huber SC (1992) Sucrose Phosphate Synthase and Sucrose Accumulation at Low Temperature. Plant Physiol **100**: 502–508

Hansen LD, Nestler C, Ringelberg D, Bajpai R (2004) Extended bioremediation of PAH/PCP contaminated soils from the POPILE wood treatment facility. Chemosphere **54**: 1481–1493

Haritash AK, Kaushik CP (2009) Biodegradation aspects of Polycyclic Aromatic Hydrocarbons (PAHs): A review. J Hazard Mater **169**: 1–15

Harms H, Schlosser D, Wick LY (2011) Untapped potential: exploiting fungi in bioremediation of hazardous chemicals. Nat Rev Microbiol **9**: 177–192

Henner P, Schiavon M, Morel J-L, Lichtfouse E (1997) Polycyclic aromatic hydrocarbon (PAH) occurrence and remediation methods. Analusis **25**: M56–M59

Herbette S, Taconnat L, Hugouvieux V, Piette L, Magniette M-LM, Cuine S, Auroy P, Richaud P, Forestier C, Bourguignon J, et al (2006) Genome-wide transcriptome profiling of the early cadmium response of *Arabidopsis* roots and shoots. Biochimie **88**: 1751–1765

Hilson P, Allemeersch J, Altmann T, Aubourg S, Avon A, Beynon J, Bhalerao RP, Bitton F, Caboche M, Cannoot B, et al (2004) Versatile Gene-Specific Sequence Tags for *Arabidopsis* Functional Genomics: Transcript Profiling and Reverse Genetics Applications. Genome Res **14**: 2176–2189

Van Hoewyk D, Takahashi H, Inoue E, Hess A, Tamaoki M, Pilon-Smits EAH (2008) Transcriptome analyses give insights into selenium-stress responses and selenium tolerance mechanisms in Arabidopsis. Physiol Plant **132**: 236–253

Hsiao TC (1973) Plant Responses to Water Stress. Annu Rev Plant Physiol **24**: 519–570

Huang X-D, El-Alawi Y, Penrose DM, Glick BR, Greenberg BM (2004) A multi-process phytoremediation system for removal of polycyclic aromatic hydrocarbons from contaminated soils. Environ Pollut Barking Essex 1987 **130**: 465–476

HuiJie L, CaiYun Y, Yun T, GuangHui L, TianLing Z (2011) Using population dynamics analysis by DGGE to design the bacterial consortium isolated from mangrove sediments for biodegradation of PAHs. Int Biodeterior Biodegrad **65**: 269–275

Islam MA, Macdonald SE (2004) Ecophysiological adaptations of black spruce (Picea mariana) and tamarack (Larix laricina) seedlings to flooding. Trees **18**: 35–42

Jans JH, Vedder H (2008) European Environmental Law. Europa Law Pub.

Jedrychowski W, Galas A, Pac A, Flak E, Camman D, Rauh V, Perera F (2005) Prenatal Ambient Air Exposure to Polycyclic Aromatic Hydrocarbons and the Occurrence of Respiratory Symptoms over the First Year of Life. Eur J Epidemiol **20**: 775–782

Jennings AA (2012) Worldwide regulatory guidance values for surface soil exposure to carcinogenic or mutagenic polycyclic aromatic hydrocarbons. J Environ Manage **110**: 82–102

Jin X-F, Shuai J-J, Peng R-H, Zhu B, Fu X-Y, Tian Y-S, Zhao W, Han H-J, Chen C, Xu J, et al (2011) Identification of candidate genes involved in responses of *Arabidopsis* to polychlorinated biphenyls based on microarray analysis. Plant Growth Regul **65**: 127–135

Johnsen AR, Wick LY, Harms H (2005) Principles of microbial PAH-degradation in soil. Environ Pollut **133**: 71–84

Jones MD, Crandell DW, Singleton DR, Aitken MD (2011) Stable-isotope probing of the polycyclic aromatic hydrocarbon-degrading bacterial guild in a contaminated soil. Environ Microbiol **13**: 2623–2632

Jones P, Vogt T (2001) Glycosyltransferases in secondary plant metabolism: tranquilizers and stimulant controllers. Planta **213**: 164–174

Juhasz AL, Stanley GA, Britz ML (2000) Degradation of High Molecular Weight PAHs in Contaminated Soil by a Bacterial Consortium: Effects on Microtox and Mutagenicity Bioassays. Bioremediation J **4**: 271–283

Kamangar F, Strickland PT, Pourshams A, Malekzadeh R, Boffetta P, Roth MJ, Abnet CC, Saadatian-Elahi M, Rakhshani N, Brennan P, et al (2005) High Exposure to Polycyclic Aromatic Hydrocarbons May Contribute to High Risk of Esophageal Cancer in Northeastern Iran. Anticancer Res **25**: 425–428

Kanaly RA, Harayama S (2000) Biodegradation of High-Molecular-Weight Polycyclic Aromatic Hydrocarbons by Bacteria. J Bacteriol **182**: 2059–2067

Karthikeyan AS, Varadarajan DK, Jain A, Held MA, Carpita NC, Raghothama KG (2007) Phosphate starvation responses are mediated by sugar signaling in Arabidopsis. Planta **225**: 907–918

Katsoyiannis A, Sweetman AJ, Jones KC (2011) PAH molecular diagnostic ratios applied to atmospheric sources: a critical evaluation using two decades of source inventory and air concentration data from the UK. Environ Sci Technol **45**: 8897–8906

Keunen E, Peshev D, Vangronsveld J, VAN DEN Ende W, Cuypers A (2013) Plant sugars are crucial players in the oxidative challenge during abiotic stress: extending the traditional concept. Plant Cell Environ. doi: 10.1111/pce.12061

Kim MG, Geng X, Lee SY, Mackey D (2009a) The Pseudomonas syringae type III effector AvrRpm1 induces significant defenses by activating the *Arabidopsis* nucleotide-binding leucine-rich repeat protein RPS2. Plant J Cell Mol Biol **57**: 645–653

Kim S-J, Kweon O, Cerniglia CE (2009b) Proteomic applications to elucidate bacterial aromatic hydrocarbon metabolic pathways. Curr Opin Microbiol **12**: 301–309

Kim S-J, Kweon O, Jones RC, Freeman JP, Edmondson RD, Cerniglia CE (2007) Complete and integrated pyrene degradation pathway in Mycobacterium vanbaalenii PYR-1 based on systems biology. J Bacteriol **189**: 464–472

Koch K (2004) Sucrose metabolism: regulatory mechanisms and pivotal roles in sugar sensing and plant development. Curr Opin Plant Biol **7**: 235 – 246

Kolb M, Harms H (2000) Metabolism of fluoranthene in different plant cell cultures and intact plants. Environ Toxicol Chem **19**: 1304–1310

Kotterman MJJ, Vis EH, Field JA (1998) Successive Mineralization and Detoxification of Benzo[a]pyrene by the White Rot FungusBjerkandera sp. Strain BOS55 and Indigenous Microflora. Appl Environ Microbiol **64**: 2853–2858

Krapp A, Berthomé R, Orsel M, Mercey-Boutet S, Yu A, Castaings L, Elftieh S, Major H, Renou J-P, Daniel-Vedele F (2011) *Arabidopsis* roots and shoots show distinct temporal adaptation patterns toward nitrogen starvation. Plant Physiol **157**: 1255–1282

Kuiper I, Lagendijk EL, Bloemberg GV, Lugtenberg BJJ (2004) Rhizoremediation: a beneficial plant-microbe interaction. Mol Plant-Microbe Interactions MPMI **17**: 6–15

Küpper H, Lombi E, Zhao FJ, McGrath SP (2000) Cellular compartmentation of cadmium and zinc in relation to other elements in the hyperaccumulator *Arabidopsis* halleri. Planta **212**: 75–84

Kvesitadze E, Sadunishvili T, Kvesitadze G (2009) Mechanisms of Organic Contaminants Uptake and Degradation in Plants. World Acad Sci Eng Technol **55**: 458

Landa P, Storchova H, Hodek J, Vankova R, Podlipna R, Marsik P, Ovesna J, Vanek T (2010) Transferases and transporters mediate the detoxification and capacity to tolerate trinitrotoluene in Arabidopsis. Funct Integr Genomics **10**: 547–559

Lao S-H, Loutre C, Brazier M, Coleman JO., Cole DJ, Edwards R, Theodoulou FL (2003) 3,4-Dichloroaniline is detoxified and exported via different pathways in *Arabidopsis* and soybean. Phytochemistry **63**: 653–661

Larcher W (2003) Physiological Plant Ecology: Ecophysiology and Stress Physiology of Functional Groups. Springer

Launen LA, Dutta J, Turpeinen R, Eastep ME, Dorn R, Buggs VH, Leonard JW, Häggblom MM (2007) Characterization of the indigenous PAH-degrading bacteria of Spartina dominated salt marshes in the New York/New Jersey Harbor. Biodegradation **19**: 347–363

Layton A, Smart AE, Chauhan A, Ripp SA, Williams D, Burton W, Moser S, Phillips JR, Palumbo AV, Sayler G (2012) Ameliorating Risk: Culturable and Metagenomic Monitoring of the 14 Year Decline of a Genetically Engineered Microorganism at a Bioremediation Field Site. OMICS J. Bioremediation Biodegrad. 9:

Lebas G (2012) Etude du métabolisme carboné et azoté de Miscanthus x giganteus. Université de Picardie Jules Verne, France

Lei A-P, Hu Z-L, Wong Y-S, Tam NF-Y (2007) Removal of fluoranthene and pyrene by different microalgal species. Bioresour Technol **98**: 273–280

Lichtenthaler H, Wellburn A (1983) Determinations of total carotenoids and chlorophylls a and b of leaf extracts indifferent solvents. Biochem Soc Trans **603**: 591–592

Lily MK, Bahuguna A, Dangwal K, Garg V (2009) Degradation of Benzo [a] Pyrene by a novel strain Bacillus subtilis BMT4i (MTCC 9447). Braz J Microbiol **40**: 884–892

Liste H-H, Alexander M (2000a) Accumulation of phenanthrene and pyrene in rhizosphere soil. Chemosphere **40**: 11–14

Liste H-H, Alexander M (2000b) Plant-promoted pyrene degradation in soil. Chemosphere **40**: 7–10

Liu H, Weisman D, Ye Y, Cui B, Huang Y, Colón-Carmona A, Wang Z (2009) An oxidative stress response to polycyclic aromatic hydrocarbon exposure is rapid and complex in *Arabidopsis thaliana*. Plant Sci **176**: 375 – 382

Lloyd JC, Zakhleniuk OV (2004) Responses of primary and secondary metabolism to sugar accumulation revealed by microarray expression analysis of the *Arabidopsis* mutant, pho3. J Exp Bot **55**: 1221–1230

Loh K-C, Cao B (2008) Paradigm in biodegradation using Pseudomonas putida—A review of proteomics studies. Enzyme Microb Technol **43**: 1–12

Loreti E, Poggi A, Novi G, Alpi A, Perata P (2005) A Genome-Wide Analysis of the Effects of Sucrose on Gene Expression in *Arabidopsis* Seedlings under Anoxia. Plant Physiol **137**: 1130–1138

Loutre C, Dixon DP, Brazier M, Slater M, Cole DJ, Edwards R (2003) Isolation of a glucosyltransferase from *Arabidopsis thaliana* active in the metabolism of the persistent pollutant 3,4-dichloroaniline. Plant J **34**: 485–493

Luch A (2005) The carcinogenic effects of polycyclic aromatic hydrocarbons. Imperial College Press, Hackensack, NJ

Lurin C, Andrés C, Aubourg S, Bellaoui M, Bitton F, Bruyère C, Caboche M, Debast C, Gualberto J, Hoffmann B, et al (2004) Genome-wide analysis of *Arabidopsis* pentatricopeptide repeat proteins reveals their essential role in organelle biogenesis. Plant Cell **16**: 2089–2103

Ma B, He Y, Chen H, Xu J, Rengel Z (2010) Dissipation of polycyclic aromatic hydrocarbons (PAHs) in the rhizosphere: synthesis through meta-analysis. Environ Pollut Barking Essex 1987 **158**: 855–861

MacGregor DR, Deak KI, Ingram PA, Malamy JE (2008) Root System Architecture in *Arabidopsis* Grown in Culture Is Regulated by Sucrose Uptake in the Aerial Tissues. Plant Cell Online **20**: 2643–2660

Maila MP, Cloete TE (2004) Bioremediation of petroleum hydrocarbons through landfarming: Are simplicity and cost-effectiveness the only advantages? Rev Environ Sci Biotechnol **3**: 349–360

Mallick S, Chatterjee S, Dutta TK (2007) A novel degradation pathway in the assimilation of phenanthrene by Staphylococcus sp. strain PN/Y via meta-cleavage of 2-hydroxy-1-naphthoic acid: formation of trans-2,3-dioxo-5-(2'-hydroxyphenyl)-pent-4-enoic acid. Microbiol Read Engl **153**: 2104–2115

Mancini R, Romano G, Sgambato A, Flamini G, Giovagnoli MR, Boninsegna A, Carraro C, Vecchione A, Cittadini A (1999) Polycyclic Aromatic Hydrocarbon–DNA Adducts in Cervical Smears of Smokers and Nonsmokers. Gynecol Oncol **75**: 68–71

Marmiroli N, Marmiroli M, Maestri E (2006) PHYTOREMEDIATION AND PHYTOTECHNOLOGIES: A REVIEW FOR THE PRESENT AND THE FUTURE. *In* I Twardowska, HE Allen, MM Häggblom, S Stefaniak, eds, Soil Water Pollut. Monit. Prot. Remediat. Springer Netherlands, Dordrecht, pp 403–416

Matsui T, Nomura Y, Takano M, Imai S, Nakayama H, Miyasaka H, Okuhata H, Tanaka S, Matsuura H, Harada K, et al (2011) Molecular Cloning and Partial Characterization of a Peroxidase Gene Expressed in the Roots of <I>Portulaca oleracea</I> cv., One Potentially Useful in the Remediation of Phenolic Pollutants. Biosci Biotechnol Biochem **75**: 882–890

Meßner B, Thulke O, Schäffner AR (2003) *Arabidopsis* glucosyltransferases with activities toward both endogenous and xenobiotic substrates. Planta **217**: 138–146

Miller RL, Garfinkel R, Horton M, Camann D, Perera FP, Whyatt RM, Kinney PL (2004) Polycyclic aromatic hydrocarbons, environmental tobacco smoke, and respiratory symptoms in an inner-city birth cohort. Chest **126**: 1071–1078

Mitsch WJ (2012) What is ecological engineering? Ecol Eng **45**: 5–12

Mittler R, Vanderauwera S, Gollery M, Van Breusegem F (2004) Reactive oxygen gene network of plants. Trends Plant Sci **9**: 490–498

Moya JL, Ros R, Picazo I (1993) Influence of cadmium and nickel on growth, net photosynthesis and carbohydrate distribution in rice plants. Photosynth Res **36**: 75–80

Mrozik A, Piotrowska-Seget Z, Łabuzek S (2003) Bacterial degradation and bioremediation of polycyclic aromatic hydrocarbons. Pol J Environ Stud **12**: 15–25

Murashige T, Skoog F (1962) A Revised Medium for Rapid Growth and Bio Assays with Tobacco Tissue Cultures. Physiol Plant **15**: 473–497

Muratova A, Hūbner T, Tischer S, Turkovskaya O, Möder M, Kuschk P (2003) Plant--rhizosphere-microflora association during phytoremediation of PAH-contaminated soil. Int J Phytoremediation **5**: 137–151

Narro ML, Cerniglia CE, Van Baalen C, Gibson DT (1992) Metabolism of phenanthrene by the marine cyanobacterium Agmenellum quadruplicatum PR-6. Appl Environ Microbiol **58**: 1351–1359

Ojajärvi IA, Partanen TJ, Ahlbom A, Boffetta P, Hakulinen T, Jourenkova N, Kauppinen TP, Kogevinas M, Porta M, Vainio HU, et al (2000) Occupational exposures and pancreatic cancer: a meta-analysis. Occup Environ Med **57**: 316–324

Panz K, Miksch K (2012) Phytoremediation of explosives (TNT, RDX, HMX) by wild-type and transgenic plants. J Environ Manage **113**: 85–92

Parlement Français (2008) LOI n° 2008-757 du 1er août 2008 relative à la responsabilité environnementale et à diverses dispositions d'adaptation au droit communautaire dans le domaine de l'environnement.

Pasternak T, Rudas V, Potters G, Jansen MAK (2005) Morphogenic effects of abiotic stress: reorientation of growth in *Arabidopsis thaliana* seedlings. Environ Exp Bot **53**: 299–314

Paul MJ, Foyer CH (2001) Sink regulation of photosynthesis. J Exp Bot **52**: 1383–1400

Paul MJ, Pellny TK (2003) Carbon metabolite feedback regulation of leaf photosynthesis and development. J Exp Bot **54**: 539–547

Peng R-H, Xiong A-S, Xue Y, Fu X-Y, Gao F, Zhao W, Tian Y-S, Yao Q-H (2008) Microbial biodegradation of polyaromatic hydrocarbons. FEMS Microbiol Rev **32**: 927–955

Perera FP, Li Z, Whyatt R, Hoepner L, Wang S, Camann D, Rauh V (2009) Prenatal Airborne Polycyclic Aromatic Hydrocarbon Exposure and Child IQ at Age 5 Years. Pediatrics **124**: e195–e202

Peshev D, Vergauwen R, Moglia A, Hideg É, Ende WV den (2013) Towards understanding vacuolar antioxidant mechanisms: a role for fructans? J Exp Bot ers377

Pilon-Smits E (2005) Phytoremediation. Annu Rev Plant Biol **56**: 15–39

Pirooznia M, Nagarajan V, Deng Y (2007) GeneVenn - A web application for comparing gene lists using Venn diagrams. Bioinformation **1**: 420–422

Pradhan SP, Conrad JR, Paterek JR, Srivastava VJ (1998) Potential of Phytoremediation for Treatment of PAHs in Soil at MGP Sites. J Soil Contam **7**: 467–480

Price J, Laxmi A, Martin SKS, Jang J-C (2004) Global Transcription Profiling Reveals Multiple Sugar Signal Transduction Mechanisms in Arabidopsis. Plant Cell Online **16**: 2128–2150

Provart T. and Z (2003) A Browser-based Functional Classification SuperViewer for *Arabidopsis* Genomics. Curr Comput Mol Biol 271–272

Pucciariello C, Parlanti S, Banti V, Novi G, Perata P (2012) Reactive oxygen species-driven transcription in *Arabidopsis* under oxygen deprivation. Plant Physiol **159**: 184–196

Pulford ID, Watson C (2003) Phytoremediation of heavy metal-contaminated land by trees—a review. Environ Int **29**: 529 – 540

Rahmani F, Hummel M, Schuurmans J, Wiese-Klinkenberg A, Smeekens S, Hanson J (2009) Sucrose Control of Translation Mediated by an Upstream Open Reading Frame-Encoded Peptide. Plant Physiol **150**: 1356–1367

Rai VK (2002) Role of Amino Acids in Plant Responses to Stresses. Biol Plant **45**: 481–487

Ramel F, Sulmon C, Bogard M, Couée I, Gouesbet G (2009) Differential patterns of reactive oxygen species and antioxidative mechanisms during atrazine injury and sucrose-induced tolerance in *Arabidopsis thaliana* plantlets. BMC Plant Biol **9**: 28

Ramel F, Sulmon C, Cabello-Hurtado F, Taconnat L, Martin-Magniette M-L, Renou J-P, Amrani AE, Couée I, Gouesbet G (2007) Genome-wide interacting effects of sucrose and herbicide-mediated stress in *Arabidopsis thaliana*: novel insights into atrazine toxicity and sucrose-induced tolerance. BMC Genomics **8**: 450

Ramel F, Sulmon C, Serra A-A, Gouesbet G, Couée I (2012) Xenobiotic sensing and signalling in higher plants. J Exp Bot **63**: 3999–4014

Ramesh A, Walker SA, Hood DB, Guillén MD, Schneider K, Weyand EH (2004) Bioavailability and Risk Assessment of Orally Ingested Polycyclic Aromatic Hydrocarbons. Int J Toxicol **23**: 301–333

Ramon M, Rolland F, Sheen J (2008) Sugar Sensing and Signaling. Arab Book e0117

Ratcliffe RG, Shachar-Hill Y (2001) Probing Plant Metabolism with Nmr. Annu Rev Plant Physiol Plant Mol Biol **52**: 499–526

Ravindra K, Sokhi R, Van Grieken R (2008) Atmospheric polycyclic aromatic hydrocarbons: Source attribution, emission factors and regulation. Atmos Environ **42**: 2895–2921

Rehmann L, Prpich GP, Daugulis AJ (2008) Remediation of PAH contaminated soils: Application of a solid–liquid two-phase partitioning bioreactor. Chemosphere **73**: 798–804

Rentz JA, Alvarez PJJ, Schnoor JL (2005) Benzo[a]pyrene co-metabolism in the presence of plant root extracts and exudates: Implications for phytoremediation. Environ Pollut **136**: 477–484

Richardson MD, Karcher DE, Purcell LC (2001) Quantifying Turfgrass Cover Using Digital Image Analysis. Crop Sci **41**: 1884–1888

Roitsch T (1999) Source-sink regulation by sugar and stress. Curr Opin Plant Biol **2**: 198–206

Rolland F, Moore B, Sheen J (2002) Sugar Sensing and Signaling in Plants. Plant Cell **14**: s185–s205

Rosa M, Prado C, Podazza G, Interdonato R, Gonzalez JA, Hilal M, Prado FE (2009) Soluble sugars: Metabolism, sensing and abiotic stress: A complex network in the life of plants. Signal Behav **4**: 288–393

Rozen S, Skaletsky H (2000) Primer3 on the WWW for general users and for biologist programmers. Methods Mol Biol Clifton NJ **132**: 365–386

Rundle A, Tang D, Hibshoosh H, Estabrook A, Schnabel F, Cao W, Grumet S, Perera FP (2000) The relationship between genetic damage from polycyclic aromatic hydrocarbons in breast tissue and breast cancer. Carcinogenesis **21**: 1281–1289

Russo L, Rizzo L, Belgiorno V (2012) Ozone oxidation and aerobic biodegradation with spent mushroom compost for detoxification and benzo(a)pyrene removal from contaminated soil. Chemosphere **87**: 595–601

Rybicki BA, Neslund-Dudas C, Nock NL, Schultz LR, Eklund L, Rosbolt J, Bock CH, Monaghan KG (2006) Prostate cancer risk from occupational exposure to polycyclic aromatic hydrocarbons interacting with the GSTP1 Ile105Val polymorphism. Cancer Detect Prev **30**: 412–422

Rylott EL, Budarina MV, Barker A, Lorenz A, Strand SE, Bruce NC (2011) Engineering plants for the phytoremediation of RDX in the presence of the co-contaminating explosive TNT. New Phytol **192**: 405–413

Salt DE, Blaylock M, Kumar NPBA, Dushenkov V, Ensley BD, Chet I, Raskin I (1995) Phytoremediation: A Novel Strategy for the Removal of Toxic Metals from the Environment Using Plants. Nat Biotechnol **13**: 468–474

Samanta SK, Singh OV, Jain RK (2002) Polycyclic aromatic hydrocarbons: environmental pollution and bioremediation. Trends Biotechnol **20**: 243–248

Sandermann Jr. H (1992) Plant metabolism of xenobiotics. Trends Biochem Sci **17**: 82–84

Sandermann Jr. H, Scheel D, Trenck T v. d. (1984) Use of plant cell cultures to study the metabolism of environmental chemicals. Ecotoxicol Environ Saf **8**: 167–182

Saraswathy A, Hallberg R (2002) Degradation of pyrene by indigenous fungi from a former gasworks site. FEMS Microbiol Lett **210**: 227–232

Sarret G, Harada E, Choi Y-E, Isaure M-P, Geoffroy N, Fakra S, Marcus MA, Birschwilks M, Clemens S, Manceau A (2006) Trichomes of Tobacco Excrete Zinc as Zinc-Substituted Calcium Carbonate and Other Zinc-Containing Compounds. Plant Physiol **141**: 1021–1034

Sattler SE, Mene-Saffrane L, Farmer EE, Krischke M, Mueller MJ, DellaPenna D (2006) Nonenzymatic Lipid Peroxidation Reprograms Gene Expression and Activates Defense Markers in *Arabidopsis* Tocopherol-Deficient Mutants. Plant Cell **18**: 3706–3720

Schamfuß S, Neu TR, Harms H, van der Meer JR, Tecon R, Wick LY (2013a) Mycelial Networks Enhance the Bioavailability of PAH in Water Unsaturated Environments. Environ. Sci. Technol.

Schamfuß S, Neu TR, van der Meer JR, Tecon R, Harms H, Wick LY (2013b) Impact of Mycelia on the Accessibility of Fluorene to PAH-Degrading Bacteria. Environ Sci Technol **47**: 6908–6915

Schneider J, Grosser R, Jayasimhulu K, Xue W, Warshawsky D (1996) Degradation of pyrene, benz[a]anthracene, and benzo[a]pyrene by Mycobacterium sp. strain RJGII-135, isolated from a former coal gasification site. Appl Environ Microbiol **62**: 13–19

Schnoor JL, Licht LA, McCutcheon SC, Wolfe NL, Carreira LH (1995) Phytoremediation of Organic and Nutrient Contaminants. Environ Sci Technol **29**: 318A–323A

Schober W, Lubitz S, Belloni B, Gebauer G, Lintelmann J, Matuschek G, Weichenmeier I, Eberlein-König B, Buters J, Behrendt H (2007) Environmental polycyclic aromatic hydrocarbons (PAHs) enhance allergic inflammation by acting on human basophils. Inhal Toxicol **19 Suppl 1**: 151–156

Schreiber R, Altenburger R, Paschke A, Küster E (2008) How to deal with lipophilic and volatile organic substances in microtiter plate assays. Environ Toxicol Chem SETAC **27**: 1676–1682

Shim D, Kim S, Choi Y-I, Song W-Y, Park J, Youk ES, Jeong S-C, Martinoia E, Noh E-W, Lee Y (2013) Transgenic poplar trees expressing yeast cadmium factor 1 exhibit the characteristics necessary for the phytoremediation of mine tailing soil. Chemosphere **90**: 1478–1486

Singleton DR, Hunt M, Powell SN, Frontera-Suau R, Aitken MD (2007) Stable-isotope probing with multiple growth substrates to determine substrate specificity of uncultivated bacteria. J Microbiol Methods **69**: 180–187

Singleton DR, Jones MD, Richardson SD, Aitken MD (2012) Pyrosequence analyses of bacterial communities during simulated in situ bioremediation of polycyclic aromatic hydrocarbon-contaminated soil. Appl Microbiol Biotechnol. doi: 10.1007/s00253-012-4531-0

Singleton DR, Powell SN, Sangaiah R, Gold A, Ball LM, Aitken MD (2005) Stable-Isotope Probing of Bacteria Capable of Degrading Salicylate, Naphthalene, or Phenanthrene in a Bioreactor Treating Contaminated Soil. Appl Environ Microbiol **71**: 1202–1209

Sitaras IE, Bakeas EB, Siskos PA (2004) Gas/particle partitioning of seven volatile polycyclic aromatic hydrocarbons in a heavy traffic urban area. Sci Total Environ **327**: 249–264

Sivaraman L, Leatham MP, Yee J, Wilkens LR, Lau AF, Marchand LL (1994) CYP1A1 Genetic Polymorphisms and in Situ Colorectal Cancer. Cancer Res **54**: 3692–3695

Sivitz AB, Reinders A, Ward JM (2008) *Arabidopsis* Sucrose Transporter AtSUC1 Is Important for Pollen Germination and Sucrose-Induced Anthocyanin Accumulation. Plant Physiol **147**: 92–100

Skipsey M, Knight KM, Brazier-Hicks M, Dixon DP, Steel PG, Edwards R (2011) Xenobiotic Responsiveness of *Arabidopsis thaliana* to a Chemical Series Derived from a Herbicide Safener. J Biol Chem **286**: 32268–32276

Smith LE, Denissenko MF, Bennett WP, Li H, Amin S, Tang M, Pfeifer GP (2000) Targeting of Lung Cancer Mutational Hotspots by Polycyclic Aromatic Hydrocarbons. J Natl Cancer Inst **92**: 803–811

Smith MR (1990) The biodegradation of aromatic hydrocarbons by bacteria. Biodegradation **1**: 191–206

Ana Sofia Duque AMDA (2013) Abiotic Stress Responses in Plants: Unraveling the Complexity of Genes and Networks to Survive. doi: 10.5772/52779

Solfanelli C, Poggi A, Loreti E, Alpi A, Perata P (2006) Sucrose-Specific Induction of the Anthocyanin Biosynthetic Pathway in Arabidopsis. Plant Physiol **140**: 637–646

Sulmon C, Gouesbet G, Amrani AE, Couée I (2006) Sugar-induced tolerance to the herbicide atrazine in *Arabidopsis* seedlings involves activation of oxidative and xenobiotic stress responses. Plant Cell Reports **25**: 489–498

Sulmon C, Gouesbet G, Binet F, Martin-Laurent F, El Amrani A, Couée I (2007) Sucrose amendment enhances phytoaccumulation of the herbicide atrazine in *Arabidopsis thaliana*. Environ Pollut **145**: 507–515

Sulmon C, Gouesbet G, Couée I, Amrani AE (2004) Sugar-induced tolerance to atrazine in *Arabidopsis* seedlings: interacting effects of atrazine and soluble sugars on psbA mRNA and D1 protein levels. Plant Sci **167**: 913–923

Sulmon C, Gouesbet G, El Amrani A, Couee I Involvement of the ethylene-signalling pathway in sugar-induced tolerance to the herbicide atrazine in *Arabidopsis thaliana* seedlings. J Plant Physiol **164**: 1083–1092

Syed K, Doddapaneni H, Subramanian V, Lam YW, Yadav JS (2010) Genome-to-function characterization of novel fungal P450 monooxygenases oxidizing polycyclic aromatic hydrocarbons (PAHs). Biochem Biophys Res Commun **399**: 492–497

Szabados L, Savouré A (2010) Proline: a multifunctional amino acid. Trends Plant Sci **15**: 89–97

Tadege M, Dupuis I, Kuhlemeier C (1999) Ethanolic fermentation: new functions for an old pathway. Trends Plant Sci **4**: 320–325

Taguchi G, Ubukata T, Nozue H, Kobayashi Y, Takahi M, Yamamoto H, Hayashida N (2010) Malonylation is a key reaction in the metabolism of xenobiotic phenolic glucosides in *Arabidopsis* and tobacco. Plant J **63**: 1031–1041

team RDC (2013) R: a language and environment for statistical computing. R foundation for statistical computing, Vienna, Austria

Técher D, Laval-Gilly P, Henry S, Bennasroune A, Formanek P, Martinez-Chois C, D'Innocenzo M, Muanda F, Dicko A, Rejšek K, et al (2011) Contribution of Miscanthus x giganteus root exudates to the biostimulation of PAH degradation: An in vitro study. Sci Total Environ **409**: 4489–4495

Técher D, Laval-Gilly P, Henry S, Bennasroune A, Martinez-Chois C, D'Innocenzo M, Falla J (2012) Prospects of Miscanthus x giganteus for PAH phytoremediation: A microcosm study. Ind Crops Prod **36**: 276–281

Techer D, Martinez-Chois C, Laval-Gilly P, Henry S, Bennasroune A, D'Innocenzo M, Falla J (2012) Assessment of Miscanthus × giganteus for rhizoremediation of long term PAH contaminated soils. Appl Soil Ecol **62**: 42–49

Thimm O, Bläsing O, Gibon Y, Nagel A, Meyer S, Krüger P, Selbig J, Müller LA, Rhee SY, Stitt M (2004) MAPMAN: a user-driven tool to display genomics data sets onto diagrams of metabolic pathways and other biological processes. Plant J Cell Mol Biol **37**: 914–939

Thum KE, Shin MJ, Palenchar PM, Kouranov A, Coruzzi GM (2004) Genome-wide investigation of light and carbon signaling interactions in Arabidopsis. Genome Biol **5**: R10

Timpa JD, Burke JJ, Quisenberry JE, Wendt CW (1986) Effects of Water Stress on the Organic Acid and Carbohydrate Compositions of Cotton Plants. Plant Physiol **82**: 724–728

Trzesicka-Mlynarz D, Ward OP (1995) Degradation of polycyclic aromatic hydrocarbons (PAHs) by a mixed culture and its component pure cultures, obtained from PAH-contaminated soil. Can J Microbiol **41**: 470–476

Al-Turky AI (2009) Microbial polycyclic aromatic hydrocarbons degradation in soil. Res J Environ Toxicol **3**: 1–8

UE (2004) Directive 2004/35/CE.

UN (1992) Report of the United Nations conference on Envrionment and Development.

Valluru R, Ende WV den (2008) Plant fructans in stress environments: emerging concepts and future prospects. J Exp Bot **59**: 2905–2916

Vavrek MC, Campbell WJ (2002) Identification of Plant Traits That Enhances Biodegradation of Oil.

Venny, Gan S, Ng HK (2012) Modified Fenton oxidation of polycyclic aromatic hydrocarbon (PAH)-contaminated soils and the potential of bioremediation as post-treatment. Sci Total Environ **419**: 240–249

Verslues PE, Zhu J-K (2005) Before and beyond ABA: upstream sensing and internal signals that determine ABA accumulation and response under abiotic stress. Biochem Soc Trans **33**: 375–379

Vervaeke P, Luyssaert S, Mertens J, Meers E, Tack FM., Lust N (2003) Phytoremediation prospects of willow stands on contaminated sediment: a field trial. Environ Pollut **126**: 275–282

Vieira Dos Santos C, Rey P (2006) Plant thioredoxins are key actors in the oxidative stress response. Trends Plant Sci **11**: 329–334

Vilchez-Vargas R, Junca H, Pieper DH (2010) Metabolic networks, microbial ecology and "omics" technologies: towards understanding in situ biodegradation processes. Environ Microbiol **12**: 3089–3104

Wang K, Zhang J, Zhu Z, Huang H, Li T, He Z, Yang X, Alva A (2012a) Pig manure vermicompost (PMVC) can improve phytoremediation of Cd and PAHs co-contaminated soil by Sedum alfredii. J Soils Sediments **12**: 1089–1099

Wang MC, Chen YT, Chen SH, Chang Chien SW, Sunkara SV (2012b) Phytoremediation of pyrene contaminated soils amended with compost and planted with ryegrass and alfalfa. Chemosphere **87**: 217–225

Wang P, Song C-P (2008) Guard-cell signalling for hydrogen peroxide and abscisic acid. New Phytol **178**: 703–718

Wang Z, Liu Z, Yang Y, Li T, Liu M (2012c) Distribution of PAHs in tissues of wetland plants and the surrounding sediments in the Chongming wetland, Shanghai, China. Chemosphere **89**: 221–227

Ward MH, Sinha R, Heineman EF, Rothman N, Markin R, Weisenburger DD, Correa P, Zahm SH (1997) Risk of adenocarcinoma of the stomach and esophagus with meat cooking method and doneness preference. Int J Cancer **71**: 14–19

Warshawsky D, Cody T, Radike M, Reilman R, Schumann B, LaDow K, Schneider J (1995) Biotransformation of benzo[a]pyrene and other polycyclic aromatic hydrocarbons and heterocyclic analogs by several green algae and other algal species under gold and white light. Chem Biol Interact **97**: 131–148

Watts AW, Ballestero TP, Gardner KH (2006) Uptake of polycyclic aromatic hydrocarbons (PAHs) in salt marsh plants Spartina alterniflora grown in contaminated sediments. Chemosphere **62**: 1253–1260

Weisman D, Alkio M, Colón-Carmona A (2010) Transcriptional responses to polycyclic aromatic hydrocarbon-induced stress in *Arabidopsis thaliana* reveal the involvement of hormone and defense signaling pathways. BMC Plant Biol **10**: 59

Wilson SC, Jones KC (1993) Bioremediation of soil contaminated with polynuclear aromatic hydrocarbons (PAHs): A review. Environ Pollut **81**: 229–249

Wind J, Smeekens S, Hanson J (2010) Sucrose: Metabolite and signaling molecule. Phytochemistry **71**: 1610–1614

Wu J, Omokawa H, Hatzios KK (1996) GlutathioneS-Transferase Activity in Unsafened and Fenclorim-Safened Rice (Oryza sativa). Pestic Biochem Physiol **54**: 220–229

Xu J, Su Z-H, Chen C, Han H-J, Zhu B, Fu X-Y, Zhao W, Jin X-F, Wu A-Z, Yao Q-H (2012) Stress responses to phenol in *Arabidopsis* and transcriptional changes revealed by microarray analysis. Planta **235**: 399–410

Xu SY, Chen YX, Wu WX, Wang KX, Lin Q, Liang XQ (2006) Enhanced dissipation of phenanthrene and pyrene in spiked soils by combined plants cultivation. Sci Total Environ **363**: 206–215

Yi H, Crowley DE (2007) Biostimulation of PAH Degradation with Plants Containing High Concentrations of Linoleic Acid. Environ Sci Technol **41**: 4382–4388

Zhan X, Zhang X, Yin X, Ma H, Liang J, Zhou L, Jiang T, Xu G (2012) H(+)/phenanthrene symporter and aquaglyceroporin are implicated in phenanthrene uptake by wheat (Triticum aestivum L.) roots. J Environ Qual **41**: 188–196

Zhan X-H, Ma H-L, Zhou L-X, Liang J-R, Jiang T-H, Xu G-H (2010) Accumulation of phenanthrene by roots of intact wheat (Triticum acstivnm L.) seedlings: passive or active uptake? BMC Plant Biol **10**: 52

Zhanf X-X, Cheng S-P, Zhu C-J, Sun S-L (2006) Microbial PAH-Degradation in Soil: Degradation Pathways and Contributing Factors. Pedosphere **16**: 555–565

Zhang J, Yin R, Lin X, Liu W, Chen R, Li X (2010) Interactive Effect of Biosurfactant and Microorganism to Enhance Phytoremediation for Removal of Aged Polycyclic Aromatic Hydrocarbons from Contaminated Soils. J Heal Sci **56**: 257–266

Zrenner R, Stitt M, Sonnewald U, Boldt R (2006) Pyrimidine and purine biosynthesis and degradation in plants. Annu Rev Plant Biol **57**: 805–836

Zurbriggen MD, Carrillo N, Hajirezaei M-R (2010) ROS signaling in the hypersensitive response. Plant Signal Behav **5**: 393–396

VU :

Le Directeur de Thèse
(Nom et Prénom)

VU :

Le Responsable de l'École doctorale

VU pour autorisation de soutenance

Rennes, le

Le Président de l'Université de Rennes 1

Guy CATHELINEAU

VU après soutenance pour autorisation de publication :

Le Président de Jury,
(Nom et Prénom)